NEUTRON TRANSMUTATION OF NUCLEAR WASTE

A Thesis
Presented to
The Academic Faculty

by

Edward Albert Hoffman

In Partial Fulfillment
of the Requirements for the Degree
Doctor of Philosophy in Nuclear and Radiological Engineering
in the George W. Woodruff School of Mechanical Engineering

Georgia Institute of Technology
July 2002

NEUTRON TRANSMUTATION OF NUCLEAR WASTE

Approved:

Weston M. Stacey, Chairman

Nolan E. Hertel

Farzad Rahnema

C. K. Chris Wang

Daniel W. Tedder

J. Wiley Davidson

Date Approved 7/12/02

TABLE OF CONTENTS

LIST OF TABLES

LIST OF FIGURES

ACRONYMS

ALWR	advanced light-water reactor	HELE	high ^{6}Li enrichment / low ^{6}Li enrichment dual coolant design
amu	Atomic Mass Units	HLW	high-level waste
ANL	Argonne National Laboratory	IDB	Integrated Data Base Report
ATW	accelerator transmutation of waste program	IEU	irradiated enriched uranium
ATWR	accelerator transmutation of waste reactor	IFR	integral fast reactor
BCM	bare critical mass	LBE	Lead bismuth eutectic
BOC	Beginning of Cycle	Li17Pb83	Lithium Lead Eutectic
BWR	boiling water reactor	LLFP	Long-lived Fission Product
DoE	U.S. Department of Energy	LLW	low-level waste
dpa	displacement per atom	LMFBR	liquid metal fast breeder reactor
DU	Depleted Uranium	LWRs	Light water reactors
ENDF	evaluated nuclear data file	MeV	Mega-electron Volts
EOC	End of Cycle	MHD	magnetohydrodynamic
EU	Enriched Uranium	MOX	mixed-oxide (PuO_2 & UO_2) light water reactor fuel
FOM	figure of merit	MRW	mass of repository waste containing one bare crictical mass
FPD	full power days	MTHM	Metric Ton of Heavy Metal
FTWR	fusion transmutation of waste reactor	MTU	Metri Ton of Initial Uranium
GW_e	GigaWatts of Electricital Energy	MWd	Megawatt-days
GW_{th}	GigaWatts of Thermal Energy	NU	Natural Uranium

PWR	pressurized water reactor	TRU	Transuranics
RB	radiation barrier for the high level waste containing one bare critcal mass	UDR	unshielded dose rate at 1 meter
SB	Solid Breeder Design	UREX	Uranium Extraction
SNF	spent nuclear fuel (enriched uranium irradiated in light water reactors	WGPu	weapons grade plutonium
SNS	spontaneous neutron source from one bare cricitcal mass	WPPPR	Working Party on Physics of Plutonium Recycle
TBR	tritium breeding ratio	YMP	Yucca Mountain Project
TG	thermal generation from one bare critical mass		

SUMMARY

Two metal fueled sub-critical fast reactor concepts, cooled by PbLi and PbBi, respectively, for a Fusion Transmutation of Waste Reactor (FTWR) were developed. Heat removal, radiation damage, etc. design constraints were applied to the FTWR to ensure a realistic and credible design. The standard linear stability model for critical systems was extended for evaluation of the linear stability of sub-critical systems, and the FTWR was shown to be stable to power excursions even when substantial positive fuel and coolant temperature coefficients exist. The reactor design concepts were calculated to remain sub-critical for a wide range of off-normal conditions.

Fuel cycle analyses were performed to evaluate the impacts of further transmutation of spent nuclear fuel on high-level and low-level waste mass flows into repositories, on the composition and toxicity of the high-level waste, on the capacity of high-level waste repositories, and on the proliferation-resistance of the high-level waste. Storage intact of LWR spent nuclear fuel, a single recycle in a LWR of the plutonium as MOX fuel, and the repeated recycle of the transuranics in critical and sub-critical fast reactors are compared. Sub-critical reactors based on both accelerator and fusion neutron sources were considered.

The overall conclusions are that repeated recycling of the transuranics from spent nuclear fuel would significantly increase the capacity of high-level waste repositories per unit of nuclear energy produced, significantly increase the nuclear energy production per unit mass of uranium ore mined, significantly reduce the radio-toxicity of the waste streams per unit of nuclear energy produced, and significantly enhance the proliferation-resistance of the material stored in high-level waste repositories.

CHAPTER I

INTRODUCTION

There is a substantial worldwide R&D activity devoted to the transmutation of spent nuclear fuel (e.g. Refs. 1-4). The objective of this activity is to technically evaluate the possibility of reducing the requirements for long-term geological repositories for the storage of high-level radioactive waste (HLW) from spent nuclear fuel (SNF), by neutron fission of the plutonium and higher actinides remaining in the spent fuel discharged from fission power reactors. Repeated recycling of the transuranics from SNF in special purpose fast spectrum reactors could reduce the toxicity of the spent nuclear fuel by a factor of about 100, limited by safety and criticality constraints [1]. These constraints could be relaxed if the reactors (fast or thermal spectrum) could be operated sub-critical, which would require a neutron source. There is a general consensus that significantly higher rates of net actinide destruction can be achieved by repeated recycling of the transuranics from SNF in sub-critical reactors driven by an external neutron source. An accelerator-spallation neutron source has been extensively studied for this application (e.g. Refs. 1-7) and D-T fusion neutron sources have recently received increased attention for this purpose (e.g. Refs. 8-13).

A HLW repository at Yucca Mountain, Nevada is currently being developed by the U.S. DoE Office of Civilian Radioactive Waste Management, which is charged with disposing of all SNF from commercial nuclear reactors and HLW resulting from atomic energy defense activities [14]. The once-through fuel cycle (OTC) is the baseline scenario for the proposed repository. In this scenario, the SNF discharged from light-water reactors (LWRs) is stored intact in the repository after a cooling period in temporary storage.

The Integrated Data Base Report [15] gives a summary of the U.S. SNF inventories and projections. The current inventory of discharged SNF has an average burnup of approximately 33 GWd/MTU, which has been consistently increasing over recent years and is projected to increase further in the future. The current installed capacity of LWRs is approximately 100 GW_e, approximately 2/3 of which

are pressurized water reactors and the remaining 1/3 are boiling water reactors. Over time, the LWRs have operated at increasing efficiencies and with higher initial enrichments, and have thus produced SNF with increasing discharge burnups. This trend will likely continue, resulting in a continued evolution of the composition of the discharged SNF.

The inventory of discharged SNF is estimated to be over 47,000 metric tonnes of initial uranium (MTU) by the end of 2002. Ongoing operation at the current nuclear power production level will produce over 2,000 MTU of additional SNF each year. In the OTC scenario, the SNF would be placed in specially designed containers and placed intact into the repository. The current repository has a statutory limit of 70,000 metric tons of heavy metal, which includes 63,000 MTU of commercial SNF. At current levels of production, the discharged SNF will exceed this limit around 2010. Either legislation will be required to increase the legal capacity or a second repository will be required. Even the most pessimistic predictions about the future of nuclear power in the U.S. project this statutory limit being exceeded by a large amount early in the century. Even if statutory limits are increased, Yucca Mountain has a finite capacity and the limit will be exceeded in the not too distant future.

At current levels of nuclear power production, a new repository with the statutory capacity of Yucca Mountain would be required every 34 years. If the U.S. were to exit the commercial nuclear power business, the SNF could be stored above ground for extended periods of time and eventually placed in one or two repositories. On the other hand, a steady or growing level of nuclear power production will ultimately require a large number of HLW repositories. A steady or growing level of nuclear power production also will eventually deplete the currently very cheap supply of fissile ^{235}U and future supplies of surplus ^{239}Pu from excess nuclear weapons. Transmutation is a credible solution to both of these problems.

The waste management solution in other industries that produce large quantities of hazardous waste materials is typically a combination of solutions including recycle, incineration, and immobilization. Solely immobilization is relied upon in the OTC scenario. Expanded nuclear fuel cycles could reduce the quantity of hazardous wastes by recycling and reduce the hazard and uncertainty by "incinerating" the hazardous and problematic components of the waste. Additionally, the chemical separation of the waste streams would allow for a more effective immobilization of the residual waste. Unlike non-radiological hazardous wastes, radiological wastes are only hazardous for a finite amount of time. Therefore,

immobilization can be effective in eliminating some or all of the hazardous material, particularly short-lived components. Non-radiological hazardous wastes will eventually re-enter the environment, and immobilization attempts to ensure that the rate is sufficiently slow to preclude harm. In the case of radiological waste, reducing the concentration of the long-lived isotopes in the waste increases the likelihood that the rate at which these wastes are re-introduced into the environment is sufficiently slow to be acceptable.

The transmutation portion of the nuclear fuel cycle is for waste management purposes and is akin in function to a hazardous waste incinerator. As with the hazardous waste incinerator, the primary goal of transmutation is to significantly reduce the hazard, real or perceived, of the feed material. An important secondary goal is to utilize the resulting energy to offset some of the cost of the incinerator.

Transmutation is generically the conversion of problematic isotopes to less problematic isotopes. The reasons isotopes are considered problematic are varied, but generally all transuranic isotopes, along with certain long-lived fission product isotopes, may be considered problematic. Fissioning of the transuranic isotopes essentially converts them into fission products, most of which are short-lived. Further transmutation of long-lived fission product isotopes would convert them to other less problematic isotopes.

Radioactive waste management involves both the HLW streams that will be disposed in geologic repositories, as well as the low-level waste streams that are disposed in near-surface burial facilities. Transmutation systems would change the composition and quantities of material that are disposed in both types of disposal systems. In addition, any transmutation system would include a substantial chemical separation system to support the recycle of the materials being transmuted. Thus, with transmutation, the final waste form(s) could be tailored to more effectively immobilize the radioactive waste. By incorporating recycle, incineration, and immobilization, the waste management system for the nuclear fuel cycle would be very different and presumably superior as a result of separation and transmutation.

The topic is complex and there are many technical issues as well as some confusion that revolves around semantics. In Chapter II, the theoretical basis for transmutation of spent nuclear fuel was studied and controlling mass, energy, and neutron balance equations were determined for critical and sub-critical systems. The basic terminology is defined. The background and current status are discussed, along with an overview of a basic fuel cycle incorporating transmutation. The basic physics and balance equations are

defined for actinides and fission product transmutation. The reaction rate and neutron balance equations are developed for critical and sub-critical reactors, including the incorporation of tritium breeding for fusion-driven sub-critical systems. The implications for designing a transmutation system are discussed.

In order to evaluate a transmutation system, measures of the performance must be defined. All components of any nuclear fuel cycle are required to satisfy all regulatory requirements. The difficulty of satisfying these regulatory requirements will directly effect the cost of the system and hence its relative attractiveness. Figures of merit (FOMs) have been developed to enable a quantitative comparison of different transmutation systems with the OTC.

In Chapter III, a broad set of FOMs is defined that try to address a broad set of performance and technical aspects of transmutation systems. The goal is a methodology to compare the wide range of potential neutron sources that could be used to transmute nuclear waste in a consistent manner that identifies and quantifies the major differences between transmutation systems. With the major differences between the different transmutation systems, judgment can be made about options that require further study and areas that require more detailed analysis.

A wide variety of nuclear fuel cycles have been proposed. Commercial LWRs operating on the OTC is the current baseline nuclear fuel cycle in the United States. The OTC is the reference fuel cycle for this study and the SNF from commercial LWRs is the basis for all subsequent fuel cycles.

Since commercial LWRs will produce an evolving composition of SNF, it was necessary to make assumptions about the composition of the SNF that will feed the transmutation systems. Two different options are typically evaluated. The first uses the composition of SNF representative of the average SNF that has been discharged and is currently in temporary storage. The second is to estimate the eventual average properties of the SNF discharged from commercial LWRs after their performance has evolved to some future optimum operation. The composition of already discharged SNF is represented by a relatively low burnup fuel with a fairly long cooling time, and the eventual average discharged SNF is expected to have a much higher burnup with a minimum cooling time. These constitute two significantly different SNF feed streams. The waste placed in Yucca Mountain will be of this first type, and it might be expected that the oldest SNF at shutdown reactors would be processed first. Eventually, the large backlog of discharged

SNF would be processed and over time the feed stream would evolve from the first type to the second. A SNF composition representative of the current inventory of SNF in temporary storage was chosen.

The impact of increased fuel burnup on the waste management properties of the LWR SNF was studied. In Chapter IV, the waste management properties of SNF as a function of burnup are reported. Uranium ore, which is the starting point for the OTC, is naturally hazardous. In order to separate the effects of irradiation from the natural properties of uranium, the entire nuclear fuel cycle including the waste streams associated with manufacturing the initial enriched uranium that is irradiated in the LWR must be considered. The material streams associated with manufacturing enriched uranium and their properties were evaluated and the results are reported in Chapter V.

The design of the fusion transmutation of waste reactor (FTWR) was based on adapting fusion and nuclear technologies that exist or are currently being developed. Two fusion-driven, heavy-metal cooled, metal-fueled, sub-critical reactors were designed for transmutation of the waste from the LWR SNF. One design is a liquid tritium breeding design based on the dual coolant/tritium breeding material (lithium lead eutectic) being developed for fusion applications.[16,17] The other is a solid tritium breeding design cooled by the liquid heavy metal coolant (lead bismuth eutectic) being developed for accelerator-driven transmutation applications.[18] The designs are described and the results of the design evaluations are reported in Chapter VI. A large set of design criteria were evaluated to ensure that a realistic and credible design was developed.

In order for transmutation to have a dramatic impact on the waste management from the nuclear fuel cycle, all transuranics would need to be nearly completely destroyed. Nuclear fuel cycles that repeatedly recycle the transuranics from the LWR SNF in the FTWR were developed and analyzed for both FTWR designs. The performance of the two FTWR fuel cycles was compared to the reference OTC. Variations of some of the major operational parameters of the FTWR were analyzed to quantify their impact on the performance of the FTWR. The fuel cycles and performance were evaluated and are reported in Chapter VII.

Many transmutation systems have been developed to a fairly advanced level. Several of these systems were evaluated for comparison with the FTWR. The feed composition was adjusted to be consistent with the FTWR and the output was then re-evaluated. The results were compared to evaluate the

differences between the FTWR and other transmutation systems and the results are reported in Chapter VIII.

In order to begin transmuting the backlog of SNF as quickly as possible, utilizing existing commercial reactors in the transmutation mission would seem to be a logical part of the nuclear fuel cycle. Mixed-oxide (MOX) fuel is used in many countries, and the U.S. is currently developing a program to partially destroy, degrade, and secure surplus weapons-grade plutonium by irradiation in MOX fuel in commercial LWRs. By recycling the plutonium in the SNF in existing LWRs, the bulk of the transuranics would be reused, producing more energy, which would offset the production of additional plutonium because less enriched uranium fuel would be used in the production of a given quantity of energy. Plutonium recycle would have other effects, such as the production of more minor actinides, and would constitute a significantly different feed stream to any subsequent transmutation system. The first variant of the OTC scenario that was analyzed was a single recycle of plutonium from the LWR SNF back to the LWRs as MOX fuel.

Only a partial reduction of the transuranic inventory results from the single recycle of plutonium as MOX fuel in a LWR. Complete transmutation systems that repeatedly recycle all TRU to ultimately fission all but the small fraction of TRU (which leaks into the waste streams) are required. These systems can be either "non-fertile" systems that contain essentially zero ^{238}U or "fertile" systems containing ^{238}U but designed for conversion ratios substantially less than unity. The actinide composition for these systems, whether fast or thermal, will be very different than existing reactors because of the much higher concentration of TRU. A much higher fraction of the TRU will be MA, and there will be a much lower concentration of the conventional fissile isotopes such as ^{235}U, ^{239}Pu, and ^{241}Pu.

Although transmutation systems may be based on thermal or fast neutron spectrum reactors, the probability of fission (hence actinide destruction) per neutron absorbed in an actinide is generally larger in a fast spectrum [19]. Sodium cooled, metal fueled fast reactor systems were chosen for comparison with the FTWR. Fuel cycles were analyzed based on the three "transmutation" systems (FTWR, ATWR and IFR) that would completely transmute the TRU in the SNF discharged from the LWRs by repeated reprocessing and recycling. The FTWR, ATWR and IFR use metallic actinide/zirconium fuel and liquid metal coolants and operate with fast neutron spectra. The FTWR (Fusion Transmutation of Waste Reactor) and ATWR

(Accelerator Transmutation of Waste Reactor) are sub-critical reactors using non-fertile fuel, and the IFR (Integral Fast Reactor) is a critical reactor using a fertile fuel with a low conversion rate in a critical reactor. The IFR fuel cycle utilizes a small fraction of the depleted uranium to produce the fertile fuel.

The overall conclusions of this study are discussed in Chapter IX and proposed future work is discussed in Chapter X. A large set of appendices that include the detailed input and results of this study and a comprehensive set of references follow this.

CHAPTER II

TRANSMUTATION OVERVIEW

Status of Spent Fuel Disposition

The U.S. Department of Energy's Office of Civilian Radioactive Waste Management is charged with disposal of the nation's high level radioactive waste and spent nuclear fuel resulting from both the commercial nuclear power industry and government defense and research programs. Due to legal challenges from the state of Nevada, budget restrictions from Congress, and various other roadblocks, the development of the permanent repository at Yucca Mountain, Nevada is significantly behind schedule and over budget. In fact, it has yet to be officially determined if this site is technically and scientifically suitable for the quantity and/or types of waste slated for disposal. The President has approved the Yucca Mountain site for the development of a nuclear waste repository. The state of Nevada has vetoed the site, but the Congress can override the veto. Even if this hurdle is cleared, it is far from certain that the repository will be licensed, or what the ultimate time scale and cost of licensing and operating the repository will be. If the nuclear industry continues indefinitely, this repository will be insufficient for the quantity of SNF generated.

In order to mitigate many of the challenges of disposing of the long-lived hazardous components, the transmutation of long-lived components of spent nuclear fuel and other radioactive waste to shorter-lived and stable isotopes has always been considered an option. The National Research Council formed a committee on Separations Technology and Transmutation Systems[20] conducted a broad systems review of the application of separation and transmutation concepts to radioactive waste disposal. This committee released its final report in 1996, which found that even though it is very unlikely that any transmutation system could eliminate the need for a repository, significant benefits could result and that the transmutation concept should be studied.

As the commercial spent nuclear fuel repository siting process continues to be delayed, transmutation will receive more attention. U.S. Senator Pete Domenici in a speech[21] at Harvard University stated the U.S. decision to stop reprocessing and development of mixed-oxide fuels was wrong and that he felt mixed-oxide (MOX) is the best technical solution for disposal of excess weapons grade plutonium. He discussed the benefits of transmutation and stated that he wanted to see Accelerator Transmutation of Waste investigated aggressively, which is currently underway. [22]

Transmutation System Overview

Current U.S. policy is to use the "once-through" fuel cycle (OTC) for commercial light-water reactors. In the OTC, the fresh enriched uranium fuel is irradiated in light-water reactors (LWRs) then stored for some period at the reactor and possibly for some time away from the reactor to allow the spent nuclear fuel (SNF) to decay to a level more easily and safely handled. After this cooling period, the intact spent nuclear fuel will be sealed in waste packages and placed in a repository. The repository will then be sealed when it has reached its capacity.

There is an infinite range of potential fuel cycles. Any separations and transmutation system has to be looked at as a potential nuclear fuel cycle and the entire fuel cycle considered as a complete system. The other separation and transmutation fuel cycles that will be analyzed are based on improving on the OTC by separating the LWR SNF and transmuting selected materials and directly disposing of the remainder of the material following some interim storage period.

In an alternative fuel cycle, which includes separation and transmutation, the spent nuclear fuel would be reprocessed after it has been allowed to decay to the desired level of radioactivity. The valuable elements are recovered for commercial use and certain problematic elements may be recovered for destruction by neutron irradiation (i.e., transmutation). The waste remaining after this process is separated into various streams (e.g., high-level, low-level) and treated for disposal. The objective of introducing the processing / transmutation stage is to reduce, but not eliminate, the requirement for long-term geologic storage of high-level waste. The resulting waste from this alternative fuel cycle is a waste form that is more durable and should perform significantly better in the repository environment than the untreated spent nuclear fuel from the OTC. Additional waste sources associated with the activation of structural materials

will be generated during the irradiation steps and would need to be considered in the evaluation of the transmutation fuel cycles.

The basic elements of the present "once-through" fuel cycle and of a generic "separation and transmutation" fuel cycle are shown in Figure 1. In both scenarios, the spent fuel will be stored at the reactor site prior to shipment. Once the spent fuel has been allowed to cool for sufficient time, it will be shipped offsite to the appropriate facility. In the "once-through" scenario, the spent fuel will be sent directly to the repository facilities where it may be stored for some additional time prior to packaging and emplacement in the repository.

In the "separation and transmutation" system, the spent fuel would be received at the reprocessing facility where it may be stored for some additional time. The spent fuel would then be processed to separate the spent fuel into various streams that would either be prepared for disposal or converted to assemblies suitable for irradiation. The assemblies would then be irradiated and the problematic isotopes would be partially transmuted. The irradiated assemblies would then be placed in storage to allow them to decay and would either be separated for further transmutation or would be prepared for disposal. The neutron source itself would produce materials that need to be handled as radioactive waste and may contain materials that require processing. Depending on the neutron source, this could include uranium fuel, tritium-producing assemblies, lead spallation targets, etc. Since all of these reactions would produce a lot of energy, a power plant would convert the thermal energy to electrical energy. Excess electricity would be sold commercially to offset the cost of separations and transmutation.

The purpose of the nuclear fuel cycles we are analyzing is to improve the waste management performance of the nuclear fuel cycle relative to the OTC. Optimization of the nuclear fuel cycle would involve the minimization of the energy production costs of the entire system including actual disposal costs. Given the current socio-political environment, it is likely that disposal of the intact SNF will be more difficult (i.e., more expensive) than originally anticipated. This is especially true when a publicly acceptable solution is paramount to proceeding to completion of a nuclear fuel cycle. In section CHAPTER III, the figures of merit will be discussed and defined for the systems to be analyzed.

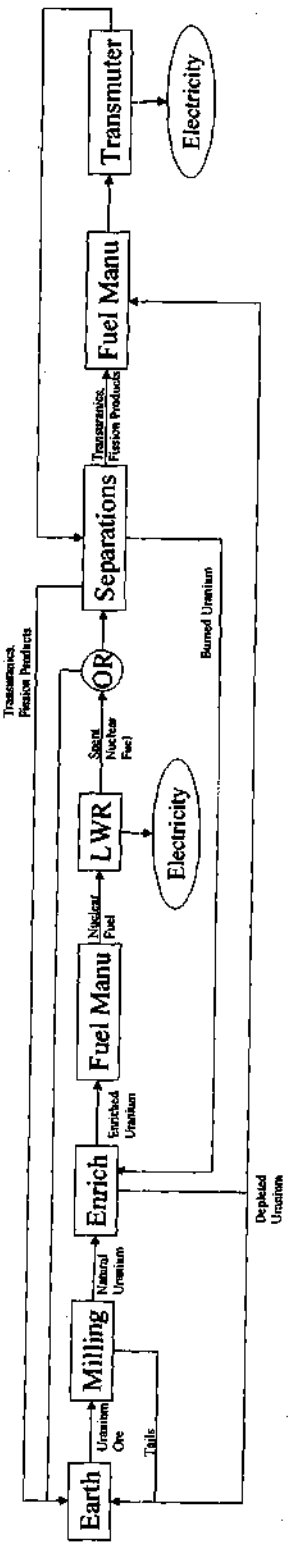

Figure 1 - Separation and Transmutation System Overview

Transmutation Basics

Transmutation focuses on two broad groups of isotopes. The first group is the residual actinides from the spent nuclear fuel. The second group is essentially everything else, which is primarily the fission products but also includes the light element activation products. The primary goal in actinide transmutation is to convert the heavy metal atoms to fission products, while the goal of fission product transmutation is to selectively transmute problematic isotopes to stable isotopes or at least isotopes that rapidly decay to stable isotopes.

Actinides

Figure 2 shows the primary reaction and decay chains for the uranium fueled light-water reactor with the cross sections for a maxwellian spectrum. The n,2n reaction for U-238 has a relatively small cross section, but due to the high U-238 concentration relative to U-235, it contributes significantly to the production of ^{237}Np. Initially, only ^{235}U and ^{238}U are present in significant quantities. The shaded isotopes in Figure 2 are present in significant quantities in LWR SNF.

The Yucca Mountain Viability Assessment[25] identifies four actinides that contribute significantly to the long-term dose predictions. These four isotopes are ^{237}Np, ^{234}U, ^{239}Pu, and ^{242}Pu. Any neutron absorption that does not result in fission will convert these to another actinide that will for the most part decay to one of these four isotopes on the time scale of the repository. These four isotopes and all isotopes that decay to one of these isotopes are shown in Figure 3 with shading. This shows that the only effective means of transmutation of the actinides is fission because capture will in general just convert one troublesome long-lived radioisotope into another.

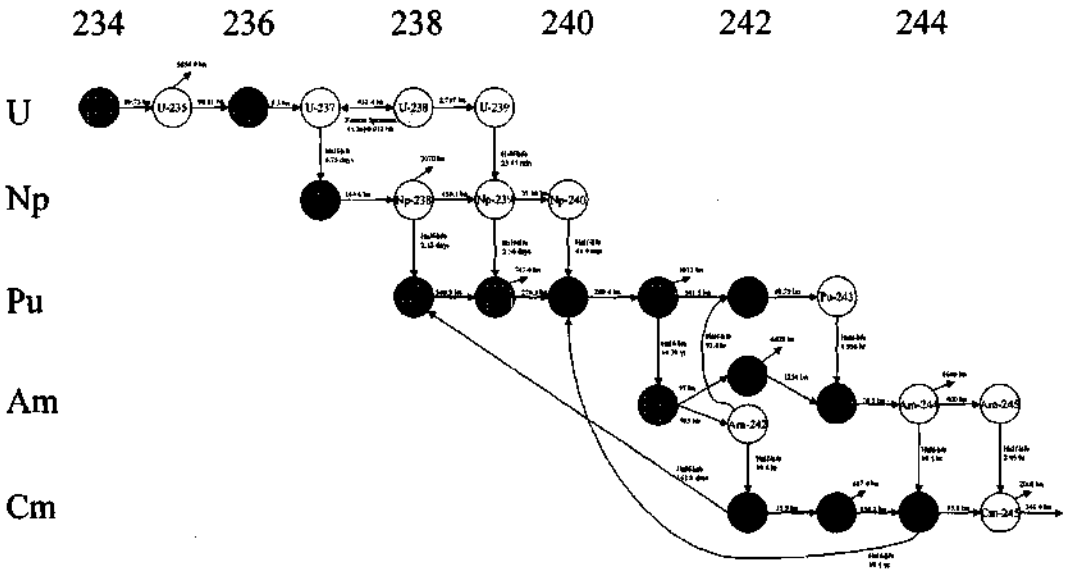

Figure 2 - Actinide Reaction and Decay Chains for Light Water Reactor Fuel

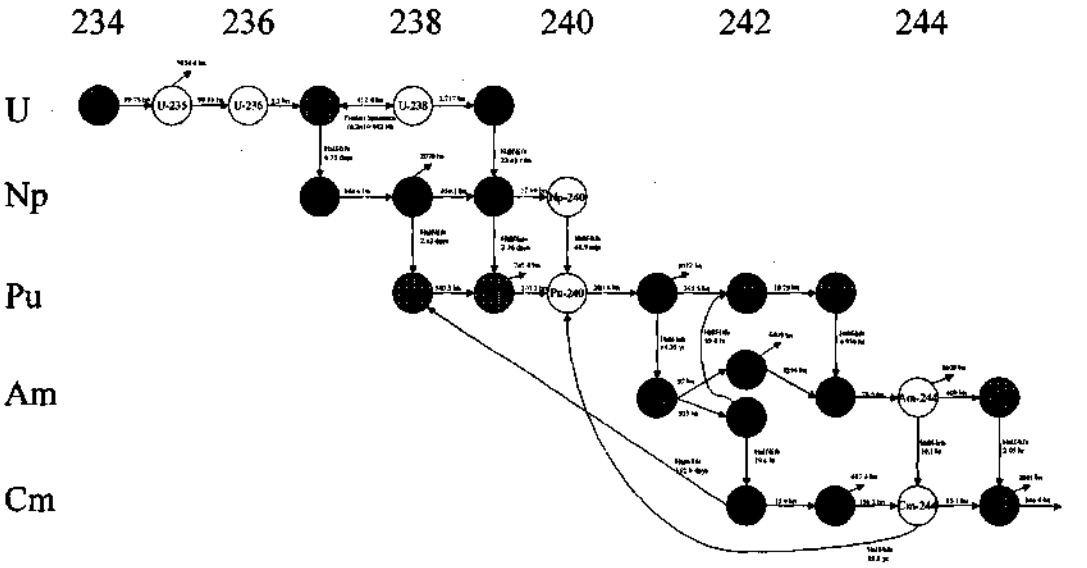

Figure 3 - Actinide Isotopes that Contribute to Repository Dose Estimates

Actinide Transmutation Energy and Mass Balance

The energy per fission is nearly constant for the actinides at approximately 1 MWd/g or 0.85 MeV/amu. This sets the total fission energy for a given mass of transuranic waste regardless of the transmutation system employed. Systems that incorporate the transuranic waste in a uranium matrix will produce greater amounts of energy per unit reduction in the transuranic inventory because of the conversion and fission of uranium. Other systems will also produce slightly more energy because of the other exoergic nuclear reactions.

The waste generated by any transmutation system can be determined by a small number of parameters. For any transmutation system starting with uranium fuel, we can determine the fraction of the transuranics that will end up in the waste knowing only the initial composition of the spent uranium fuel, the recovery fractions for the separations processes, the fractional burnup of the transuranics in each pass through the transmutation reactor, and the conversion rate in the transmutation reactor. The equations are developed for a two step process. The first step extracts the uranium from the transuranics and fission products (UREX). The second step removes the remaining actinides from the fission products (TRU-1). This relationship includes the uranium that is not recovered in the UREX process as transuranics, since most of this will be converted to transuranics during irradiation. A separate recovery fraction is specified for the discharged transmutation system fuel (TRU-2). The following equation shows this relationship.

The conversion rate (C_U) and fission rate (F_U) of uranium relative to the mass of heavy metal fissioned (F_{HM}) are defined as follows.

$$C_U = M_{U \to Np,Pu} / F_{HM}$$
$$F_U = M_{U \to fis} / F_{HM}$$

where $M_{U \to Np,Pu}$ is the mass of uranium converted to transuranics and $M_{U \to fis}$ is the mass of uranium that fissions.

The total transuranic waste (W_{TRU}^{Total}) is determined by the number of times that it is recycled. This will include the residual unfissioned transuranics from the last transmutation step plus the waste lost in recycling.

$$W_{TRU}^{Total} = M_{TRU}^{N} + \sum_{i=0}^{N-1} W_{TRU}^{i}$$

Where N is the number of cycles.

The total mass of heavy metal fissioned (F_{HM}^{Total}) is determined by the number of times that it is recycled. This will include the initial energy generated in the light water reactor plus all the heavy metal fissioned during the recycle of the transuranics. This can be expressed as follows where N is the number of cycles.

$$F_{HM}^{Total} = BU + \sum_{i=1}^{N} F_{HM}^{i}$$

Where N is the number of cycles.

Table 1 shows the equations that govern performance during each pass through the transmutation reactor assuming the same performance parameters during each pass. The initial mass of transuranics (M_{TRU}^{i}) is a function of burnup, design, and operation of the LWR. As long as the conversion rate is not sufficiently high to offset fission and losses, the residual mass of transuranics will be reduced in each subsequent recycle and will decline to zero after and infinite number of recycles.

Table 1 - Transmutation Summary Equations

Recycle	Transuranic Mass Loaded (L^i_{TRU})	Heavy Metal Fissioned (F^i_{HM})	Transuranic Mass Discharged (M^i_{TRU})	Transuranic Mass Lost to Waste (W^i_{TRU})
LWR	0	BU	M^0_{TRU}	$(f^{TRU}_{UREX} + (1 - f^{TRU}_{UREX}) f_{TRU-1}) M^0_{TRU}$
1	$(1 - f^{TRU}_{UREX} - (1 - f^{TRU}_{UREX}) f_{TRU-1}) M^0_{TRU}$	$\frac{f^{HM}_{BU}}{f^{TRU}_{mass}} L^1_{TRU}$	$(1 - \frac{f^{HM}_{BU}(1 - C_U - F_U)}{f^{TRU}_{mass}} L^1_{HM}$	$f_{TRU-2} M^1_{TRU}$
2	$(1 - f_{TRU-2}) M^1_{TRU}$	$\frac{f^{HM}_{BU}}{f^{TRU}_{mass}} L^2_{TRU}$	$(1 - \frac{f^{HM}_{BU}(1 - C_U - F_U)}{f^{TRU}_{mass}}) L^2_{HM}$	$f_{TRU-2} M^2_{TRU}$
n	$(1 - f_{TRU-2}) M^n_{TRU}$	$\frac{f^{HM}_{BU}}{f^{TRU}_{mass}} L^n_{TRU}$	$(1 - \frac{f^{HM}_{BU}(1 - C_U - F_U)}{f^{TRU}_{mass}} L^n_{HM}$	$f_{TRU-2} M^n_{TRU}$

The limits can be evaluated for an infinite number of recycles. The results for the total mass of transuranics that end up in the waste stream are expressed as the following.

$$W^{\infty}_{TRU} = W^0_{TRU} + \sum_{i=1}^{\infty} W^i_{TRU}$$

$$W^{\infty}_{TRU} = M^0_{TRU}\left\{(f^{TRU}_{UREX} + (1 - f^{TRU}_{UREX}) f_{TRU-1}) + (1 - f^{TRU}_{UREX} - (1 - f^{TRU}_{UREX}) f_{TRU-1}) f_{TRU-2} \sum_{i=1}^{\infty} (1 - \frac{f^{HM}_{BU}(1 - C_U - F_U)}{f^{TRU}_{mass}})^i (1 - f_{TRU-2})^{i-1}\right\}$$

$$W^{\infty}_{TRU} = M^0_{TRU}\left\{\begin{array}{l}(f^{TRU}_{UREX} + (1 - f^{TRU}_{UREX}) f_{TRU-1}) + \\ (1 - f^{TRU}_{UREX} - (1 - f^{TRU}_{UREX}) f_{TRU-1}) f_{TRU-2} (1 - \frac{f^{HM}_{BU}(1 - C_U - F_U)}{f^{TRU}_{mass}}) / (1 - (1 - \frac{f^{HM}_{BU}(1 - C_U - F_U)}{f^{TRU}_{mass}})(1 - f_{TRU-2}))\end{array}\right\}$$

The total mass of heavy metal that is fissioned for an infinite recycle is expressed as the following.

$$F^{\infty}_{HM} = BU + \sum_{i=1}^{\infty} F^i_{TRU} = BU + M^0_{TRU} \frac{f^{HM}_{BU}}{f^{TRU}_{mass}} (1 - f^{TRU}_{UREX} - (1 - f^{TRU}_{UREX}) f_{TRU-1}) \sum_{i=1}^{\infty} (1 - \frac{f^{HM}_{BU}(1 - C_U - F_U)}{f^{TRU}_{mass}})^{i-1} (1 - f_{TRU-2})^{i-1}$$

$$F^{\infty}_{HM} = BU + M^0_{TRU} \frac{f^{HM}_{BU}}{f^{TRU}_{mass}} (1 - f^{TRU}_{UREX} - (1 - f^{TRU}_{UREX}) f_{TRU-1}) / (1 - (1 - \frac{f^{HM}_{BU}(1 - C_U - F_U)}{f^{TRU}_{mass}})(1 - f_{TRU-2}))$$

Discharge Burnup and System Burnup Definitions

There are two separate burnups that are referred to in this analysis. These are the discharge burnup and the system burnup, which have significantly different meanings.

The discharge burnup (BU) is the traditional definition of burnup expressed as the fraction of heavy metal fissioned. The residual heavy metal that will either go to the waste or be recycled is unity minus the discharge burnup.

The system burnup (BU_{sy}) is the effective burnup of the transmutation system. This is the ratio of the feed minus the waste to the feed or unity minus the ratio of the waste to the feed. The feed and waste terms can be defined to suit the purpose of the system being analyzed. For this analysis, the feed is the transuranics in the SNF from the OTC and the waste is the transuranics that are lost in the various processing steps. If all processes were perfect, the system burnup would be 100% for infinite recycle regardless of the discharge burnup. If a limited number of recycles is performed, the residual unfissioned transuranics would be included as part of the waste stream. For the infinite recycle of LWR SNF transuranics as described in the previous section the system burnup would be defined by the following equation.

$$BU_{sy} = 1 - \frac{W_{TRU}^{\infty}}{M_{TRU}^{0}}$$

Effect of Conversion Rate and Uranium Loading

The conversion rate from uranium to transuranics (C_U) and the fission rate of uranium (F_U) are a strong function of the design (spectrum), loading, and burnup of transuranics for different transmutation reactors. These values can be estimated based on the fission and capture cross sections for uranium relative to the transuranic fission. For a design of the Li17Pb83 cooled FTWR the microscopic cross sections are 1.0 for transuranic fission, 0.2721 for uranium absorption and 0.0648 for uranium fission. The differential equation for the time dependent concentrations of uranium and transuranics are the following where ($[\phi t]$) is the normalized fluence.

$$\frac{dU}{d[\phi t]} = -(\sigma_f^U + \sigma_c^U)U$$

$$\frac{dTRU}{d[\phi t]} = -\sigma_f^{TRU} TRU + \sigma_{trn}^U U$$

The normalized fluence is calculated that gives the specified heavy metal burnup, and then the integral uranium conversion and fission parameters can be determined.

Figures 4 - 6 show the behavior for a transmutation reactor with the relative cross sections described above. Figure 4 shows the net reduction in the transuranics and excess fissions as a function of the transuranic loading for a 25% heavy metal burnup. The excess fissions are the number of fissions above the net reduction in transuranics or the effective fission rate of the uranium. This is the fractional increase in the number of fissions required for the reduction of a given amount of transuranics because of the fission and capture of the uranium. The larger transuranic fission cross section causes the transuranic burnup to increase as the loading decreases until it peaks at around 35% transuranic / 65% uranium. The excess fissions increases exponentially as the uranium mass increases. Figure 5 shows the mass of transuranics that will end up in the waste stream. This shows the same behavior as the transuranic burnup. Figures 4 - 5 show that the addition of uranium can reduce the mass of transuranic that end up in the waste for a given loading of heavy metal and fraction burnup. This comes at the expense of a larger total number of fissions to destroy the entire inventory of transuranics. Figure 6 shows the transuranic waste as a function of burnup. The transuranic waste will increase rapidly at burnups less than roughly 15% and decreases slowly at higher burnups.

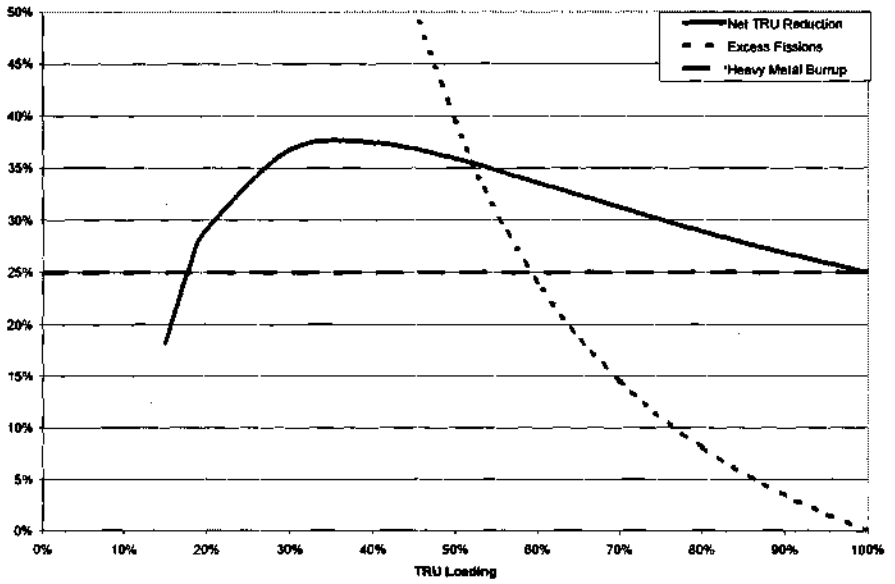

Figure 4 - Transuranic Burnup and Excess Fissions versus TRU Loading

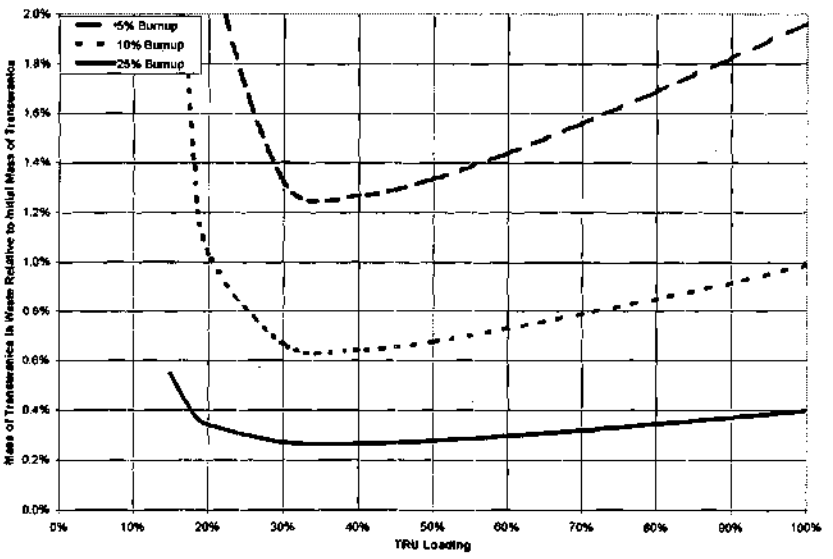

Figure 5 - Transuranic Waste versus Transuranic Loading for Infinite Recycle

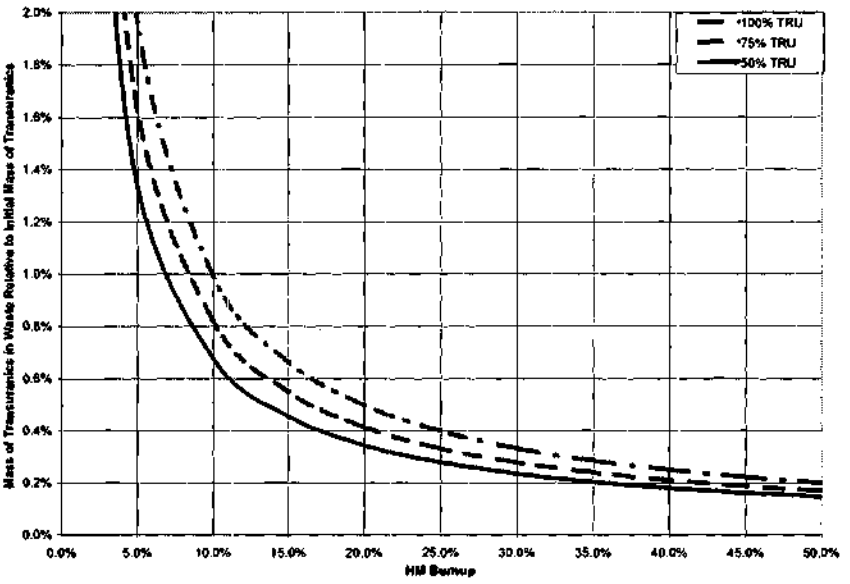

Figure 6 - Transuranic Waste versus Heavy Metal Burnup

MOX Offset

In addition to the effects described above, if the transmutation reactor is a net producer of electricity, the transmutation reactor will offset the production of transuranics from the LWR. The offset of production will occur because less LWRs will be needed to meet electrical demands. This also occurs when plutonium is recycled and used to create mixed oxide (MOX) fuel in existing reactors. The transuranics that would have been produced in the uranium fuel are not produced, therefore reducing the overall inventory of transuranics even if actual reduction in transuranic mass in the MOX fuel is neglected. The magnitude of the offset is a function of the plutonium concentration in the spent light water reactor fuel (f_{Pu}^{U}), the transuranic loading in the MOX fuel (m_{Pu}^{MOX}), the discharge burnup of the uranium fuel (BU_U), and the discharge burnup of the MOX fuel (BU_{MOX}). The mass of plutonium in the discharged uranium fuel is: $M_{Pu} = f_{Pu}^{U} M_U$. This would produce a fixed quantity of MOX fuel: $M_{MOX} = \frac{f_{Pu}^{U} M_U}{m_{Pu}^{MOX}}$. The energy produced by the uranium fuel is $E_U = BU_U M_U$. The energy produced by the MOX fuel is

$E_{MOX} = BU_{MOX} M_{MOX} = BU_{MOX} \frac{f_{Pu}^{U} M_U}{m_{Pu}^{MOX}}$. The fraction of energy produced by the MOX fuel is

$f_E^{MOX} = \frac{E_{MOX}}{E_U + E_{MOX}} = \frac{f_{Pu}^{U} BU_{MOX}}{f_{Pu}^{U} BU_{MOX} + m_{Pu}^{MOX} BU_U}$. If the burnup of the MOX fuel and the uranium fuel are the same and the plutonium concentration in the spent uranium fuel is 1% and the plutonium loading in the MOX fuel is 3.5%, the fraction of energy produced by the MOX fuel would be 22%. This would be a reduction of 22% in the mass of uranium spent fuel produced per unit energy and therefore a reduction in the transuranic inventory by 22% per unit energy produced versus the OTC before any reduction of the transuranic mass that would occur in the MOX fuel are taken into account. The offset effect is a very large component of the MOX fuel cycle and will increase with each additional recycle of the plutonium.

Actinide Transmutation Neutron Balance

The transmutation of actinides has been proposed in a wide variety of reactors including fast and thermal spectrums as well as critical and sub-critical reactors. In order for transmutation to be beneficial, the transuranics will need to be fissioned essentially completely. The composition will change as the isotopes undergo neutron capture and radioactive decay. The neutron balance for an isotope can be performed for a given spectrum. This calculates the average number of absorptions (n_{abs}) an isotope undergoes before it fissions and the average number of neutrons produced by fission ($\bar{\nu}$). The neutron surplus (n_{sur}) is the excess neutron produced in the process of completely fissioning the original isotope. The more excess neutrons, in general, the easier it will be to design a system that completely fissions a given isotope. Isotopes with very small or negative neutron surplus will require the surplus neutrons from other isotopes or externally supplied neutrons for complete fission. The reaction and decay chain is followed until there is a negligible quantity left. Each isotope either absorbs a neutron or decays to another isotope. The probability of absorption in isotope j is based on the average flux ($\bar{\phi}$), which is the flux averaged over operation, storage, and processing. This is expressed as following.

$$p_{abs,j} = \frac{\bar{\phi}\sigma_{abs,j}}{\bar{\phi}\sigma_{abs,j} + \lambda_j}$$

The probability of fission of isotope j as a result on the neutron capture is the following.

$$p_{fis,j} = \frac{\sigma_{fis,j}}{\sigma_{abs,j}}$$

The number of neutrons absorbed by isotope j is the following.

$$n_{abs,j} = C_j p_{abs,j}$$

The number of neutrons produced by fission of isotope j is the following.

$$\bar{\nu}_j = \nu_j p_{fis,j} n_{abs,j}$$

The concentration of isotope 1 (C_1) is unity and the concentration of all subsequent isotopes in the reaction-decay chain is calculated based on the reaction probabilities. The original isotope is followed down through all branches of the reaction-decay chain and the neutrons absorbed, fission neutrons produced, and surplus neutrons is calculated as follows.

$$n_{abs} = \sum_{j=1}^{\infty} \bar{n}_{abs} \; ; \; \bar{\nu} = \sum_{j=1}^{\infty} \bar{\nu}_j \; ; \; n_{sur} = \bar{\nu} - n_{abs}$$

This number is sensitive to the fraction of ^{241}Pu that decays since the ^{241}Am has a much lower fission probability than ^{241}Pu. This is also true for other isotopes such as ^{238}Pu, but in general this method will identify the isotopes that will be most difficult to transmute.

Table 2 and 3 show the cross sections, average number of neutrons required to produce fission and the average number of neutrons produced by the fission for a fast reactor and LWRs, respectively. The cross sections are normalized to the neutron absorption cross sections for U-238 and were taken from the ORIGEN-S cross section libraries for a liquid metal fast breeder reactor (LMFBR) in SCALE 4.4.[42] The spectrum has a very large effect on the neutron balance. In general, the harder the spectrum the less neutrons required to produce fission and the more neutrons produced by fission. Figures 7 and 8 show the excess neutrons for fast and light water reactors, respectively. Figures 7 shows that in a fast spectrum all of the isotopes have a neutron surplus and most have a significantly large neutron surplus. Figures 8 shows that in a LWR spectrum most of the isotopes have a small or negative neutron surplus. The number of neutrons produced per absorption in a given isotope (η-1) shows that only a few isotopes in an LWR are producing more neutrons than they are absorbing, while in the fast reactor this number increases significantly.

Table 4 shows a comparison between the fast reactor and the LWR. In general, the number of neutrons produced by fission is only slightly higher in the fast reactor than in the LWR, while the average number of neutrons required to produce fission is significantly less in the fast reactor for most isotopes. In particular, Np-237 requires only 45% as many neutrons to produce fission in a fast reactor as in a LWR. Pu-238 requires 65%, Pu-238 requires 39% and Pu-240 requires 59%. Some of the major constituents of the LWR transuranics will require far less neutrons to fission in a fast spectrum. One advantage of the thermal spectrum is that most cross sections relative to U-238 absorption are much larger. This could allow for the design of a transmutation system with a small transuranic conversion rate in a thermal spectrum using a U-238 fuel matrix.

Table 2 - Fast Reactor Neutron Balances

Isotope	σ_{abs}	σ_{fis}	ν	η-1	n_{abs}	$\bar{\nu}$	n_{sup}
Th232	1.35	0.04	2.42	-0.93	2.16	2.52	0.36
U233	10.42	9.26	2.51	1.23	1.19	2.52	1.33
U234	2.82	1.50	2.71	0.44	1.73	2.62	0.89
U235	7.63	5.97	2.43	0.90	1.56	2.52	0.97
U236	2.29	0.34	2.76	-0.59	2.55	2.85	0.31
U238	1	0.13	2.76	-0.65	2.25	2.92	0.67
Np237	3.31	1.06	3.04	-0.03	1.82	2.87	1.05
Pu238	4.71	4.06	2.76	1.37	1.20	2.79	1.59
Pu239	6.91	5.44	2.89	1.27	1.42	2.94	1.52
Pu240	2.26	1.04	3.16	0.45	1.99	3.12	1.14
Pu241	8.59	7.32	2.95	1.51	1.32	2.96	1.64
Pu242	1.82	0.82	2.82	0.26	2.16	3.03	0.86
Am-241	4.27	1.36	3.52	0.12	1.84	3.09	1.26
Am242m	6.56	5.38	3.53	1.89	1.38	3.47	2.09
Am243	2.33	0.70	3.01	-0.10	2.11	3.20	1.09
Cm244	2.31	1.21	3.24	0.70	1.58	3.28	1.69
Cm245	8.37	7.20	3.31	1.85	1.23	3.31	2.09
Cm246	1.77	0.88	3.32	0.65	1.62	3.34	1.71
Cm247	7.38	6.32	3.32	1.84	1.24	3.36	2.12
Cm248	1.76	0.86	3.32	0.62	1.68	3.58	1.90
Cf249	9.94	7.49	3.71	1.80	1.32	3.83	2.51
Cf250	4.81	3.59	4.10	2.06	1.31	4.19	2.88
Cf251	7.17	5.97	4.49	2.73	1.22	4.45	3.23
Cf252	4.78	3.64	4.40	2.35	1.32	4.26	2.95

Note: Cross sections normalized to the U-238 absorption cross section

Table 3 - Light Water Reactor Neutron Balances

Isotope	σ_{abs}	σ_{fis}	ν	η-1	n_{fis}	$\bar{\nu}$	n_{surp}
Th232	2.98	0.02	2.42	-0.98	2.31	2.50	0.20
U233	59.58	52.96	2.50	1.22	1.32	2.50	1.19
U234	21.04	0.53	2.71	-0.93	2.86	2.52	-0.33
U235	51.92	42.22	2.43	0.98	1.91	2.52	0.61
U236	7.50	0.29	2.76	-0.89	4.85	2.91	-1.94
U238	1	0.10	2.76	-0.72	2.98	2.92	-0.07
Np237	34.81	0.53	2.61	-0.96	4.01	2.92	-1.09
Pu238	34.60	2.42	2.75	-0.81	3.05	2.92	-0.13
Pu239	158.39	101.33	2.88	0.84	2.21	2.93	0.73
Pu240	142.36	0.58	3.16	-0.99	3.35	3.03	-0.32
Pu241	150.75	110.14	2.94	1.15	2.14	3.04	0.90
Pu242	33.79	0.43	2.81	-0.96	4.24	3.31	-0.93
Am-241	105.18	1.07	3.09	-0.97	3.78	2.97	-0.81
Am242m	756.32	629.61	3.18	1.65	1.55	3.20	1.65
Am243	48.40	0.43	3.00	-0.97	3.28	3.31	0.03
Cm244	12.97	0.89	3.23	-0.78	2.30	3.32	1.02
Cm245	201.28	172.07	3.30	1.82	1.40	3.32	1.93
Cm246	5.37	0.00	3.31	-1.00	2.73	3.46	0.73
Cm247	79.53	53.89	3.31	1.24	1.73	3.46	1.73
Cm248	7.66	0.00	3.32	-1.00	2.27	3.77	1.51
Cf249	261.68	233.45	3.70	2.30	1.27	3.77	2.51
Cf250	626.40	0.00	4.09	-1.00	2.48	4.38	1.90
Cf251	719.09	470.85	4.48	1.93	1.48	4.38	2.90
Cf252	9.98	6.81	4.40	2.00	1.40	4.20	2.80

Note: Cross sections normalized to the U-238 absorption cross section

Table 4 - Neutron Balances Comparison

Isotope	$\frac{n_{fis}^{FR}}{n_{fis}^{LWR}}$	$\frac{\bar{\nu}_{fis}^{FR}}{\bar{\nu}_{fis}^{LWR}}$
Th232	0.94	1.01
U233	0.91	1.01
U234	0.61	1.04
U235	0.82	1.00
U236	0.52	0.98
U238	0.75	1.00
Np237	0.45	0.98
Pu238	0.39	0.95
Pu239	0.65	1.00
Pu240	0.59	1.03
Pu241	0.62	0.97
Pu242	0.51	0.92
Am-241	0.49	1.04
Am242m	0.89	1.08
Am243	0.64	0.96
Cm244	0.69	0.99
Cm245	0.88	1.00
Cm246	0.59	0.96
Cm247	0.72	0.97
Cm248	0.74	0.95
Cf249	1.04	1.01
Cf250	0.53	0.96
Cf251	0.82	1.02
Cf252	0.94	1.01

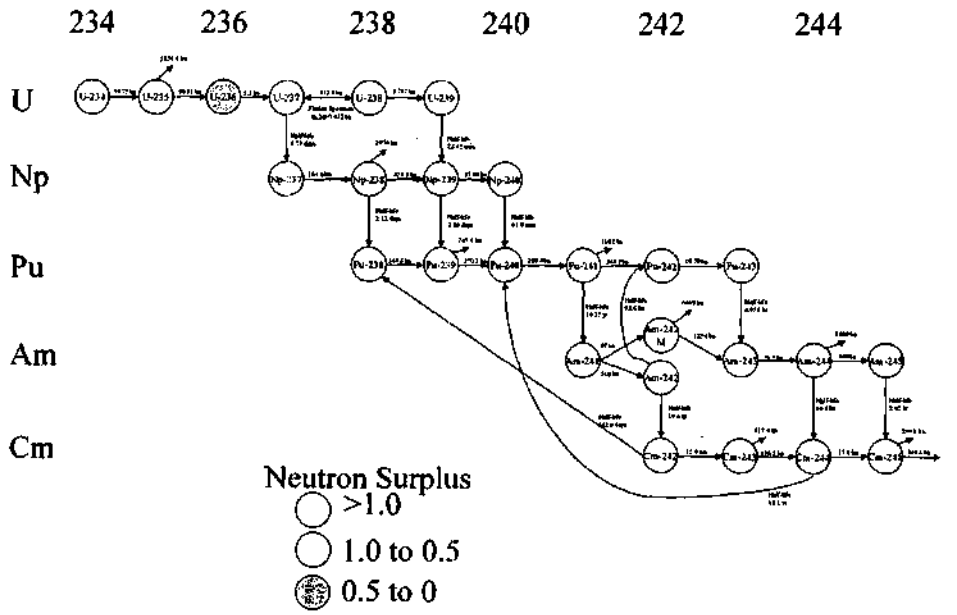

Figure 7 - Neutron Balance for Fast Reactor

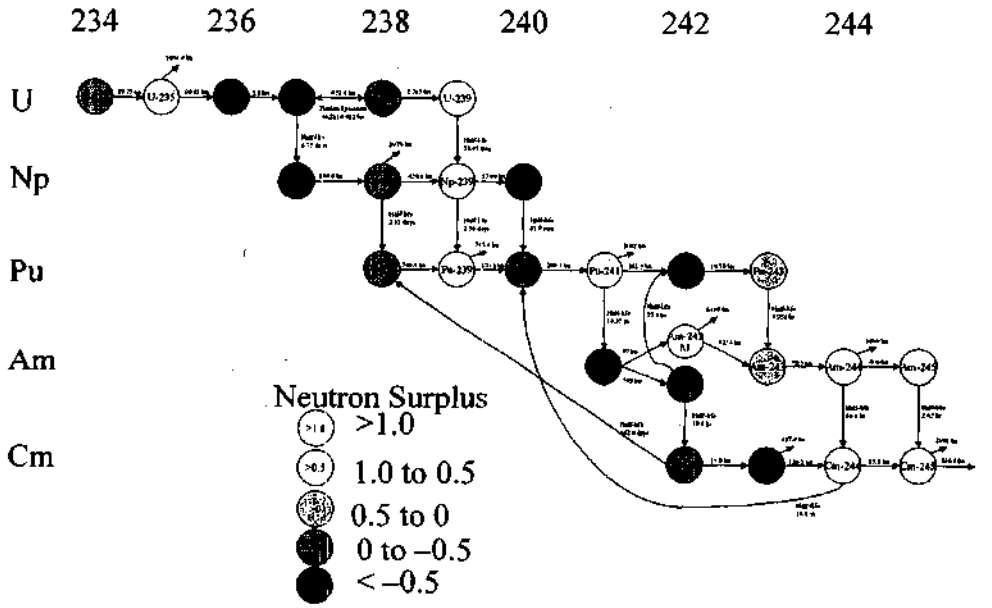

Figure 8 - Neutron Balance for Light Water Reactor

Fission Product Transmutation

Transmutation of fission products focuses on three main areas. Since they are already radioactive, is it practical to transmute them at a sufficient high rate to make improvements over the natural radioactive decay rate? How much material do we need to load in order to transmute the material at a rate at least as great as it is being produced? Finally, how often do the fission products need to be reprocessed?

Effective Half-lives

The fission products that are considered for transmutation are obviously radioactive or they would not be of concern. Therefore, natural decay is transmuting them with the radiological half-life of the given isotope. In order for transmutation to be of any benefit, the transmutation rate must be of the order of the decay rate and most likely significantly higher. This can be quantified by the effective half-life. The total transmutation rate is defined by the following equation.

$$\frac{dN}{dt} = -(\lambda_{rad} + \phi\sigma)N$$

The effective half-life is then defined by the following equation.

$$T_{1/2}^{eff} = \frac{\ln 2}{\lambda_{rad} + \phi\sigma}$$

As can be seen from this equation, the effective half-life is a function of the flux level (ϕ) and the microscopic cross section (σ) for a given neutron spectrum. For the system to be effective, the effective half-life would be expected to be a relatively small fraction of the radiological half-life and probably on the order of 10 years. Table 5 gives a number of isotopes considered to be problematic and considered for transmutation.[20] As can be seen from this table transmutation of Cs-137 and Sr-90 would require very high thermal fluxes to produce a significant transmutation rate because of the small cross sections. Tc-99 and I-

129, the long-lived fission products of most concern, would require fairly large, but not unreasonably high, thermal fluxes in order to transmute them at a significant rate.

Table 6 gives the result for fission spectrum average cross sections. The fast flux levels would have to be much higher and most likely impractical for fission product transmutation.

Table 5 - Long-lived Fission Product Transmutation in a Thermal Flux

Isotope	Half-Life (yr)	Maxwell Average Radiative Capture	Thermal Flux for 50% Reduction in Effective Half-life (n/cm^2-sec)	Thermal Flux for 10 year Effective Half-Life (n/cm^2-sec)
^{99}Tc	211,100	17.4900	6E+09	1E+14
^{129}I	15,700,000	23.8800	6E+07	9E+13
^{90}Sr	28.78	0.1330	6E+15	1E+16
^{137}Cs	30.07	0.2217	3E+15	7E+15
^{126}Sn	100,000	0.0798	3E+12	3E+16
^{79}Se	650,000	44.3300	8E+08	5E+13
^{135}Cs	2,300,000	7.7120	1E+09	3E+14
^{14}C	5,730	very small	very large	very large

Table 6 - Long-lived Fission Product Transmutation in a Fast Flux

Isotope	Half-Life (yr)	Fission Spectrum Average Radiative Capture	Fast Flux for 50% Reduction in Effective Half-life (n/cm^2-sec)	Fast Flux for 10 year Effective Half-Life (n/cm^2-sec)
^{99}Tc	211,100	0.0871	1.E+12	3.E+16
^{129}I	15,700,000	0.0630	2.E+10	3.E+16
^{90}Sr	28.78	0.0042	2.E+17	3.E+17
^{137}Cs	30.07	0.0050	1.E+17	3.E+17
^{126}Sn	100,000	0.0044	5.E+13	5.E+17
^{79}Se	650,000	0.0300	1.E+12	7.E+16
^{135}Cs	2,300,000	0.0276	3.E+11	8.E+16
^{14}C	5,730	very small	very large	very large

Long-lived Fission Product Loading

The quantity of fission product that must be loaded is determined by the production rate of that isotope. At equilibrium, the transmutation rate must be equal to the production rate. Tc-99 and I-129 are discharged from LWRs at an approximate rate of 25.6 kg/GW_e-yr and 5.9 kg/ GW_e-yr, respectively. We can determine the quantity of material the must be loaded based on an average flux to reach an equilibrium inventory. This is determined by the following equation.

$$\dot{P}_{eq} = \frac{-dN_{eq}}{dt} = (\lambda_{rad} + \phi\sigma)N_{eq}$$

If we generate a thermal flux of 10^{13} n/cm^2-sec, the resulting inventory of Tc-99 and I-129 would be 4,600 kg/GW_e and 783 kg/GW_e, respectively. This would only offset the production by the LWRs and if the transmutation system included the transuranics for the LWRs, the long-lived fission products resulting from the transmutation of the LWR transuranics would also have to be transmuted.

The fission product yield of transuranics varies significantly with isotope and neutron spectrum and was estimated from England and Rider.[23] The fission yield for Tc-99 for Pu-239 is 6.2% for thermal neutrons and 6.0% for fission spectrum neutrons. U-235 and Pu-241 show similar yields. The fission yield of I-129 is 1.4% for thermal neutrons and 1.5% for fission spectrum neutrons. U-235 has a yield of 0.54% for thermal neutrons and 0.84% for fission spectrum neutrons. Pu-241 has a yield of 0.82% for thermal neutrons. The fission yields from transmutation of the LWR transuranics will be approximately 6.1% for Tc-99 and approximately 1% for I-129.

The LWR will contain approximately 360 kg of transuranics per GW_e-yr. The total production of the long-lived fission products will be proportional to the number of fissions required to produce a net reduction of 360 kg as described in section 0. For a uranium-free transmutation reactor, the transuranics will produce an additional 9.1 kg of Tc-99 and 1.9 kg of I-129. This would increase the equilibrium loadings of each by approximately a third.

Long-lived Fission Product Neutron Balance

The transmutation chains for Tc-99 and I-129 are shown in Figures 9 and 10, respectively. Included in this figure are the 0.025 eV radiative capture cross sections and half-lives. Two isotopes of iodine are present in significant quantities in the spent LWR fuel, and without isotopic separation the stable I-127 will also be transmuted along with the LLFP isotope I-129.

The Tc-99 chain shows that it will be converted to the very short-lived Tc-100. Tc-100 will quickly decay to stable Ru-100. Ru-100 has a relatively small cross section relative to Tc-99 and will not present a large parasitic absorption problem until a fairly large fraction of the Tc-99 has been transmuted.

I-129, on the other hand, presents a more problematic situation for transmutation and neutron economy. First, without isotopic separation, the stable I-127 will have to be transmuted completely in order for the I-129 to be transmuted completely. I-127 is present at about one atom for every 5.5 atoms of I-129 in discharge LWR SNF. Therefore, 15% of the neutrons will go to transmuting I-127. The relatively small I-127 cross section will result in the buildup of I-127 as the iodine is repeatedly recycled. At equilibrium, I-127 would compromise approximately 44% of the iodine inventory and nearly double the iodine loading. Transmutation of iodine results in the production of the noble gas xenon. The xenon isotopes have fairly large cross sections. Achieving high fractional burnup in iodine will result in significant parasitic absorption further increasing the number of neutrons that must be committed to transmuting I-129.

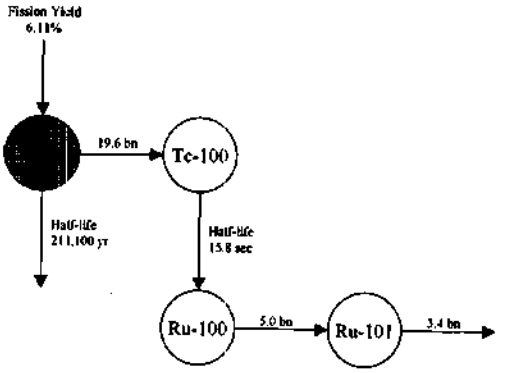

Figure 9 - Tc-99 Transmutation Chain

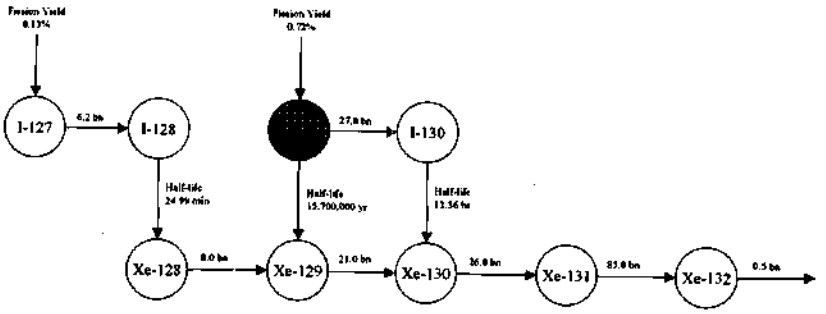

Figure 10 - I-129 Transmutation Chain

Sub-critical Transmutation Reactors

The sub-critical transmutation reactors are driven by an external neutron source strength (S). The external source of neutrons is multiplied by the fission of the transuranic waste and to a much lesser extent (n,2n) reactions. The sub-critical multiplication is defined in terms of the effective neutron multiplication factor (k_{sub}). This is calculated from the multiplication of the source neutrons where the total neutron production rate ($\dot{N}$) is calculated and then k is calculated from the sub-critical neutron multiplication equation.

$$\dot{N} = \bar{\nu}\dot{F} + S = \frac{S}{1-k_{sub}}$$

The fission rate ($\dot{F}$) can then be determined based on the source strength and average number of neutrons emitted per fission ($\bar{\nu}$).

$$\dot{F} = \frac{k_{sub}S}{\bar{\nu}\left(1-k_{sub}\right)}$$

The absorption rate ($\dot{A}_{HM}$) in the heavy metal is related to the fission rate by average number of neutrons emitted per absorption in the heavy metal ($\bar{\eta}$) by the following equation.

$$\bar{\eta}\dot{A}_{HM} = \nu\dot{F}_{HM}$$

All neutrons in the system will ultimately be absorbed either in the heavy metal fuel and used for transmutation or absorbed in other materials such as fission products, structural materials, or the surrounding materials after they leak out of the reactor. This allows us to determine the absorption rates in the system, which can be written as follows.

$$\dot{N} = \dot{A}_{HM} + \dot{A}_{loss}$$

$$\dot{A}_{loss} = S + \dot{A}_{HM}\left(\overline{\eta} - 1\right)$$

For a critical reactor, the source term would be removed from this equation. As can be seen, the sub-critical system can theoretically operate with any mixture of isotopes, including isotopes where $\overline{\eta} - 1$ would be negative. In the critical system, the only parameter controlling the neutron balance is the manipulation of the loss term (e.g., control rods), while for a sub-critical system it is possible to manipulate the loss term and the source term.

If long-lived fission products are included in the transmutation system, the absorption rate in the long-lived fission products will need to be a fraction of the fission rate to maintain the equilibrium long-lived fission product inventory. This further limits the amount of neutrons that are "lost" in the transmutation reactor. This relationship can be written as follows.

$$\dot{A}_{llfp} = \alpha_{llfp}\dot{F}$$

$$\dot{A}_{loss} = S + \dot{A}_{HM}\left(\overline{\eta} - 1\right) - \alpha_{llfp}\dot{F}$$

$$\dot{A}_{loss} = S\left(1 + \frac{k_{sub}}{1 - k_{sub}}\left(1 - \frac{1}{\overline{\eta}} - \frac{\alpha_{llfp}}{\overline{\nu}}\right)\right)$$

The transmutation system must then be designed in a manner that satisfies these neutron balances. As can be seen all rates are proportional to the source strength and a function of the neutron multiplication of the system.

In general, the sub-critical neutron multiplication factor (k_{sub}) calculated from the source multiplication is not the same value as the effective neutron multiplication factor (k_{eff}) of the system determined by the eigenvalue of the fundamental mode of the neutron distribution. As the system approaches criticality the source driven flux distribution and the fundamental mode will begin to converge and both the sub-critical k and the eigenvalue will approach unity.

Fusion Sub-Critical Transmutation Reactors

Using a fusion source adds an additional requirement on the system. This is the requirement for the transmutation reactor to be tritium self-sufficient. Tritium is produced by the fission of both lithium-6 and lithium-7. Lithium-6 has a larger tritium production cross section in a fission spectrum, while lithium-7 has a much larger cross section at the 14.1 MeV fusion neutron energy. Lithium-7 has a threshold at 2.82 MeV. Natural lithium is 7.5% Li-6 and 92.5% Li-7. Lithium-6 has a large resonance and a very large thermal cross section for tritium production, which makes tritium production much easier in softer spectrums.

Table 7 - Tritium Production Cross Sections

Isotope	Atom Fraction	14 MeV	Fission Spectrum	Resonance Integral	Maxwell Average
Li-6	7.5%	28.0 mbn	330.7 mbn	424.9 bn	833.4 bn
Li-7	92.5%	302.9 mbn	20.0 mbn	0	0
Natural Lithium		282.3 mbn	43.3 mbn	31.9 bn	62.5 bn

Note: Data from Table of Nuclides maintained by the Korea Atomic Energy Research Institute. [24]

A number of relationships for the fusion driven sub-critical system can be developed from the basic physics. The Q for D-T fusion is 17.6 MeV. The Q for Li-6(n,α)T is 4.8 MeV. The Q for Li-7(n,n'α)T is -2.5 MeV. The system will have to produce more than 1 tritium for every fusion to compensate for losses and most will be produced from lithium-6 because most neutrons in a fission/fusion hybrid system will be produced below the Li-7 threshold. Tritium production multiplies the fusion power by roughly 25% to

30%. There are other exothermic and endothermic reactions and variations in the fission energy that will effect the total power of the system. These are relatively small and vary with time.

The fission rate can be related to the fusion power with the following simple relationship based on the relationship between the source strength and fission rate, where the average mass of the fissionable isotopes is approximately 239 g/mole.

$$P_{fis}[MW] = \alpha \dot{F} = 12.2 \frac{k_{sub}}{\bar{\nu}(1-k_{sub})} P_{fus}[MW]$$

This can be further expanded to determine the total power level of the system, where Q_p is the plasma energy multiplication factor for the auxiliary power used to provide external heating and current drive to the fusion plasma.

$$P_{tot} = P_{fis} + P_{fus} + P_{other}$$

$$P_{other} = P_{trit} + P_{aux} + P_{minor}$$

$$P_{tot}[MW] = \left(12.2 \frac{k_{sub}}{\bar{\nu}(1-k_{sub})} + 1.25 + \frac{1}{Q_p} \right) P_{fus}[MW]$$

Fusion Sub-critical Reactor Neutron Balance

The neutron balance in a fusion driven transmutation reactor must be tritium self-sufficient. Therefore, the absorption rate in lithium will be proportional to the source strength such that enough tritium is produced to account for fusion and all losses including radioactive decay. This reduces the neutrons that can be allowed to be lost from the system, while operating at the same neutron multiplication factor. This can be expressed by the following.

$$\dot{A}_{Li} = \alpha_{Li} S$$

$$\dot{A}_{loss} = S\left(1-\alpha_{Li}+\frac{k_{sub}}{1-k_{sub}}\left(1-\frac{1}{\overline{\eta}}-\frac{\alpha_{llfp}}{\overline{\nu}}\right)\right)$$

We can therefore estimate the neutron absorption probabilities that the system must be designed to achieve. Rewriting the neutron balance equation for the absorption rates in the reactor.

$$\dot{A}_{HM}+\dot{A}_{llfp}+\dot{A}_{Li}+\dot{A}_{loss}=\overline{\nu}\dot{F}+S=\frac{S}{1-k_{sub}}=\dot{N}$$

The probability of a neutron resulting in any particular reaction is the rate of that reaction divided by the total neutron production rate ($\dot{N}$). This leads to the following probabilities.

Probability of fission: $P_{fis}=\frac{\dot{F}}{\dot{N}}=\frac{k_{sub}}{\overline{\nu}}$

Probability of absorption in the heavy metal: $P_{HM}=\frac{\dot{A}_{HM}}{\dot{N}}=\frac{k_{sub}}{\overline{\eta}}$

Probability of absorption in long-lived fission products: $P_{HM}=\frac{\dot{A}_{llfp}}{\dot{N}}=\frac{\alpha_{llfp}k_{sub}}{\overline{\nu}}$

Probability of absorption in lithium: $P_{Li}=\frac{\dot{A}_{Li}}{\dot{N}}=\alpha_{Li}(1-k_{sub})$

Probability of neutron loss or leakage: $P_{loss}=\frac{\dot{A}_{loss}}{\dot{N}}=1-\frac{k_{sub}}{\overline{\eta}}-\frac{\alpha_{llfp}k_{sub}}{\overline{\nu}}-\alpha_{Li}(1-k_{sub})$

These probabilities hold for a critical reactor (k=1) and for an accelerator driven sub-critical reactor (α_{Li} =0). Many of these parameters are known approximately. Most of these parameters are time dependent and will represent cycle averaged values. Typical parameters for the discharge LWR transuranics in a uranium-free transmutation reactor are $\overline{\nu}$ ~2.9,2.9; $\overline{\eta}$ ~2.1,1.3 for a fast reactor and LWR spectrums, respectively. The lithium and long-lived fission product parameters are roughly independent of

spectrum and are α_{Li}~1.1, and α_{llfp}~0.3. The neutron multiplication of the system is then a design parameter that determines the fate of the neutrons.

Tables 8 and 9 show the results for a fast reactor and LWR spectrums, respectively. The probabilities for fission, long-lived fission product transmutation, and lithium absorption are essentially the same. The larges difference is in the large fraction of neutrons in the LWR spectrum that must be absorbed by the heavy metal and the resulting smaller fraction of neutrons that can be lost to fission products, structural material, control elements, and leakage. This does not directly indicate more difficulty in a softer spectrum because the thermal cross sections of the heavy metals and lithium-6 are much larger at thermal energies, making achieving these probabilities somewhat easier, but in a fast critical reactor more than 40% of the neutrons must lost, while less than 15% of the neutrons can be lost in a LWR spectrum. The fast reactor will have a very large surplus of neutrons even when the production of tritium and LLFP transmutation are included.

Table 8 - Reaction Rate Probabilities in a Fast Reactor Spectrum

k_{sub}	Fission	HM abs	LLFP	Lithium	Loss
Critical	34%	48%	10%	0%	42%
0.97	33%	46%	10%	3%	40%
0.95	33%	45%	10%	6%	39%
0.90	31%	43%	9%	11%	37%
0.85	29%	40%	9%	17%	34%
0.80	28%	38%	8%	22%	32%
0.75	26%	36%	8%	28%	29%
0.70	24%	33%	7%	33%	26%
0.65	22%	31%	7%	39%	24%
0.60	21%	29%	6%	44%	21%

Table 9 - Reaction Rate Probabilities in a LWR Spectrum

k_{sub}	Fission	HM abs	LLFP	Lithium	Loss
critical	34%	77%	10%	0%	13%
0.97	33%	75%	10%	3%	12%
0.95	33%	73%	10%	6%	12%
0.90	31%	69%	9%	11%	10%
0.85	29%	65%	9%	17%	9%
0.80	28%	62%	8%	22%	8%
0.75	26%	58%	8%	28%	7%
0.70	24%	54%	7%	33%	6%
0.65	22%	50%	7%	39%	5%
0.60	21%	46%	6%	44%	4%

Transmutation System Design

There are two modes of operation of the transmutation system. The first is to burn down the backlog of LWR SNF that has accumulated and will continue to accumulate until the transmutation system has reached a level where the destruction rate exceeds the production rate. The second mode is after the backlog has been burned down and the transmutation system operates at an equilibrium. At equilibrium, the inventories of transuranics and long-lived fission products will be proportional to the nuclear energy power level. The equilibrium levels will be a function of the designs of the system, particularly the cooling time and the amount of fuel in storage awaiting processing.

To burn up the backlog, a fixed number of full power years of transmutation reactor operations will be required to burn down a given quantity of waste. This can be expressed in terms of the fission energy of the transmutation reactors (GW_{th}·yr). At equilibrium, an individual transmutation reactor will support a certain given capacity of LWRs. This can then be expressed as a ratio of the fission power of the LWRs to the combined fission power of LWRs and the transmutation reactors.

The mass of backlog material (M_{TRU}^{Back}) that has accumulated in discharged LWR SNF is a function of when the transmutation reactors begin operation. The physical number of transmutation reactors required will then be a function of their size (fission power), capacity factor, and lifetime. In terms of fission energy, the number required is given by the following equation.

$$Transmuters[GWyr - fission] = 2.7 \frac{F_{HM}^{\infty} - BU}{M_{TRU}^{0}} M_{TRU}^{Back}[MT]$$

The results are a function of conversion and fission rate of uranium and to a lesser extent the operation of the chemical separation systems.

For the equilibrium situation, the result is essentially the same, but it is related to the rate of production of transuranics by the LWRs.

$$Transmuters[GWyr^{transmuter} / GWyr^{LWR}] = 2.7 \frac{F_{HM}^{\infty} - BU}{M_{TRU}^{0}} \dot{M}_{TRU}[MT / GWyr^{LWR}]$$

A typical LWR produces approximately 360 kg/GW_e-yr or 121 kg/GW_{th}-yr. If we assume the separations process is perfect and uranium-free transmutation reactors are used, the LWRs will produce approximately 75% of the fission energy. If plutonium is recycled as MOX fuel, and a 30% reduction in the transuranic discharge per unit energy of LWRs is achieved, the LWRs would produce 81% of the fission energy and the number of transmutation reactors required would be reduced by 30%. If uranium matrix is used in the transmutation reactors, the fraction of energy produced by the transmutation reactors will increase asymptotically to unity as the conversion and fission rate of uranium approach unity.

For uranium-free fuel, the contribution of uranium to the total fissions is zero and the smallest number of transmutation reactors will be required, regardless of the spectrum. For thermal spectra, a U-238 matrix can be designed to have very low conversion and fission rates in the uranium. Even with relatively dilute amounts of transuranics, this is true because of the relatively small U-238 cross sections. If these assemblies are placed in a LWR, they will not only destroy the transuranic waste, but will offset the production of new transuranics that would have occurred in enriched uranium fuel that would otherwise have been irradiated. This will result in the smallest number of non-LWR transmutation facilities to support LWRs. In fast spectra, the conversion and fission rates in a U-238 matrix will be significant, even with fairly high concentrations of transuranics. The small relative cross sections of U-238 at thermal energies is lost as the energy of the neutron spectrum is increased. This results in a much higher number of transmutation reactors required to support the LWRs.

CHAPTER III

WASTE MANAGEMENT AND SYSTEM PERFORMANCE FIGURES OF MERIT

How do we measure the performance of the system shown in Figure 1? The system will be designed to satisfy all regulatory requirements. The difficulty of satisfying these regulatory requirements will directly effect the cost of the system, which when compared to the alternatives and accounting for differing financial risk will determine the option chosen. The public perception has a significant effect on the ease, difficulty, or complete preclusion of licensing a facility. This is a major component of financial risk. These financial aspects are far beyond the scope or capabilities of this study. Therefore, surrogate figures of merit (FOMs) need to be developed to address the major factors such as size and technical difficulty of performing each step identified in Figure 1. These FOMs can then be used to make relative comparisons of the different options analyzed and identify the more promising options that should be studied in more detail.

The transmutation portion of the nuclear fuel cycle is for waste management purposes and is akin in function to a hazardous waste incinerator. Its primary goal is to significantly reduce the hazard, real or perceived, of the feed material and secondly, to utilize the resulting energy to offset some of the cost of the incinerator. Our systems analysis will focus on quantifying criteria and figures of merit related to the waste management aspects of the system and the overall performance of the system.

FOMs need to be evaluated that cover the range of issues that will impact the choice of a technology used to achieve the waste management goals and to allow engineering judgment as to which paths to evaluate in further detail. The importance of the different components is very subjective and changes with public opinion. In order to attempt to cover the widest range of issues and provide a broad set of indicators, a wide range of figures of merit were chosen. The figures of merit are defined in the following subsections. These figures of merit attempt to address the issues related to separations, high-level waste disposal, low-level waste disposal, repository performance, shipping, proliferation, public perception,

and cost, but the focus will be on the high level waste, since this currently appears to be the most pressing issue.

The current baseline for the Yucca Mountain Project and for the accelerator transmutation of waste (ATW) program is based on the projection of the end of nuclear power in the United States and a limited quantity of spent nuclear fuel (SNF) requiring disposal. If this is the ultimate fate, it's hard to envision strong public support for a new nuclear energy system or sufficient technical resources to support a dying industry. Nevertheless, this is the current baseline, so the figures of merit will be evaluated on a per unit mass of enriched uranium irradiated in LWRs. This can be scaled for a limited input scenario that would be consistent with the current baseline design for Yucca Mountain.

If the demise of the U.S. nuclear energy is not imminent and persists well into the future, a steady supply of LWR SNF will be produced. A system could still be acceptable even if it produced more "waste" if it produces more useful energy. The system that produces the least "waste" per unit useful energy produced would be the preferred waste management system. Therefore, all waste management figures of merit will be normalized to a per unit energy produced basis.

Waste Management Figures of Merit

Repository Dose Contributing Isotopes

The quantity of the isotopes contributing most significantly to the predicted dose rates to an "average" individual withdrawing water from a well penetrating the maximum plume concentration 20 km from the repository as determined in the Yucca Mountain Viability Assessment[25] will be quantified. The time behavior of the predicted dose rate is shown in Figure 11 reproduced from the Yucca Mountain Viability Assessment. The ideal parameter would be the comparison of calculated doses for disposal of the different materials, but this is well beyond the scope of this study. Assuming that the waste form of the transmutation waste is at least as good as that analyzed in the Viability Assessment, a lower quantity will produce a lower dose rate. This reduction will not be proportional and may be very small for isotopes that have low saturation levels. The improvement of waste form will not be addressed, but should improve the performance of the repository very significantly. The values shown in Table 10 were taken from the total system performance assessment in the Yucca Mountain Viability Assessment.[25] Table 10 includes

calculated dose rates at several times and the relative contributions at those times. The peak values shown in this table is the peak value for each isotope, which do not occur at the same time, and are shown relative to the maximum calculated dose of 300 mRem/yr that occurs in the 200,000 to 300,000 year timeframe.

Table 10 - Repository Dose By Isotope

Time (yr)	10,000	100,000	Peak	1,000,000
Dose Rate (mRem/yr)	0.04	5	300	45
Tc-99	75%	8.0%	0.7%	02%
I-129	25%	4.0%	0.5%	1.1%
Np-237		9.0%	100.0%	86.7%
U-234		0.4%	2.0%	0.7%
Pu-239		0.1%	1.3%	
Pu-242			30.0%	12.2%

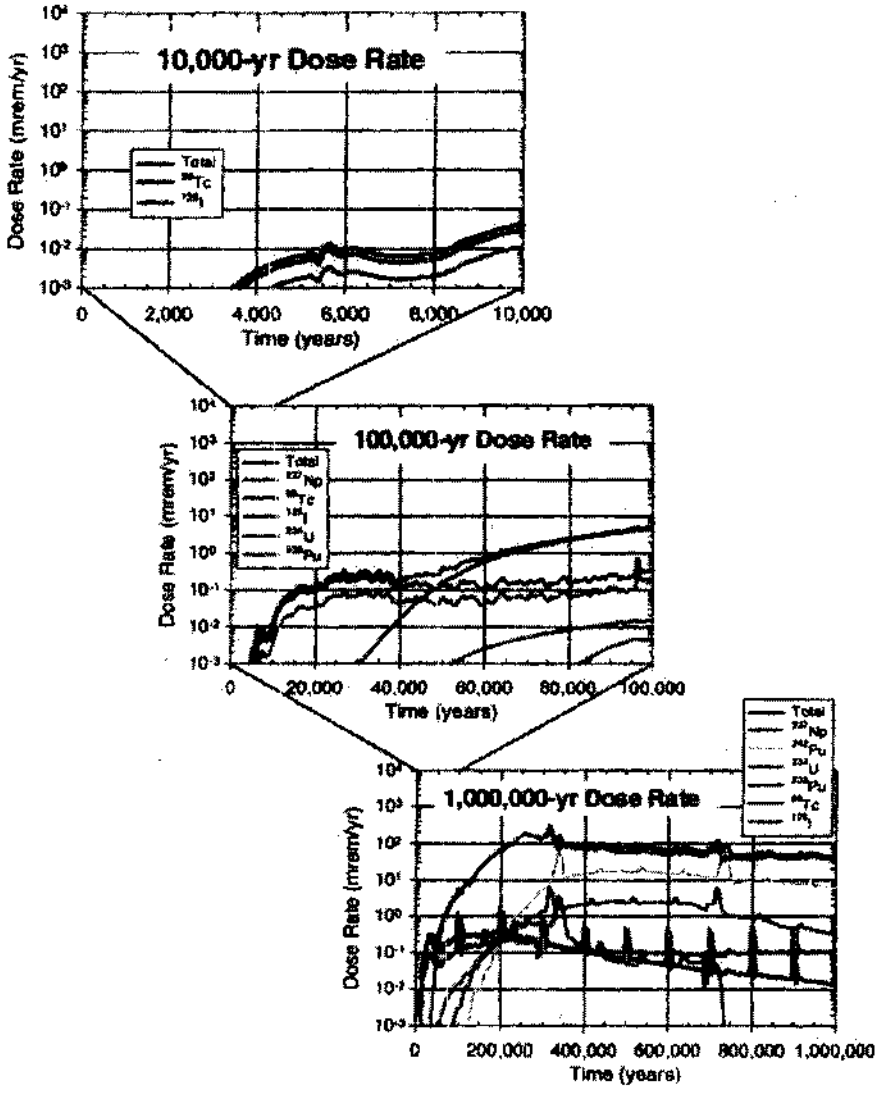

Figure 11 - Dose Rate Estimates From Repository Waste

Tc-99 is a soluble long-lived fission product. From the Yucca Mountain Viability Assessment it constitutes 75% of the peak dose at 10,000 years. The peak Tc-99 dose rate is approximately 2 mRem/yr or 0.7% of the peak dose rate. The total Tc-99 includes the decay of other fission products that will decay to Tc-99 on the time scale of the repository. These other fission products included in the total Tc-99 are Tc-99m, Mo-99, Nb-99, and Zr-99.

I-129 is a soluble long-lived fission product. From the Yucca Mountain Viability Assessment it constitutes 25% of the peak dose at 10,000 years. The peak I-129 dose rate is approximately 1.5 mRem/yr or 0.5% of the peak dose rate.

Np-237 is a transuranic isotope produced by a number of different reaction and decay paths. From the Yucca Mountain Viability Assessment it dominates the dose rate at time periods significantly beyond 10,000 years. The peak Np-237 dose rate is approximately 300 mRem/yr or 100% of the peak dose rate. The total Np-237 includes the decay of other actinides that will decay to Np-237 on the time scale of the repository. These other actinides included in the total Np-237 are U-237, Pu-237, Pu-241, Am-241, Cm-241, Am-245, Bk-245, Cf-249, and Cm-245.

U-234 occurs naturally in uranium as a daughter of U-238 it is also produced by a number of different reaction and decay paths. From the Yucca Mountain Viability Assessment it contributes to the dose rate at time periods significantly beyond 10,000 years. The peak U-234 dose rate is approximately 6 mRem/yr or 2% of the peak dose rate. The total U-234 includes the decay of other actinides that will decay to U-234 on the time scale of the repository, which does not include U-238. These other actinides included in the total U-234 are Pa-234, Th-234, Np-238, Pu-238, Cm-242, 82.7% of the Am-242, 82.78% of Am-242m, and Cf-246.

Pu-239 is a transuranic isotope produced by a number of different reaction and decay paths. From the Yucca Mountain Viability Assessment it contributes to the dose rate at time periods significantly beyond 10,000 years. The peak Pu-239 dose rate is approximately 4 mRem/yr or 1.3% of the peak dose rate. The total Pu-239 includes the decay of other actinides that will decay to Pu-239 on the time scale of the repository. These other actinides included in the total Pu-239 are U-239, Np-239, Cm-243, Am-243, and Pu-243.

Pu-242 is a transuranic isotope produced by a number of different reaction and decay paths. From the Yucca Mountain Viability Assessment it contributes to the dose rate at time periods significantly beyond 100,000 years. The peak Pu-242 dose rate is approximately 90 mRem/yr or 30% of the peak dose rate. The total Pu-242 includes the decay of other actinides that will decay to Pu-242 on the time scale of the repository. These other actinides included in the total Pu-242 are 17.3% of Am-242, 17.22% of Am-242m, and Cm-246.

Masses

The simplest measure of performance is mass. Several categories of elements will be summarized in terms of mass. For the heavy elements, the only option for complete elimination is fission. The masses of these isotopes will determine the minimal size of the waste management system for complete elimination. Without addition production (i.e., breeding or conversion), approximately 1 megawatt-day of fission energy will be produced by the fission of 1 gram of heavy metal.

Plutonium is an element that strongly impacts public perception of the nuclear fuel cycle. Plutonium is also important as a proliferation concern. Reduced quantities of plutonium would be a strong selling point of any transmutation system; while the plutonium separation required for recycle will be a point of particularly contention due to the both real and perceived concerns for proliferation.

The total quantity of *transuranic elements* determines how much material must be fissioned for a complete elimination of man-made heavy elements. This will provide a good estimate of the total size of the system that will be required to accomplish a very significant reduction in the transuranic, man-made, elements. The presence of uranium in the system will result in production of additional transuranics that will increase the overall size in terms of energy production required.

Minor actinides tend to be more radioactive and problematic to handle during recycle. The minor actinides also tend to have less than ideal reactor physics properties. The larger the quantity of minor actinides, the more difficult the waste management problem, in general.

The largest component of any scenario will be the *uranium*. The mass of uranium will be its primary impact on the waste management system. The uranium will exist in two separate streams. The first is the enriched uranium that will initially be irradiated in the light-water reactor. The recovered enriched uranium will not be considered further in this analysis. The second is the depleted uranium stream. The

bulk of the mass will be contained in this stream. At very long time periods, many of the waste management parameters will be controlled by the decay of the depleted uranium.

Toxicity

Toxicity is a measure based solely on the isotopic composition of a material at any given time. This is primarily a measure of the radioactivity of a material and is not a good measure of the risk posed by a material placed in a geologic repository. The toxicity index (TI) is a measure used to quantify the toxicity of a material. Values for the TI can be determined for the material in either water or air. The TI for water is defined as follow[20]:

$$TI_w = \sum(\lambda_i N_i / C_{iw}) = \sum(A_i / C_{iw})$$

λ_i = Decay constant for i^{th} element (s^{-1})
N_i = Number of atoms for i^{th} element
A_i = Activity of i^{th} element (Bq)
$C_{i,w}$ = Maximum permissible concentration of i^{th} element in water (Bq/m^3)

In general, the short-lived isotopes are the most toxic but easiest to contain for sufficient time, while the long-lived isotopes are the least toxic but most difficult to contain for sufficient time. The Nuclear Regulatory Commission requires containment by the waste package for a period of at least 300 - 1000 years[20] and subsequent releases from the repository must be within specified dose limits. Assuming this is achieved, the very short-lived isotopes ($t_{1/2} < 50$ years) will have decayed almost completely away and have little chance of reaching the population.

One objective of transmutation would be to reduce the overall toxicity of the spent nuclear fuel (SNF) after the time period when containment can be assured. Even though TI is not a good measure of risk, it is to some degree the upper bound of the risk presented by the material, under the worse conceivable circumstances, even if such circumstances are not scientifically credible. If the TI were reduced for time periods beyond 1000 years, the upper bound of the potential for the SNF to cause harm would be reduced.

The advantage of using the TI is that it is simple to calculate and is a material property that is not a function of the site and/or scenario. This parameter has been used by some evaluators in determining the benefits of transmutation[20,26,27].

The toxicity index is calculated by the ORIGEN-S[28] computer code. The TI is the quantity of water required to dilute the material to the maximum permissible concentration for continuous ingestion.[29] The TI is time dependent as more or less toxic isotopes decay to less or more toxic isotopes. Each of the available actinides and fission products was allowed to decay for 1,000,000 years and the TI at many times was compiled in a database. For isotopes that do not decay directly to stable isotopes, the TI will be a composite of all isotopes in the chain. By assigning the TI to the original parent isotope, it identifies which isotope must be destroyed today to reduce the TI at some point in the future. Tables 113 and 114 in Appendix A contain the toxicity indices as a function of time for the actinide and fission product isotopes, respectively.

Decay Heat

The quantity of material that may be placed in the repository is limited by the temperature change in the immediate vicinity of the waste package and at a distance far from the waste, which are dominated by the decay power and integrated decay energy, respectively. The actual limits on decay heat have not yet been determined but may be as high as 85 kW/acre, with a more typical value of 57 kW/acre. If the decay heat from the waste were to be reduced, the quantity of material that could be placed in the repository would be increased. There are various scenarios for reducing decay heat, including separation of cesium and strontium to reduce the decay power. [20] The decay heat also affects the ease of handling the material, which will impact the design of storage, shipping, and processing facilities.

The decay heat is calculated by the ORIGEN-S[28] computer code. The decay heat is the power in watts from radioactive decay. The decay heat is time dependent. Each of the available actinides and fission products was allowed to decay for 1,000,000 years and the decay heat at many times was compiled in a database. For isotopes that do not decay directly to stable isotopes, the decay heat will be a composite of all isotopes in the chain. By assigning the decay heat to the original parent isotope, it identifies which isotope must be destroyed today to reduce the decay heat at some point in the future. Tables 115 and 116 in

Appendix B contain the decay heat as a function of time for the actinide and fission product isotopes, respectively.

Integral Decay Energy

The quantity of material that may be placed in the repository is limited by the temperature change in the immediate vicinity of the waste package and at a distance far from the waste, which are dominated by the decay power and integrated decay energy, respectively. Removal of actinides would dramatically reduce the integrated decay energy[20,30] by reducing the "thermal half-life" from several hundred years to ~30 years. By ventilating the repository during operation a significant amount of the total decay heat can be removed prior to closure in order to allow significantly more waste to be loaded[30]. The integral decay energy will determine the total amount of energy deposited in the repository over a given time period.

The integral decay energy in joules was determined by integrating the decay heat over the time steps with the assumption of a constant half-life over the time period. Tables 117 and 118 in Appendix C contain the integral decay energy as a function of time for the actinide and fission product isotopes, respectively.

Unshielded Dose Rate

The difficulty of handling the materials, whether for shipping, storage, or processing, will be a function of the photon and neutron emission rates as well as the spectrum of these particles. In order to give an indication of the relative difficulty of handling the different waste streams, the unshielded dose rate (REM/hr) at 1 meter will be used as a figure of merit. There will be significant self-shielding which is dependent on the form of the waste. This is far too difficult to take into account at this level of analysis so the unshielded dose rate is used. There are two sources of neutrons. The first is from spontaneous fission. The second source is from α,n reactions. The spontaneous neutron source is independent of the surrounding medium. The unshielded dose rate is calculated separately for the photons, spontaneous fission neutrons, and the α,n neutrons. The dose conversion factors were taken from the MCNP manual.[31]

The emission rates and spectrum were calculated by the ORIGEN-S[28] computer code. Each of the available actinides and fission products was allowed to decay for 1,000,000 years and the emission rate by energy group was multiplied by the dose conversion factors to determine the unshielded dose rate. This was performed at several times and the results were compiled in a database that is multiplied by the

concentration in the material stream of interest. For isotopes that do not decay directly to stable isotopes, the dose rate will be a composite of all isotopes in the chain. By assigning the value to the original parent isotope, it identifies which isotope must be destroyed today to reduce the dose rate at some point in the future.

The low energy photons (E <100 keV) were neglected from the calculation because of the relative ease of shielding. Table contains the unshielded photon dose rate for the actinide isotopes. Tables 119 and 120 in Appendix D contain the unshielded photon dose rate as a function of time for the actinide and fission product isotopes, respectively.

Only actinide isotopes undergo spontaneous fission. Table 121 in Appendix E contains the unshielded spontaneous neutron dose rate for the actinide isotopes.

The neutron emission produced by α,n reactions is a strong function of the material. The dose rate from α,n reactions will only given an indication of the relative magnitude of the actual dose rate that will occur for materials of the same form. For materials that are in different forms such as oxide fuels and metal fuels, the comparison has no value. The only significant source of alpha particles is from actinide isotopes. Table 122 in Appendix F contains the unshielded α,n neutron dose rate for the actinide isotopes.

Proliferation

Proliferation of nuclear explosives is one of the concerns associated with any nuclear fuel cycle. International safeguards will be in place to ensure that this does not occur. The properties of the materials involved in the nuclear fuel cycle will determine the relative difficulty required to convert the nuclear materials to a nuclear explosive. Since the assumption is that international safeguards are in place and this analysis is based on the United States, which already has a stockpile of nuclear weapons, the covert diversion of material for clandestine purposes is the only area that will be analyzed.

Producing a nuclear explosive will require the following steps: 1) acquiring the mass required to produce the explosive; 2) purifying the material for use in the explosive; 3) construction of the explosive device; and 4) achieving a significant yield from the explosive. The material properties related to the relative difficulty at succeeding at each of these steps will be quantified. The attributes that will be evaluated are based on Beller.[32] These include the bare critical mass (BCM), thermal generation (TG), spontaneous neutron source (SNS), and the inherent radiation barrier (RB). In addition, one BCM will be

diluted in a large mass of material in the repository making it a physical impediment to the covert removal of the material.

The *bare critical mass* will be calculated for all transuranic (BCM_{TRU}) and for the plutonium (BCM_{Pu}). The other attributes will be calculated for the material at its purest form in the separation process and the high-level waste that is destined for the repository. All values will be normalized to the BCM_{Pu} and the BCM_{TRU} to account for the relative quantities of material that would be needed. All parameters in the repository are time dependent. For example, Pu-241 & Pu-238 will both decay to isotopes with significantly larger critical masses with the relatively short half-lives of 14.35 yrs and 87.7 yrs, respectively. The repository parameters will be evaluated at a number of time steps.

The bare critical mass is calculated using MCNP4B.[31] The radius of a sphere with the given concentration is adjusted until the critical radius for the bare sphere is determined. This procedure is repeated for the plutonium sphere and for the transuranic sphere at each of the point of interest.

The *thermal generation* is related to achieving a significant yield. Therefore, the fission products and other actinides will not be included in the calculation of these values. The thermal generation is the decay heat at time zero of one bare critical mass of plutonium or transuranics.

A high *spontaneous neutron source* (SNS) is seen as a non-proliferation benefit, by increasing the likelihood of premature detonation and low yield. Therefore, the fission products and other actinides will not be included in the calculation of these values. The SNS is the source strength at time zero of one bare critical mass of plutonium or transuranics.

The spontaneous neutron emission rate is calculated by the ORIGEN-S[28] computer code. Table 123 in Appendix G contains the spontaneous neutron emission rate for the actinide isotopes.

The fission products and other actinides are included in the *inherent radiation barrier* calculations because this is related to the difficulty of handling the material while it is being purified for use in the explosive. The inherent radiation barrier is the unshielded dose rate for the photons and spontaneous neutrons at time zero for the quantity of material that contains one bare critical mass of plutonium or transuranics. The α,n dose rate is neglected.

The *mass of repository waste* (MRW) including fission products and actinides that contains one BCM will be calculated. The fission products and actinides will be diluted when they are placed in the

waste form that will be used for disposal. This additional mass is neglected, even though it will most likely be very large for the waste streams from the chemical separation systems.

System Performance Parameters

The cost of electricity will be determined by the total of all expenses and the *total electrical energy generated* by all processes of the nuclear fuel cycle. The total electrical energy production includes the electrical energy production in the LWRs plus the net electrical production of the transmutation reactors. If transmutation results in increased electrical output, the additional expenses would be spread over a large quantity of electricity. In addition, since a greater positive benefit results, i.e., more electricity, a proportionally larger quantity of waste would not imply an inferior system. In addition, the expense of handling more hazardous materials would also be spread over a large quantity of electricity.

The FOMs normalized to the initial mass of uranium irradiated in the LWRs are a measure of the concentration of the hazard. The FOMs normalized to the electrical energy production are a measure of the rate of production of the particular hazard. The FOMs will be normalized to both to measure the impact on the concentration and production rate. Systems will look different if the have a high rate of less hazardous waste or a low rate of more hazardous waste and quantifying the hazard concentration and the hazard production rate will try to quantify this effect.

The greater material that can be destroyed in a single pass or *cycle burnup*, the smaller the capacity of reprocessing facilities that is required to support the nuclear fuel cycle. Reprocessing is very expensive and higher burnups in each pass through the transmutation reactor will lower the reprocessing costs as well as reduce the quantity of transuranics that leaks into the waste streams.

The minimum energy production is produced when only fission of the transuranics occurs without any other reactions that produce energy. This includes the breeding of addition transuranics and fusion energy. The large backlog of LWR SNF suggests there is significant benefit in reducing this inventory as quickly as possible. Therefore, lower *energy production per unit reduction* would result in a greater reduction in the inventory on a per unit net electric basis. This figure of merit will only be calculated on thermal power because cost considerations would suggest that a higher thermal efficiency would save money and not be beneficial, even though it would increase the size of the system as measured by net electrical output.

CHAPTER IV

ONCE-THROUGH CYCLE

The once-through fuel cycle (OTC) is the baseline scenario for the proposed repository at Yucca Mountain, Nevada. The repository is currently being developed by the U.S. DoE Office of Civilian Radioactive Waste Management, which is charged with disposing of all spent nuclear fuel from commercial nuclear reactors and high-level radioactive waste resulting from atomic energy defense activities.[33] The OTC is shown in Figure 12. Three waste streams are considered for the OTC. There is one high-level waste (HLW) stream composed of the intact SNF that will be disposed in a geologic repository. The OTC has two low-level waste (LLW) streams associated with producing the enriched uranium that is irradiated in the LWR: the mill tailings (uranium daughters) and the depleted uranium.

The Integrated Data Base Report[34] (IDB) gives a summary of the U.S. SNF inventories and projections. The current inventory of discharged SNF has an average burnup of approximately 33 GWd/MTU, which has been consistently increasing over recent years and is projected to increase still further in the future as shown in Table 11. The current installed capacity of LWRs is approximately 100 GWe, of which about 2/3 is pressurized water reactors (PWR) and the remaining 1/3 is boiling water reactors (BWRs). In the IDB, it is assumed that the U.S. will shutdown all reactors at the expiration of the current license. However, it appears that many of the existing reactors will have their operating licenses extended by 20 years. Overtime, they have operated at increasing efficiencies and produce SNF with higher initial enrichment and discharge burnup, and this trend will most likely continue. This will result in a continued evolution of the composition of the discharge SNF.

There is a large backlog of SNF, estimated to be over 47,000 MTU by the end of 2002. The transmutation reactor systems were evaluated using a SNF composition that is based on the current backlog SNF.

This section will evaluate the impact of burnup on the waste management and feed properties of PWR SNF. The composition of the backlog SNF characteristics was determined and used to evaluating the transmutation reactors.

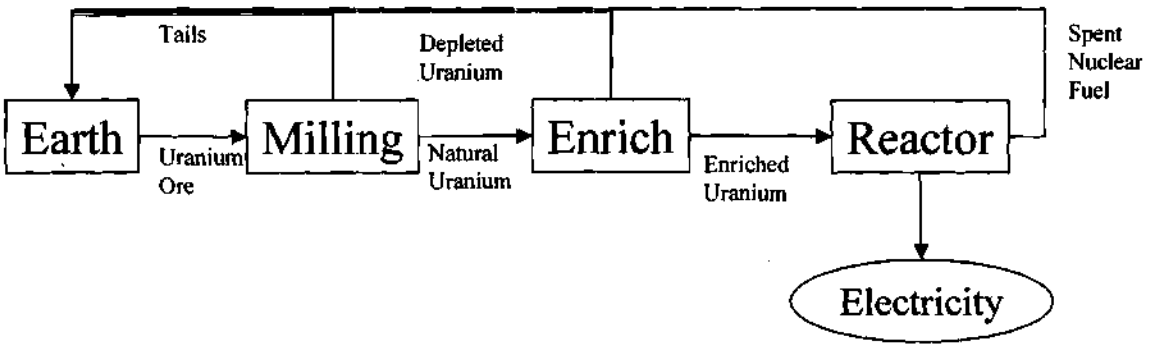

Figure 12 - Once-Through Fuel Cycle

Table 11 - LWR Fuel Data

LWR Type	Year Fuel is Loaded	Fuel Enrichment (% U-235)	Design Burnup (GWd/MTU)
BWR	1993	3.14	36
	1996	3.12	40
	2000	3.47	43
	2010	3.58	46
PWR	1993	3.84	42
	1997	4.11	46
	2001	4.38	50
	2008	4.74	55

All Data taken from the IDB[34]

Reference OTC Characteristics

The IDB reference characteristics for a PWR were chosen as the basis for evaluating the OTC and determining the detail isotopic composition of the SNF that will feed the transmutation fuel cycles. The details of the reference PWR fuel assemblies are given in Table 12. This design was evaluated at burnup levels and enrichments given in Table 11. The backlog inventory was approximated by a PWR with a burnup of 33 GWd/MTU with an initial enrichment of 3.15 % U-235 and a storage time of 25 years. This level was chosen to approximate the composition of the backlog SNF as specified in the Yucca Mountain

Project (YMP) draft environment impact statement[35] and is referred to as the reference fuel cycle. Table 13 compares the transmutation reactor feed calculated in this study with the results from the YMP data, and the value used in the Argonne National Laboratory (ANL) Accelerator Transmutation of Waste studies.[36] The results were in generally good agreement with the other calculations as can be seen in Table 13.

The average thermal efficiency of nuclear power plants was 33.76% in 1998.[37] This value is used to normalize the results to the electrical energy production.

Table 12 - Base Case Fuel Pin Design (17x17 PWR)

Parameter	Value	Source
Clad OD (cm)	0.9500	34
Clad Diametrical Thickness (cm)	0.1143	38
Diametrical Gap (cm)	0.0165	38
Fuel OD (cm)	0.8192	38
Active Fuel Length (m)	3.658	34
Fuel pins per assembly	264	34
Pin Pitch (cm)	1.25984	38
HM Concentration per Assembly (MT)	0.46	34
Assembly Power (MW)	18.4	38
Cycles in Core	3	38
Fuel Temperature (K)	850	42
Moderator Temperature (K)	579	42
Moderator Pressure (psi)	2250	42
Cycle average boron concentration (ppm)	1000	42
Power Density (MW/MTHM)	39.8	Calculated
Cycle Length (days)	Variable	Calculated
Down time between cycles (days)	60	Assumed

Table 13 - Transmutation Reactor Feed Comparison

	HM Weight Fraction of Feed			Absolute Difference with		Relative Difference with	
	Calculated	ANL[36]	YMP[35]	ANL	YMP	ANL	YMP
U235	0.0038%	0.0040%	0.0040%	-0.0002%	-0.0002%	-4.1%	-4.1%
U236	0.0018%	0.0020%	0.0020%	-0.0002%	-0.0002%	-11.8%	-11.8%
U238	0.4231%	0.4780%	0.4190%	-0.0549%	0.0041%	-11.5%	1.0%
Np237	4.3147%	5.0230%	5.6010%	-0.7083%	-1.2863%	-14.1%	-23.0%
Pu238	1.2393%	1.2720%	1.7250%	-0.0327%	-0.4857%	-2.6%	-28.2%
Pu239	53.8669%	53.1960%	52.1720%	0.6709%	1.6949%	1.3%	3.2%
Pu240	21.2638%	21.5340%	21.0850%	-0.2702%	0.1788%	-1.3%	0.8%
Pu241	3.8678%	3.7820%	3.5400%	0.0858%	0.3278%	2.3%	9.3%
Pu242	4.6785%	4.6860%	4.6230%	-0.0075%	0.0555%	-0.2%	1.2%
Am241	9.1778%	8.9670%	9.4310%	0.2108%	-0.2532%	2.4%	-2.7%
Am242m	0.0067%	0.0140%	0.0190%	-0.0073%	-0.0123%	-52.3%	-64.9%
Am243	1.0245%	0.9260%	1.1990%	0.0985%	-0.1745%	10.6%	-14.5%
Cm243	0.0018%	0.0020%	0.0030%	-0.0002%	-0.0012%	-11.2%	-40.8%
Cm244	0.1157%	0.1040%	0.1560%	0.0117%	-0.0403%	11.2%	-25.8%
Cm245	0.0125%	0.0090%	0.0190%	0.0035%	-0.0065%	39.1%	-34.1%
Cm246	0.0010%	0.0010%	0.0020%	0.0000%	-0.0010%	-0.6%	-50.3%
TRU	99.5712%	99.5160%	99.5750%	0.0552%	-0.0038%	0.1%	0.0%
U	0.4288%	0.4840%	0.4250%	-0.0552%	0.0038%	-11.4%	0.9%
Np	4.3147%	5.0230%	5.6010%	-0.7083%	-1.2863%	-14.1%	-23.0%
Pu	84.9164%	84.4700%	83.1450%	0.4464%	1.7714%	0.5%	2.1%
MA	14.6548%	15.0460%	16.4300%	-0.3912%	-1.7752%	-2.6%	-10.8%

Fuel Enrichment

In order to completely account for all isotopes in the uranium, the quantity of U-234 that ends up in the enriched uranium versus the depleted uranium was estimated. The relative quantities of U-234 to U-235 were estimated using the method in Cochran.[39] The theoretical separation of two isotopes of uranium in UF_6 by gaseous diffusion is given by the following equation.

$$\alpha_1^2 = (M_1 + 6 * M_F)/(M_2 + 6 * M_F)$$

Where M_1 and M_2 are the masses of the heavier and lighter uranium isotopes, respectively.

This value is reduced by the actual efficiency of the system. The number of pass required to given the ratio of U-235 to U-238 as determined by the specified enrichment is given by the following equation.

$$^{0}A_{238}^{235}(f\alpha_{238}^{235})^{N} = {}^{N}A_{238}^{235}$$

Where

$^{0}A_{238}^{235}$ = initial atom ratio of U-235 to U-238,

$^{N}A_{238}^{235}$ = is the target atom ratio of U-235 to U-238,

N = is the number of passes required to achieve the target, and

f = is separation reduction factor.

The atom ratio of U-234 to U-235 is then calculated using the same methodology for N passes required to achieve the target U-235 to U-238 ratio. The uranium tails were assumed to be 0.2% U-235 and the mass and composition of the tails was determined by solving the mass balance equation for a unit mass of enriched uranium with the calculated composition determined by its enrichment.

The separation reduction factor was adjusted to give agreement with Rahnema.[40] The theoretical separation efficiency was reduced by the factor 99.895% in order to achieve good agreement. The calculated atom fractions for each isotope of uranium are compared with the three enrichments from

Rahnema. The enriched uranium composition is in good agreement with Rahnema over the range of enrichments of 1.6% to 3.95%, which covers most of the range of interest for this study.

Table 14 - Comparison of Estimated Enriched Uranium Isotopic Composition

	Enrichment (w/o U-235)					
	1.6%		2.8%		3.95%	
	Calculated	Rahnema	Calculated	Rahnema	Calculated	Rahnema
U-234	0.0135%	0.0140%	0.0253%	0.0256%	0.0373%	0.0367%
U-235	1.6201%	1.6202%	2.8348%	2.8349%	3.9985%	3.9985%
U-238	98.3663%	98.3658%	97.1399%	97.1394%	95.9642%	95.9648%

Fuel Cycle Isotopic Data

The depletion of the LWR fuel was simulated using the SAS2H Module of the SCALE 4.4[42] code package using the parameters in Table 12. The SCALE 4.4 code package is a Nuclear Regulatory Commission approved code for light water reactor applications and was run for a basic PWR assembly depletion calculation. The SAS2H Module performs 1-D neutron transport analyses of the reactor fuel assembly using the larger unit-cell (assembly) within an infinite lattice. In the SAS2H Module, time dependent nuclide cross sections are used in a point-depletion to determine the burnup-dependent fuel composition used for the next spectrum calculation. The 33-group ENDF/B-V library was used and the cross sections of all isotopes (128 heavy isotopes and 879 fission products) were updated after each transport calculation.

The burnup, enrichment, energy generated, and natural uranium required are given in Table 15. The enrichment of the 33 GWd/MTU SNF was used to approximate the backlog inventory of SNF, when irradiated in a PWR. The enrichment for the other burnups was taken from the projections in the IDB.[34] The detailed isotopic composition of the LWR SNF used to calculate all FOMs is given in Table 125 in Appendix I. The natural uranium requirements increase per unit mass of LWR fuel, but decrease when normalized to the electrical generation.

Table 15 - Burnup and Enrichment for OTC

Enrichment (w/o U-235)	Burnup (GW_{th}-d/MTU)	Natural Uranium (MT/MTU)	Electrical Energy (GW_e-yr/MTU)	Natural Uranium (MT/GW_e-yr)
3.15	33	5.77	0.0305	189
3.84	42	7.12	0.0388	184
4.11	46	7.65	0.0425	180
4.38	50	8.18	0.0462	177
4.74	55	8.89	0.0508	175

Effect of Burnup on OTC Waste

The results are summarized in this section. The FOMs are given based on the concentration, which is the value of the FOM normalized to the metric tonne of initial uranium (MTU) that was irradiated. This value is a measure of the concentration of the particular FOM in a given mass of SNF. The FOMs are also given based on the production rate, which is the value of the FOM normalized to the electrical generation (GW_e-yr). This is a measure of the rate of production of the particular FOM for a given level of nuclear power. In general, the FOM concentrations increase with burnup, in other words the SNF becomes more hazardous as the burnup increases. On the other hand, FOM production rate is nearly independent of burnup. At higher burnups, there will be smaller quantities of more hazardous waste. This suggests that burnup will have little net effect on waste management.

Effect of Burnup on Repository Isotopes

The results for the repository isotopes are given in Table 16. Figure 13 shows the repository isotope concentrations as a function of burnup and Figure 14 shows the repository isotope production rate as a function of burnup. The concentration of repository isotopes increases with burnup. The rate of increase is nearly linear; therefore, when normalized to energy production, the effect of burnup nearly disappears. For a given energy production, the quantity of repository isotopes is nearly independent of the discharge burnup.

The long-lived fission products (LLFP) concentration increases with burnup, but the rate remains nearly constant when normalized to energy production. The LLFP concentration in the reference fuel cycle is 781 g of Tc-99 and 181 g I-129 for each MTU of SNF. The concentration of both increases significantly with burnup. When normalized to the electrical energy produced, the reference scenario rate of production of the LLFP is 25.6 kg of Tc-99 and 5.9 kg of I-129 per GW_e-yr. The rates decline slightly with burnup.

The actinide repository isotopes increase at varying rates with burnup. When normalized to energy production, the production rate of U-234 and Pu-242 increase with burnup, while the production rates of Pu-239 and Np-237 decline slightly. Np-237, which is the most significant isotope, declines slightly, but overall burnup will have little effect on the actinide repository isotopes.

The reference fuel cycle SNF has a Np-237 concentration of 1.9 kg/MTU, which increases significantly with burnup. The production rate of Np-237 is 63 kg/GW_e-yr, which declines slightly with burnup. The U-234 concentration is 328 g U-234/MTU, which increases rapidly with burnup. The U-234 production rate is 11 kg/GW_e-yr, which increases significantly with burnup. The Pu-239 concentration is 6.1 kg/MTU, which increases significantly with burnup. The Pu-239 production rate is 200 kg/ GW_e-yr, which declines significantly with burnup. The Pu-242 concentration is 521 g/MTU, which increases rapidly with burnup. The Pu-242 production rate is 17 kg/ GW_e-yr, which increases slightly with burnup.

Table 16 - OTC Repository Isotope Concentrations (MT/MTU)

Burnup (GWd/MTU)	Tc-99	I-129	Np-237	U-234	Pu-239	Pu-242
33	7.81E-04	1.81E-04	1.91E-03	3.28E-04	6.11E-03	5.21E-04
42	9.70E-04	2.27E-04	2.36E-03	4.51E-04	6.63E-03	6.96E-04
46	1.05E-03	2.49E-04	2.56E-03	5.11E-04	6.83E-03	7.76E-04
50	1.13E-03	2.70E-04	2.74E-03	5.73E-04	7.00E-03	8.58E-04
55	1.23E-03	2.94E-04	2.97E-03	6.60E-04	7.26E-03	9.54E-04

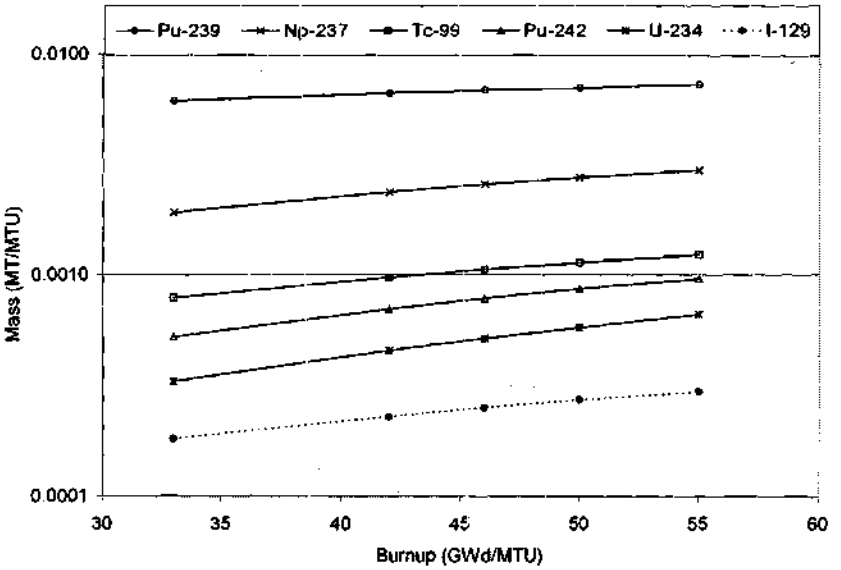

Figure 13 - Repository Isotope Concentrations for OTC Scenario

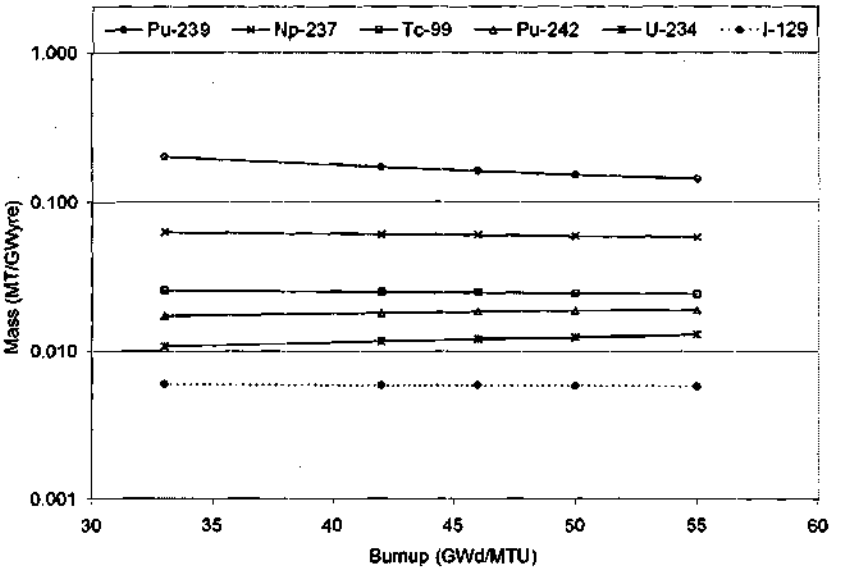

Figure 14 - Repository Isotopes Discharge Rates for OTC Scenario

Effect of Burnup on Waste Material Composition

The summary of the actinide masses are given in Table 17. Figure 15 shows the concentration as a function of burnup and Figure 16 shows production rate as a function of burnup. The concentration of transuranics increases with burnup, while the rate of production declines with burnup. The composition of transuranic shifts to higher actinides as the burnup increases, which results in transuranics with a lower fraction of plutonium. Overall, far less heavy metal will need to be handled and processed for systems operating at higher burnups and the production rate of transuranics will decline slightly.

The reference fuel cycle SNF has a plutonium concentration of 9.5 kg/MTU of SNF, which increases with burnup. The production rate of plutonium is 310 kg/GW_e-yr, which decreases significantly with burnup. The transuranic concentration is 11 kg/MTU, which increases with burnup. The transuranic production rate is 360 kg/GW_e-yr, which decreases with burnup. The minor actinide concentration is 0.1 kg/MTU, which increases with burnup. The minor actinide concentration is 3.4 kg/GW_e-yr, which increases with burnup.

The bulk of the material is the uranium. The reference fuel cycle SNF has a residual uranium concentration of 955 kg/MTU, which decreases with burnup. The uranium production rate is 31 MT/GW_e-yr, which decreases significantly with burnup. The total heavy metal concentration is 966 kg/MTU, which decreases with burnup. The heavy metal production rate is 32 MT/GW_e-yr, which decreases significantly with burnup.

Table 17 - Data for OTC Actinide Mass (MT/MTU)

Burnup (GWd/MTU)	Pu	TRU	MA	U	Actinides
33	9.46E-03	1.11E-02	1.05E-04	9.55E-01	9.66E-01
42	1.17E-02	1.27E-02	1.48E-04	9.45E-01	9.57E-01
46	1.22E-02	1.34E-02	1.63E-04	9.42E-01	9.55E-01
50	1.27E-02	1.40E-02	1.77E-04	9.35E-01	9.49E-01
55	1.33E-02	1.48E-02	1.97E-04	9.26E-01	9.41E-01

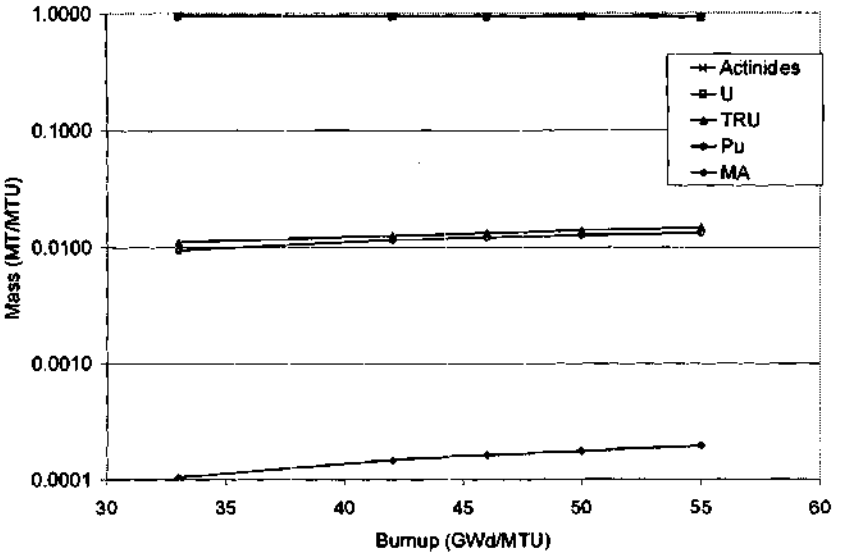

Figure 15 - Mass of Actinides Discharged per MTU Loaded for OTC Scenario

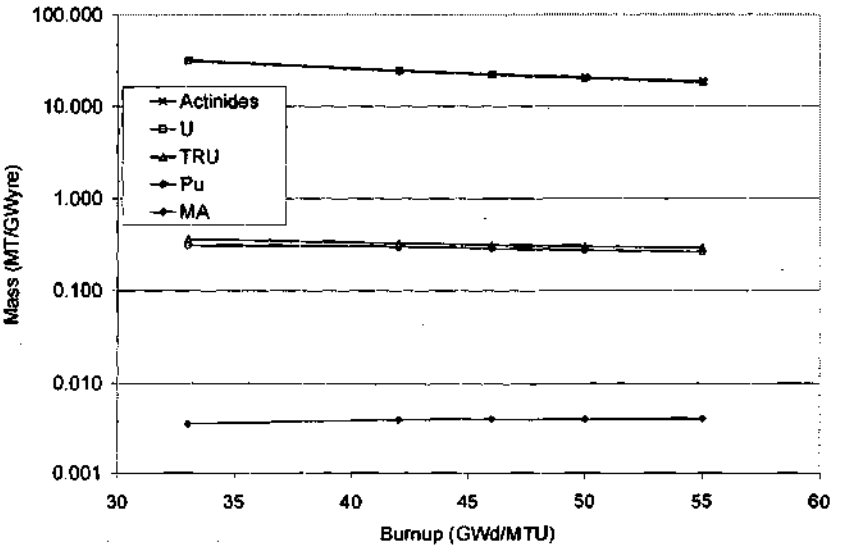

Figure 16 - Mass of Actinides Discharged per GW_e-yr Produced for OTC Scenario

Effect of Burnup on Waste Material Toxicity

The toxicity was calculated and is included in Table 18. Figure 17 shows the toxicity concentration as a function of burnup and time. Figure 18 shows the toxicity production rate as a function of burnup and time. The toxicity concentration increases versus burnup for all times. When normalized to the electrical generation, the toxicity production rate decreases slightly at higher burnups. Operation at higher burnups will reduce the total toxicity generated over the range of burnups considered.

The top two parent isotopes and their contribution to toxicity versus time after discharge are shown in Table 19. Initially, the fission products dominate the toxicity and in particular, Sr-90 contributes the larges amount to toxicity. After the highly toxic fission products have decayed away, the actinides and their daughters begin to dominate the toxicity. Pu-241 and its daughters contribute the highest fraction to toxicity at 1000 years. At 1,000,000 years, the daughter products of U-238 and U-234 (Pu-238 decays to U-234) are the largest contributors to toxicity. This shows that fissioning the plutonium will make a significant contribution to reducing the toxicity in the 1,000 to 10,000 year time frame. If the very long-term toxicity is to be reduced significantly, the uranium must also be transmuted.

Figure 19 shows the toxicity of the reference SNF. The radioactive decay will result in a continual evolution of the composition of the SNF. In order to determine the materials that need to be transmuted today to affect the toxicity at some point in the future, the time dependent toxicity attributed to each isotope or group is the toxicity of all isotopes present as a result of decay from the original isotope or group.

For example, the individual isotope ^{241}Pu is shown separately in Figure 19. ^{241}Pu has a half-life of 14 years and there is only a very small concentration of parent isotopes for ^{241}Pu in the SNF. Therefore, the actual mass of ^{241}Pu will decay away nearly completely in 200 years. The ^{241}Pu will decay to ^{241}Am, which has a half-life of 430 years and will also decay completely on the time scale of the repository. ^{241}Am decays to ^{237}Np, which has a 2 million year half-life. The ^{241}Pu toxicity curve shows that initially it constitutes a very small fraction of the toxicity, but at a few hundred years, after all of the ^{241}Pu has decayed, its daughter products will constitute a very large fraction of the toxicity. After the ^{241}Am decays away in a few thousand years, the ^{241}Pu contribution to toxicity is very small, but eventually the radioactive daughters of ^{237}Np controlled by the 150 thousand year half-life of ^{233}U will build to secular equilibrium with ^{237}Np, and the 14 year half-life isotope ^{241}Pu will contribute a small but significant fraction of the toxicity of the SNF

at one million years as shown in Figure 19. The original ^{241}Pu present in the SNF must be fissioned in order to destroy the toxicity of the ^{237}Np and its daughters present at one million years that were initially ^{241}Pu.

Figure 19 shows that fission products that decay away in a few hundred years dominate the short-term toxicity. After the fission products have decayed away, the toxicity is dominated by the transuranics for approximately 100,000 years. Beyond 100,000 years, the residual irradiated enriched uranium (IEU) will be the largest contributor to toxicity. By one million years, only a few transuranics isotopes have half-lives sufficiently long to remain in any significant quantities and all other transuranics isotopes will have decayed away, many of them back to ^{238}U and ^{235}U. The long-lived fission products represent an extremely small fraction of the toxicity.

Table 18 - Toxicity Concentration (m^3 H_2O/MTU) for OTC

	Time After Discharge (yr)						
Burnup (GWd/MTU)	0	100	500	1,000	10,000	100,000	1,000,000
33	4.63E+11	2.38E+10	7.59E+08	4.31E+08	1.05E+08	5.83E+07	2.81E+07
42	1.07E+12	3.01E+10	9.24E+08	5.13E+08	1.19E+08	7.77E+07	3.24E+07
46	1.11E+12	3.28E+10	9.86E+08	5.45E+08	1.25E+08	8.72E+07	3.45E+07
50	1.14E+12	3.55E+10	1.04E+09	5.72E+08	1.31E+08	9.67E+07	3.65E+07
55	1.18E+12	3.88E+10	1.11E+09	6.06E+08	1.38E+08	1.10E+08	3.92E+07

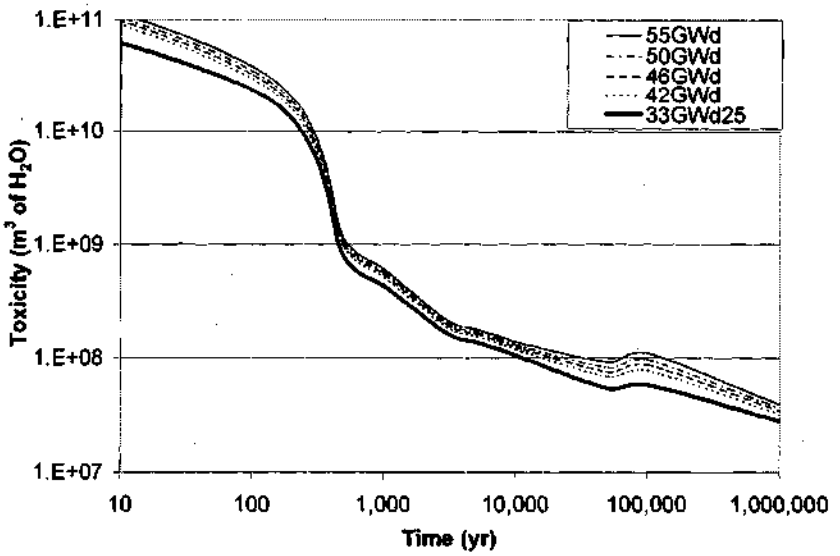

Figure 17 - Toxicity versus Time per MTU for OTC Scenario

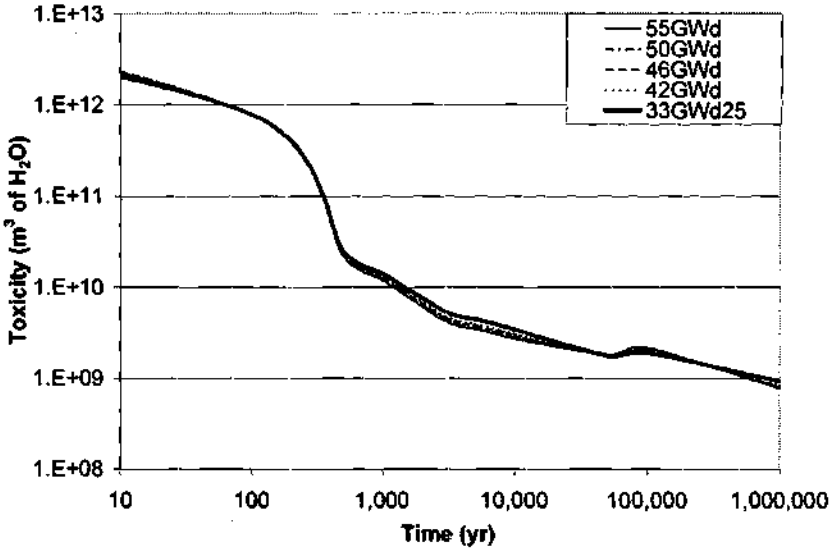

Figure 18 - Toxicity versus Time per GW_e-yr Produced for OTC Scenario

Table 19 - Parent Isotopes with Largest Contribution to Toxicity

	Time after Discharge (yr)											
Burnup	0		100		1,000		10,000		100,000		1,000,000	
33	Sr 90	25%	Sr 90	42%	Am241	19%	Pu239	25%	U234	22%	U238	22%
	Ce144	12%	Am241	1%	Pu240	10%	Pu240	16%	Pu238	16%	U234	8%
42	Sr 90	14%	Sr 90	42%	Pu241	26%	Pu239	23%	Pu238	23%	U238	19%
	Sr 89	13%	Pu241	2%	Pu240	10%	Pu240	16%	U234	16%	Pu238	9%
46	Sr 90	14%	Sr 90	42%	Pu241	26%	Pu239	23%	Pu238	25%	U238	17%
	Sr 89	12%	Pu241	2%	Pu240	10%	Pu240	16%	U234	15%	Pu238	10%
50	Sr 90	15%	Sr 90	42%	Pu241	26%	Pu239	22%	Pu238	26%	U238	16%
	Sr 89	12%	Pu241	2%	Pu240	10%	Pu240	16%	U234	14%	Pu238	11%
55	Sr 90	16%	Sr 90	42%	Pu241	26%	Pu239	22%	Pu238	28%	U238	15%
	Sr 89	11%	Pu241	2%	Pu240	9%	Pu240	16%	U234	13%	Pu238	13%

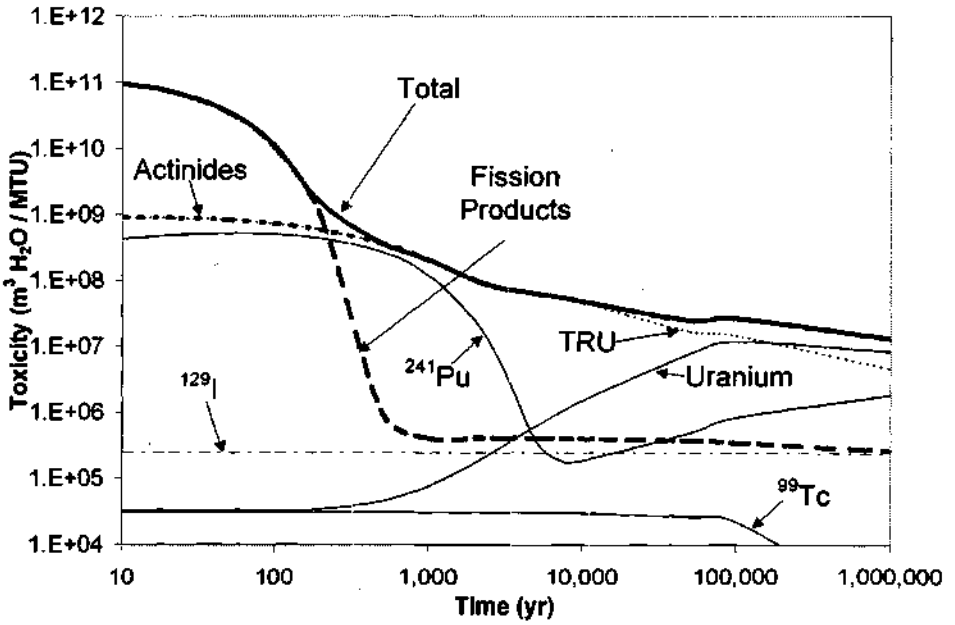

Figure 19 - Toxicity of Representative SNF

(Note: All groups are for parent isotopes at discharge and includes all daughter products that accumulate over time.)

Effect of Burnup on Waste Material Decay Heat

The decay heat was calculated and is included in Table 20. Figure 20 shows the decay heat concentration as a function of burnup and time. Figure 21 shows the decay heat production rate as a function of burnup and time. The decay heat concentration increases versus burnup for all times. When normalized to the electrical generation, the decay heat production rate decreases slightly from burnup. Individual assemblies will have higher decay heat as the burnup increases and therefore will require additional cooling prior to shipment. The decay heat of the 55 GWd/MTU SNF will have a higher decay heat at 10 years than the 33 GWd/MTU SNF has at 5 years. The rate of production of decay heat declines slightly with burnup, which will have little impact on the heat load of waste sent to a repository.

The top two parent isotopes and their contribution to decay heat versus time after discharge are shown in Table 21. Initially, the fission products dominate the decay heat. After the highly radioactive fission products have decayed away, the actinides and their daughters begin to dominate the decay heat. The decay heat at long times in the future is of little concern, since any handling of the waste will occur in the first 100 years, beyond this the decay heat is sufficiently low to not present any handling difficulties.

Table 20 - Decay Heat Concentration (W/MTU) for OTC

	Time after Discharge (yr)						
Burnup (GWd/MTU)	0	10	100	1,000	10,000	100,000	1,000,000
33	3.89E+03	1.18E+03	3.04E+02	6.12E+01	1.52E+01	1.19E+00	4.27E-01
42	5.87E+04	1.55E+03	4.02E+02	7.26E+01	1.70E+01	1.41E+00	5.12E-01
46	5.86E+04	1.73E+03	4.41E+02	7.70E+01	1.77E+01	1.51E+00	5.50E-01
50	5.93E+04	1.91E+03	4.79E+02	8.08E+01	1.84E+01	1.60E+00	5.86E-01
55	6.04E+04	2.14E+03	5.29E+02	8.55E+01	1.93E+01	1.74E+00	6.32E-01

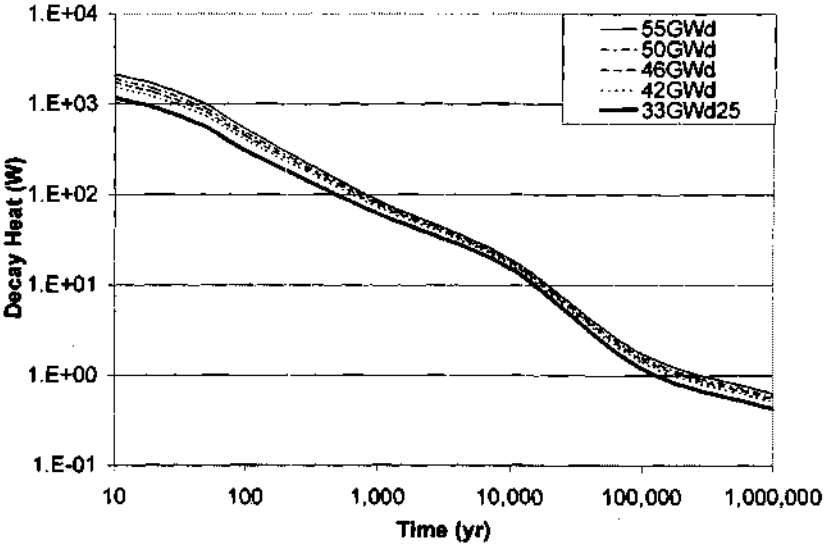

Figure 20 - Decay Heat versus Time per MTU for OTC Scenario

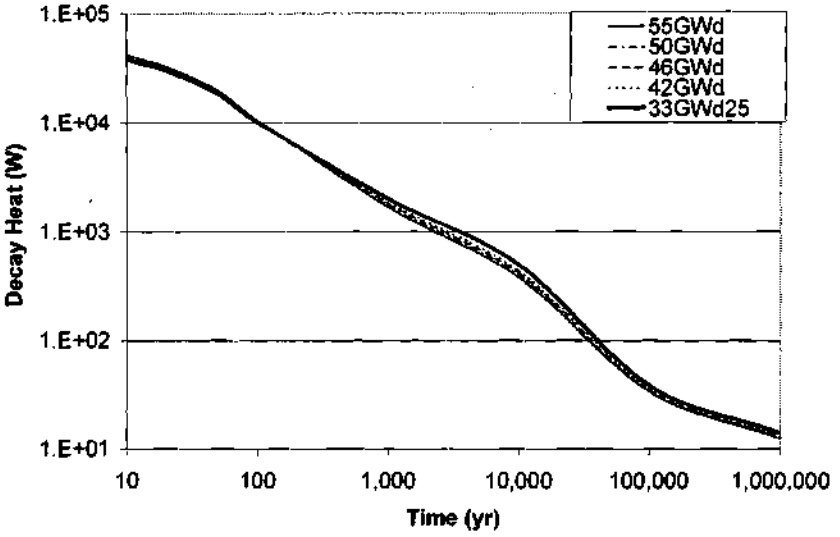

Figure 21 - Decay Heat versus Time per GW_e-yr Produced for OTC Scenario

Table 21 - Parent Isotopes with Largest Contribution to Decay Heat

	Time after Discharge (yr)											
Burnup	0		100		1,000		10,000		100,000		1,000,000	
33	Cs134	19%	Ce144	20%	Cs137	16%	Am241	18%	Pu239	26%	Am241	15%
	Ce144	9%	Ru106	14%	Sr 90	16%	Pu240	11%	U234	6%	U238	9%
42	Pr144	8%	Ce144	17%	Cs137	16%	Pu241	25%	Pu239	23%	Pu241	20%
	Zr 95	7%	Ru106	13%	Sr 90	15%	Pu240	11%	Pu238	7%	Np237	8%
46	Pr144	8%	Ce144	16%	Cs137	15%	Pu241	25%	Pu239	22%	Pu241	20%
	Zr 95	7%	Ru106	13%	Sr 90	15%	Pu240	11%	Pu238	8%	Np237	8%
50	Pr144	8%	Ce144	16%	Cs137	15%	Pu241	25%	Pu239	21%	Pu241	20%
	Zr 95	7%	Ru106	13%	Sr 90	14%	Pu240	11%	Pu238	9%	Np237	9%
55	Pr144	8%	Ce144	15%	Cs137	15%	Pu241	25%	Pu239	20%	Pu241	19%
	Zr 95	7%	Ru106	13%	Sr 90	14%	Pu240	10%	Pu238	10%	Np237	9%

Effect of Burnup on Waste Material Integral Decay Energy

The integral decay energy was calculated and is included in Table 22. Figure 22 shows the integral decay energy concentration as a function of burnup and time. Figure 23 shows the integral decay energy production rate as a function of burnup and time. The integral decay energy concentration increases versus burnup for all times. When normalized to the electrical generation, the integral decay energy production rate decreases slightly from burnup, except for the backlog material (33 GWd/MTU). The integral decay energy of the waste sent to the repository will not vary significantly based on the SNF burnup.

The top two parent isotopes and their contribution to integral decay energy versus time after discharge are shown in Table 23. Initially, the fission products dominate the integral decay energy. Nearly as much energy is released in the first 100 years as is released in the next 900 years. This would allow storage outside the repository or ventilation of the repository to significantly reduce the heat load. After the highly radioactive fission products have decayed away, the actinides and their daughters begin to dominate the integral decay energy. Pu-241 and its daughters contribute the highest fraction to integral decay energy at 10,000 years. By transmuting plutonium and other heat management strategies for the fission products, the heat load in the repository can be dramatically reduced.

Table 22 - Integral Decay Energy Concentration (J/MTU) for OTC

	Time After Discharge (yr)						
Burnup (GWd/MTU)	0	10	100	1,000	10,000	100,000	1,000,000
33	0.00E+00	8.84E+11	2.52E+12	5.76E+12	1.30E+13	2.55E+13	4.07E+13
42	0.00E+00	1.33E+12	3.49E+12	7.53E+12	1.58E+13	2.97E+13	4.83E+13
46	0.00E+00	1.43E+12	3.82E+12	8.18E+12	1.68E+13	3.15E+13	5.15E+13
50	0.00E+00	1.53E+12	4.14E+12	8.78E+12	1.78E+13	3.30E+13	5.45E+13
55	0.00E+00	1.65E+12	4.57E+12	9.57E+12	1.91E+13	3.51E+13	5.85E+13

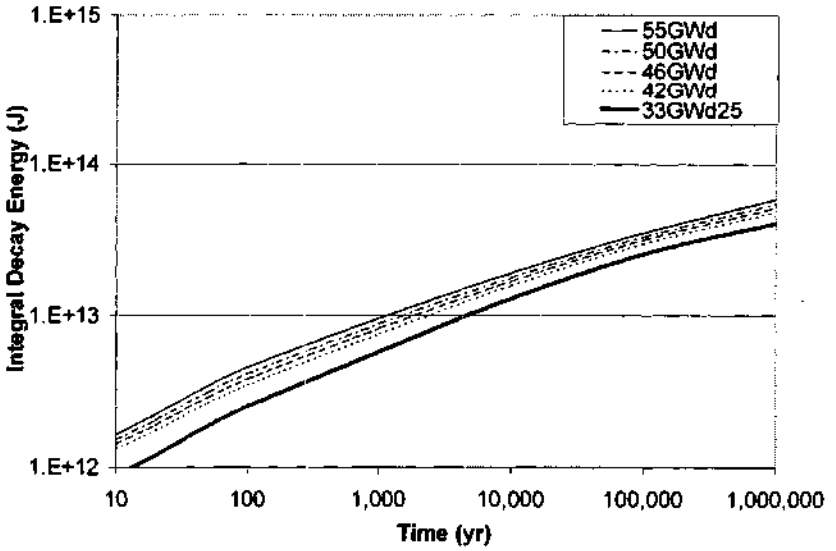

Figure 22 - Integral Decay Energy per MTU Versus Time for OTC Scenario

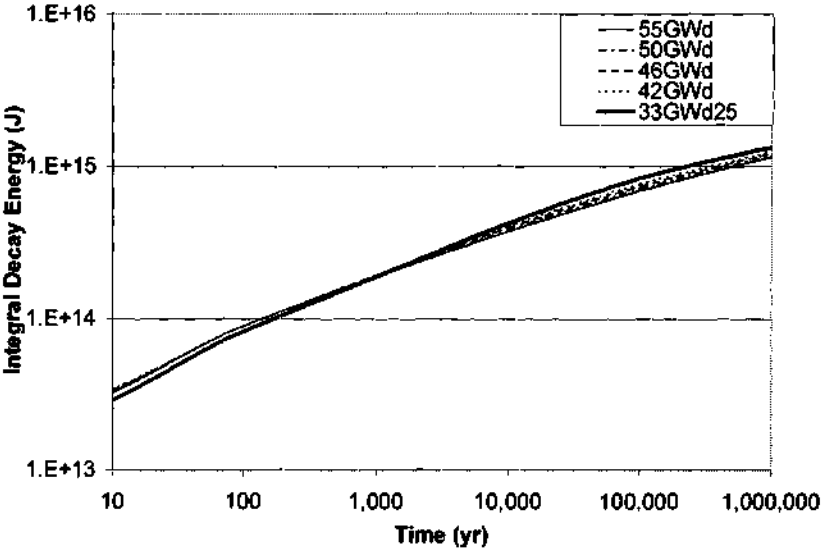

Figure 23 - Integral Decay Energy per GW_e-yr Produced Versus Time for OTC Scenario

Table 23 - Parent Isotopes with Largest Contribution to Integral Decay Energy

	Time after Discharge (yr)									
Burnup	100		1,000		10,000		100,000		1,000,000	
33	Ce144	19%	Ce144	11%	Am241	15%	Pu239	22%	Pu239	18%
	Cs134	13%	Ru106	8%	Pu241	6%	Pu240	10%	Am241	7%
42	Zr 95	10%	Ce144	8%	Pu241	18%	Pu239	20%	Pu239	16%
	Ce144	7%	Cs134	7%	Cs137	5%	Pu240	10%	Pu241	9%
46	Zr 95	9%	Cs134	7%	Pu241	17%	Pu239	19%	Pu239	15%
	Ce144	7%	Ce144	7%	Cs137	6%	Pu240	10%	Pu241	9%
50	Zr 95	9%	Cs134	8%	Pu241	17%	Pu239	19%	Pu239	15%
	Cs134	8%	Ce144	7%	Cs137	6%	Pu240	9%	Pu241	9%
55	Zr 95	9%	Cs134	8%	Pu241	16%	Pu239	18%	Pu239	14%
	Cs134	8%	Ce144	6%	Cs137	6%	Pu240	9%	Pu241	9%

Effect of Burnup on Waste Material Radiological Properties

The following parameters are focused on the difficulty of handling the materials. In particular, the relative amount of shielding that would be required to ship, store, or process the waste. Overall, the higher the burnup, the more shielding that would be required to handle the material or longer decay times will be required. In generally, it increases slower than the net electrical generation of the SNF. The photon dose rate of the 55 GWd/MTU SNF will is higher at 10 years than the 33 GWd/MTU SNF is at 5 years.

The photon dose rate was calculated and is included in Table 24. Figure 24 show the photon dose rate concentration as a function of burnup and time. Figure 25 shows the photon dose rate production rate as a function of burnup and time. The photon dose rate concentration increases versus burnup for all times. When normalized to the electrical generation, the photon dose rate production rate still increases versus burnup, but the differences are small at most times.

The top two parent isotopes and their contribution to photon dose rate versus time after discharge and are shown in Table 25. Initially, the fission products dominate the photon dose rate. After the highly radioactive fission products have decayed away, the actinides and their daughters begin to dominate the photon dose rate. The photon dose rate at long times in the future is of little concern, since any handling of the waste will occur in the first 100 years, beyond this the photon dose rate is sufficiently low to not present any handling difficulties.

Table 24 - Unshielded Photon Dose Rate Concentration (REM/hr/MTU) for OTC

	Time after Shutdown (yr)						
Burnup (GWd/MTU)	0	10	100	1,000	10,000	100,000	1,000,000
33	2.04E+05	4.07E+04	4.10E+03	3.36E+00	2.05E+00	1.73E+00	8.07E-01
42	2.89E+06	5.23E+04	5.17E+03	4.94E+00	2.90E+00	2.29E+00	9.44E-01
46	2.93E+06	5.77E+04	5.66E+03	5.75E+00	3.32E+00	2.55E+00	1.01E+00
50	2.96E+06	6.28E+04	6.11E+03	6.57E+00	3.75E+00	2.82E+00	1.07E+00
55	3.02E+06	6.93E+04	6.70E+03	7.60E+00	4.30E+00	3.19E+00	1.15E+00

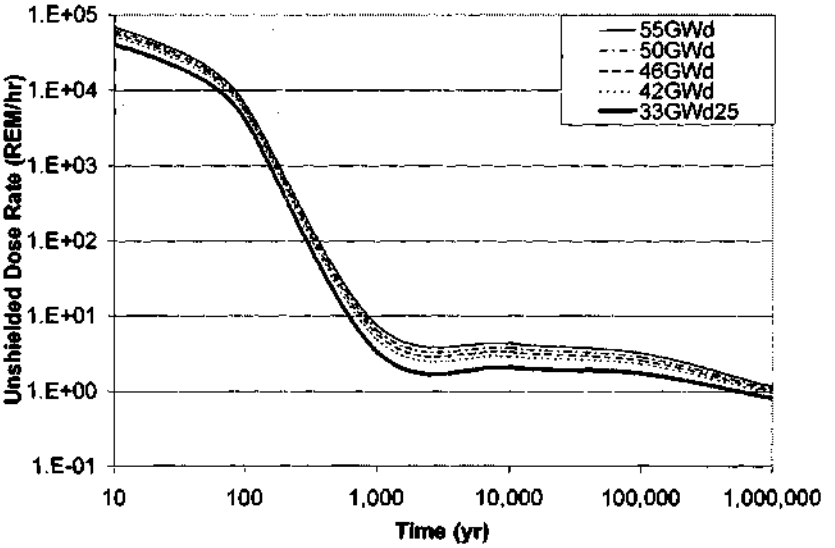

Figure 24 - Unshielded Dose Rate from Photon Emission per MTU Versus Time for OTC Scenario

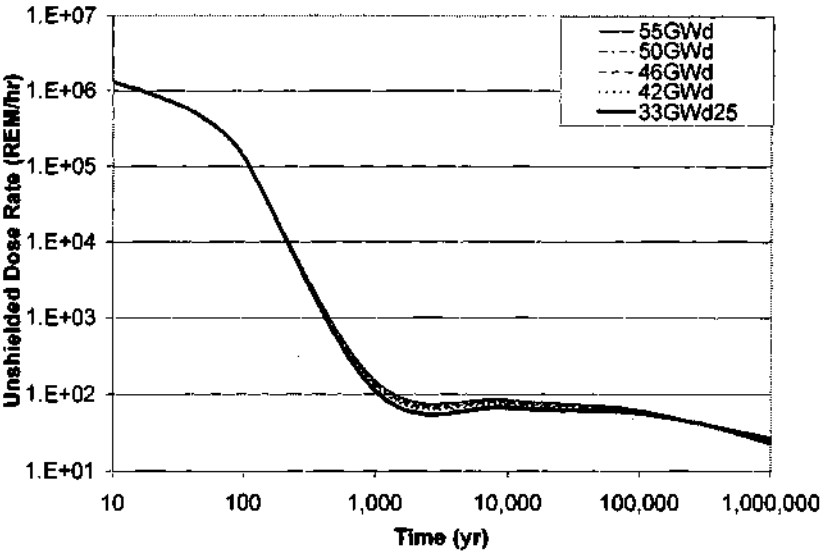

Figure 25 - Unshielded Dose Rate from Photon Emission per GW_e-yr Produced Versus Time for OTC Scenario

Table 25 - Parent Isotopes with Largest Contribution to Photon Dose Rate

	Time after Shutdown (yr)									
Burnup (GWd/MTU)	0		100		1,000		10,000		1,000,000	
33	Cs134	35%	Cs134	21%	Cs137	36%	Am243	33%	U238	18%
	Ba137m	9%	Ru106	11%	Cs134	6%	Sn126	10%	Am241	9%
42	Nb 95	14%	Cs134	20%	Cs137	35%	Am243	35%	U238	15%
	Zr 95	13%	Ru106	8%	Cs134	7%	Sn126	8%	Pu241	12%
46	Nb 95	13%	Cs134	21%	Cs137	35%	Am243	36%	U238	14%
	Zr 95	13%	Ru106	8%	Cs134	7%	Sn126	8%	Pu241	12%
50	Nb 95	13%	Cs134	22%	Cs137	35%	Am243	37%	U238	13%
	Zr 95	13%	Ru106	8%	Cs134	7%	Sn126	7%	Pu241	12%
55	Nb 95	13%	Cs134	22%	Cs137	34%	Am243	37%	U238	12%
	Zr 95	12%	Ru106	7%	Cs134	7%	Sn126	7%	Pu241	12%

The spontaneous neutron source dose rate was calculated and is included in Table 26. Figure 26 shows the unshielded spontaneous neutron source dose rate concentration as a function of burnup and time. Figure 27 shows the unshielded spontaneous neutron source dose rate production rate as a function of burnup and time. The spontaneous neutron source dose rate concentration increases versus burnup for all times, but the difference reduces over time. When normalized to the electrical generation, the spontaneous neutron source dose rate production rate still increases versus burnup, but the differences become very small at large decay times.

The top two parent isotopes and their contribution to spontaneous neutron source dose rate versus time after discharge and are shown in Table 27. The fission products do not undergo spontaneous fission; therefore they do not contribute to the spontaneous neutron source dose rate. Curium-244 dominates the spontaneous neutron source for the first 1,000 years. The spontaneous neutron source dose rate at long times in the future is of little concern, since any handling of the waste will occur in the first 100 years, beyond this the spontaneous neutron source dose rate is sufficiently low to not present any handling difficulties.

Table 26 - SNS Dose Rate Concentration (REM/hr/MTU) for OTC

	Time after Shutdown (yr)						
Burnup (GWd/MTU)	0	10	100	1,000	10,000	100,000	1,000,000
33	1.50E-01	1.04E-01	7.72E-03	4.02E-03	2.00E-03	7.67E-04	1.55E-04
42	7.65E-01	4.77E-01	2.20E-02	6.04E-03	2.79E-03	1.02E-03	2.02E-04
46	9.58E-01	6.10E-01	2.77E-02	7.39E-03	3.28E-03	1.15E-03	2.26E-04
50	1.17E+00	7.56E-01	3.42E-02	8.99E-03	3.83E-03	1.28E-03	2.50E-04
55	1.46E+00	9.55E-01	4.33E-02	1.14E-02	4.64E-03	1.43E-03	2.78E-04

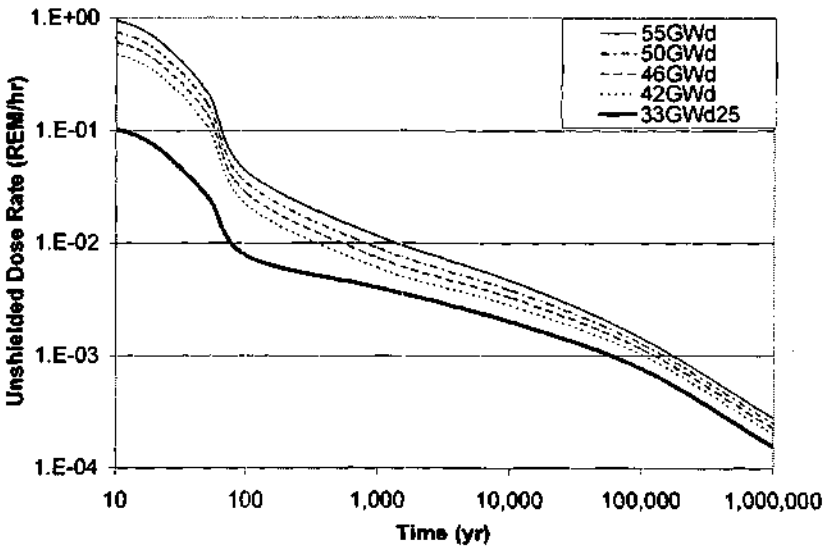

Figure 26 - Unshielded Dose Rate from Spontaneous Neutron Emission per MTU Versus Time

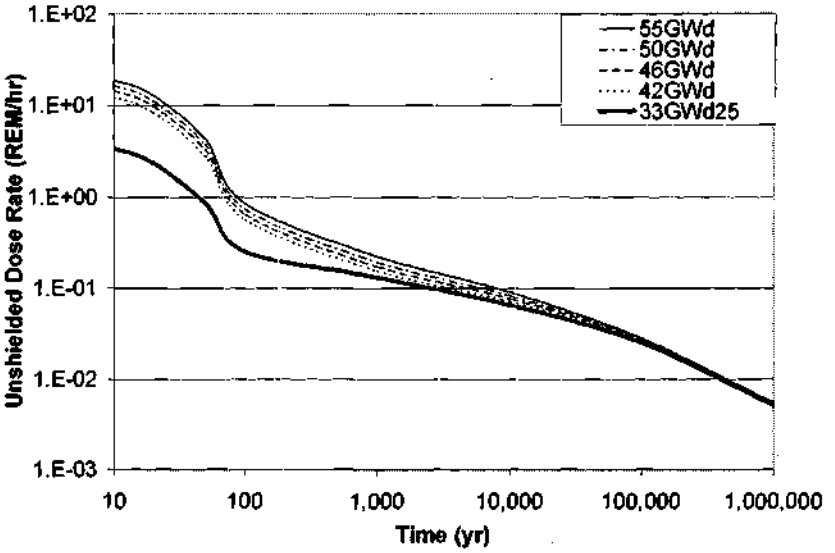

Figure 27 - Unshielded Dose Rate from Spontaneous Neutron Emission per GW_e-yr Versus Time for OTC Scenario

Table 27 - Parent Isotopes with Largest Contribution to Spontaneous Neutron Source Dose Rate

	Time After Discharge (Yr)									
Burnup	0		100		1,000		10,000		1,000,000	
33	Cm244	45%	Cm244	45%	Cm244	44%	Pu240	26%	Pu242	42%
	Pu240	1%	Pu240	1%	Pu240	1%	Pu242	10%	U238	4%
42	Cm244	42%	Cm244	45%	Cm244	46%	Pu240	19%	Pu242	43%
	Cm242	4%	Cm242	1%	Pu240	0%	Cm246	17%	U238	3%
46	Cm244	42%	Cm244	45%	Cm244	46%	Cm246	21%	Pu242	43%
	Cm242	3%	Cm242	1%	Cm246	0%	Pu240	16%	U238	3%
50	Cm244	43%	Cm244	45%	Cm244	46%	Cm246	24%	Pu242	43%
	Cm242	3%	Cm242	1%	Cm246	0%	Pu240	14%	U238	2%
55	Cm244	44%	Cm244	45%	Cm244	46%	Cm246	27%	Pu242	43%
	Cm242	2%	Cm242	0%	Cm246	0%	Pu240	11%	U238	2%

The α,n neutron source dose rate was calculated and is included in Table 28. Figure 28 shows the unshielded α,n neutron source dose rate concentration as a function of burnup and time. Figure 29 shows the unshielded α,n neutron source dose rate production rate as a function of burnup and time. The α,n neutron source dose rate concentration increases versus burnup for all times. When normalized to the electrical generation, the α,n neutron source dose rate production rate still increases versus burnup at times less than 100 years, but beyond a few hundred years the α,n neutron source dose rate will decrease with burnup.

The top two parent isotopes and their contribution to spontaneous neutron source dose rate versus time after discharge and are shown in Table 29. In general, the fission products do not undergo α decay, and therefore they do not contribute to the α,n neutron source dose rate. Curium dominates the α,n neutron source for the first 1,000 years. The α,n neutron source dose rate at long times in the future is of little concern, since any handling of the waste will occur in the first 100 years, beyond this the spontaneous neutron source dose rate is sufficiently low to not present any handling difficulties.

Table 28 - Unshielded α,n Neutron Dose Rate Concentration (REM/hr/MTU) for OTC

	Time after Shutdown (yr)						
Burnup (GWd/MTU)	0	10	100	1,000	10,000	100,000	1,000,000
33	7.18E-03	7.10E-03	5.56E-03	1.55E-03	3.50E-04	2.95E-05	1.40E-05
42	2.58E-02	1.08E-02	7.55E-03	1.85E-03	3.91E-04	3.53E-05	1.69E-05
46	2.82E-02	1.28E-02	8.33E-03	1.96E-03	4.08E-04	3.79E-05	1.83E-05
50	3.04E-02	1.50E-02	9.08E-03	2.06E-03	4.24E-04	4.05E-05	1.95E-05
55	3.33E-02	1.79E-02	1.01E-02	2.18E-03	4.44E-04	4.40E-05	2.10E-05

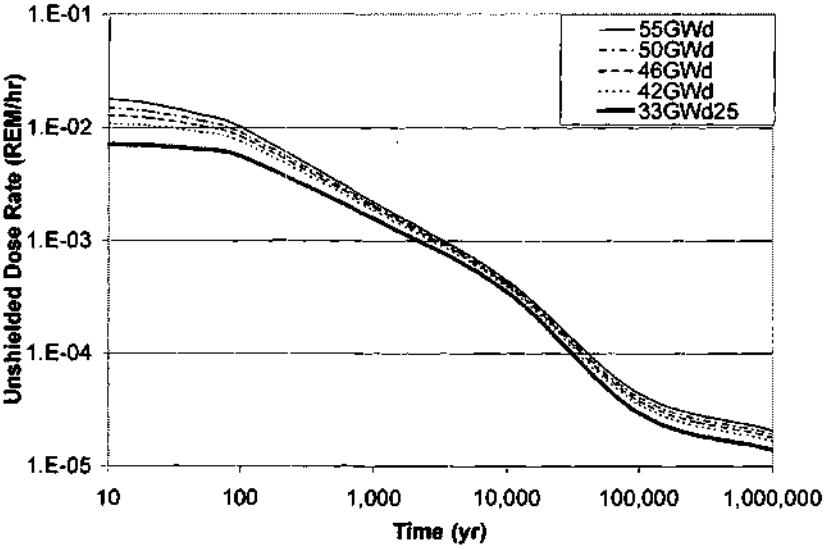

Figure 28 - Unshielded Dose Rate from α,n Neutron Emission per MTU Versus Time

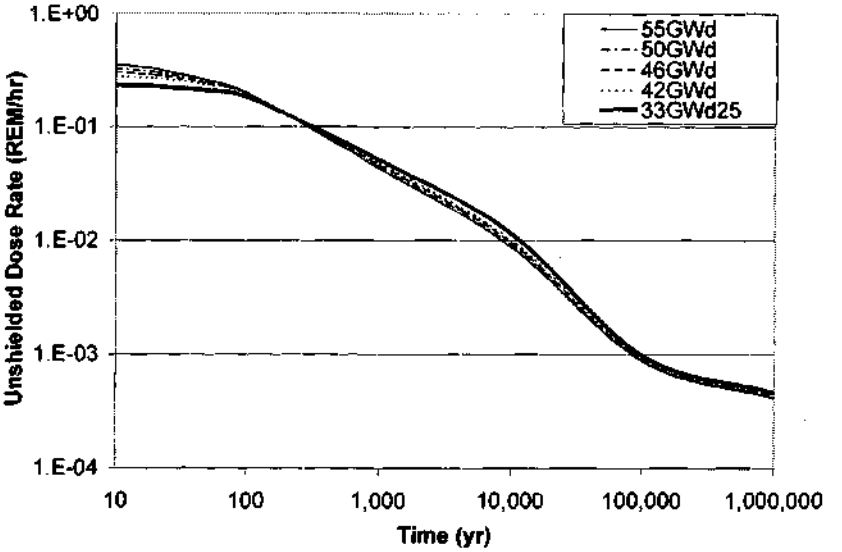

Figure 29 - Unshielded Dose Rate from α,n Neutron Emission per GW_e-yr Produced Versus Time for OTC Scenario

Table 29 - Parent Isotopes with Largest Contribution to Spontaneous Neutron Source Dose Rate

	Time After Shutdown (Yr)									
Burnup (GWd/MTU)	0		100		1,000		10,000		1,000,000	
33	Am241	20%	Am241	20%	Am241	20%	Am241	19%	Am241	17%
	Pu238	14%	Pu238	14%	Pu238	13%	Pu240	10%	Np237	8%
42	Cm242	27%	Cm244	17%	Pu238	16%	Pu241	26%	Pu241	23%
	Cm244	10%	Pu238	13%	Cm244	16%	Pu240	10%	Np237	9%
46	Cm242	24%	Cm244	19%	Cm244	17%	Pu241	26%	Pu241	22%
	Cm244	12%	Pu238	14%	Pu238	17%	Pu240	10%	Np237	9%
50	Cm242	22%	Cm244	21%	Cm244	18%	Pu241	26%	Pu241	22%
	Cm244	13%	Pu238	14%	Pu238	17%	Pu240	10%	Np237	10%
55	Cm242	19%	Cm244	22%	Cm244	19%	Pu241	26%	Pu241	22%
	Cm244	15%	Pu238	14%	Pu238	17%	Pu240	9%	Np237	10%

Effect of Burnup on Proliferation Properties

The FOMs related to proliferation have been calculated. These parameters have been calculated from discharge to 1 million years, since proliferation concerns exist even after the waste has been placed in the repository. The burnup seems to have a relatively small effect on the proliferation resistance of the SNF. In general, the quantities that will be produced are reduced as the burnup increases. For times less than 1,000 years, the radiation barrier will be high. In the 1,000 to 10,000 year time frame, the physical barriers to proliferation (i.e., radiation barrier, mass of radioactive waste) will be low and the technical barriers (i.e., spontaneous neutron source, decay heat, and bare critical mass) will be near their minima. Beyond 100,000 years, a large mass of radioactive waste would need to be processed to recover on bare critical mass and the bare critical mass has increased dramatically.

Table 30 and 31 shows the bare critical mass (BCM) of transuranics and plutonium, respectively. At 1 million years, the plutonium is essentially pure Pu-242, and the only other transuranic is Np-237. These tables show that the BCM is time dependent and varies slightly over the first 10,000 years and then increases significantly by 1 million years. The BCM increases slightly with burnup at all times. The plutonium BCM is less than the transuranic BCM except at decay times beyond a few hundred thousand years.

Table 30 - OTC Bare Critical Mass of Transuranics (kg)

	Time after Discharge (yr)						
Burnup (GWd/MTU)	0	10	100	1,000	10,000	100,000	1,000,000
33	16.08	16.21	16.61	17.45	17.64	46.76	74.39
42	15.65	16.15	17.27	18.22	18.59	49.31	74.44
46	15.75	16.27	17.51	18.59	18.94	50.06	74.81
50	15.87	16.45	17.85	18.90	19.29	51.17	74.36
55	16.04	16.64	17.92	19.16	19.58	51.48	74.47

Table 31 - OTC Bare Critical Mass of Plutonium (kg)

	Time after Discharge (yr)						
Burnup (GWd/MTU)	0	10	100	1,000	10,000	100,000	1,000,000
33	14.62	14.60	14.72	14.61	13.56	23.31	92.84
42	14.70	14.80	15.02	15.00	13.94	25.83	93.04
46	14.80	14.89	15.24	15.20	14.01	26.65	92.60
50	14.90	14.98	15.32	15.24	14.23	27.57	92.20
55	14.96	15.03	15.44	15.34	14.35	28.53	93.02
WGPu	10.70						

Tables 32 and 33 show the BCM production rate normalized to net electrical generation for transuranic and plutonium, respectively. The BCM production rate declines with burnup, especially for plutonium.

Table 32 - OTC Bare Critical Mass of Transuranics Production Rate (BCM/GW_e-yr)

	Time after Discharge (yr)						
Burnup (GWd/MTU)	0	10	100	1,000	10,000	100,000	1,000,000
33	22.63	22.40	21.70	19.79	14.58	1.85	0.65
42	20.70	20.01	18.49	16.74	12.32	1.69	0.63
46	19.76	19.08	17.47	15.71	11.61	1.64	0.62
50	18.92	18.21	16.53	14.87	11.01	1.58	0.61
55	18.06	17.36	15.84	14.11	10.48	1.56	0.61

Table 33 - OTC Bare Critical Mass of Plutonium Production Rate (BCM/GW_e-yr)

	Time after Discharge (yr)						
Burnup (GWd/MTU)	0	10	100	1,000	10,000	100,000	1,000,000
33	21.22	20.86	19.93	19.10	14.26	1.10	0.03
42	20.40	19.14	16.90	16.01	11.97	0.95	0.03
46	19.33	18.14	15.82	14.99	11.30	0.91	0.03
50	18.39	17.27	15.04	14.25	10.64	0.87	0.03
55	17.52	16.45	14.23	13.47	10.10	0.83	0.03

The radiation barrier (RB) of one BCM for transuranics and plutonium are shown in Tables 34 and 35, respectively. The RB decreases rapidly with time and reaches a minimum at around 10,000 years, but remains low, thereafter. The RB decreases slightly with burnup at discharge, but increases with burnup for 10 or more years after discharge. The RB for plutonium is nearly the same as the transuranics except at long decay times. Higher burnups will produce a more effective radiation barrier for a longer period of time, but on the time scale of the repository, this is insignificant.

Table 34 - OTC Transuranic Radiation Barrier (REM/hr/BCM)

	Time after Discharge (yr)						
Burnup (GWd/MTU)	0	10	100	1,000	10,000	100,000	1,000,000
33	3.0E+05	6.0E+04	2.0E+04	6.8E+03	4.7E+00	3.6E+01	6.0E+01
42	3.6E+06	6.7E+04	2.3E+04	8.0E+03	6.2E+00	4.1E+01	5.8E+01
46	3.5E+06	7.1E+04	2.4E+04	8.4E+03	6.8E+00	4.3E+01	5.7E+01
50	3.4E+06	7.5E+04	2.6E+04	8.9E+03	7.5E+00	4.5E+01	5.7E+01
55	3.3E+06	7.9E+04	2.7E+04	9.4E+03	8.2E+00	4.7E+01	5.7E+01

Table 35 - OTC Plutonium Radiation Barrier (REM/hr/BCM)

	Time after Discharge (yr)						
Burnup (GWd/MTU)	0	10	100	1,000	10,000	100,000	1,000,000
33	3.2E+05	6.4E+04	2.2E+04	7.0E+03	4.8E+00	6.1E+01	1.3E+03
42	3.6E+06	7.0E+04	2.5E+04	8.3E+03	6.4E+00	7.2E+01	1.2E+03
46	3.6E+06	7.5E+04	2.7E+04	8.9E+03	7.0E+00	7.7E+01	1.1E+03
50	3.5E+06	7.9E+04	2.8E+04	9.3E+03	7.8E+00	8.2E+01	1.1E+03
55	3.4E+06	8.3E+04	3.0E+04	9.8E+03	8.5E+00	8.8E+01	1.1E+03

The spontaneous neutron source (SNS) of one BCM for transuranics and plutonium are shown in Tables 36 and 37, respectively. The SNS for transuranics declines for the first 1,000 years and then increases slowly. On the other hand, the SNS for plutonium generally increases with time. The SNS for plutonium is initially orders of magnitude less than the transuranics. The difference decreases slowly with time and beyond a few tens of thousands of years the SNS of the transuranics is less than plutonium. The SNS increases with burnup. The transuranics will be technically more challenging to produce a significant yield because of the high spontaneous neutron emission rate, but it does decline to levels similar to reactor grade plutonium in the 1,000 to 10,000 year time frame.

Table 36 - OTC Transuranic Spontaneous Neutron Source (n/s/BCM)

	Time after Discharge (yr)						
Burnup (GWd/MTU)	0	10	100	1,000	10,000	100,000	1,000,000
33	2.2E+08	1.5E+08	1.2E+07	6.6E+06	4.4E+06	1.3E+07	7.2E+06
42	1.4E+09	6.3E+08	3.1E+07	9.2E+06	5.8E+06	1.5E+07	7.7E+06
46	1.6E+09	7.8E+08	3.8E+07	1.1E+07	6.5E+06	1.6E+07	8.1E+06
50	1.9E+09	9.3E+08	4.6E+07	1.3E+07	7.4E+06	1.7E+07	8.3E+06
55	2.2E+09	1.1E+09	5.5E+07	1.6E+07	8.6E+06	1.8E+07	8.6E+06

Table 37 - OTC Plutonium Spontaneous Neutron Source (n/s/BCM)

	Time after Discharge (yr)						
Burnup (GWd/MTU)	0	10	100	1,000	10,000	100,000	1,000,000
33	5.8E+06	5.8E+06	5.8E+06	5.3E+06	4.0E+06	2.2E+07	1.6E+08
42	5.8E+06	6.2E+06	6.5E+06	6.0E+06	4.6E+06	2.7E+07	1.6E+08
46	6.1E+06	6.5E+06	6.9E+06	6.2E+06	4.9E+06	2.9E+07	1.6E+08
50	6.4E+06	6.8E+06	7.2E+06	6.4E+06	5.1E+06	3.1E+07	1.6E+08
55	6.7E+06	7.1E+06	7.5E+06	6.7E+06	5.4E+06	3.2E+07	1.6E+08
WGPu	6.0E+05						

The decay heat (DH) of one BCM for transuranics and plutonium are shown in Tables 38 and 39, respectively. The DH for transuranics and plutonium declines for the first 10,000 years, and is higher at 100,000 years. At 1 million years, the DH is less than at 100,000 years for both transuranics and plutonium and the transuranics are at the lowest value at 1 million years. On the other hand, the DH for plutonium generally increases with time. The DH for plutonium is initially orders of magnitude less than the transuranics. The difference decreases slowly with time and beyond a few tens of thousands of years the DH of the transuranics is less than plutonium. The DH increases with burnup except at long decay times. The transuranics will be technically more challenging to produce because of the higher decay heat, but it does decline to levels similar to reactor grade plutonium in the 1,000 to 10,000 year time frame.

Table 38 - OTC Transuranic Decay Heat (W/BCM)

	Time after Discharge (yr)						
Burnup (GWd/MTU)	0	10	100	1,000	10,000	100,000	1,000,000
33	3.8E+02	3.8E+02	3.2E+02	1.0E+02	3.4E+01	1.3E+01	1.9E+00
42	3.4E+03	4.9E+02	3.9E+02	1.1E+02	3.5E+01	1.3E+01	1.9E+00
46	3.7E+03	5.6E+02	4.2E+02	1.1E+02	3.5E+01	1.2E+01	2.0E+00
50	4.0E+03	6.3E+02	4.4E+02	1.2E+02	3.5E+01	1.2E+01	2.0E+00
55	4.4E+03	7.2E+02	4.7E+02	1.2E+02	3.6E+01	1.2E+01	2.0E+00

Table 39 - OTC Plutonium Decay Heat (W/BCM)

	Time after Discharge (yr)						
Burnup (GWd/MTU)	0	10	100	1,000	10,000	100,000	1,000,000
33	1.7E+02	1.6E+02	1.1E+02	4.6E+01	3.4E+01	2.2E+01	1.1E+01
42	2.3E+02	2.4E+02	1.5E+02	4.7E+01	3.5E+01	2.1E+01	1.1E+01
46	2.5E+02	2.7E+02	1.7E+02	4.8E+01	3.5E+01	2.1E+01	1.1E+01
50	2.8E+02	3.0E+02	1.9E+02	4.8E+01	3.5E+01	2.1E+01	1.1E+01
55	3.2E+02	3.4E+02	2.1E+02	4.8E+01	3.5E+01	2.1E+01	1.1E+01
WGPu	2.4E+01						

The mass of radioactive waste (MRW) of one BCM for transuranics and plutonium are shown in Tables 40 and 41, respectively. The MRW for transuranics and plutonium increases with time, but has only increased a small amount by 10,000 years. The MRW decreases with burnup. At very long times, the quantity of material required to be processed would become a significant barrier, but until greater than 10,000 years the quantity only changes slightly from the original value.

Table 40 - OTC Transuranic Mass of Radioactive Waste (MT/BCM)

	Time after Discharge (yr)						
Burnup (GWd/MTU)	0	10	100	1,000	10,000	100,000	1,000,000
33	1.45	1.46	1.51	1.66	2.25	17.76	50.71
42	1.24	1.29	1.39	1.54	2.09	15.29	41.16
46	1.19	1.23	1.35	1.50	2.03	14.37	38.18
50	1.14	1.19	1.31	1.46	1.97	13.66	35.31
55	1.09	1.13	1.24	1.39	1.88	12.65	32.47

Table 41 - OTC Plutonium Mass of Radioactive Waste (kg/BCM)

	Time after Discharge (yr)						
Burnup (GWd/MTU)	0	10	100	1,000	10,000	100,000	1,000,000
33	1.55	1.57	1.65	1.72	2.30	29.85	1,135.69
42	1.26	1.35	1.53	1.61	2.15	27.12	855.39
46	1.22	1.30	1.49	1.57	2.08	25.97	763.16
50	1.18	1.25	1.44	1.52	2.03	24.94	685.88
55	1.12	1.20	1.38	1.46	1.95	23.70	621.63

Transuranic Inventory

The transuranic inventory in SNF for the OTC will continue to increase with time. The growth over the next century will only be slowed by a negligible amount of radioactive decay. Figure 30 shows the transuranic inventory for a constant level of nuclear power (100 GWe). The transuranic inventory will double over the next 40 years. The inventory depends on the average burnup of the SNF and will be slightly lower at higher average SNF burnups. Of course, if the nuclear power level increases the rate of production will increase and the transuranic inventories will increase more rapidly, and if the nuclear power level declines the rate of production will also decline and the transuranic inventories will increase more slowly.

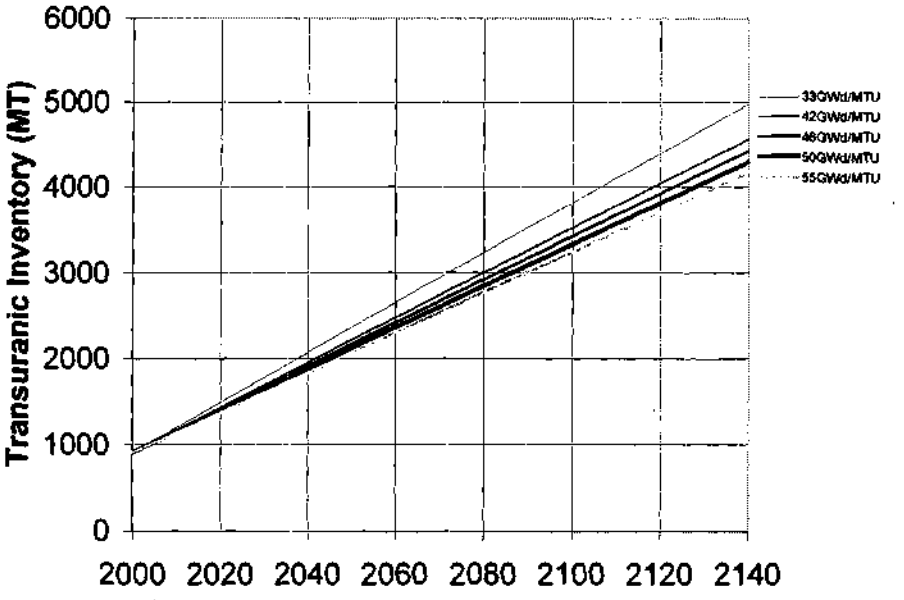

Figure 30 - OTC Transuranic Inventory

CHAPTER V

URANIUM ORE

Scenario Description

Uranium ore as it exists in nature is a toxic substance. The OTC will require a certain amount of uranium ore that will be processed and irradiated, which will result in a number of different waste streams. None of the fuel cycles evaluated will fission more than a very small fraction of the original uranium. Therefore, the long-term properties of the total system waste will eventually return to levels very close to that of the original uranium ore. The evaluation of the uranium ore provides a baseline against which to compare the impact of irradiation on the properties of the waste from the properties of the original uranium ore as mined.

Uranium ore is composed of two parent isotopes of uranium, U-238 and U-235, in equilibrium with their radioactive daughters. The uranium ore is separated into two streams when it is mined. The first is the natural uranium that contains U-238, U-235, and U-234. The second is the mill tails that contain all other elements. The natural uranium feeds the OTC and the tails are disposed. There are no waste streams that would end up in a repository for unirradiated uranium ore.

Reference Quantity

The quantity of uranium ore required is based on the natural uranium needed for the OTC. No losses are considered in the mining and milling process. The natural uranium needed will be determined by the U-235 enrichment of the fuel and deplete uranium tails. The quantities will be evaluated for the reference PWR fuel design used to evaluated the reference OTC. The radioactive decay chain data is given in Table 133 in Appendix K. The naturally occurring ratio is 99.28 moles of U-238 and U-234 to 0.72 moles of U-235. The U-234 is present at its equilibrium concentration with U-238. The decay data was taken from the Table of Nuclides[24] and the Universal Nuclide Chart and Radioactive Decay Applet.[41]

Methodology

At equilibrium the concentration of the radioactive daughters is constant and is achieved when the production rate by radioactive decay from all parents to a given isotope is equal to its decay to all of its daughters. The calculations were performed starting with U-238 and U-235 and all daughter concentrations calculated until a stable isotope is reached. The following equation was used to hand calculate all the daughter concentrations.

Production Rate = Decay Rate

$$\sum_p f_d^p \frac{\ln(2)}{T_{1/2}^p} N_p^\infty = \frac{\ln(2)}{T_{1/2}^d} N_d^\infty \Rightarrow N_d^\infty = T_{1/2}^d \sum_i \frac{f_d^i}{T_{1/2}^p} N_p^\infty$$

Where

N_d^∞ = equilibrium concentration of daughter isotope d;

N_p^∞ = equilibrium concentration of parent isotope p;

f_d^p = branching ratio of parent isotope p to daughter isotope d;

$T_{1/2}^d$ = half-life of daughter isotope d;

$T_{1/2}^p$ = half-life of parent isotope p.

The equilibrium compositions were also estimated using the ORIGEN-S module of the SCALE 4.4[42] code package. The U-238 and U-235 were allowed to decay for 2 million years. This is more than 8 times the half-life of U-234, which is the longest-lived daughter and controls the decay of the U-238 daughters.

Uranium Ore Isotopic Data

Table 42 shows the composition of one mole of natural uranium at equilibrium. The results of ORIGEN-S calculations show good agreement with the calculations using the data given in Table 133. The small differences will result in small time variations in the aggregate values over time.

Table 42 - Composition of Natural Uranium at Equilibrium

Isotope	Equilibrium Calculations	ORIGEN-S	Isotope	Equilibrium Calculations	ORIGEN-S
Hg206	6.5331E-21		Rn222	2.3229E-12	2.38E-12
Pb209	1.1528E-21		Rn219	1.2837E-18	1.28E-18
Tl206	5.7044E-21	2.39E-21	Rn222	2.3229E-12	2.38E-12
Tl207	9.2519E-17	9.23E-17	Fr223	5.9052E-18	5.84E-18
Tl210	1.0969E-19		Ra223	3.2028E-13	3.20E-13
Pb210	5.1703E-09	5.06E-09	Ra226	3.5504E-07	3.63E-07
Pb211	7.0216E-16	7.01E-16	Ac227	2.2274E-10	2.22E-10
Pb214	1.1305E-14	1.16E-14	Th227	5.1709E-13	5.16E-13
Bi210	3.0456E-12	3.11E-12	Th230	1.6727E-05	1.71E-05
Bi211	4.1624E-17	4.15E-17	Th231	2.9783E-14	2.97E-14
Bi214	8.3958E-15	8.58E-15	Th234	1.4661E-11	1.47E-11
Po210	8.4068E-11	8.59E-11	Pa231	3.3514E-07	3.35E-07
Po211	4.6837E-22	4.59E-22	Pa234m	4.9426E-16	4.94E-16
Po214	1.1551E-21	1.18E-21	Pa234	2.2077E-16	2.21E-16
Po215	5.7736E-22	5.76E-22	U234	5.4477E-05	5.44E-05
Po218	1.3079E-15	1.34E-15	U235	7.2000E-03	7.19E-03
At218	2.1095E-21		U238	9.9275E-01	9.92E-01
Rn218	4.9221E-26		U235	7.2000E-03	7.19E-03
Rn219	1.2837E-18	1.28E-18	U238	9.9275E-01	9.92E-01

Waste Management Figures of Merit

The uranium ore will eventually be separated into three separate streams in the OTC. These are the mill tailings, deplete uranium or tails from enrichment process, and the enriched uranium that will be irradiated in the light-water reactors (LWRs). The enriched uranium will contain significantly higher concentration of U-235 and U-234 than natural uranium and these isotopes will be significantly reduced in the depleted uranium. When the waste management parameters are taken in aggregate, the parameters will remain constant and equal to that of the uranium ore because all chains in one stream will be exactly offset in the other two streams. The waste management figures of merit have been calculated based on the reference OTC fuel cycle, which requires an estimated 5.77 MT of natural uranium. The natural uranium is separated into 1 MT of enriched uranium and 4.77 MT of depleted uranium. The compositions of the natural uranium, enriched uranium and depleted uranium streams are given in Table 43. The waste management figures of merit for these quantities of material were evaluated. Each figures of merit is evaluated in two separate figures. The first show the results for the uranium ore, mill tailings, natural uranium, enriched uranium, and depleted uranium. The second shows the results for uranium ore and the

three naturally occurring uranium isotopes with their daughters that will accumulate after starting with only that isotope at time zero.

Except for neutron emission, the uranium daughters dominate the FOMs. For example, the toxicity of the natural uranium increases by two orders of magnitude when the daughters reach equilibrium. The U-234 in the natural uranium is treated separately from the U-234 produced by U-238 decay, which is included in its daughter products. The U-234 concentration in the enriched uranium is at a super-equilibrium concentration and will eventually fall to the equilibrium concentration driven by the lower U-238 concentration. The U-234 concentration in the depleted uranium is at a sub-equilibrium concentration and will eventually rise to the equilibrium concentration driven by the higher U-238 concentration. Since the total U-238 concentration is unchanged by irradiation the net change in total U-234 as a function of time is zero. The decay of the U-234 from the natural uranium explains some of the time behavior of the different uranium streams.

U-238 quickly reaches equilibrium with the pre-U-234 daughters. The approach to U-234 equilibrium is very slow because of its 245,500 year half-life, which controls the buildup of the U-238 daughters. U-235 daughter buildup is controlled by Pa-231, which has a 32,760 year half-life. The mill tailings decay is controlled by the decay of the Th-230, which has a 75,380 year half-life. U-234 considered independent of its U-238 parent will decay significantly during the 1,000,000 year time period considered. The buildup of its daughters will be controlled by the decay of Th-230 has a half-life that is approximately 1/3 that of U-234. Therefore U-234 will only achieve a secular equilibrium with its daughter products.

Table 43 - Composition of Uranium Ore Streams

Stream	Natural Uranium (NU)	Enriched Uranium (EU)	Depleted Uranium (DU)
Mass (MT)	5.77	1.00	4.77
U-234	0.00536%	0.02845%	0.00052%
U-235	0.71097%	3.15002%	0.20000%
U-238	99.28367%	96.82153%	99.79948%

Waste Material Composition Summary

The mass of material and mass of the repository dose contributing isotope U-234 are given in Table 44. The quantity of material is given in Table 44. The only actinide element present in significant quantities is uranium. The majority of the mass is contained in the depleted uranium. Approximately 8% of the U-234 mass is included in the depleted uranium and will be include in the low-level waste stream.

Table 44 - Uranium Ore Mass Summary

Component	Mass (MT)	U-234 (MT)
Uranium Ore	5.77	3.09E-04
Mill Tails	9.72E-05	4.06E-15
Natural Uranium	5.77	3.09E-04
Depleted Uranium	4.77	2.47E-05
Enriched Uranium	1.00	2.85E-04

Waste Material Toxicity Summary

Figure 31 shows the time dependence of the toxicity for the uranium streams and for the original uranium ore. Figure 32 shows the time dependence of the uranium tails, and each of the three uranium isotopes. The uranium streams contain a high level of toxicity. In the near-term, the mill tails that are part of the low-level waste stream dominates the toxicity. At very long times, most of the toxicity will be in the depleted uranium, which will be unaffected by irradiation in light-water reactors and will be disposed in a low-level waste facility.

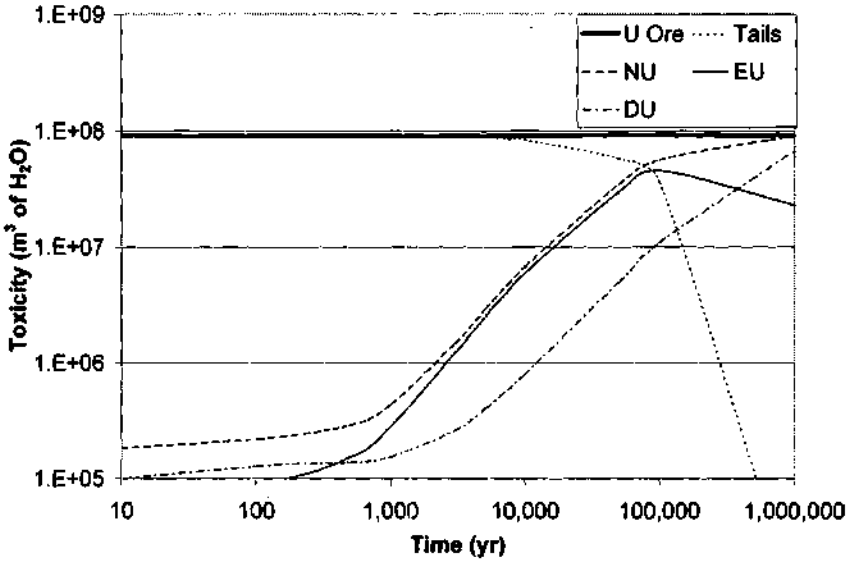

Figure 31 - Toxicity of Uranium Ore Streams Required To Produce One Metric Tonne of Enriched Uranium

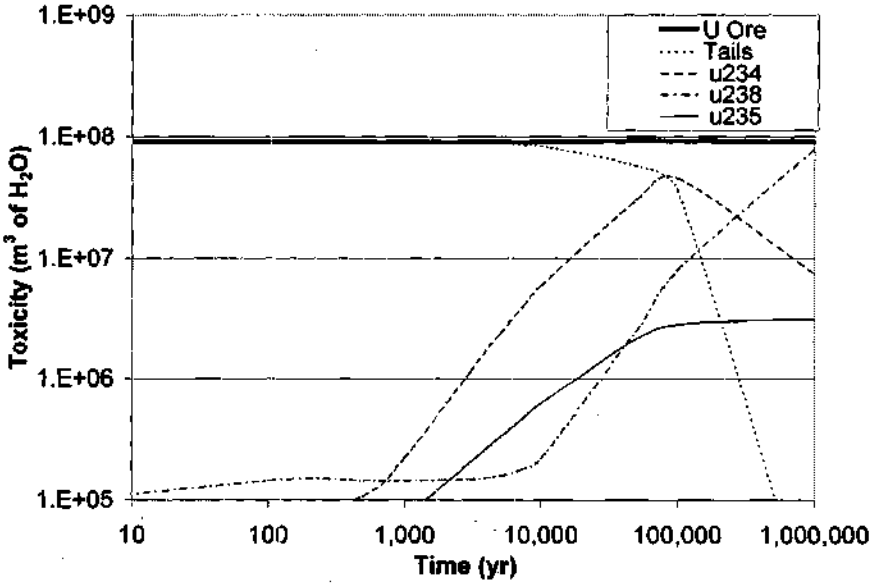

Figure 32 - Toxicity of Uranium Isotopes Required To Produce One Metric Tonne of Enriched Uranium

Waste Material Decay Heat Summary

Figure 33 shows the time dependence of the decay heat for the uranium streams and for the original uranium ore. Figure 34 shows the time dependence of the uranium tails, and each of the three uranium isotopes. The decay heat at all times is very low for the uranium streams.

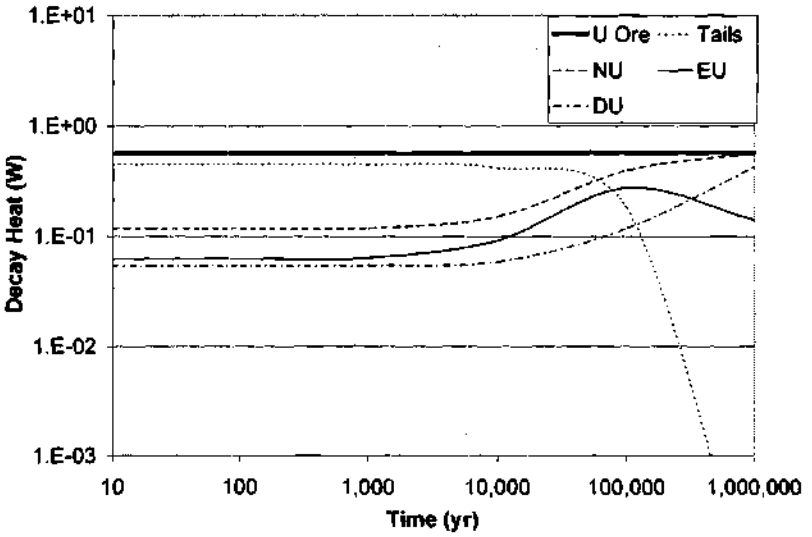

Figure 33 - Decay Heat of Uranium Ore Streams Required To Produce One Metric Tonne of Enriched Uranium

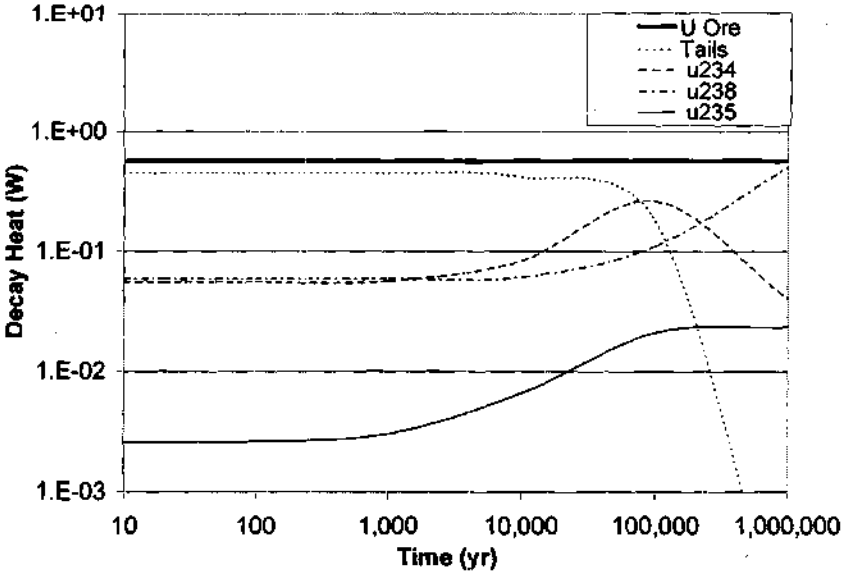

Figure 34 - Decay Heat of Uranium Isotopes Required To Produce One Metric Tonne of Enriched Uranium

Waste Material Integral Decay Energy Summary

Figure 35 shows the time dependence of the integral decay energy for the uranium streams and for the original uranium ore. Figure 36 shows the time dependence of the uranium tails, and each of the three uranium isotopes. The integral decay energy is small for the uranium streams.

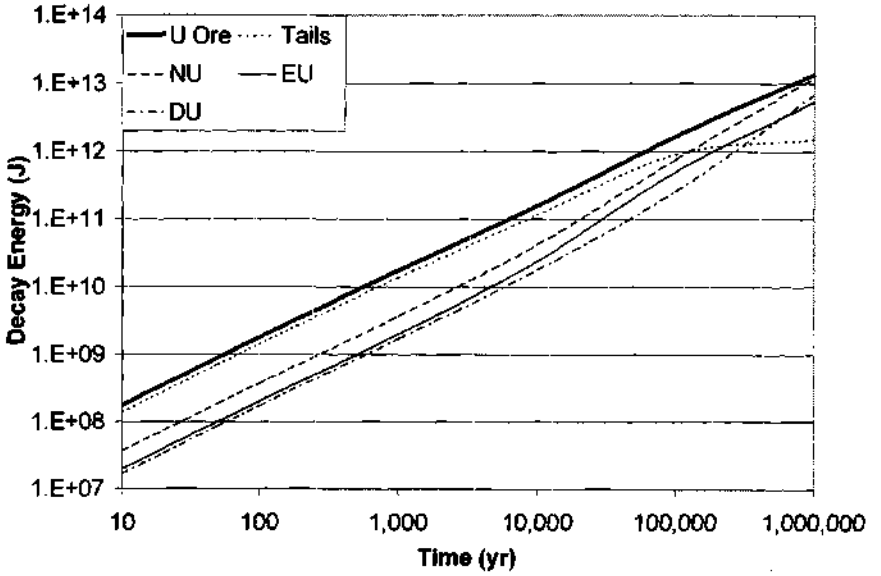

Figure 35 - Integral Decay Energy of Uranium Streams Required To Produce One Metric Tonne of Enriched Uranium

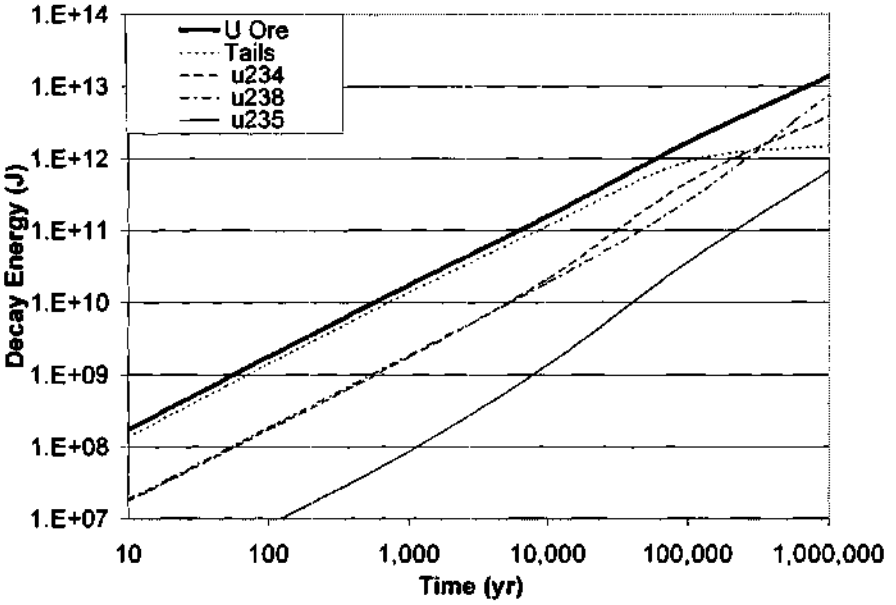

Figure 36 - Integral Decay Energy of Uranium Isotopes Required To Produce One Metric Tonne of Enriched Uranium

Waste Material Radiological Summary

Figure 37 shows the time dependence of the photon dose rate for the uranium streams and for the original uranium ore. Figure 38 shows the time dependence of the uranium tails, and each of the three uranium isotopes. The large mass and high atomic number of uranium will result in a large self-shielding of the photon dose rates. The photon dose rate behaves essentially the same as the toxicity.

Figure 39 shows the time dependence of the SNS dose rate for the uranium streams and for the original uranium ore. Figure 40 shows the time dependence of the uranium tails, and each of the three uranium isotopes. The SNS dose rates are small and are nearly 100% from U-238.

Figure 41 shows the time dependence of the α,n dose rate for the uranium streams and for the original uranium ore. Figure 42 shows the time dependence of the uranium tails, and each of the three uranium isotopes. In the near-term, the mill tails have a much higher activity, which translates into a higher α,n dose rate because all the short-lived isotopes are in this streams. As the uranium daughter products build up in the separated uranium, the α,n dose rates will increase and be eventually dominated by the U-238, which is mostly in the depleted uranium.

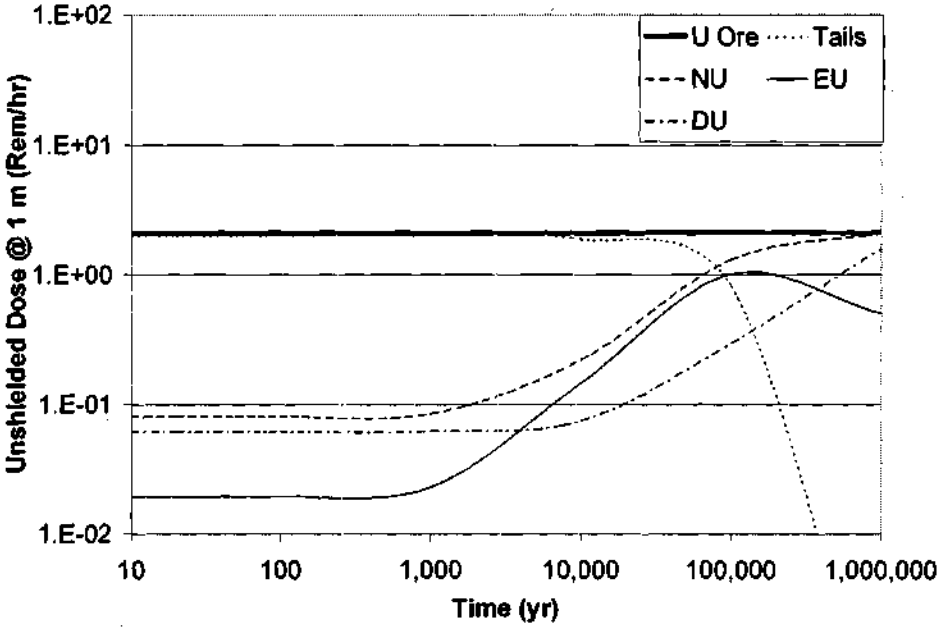

Figure 37 - Unshielded Dose Rate from Photon Emission of Uranium Streams Required To Produce One Metric Tonne of Enriched Uranium

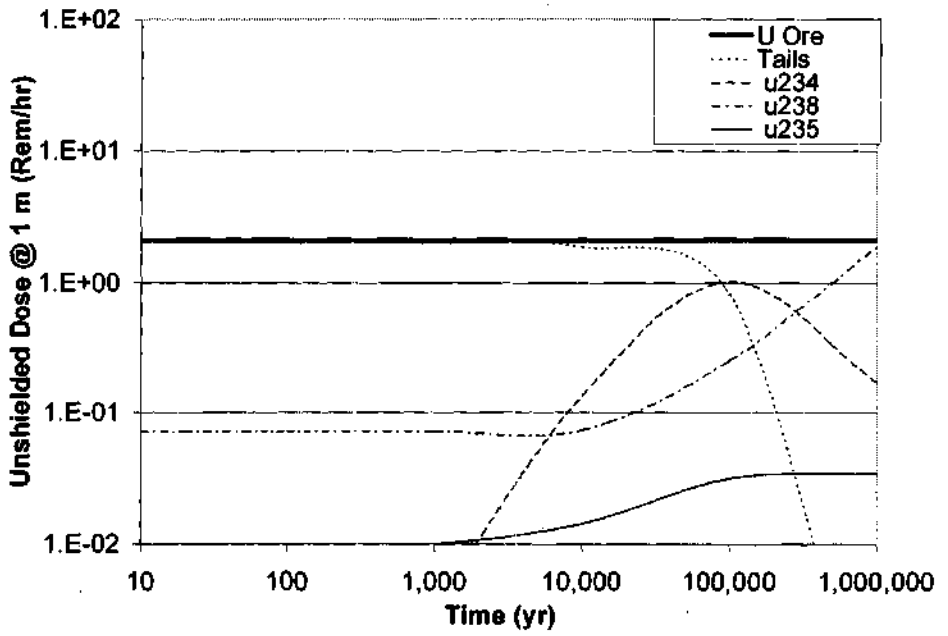

Figure 38 - Unshielded Dose Rate from Photon Emission of Uranium Isotopes Required To Produce One Metric Tonne of Enriched Uranium

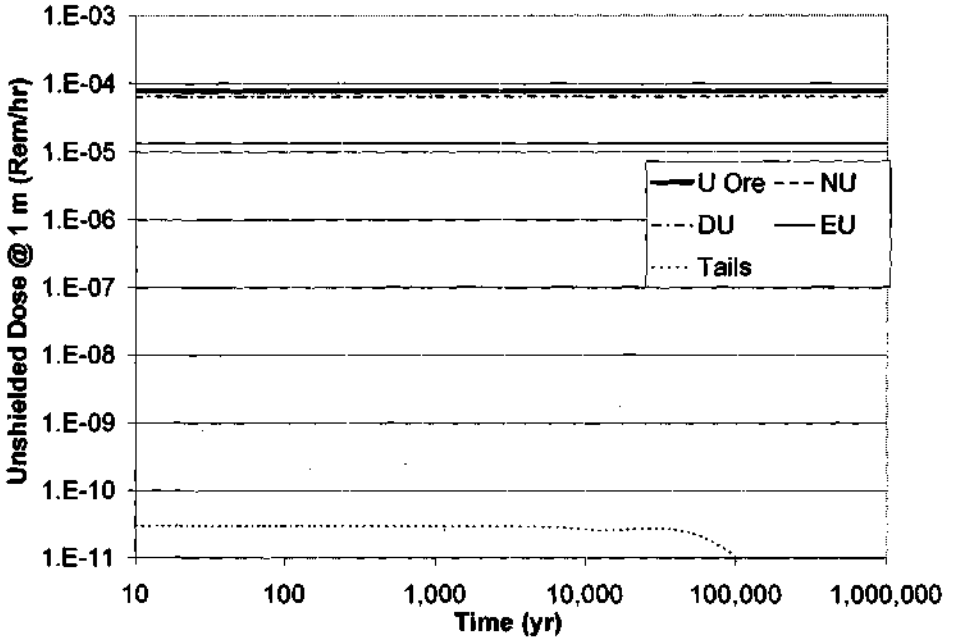

Figure 39 - Unshielded Dose Rate from Spontaneous Neutron Emission of Uranium Streams Required To Produce One Metric Tonne of Enriched Uranium

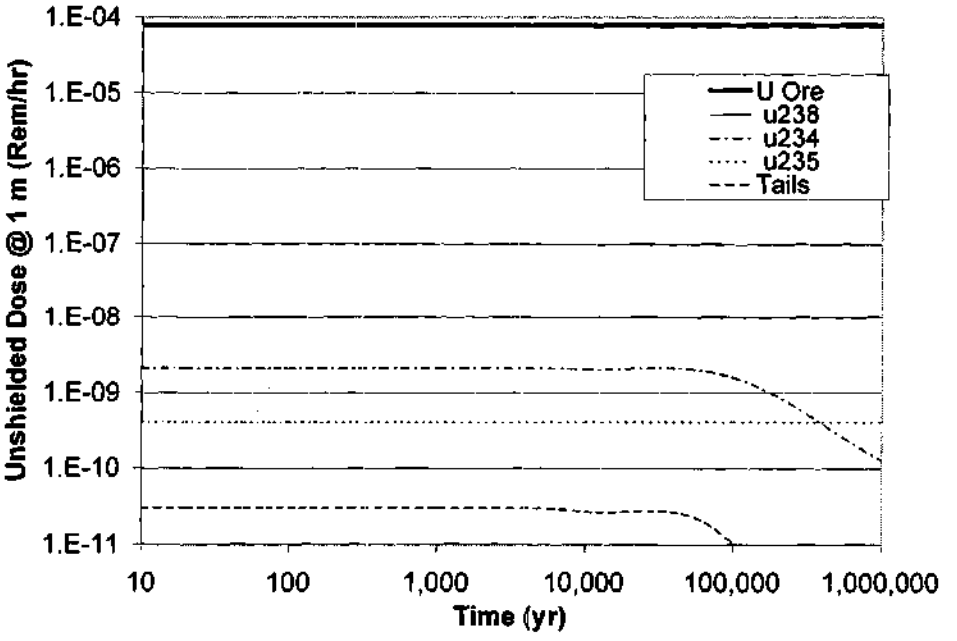

Figure 40 - Unshielded Dose Rate from Spontaneous Neutron Emission of Uranium Isotopes Required To Produce One Metric Tonne of Enriched Uranium

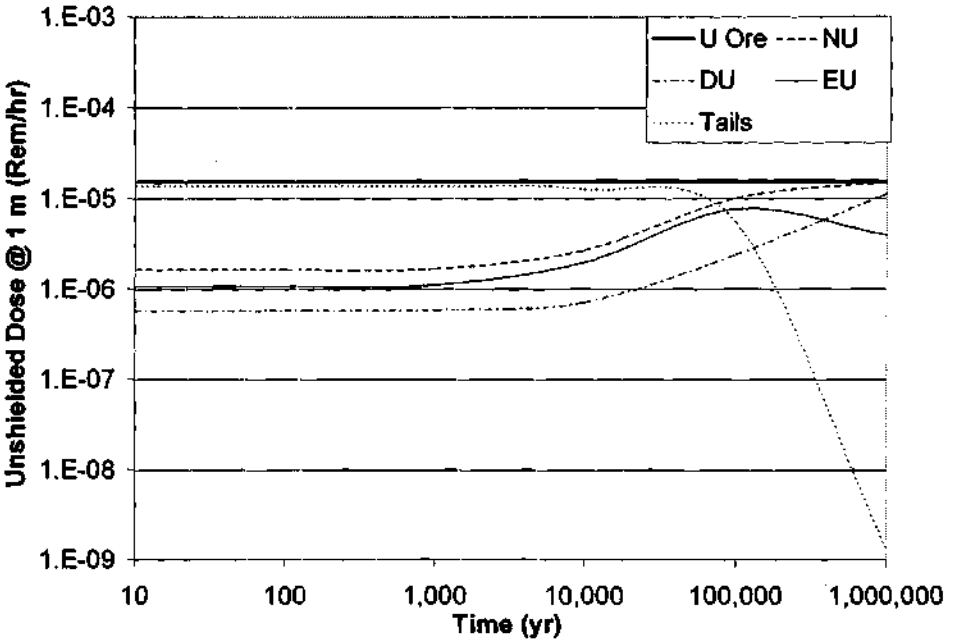

Figure 41 - Unshielded Dose Rate from α,n Neutron Emission of Uranium Streams Required To Produce One Metric Tonne of Enriched Uranium

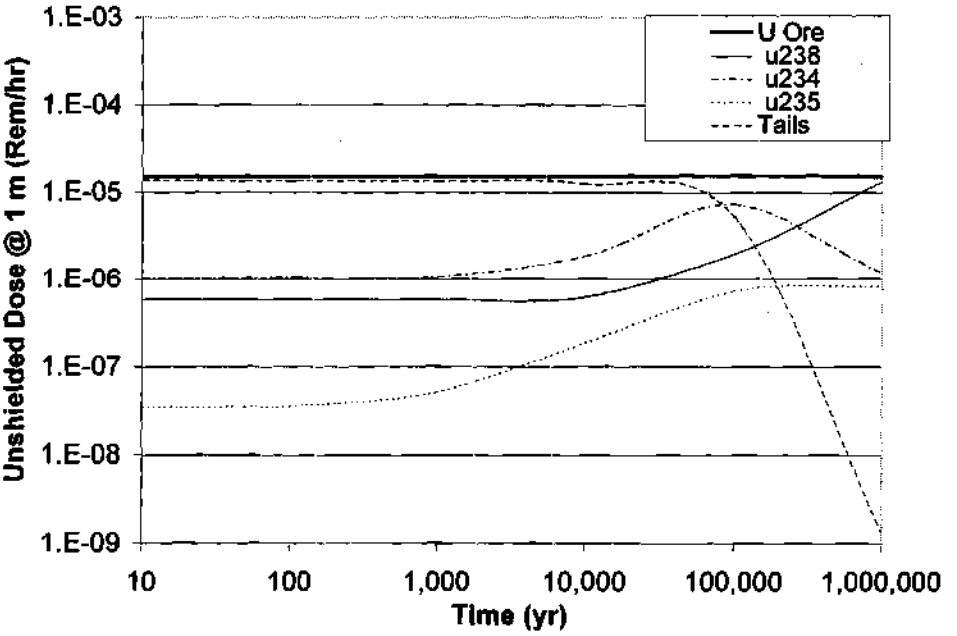

Figure 42 - Unshielded Dose Rate from α,n Neutron Emission of Uranium Isotopes Required To Produce One Metric Tonne of Enriched Uranium

Proliferation Summary

It is not possible to make any of the uranium streams into a bare critical configuration without moderation. Therefore, all proliferation parameters are meaningless.

CHAPTER VI

FUSION-DRIVEN TRANSMUTATION OF WASTE REACTOR DESIGN ANALYSIS

Fusion-Driven Transmutation of Waste Reactor Reference Design

The goal of the design of the Fusion-Driven Transmutation of Waste Reactor (FTWR) sub-critical reactor was to use nuclear and processing technologies that exist or are being developed to the maximum extent possible. The fusion neutron source constrains the geometry of the blanket region and the neutron source strength. The design for the fusion neutron source developed by Stacey et al.[43] was used without modification. The blanket design that is based on the technologies being developed by Argonne National Laboratory (ANL) for the Accelerator-driven Transmutation of Waste (ATW) sub-critical reactor was modified to conform to the geometrical constraints of the FTWR blanket.

The power level of the FTWR was set at 3000 MW thermal for the blanket, primarily produced in the sub-critical reactor. The FTWR was designed to break even on electricity at this power level as described in Stacey.[43]

Sub-Critical Reactor Adaptation

The basic goal of the design of the FTWR was to adapt the design of the sub-critical reactor being developed by ANL for the ATW.[64] The reactor will be a heavy metal cooled, metal fueled, sub-critical design. The FTWR will consist of one large sub-critical reactor driven by a fusion neutron source, while the ATW will consists of multiple, most likely four, smaller sub-critical reactors driven by spallation neutron sources produced by splitting the proton beam from a single large accelerator. The major difference is that the FTWR is driven by a fusion neutron source, which leads to a number of differences in the design. A comparison of the major characteristics of the ATW and FTWR designs is given in Table 45.

The need for the FTWR to be tritium self-sufficient requires the addition of lithium to the system. Lithium can be added in either solid or liquid form. Both types of designs are examined. A solid breeder design can be cooled with the same heavy metal alloy, lead bismuth eutectic (LBE), as the ATW. For the

liquid breeder design, the heavy metal coolant must be alloyed with the lithium. The amount of lithium required results in a significantly different alloy. Therefore, the lithium lead eutectic (Li17Pb83) being developed for fusion applications was chosen.

The second major difference is the geometry of the sub-critical reactor. The ATW sub-critical reactor is a relatively small cylindrical reactor surrounding a small cylindrical spallation neutron source. The FTWR is a very large cylindrical reactor in the located outboard blanket of the toroidal fusion reactor.

The fuel pin diameter was chosen to limit the transuranic loading to less than 45 volume percent and ensuring thermal performance. The height of the sub-critical reactor was chosen to be 75% of the height of the plasma chamber. The solid breeder design will add addition assemblies in which the fuel is replaced with the solid breeder and placed as additional rows of the reactor.

Table 45 - Comparison of FTWR and ATW Designs

Parameter	FTWR	ATW[64]
Sub-critical Reactor		
Inner Radius	4.0 m	0.4 m
Outer Radius	4.4 m	1.3 m
Height	2.3 m	1.1 m
Volume	24.1 m^3	5.2 m^3
Power	3000 MW	840 MW (3360 MW)
Power Density	124 kW/l	160 kW/l
Fuel Loading	27 MTHM	2.3 MTHM (9.2 MTHM)
Maximum Neutron Multiplication	0.95	0.97
Assemblies	217 pin hexagonal	217 pin hexagonal
Fuel	TRU-10Zr/Zr	TRU-10Zr/Zr
Cladding	HT-9	HT-9
Coolant	LBE or Li17Pb83	LBE

Note: A single accelerator may drive multiple sub-critical reactors.
Four units is the current conceptual design.

Neutron Source Design

The neutron source design includes the design of the plasma chamber, first wall, and the magnetic confinement system, which was developed by Stacey et al.[43] This design also sets the overall dimension of the blanket region between the first wall and the toroidal field coils. Table 46 gives the dimension of the neutron source design. The design of the FTWR will use this fusion neutron source design and modify the blanket within the limitations of the design.

Table 47 gives the design information for the toroidal field coils and the central solenoid. Table 48 gives the design information for the first wall. The data is based on Stacey unless otherwise noted.

Table 46 - Fusion Neutron Source Design

Parameter	Dimension (m)
Major radius, R_o	3.1
Minor radius, a	0.89
Elongation, κ	1.7
Flux Core Radius	1.24
Solenoid Thickness	0.18
Toroidal Field Coil Thickness	0.39
First Wall Thickness	0.025
Inner Blanket Thickness	0.4
Inner Gap	0.1

Table 47 - Magnets Materials and Properties

Component	Material	Toroidal Field Coil Volume Fraction	Central Solenoid Volume Fraction	Density (g/cc)
Structure	Steel (HT-9 used for calculations)	3%	20%	9.27
Coolant	Liquid Nitrogen	5%	5%	0.84
Conductor	Oxygen-Free High Conductivity copper	92%	75%	8.92[44]
Insulators	Ceramic	~0	~0	

Table 48 - First Wall Materials and Properties

Component	Material	Volume Fraction	Density (g/cc)
Structure	HT-9	67.3%	9.27
Coolant	LBE or Li17Pb83	12.7%	See page 109
Plasma Facing	Beryllium	20.0%	1.848[44]

Fusion Neutron Source Distribution

The determination of the actual fusion neutron source density is determined by operation parameters and is beyond the scope of this analysis. As a result of the large neutron multiplication of the sub-critical reactor, the neutron flux is not highly sensitive to deviations in the fusion neutron source distribution. The maximums and limits of the fusion neutron source were estimated from plasma density profiles from experiments in DIII-D.[45] The boundaries of the RZ fusion source are shown in Figure 43 and the equations for determining the parameters for the fusion neutron source are given in Table 49. The fusion neutron source was assumed to have a parabolic shape between the maximum value and the edge of the plasma and is estimated by the following equation. The resulting neutron source distribution is shown in Figure 44.

$$F(r,z) = F_{max} * (1-((r-r_{max})/(r_{lim}-r_{max}))^2) * (1-((z-z_{max})/(z_{lim}-z_{max}))^2)$$

Where

for $r \le r_{max}$

$r_{lim} = r_1$ and $z_{lim} = z_2$

for $r_{max} < r \le r_2$ and $z \le z_1$

$r_{lim} = r_3$ and $z_{lim} = z_2$

for $r > r_2$ and $z \le z_1$

$$r_{lim} = r_3 \text{ and } z_{lim} = z_1 + \frac{z_2 - z_1}{r_3 - r_2}(r_3 - r)$$

for $r_{max} < r \le r_2$ and $z > z_1$

$$r_{lim} = r_2 + \frac{r_3 - r_2}{z_2 - z_1}(z - z_1) \text{ and } z_{lim} = z_2$$

for $r > r_2$ and $z > z_1$

$$r_{lim} = r_2 + \frac{r_3 - r_2}{z_2 - z_1}(z - z_1),\ z_{lim} = z_1 + \frac{z_2 - z_1}{r_3 - r_2}(r_3 - r), \text{ and}$$

$F(r,z) = 0$ for $r \ge r_{lim}$ or $z \ge z_{lim}$

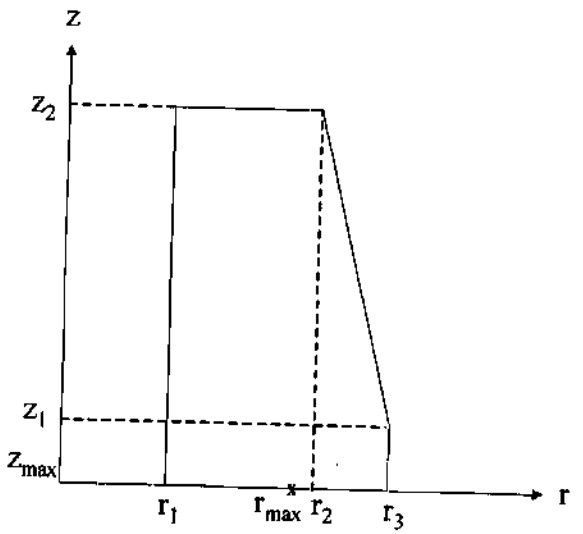

Figure 43 - Fusion Neutron Source Limits

Table 49 - Fusion Neutron Source Distribution Parameters

Parameters	Formula	Value (m)
r_{max}	R+.1a	3.19
z_{max}	0	0
r_1	R-a	2.21
r_2	R+a/3	3.40
r_3	R+a	3.99
z_1	aκ/3	0.51
z_2	aκ	1.52

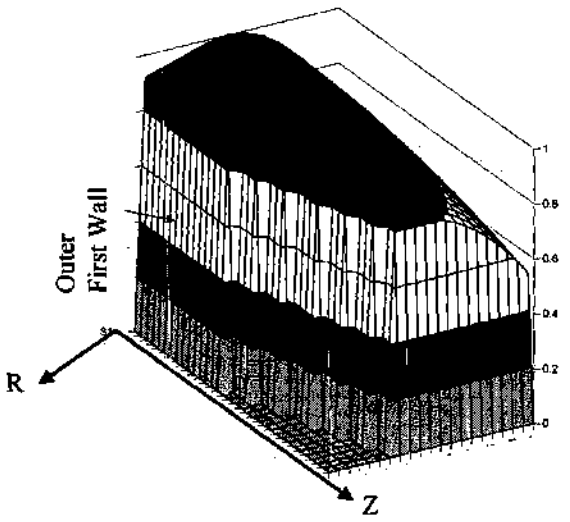

Figure 44 - Fusion Neutron Source Distribution

Blanket Design

The blanket, the region between the plasma chamber and the toroidal field coils, consist of six different systems. These are the first wall, the sub-critical reactor, the tritium breeding/neutron reflector region, the magnet shield, the vacuum vessel, and the control rod region. The first wall was designed as part of the neutron source design. The schematic representation of the FTWR is shown in Figure 45 with a close-up of the FTWR blanket shown in Figure 46. More detailed figures are included in the following sections. For design purposes, the blanket is divided into three regions. These are designated as the inner blanket, upper blanket, and the outer blanket. The lower blanket, or divertor, was neglected in this analysis.

The lower blanket was assumed to be symmetric about the mid-plane for modeling purposes, which allowed only the upper half of the FTWR to be modeled.

The inner blanket is located on the inboard side of the plasma chamber. This region is 40 cm including 10 cm of gap. The primary function of the inner blanket is to reduce the irradiation damage to the toroidal field coils to allowable levels.

The upper blanket is located above the plasma chamber. The thickness of this region is not constrained by the neutron source design. The primary function of the upper blanket is to reduce the irradiation damage to the toroidal field coils to allowable levels. No gap was included in the upper blanket.

The outer blanket is located on the outboard side of the plasma chamber. The thickness of this region is not constrained by the neutron source design. This region includes the sub-critical reactor and shielding for the toroidal field coils. No gap was included in the outer blanket.

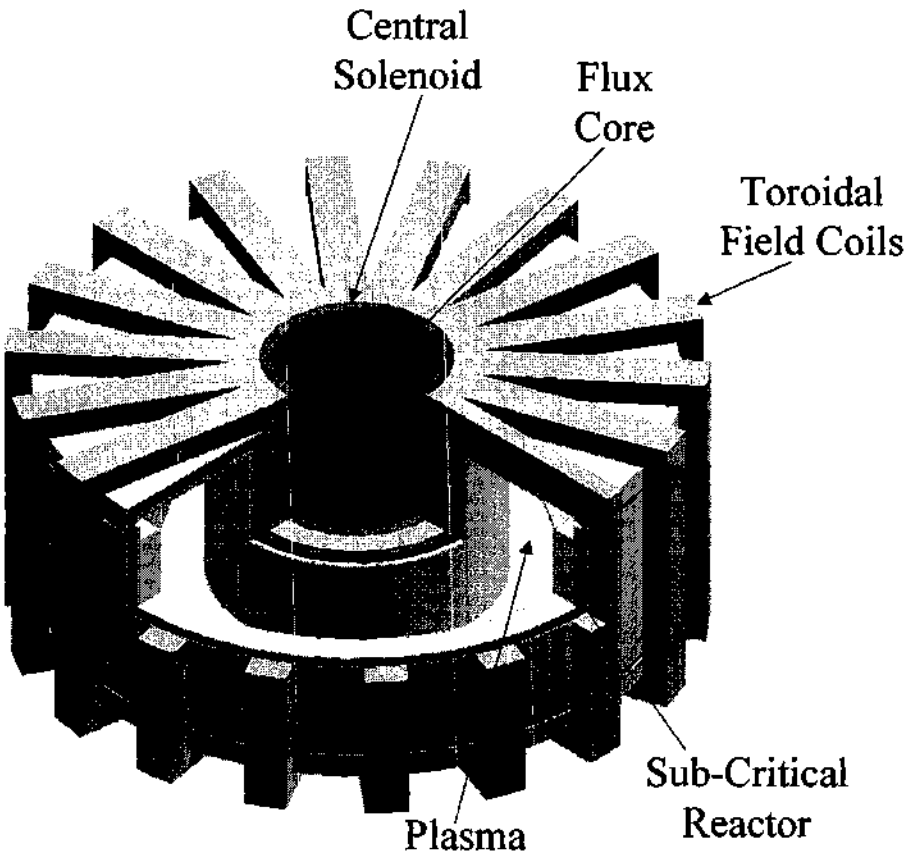

Figure 45 - FTWR Schematic

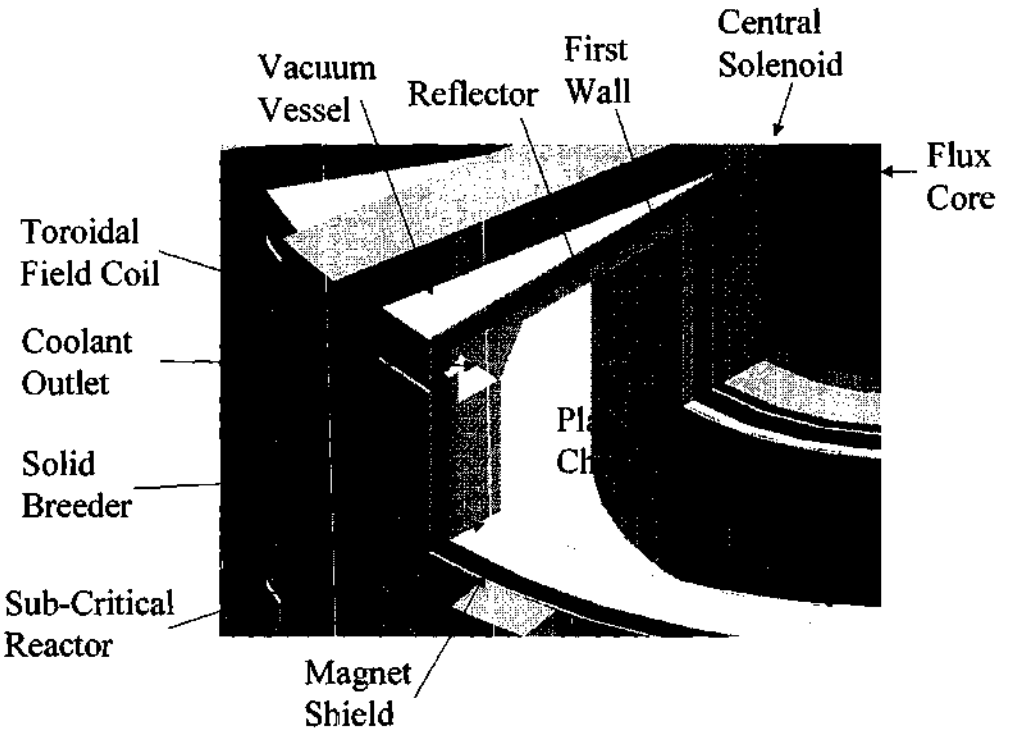

Figure 46 - FTWR Schematic Close-up

First Wall Design

The first wall for the fusion source was taken from Stacey et al.[43] This first wall design will be used. The first wall is 2.5 cm thick, which consists of a plasma facing layer of beryllium that is 0.5 cm thick and a 2.0 cm structural layer. The structural layer is HT-9 cooled by 0.9 cm diameter coolant channels spaced at a distance of 2.0 cm. This design incorporated temperature and stress limits in the analysis.

Vacuum Vessel

The vacuum vessel is located just inside the toroidal field coils. The vacuum vessel is a steel pressure vessel that maintains the vacuum required in the plasma chamber. The vacuum vessel thickness is 3 cm of HT-9, which is consistent with Hoffman.[46] There is a gap of 10 cm between the vacuum vessel and the toroidal field coils to account for assembly and manufacturing tolerances as per Stacey et al.[43]

Magnet Shielding

Just inside the vacuum vessel is the shielding for the magnets. This region is designed to ensure that the magnets will be sufficiently shielded to ensure that they will last for the life of the facility. The basic design of the shield was taken from the ATW design.[64] The composition of the shield is given in Table 50. The coolant for the shield is LBE for the solid breeder design and the high-enriched Li17Pb83 for the liquid breeder design.

Table 50 - Magnet Shield Materials and Properties

Component	Material	Volume Fraction	Density (g/cc)
Structure	HT-9	24.0%	7.76
Coolant	LBE or Li17Pb83	18.4%	See page 109
Neutron Shield	B_4C w/ B enriched to 20% B-10	44.8%	2.51

Tritium Breeding / Neutron Reflector

Inside the magnet shield and outside the first wall and sub-critical reactor is the tritium breeding/neutron reflector region. The function of this region is to maximize the utilization of the neutrons by either capturing the neutrons and producing tritium or reflecting them into the sub-critical reactor. Two different designs were developed using two different coolants, Li17Pb83 and LBE. This results in two significantly different breeder/reflector designs. The Li17Pb83 cooled design is a liquid tritium breeder design and the LBE cooled design is a solid tritium breeder design

For the liquid breeder design, this region will consist of the Li17Pb83 coolant and steel. The lithium will be enriched to the level necessary to ensure tritium self-sufficiency. The steel will at a minimum will provide the structural support needed to contain the flow of the liquid breeder. The atom density of steel is far higher than that of Li17Pb83 and the microscopic cross sections are not significantly different in the energy range of interest. By increase the steel content, the amount of shield needed may be significantly reduced with a relatively small impact allowing a larger reflector region and possible lower lithium enrichments. For the liquid breeder design, the ^6Li concentration in the reactor region increases the coolant temperature reactivity coefficient because of the large neutron absorption cross section. To control

this and still allow for tritium self-sufficiency, the liquid breeder design has two separate coolant systems. A low ^{6}Li enrichment for the fuel region and a high ^{6}Li enrichment to ensure tritium self-sufficiency that flows through the rest of the FTWR. This design is referred to as the high enrichment / low enrichment (HELE) design. The solid breeder (SB) design does not have this problem because of the low absorption of lead and bismuth.

The tritium production takes place everywhere lithium is present and is primarily produced by reaction in ^{6}Li. The Li17Pb83 cools the entire blanket system including the sub-critical reactor, neutron reflector, magnet shield, and first wall resulting in tritium production throughout. Despite the flux levels being the highest in the sub-critical reactor, the very low ^{6}Li enrichment and coolant fraction result in only a small fraction of the tritium being produced in the sub-critical reactor coolant. Most tritium production takes place just outside the reactor where neutrons leak from the sub-critical reactor into the adjacent region cooled by Li17Pb83 that with highly enriched lithium. Significant quantities of tritium are also produced in the first wall coolant and inboard and above the first wall.

For the solid breeder design, the tritium breeding/neutron reflector region will consist of two distinct regions. One for tritium breeding and one for neutron reflection. The solid tritium breeder elements will need to be removed after each cycle and must be easily manufactured. Using the same pin dimensions as the fuel pins seemed a logical starting point. Solid breeder assemblies of the same height and pin size were placed just outside the sub-critical reactor creating an extra ring of assemblies in the neutron reflector region between the reactor and magnet shield. This design is easily accessible after each cycle. To produce sufficient tritium, the pitch to diameter ratio of the breeder assemblies was reduced to 1.5 to increase the lithium density and still allow more than adequate coolant because of the much lower power density outside the core region. To reduce the lithium enrichment, lithium rods could replace fuel pins in the fuel assemblies similar to the placement of burnable poison in PWR assemblies. This would also provide the ability to flatten power peaking and, if absorption rates in the ^{6}Li were sufficiently high, to act as burnable poisons.

The remainder of this region in the solid breeder design will be LBE coolant and steel that will be designed to limit the radiation damage to the magnets, while reflecting some of the neutrons into the solid breeder regions to improve the neutron economy. The solid breeder will be Li_2O at 85% theoretical density,

the density of natural lithium oxide is 2.1 g/cc[46] and the atom density of enriched lithium oxide is assumed to be the same.

The density of Li17Pb83 with natural lithium was calculated using the following formula from Zinkle.[47] The density of Li17Pb83 with isotopically modified lithium, enriched or depleted in ^{6}Li, was assumed to have the same atom density as natural lithium lead at the same operating temperature. The other properties used in the thermal calculations were also taken from Zinkle.[47]

$$\rho(T) = 10450*(1-0.000161*T)\ [kg/m^3]$$
T in K.

The temperature dependence data for LBE was taken from Martynov.[48] The density is calculated using the linear least squares fit of the data given by the following equation. The other properties used in the thermal calculations were also calculated in the same manner for the data in Martynov.[48]

$$\rho(T) = 11060-1.216*T\ [kg/m^3]$$
T in K.

The composition of the various tritium breeding/neutron reflector regions is given in Tables 51, 52, and 53.

Table 51 - Inner Reflector Region

Component	Material	Volume Fraction
Structure	HT-9	70%
Coolant	LBE or Li17Pb83	30%

Table 52 - Other Reflector Regions

Component	Material	Volume Fraction
Structure	HT-9	15%
Coolant	LBE or Li17Pb83	85%

Table 53 - Solid Breeder Region

Component	Material	Volume Fraction
Structure	HT-9	13.82%
Coolant	LBE	59.69%
Solid Breeder	Li_2O	26.48% @ 100% density

Sub-critical Reactor

The sub-critical reactor region consists of the region containing the fuel assemblies, located just outside the outboard first wall and the reactor coolant inlet and outlet regions. For the solid breeder, the coolant is the same in all regions and the reactor coolant inlet and outlet regions will have the same composition as the neutron reflector regions. For the liquid breeder design, the strong absorption of Li-6 in the coolant results in a significant increase in the reactivity as the coolant flowing through the core is heated and the density of the coolant and therefore Li-6 is reduced. To mitigate this effect, the liquid breeder will have a low lithium enrichment coolant flowing through the fuel region and a high enrichment coolant flowing through all other regions. The low lithium enrichment coolant will flow from outside the toroidal field coil in the bottom and out of the top of the reactor region and then back outside the toroidal field coils to the heat exchangers. This region is sized so that the flow area of the coolant normal to the flow path is greater than or equal to the flow area of the coolant in the reactor region as it flows past the fuel pins.

The fuel assemblies are triangular pitch hexagonal fuel assemblies. To produce a relatively uniform thickness fuel region as shown in Figure 48, some of assemblies will be "half" assemblies. The assemblies are 217 pin hexagonal fuel assemblies, seven of which are structural pins. The half assemblies will include 117 pins, 5 of which are structural pins. The cross section of a fuel assembly is shown in Figure 47. The fuel assemblies are centered on the mid-plane of the plasma chamber and are 75% of the height of the plasma chamber. The structure of the first wall will be segmented to form a polygon circumscribing the plasma chamber. The segments will be sized for two columns of assemblies per segment. A coolant channel will surround the fuel in each segment with voids between each of the segment. The coolant channel shell is 0.25 cm thick with reinforcing between channels as needed. The arrangement of the sub-critical reactor region including the assemblies, coolant channels, and first wall is shown in Figure 48.

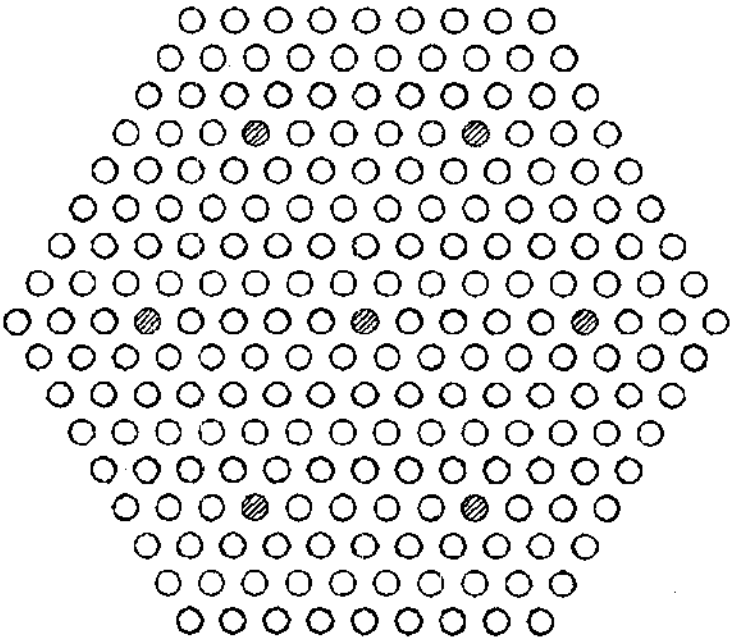

Figure 47 - Fuel Assembly Cross Section

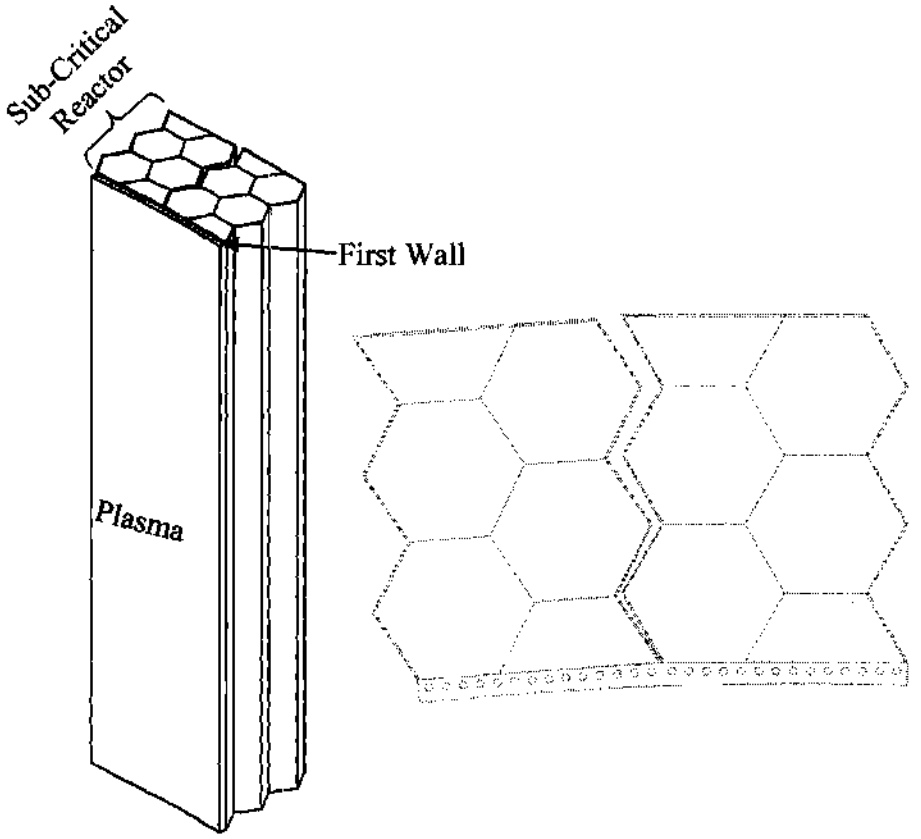

Figure 48 - Sub-Critical Reactor Schematic

Control Rods

The control elements will be located in voided regions between the fuel channels. They will be controlled from above and located in the gaps between the toroidal field coils as shown in Figure 49. The number of locations available will be subject to the details of the design of the FTWR. This will include the design of the toroidal field coils, the orientation of the sub-critical reactor, the ability to refuel the reactor, and other considerations. Figure 49 suggest that control rod locations will be available in roughly 60% of the fuel channel gaps. The control rods will be steel clad, B_4C elements of different sizes design to fit in the gaps between the fuel channels. The B-10 concentration was assumed to be 20%, which is the same as in the B_4C in the magnet shielding. For the design, 50% of the locations were assumed to be available and the cladding was assumed to be 10% of the control rod volume. Therefore, 50% of the void in Table 54 will be filled with control rods, the remaining 50% of the void will still be void after the control rods are fully inserted.

Under normal operating conditions, the control rods will be removed completely from the reactor. The change in reactivity associated with fuel burnup will be compensated by the fusion power. There are many ways this system could be operated. This scheme results in the lowest parasitic loss of neutrons because none are lost to the control elements, which minimizes the heavy metal loading and fusion power combination. This operational scheme was also chosen for its simplicity and is a reasonable starting point. Other scenarios may ultimately yield better performance.

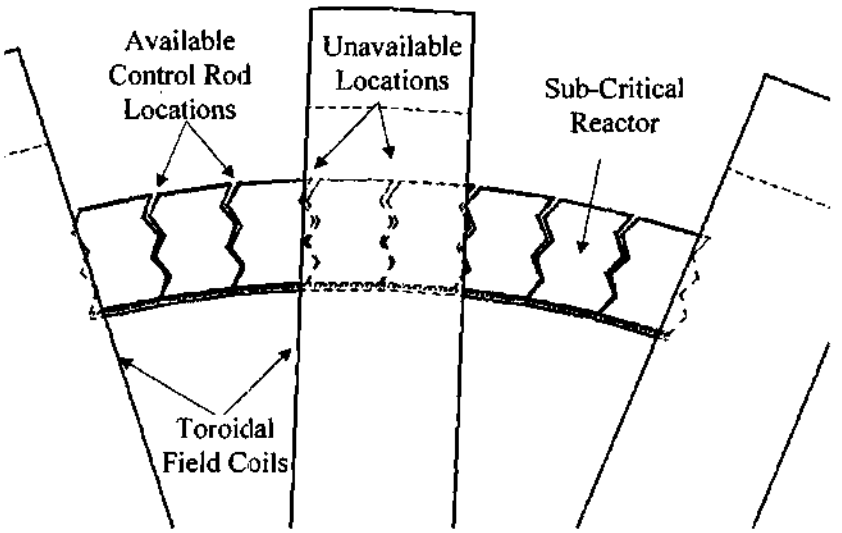

Figure 49 - Control Rod Locations

Nuclear Analysis

The nuclear analysis was performed with the same codes and similar methodology used in the ANL ATW design studies.[64,62] The fuel cycle analysis was performed with the REBUS[49] fuel cycle code. Within this code, the neutronics calculations were 2-D discrete ordinates transport calculations using the DANT[50] code with material-dependent multi-group cross section libraries based on the ENDF/B-V.2 nuclear data library processed using the MCC-2[51] and SDX[52] codes for a 34 group energy structure. The REBUS input specifies the compositions, geometries, and all other necessary fuel cycle parameters. The neutronics calculations were performed using an R-Z geometry model, with R in the direction of the major radius. The details of the input and operation of the codes are described in the following sub-sections.

TWODANT RZ Model

The neutronics model used to analyze the FTWR was a 2-D RZ model symmetric about the mid-plane of the plasma chamber. For modeling purposes the fuel region was divided into five radial and five axial regions. The axial regions allow for axial variation in the fuel composition resulting from the non-uniform flux distribution. The material volume fractions of the 5 radial fuel regions is given in Table 54. The fuel volume in each of the radial regions are the same, but constitutes a smaller fraction as the distance from the plasma increases because of the geometry shown in Figure 47.

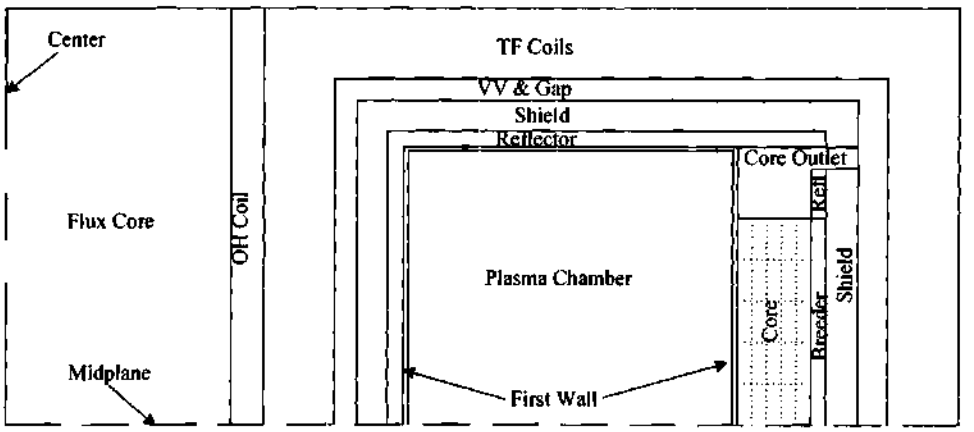

Figure 50 - RZ Model

Table 54 - Fuel Region Volume Fraction

Radial Region	Fuel (100% density)	Structure & Clad	Coolant	Void
Inner	19.46%	11.56%	67.65%	1.33%
2	19.09%	11.33%	66.33%	3.25%
3	18.72%	11.12%	65.07%	5.09%
4	18.37%	10.91%	63.85%	6.87%
Outer	18.03%	10.71%	62.68%	8.58%

Cross Section Generation

The MCC-2 computer code, along with SDX, was used to create the region dependent cross section library. The energy structure was based on a standard 33-group structure with an extra energy group added in the highest energy group to better represent the 14 MeV DT fusion source neutrons. An MCC-2 calculation is run for each of the regions of the FTWR to generate regionally dependent cross sections. The SDX code then merges the cross sections into a single library for use in the transport calculations.

The composition of the fuel region was initially estimated from previous calculations. The calculated beginning of cycle compositions from the REBUS equilibrium cycle calculations was then used to regenerate the cross section libraries which were then used in the subsequent depletion and safety calculations. The effect on the beginning of cycle reaction rates was typically small and this new library would be used to rerun the equilibrium calculations if the differences appeared significant.

Lumped Fission Products

In a fast neutron spectrum, there are not any fission products with giant cross sections as there are in a thermal spectrum. In order to greatly speed the calculations without a significant decrease in accuracy, the fission products are treated by a number of lumped "isotopes." The lumped isotopes are divided into two groups. These are the rare earth (RE) fission products and all other fission products (FP). Since the chemistry of the rare earth elements is similar to that of the actinides, it is assumed that a small fraction of them will not be removed and be recycled with the transuranics. The other fission products are assumed to be separated completely.

The fission product groups are based on their source. The source is either the fissioning isotope for fission products produced in the FTWR or rare earth elements that were not removed from the LWR feed.

The compositions of the fission product lumps produced by fast fission in the FTWR were estimated using SCALE 4.4.[42] Individual isotopes are irradiated to fairly high burnup using the fast reactor cross sections, so that the concentrations approaches the steady state level. The compositions of the fission product lumps are given in Table 130 in Appendix J. This is consistent with the method used to estimate the fission product lumps in the ANL ATW calculations.[63]

Lumps were created for five isotopes with fission product yield data in SCALE 4.4. These are U-235, U-238, Pu-239, Pu-240, and Pu-241. The fission of the actinides is assumed to result in 1 rare earth lump and 1 fission product lump of the lumps for the isotope of the nearest mass. The fission product lumps are used in the burnup chains as given in Table 126 in Appendix J.

MCNP Model

The geometry of the FTWR is more complex than a typical fast reactor. In order to verify the results of the simplified two-dimensional RZ model used for developing the FTWR designs, a detailed three-dimensional MCNP model was created. The neutron multiplication and tritium production rates are the most important parameters for the design of the FTWR. These parameters are calculated using the detailed MCNP model and compared to the simplified REBUS/TWODANT RZ model. The neutron multiplication was performed using an actinide isotopic vector consistent with the equilibrium fuel cycle loading without any fission products. The enrichment of the fuel was adjusted to achieve a neutron multiplication factor in the FTWR operating range. The REBUS/TWODANT RZ model is shown in Figure 50. The same dimensions are used in the MCNP model, with the first wall, fuel region, and solid breeders modeled discretely. Figure 51 shows the first wall, fuel region, and solid breeder MCNP model for the SB design. Figure 52 shows a more detailed view of the first wall and fuel regions. The solid breeder region is replaced with a homogenous coolant / structure region in the HELE design.

The actual boundary conditions on the left and right sides of the wedge are periodic. This model used reflective boundary conditions because the periodic boundary conditions only apply to rectangular geometries and not to radial geometries. There are relatively small differences between these two boundary conditions for this model. Neutrons crossing either boundary will see nearly the same arrangement within a few centimeters of the boundary.

The three dimensional model shows a number of features that are not present in a typical reactor design. The first wall is composed of 90 flat segments that form a 90-sided polygon that circumscribe the plasma. The fuel assemblies are placed so that they fit together as tightly as possible and the first wall is bent at the joints. This results in gaps at each joint that are relatively narrow at the first wall and generally increase as you move outward. The fuel assemblies for each of the 90 segments are contained inside a steel shell that will act as a coolant channel, provide structural support, and maintain voided locations between assemblies for insertion of control rods. Since the coolant is heavy metal, it is desirable to have the control rods in voided locations. This allows for easier insertion and avoids the potential that they would float out of the core in the event if they were to break off.

Since the assembly "flats" are placed parallel to the first wall segment and not arranged as ever growing rings as in a typical reactor, the assemblies cannot be arranged to fit perfectly together. This results in some open pin locations.

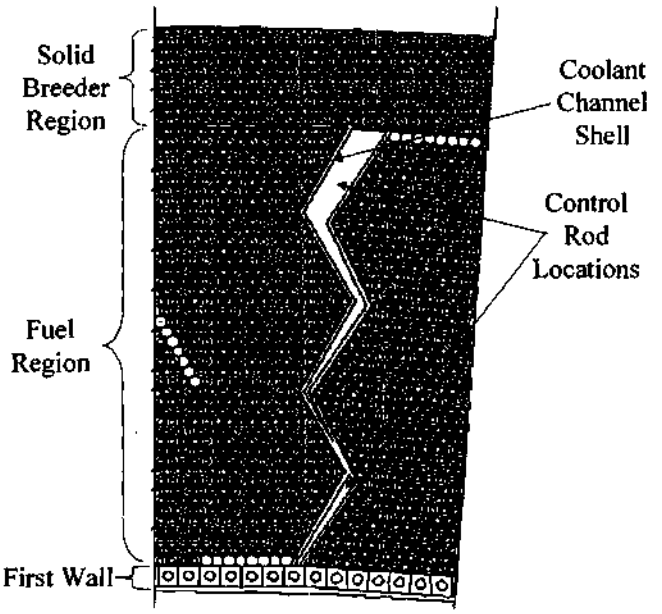

Figure 51 - Outer Blanket MCNP Model for the SB design

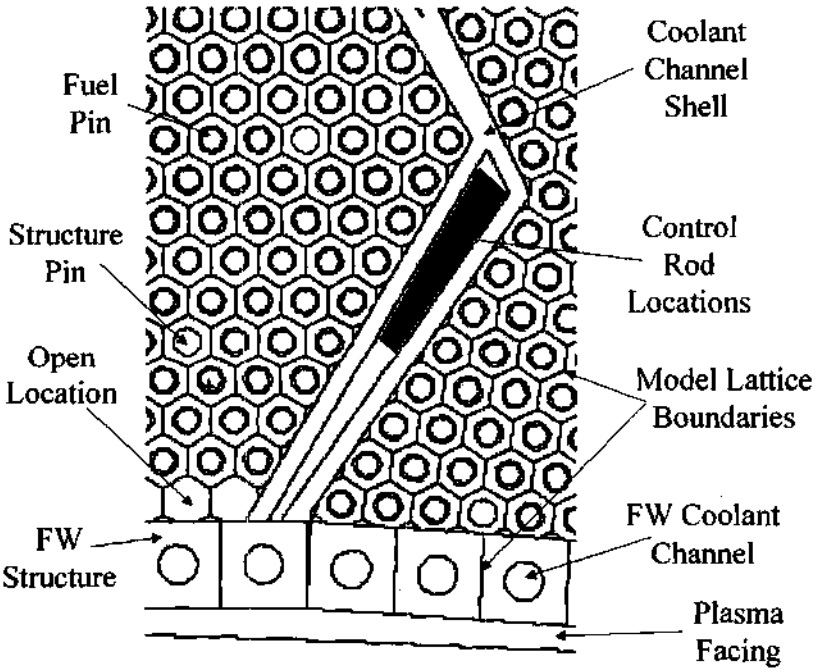

Figure 52 - Detail of Outer Blanket MCNP Model

TWODANT - MCNP Comparison

Four different cases were run to estimate the bulk neutron parameters for the two different designs. These cases had the fuel enrichment (ratio of actinides to zirconium) adjusted to give a range of conditions over which the FTWR will operate. Four parameters were estimated. These are the neutron multiplication factor (k_{sub}), the neutron multiplication (M), the tritium breeding ratio (TBR), and the number of fissions per fusion (F/F). The results are given in Table 55. For the sub-critical calculations, the results are not normalized as they are in an eigenvalue calculation. The total neutron production rate is M times the source, where $M= 1 / (1-k_{sub})$ and therefore small differences in k_{sub} result in significant differences in the number of neutrons available. For example, the case 1 HELE results show a difference in k_{sub} of 0.4%, which corresponds to a 6% difference in the neutron population. The significance of this difference is that there are 6% less neutrons available to produce tritium and this explains most of the 10% difference in the TBR. The statistical error for the neutron multiplication or neutron multiplication factor is not calculated in MCNP. For the TBR, the statistical error varies from approximately 3% for case 1 to approximately 5% for case 4.

The SB design has slightly larger differences in k_{sub}, which translate into large differences in TBR. The solid breeder also seems to be more sensitive to differences in k_{sub}, which is nearly all fission multiplication. All neutrons that reach the solid breeder must pass through the core before reaching the solid breeder. Differences in k_{sub}, will significantly impact the number of neutrons leaking out the external surface of the core and into the solid breeder region. The HELE design produces a large fraction of its tritium in the same region as the solid breeder, but also produces large amounts of tritium on the inboard side and above the plasma, which is going to be driven more by fusion neutrons than the region outside the core.

The axial power distribution was calculated for case 3. The results are given in Table 56. The core was divided into 5 axial regions of equal height. The bottom region begins at the midplane or center of the FTWR. The statistical errors for the MCNP calculations were generally less than 2%. The results show good agreement. MCNP predicts slightly higher power at the midplane and at the ends, but these differences are relatively small.

The flux volume ($\int_{V,E} \phi(E,\vec{r})\delta E\,\delta\vec{r}$) for the major regions of the FTWR was calculated for the case 3 HELE design. The results are given in Table 57. The maximum difference in the neutron multiplication was -6%. The largest error was -13% in the magnets. This is not surprising because this region is farthest from the plasma, and a slightly larger mesh size is used in the TWODANT calculation because this region has little effect on the neutron balance in the rest of the FTWR. The baffle shows a 9% higher value in MCNP. This is consistent with the higher fission rate at the end of the fuel predicted by MCNP. The first wall shows a 10% difference, which is slightly more than the difference in the neutron multiplication. The core region shows a 4% difference and this is where the bulk of the neutrons are produced and is a little smaller than difference in the neutron multiplication.

Overall, the results verify that the TWODANT results are sufficiently accurate. TWODANT consistently under predicts the TBR relative to MCNP, indicating that the relatively high ^{6}Li enrichment required for tritium self-sufficiency is quite conservative. There is good agreement between TWODANT and MCNP on the sub-critical neutron multiplication factor, which indicates the fuel cycle analysis will result in good estimates of the cycle length, and other design parameters, and significant design changes will not result from more detailed design analysis.

Table 55 - Results of MCNP and TWODANT Comparisons

		HELE			SB		
		MCNP	TWODANT	Difference	MCNP	TWODANT	Difference
Case 1	Neutron Multiplication Factor	0.940	0.936	0%	0.938	0.927	-1%
	Neutron Multiplication	16.626	15.708	-6%	16.120	13.708	-16%
	Tritium Breeding Ratio	2.059	1.868	-10%	1.771	1.361	-26%
	Fissions per Fusion	4.788	4.708	-2%	4.647	4.052	-14%
Case 2	Neutron Multiplication Factor	0.933	0.929	0%	0.911	0.899	-1%
	Neutron Multiplication	14.826	14.140	-5%	11.179	9.872	-12%
	Tritium Breeding Ratio	1.829	1.696	-8%	1.176	0.957	-21%
	Fissions per Fusion	4.195	4.191	0%	3.008	2.777	-8%
Case 3	Neutron Multiplication Factor	0.906	0.901	-1%	0.884	0.870	-2%
	Neutron Multiplication	10.649	10.065	-6%	8.584	7.670	-11%
	Tritium Breeding Ratio	1.338	1.247	-7%	0.870	0.726	-18%
	Fissions per Fusion	2.813	2.837	1%	2.152	2.047	-5%
Case 4	Neutron Multiplication Factor	0.872	0.871	0%	0.851	0.839	-1%
	Neutron Multiplication	7.836	7.774	-1%	6.725	6.202	-8%
	Tritium Breeding Ratio	1.001	0.994	-1%	0.640	0.573	-11%
	Fissions per Fusion	1.882	2.074	10%	1.541	1.565	2%

Table 56 - Axial Power Distribution Comparison of MCNP and TWODANT for Case 3

Design	HELE		SB	
Model	MCNP	TWODANT	MCNP	TWODANT
Bottom (nearest midplane)	23.8%	23.0%	23.2%	22.4%
2	22.9%	23.1%	22.6%	22.8%
3	21.0%	21.3%	20.8%	21.1%
4	18.2%	18.6%	18.3%	18.9%
Top	14.2%	14.0%	15.1%	14.8%

Table 57 - Flux Distribution Comparison TWODANT results with MCNP for HELE Case 3

Region	Difference
Core	-4%
First Wall	-10%
Reflector	-1%
Shield	3%
Baffle	9%
Vacuum Vessel	-5%
Magnets	-13%

Design Requirements

This section includes the requirements that were used in determining the size and compositions of the FTWR. Each subsection addresses the design requirements for a specific area of the design, the methodology used to evaluate the requirements, and a comparison of the results with the requirement.

Tritium Self-Sufficient

The FTWR must be tritium self-sufficient. An external source of tritium will only provide the initial inventory of tritium required to start the first cycle and run the FTWR until tritium produced by the FTWR is recovered. The FTWR will be self-sufficient for the remainder of its operations.

Tritium Inventory

Because the fusion rate and tritium production will be time dependent, a simple tritium breeding ratio calculation is insufficient. In order to satisfy the requirement for tritium self-sufficiency, the tritium inventory at the beginning of each subsequent cycle needs to be at least as large as the tritium inventory at the first cycle. This is expressed by the following equation.

$$T_{BOC}^{1} \leq T_{BOC}^{n} = T_{EOC}^{n-1} e^{-\lambda_T t_{down}}$$

There are two distinctly different methods of producing tritium. These are solid breeders and liquid breeders. The solid breeders are left in the reactor for an entire cycle and then removed and processed to recover the tritium for the next cycle. The liquid breeders will be continuously processed to recover the tritium, which will be available for use with only a short delay associated with the processing time. For the solid breeder, the entire inventory of tritium that will be consumed over the cycle must be available at the beginning of the cycle. For the liquid breeder, the beginning of cycle tritium inventory only needs to be large enough to operate the fusion reactor until the tritium produced in the liquid coolant can be processed an made available. The beginning of cycle inventory needs to be sufficient to allow for operation during the time (t_{BOC}), which the tritium produced in the blanket, will be unavailable. For the liquid breeder, 45 days supply was assumed. For solid breeders, the tritium will be unavailable over the entire cycle. The end of cycle tritium inventory needs to be sufficient to allow for decay during outages between cycles with a maximum down time (t_{down}) of greater than equal to the assumed limit of 90 days. Any extended outages beyond the maximum down time would need to be compensate for with external sources of tritium.

The consumption of tritium consists of fusion, losses in the tritium processing systems, and radioactive decay. The tritium inventory available at the beginning (T_{BOC}^{0}) must be sufficient so that it is greater than zero at t_{BOC}. The equation for beginning of cycle tritium inventory as a function of time is defined by the following equations. The equations are solved starting with the inventory at t_{BOC} which is

set to zero, and then at the preceding time interval boundary, and each preceding time interval boundary until the initial inventory is calculated.

$$T_{BOC}^{0} = \int_{0}^{t_{BOC}} \frac{dT_{BOC}(t)}{dt} dt = \int_{0}^{t_{BOC}} (-\lambda T_{BOC}(t) - (1+\alpha_T^F)\dot{F}(t)) dt$$

Where

$$T_{BOC}^{i-1}(t) = T_{BOC}^{i} e^{-\lambda(t_{i-1}-t_i)} - \frac{A_i}{\lambda}(1-e^{-\lambda(t_{i-1}-t_i)}) - \frac{A_i'}{\lambda^2}(\lambda(t_{i-1}-t_i)-1+e^{-\lambda(t_{i-1}-t_i)});$$

$$A_i = (1+\alpha_T^F)\dot{F}_{i-1};\ A_i' = (1+\alpha_T^F)\frac{(\dot{F}_i - \dot{F}_{i-1})}{t_i - t_{i-1}};\ \text{and}\ T_{BOC}^{t_{BOC}} = 0$$

For i, where $t_{i-1} < t_{BOC} \le t_i$

$$T_{BOC}^{i-1}(t_{BOC}) = -\frac{A_i}{\lambda}(1-e^{-\lambda(t_{i-1}-t_{BOC})}) - \frac{A_i'}{\lambda^2}(\lambda(t_{i-1}-t_{BOC})-1+e^{-\lambda(t_{i-1}-t_{BOC})})$$

For $i = 1$

$$T_{BOC}^{0} = T_{BOC}^{1} e^{\lambda t_1} - \frac{A_1}{\lambda}(1-e^{\lambda t_1}) - \frac{A_1'}{\lambda^2}(-\lambda t_1 - 1 + e^{\lambda t_1})$$

For the solid breeder, the tritium will be treated as two separate inventories. The first is the external inventory that will be available for use in the fusion reactor. The second is the internal inventory of tritium that is created in the solid breeder that will be used in the next cycle. For the liquid breeder systems the processing will be relatively quickly and the internal and external tritium inventory are treated as a single inventory. The tritium production rate is reduced by the term α_T^I. This term takes into account all non-radioactive losses that occur from the time of creation of the tritium until the tritium is available for use and the uncertainties in the reactions rates and geometrical modeling errors. The tritium fusion rate is increased by the term α_T^F. This term takes into account all non-radioactive losses that occur in the external fuel cycle as the tritium is cycled through the fusion reactor. The methodology, model, and values used to estimate these parameters were based on the model developed by Abdou[53]. Table 58 shows the values of the parameters defined by Abdou[53] used to estimate the non-radioactive loss of tritium. Table 59 includes assumptions used in this analysis and the resulting tritium loss parameters. Errors in this

parameters result in an error in the predicted lithium-6 enrichment required for tritium self-sufficiency. The lithium-6 enrichment is not approaching a limiting value so this will not have a significant impact on the design.

Figure 53 shows the tritium system model. The following equations represent the loss terms used for the tritium system. The reduction in tritium production rate (α_T^I) is 5.1% and the average number of tritium atoms lost per fusion (α_T^F) is 2.3%, which results in a total tritium reduction factor (α_T) of 7.2%. The cycle average tritium breeding ratio (TBR) neglecting radioactive decay was calculated for comparison purposes and is 1.08 for both the solid and liquid breeder systems is required.

$$\alpha_T^I = 1-(1-\varepsilon_1)(1-\varepsilon_2)(1-\varepsilon_4)(1-E)$$

$$\alpha_T^F = \frac{1-(1-\beta-f_1-f_{fw})(1-\varepsilon_6)(1-\varepsilon_4)}{\beta}-1$$

$$\alpha_T = 1-\frac{1-\alpha_T^I}{1+\alpha_T^F}$$

$$TBR = \frac{1}{1-\alpha_T} = \frac{1+\alpha_T^F}{1-\alpha_T^I}$$

Table 58 - Model Parameters for Tritium Cycle from Abdou[53]

Parameter	Liquid Breeder	Solid Breeder	Definition
ε_1	0	0	Loss in Blanket
ε_2	0.001	0.001	Loss in Breeder Processing
ε_4	0	0	Loss in Fuel Cleanup and Isotope Separation
β	0.05	0.05	Fractional burnup in plasma
f_l	0.0001	0.0001	Leakage from plasma to limiter
ffw	0.0001	0.0001	Leakage from plasma to first wall
ε_6	0.001	0.001	Loss in plasma exhaust processing

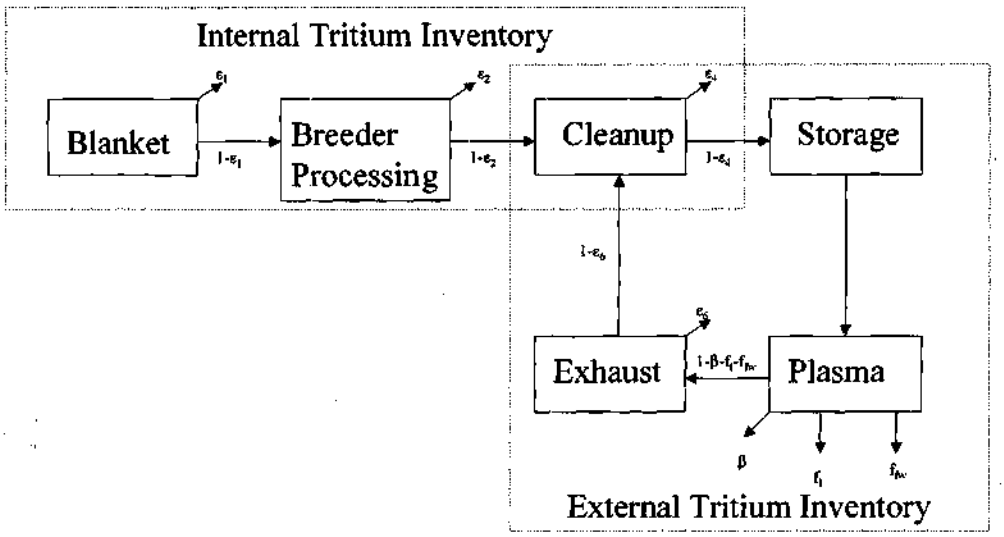

Figure 53 - Tritium Cycle

Table 59 - Parameter Used for Tritium Inventory Calculations

E	0.05	0.05	Assumed error in tritium production calculations
α_T^I	5.095%	5.095%	Total reduction factor for tritium production
α_T^F	2.2996%	2.2996%	Tritium atoms lost per fusion reaction
α_T	7.2284%	7.2284%	Total reduction factor for tritium production
TBR	1.077916	1.077916	Required cycle average tritium breeding ratio neglecting radioactive decay
t_{down}	90	90	Down time between cycles (days)
t_{BOC}	30	Cycle	Time to make produced tritium available (days)

Liquid Breeder Tritium Inventory

The time dependent tritium is a function of the fusion rate ($\dot{F}$), tritium production rate ($\dot{T}$), fractional loss of tritium (α_T), and the radioactive decay of the tritium. The differential tritium inventory is given by the following equation

$$\frac{dT(t)}{dt} = -\lambda T(t) - (1+\alpha_T^F)\dot{F}(t) + (1-\alpha_T^I)\dot{T}(t)$$

The fusion rate and tritium production rate are calculated at the beginning and end of each time step in the fuel depletion calculations. This equation was evaluated assuming a linear change in the fusion rate and tritium production rate over each time step of the depletion calculations. This results in the time dependent tritium inventory over a time step is the following.

$$T_i(t) = \frac{A_i + A_i'(t_i - t_{i-1})}{\lambda} - \frac{A_i'}{\lambda^2} + (T_{i-1} - \frac{A_i}{\lambda} + \frac{A_i'}{\lambda^2})e^{-\lambda(t_i - t_{i-1})}$$

Where

$$A_i = (1-\alpha_T^I)\dot{T}_{i-1} - (1+\alpha_T^F)\dot{F}_{i-1} \text{ and } A_i' = \frac{(1-\alpha_T^I)(\dot{T}_i - \dot{T}_{i-1}) - (1-\alpha_T^F)(\dot{F}_i - \dot{F}_{i-1})}{t_i - t_{i-1}}$$

The initial inventory, maximum shutdown between cycles, and fraction losses of tritium are needed to evaluate this requirement. The design is not very sensitive the initial inventory or shutdown time. A higher initial inventory will require slightly higher tritium production to offset the higher radioactive decay rate and longer shutdown time will require slightly higher end of cycle tritium inventories to allow for the additional decay.

Solid Breeder Tritium Inventory

The solid breeders will be removed at the end of each cycle and the tritium that is produced over the cycle will be unavailable until the beginning of the next cycle. There will be two separate inventories of

tritium. These are the internal inventory of tritium that accumulates in the solid breeder and the external inventory that will be consumed over the course of the cycle.

The time dependent external tritium is a function of the fusion rate ($\dot{F}$), fractional loss of tritium (α_T^F), and the radioactive decay of the tritium. The differential external tritium inventory is given by the following equation

$$\frac{dT_E(t)}{dt} = -\lambda T_E(t) - (1+\alpha_T^F)\dot{F}(t)$$

The fusion rate is calculated at the beginning and end of each time step in the fuel depletion calculations. This equation was evaluated assuming a linear change in the fusion rate over each time step of the depletion calculations. This results in the time dependent external tritium inventory over a time step is the following.

$$T_E^i(t) = T_E^{i-1}e^{-\lambda(t-t_{i-1})} - \frac{A_i}{\lambda}(1-e^{-\lambda(t-t_{i-1})}) - \frac{A_i'}{\lambda^2}(\lambda(t-t_{i-1}) - 1 + e^{-\lambda(t-t_{i-1})})$$

Where

$$A_i = (1+\alpha_T^F).\dot{F}_{i-1} \text{ and } A_i' = (1+\alpha_T^F)\frac{(\dot{F}_i - \dot{F}_{i-1})}{t_i - t_{i-1}}$$

The time dependent internal tritium inventory is a function of the production rate ($\dot{T}$), and the radioactive decay of the tritium. The differential tritium inventory is given by the following equation

$$\frac{dT_I(t)}{dt} = -\lambda T_I(t) + \dot{T}_I(t)$$

The tritium production rate is calculated at the beginning and end of each time step in the fuel depletion calculations. This equation was evaluated assuming a linear change in the tritium production rate over each time step of the depletion calculations. This results in the time dependent internal tritium inventory over a time step is the following.

$$T_I^i(t) = T_I^{i-1} e^{-\lambda(t-t_{i-1})} + \frac{(1-\alpha_T^I)\dot{T}_{i-1}}{\lambda}(1-e^{-\lambda(t-t_{i-1})}) +$$
$$\frac{(1-\alpha_T^I)(\dot{T}_i - \dot{T}_{i-1})}{\lambda^2(t_i - t_{i-1})}(\lambda(t-t_{i-1}) - 1 + e^{-\lambda(t-t_{i-1})})$$

Equilibrium Cycle Tritium

The fusion rate, tritium production rate, and tritium inventory are variable over the cycle. The depletion of lithium-6 in the SB design is also modeled in the REBUS code. Table 60 summarizes the tritium results. Both designs require a high lithium-6 enrichment to achieve tritium self-sufficiency. This is true because there is very little lithium-6 in the core region for the HELE design and none for the SB design. Addition of moderators in the breeder regions may help reduce the lithium-6 enrichment, but this shows that the FTWR design can be tritium self-sufficient. The peak tritium inventory of the SB design is more than 10 times that of the HELE design.

Table 61 shows the instantaneous TBR over the cycle. Figures 54 and 55 show the tritium inventory for the HELE and SB designs, respectively. Both designs are initially producing a lot more tritium than they are consuming at the BOC when the neutron multiplication is high and the fusion power is

low. As the neutron multiplication falls and the fusion power increases, the tritium consumption increase by a factor of approximately 2.5, while the TBR falls. The excess tritium produced early in the cycle is quickly consumed and the tritium inventory is falling very rapidly at the EOC. This is shown in Figures 54 and 55 by the rapid rise and even more rapid decline in the tritium inventory. Small differences in the lithium-6 enrichment make small changes in the TBR, which translates into dramatic differences in the EOC tritium inventory. The larger instantaneous tritium breeding ratios in the SB design results from the much larger decay rate that results from the larger inventory of tritium. The decay rate in the SB design is approximately 14% of the tritium production rate in the SB design.

Table 60 - Equilibrium Cycle Tritium Data

	HELE	SB
BOC Inventory (kg)	0.18	11.02
EOC Inventory (kg)	0.59	12.09
Peak Inventory (kg)	1.09	12.40
Maximum Down Time (days)	7,738	598
Fuel Coolant Lithium Enrichment	0.5%	N/A
Breeder Lithium Enrichment	75.0%	90.0%

Table 61 - Equilibrium Cycle Instantaneous Tritium Breeding Ratios

	HELE		SB	
Time Step	Time (days)	TBR	Time (days)	TBR
BOC	0	1.69	0	1.93
1	56	1.52	54	1.76
2	113	1.39	108	1.62
3	169	1.28	162	1.50
4	226	1.19	216	1.40
5	282	1.12	270	1.31
6	338	1.05	324	1.23
7	395	1.00	378	1.16
8	451	0.95	432	1.10
9	508	0.91	486	1.04
EOC	564	0.87	540	0.99

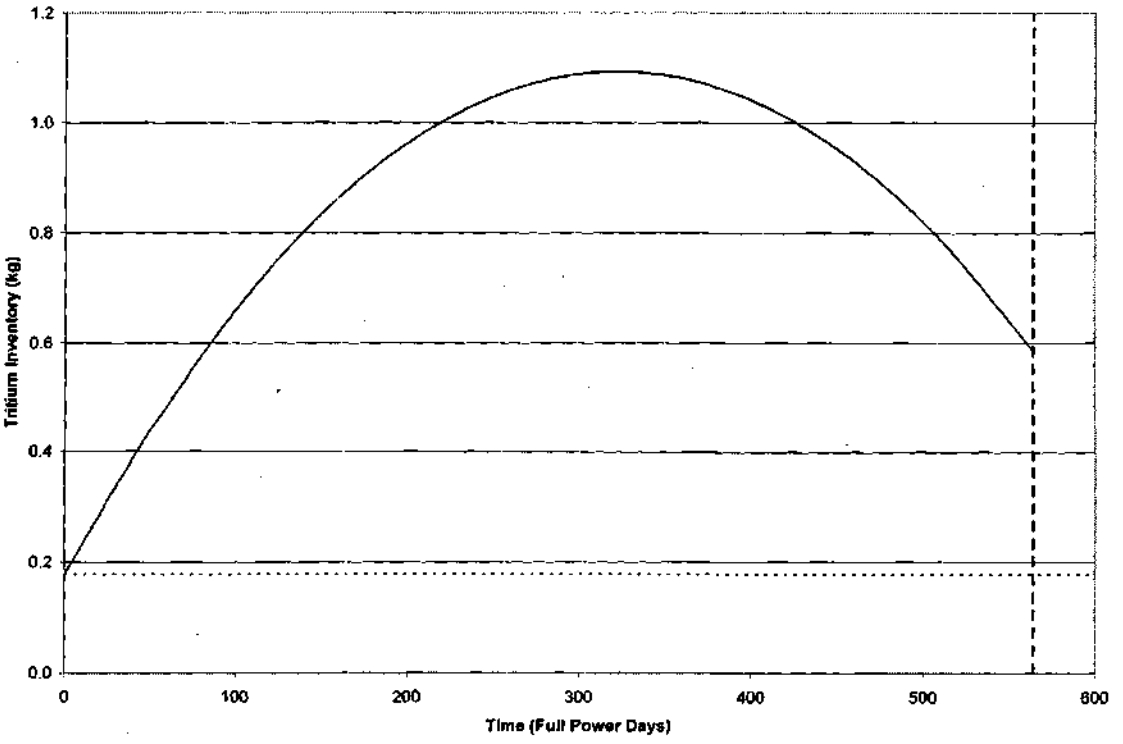

Figure 54 - HELE Design Tritium Inventory

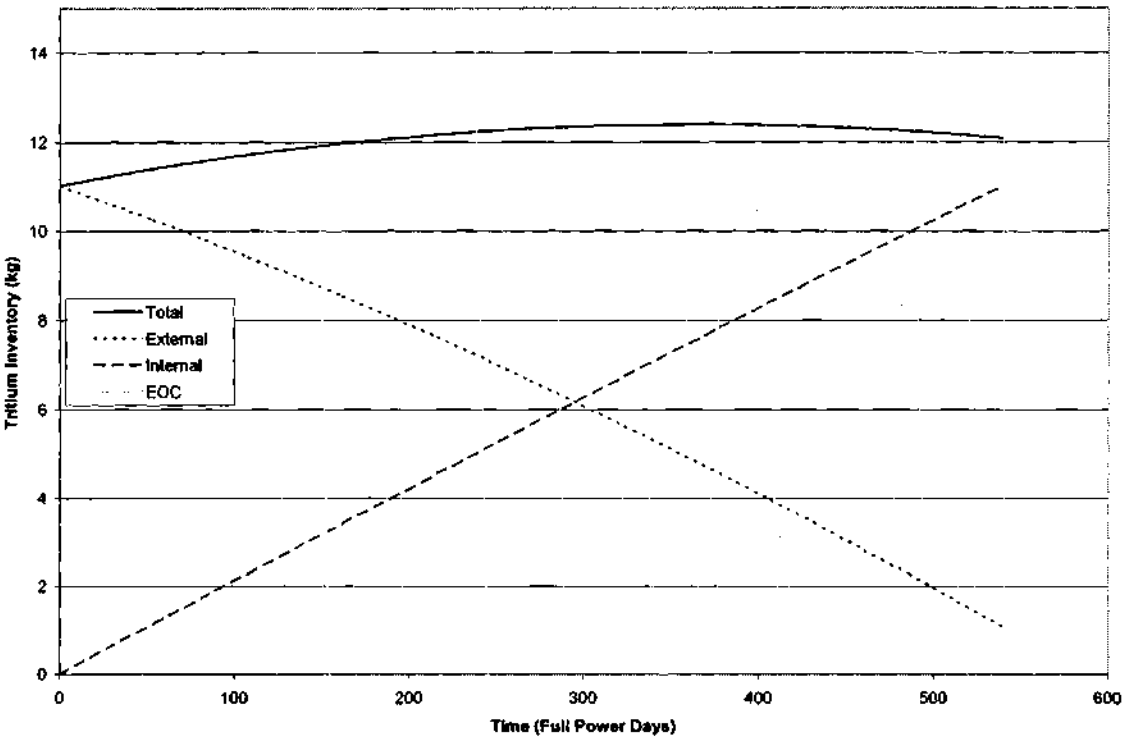

Figure 55 - SB Design Tritium Inventory

Fuel Composition Limits

The fuel is a transuranic zirconium alloy (TRU-10Zr) dispersed in a zirconium matrix. The relative amounts of actinides and zirconium in the fuel region are adjusted to achieve the desired neutron multiplication at the beginning of each cycle. The smear density of the fuel is 85% and the transuranic loading is limited to 45% by volume.[54] The FTWR design is operating at this limit and the length of the fuel cycle is limited by this constraint.

Coolant Limits

The coolant temperature in the hottest channel and the coolant velocity will be constrained to limit the corrosion and erosion rates to an acceptable level. The inlet temperature will be limited to avoid freezing of the coolant. The coolant velocity will be calculated to limit the temperature rise in the core. From the ANL ATW study,[64] the coolant velocity needs to be below 2.0 m/s. The ATW Roadmap[18] gives a temperature rise of 170 K for the Russian LBE cooled reactors while the MIT LBE reactor design study[55]

used temperature rise of 250 K in the hot channel. The values from the MIT study were assumed to be achievable. The properties and values used for the coolant and the associated references are given in Table 62.

Table 62 - Heavy Metal Coolant Properties

Property	Li17Pb83		LBE	
	Value	Reference	Value	Reference
Melting Temperature (C)	233.85 (507 K)	47	125	55
Boiling Temperature (C)			1670	55
Inlet Temperature (C)	275	16	290	55
Maximum Outlet Temperature (C)	480	17	540	55
Maximum ΔT (C)	205		250	
Heat Capacity (J/kg-K)	195-0.009116T	47	146.2	55

By setting the temperature rise in the hottest channel at its limit, the necessary flow rate can be determined. The mass flow rate is determined from the following equation.

$$P = \dot{m} C_p (T_{out}^{\max} - T_{in}) / f_{rad}$$

Where P is the power in the region, $\dot{m}$ is the mass flow rate, C_p is the coolant heat capacity, $T_{out}^{\max}$ is the maximum outlet temperature, T_{in} is the coolant inlet temperature, and f_{rad} is the hot channel peaking factor.

The average temperature rise is calculated using the following equation and the average coolant temperature was the average of the inlet and outlet temperatures.

$$P = \dot{m} C_p (\bar{T}_{out} - T_{in}) = 2\dot{m} C_p (T_C^{Ave} - T_{in})$$

Table 63 includes the results for the flow rate calculations. The average linear power and coolant velocity are well below the design limits. If MHD forces can be mitigated, the FTWR has a large margin in the thermohydraulic design to allow operation at much high power level.

Table 63 - Equilibrium Cycle Flow Rate Calculation Results

Design	HELE		SB	
Time	BOC	EOC	BOC	EOC
Fuel Region Power (MW)	2,904	2,880	2,922	2,899
Hot Channel Factor	1.11	1.11	1.11	1.11
Coolant Velocity (m/s)	1.15	1.14	0.95	0.94
Coolant Velocity Limit (m/s)	2.0	2.0	2.0	2.0
Average Outlet Temperature (C)	460	460	515	515

Fuel Temperature Limit

The peak fuel temperature must be kept below the fuel melting point. The fuel solidus temperature is 840 °C from the ANL ATW studies.[64,62] This limits the linear power (q'_{lim}) in the fuel region. The linear power limit, heat transfer coefficient, and average fuel temperature were calculated using the equations from Lamarsh[56] for a fuel pin. The equation for the peak fuel temperature is the following.

$$q'_{lim} = \frac{(T_F^{max} - T_c)}{\frac{1}{4\pi k_F} + \frac{\ln(1 + t_{clad}/r_F)}{2\pi k_{clad}} + \frac{1}{2\pi r_p h}} \geq q'_{max} = \frac{f P_F}{n_F H}$$

The effective fuel matrix conductivity was a volume weighted average of the conductivity of the zirconium and the transuranic fuel. The zirconium thermal conductivity is 22.2 W/m-K and the unirradiated fuel thermal conductivity is 13.8 W/m-K, which was reduced by 50% to account for irradiation per the ANL Study.[62]

The parameters used to evaluate the linear power limit are given in Table 64. The results of the linear power limit calculations are given in Table 65. There is a large margin for the linear power limits. This combined with the large margin in the coolant flow rate provides a large margin for greater peaking than is predicted by the model and the potential for increased power level and net production of electricity.

Table 64 - Parameter Used for Linear Power Limit Calculations

Parameter	Definition (units)	Li17Pb83 Value	LBE Value	ANL Study[62]
T_F^{max}	Fuel Temperature Limit (C)	840 (1,113 K)	840 (1,113 K)	840 (1,113 K)
h	Heat Transfer Coefficient (W/m^2-K)	28,783	17,654	37,700
H	Fuel Length (m)	2.28	2.28	
r_F	Pin Radius (m)	0.0026162	0.0026162	
t_{clad}	Clad Thickness (m)	0.0005588 (0.22 in)	0.0005588 (0.22 in)	
k_F	Effective Fuel Matrix Conductivity (W/m-K)	15.28	15.28	17.6
k_{clad}	Clad Conductivity (W/m-K)	26.8	26.8	26.8
n_F	Number of Fuel Pins	94,696	94,696	

Table 65 - Equilibrium Cycle Results For Linear Power Limit Calculations

Design	HELE		SB	
Time	BOC	EOC	BOC	EOC
Fuel Region Power (MW)	2,904	2,880	2,922	2,899
Peaking Factor	1.43	1.31	1.68	1.56
Average Linear Power Limit	382	418	259	279
Average Linear Power	135	133	135	133

Radiation Damage Limits

There are three regions that the radiation damage limits are evaluated. The fuel is clad with steel similar to HT-9. The cladding must be able to withstand the radiation damaging during the residence time of the fuel in the reactor, which is 5 cycles or approximately 7.5 full power years. The radiation damage limit for the cladding is set at 200 dpa.[57] The design limit used in the ANL studies[64,62] is a fast neutron fluence of 4×10^{23} n/cm^2 which results in a similar level of dpa to the limit used in this analysis.

The structural material in the first wall is made of the same material as the fuel cladding. The limit is also set at 200 dpa for the first wall. The first wall will be replaced prior to reaching this limit.

The magnets are designed as lifetime components. There is significant uncertainty in the radiation damage limits to the magnet insulators. The limits for the magnet insulators are 10^{11} rads for organic

insulators and $4x10^{22}$ fast neutrons per cm^2 for the inorganic insulators.[58] The inorganic insulators are more resistant to radiation damage and present a less stringent limit. This is the limit that will be used in this analysis.

Table 66 summarizes the radiation damage results. The first wall will need to be replaced after approximately 9 cycles or 2 or 3 times over the life of the facility for both the HELE and SB designs. The fuel cladding has a large margin to its limit providing a large margin for detailed pin peaking burnups that may be significantly above the maximum assembly average damage rates. The peak fast neutron fluence to the magnets over the life of the FTWR is right at the limit for both designs. This value is calculated at the surface of the magnets and will be attenuated by some of the structural material surrounding the insulators. The magnets will most likely limit the life of the plant and the current design allows for an operational life of almost 40 full power years.

Table 66 - Equilibrium Cycle Irradiation Damage Results

	HELE	SB	Limit
First Wall (DPA/Cycle)	20	21	200
Fuel Cladding (DPA)	146	145	200
Magnet Fast Fluence (n/cm2-sec)	4.16E+22	4.04E+22	4E+22

Reactivity Compensation

There are a number of options to compensate for the change in reactivity as the fuel is burned. This includes varying the enrichment of the lithium over the cycle for lithium lead cooled designs, control rods, declining power, the neutron source strength, or any combination. This design compensates for burnup by increase the neutron source strength over the cycle in order to maintain a constant power level in the blanket. This imposes a limit on the end of cycle source strength corresponding to the design limit fusion power of 150 MW.[43] The swing in reactivity over a cycle was limited by the fuel composition limit.

The neutron multiplication factor and fusion power ranges are given in Table 67. The end of cycle fusion power is design to be at the limit of 150 MW. The HELE design has a slightly larger swing in reactivity, which still has a low BOC neutron multiplication factor of 0.925.

Table 67 - Equilibrium Cycle Summary

Design	HELE		SB	
Time	BOC	EOC	BOC	EOC
Neutron Multiplication Factor	0.925	0.836	0.913	0.837
Fusion Power (MW)	62	150	73	150

Sub-Critical Reactor Stability

The stability of the reactor is important to its safe and efficient operation. The reactor stability equations based on the point kinetics equations were evaluated for a sub-critical reactor. The standard stability analysis methodology for a critical reactor was modified for a source driven sub-critical reactor. The properties of the FTWR were estimated and used to evaluate the conditions under which the FTWR would be stable.

Neutron Population In A Sub-Critical Reactor Without Feedback

The first step was to evaluate the no feedback conditions for the neutron balance equations. For the source driven sub-critical reactors, the Z(s) transfer function changes slightly from the critical reactor. This results from the initial negative reactivity (ρ_0) of the sub-critical ($k < 1$) reactor. For a critical reactor, the initial reactivity of the system is zero.

The equations determining the neutron (n) and delayed neutron precursor concentrations in a sub-critical reactor driven by an external neutron source (S) are the following.

$$\frac{\partial n(t)}{\partial t} = \left(\frac{\rho(t) - \beta}{\Lambda} \right) n(t) + \sum \lambda_i C_i(t) + S(t)$$

$$\frac{\partial C_i(t)}{\partial t} = \left(\frac{\beta_i}{\Lambda} \right) n(t) - \lambda_i C_i(t)$$

$$\rho(t) = \frac{k(t) - 1}{k(t)}$$

$$\beta = \sum_i \beta_i$$

β_i is the delayed neutron fraction for precursor group i.

$C_i(t)$ is the concentration of delay neutron precursor group i.

λ_i is the decay constant for neutron emission from neutron precursor group i.

The initial conditions are the following.

$$\rho_0 < 0 \,;\; n_0 = \frac{-\Lambda S_0}{\rho_0} \,;\; C_{i,0} = \frac{-\beta_i S_0}{\lambda_i \rho_0} \,; \text{ and } n_1(0) = 0$$

These equations were solved using the standard linear analysis methodology[59] by expanding about an equilibrium solution with the assumption that perturbations from the initial conditions are small and products of perturbations can be neglected.

$$n(t) = n_0 + n_1(t)$$
$$C_i(t) = C_{i,0} + C_{i,1}(t)$$
$$S(t) = S_0 + S_1(t)$$
$$\rho(t) = \rho_0 + \rho_{ex}(t)$$

Laplace transforming then results in the following relation among the transformed neutron density perturbations, reactivity, and source.

$$n_1(s) = Z(s)\left(n_0\rho_{ex}(s) + \Lambda S_1(s)\right),$$

where

$$Z(s) = \frac{1}{s}\left(\Lambda - \frac{\rho_0}{s} + \sum_{i=1}^{6}\frac{\beta_i}{s+\lambda_i}\right)^{-1}$$ is the zero power transfer function.

Neutron Population In A Sub-Critical Reactor With Feedback

The neutron balance equations are then expanded to include a two-temperature feedback model. The neutron population is written in terms of the perturbed fission power (P_1) and the neutron precursors are normalized accordingly. The equations governing the deviations of the fuel temperature (T_F) and coolant temperature (T_M) from their equilibrium values are the following.

$$\frac{\partial T_F(t)}{\partial t} = aP_1(t) - \omega_F T_F(t)$$
$$\frac{\partial T_M(t)}{\partial t} = bT_F(t-\Delta t) - \omega_M T_M(t)$$

where Δt is the time delay between changes in the fuel temperature and the effect on the coolant temperature. The other parameters are defined in the remainder of this section and in Table 68.

The reactivity equation is modified as follows.

$$\rho(t) = \rho_0 + \rho_{ex}(t) + \alpha_F T_F(t) + \alpha_M T_M(t),$$

where α_F and α_M are the fuel and coolant temperature coefficients of reactivity.

This may be rewritten in the following form.

$$\rho(t) = \rho_0 + \rho_{ex}(t) + \int_0^t f(t-\tau) P_1(\tau) \partial\tau$$

The additional initial conditions are the following.

$$P_1(0) = T_F(0) = T_M(0) = 0$$

Laplace transforming these equations results in the following equation.

$$P_1(s) = \frac{Z(s)\left(P_0 \rho_{ex}(s) + \Lambda S_1(s)\right)}{1 - P_0 F(s) Z(s)}$$

where the feedback transfer function F(s) is

$$F(s) = \frac{\alpha_F a}{s+\omega_F} + \frac{\alpha_M abe^{-s\Delta t}}{(s+\omega_F)(s+\omega_M)}$$

Poles of the above equation for $P_1(s)$, which are the roots of $1 - P_0 F(s)Z(s) = 0$ determine the stability of the reactor.

The reactor will be stable if the real portion of all roots is negative and unstable if the real portion of any of the roots is positive.

FTWR Reactivity Feedback Properties

This section defines the parameters used in the reactor stability model. The definition of the individual parameters and their value is given in Table 68. The fuel temperature time constant is estimated by the following equation.

$$\tau_F = \frac{1}{\omega_F} = \frac{\rho_F C_p^F r_F^2}{k_F}$$

The coolant temperature time constant is estimated by the following equation

$$\tau_M = \frac{1}{\omega_M} = \frac{\rho_{Cl} C_p^{Cl} \pi\left((r_F + t_{cl})^2 - r_F^2\right)}{2\pi(r_F + t_{cl})h} + \frac{H_F}{2v}\left(1 + \frac{\rho_F C_p^F \pi r_F^2}{\rho_{Cl} C_p^{Cl} \pi\left((r_F + t_{cl})^2 - r_F^2\right)}\right)$$

The parameter that relates the change in power to change in temperature is given by the following equation.

$$a = \frac{1}{\rho_F C_p^F V_F}$$

The relationship between the changes in average fuel temperature and average coolant temperature is the following.

$$P_f = 2\dot{m}C_p\left(T_M^{ave} - T_M^{in}\right) = C_K^F\left(T_F^{ave} - T_M^{ave}\right)$$

This equation can then be used to relate the average change in the coolant temperature to the average change in fuel temperature.

$$\frac{\Delta T_M^{ave}}{\Delta T_F^{ave}} = \frac{C_K^F}{C_K^F + 2\dot{m}C_p}$$

The parameter that relates the change in coolant temperature to the change in the fuel temperature is estimated by the following equation.

$$b = \frac{\Delta T_M^{ave} / \Delta T_F^{ave}}{\tau_F}$$

Table 68 - Parameters for Stability Model

Parameter	Definition	Units	Li17Pb83	Value for LBE
ρ_F	Volume weighted fuel density	kg/m^3	9847	9847
C_p^F	Volume weighted fuel heat capacity	J/kg-K	193	193
r_F	Fuel pin radius	m	0.0026162	0.0026162
k_F	Effective Fuel Matrix Conductivity (W/m-K)	W/m-K	15.28	15.28
τ_F		sec	0.53	0.50
ρ_{Cl}	Clad Density	kg/m^3	7762	7762
C_p^{Cl}	Cladding heat capacity	J/kg-K	68.3	68.3
t_{cl}	Cladding thickness	m	0.0005588	0.0005588
h	Heat Transfer Coefficient	W/m^2-K	28,783	17,654
H_F	Fuel Length	m	2.28	2.28
v	Coolant Velocity	m/s	1.2	1.2
τ_M		sec	1.23	1.29
V_F	Fuel Volume	m^3	4.85	4.85
a			1.8E-7	1.8E-7
P_f	Fission Power	W	2900	2900
$\dot{m}$	Coolant mass flow rate	kg/s	83,000	96,000
C_p	Coolant heat capacity	J/kg-K	146	189
T_M^{ave}	Average coolant temperature	K	640	667
T_M^{in}	Coolant inlet temperature	K	548	563
T_F^{ave}	Average fuel temperature	K	719	758
b			0.86	0.68

Stability Analysis

The stability was determined for Li17Pb83 and LBE cooled designs. These two designs have similar properties and have very similar stable regions. The stability was analyzed as a function of the coolant and fuel temperature coefficients for nominal operating conditions as a function of neutron multiplication factor. The stability of a large array of points was determined and the line of stability appeared to be nearly linear over the region that was sampled. A linear least squared fit was performed and the fitting parameters are given in Table 69. Figures 56 and 57 show the line of stability as a function of neutron multiplication factor for the HELE and SB designs, respectively. For the sub-critical FTWR, both designs would be stable even with fairly large positive reactivity coefficients. For the critical system, both coolant and fuel temperature coefficients cannot be positive.

Table 69 - Slope and Intercept of Lines of Stability

	k=0.90		k=0.95		k=0.97		k=1	
	Slope	Intercept	Slope	Intercept	Slope	Intercept	Slope	Intercept
HELE	-0.449	11.449	-0.449	5.394	-0.451	3.138	-0.466	-0.041
SB	-0.449	11.456	-0.449	5.397	-0.450	3.161	-0.452	-0.217

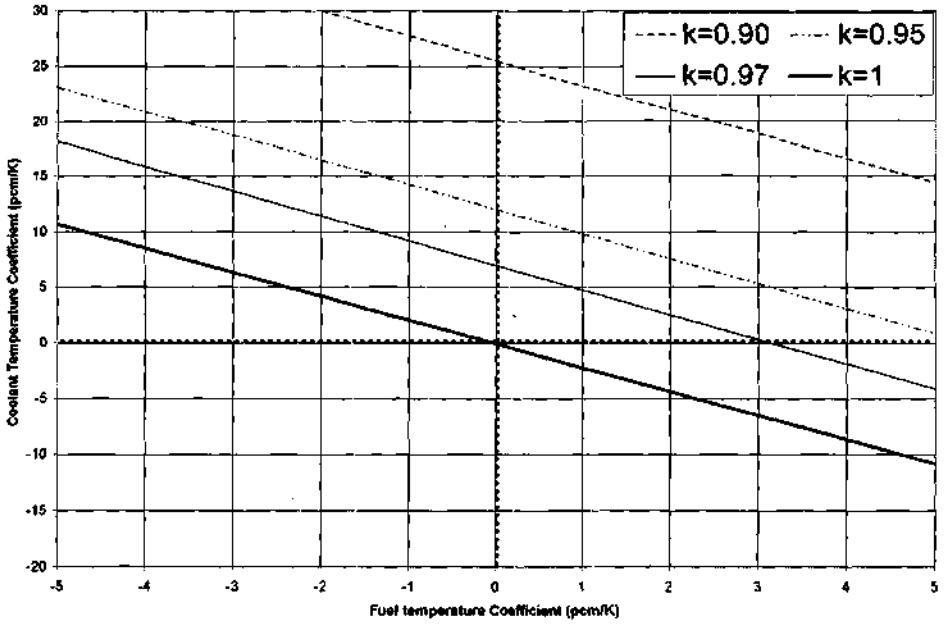

Figure 56 - Line of Stability For The HELE Design As A Function Of The Temperature Coefficients

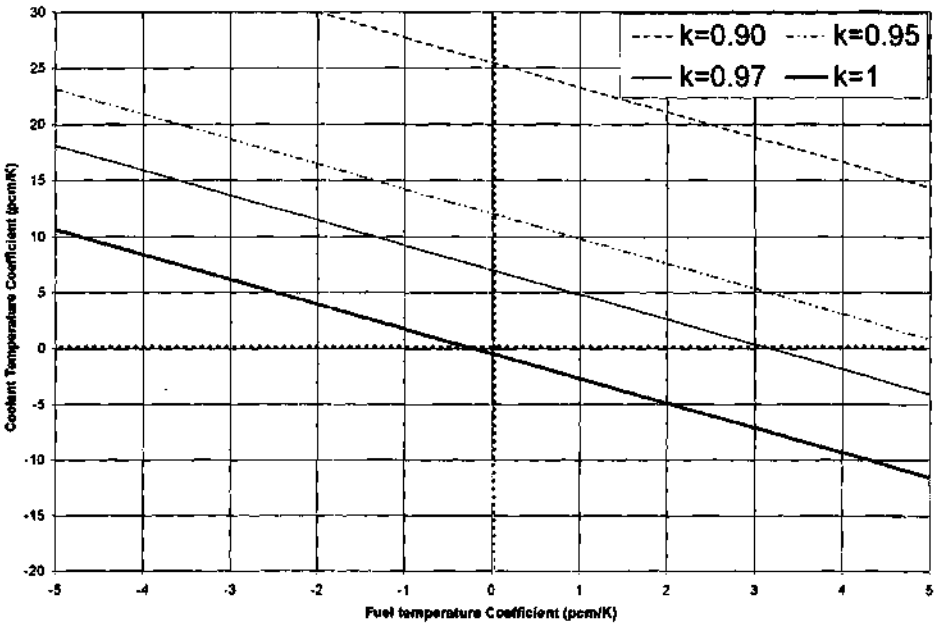

Figure 57 - Line of Stability For The SB Design As A Function Of The Temperature Coefficients

Reactivity Coefficients Limits

The stable sub-critical reactor will not be subject to runaway power in the advent of an accidental reactivity insertion as long as $\rho < |\rho_0| + \beta$. If there is sufficient margin to allow for the increase in power, there will not be damage to the core as a result of an accidental reactivity insertion. Even with positive reactivity coefficients, the feedback will be limited because of the sub-criticality of the system. As long as the new equilibrium level, represents a relatively small change relative to the original conditions the operation of the reactor is assumed to be manageable. The requirement imposed on the design is that the reactivity coefficients are sufficiently small to prevent large changes in the fission power as a result of minor perturbations in the source strength or inlet temperature. The reactivity coefficients considered are the coolant temperature coefficient and the fuel Doppler temperature coefficient. The thermal expansion of the core was not calculated, but should be a significant negative feedback mechanism because of the resulting increase in neutron leakage and increased absorption of the Li-6 in the Li17Pb83 design.

To improve operability, by limiting power fluctuations resulting from reactivity feedback, it would be desirable for the temperature coefficients to be negative. For the solid breeder (SB) design, both the fuel

Doppler and coolant coefficients are negative. However, since decreasing the Li17Pb83 density reduces the absorption cross section, it is necessary to reduce the ^{6}Li enrichment to obtain a negative coolant coefficient at BOC in the liquid breeder (HELE) design. The EOC coolant temperature coefficient is still slightly positive. The thermal expansion was not accounted for and is expected to make the coolant temperature coefficient negative and may allow for a significantly higher Li-6 concentration in the reactor coolant system, which would greatly reduce the enrichment required in the rest of the FTWR. The temperature coefficients of reactivity for the FTWR are given in Table 70.

Table 70 - Equilibrium Cycle Temperature Coefficients

Design	HELE		SB	
Time	BOC	EOC	BOC	EOC
Coolant Temp Coefficient (pcm/C)	-0.25	0.13	-1.37	-1.11
Doppler Temp Coefficient (pcm/C)	-0.01	-0.03	-0.03	-0.02

Criticality Safety

The design will be required to remain sub-critical under a number of very limiting off-normal conditions. The basic assumptions for the analysis of off-normal conditions are that the source will be turned off and control rods will be inserted into the reactor. The control rods are assumed to remain outside of the reactor during normal operation. In order to be able to tolerate rather large reactivity insertions associated with off-normal conditions, the maximum (BOC) value of the multiplication factor under normal operating conditions was limited to 0.95. The beginning of cycle neutron multiplication factor of 0.97 was used in the ANL ATW studies.[64,62] The FTWR is a higher leakage design and therefore requires a more reactive fuel to achieve the same neutron multiplication factor. This suggests a lower neutron multiplication factor to achieve the same level of safety.

The 4 batch fuel cycle would be limited by this constraint, while the 5 batch fuel cycle that was chosen is limited by the maximum fuel loading.

Off-normal Conditions without Fuel Damage

Five off-normal conditions were evaluated. The fuel is assumed to remain undamaged. In the event that there is a failure of the first wall which results in the plasma chamber becoming flooded. The first wall coolant is assumed to completely flood the chamber and cool to the freezing point. Voiding will more than likely damage the fuel, but the condition of all of the fuel becoming uncovered was evaluated. A combination of flooded plasma chamber and uncovered fuel was evaluated. The outer reflector/breeder region that contains the highly absorbent Li-6 in the liquid breeder design may be drained and this condition was evaluated. The last condition was all of the coolant drained from the outer blanket.

Fuel Damage Accidents

Fuel damage and fuel melting accidents will probably result in more limiting criticality safety accidents. These accidents are far beyond the capabilities of this analysis. The reconfiguration of the fuel into a critical configuration is possible. The dissolution, fuel sweep out, and rearrangement of the fuel involve very complex phenomena. These issues were addressed in some detail for heavy metal cooled reactors in Wider[60] and Maschek.[61] Their results suggest that the FTWR should be able to be designed for this type of accident without significant modification.

Safety Calculations

In order to perform the criticality safety calculations, the appropriate concentrations from the depletion calculations are perturbed and the transport calculations are performed. The source is assumed to be turned off early in the transient, so these calculations are performed as criticality (eigenvalue) calculations. The eigenvalue of the original configuration with and without control rods is also calculated for comparison with the source driven neutron multiplication factor and to show the change in eigenvalue associated with the particular perturbation.

Criticality Safety Results

Table 71 gives the results for the accident conditions that were evaluated. The HELE design has a very large margin to critical for all conditions considered. The SB design is near critical with the plasma chamber flooded, because the LBE makes an effective reflector without containing the more absorbent lithium. The HELE design satisfies the safety conditions analyzed, while the SB design does not quite meet these criteria with the relatively conservative assumptions about control rods. More thorough analysis, particularly a slight increase in control rods or boron enrichment in the control rods, will probably allow the SB design to remain sub-critical with the plasma chamber flooded.

Table 71 - Criticality Safety Calculations at Beginning of Equilibrium Cycle

Design	HELE	SB
Source Off	0.951	0.937
Control Rods In	0.896	0.895
Plasma Chamber Flooded	0.932	1.001
Core Void	0.899	0.868
Plasma Chamber Flooded & Core Void	0.950	0.984
Reflector Drained	0.857	0.882
Outer Blanket Drained	0.845	0.847

Reactor Tiltiness

The fuel region was divided into 4 rings of uniform volume and 3 polar regions with a volume of one half of an assembly, one assembly, and the remainder of one quarter of the reactor. The model has reflective boundary conditions and simulates two perturbed assemblies 180 degrees apart. The concentrations in one half of an assembly were perturbed separately in each radial ring to determine the effect on the power density on the perturbed assembly, and on its nearest neighbors as a function of radial location.

There was only a slight impact on the neighbor assemblies, while there was a large impact on the perturbed assembly. Radial location didn't have a large effect on the perturbed assembly. Even with a large increase in heavy metal loading in a single assembly, only a small increase in peaking factor from 1.20 to 1.28 occurred. Peaking appears that it will not be a large problem that will require tight composition controls.

The core doesn't seem to tilt radially from increased fuel loadings. The power in the individual assembly goes up, but there is almost no effect even on the neighboring assemblies. It seems since the source is uniform and the core is so unconnected, the increased reactivity of an assembly or area just increases the power locally. For the sub-critical reactor, there is no requirement that the power elsewhere goes down to compensate for an increase elsewhere, but this would be a very small effect.

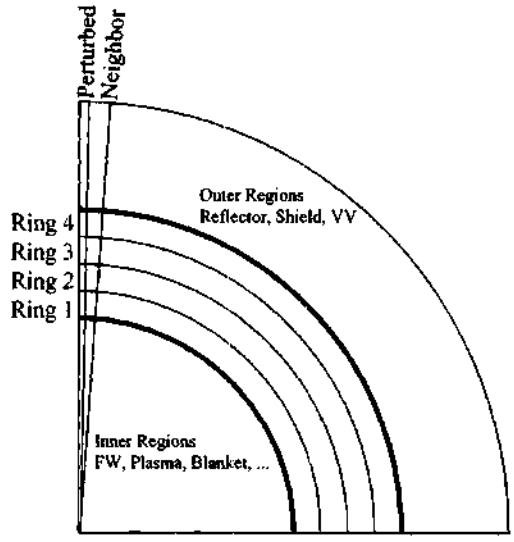

Figure 58 - FTWR Rθ Model Used for Analysis of Power Tilts

CHAPTER VII

FUSION TRANSMUTATION OF WASTE REACTOR FUEL CYCLE ANALYSIS

Scenario Description

A scenario was adapted from the fuel cycle proposed in the ATW Roadmap[22] and the design development for the ATW at Argonne National Laboratory.[64, 62] The transuranic waste recovered from the OTC will be transmuted in the FTWR. The discharge fuel from the FTWR will be recycled and mixed with transuranics from the OTC. The repeated recycle of the transuranics will completely transmute the transuranic waste from the OTC. The only waste will be the fission products (FP) and the small fraction of transuranics that are lost in the imperfect separations process. Figure 59 shows the FTWR fuel cycle. The FTWR fuel cycle includes the three waste streams from the OTC, but it separates the LWR SNF into three separate streams. These are the fission products, which are disposed in the repository, the recovered uranium, which is treated as LLW, and the transuranic elements, which feed the FTWR. The fission products are repeatedly separated and all actinides recycled with "fresh" transuranic makeup material from LWR SNF. The separation processes are not perfect, and some of the actinides will follow the fission products into the HLW streams. The pyroprocessing waste is broken into two components. Theses are the waste from the Pyro A processing (LWR FP Waste) and the Pyro B processing (FTWR FP Waste) as described in the section 0.

All streams and components of the FTWR fuel cycle and the OTC are given in Table 72. Table 72 defines the waste streams that are generated by the FTWR fuel cycle. This shows each stream generated in each step of the fuel cycle and the aggregate groupings that are analyzed to assess the performance of the FTWR fuel cycle.

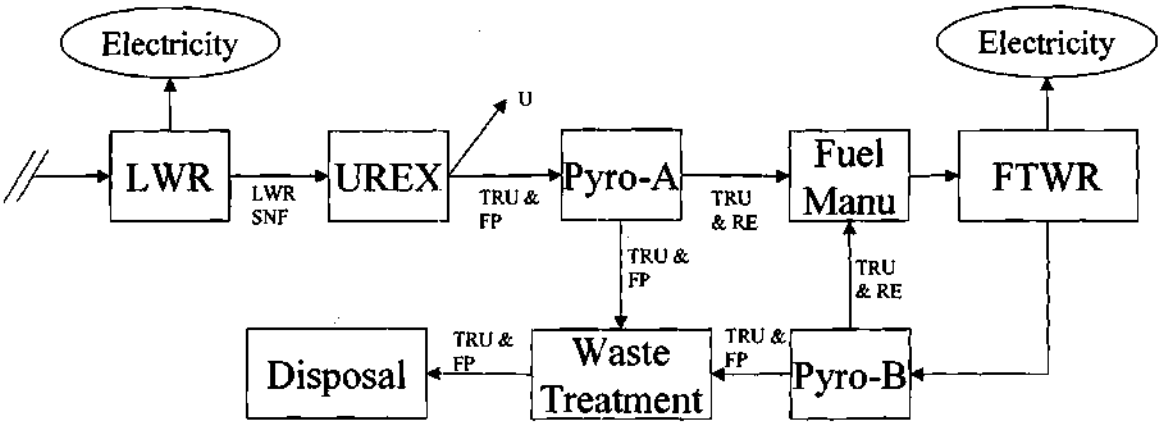

Figure 59 - Fusion Transmutation of Waste Reactor Fuel Cycle

Table 72 - Waste Management System Components

Source	Components				
Earth	Uranium Ore (U Ore)				
Uranium Ore (U Ore)	Natural Uranium (NU)	Mill Tails (Tails)			
Natural Uranium (NU)	Enriched Uranium (EU)	Depleted Uranium (DU)			
Enriched Uranium (EU)	Irradiated EU (LWR SNF)				
LWR SNF	Recovered Uranium (RU)	LWR SNF Processing Waste (LWR Waste)	FTWR Feed		
FTWR Feed Reload	FTWR Charge				
FTWR Charge	Irradiated FTWR Charge (FTWR Discharge)				
Irradiated FTWR Charge (FTWR Discharge)	FTWR Reload	FTWR Waste			
Aggregate Groups	Components				
OTC Fuel Cycle	LWR SNF	DU	Tails		
FTWR Fuel Cycle	FTWR Waste	LWR Waste	RU	DU	Tails
OTC Repository Waste	LWR SNF				
FTWR Repository Waste	FTWR Waste	LWR Waste			

Equilibrium Fuel Cycle

The reference fuel cycle for the FTWR is the equilibrium fuel cycle. The performance of the equilibrium fuel cycle will determine the long-term impact and behavior of a fuel cycle incorporating the FTWR. The equilibrium cycle is the cycle that would result after the FTWR fuel has been repeatedly recycled to the point that the charged and discharged fuel compositions have reached a relatively stable composition when the FTWR is operated under the given set of operating conditions. The expectation is that initial cycles would be designed to approximate the behavior of the equilibrium cycle to minimize changes in cycle behavior over time. Any deviations during the initial cycles will have minimal impact on the overall performance of the FTWR or any other fuel cycle.

Equilibrium Fuel Cycle Analysis

Calculations were performed to determine the composition and behavior of the equilibrium fuel cycle. The equilibrium fuel cycle was designed to satisfy the design requirements as described in chapter 0. The fresh fuel will be loaded in the outer radial region of the sub-critical reactor and be stepped inward one ring during each irradiation step. After irradiation in the innermost ring of the sub-critical reactor, it will be discharged for processing. The irradiated fuel discharged from the FTWR is processed and the recovered transuranics blended with LWR feed and remanufactured in a single cycle. The transuranics in "spent" FTWR fuel discharged in cycle *i* will be processed during cycle i+1 and be returned to the reactor in "fresh" fuel loaded in the outer most region in cycle i+2. The reprocessing time and refabrication time are assumed to be 150 days each. After discharge, the fuel is assumed to cool until 300 days prior to the next cycle at which point it begins the reprocessing and refabrication process.

Equilibrium Fuel Cycle Calculations

The REBUS code is used extensively at Argonne National Laboratory for fuel cycle analysis and design of fast reactors and their associated fuel cycles. This fuel cycle code integrates the transport calculations performed with the TWODANT code and the time dependent depletion calculations.

The equilibrium cycle concentrations are calculated using a relatively small number of depletion time steps. Even so, these calculations are very time consuming. In order to get a more detailed time dependent behavior, the beginning of equilibrium cycle concentrations was depleted using the non-

equilibrium mode of REBUS with more time steps. This more detailed depletion is then used to calculate the integral parameters such as irradiation damage and tritium inventory.

The tritium production cross sections were taken from the JEF-2.2 cross section set.[24] The energy dependent tritium production cross sections are collapsed using the spectrum calculated by MCC-2 for the region in which the lithium is located.

The displacement per atom (DPA) radiation damage cross sections were taken from Hill[63] for iron, nickel, and chromium, which are the primary components of the cladding and first wall.

Transmutation Fuel Cycle Input

Many of the performance parameters are very sensitive to the performance of the waste processing systems. The UREX system is assumed to recover 99.995% of the uranium.[36] The remainder of the material is assumed to be sent for pyroprocessing for purification of the transmutation feed. The pyroprocessing (Pyro A) of the stream of material from the UREX processing is assumed to remove all non-rare earth fission products, all suburanic (Z<92) heavy metal elements, and 95% of the rare earth fission products. The Pyro A processing recovers 99.9% of the uranium and transuranic elements[64] with 0.1% of these elements leaking into the fission product waste stream. The discharged transmutation reactor fuel is purified in a separate pyroprocessing (Pyro B) system, which is assumed to perform the same as Pyro A.

The composition of the reference design SNF along with the compositions of the different streams of material including the transmutation reactor feed is given in Table 124 in Appendix H. Table 13 compares the transmutation reactor feed used in this study with composition used in the ANL ATW studies[36] and the transmutation reactor feed composition based on the Yucca Mountain Environmental Impact Statement.[35] This shows generally good agreement. The Np-237 composition is lower than the others by roughly 1% and the Pu-239 is slightly higher by roughly 1%.

Depletion Chains

The data for the depletion chains used in the REBUS model are given in Appendix J. The depletion chains used for the FTWR fuel cycle are given in Table 126. The lithium chains are not used for the liquid breeder design, since the lithium is also the coolant and will flow through the system and the tritium will be continuously extracted. Table 127 shows the depletion chain for the solid breeder. Table 128

defines the reaction types used in Tables 126 and 127. Table 129 gives the half-lives and branching fractions for the radioactive decay.

Equilibrium Fuel Cycles

There are many design approaches that can be taken to develop and optimize the operation of the FTWR. The reference design focused on maximizing the fuel burnup, while limiting refueling outages. Initial studies resulted in the increase of the number of fuel batches from three to five. At three and four batch loading, the cycle lengths were very long, two or more years, while the burnup was limited by the BOC k_{sub}. At five batches, the fuel enrichment became limiting and the BOC k_{sub} was reduced, but the cycle length was still approximately 1.5 full power years. The optimum batch size seems to be either 4 or 5. Five batches were chosen because it results in higher burnup and lower BOC k_{sub}.

The summary of the equilibrium fuel cycles for the reference FTWR designs is given in Table 73. The HELE and SB reference designs will operate very similarly. The BOC k_{sub} is limited by the fuel enrichment at the BOC. Both designs will fission over 99% of the original LWR TRU from approximately 100 MTU of LWR SNF per full power year.

Table 73 - Equilibrium Cycle Summary

Design	HELE	SB
Cycle Length (Full Power Days)	564	540
BOC HM Loading (MT)	27	27
BOC Neutron Multiplication Factor	0.925	0.913
EOC Neutron Multiplication Factor	0.836	0.837
Fuel Enrichment	45%	45%
Fresh Fuel Batch Size (MT)	6.2	6.2
Fuel Batches	5	5
Discharge Burnup	29%	28%
TRU Burnup	99.65%	99.66%
LWR SNF Transmuted (MTU/cycle)	155	148
LWR SNF Transmuted (MTU/Full Power Year)	101	100
Total Cycles	26	27
LWR SNF Transmuted (MTU/FTWR)	4,035	4,009
TRU Burnup Rate (MWd/g)	0.96	0.96

Equilibrium Fuel Cycle Power Summary

The FTWR is designed to operate at a blanket power level of 3000 MW. The fusion source is adjusted to maintain this level throughout the cycle. The total system power includes this 3000 MW, plus the 20% of the fusion power that is carried by the α particles and the power from the current drive. The 80% of the fusion energy carried by the neutrons is deposited in the blanket and is included in the 3000 MW blanket power. The fusion source operates at a Q_p of 2.0, which corresponds to an external plasma heating power level from the current drive that is 50% of the fusion power. The power deposited in the plasma from the α particles and the current drive will be deposited on the first wall and diverter and are included in the total thermal power of the system. The "other" power is the power produced by exothermic reactions, and lost to endothermic reactions. The other power falls over the cycle.

Tables 74 and 76 show the system power behavior over the equilibrium cycle for HELE and SB designs, respectively. Both designs show nearly the same behavior. The fusion power rises from approximately 60 MW to the design limit of 150 MW. Tables 75 and 77 show the distribution of the 3000 MW of blanket power over the equilibrium cycle for the HELE and SB designs, respectively. The first wall power increases significantly as the fusion power increases; otherwise the variations are only a few percent or less in each region.

Table 74 - Equilibrium Cycle Power Data for the HELE FTWR

Time (FPD)	Blanket (MW)	Fusion (MW)	Fission (MW)	Other (MW)	Total (MW)
0	3,000	62	2,910	40	3,044
56	3,000	71	2,908	35	3,050
113	3,000	79	2,905	31	3,056
169	3,000	88	2,902	27	3,061
226	3,000	96	2,899	24	3,067
282	3,000	105	2,896	20	3,074
338	3,000	114	2,893	16	3,080
395	3,000	123	2,890	12	3,086
451	3,000	131	2,887	8	3,092
508	3,000	140	2,883	4	3,098
564	3,000	150	2,880	0	3,105

Table 75 - Distribution of the Blanket Power in the HELE FTWR

Time (FPD)	Blanket (MW)	First Wall (MW)	Reactor Core (MW)	Reflector (MW)	Shield (MW)
0	3,000	8	2,903	32	56
56	3,000	8	2,900	33	57
113	3,000	8	2,898	33	59
169	3,000	9	2,895	34	60
226	3,000	9	2,893	35	61
282	3,000	9	2,891	36	62
338	3,000	10	2,888	36	63
395	3,000	10	2,886	37	65
451	3,000	10	2,883	38	66
508	3,000	11	2,881	39	67
564	3,000	11	2,878	40	68

Table 76 - Equilibrium Cycle Power Data for the SB FTWR

Time (FPD)	Blanket (MW)	Fusion (MW)	Fission (MW)	Other (MW)	Total (MW)
0	3,000	73	2,901	40	3,051
54	3,000	80	2,900	36	3,056
108	3,000	87	2,898	32	3,061
162	3,000	95	2,895	29	3,066
216	3,000	102	2,893	26	3,072
270	3,000	110	2,890	22	3,077
324	3,000	117	2,887	19	3,082
378	3,000	125	2,885	15	3,087
432	3,000	133	2,882	12	3,093
486	3,000	140	2,879	8	3,098
540	3,000	148	2,877	5	3,104

Table 77 - Distribution of the Blanket Power in the SB FTWR

Time (FPD)	Blanket (MW)	First Wall (MW)	Reactor Core (MW)	Reflector (MW)	Shield (MW)
0	3,000	7	2,890	50	50
54	3,000	8	2,888	50	52
108	3,000	8	2,886	51	53
162	3,000	8	2,884	51	54
216	3,000	8	2,882	52	55
270	3,000	9	2,880	52	56
324	3,000	9	2,878	53	57
378	3,000	9	2,876	53	58
432	3,000	10	2,874	54	60
486	3,000	10	2,872	55	61
540	3,000	10	2,870	55	62

Fuel Cycle Isotopic Data

The isotopic data used to calculate the FOMs was calculated using the methodology described in this section. The detailed isotopic composition of the FTWR waste is given in Table 132 in Appendix J. These results were used to calculate all FOMs. The softer spectrum in the HELE design because of the presences of lithium in the coolant produced an equilibrium FTWR with higher concentrations of the higher actinides such as curium and californium and slightly less of the major components such as plutonium and neptunium. These differences are fairly small and will have a slight impact on the figures of merit.

Waste Management Figures of Merit

The waste management figures of merit for the HELE and SB FTWR fuel cycles are presented in comparison with several components of the OTC so the impact of transmutation can be evaluated. The results are compared to the SNF to show the effect of transmutation of the LWR SNF. They are also compared to the SNF where the uranium is neglected so the impact of the irradiation can be separated from the effect of chemical separation of the SNF. The results are also compared to the properties of the unirradiated uranium ore that originally was used to create the LWR fuel. This shows the overall effect of the nuclear fuel cycle compared with the natural hazard of the uranium ore.

The results for the HELE and SB FTWR are nearly identical. In general, the increased production of fission products increases the radiological FOMs and the decay heat. The long-term effect on the repository waste is generally several orders of magnitude reduction in the FOMs. For all waste streams, the long-term FOMs are dominated by the uranium and are essentially unchanged.

Waste Material Composition Summary

The results for the repository isotopes are given in Table 78. Figures 60 and 61 show the results for the repository waste streams and all waste streams, respectively.

The fission of the transuranics results in addition fission products. As a result, the Tc-99 inventory is increased by approximately 25% and the I-129 is increased by approximately 33%. The difference is not the same for both isotopes because the fissioning isotopes and spectrum are dramatically different in the FTWR, which produces a different fission product yield than occurs in the LWRs.

The fission of the transuranics greatly reduces the inventory of actinide isotopes sent to the repository. The amount of Np-237 sent to the repository will be reduced by approximately 99.7% and should have a significant impact on long-term dose predictions that are dominated by Np-237.

The U-234 sent to the repository is reduced by approximately 98%. This is less than the other repository isotopes because a larger fraction of the higher actinide isotopes decay to U-234 in the FTWR or on the time scale of the repository. The shift to higher actinides, such as Np-237 to Pu-238, results in the U-234 concentration increasing from essential zero in the LWR SNF feed stream to approximately 2% in the equilibrium FTWR fuel. Separation of the uranium from the SNF will result in approximately 10 times as much U-234 being disposed in LLW facilities, assuming the uranium is not recycled. For all waste streams, the U-234 is reduced by only 37%.

The amount of Pu-239 sent to the repository will be reduced by approximately 99.7%. This should have a significant impact on long-term dose predictions as well as greatly reducing the concerns for a future critical configuration in the repository and the potential for proliferation of the repository waste.

The Pu-242 is reduced dramatically in the FTWR. The amount of Pu-242 sent to the repository will be reduced by approximately 99.3%. This is slightly less than the other repository isotopes, except U-234, because of the shift to higher actinides in the FTWR.

Table 78 - Data for FTWR Repository Isotopes (MT/MTU)

	Repository Isotopes Mass (MT)					
Component	Tc-99	I-129	Np-237	U-234	Pu-239	Pu-242
Uranium Ore				3.09E-04		
Enriched Uranium				2.84E-04		
OTC Repository Waste	7.81E-04	1.81E-04	1.90E-03	3.26E-04	6.01E-03	5.21E-04
OTC Repository Waste (w/o U)	7.81E-04	1.81E-04	1.90E-03	1.34E-04	6.01E-03	5.21E-04
HELE Repository Waste	1.06E-03	2.59E-04	6.25E-06	2.71E-06	1.33E-05	3.72E-06
SB Repository Waste	1.05E-03	2.56E-04	6.01E-06	2.57E-06	1.29E-05	3.54E-06
OTC LLW				2.47E-05		
HELE LLW				2.16E-04		
SB LLW				2.16E-04		
OTC	7.81E-04	1.81E-04	1.90E-03	3.50E-04	6.01E-03	5.21E-04
HELE Fuel Cycle	1.06E-03	2.59E-04	6.25E-06	2.19E-04	1.33E-05	3.72E-06
SB Fuel Cycle	1.05E-03	2.56E-04	6.01E-06	2.19E-04	1.29E-05	3.54E-06

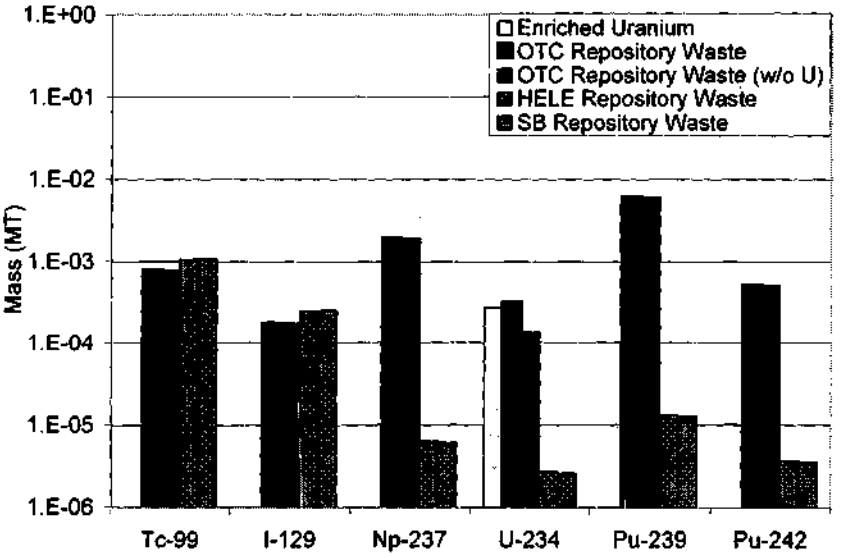

Figure 60 - Repository Isotopes Discharged per MTU for FTWR Scenario (Repository Waste Streams)

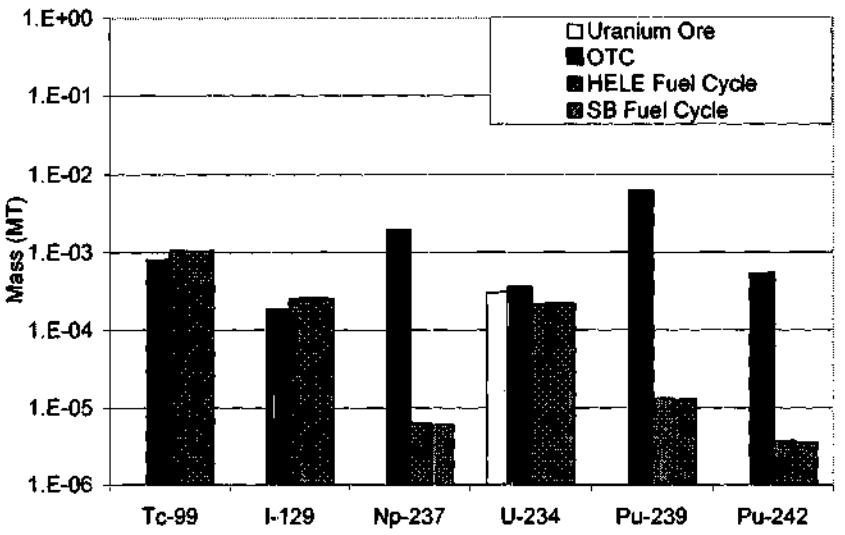

Figure 61 - Repository Isotopes Discharged per MTU for FTWR Scenario (All Waste Streams)

Masses

The actinide mass summary is given in Table 79 and compared with the uranium ore, the OTC, and the OTC neglecting the uranium. Figures 62 and 63 show the results for the repository waste streams and all waste streams, respectively. The mass of plutonium, transuranics, and minor actinides sent to the repository will be reduced by 99.7%, 99.7%, and 99.0%, respectively.

The mass of uranium sent to the repository is reduced from 0.95 MT/MTU to approximately 1 g/MTU. The uranium in the LWR SNF is separated and disposed in a LLW facility if it is not recycled. The mass or uranium in all waste streams is nearly unaffected because the uranium is not recycled and only a small fraction of the original uranium in the uranium ore is fissioned in the LWR.

Table 79 - Data for FTWR Actinide Mass (MT/MTU)

	Actinide Mass (MT)			
Component	Pu	TRU	MA	U
Uranium Ore				5.77E+00
Enriched Uranium				1.00E+00
OTC Repository Waste	1.04E-02	1.10E-02	6.46E-04	9.55E-01
OTC Repository Waste (w/o U)	1.04E-02	1.10E-02	6.46E-04	1.28E-05
HELE Repository Waste	3.13E-05	3.80E-05	6.67E-06	1.42E-06
SB Repository Waste	3.01E-05	3.65E-05	6.40E-06	1.35E-06
OTC LLW				4.77E+00
HELE LLW				5.73E+00
SB LLW				5.73E+00
OTC	1.04E-02	1.10E-02	6.46E-04	5.73E+00
HELE Fuel Cycle	3.13E-05	3.80E-05	6.67E-06	5.73E+00
SB Fuel Cycle	3.01E-05	3.65E-05	6.40E-06	5.73E+00

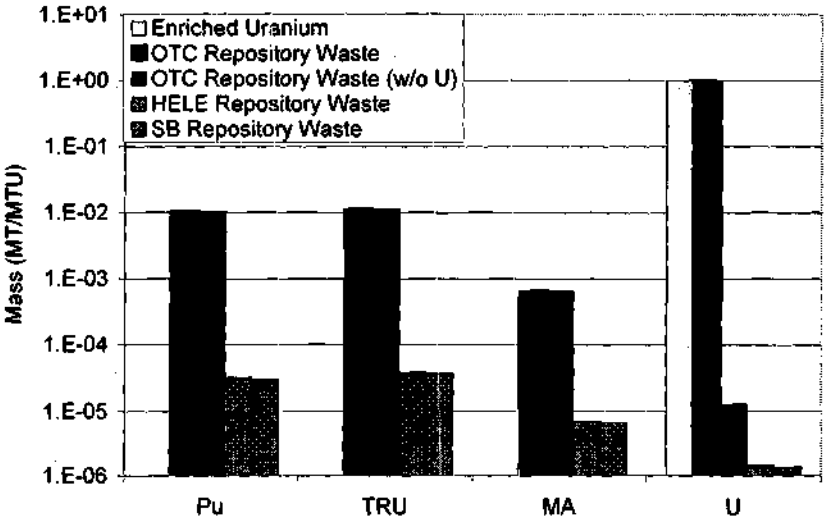

Figure 62 - Actinides Discharged per MTU for FTWR Scenario (Repository Waste Streams)

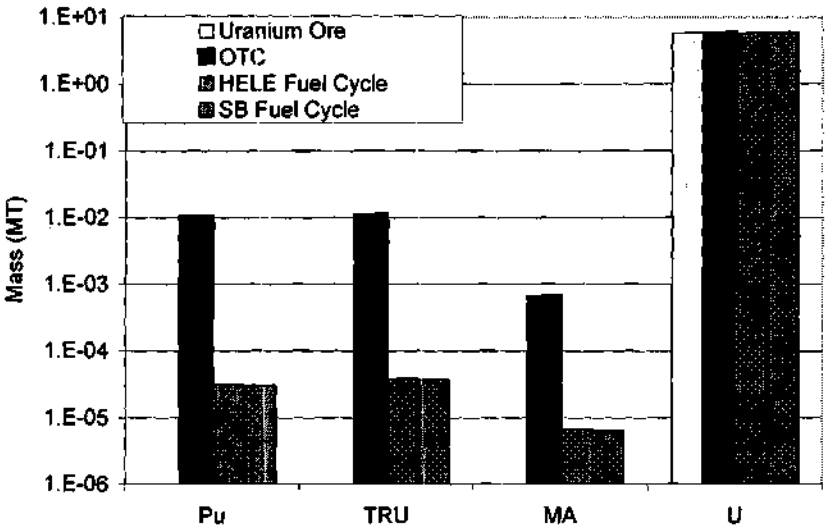

Figure 63 - Actinides Discharged per MTU for FTWR Scenario (All Waste Streams)

Waste Material Toxicity Summary

The toxicity summary is given in Table 80. Figures 64 and 65 show the toxicity for the repository waste streams and all waste streams, respectively. The toxicity of the FTWR waste is initially greater than the OTC because of the greater quantity of fission products. They are equal at about 100 years. The repository waste for the FTWR falls well below the OTC by 1,000 years. The toxicity of the repository waste falls below that of the original uranium ore used to create the nuclear fuel in several hundred years for the FTWR, while it takes about 10,000 years for the OTC. When all waste streams are considered, there is almost no effect beyond 100,000 years. The FTWR waste decays to near the level of the uranium ore in less than 1,000 year. The OTC has a longer-term component associated with the transuranics.

When all waste streams are considered, the bulk of the long-term toxicity will be in the depleted uranium. The fission products dominate the toxicity for the first few hundred years and will be unaffected by transmutation. Over the several thousand year timeframe, the FTWR destroys the toxicity associated with the transuranics and greatly reduces the toxicity placed in the repository beyond 1,000 years.

Table 80 - Comparison of FTWR Toxicity (m^3 H_2O/MTU)

	Time After Discharge (yr)					
Component	0	100	1,000	10,000	100,000	1,000,000
Uranium Ore	9.1E+07	9.1E+07	9.1E+07	9.0E+07	9.2E+07	9.1E+07
Enriched Uranium	6.9E+04	9.2E+04	2.8E+05	6.0E+06	4.5E+07	2.3E+07
OTC Repository Waste	4.6E+11	2.4E+10	4.4E+08	1.0E+08	5.8E+07	2.8E+07
OTC Repository Waste (w/o U)	4.6E+11	2.4E+10	4.4E+08	1.0E+08	2.8E+07	9.6E+06
HELE Repository Waste	8.4E+13	2.6E+10	2.9E+06	1.7E+06	1.5E+06	9.0E+05
SB Repository Waste	9.1E+13	2.6E+10	3.0E+06	1.7E+06	1.5E+06	8.9E+05
OTC LLW	9.1E+07	9.1E+07	9.0E+07	8.4E+07	4.7E+07	6.8E+07
HELE FTWR LLW	9.1E+07	9.1E+07	9.1E+07	8.8E+07	7.7E+07	8.6E+07
SB FTWR LLW	9.1E+07	9.1E+07	9.1E+07	8.8E+07	7.7E+07	8.6E+07
OTC	4.7E+11	2.4E+10	5.3E+08	1.9E+08	1.0E+08	9.6E+07
HELE Fuel Cycle	8.4E+13	2.6E+10	9.3E+07	9.0E+07	7.8E+07	8.7E+07
SB Fuel Cycle	9.1E+13	2.6E+10	9.3E+07	9.0E+07	7.8E+07	8.7E+07

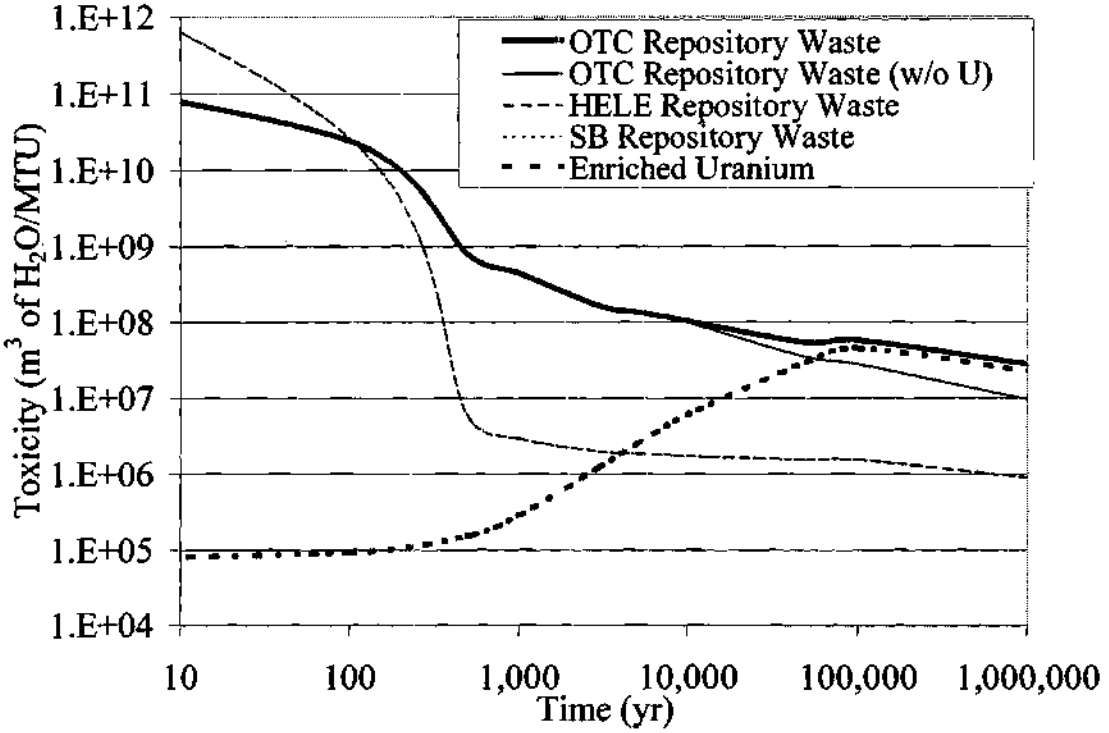

Figure 64 - Toxicity versus Time per MTU for FTWR Scenario (Repository Waste Streams)

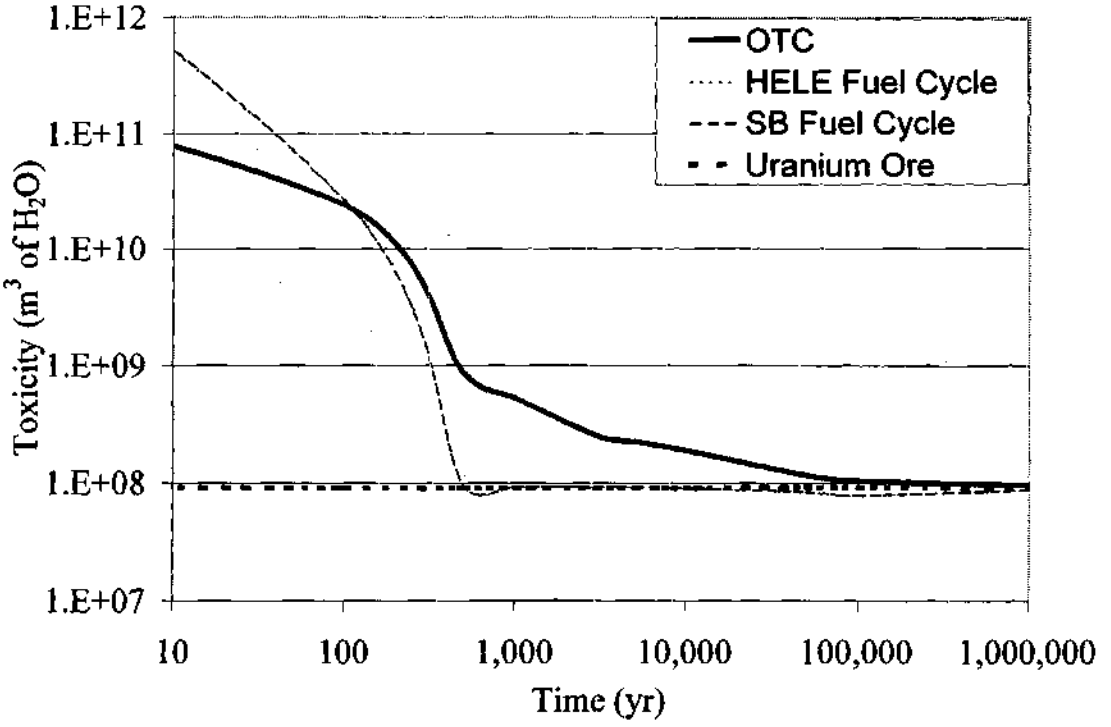

Figure 65 - Toxicity versus Time per MTU for FTWR Scenario (All Waste Streams)

Waste Material Decay Heat Summary

The decay heat summary is given in Table 81. Figures 66 and 67 show the decay heat for the repository waste streams and all waste streams, respectively. The decay heat of the FTWR waste is initially greater than the OTC because of the greater quantity of fission products, but the FTWR falls below the OTC waste in a few years. The large amount of energy released by the transuranics and their daughters keeps the decay of the OTC waste high for a significant period of time. The FTWR will greatly reduce the level of decay in the repository. This will allow a much greater loading of waste for a heat load limited repository.

Table 81 - Data for FTWR Decay Heat (W/MTU)

	Time After Discharge (yr)							
Component	0	1	10	100	1,000	10,000	100,000	1,000,000
Uranium Ore	5.7E-01	5.7E-01	5.7E-01	5.7E-01	5.7E-01	5.7E-01	5.7E-01	5.7E-01
Enriched Uranium	6.1E-02	6.3E-02	6.3E-02	6.3E-02	6.4E-02	9.3E-02	2.8E-01	1.4E-01
OTC Repository Waste	5.5E+03	9.7E+03	1.2E+03	3.2E+02	6.2E+01	1.5E+01	1.2E+00	4.2E-01
OTC Repository Waste (w/o U)	5.5E+03	9.7E+03	1.2E+03	3.2E+02	6.2E+01	1.5E+01	9.8E-01	3.0E-01
HELE Repository Waste	1.3E+05	1.3E+04	1.2E+03	1.2E+02	2.6E-01	8.0E-02	2.1E-02	2.3E-03
SB Repository Waste	1.2E+05	1.3E+04	1.1E+03	1.2E+02	2.5E-01	7.8E-02	2.0E-02	2.2E-03
OTC LLW	5.1E-01	5.1E-01	5.1E-01	5.1E-01	5.0E-01	4.8E-01	3.0E-01	4.3E-01
HELE LLW	5.6E-01	5.6E-01	5.6E-01	5.6E-01	5.6E-01	5.5E-01	4.9E-01	5.5E-01
SB LLW	5.6E-01	5.6E-01	5.6E-01	5.6E-01	5.6E-01	5.5E-01	4.9E-01	5.5E-01
OTC	5.5E+03	9.7E+03	1.2E+03	3.2E+02	6.3E+01	1.6E+01	1.5E+00	8.5E-01
HELE Fuel Cycle	1.3E+05	1.3E+04	1.2E+03	1.2E+02	8.1E-01	6.3E-01	5.1E-01	5.5E-01
SB Fuel Cycle	1.2E+05	1.3E+04	1.1E+03	1.2E+02	8.0E-01	6.2E-01	5.1E-01	5.5E-01

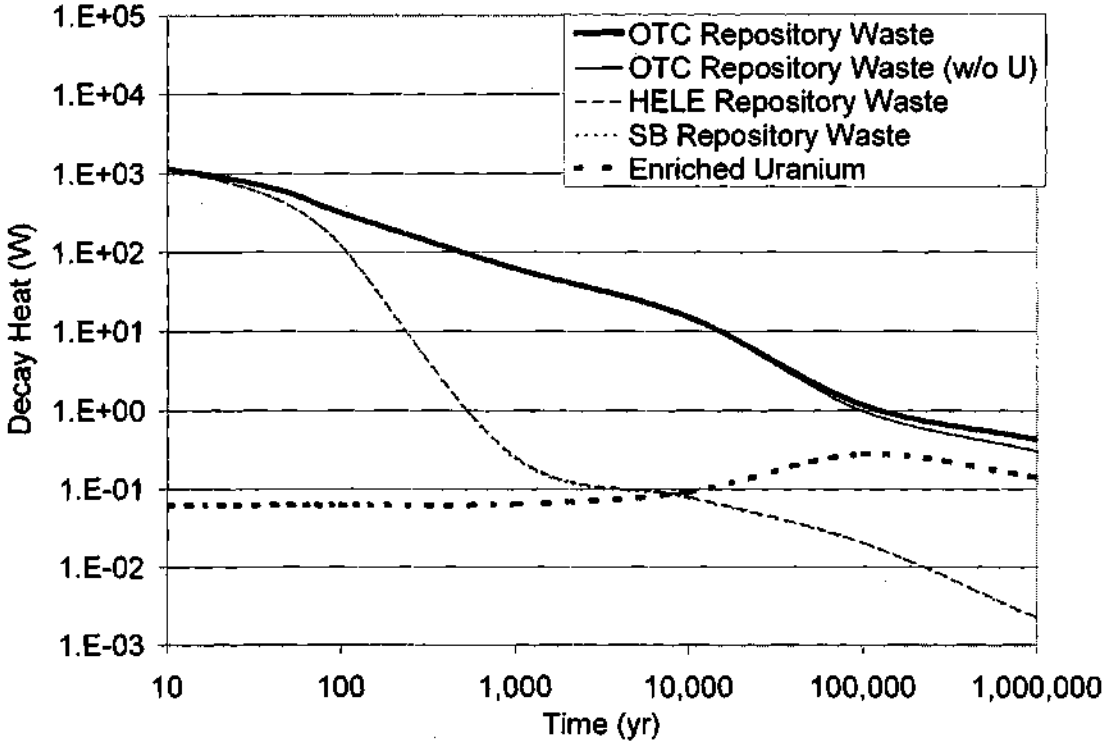

Figure 66 - Decay Heat versus Time per MTU for FTWR Scenario (Repository Waste Streams)

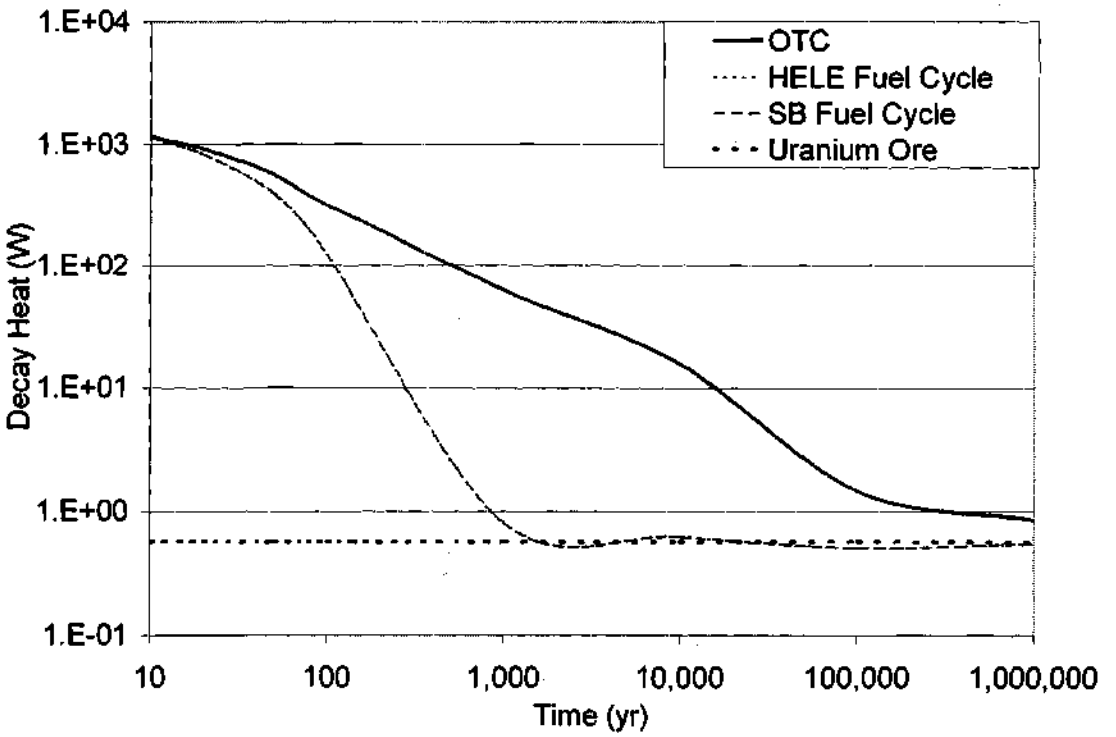

Figure 67 - Decay Heat versus Time per MTU for FTWR Scenario (All Waste Streams)

Waste Material Integral Decay Energy Summary

The integral decay energy summary is given in Table 82. Figures 68 and 69 show the decay energy for the repository waste streams and all waste streams, respectively. The integral decay energy from the FTWR repository waste increases very slowly beyond 100 years, while the OTC repository waste releases significantly more energy beyond 100 years. The lower quantity of decay energy released by the FTWR waste will result in a small change in the bulk repository temperature.

Table 82 - Data for FTWR Integral Decay Energy (J/MTU)

	Time After Discharge (yr)							
Component	0	1	10	100	1,000	10,000	100,000	1,000,000
Uranium Ore	0	1.2E+07	1.7E+08	1.8E+09	1.8E+10	1.6E+11	1.7E+12	1.4E+13
Enriched Uranium	0	2.0E+06	2.0E+07	2.0E+08	2.0E+09	2.4E+10	5.0E+11	5.3E+12
OTC Repository Waste	0	1.8E+11	9.1E+11	2.6E+12	5.9E+12	1.3E+13	2.5E+13	4.1E+13
OTC Repository Waste (w/o U)	0	1.8E+11	9.1E+11	2.6E+12	5.9E+12	1.3E+13	2.5E+13	3.7E+13
HELE Repository Waste	0	3.7E+11	1.2E+12	2.5E+12	2.6E+12	2.7E+12	2.8E+12	3.0E+12
SB Repository Waste	0	3.6E+11	1.2E+12	2.5E+12	2.6E+12	2.7E+12	2.8E+12	2.9E+12
OTC LLW	0	1.0E+07	1.5E+08	1.6E+09	1.6E+10	1.3E+11	1.2E+12	8.3E+12
HELE LLW	0	1.2E+07	1.7E+08	1.8E+09	1.7E+10	1.5E+11	1.5E+12	1.2E+13
SB LLW	0	1.2E+07	1.7E+08	1.8E+09	1.7E+10	1.5E+11	1.5E+12	1.2E+13
OTC	0	1.8E+11	9.1E+11	2.6E+12	5.9E+12	1.3E+13	2.7E+13	4.9E+13
HELE Fuel Cycle	0	3.7E+11	1.2E+12	2.5E+12	2.7E+12	2.8E+12	4.3E+12	1.5E+13
SB Fuel Cycle	0	3.6E+11	1.2E+12	2.5E+12	2.6E+12	2.8E+12	4.3E+12	1.5E+13

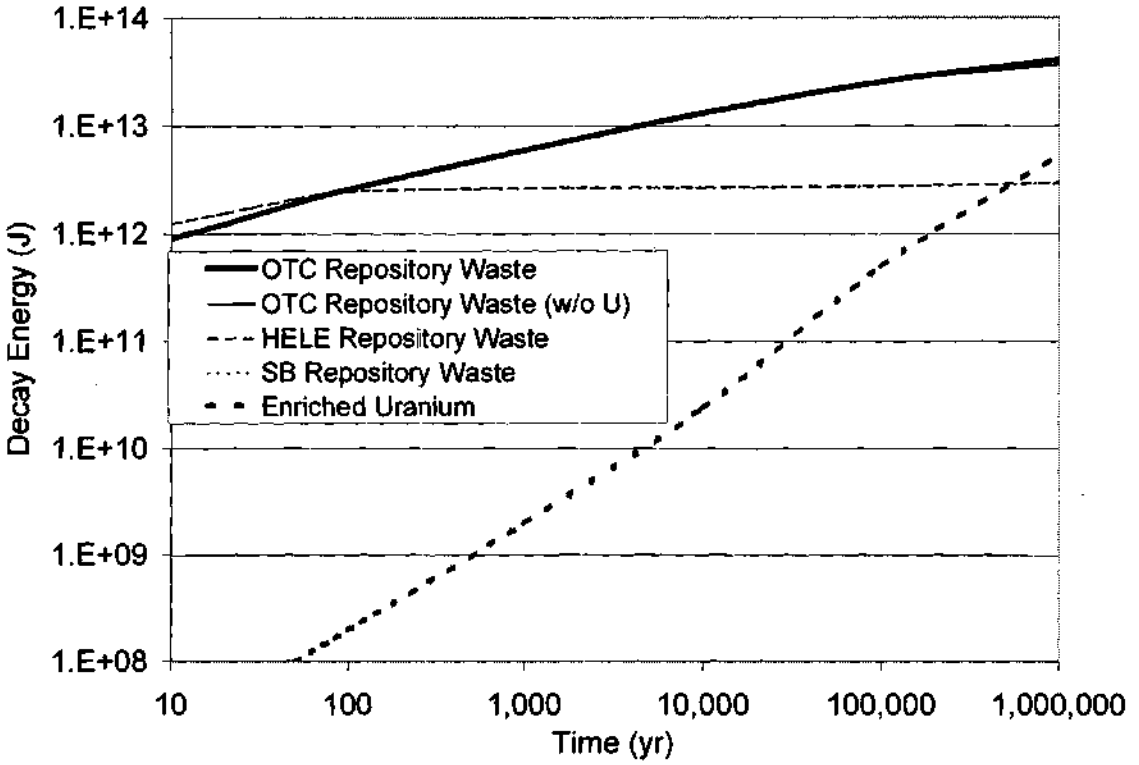

Figure 68 - Integral Decay Energy per MTU for FTWR Scenario (Repository Waste Streams)

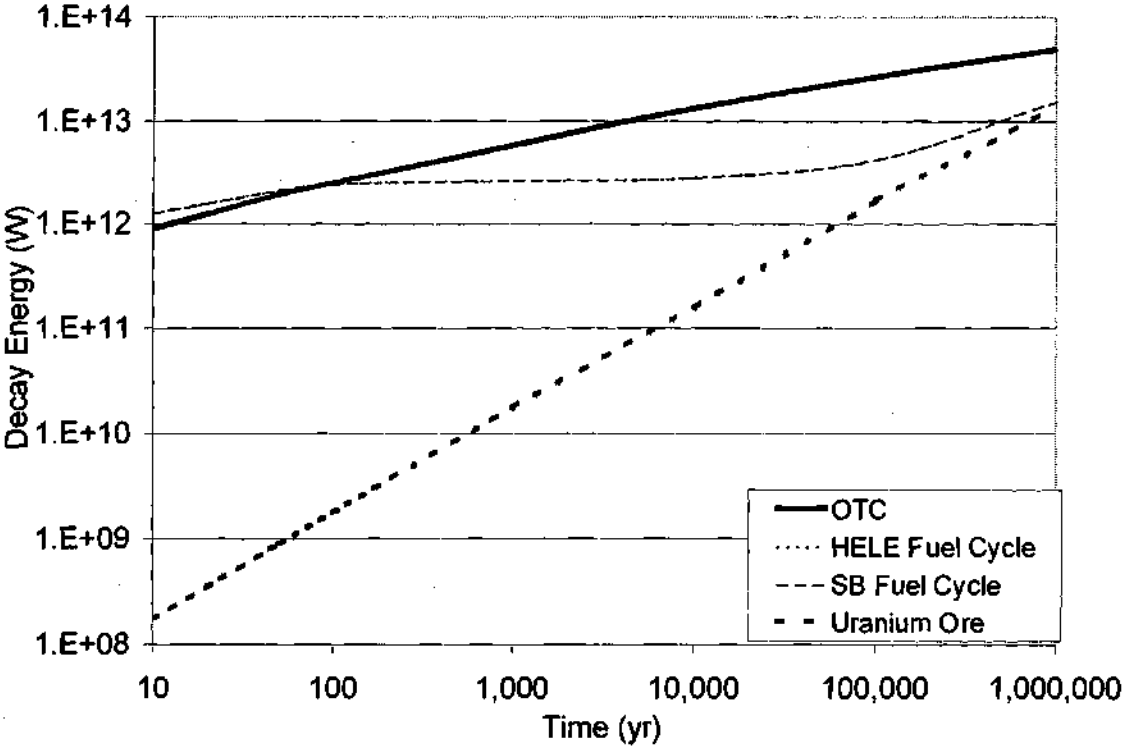

Figure 69 - Integral Decay Energy per MTU for FTWR Scenario (All Waste Streams)

Waste Material Radiological Summary

The following parameters are focused on the difficulty of handling the materials. In particular, the relative amount of shielding that would be required to ship, store, or process the waste.

The photon dose rate summary is given in Table 83. Figures 70 and 71 show the photon dose rate for the repository waste streams and all waste streams, respectively. The photon dose rate of the FTWR waste is initially greater than the OTC because of the greater quantity of fission products. They are equal at about 100 years. The photon dose rate of the repository waste falls below that of the original uranium ore used to create the nuclear fuel in approximately 1,000 years for the FTWR, and about twice as long for the OTC. Beyond 100,000 years, the FTWR repository waste falls significantly below the OTC repository waste. When all waste streams are considered, there is almost no effect beyond 1,000 years. The FTWR and OTC waste decays to near the level of the uranium ore in less than 1,000 year. The photon dose rate at long times in the future is of little concern, since any handling of the waste will occur in the first 100 years, beyond this the photon dose rate is sufficiently low to not present any handling difficulties.

Table 83 - Data for FTWR Photon Dose Rate (REM/hr/MTU)

	Time After Discharge (yr)							
Component	0	1	10	100	1,000	10,000	100,000	1,000,000
Uranium Ore	2.1E+00	2.1E+00	2.1E+00	2.1E+00	2.1E+00	2.1E+00	2.1E+00	2.1E+00
Enriched Uranium	7.3E-03	1.9E-02	1.9E-02	1.9E-02	2.3E-02	1.5E-01	1.0E+00	5.0E-01
OTC Repository Waste	2.0E+05	2.4E+05	4.1E+04	4.1E+03	3.4E+00	2.0E+00	1.7E+00	8.0E-01
OTC Repository Waste (w/o U)	2.0E+05	2.4E+05	4.1E+04	4.1E+03	3.3E+00	2.0E+00	1.0E+00	3.8E-01
HELE Repository Waste	2.6E+06	3.0E+05	4.9E+04	5.1E+03	1.1E+00	1.1E+00	5.7E-01	3.6E-03
SB Repository Waste	3.7E+06	3.3E+05	5.3E+04	5.4E+03	1.3E+00	1.2E+00	6.4E-01	3.8E-03
OTC LLW	2.1E+00	2.1E+00	2.1E+00	2.1E+00	2.1E+00	1.9E+00	1.1E+00	1.6E+00
HELE LLW	2.1E+00	2.1E+00	2.1E+00	2.1E+00	2.1E+00	2.0E+00	1.8E+00	2.0E+00
SB LLW	2.1E+00	2.1E+00	2.1E+00	2.1E+00	2.1E+00	2.0E+00	1.8E+00	2.0E+00
OTC	2.0E+05	2.4E+05	4.1E+04	4.1E+03	5.4E+00	4.0E+00	2.8E+00	2.4E+00
HELE Fuel Cycle	2.6E+06	3.0E+05	4.9E+04	5.1E+03	3.2E+00	3.1E+00	2.4E+00	2.0E+00
SB Fuel Cycle	3.7E+06	3.3E+05	5.3E+04	5.4E+03	3.4E+00	3.2E+00	2.4E+00	2.0E+00

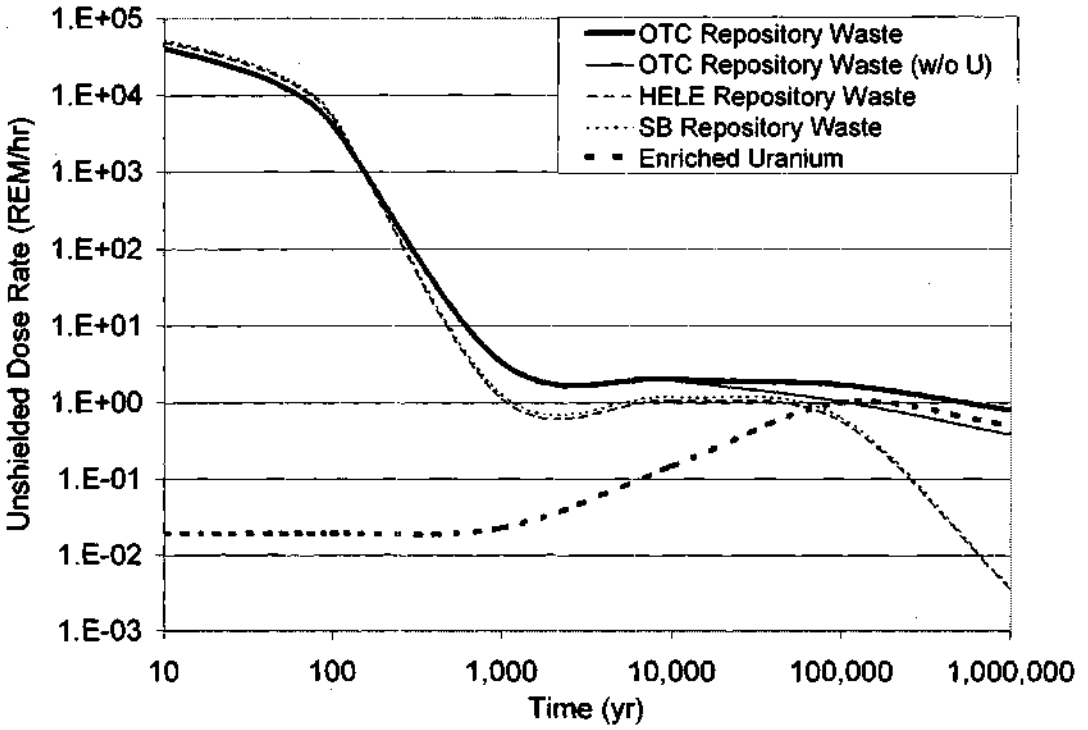

Figure 70 - Unshielded Dose Rate from Photon Emission per MTU for FTWR Scenario (Repository Waste Streams)

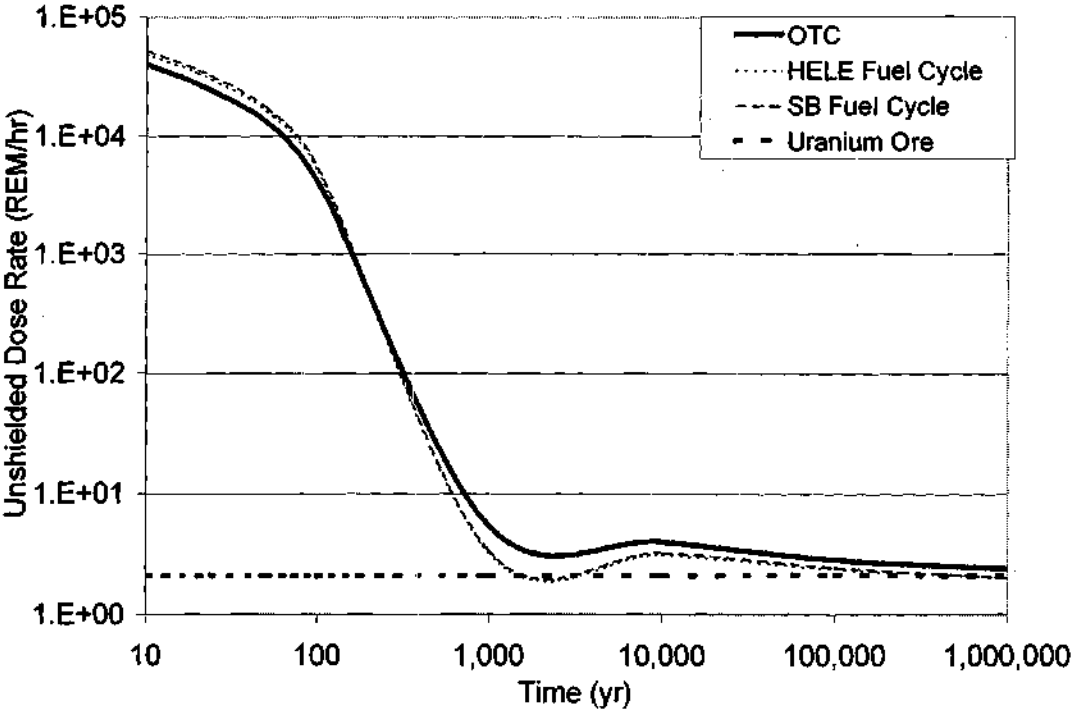

Figure 71 - Unshielded Dose Rate from Photon Emission per MTU for FTWR Scenario (All Waste Streams)

The spontaneous neutron source (SNS) dose rate summary is given in Table 84. Figures 72 and 73 show the SNS dose rate for the repository waste streams and all waste streams, respectively. The SNS dose rate is of the FTWR repository waste is more than an order of magnitude less than the OTC SNF at all times. When all waste streams are considered, the difference is still large, but decreases with time, but is still a factor of 3 at one million years.

Table 84 - Data for FTWR SNS Dose Rate (REM/hr/MTU)

	Time After Discharge (yr)							
Component	0	1	10	100	1,000	10,000	100,000	1,000,000
Uranium Ore	7.8E-05	7.8E-05	7.8E-05	7.8E-05	7.8E-05	7.8E-05	7.8E-05	7.8E-05
Enriched Uranium	1.3E-05	1.3E-05	1.3E-05	1.3E-05	1.3E-05	1.3E-05	1.3E-05	1.3E-05
OTC Repository Waste	6.5E-01	4.2E-01	2.6E-01	1.3E-02	4.0E-03	2.0E-03	7.7E-04	1.5E-04
OTC Repository Waste (w/o U)	6.5E-01	4.2E-01	2.6E-01	1.3E-02	4.0E-03	2.0E-03	7.5E-04	1.4E-04
HELE Repository Waste	5.8E-03	4.9E-03	3.3E-03	4.4E-04	3.0E-04	1.1E-04	3.1E-05	5.1E-06
SB Repository Waste	5.5E-03	4.6E-03	3.2E-03	4.1E-04	2.8E-04	1.0E-04	2.9E-05	4.8E-06
OTC LLW	6.5E-05	6.5E-05	6.5E-05	6.5E-05	6.5E-05	6.5E-05	6.5E-05	6.5E-05
HELE LLW	7.8E-05	7.8E-05	7.8E-05	7.8E-05	7.8E-05	7.8E-05	7.8E-05	7.8E-05
SB LLW	7.8E-05	7.8E-05	7.8E-05	7.8E-05	7.8E-05	7.8E-05	7.8E-05	7.8E-05
OTC	6.5E-01	4.3E-01	2.6E-01	1.3E-02	4.1E-03	2.1E-03	8.3E-04	2.2E-04
HELE Fuel Cycle	5.9E-03	5.0E-03	3.4E-03	5.1E-04	3.8E-04	1.9E-04	1.1E-04	8.3E-05
SB Fuel Cycle	5.6E-03	4.7E-03	3.2E-03	4.9E-04	3.6E-04	1.8E-04	1.1E-04	8.3E-05

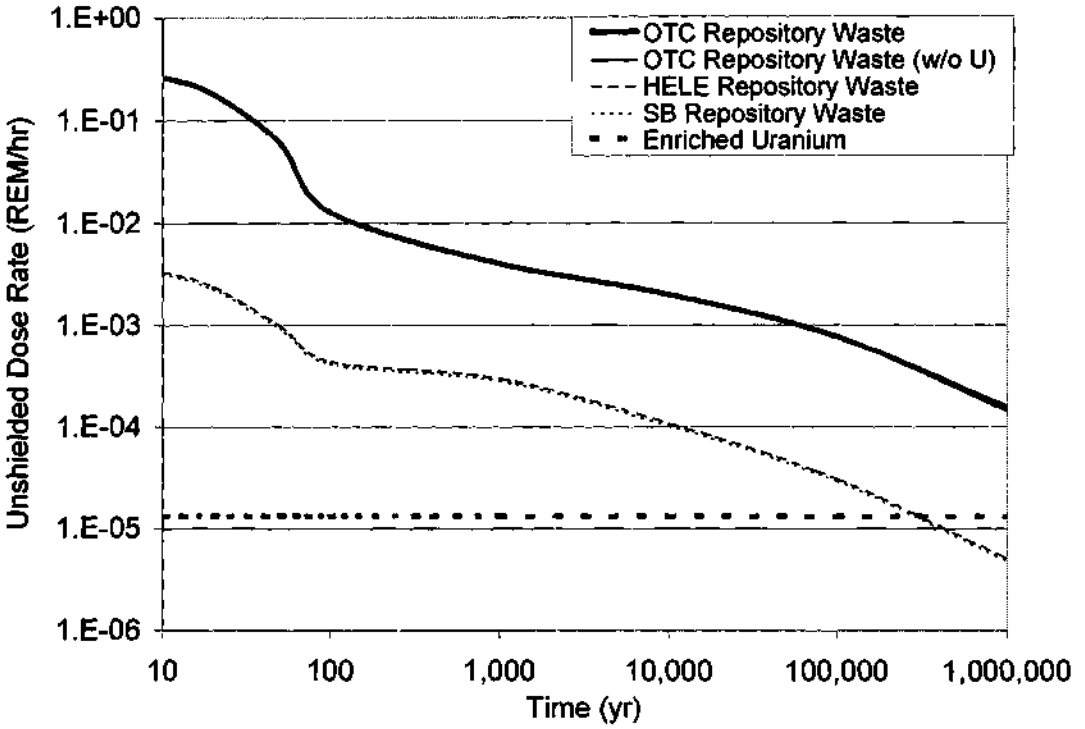

Figure 72 - Unshielded Dose Rate from Spontaneous Neutron Emission per MTU for FTWR Scenario (Repository Waste Streams)

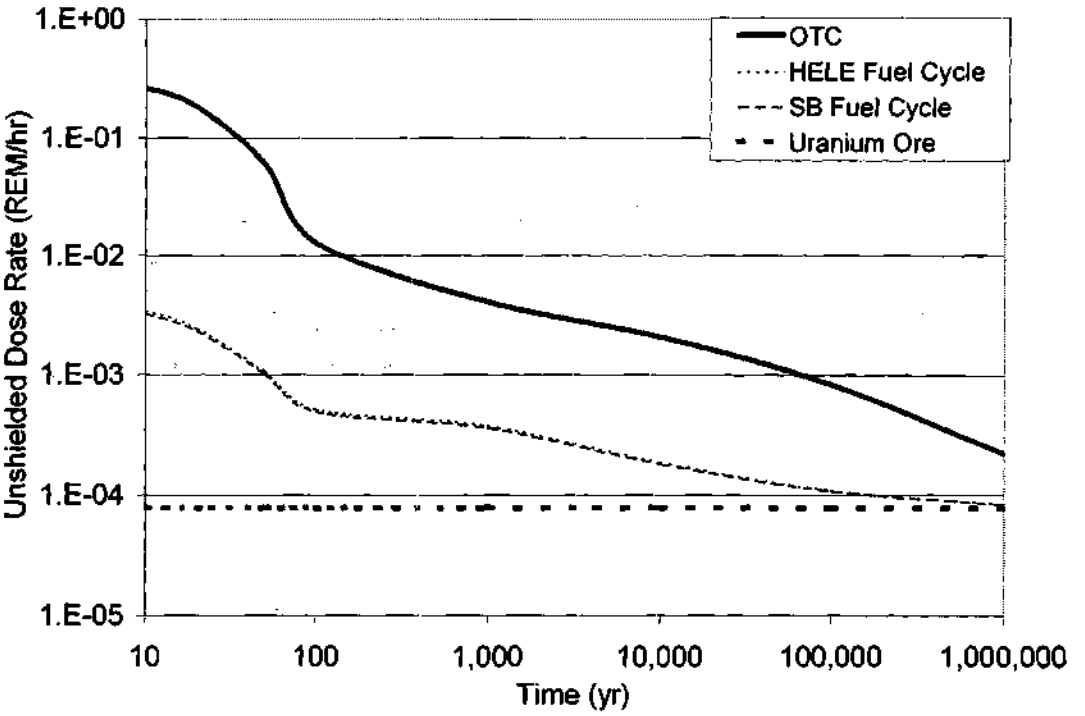

Figure 73 - Unshielded Dose Rate from Spontaneous Neutron Emission per MTU for FTWR Scenario (All Waste Streams)

The α,n dose rate summary is given in Table 85. Figures 74 and 75 show the SNS dose rate for the repository waste streams and all waste streams, respectively. The α,n dose rate for the FTWR repository waste is more than an order of magnitude less than the OTC SNF at all times. When all waste streams are considered, the difference is still large, but decreases with time, but is still a factor of 3 at one million years.

Table 85 - Data for FTWR α,n Neutron Dose Rate (REM/hr/MTU)

	Time After Discharge (yr)							
Component	0	1	10	100	1,000	10,000	100,000	1,000,000
Uranium Ore	1.5E-05	1.5E-05	1.5E-05	1.5E-05	1.5E-05	1.5E-05	1.5E-05	1.5E-05
Enriched Uranium	1.1E-06	1.1E-06	1.1E-06	1.1E-06	1.1E-06	2.0E-06	7.7E-06	3.9E-06
OTC Repository Waste	6.6E-02	1.9E-02	6.9E-03	5.9E-03	1.6E-03	3.5E-04	2.9E-05	1.4E-05
OTC Repository Waste (w/o U)	6.6E-02	1.9E-02	6.9E-03	5.9E-03	1.6E-03	3.5E-04	2.4E-05	1.1E-05
HELE Repository Waste	2.7E-04	1.2E-04	6.9E-05	3.3E-05	5.8E-06	1.3E-06	1.2E-07	4.5E-08
SB Repository Waste	2.6E-04	1.1E-04	6.6E-05	3.1E-05	5.6E-06	1.2E-06	1.2E-07	4.3E-08
OTC LLW	1.4E-05	1.4E-05	1.4E-05	1.4E-05	1.4E-05	1.3E-05	7.7E-06	1.1E-05
HELE LLW	1.5E-05	1.5E-05	1.5E-05	1.5E-05	1.5E-05	1.5E-05	1.3E-05	1.4E-05
SB LLW	1.5E-05	1.5E-05	1.5E-05	1.5E-05	1.5E-05	1.5E-05	1.3E-05	1.4E-05
OTC	6.6E-02	1.9E-02	7.0E-03	5.9E-03	1.6E-03	3.6E-04	3.7E-05	2.5E-05
HELE Fuel Cycle	2.9E-04	1.4E-04	8.4E-05	4.8E-05	2.1E-05	1.6E-05	1.3E-05	1.4E-05
SB Fuel Cycle	2.7E-04	1.3E-04	8.1E-05	4.6E-05	2.0E-05	1.6E-05	1.3E-05	1.4E-05

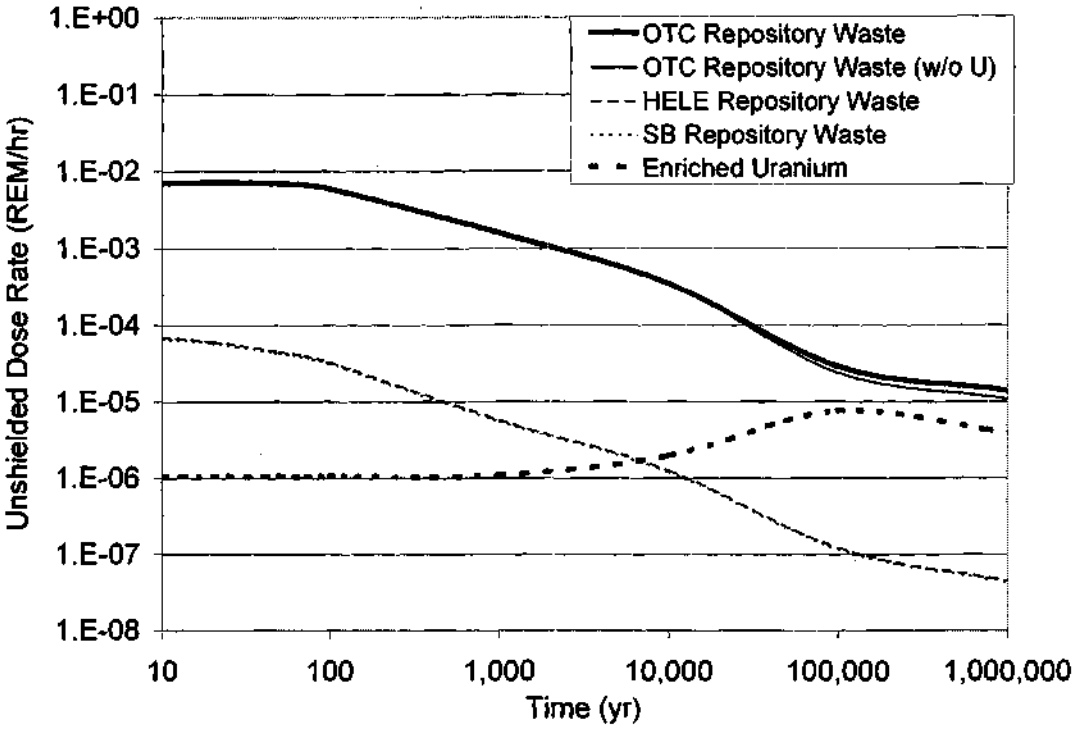

Figure 74 - Unshielded Dose Rate from α,n Neutron Emission per MTU Versus Time for FTWR Scenario (Repository Waste Streams)

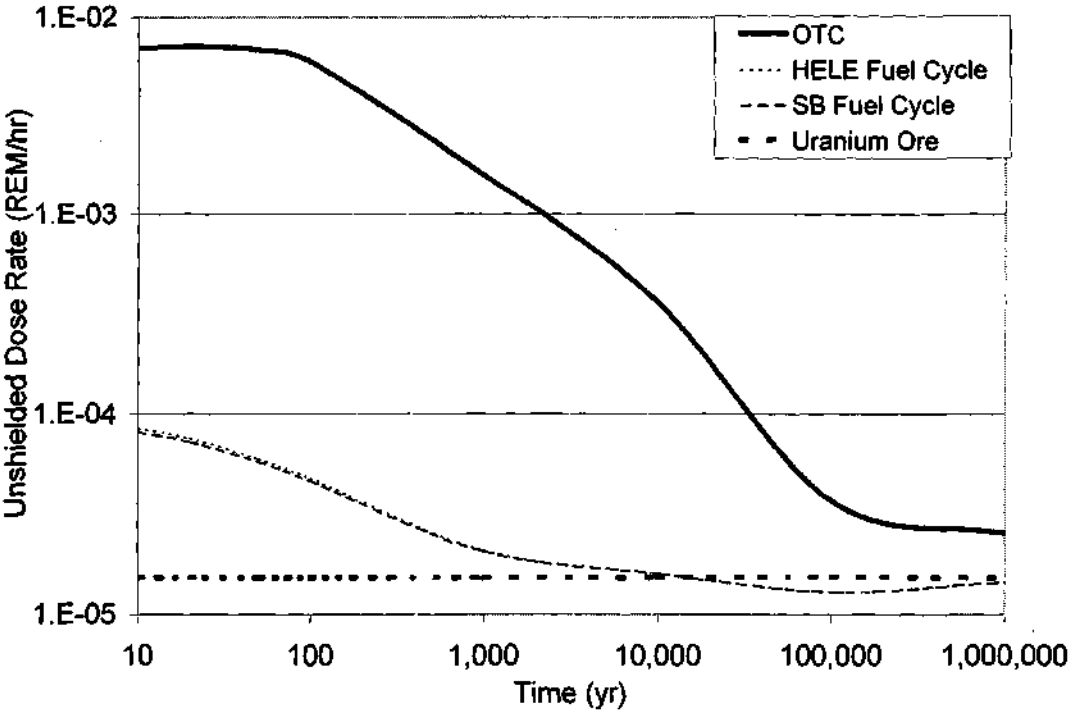

Figure 75 - Unshielded Dose Rate from α,n Neutron Emission per MTU Versus Time for FTWR Scenario (All Waste Streams)

Proliferation Summary

The proliferation parameters are almost identical for the HELE and SB FTWR designs. The FTWR destroys nearly all of the transuranics and the residual transuranics in the waste stream will be very dilute and have a degrade isotopic vector. The FTWR waste will preset very significant technological and physical barriers to the proliferation of nuclear explosives.

The BCM of transuranics and plutonium for the material from the FTWR fuel cycle and the OTC is compared in Tables 86 and 87, respectively. The FTWR increases the BCM at all times, but especially over the first 10,000 years.

Table 86 - FTWR Bare Critical Mass of Transuranics (kg)

	Time after Discharge (yr)						
Fuel Cycle	0	10	100	1,000	10,000	100,000	1,000,000
OTC	16.08	16.21	16.61	17.45	17.64	46.76	74.39
HELE	22.02	22.50	24.47	27.13	26.91	61.91	76.13
SB	21.77	22.26	24.14	26.69	26.55	61.70	76.31

Table 87 - FTWR Bare Critical Mass of Plutonium (kg)

	Time after Discharge (yr)						
Fuel Cycle	0	10	100	1,000	10,000	100,000	1,000,000
OTC	14.62	14.60	14.72	14.61	13.56	23.31	92.84
HELE	20.94	21.41	22.67	23.30	20.87	48.59	91.14
SB	20.61	20.95	22.13	22.72	20.53	47.66	91.54
WGPu	10.70						

The BCM production rates of transuranics and plutonium for the material from the FTWR fuel cycle and the OTC are compared in Tables 88 and 89, respectively. By fissioning nearly all of the transuranics, the FTWR fuel cycle greatly reduces the rate of production of BCM quantities of material. At the current level of LWRs, ~100 GWe, the OTC generates over 2,000 BCM worth of transuranics every years. The FTWR fuel cycle would only produce 4 BCMs per year.

Table 88 - FTWR Bare Critical Mass of Transuranics Production Rate (BCM/GW_e-yr)

	Time after Discharge (yr)						
Fuel Cycle	0	10	100	1,000	10,000	100,000	1,000,000
OTC	22.628	22.402	21.700	19.791	14.582	1.8464	0.6468
HELE	0.041	0.040	0.036	0.030	0.021	0.0040	0.0016
SB	0.043	0.042	0.037	0.031	0.022	0.0042	0.0017

Table 89 - FTWR Bare Critical Mass of Plutonium Production Rate (BCM/GW_e-yr) Cycles

	Time after Discharge (yr)						
Fuel Cycle	0	10	100	1,000	10,000	100,000	1,000,000
OTC	21.218	20.859	19.925	19.099	14.261	1.0986	0.02888
HELE	0.035	0.034	0.030	0.027	0.019	0.0022	0.00019
SB	0.037	0.036	0.032	0.028	0.020	0.0022	0.00019

The radiation barrier for the transuranics and plutonium provided by the waste from the FTWR fuel cycle and the OTC is compared in Tables 90 and 91, respectively. The FTWR waste provides a much larger radiation barrier than the OTC SNF at all times. The radiation barrier of the FTWR waste for more than one million years is greater than the radiation barrier of the LWR SNF feed at any time. This is primarily a result of the very high ratio of fission products to transuranics in the FTWR waste. On a mass basis, there are initially 400 times more fission products than transuranics in the FTWR waste, while in the OTC the ratio is about 3 to 1.

Table 90 - FTWR Transuranic Radiation Barrier (REM/hr/BCM)

	Time after Discharge (yr)						
Fuel Cycle	0	10	100	1,000	10,000	100,000	1,000,000
OTC	3.0E+05	6.0E+04	2.0E+04	6.8E+03	4.7E+00	3.6E+01	6.0E+01
HELE	1.9E+09	4.6E+07	1.2E+07	9.5E+06	1.0E+07	2.6E+07	2.0E+07
SB	1.8E+09	4.5E+07	1.2E+07	9.1E+06	9.5E+06	2.5E+07	1.9E+07

Table 91 - FTWR Plutonium Radiation Barrier (REM/hr/BCM)

	Time after Discharge (yr)						
Fuel Cycle	0	10	100	1,000	10,000	100,000	1,000,000
OTC	3.2E+05	6.4E+04	2.2E+04	7.0E+03	4.8E+00	6.1E+01	1.3E+03
HELE	2.2E+09	5.5E+07	1.4E+07	1.1E+07	1.1E+07	4.8E+07	1.7E+08
SB	2.1E+09	5.3E+07	1.4E+07	1.0E+07	1.0E+07	4.6E+07	1.7E+08

The spontaneous neutron source from one BCM of transuranics and plutonium for the material from the FTWR fuel cycle and the OTC is compared in Tables 92 and 93, respectively. The transuranic and plutonium isotopic vectors of the FTWR materials result in an increase in the SNS. The SNS of the FTWR material is generally larger than the LWR SNF material at discharge from the reactor. The SNS of the transuranics falls with time while that of the plutonium rises with time.

Table 92 - FTWR Transuranic Spontaneous Neutron Source (n/s/BCM)

	Time after Discharge (yr)						
Fuel Cycle	0	10	100	1,000	10,000	100,000	1,000,000
OTC	2.2E+08	1.5E+08	1.2E+07	6.6E+06	4.4E+06	1.3E+07	7.2E+06
HELE	4.6E+09	2.7E+09	4.1E+08	3.4E+08	1.7E+08	2.6E+08	1.0E+08
SB	4.1E+09	2.4E+09	3.2E+08	2.5E+08	1.2E+08	1.7E+08	6.9E+07

Table 93 - FTWR Plutonium Spontaneous Neutron Source (n/s/BCM)

	Time after Discharge (yr)						
Fuel Cycle	0	10	100	1,000	10,000	100,000	1,000,000
OTC	5.8E+06	5.8E+06	5.8E+06	5.3E+06	4.0E+06	2.2E+07	1.6E+08
HELE	2.0E+07	2.0E+07	2.0E+07	1.9E+07	1.6E+07	7.2E+07	1.6E+08
SB	1.9E+07	1.9E+07	2.0E+07	1.8E+07	1.5E+07	7.0E+07	1.6E+08
WGPu	6.0E+05						

The decay heat from one BCM of transuranics and plutonium for the material from the FTWR fuel cycle and the OTC is compared in Tables 94 and 95, respectively. The decay heat of the FTWR transuranics and plutonium are initially more than an order of magnitude higher than the OTC. This differences disappear with time. The FTWR waste still produces twice as much heat as the OTC material at 1,000 years.

Table 94 - FTWR Transuranic Decay Heat (W/BCM)

	Time after Discharge (yr)						
Fuel Cycle	0	10	100	1,000	10,000	100,000	1,000,000
OTC	3.8E+02	3.8E+02	3.2E+02	1.0E+02	3.4E+01	1.3E+01	1.9E+00
HELE	6.9E+03	1.8E+03	9.4E+02	1.9E+02	6.3E+01	1.0E+01	2.6E+00
SB	7.3E+03	1.7E+03	9.2E+02	1.9E+02	6.0E+01	1.0E+01	2.5E+00

Table 95 - FTWR Plutonium Decay Heat (W/BCM)

	Time after Discharge (yr)						
Fuel Cycle	0	10	100	1,000	10,000	100,000	1,000,000
OTC	1.7E+02	1.6E+02	1.1E+02	4.6E+01	3.4E+01	2.2E+01	1.1E+01
HELE	1.1E+03	1.0E+03	6.4E+02	9.9E+01	6.2E+01	1.8E+01	1.1E+01
SB	1.1E+03	9.9E+02	6.2E+02	9.5E+01	6.1E+01	1.8E+01	1.1E+01
WGPu	2.4E+01						

The mass of radioactive waste that would need to be processed to separate one BCM of transuranics and plutonium from the waste from the FTWR fuel cycle and the OTC is compared in Tables 96 and 97, respectively. Nearly 10 times as much FTWR waste would need to be processed. This does not include the dilution of the radioactive waste from the FTWR when it is converted to the final waste form for disposal in the repository. The large mass of material required will provide a significant barrier to proliferation of the final waste forms in the FTWR fuel cycles.

Table 96 - FTWR Transuranic Mass of Radioactive Waste (MT/BCM)

	Time after Discharge (yr)						
Fuel Cycle	0	10	100	1,000	10,000	100,000	1,000,000
OTC	1.4	1.5	1.5	1.7	2.2	17.8	50.7
HELE	9.5	9.8	11.1	13.3	18.9	98.5	242.4
SB	8.8	9.0	10.2	12.2	17.2	89.6	219.3

Table 97 - FTWR Plutonium Mass of Radioactive Waste (MT/BCM)

	Time after Discharge (yr)						
Fuel Cycle	0	10	100	1,000	10,000	100,000	1,000,000
OTC	1.5	1.6	1.6	1.7	2.3	29.9	1,135.7
HELE	11.2	11.6	13.1	14.8	20.6	182.2	2,098.0
SB	10.3	10.6	12.0	13.5	18.8	168.2	2,006.9

Transuranic Inventory

A scenario for deployment of FTWRs was developed. This was intend to identify the level and time frame required to stabilize the transuranic inventory at current levels. The availability of the FTWR was then adjusted to represent the behavior for different levels. The 0% or OTC case shows the transuranic inventory for a 100 GWe of LWRs operated indefinitely. The 60% is the nominal case. One FTWR was placed in service in 2020, followed by one per year beginning in 2030, two per year in 2040, which continued until the inventory stabilized at current levels. Beyond that time, the FTWRs were commission to replace the equilibrium fleet, when they reached the end of life.

Figure 76 shows the inventory of transuranic waste as a function of time for the above scenario, for different assumptions about the availability of the FTWR. The higher the availability in the 'slow growth' and 'fast growth' phases defined above, the earlier in time the maximum inventory occurs and the lower are both the maximum and equilibrium inventories. With the reference availability (60%), the transuranic inventory would begin to decline after 2050 and would approach equilibrium by approximately 2120. The peak FTWR fleet would be approximately 70 FTWRs or over 200 GWth of fission power. The peak transuranic inventory would be approximately 3.7 times current levels. Transmutation will require a

large number of FTWRs over a long period of time. Equilibrium will not be achieved for nearly 125 years. At equilibrium, each FTWR would support approximately 3 GWe of LWRs.

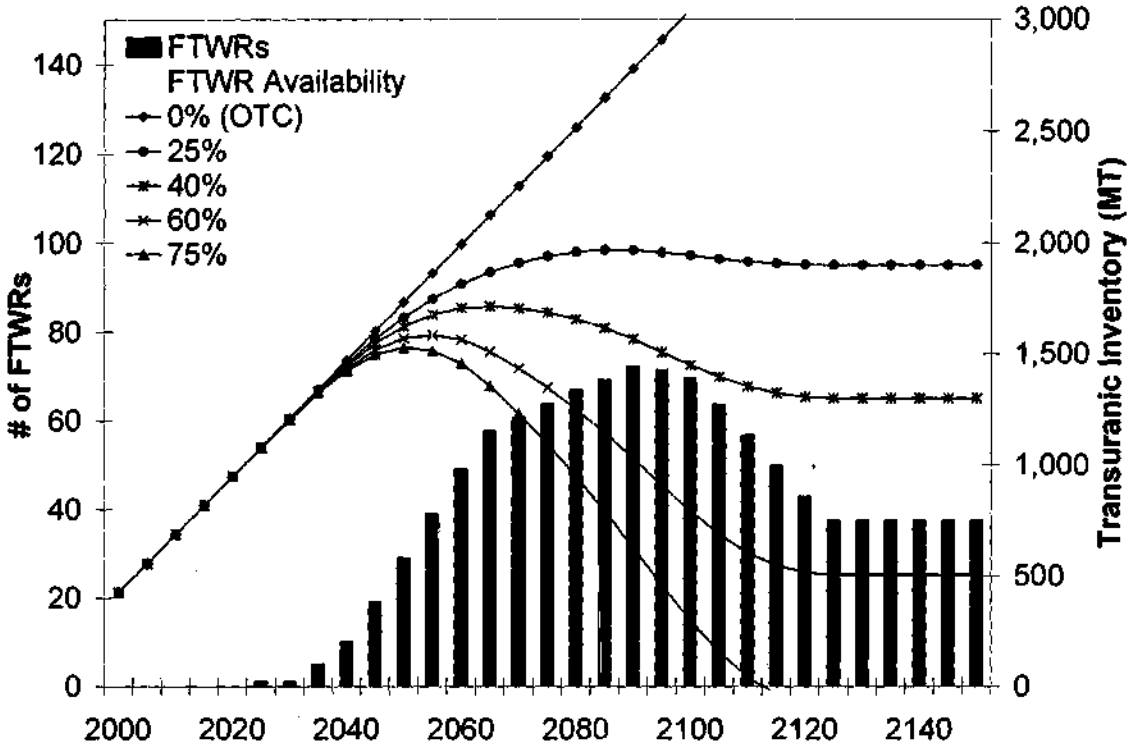

Figure 76 - Transuranic Inventory and FTWR Design

Other FTWR Fuel Cycles & Operational Schemes & Studies

The FTWR is a very flexible design that can be operated under a wide range of operational scenarios. Some of these variables will be analyzed in varying level of details to determine potential improvements in the operation of the FTWR and the impact of changes in the feed stream of transuranics.

Control Rods

Control rods are included in the design as a safety feature for emergency shutdown and to maintain sub-criticality under accident conditions. Control rods could be used to offset reactivity changes resulting from fuel burnup. Figure 77 and 78 show time dependent behavior of the neutron multiplication factor and the fusion power, respectively, for one potential operational scheme where control rods would be utilized.

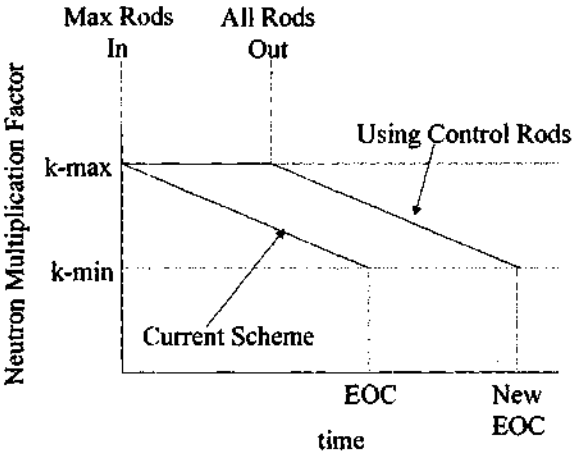

Figure 77 - Neutron Multiplication Factor Operating with Control Rods

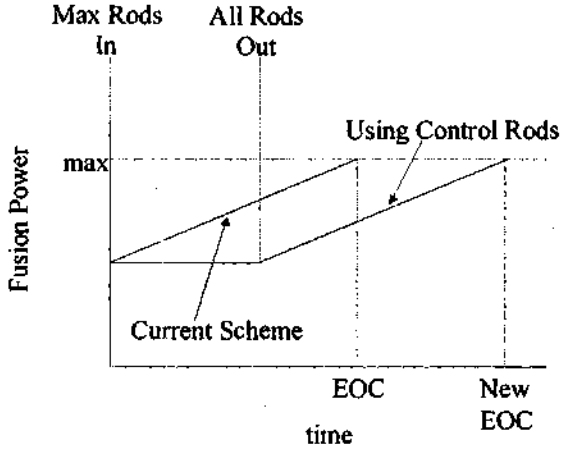

Figure 78 - Fusion Power Operating with Control Rods

This would allow for a larger BOC fuel loading and reduce the cycle average fusion power required to drive the FTWR. In the equilibrium fuel cycle, the fuel loading is near the limit, so the other option would allow for a longer fuel cycle and operation with a reduced number of batches in the core. With the same average discharge burnup (BU_{dis}), going from 5 batches to 4 batches would increase the cycle length by 25%. This would decrease the BOC core average burnup causing a more reactive core compensated by the control rods. The EOC core average burnup would increase by 4%, which would cause

the core to be less reactive and would limit the cycle length increase slightly. Utilizing the control rods would also reduce the shutdown margin.

The BOC cycle average burnup for an N batch core is given by the following equation.

$$BU_{BOC}^{Ave} = \sum_{i=0}^{N-1} \frac{iBU_{dis}}{N^2} = \frac{BU_{dis}}{N^2} \sum_{i=0}^{N-1} i$$

The EOC cycle average burnup for an N batch core is given by the following equation.

$$BU_{EOC}^{Ave} = \sum_{i=1}^{N} \frac{iBU_{dis}}{N^2} = \frac{BU_{dis}}{N^2} \sum_{i=1}^{N} i$$

Power Coastdown

Allowing the fission power to fall after the maximum fusion power has been reached is another way to extend the length of the fuel cycle. This would have essentially the same effect as using the control rods. The difference being that the BOC average burnup and fuel loading would be least affected and the EOC average burnup would be increased. Coasting down would greatly increase the cycle average fusion power and therefore the tritium requirements would be increased dramatically. Figure 79,80, and 81 show time dependent behavior of the neutron multiplication factor, the fusion power, and the blanket power, respectively, for one potential operational scheme where control rods would be utilized.

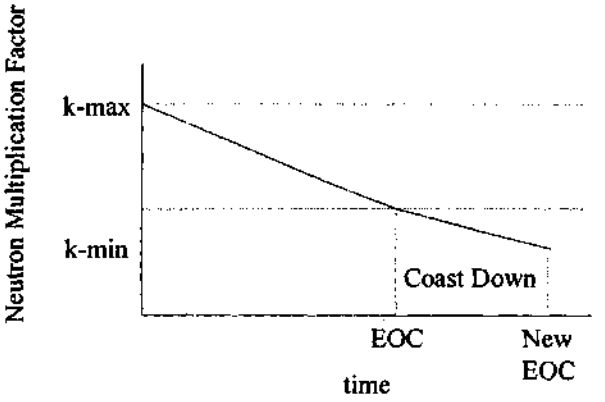

Figure 79 - Neutron Multiplication Factor Operating with End of Cycle Power Coastdown

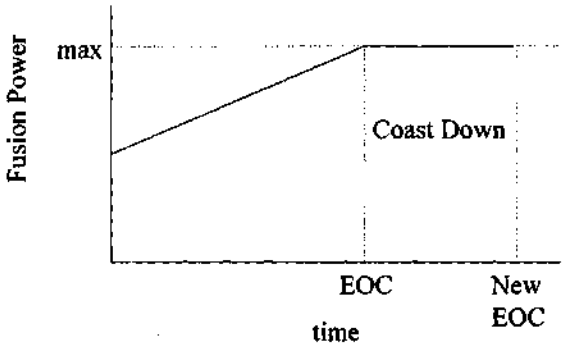

Figure 80 - Fusion Power Operating with End of Cycle Power Coastdown

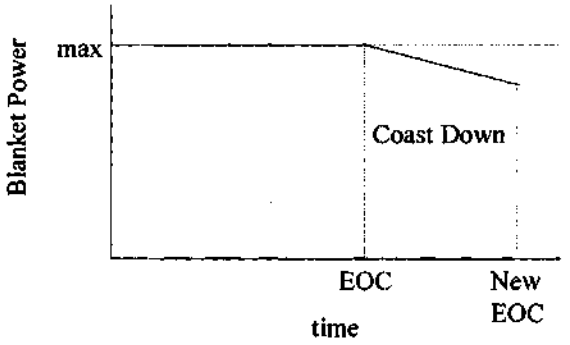

Figure 81 - Blanket Power Operating with End of Cycle Power Coastdown

Integral Burnable Poison Rods

By replacing a number of fuel rods with burnable poison rods, the power within the core could be flattened and the initial loading of heavy metals could be increased allowing for a slightly longer fuel cycle. Because of the fast spectrum, these effects are relatively small. If these rods contained lithium, it would allow for a greater loading of lithium-6 in the core where the majority of the neutrons exist. This would result in greater tritium production and reduce the enrichment of lithium-6 needed outside the core. This would be particularly beneficial in the SB design because it requires greater tritium production and the only location of lithium currently in this design is outside the core. Replacing the fuel rods requires the enrichment to be increased to compensate for the smaller number of fuel rods and the greater absorption. For the equilibrium cycle, the enrichment is at the limit and cannot be increased, so the fuel cycle would have to be shortened to compensate.

Rare Earth Removal

A fraction (5%) of the rare earth element fission products are assumed to follow the transuranics and these isotopes will act as neutron poisons. To estimate the benefit of improving the processing system, the BOC neutron multiplication factor was calculated for a case with the rare earth concentrations assuming perfect chemical separation with none of the rare earth elements being recycled. The neutron multiplication increased 0.002. The fast spectrum limits the impact of the separations on the performance of the FTWR making performance of the chemical separation systems less important neutronically.

Minor Actinides Only

The FTWR cannot be operated only on minor actinides. The neutron multiplication of the FTWR fully loaded with minor actinides from the LWR SNF was calculated. The neutron multiplication factor was 0.446. This is too low for the system to operate efficiently. For systems that would efficiently recycle the plutonium, the minor actinides alone could not be transmuted in the FTWR. Some plutonium would have to be sent along with the minor actinides to achieve a sufficiently high neutron multiplication factor.

Long-Lived Fission Product Transmutation

The feasibility of transmuting the long-lived fission products was studied for the HELE design. Figure 51 shows the layout of this design. The region outside the core contains rods containing either Tc-99, or I-129 and I-127. The technetium was assumed to be in metal form. The iodine was assumed to be in the form of ^{7}LiI. The ratio of I-127 to I-129 was set so that both would be destroyed at rates proportional to there fission yields.

Two cases were evaluated. The first would be a hard spectrum transmutation reactor where the region outside the core is composed of fission product rods surrounded by high-enriched Li17Pb83 coolant. The second would be a softer spectrum transmutation reactor with a buffer region outside the core containing high-enriched Li17Pb83 coolant region followed by fission product rods in a graphite matrix. The goal of the calculations was to determine if Tc-99 and I-129 could be transmuted at a sufficiently high rate to offset the equilibrium production of these isotopes in the LWRs and FTWR. The FTWR still must be tritium self-sufficient. The Li-6 enrichment in the high enriched Li17Pb83 coolant was increased to 90% to verify that sufficient tritium could still be produced.

The harder spectrum fission product transmutation reactor is unable to produce sufficiently high transmutation rates to offset their production rates. The fission products would be transmuted at roughly 50% of the rate they are produced. On the other hand with the graphite moderation, it appears that all criteria can be met. With approximately 5 cm of reflector between the core and the graphite matrix, the neutron multiplication only changed slightly, and the tritium breeding ratio was well above the base value. It appears that about 12 MT of Tc-99 and 2 MT I-129 needs to be loaded to achieve the required transmutation rates.

The SNF inventory that would have to be processed to separate 12 MT of Tc-99 and 2 MT of I-129 is approximately 15,000 MTU and 11,000 MTU, respectively. The FTWR will only require approximately 2,000 MT of SNF for the initial load of transuranics. Over the lifetime of a single FTWR, the transuranic content of approximately 4,000 MTU of SNF will be fissioned. The reaction rates are achievable, but it would take an extremely long time to separate the quantities of fission products needed to achieve these rates. The fission products must be subjected to high thermal fluxes in order to reduce the required inventory to levels consistent with the processing rates of the SNF that will occur for transuranic transmutation. The inventories need to be approximately the quantities that exist in the initial 2,000 MT of SNF that will be processed to create the initial loading of transuranics. This is 1.6 MT of Tc-99 and 0.4 MT of I-129. A factor of 8 reduction for Tc-99 and a factor of 5 reduction for the I-129.

In order to make LLFP transmutation practical, the average thermal flux needs to be increased dramatically, which does not seem to be achievable in the fast spectrum of the FTWR core or in moderated assemblies outside of the core. There are sufficient neutrons available in the FTWR to perform LLFP transmutation, but the hard spectrum suggests that it maybe impractical. The additional of hydrogen moderation was not explored, but appears to be the only possibility to increase the thermal flux and reduce the LLFP loading to reasonable and practical levels.

High Burn LWR SNF

The HELE FTWR calculations were run using the input from the 55 GWd/MTU SNF. This higher burnup may be typical of future discharges from LWRs. The amount of minor actinides increases with burnup and the fraction of Pu-239 decreases with burnup producing a less reactive transuranic feed to the FTWR. The enrichment in the equilibrium cycle needs to be increased by 4% to achieve the same

performance as the feed from the backlog SNF. This would exceed the enrichment limit, but suggests that the high burn LWR SNF would only result in small changes in the operation of the FTWR. In particular, the cycle length would need to be shortened slightly to reduce the enrichment to the limit. Otherwise, the equilibrium FTWR does not appear to be very sensitive to the LWR SNF burnup.

The composition of the equilibrium fuel cycle would have a significantly different composition despite similar performance. The fraction of Pu is virtually unchanged, but it contains significantly higher fractions of Pu-238, Pu-241, and Pu-242, and a significantly lower fraction of Pu-239. The fraction of Np-237 increases significantly. The Am concentration is about the same, but contains more Am-243 and less Am-241 and Am-242m. The concentration of Cm increases by approximately 50%, but is still relatively small. These changes in the isotopic composition will have some impact on the resulting FOMs.

First Cycle FTWR - Fresh TRU

The HELE design was run without recycle to estimate the performance in the first few cycles. Operating under the same conditions, the first cycles of the FTWR will have a reduced inventory of transuranics as expected. The enrichment is reduced from 45% to approximately 38%. The BOC neutron multiplication factor increases from 0.925 to 0.945 and both have an EOC neutron multiplication factor of 0.836. The BOC fusion power decreases from 62 MW to 44 MW because of the increased neutron multiplication. This will reduce the cycle average fusion power and the required tritium production. The operation will change as the fuel is repeatedly recycled, but the changes do not appear to be dramatic. The required lithium enrichment, fuel loading, and BOC fusion power will slowly increase. The cycle length appears as if it will not change significantly.

CHAPTER VIII

ALTERNATIVE FUEL CYCLE COMPARISON

Many transmutation systems have been developed to a fairly advanced level. Several of these systems were evaluated for comparison with the FTWR. The feed composition was adjusted to be consistent with the FTWR and the output was then re-evaluated. The results were compared to evaluate the differences between the FTWR and other transmutation systems.

In order to begin transmuting the backlog of SNF as quickly as possible, utilizing existing commercial reactors in the transmutation mission would seem to be a logical part of the nuclear fuel cycle. Mixed-oxide (MOX) fuel is used in many countries, and the U.S. is currently developing a program to partially destroy, degrade, and secure surplus weapons-grade plutonium by irradiation in MOX fuel in commercial LWRs. By recycling the plutonium in the SNF in existing LWRs, the bulk of the transuranics would be reused, producing more energy, which would offset the production of additional plutonium because less enriched uranium fuel would be used in the production of a given quantity of energy. Plutonium recycle would have other effects, such as the production of more minor actinides, and would constitute a significantly different feed stream to any subsequent transmutation system. The first variant of the OTC scenario that was analyzed was a single recycle of plutonium from the LWR SNF back to the LWRs as MOX fuel

Only a partial reduction of the transuranic inventory results from the single recycle of plutonium as MOX fuel in a LWR. Complete transmutation systems that repeatedly recycle all TRU to ultimately fission all but the small fraction of TRU (which leaks into the waste streams) are required. These systems can be either "non-fertile" systems that contain essentially zero ^{238}U or "fertile" systems containing ^{238}U but designed for conversion ratios substantially less than unity. The actinide composition for these systems, whether fast or thermal, will be very different than existing reactors because of the much higher

concentration of TRU. A much higher fraction of the TRU will be MA, and there will be a much lower concentration of the conventional fissile isotopes such as ^{235}U, ^{239}Pu, and ^{241}Pu.

Although transmutation systems may be based on thermal or fast neutron spectrum reactors, the probability of fission (hence actinide destruction) per neutron absorbed in an actinide is generally larger in a fast spectrum [65]. Sodium cooled, metal fueled fast reactor systems were chosen for comparison with the FTWR. Fuel cycles were analyzed based on the three "transmutation" systems (FTWR, ATWR and IFR) that would completely transmute the TRU in the SNF discharged from the LWRs by repeated reprocessing and recycling. The FTWR, ATWR and IFR use metallic actinide/zirconium fuel and liquid metal coolants and operate with fast neutron spectra. The FTWR and ATWR are sub-critical reactors using non-fertile fuel, and the IFR is a critical reactor using a fertile fuel with a low conversion rate in a critical reactor. The IFR fuel cycle utilizes a small fraction of the depleted uranium to produce the fertile fuel.

MOX Recycle

The recycle of plutonium from the spent nuclear fuel (SNF) of light-water reactors (LWRs) back to the LWRs would significantly reduce the quantity of feed material requiring destruction for a given amount of energy production. By recycling the plutonium back in LWRs, the bulk of the transuranic material is reused and produces more energy and offsets the production of additional plutonium because less enriched uranium fuel would be used in the production of a given quantity of energy. Plutonium recycle will have other effects such as the production of more minor actinides and would constitute a significantly different feed stream to any transmutation system. This scenario looks at a single recycle of plutonium as mixed-oxide (MOX) fuel in LWRs. The basic differences in waste from the once-through cycle (OTC) and the single MOX recycle are quantified. The waste streams are essentially the same as the OTC with the addition of the waste streams resulting from the processing of the enriched uranium spent fuel. These new streams include a high-level waste (HLW) stream that is composed of the fission products and minor actinides, and a low-level waste (LLW) stream that is composed of the separated uranium. Figure 82 shows the fuel cycle for the single MOX recycle.

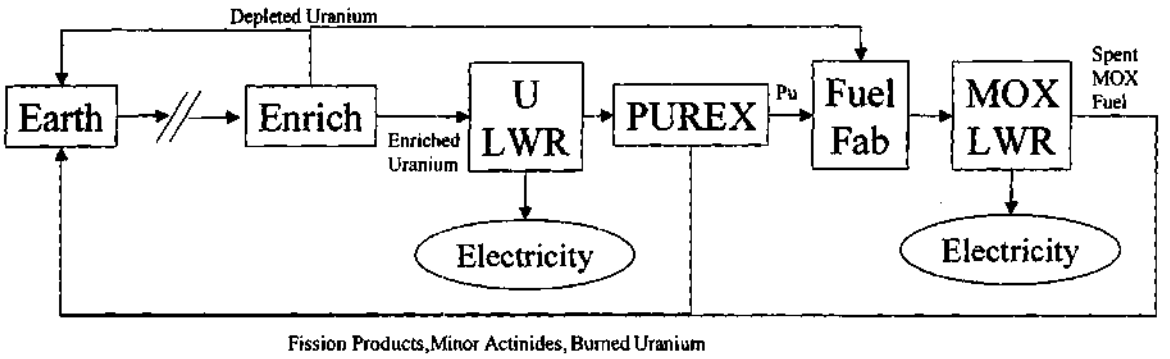

Figure 82 - Single Mixed Oxide Recycle Fuel Cycle

Reference MOX Fuel Characteristics

The reference design was taken from the Working Party on Physics of Plutonium Recycle (WPPPR).[66] This specified all irradiation parameters. Table 98 gives the composition of the MOX fuel. The power density is 38.3 MW/MTHM and the discharge burnup is 50 GWd/MTHM. The original enriched uranium fuel was irradiated to 33 GWd/MTHM. The details of this scenario represent plutonium of existing quality being irradiated to the higher burnup levels that are currently achieved. The MOX fuel is very sensitive to the discharge burnup of the enriched uranium, storage time, and discharge burnup of the MOX fuel. This case looks at the example exactly as used in the WPPPR benchmark, which happens to be consistent with the transmutation system calculations. The reference parameters are summarized in Table 100.

MOX Fuel Cycle Isotopic Data

The depletion of the MOX fuel was simulated using the SAS2H Module of the SCALE 4.4 code package using the parameters from the WPPPR volume II.[66] The SAS2H Module performs 1-D neutron transport analyses of the reactor fuel assembly using the larger unit-cell (assembly) within an infinite lattice. In the SAS2H Module, time dependent nuclide cross sections are used in a point-depletion to determine the burnup-dependent fuel composition used for the next spectrum calculation. The 33-group ENDF/B-V library was used and the cross sections of all isotopes (128 heavy isotopes and 879 fission products) were updated after each transport calculation.

The WPPPR Volume II was a benchmark study for MOX fuel and the calculations were performed by a number of different codes and organizations. The results calculated here were compared with those from the benchmark study for the major actinide isotopes. The results were within the range of results and typically did not differ significantly from the average results. Table 99 compares the concentrations of the major actinide isotopes with the average values calculated in the WPPPR study. The detailed composition of the spent MOX fuel is given in Table 134 in Appendix L.

Table 98 - Composition of MOX Fuel

Isotope	Concentration
U-234	2.4626×10^{17}
U-235	5.1515×10^{19}
U-238	2.0295×10^{22}
Pu-238	2.1800×10^{19}
Pu-239	7.1155×10^{20}
Pu-240	2.7623×10^{20}
Pu-241	1.4591×10^{20}
Pu-242	4.7643×10^{19}

Table 99 - Comparison of Major Actinide Isotope in Discharged MOX Fuel

Isotope	Calculated	WPPPR Average	Error
U234	5.53E-07	4.74E-07	-14%
U235	1.98E-05	1.98E-05	0%
U236	6.40E-06	6.16E-06	-4%
U238	1.95E-02	1.96E-02	0%
Np237	4.06E-06	3.62E-06	-11%
Pu238	2.08E-05	1.97E-05	-5%
Pu239	3.16E-04	2.94E-04	-7%
Pu240	2.36E-04	2.42E-04	2%
Pu241	1.52E-04	1.51E-04	-1%
Pu242	9.69E-05	9.43E-05	-3%
Am241	1.18E-05	1.05E-05	-11%
Am242m	3.53E-07	2.18E-07	-38%
Am243	3.08E-05	2.69E-05	-12%
Cm242	3.16E-06	3.17E-06	1%
Cm243	1.52E-07	1.32E-07	-13%
Cm244	1.85E-05	1.69E-05	-9%
Cm245	1.71E-06	1.78E-06	4%

Integral Fast Reactor

The integral fast reactor (IFR) concept has been well studied. This system is intermediate between a sub-critical fast reactor and the critical thermal light water reactors. This system will burn all the transuranics, but the inclusion of uranium reduces the rate at which this occurs. The IFR fuel cycle is nearly identical to the FTWR fuel cycle. The sub-critical FTWR is replaced with the critical IFR designed to burn transuranics (conversion rate <1). A small fraction of the depleted uranium is blended with the transuranics from the LWR to form the fuel for the IFR. Figure 83 shows the IFR fuel cycle.

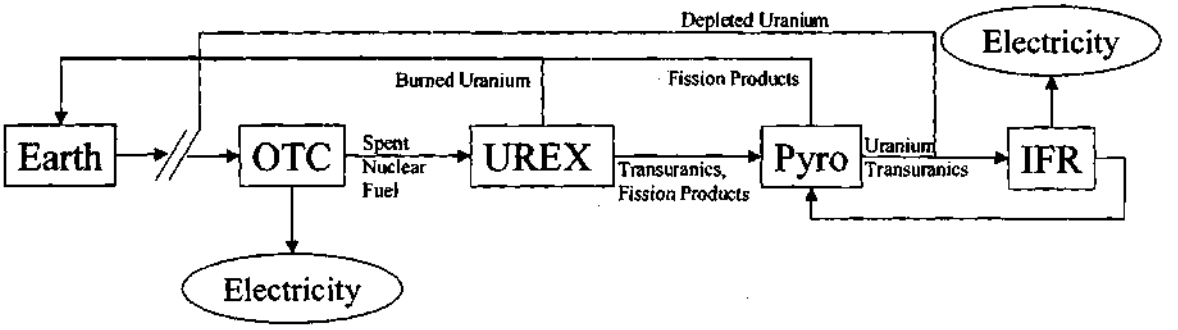

Figure 83 - Integral Fast Reactor Fuel Cycle

Reference IFR Characteristics

The IFR[4,67] is a 840 MW_{th} sodium-cooled, metal fueled, critical reactor. The IFR is a cylindrical reactor with a radius of 161 cm, and a fuel height of 48 cm. The height of the IFR is reduced to increase leakage and reduce the conversion rate. The fuel is the U/TRU-10Zr metal alloy with a charge of approximately 72% U and 28% TRU. The fuel is clad with a steel similar to HT-9. Additional details of the IFR design are provided in Ref. 67.

The IFR design and fuel cycle were developed for SNF feed from an advanced light-water reactor (ALWR) operated to 50 GWd/MTU. For the purposes of this paper, the representative SNF given in Table 101 was used in this analysis. No other changes were made to the reactor design or fuel cycle. The IFR reactor operates on a 310 day cycle with a 7 batch refueling scheme. The reference parameters are summarized in Table 100.

The BOC fuel loading for a single IFR reactor is 13.89 MT of heavy metal of which 3.78 MT are TRU. The heavy metal loading for the IFR given in Ref. 4 was 13.89 for the ALWR SNF feed. The discharge TRU burnup calculated in this analysis was 18.0% compared with 18.6% for the ALWR feed. The burnup reactivity loss calculated in this analysis was 2.08% compared with 2.34% for the ALWR feed. The TRU charge enrichment was 28.0% in this analysis compared with 32.4% for the ALWR feed. In this analysis 20% less TRU is fissioned in each pass through the reactor than was calculated for the ALWR feed. The conversion rate in this analysis is 0.59 compared with 0.51 for the ALWR feed. The TRU reduction is 99.44% for this analysis compared with 99.5% for the ALWR feed. Overall, there are some significant differences with the results calculated in Ref. 4 because of the different SNF feeds, but better

optimization for the SNF feed used in this analysis should not significantly effect the conclusions of this study.

IFR Fuel Cycle Isotopic Data

The FTWR, ATWR and IFR fuel cycles were analyzed using the REBUS-3 fuel cycle analysis code, [68] in which the performance of the external cycle is explicitly modeled. The same techniques were used to produce the multigroup cross sections and perform the neutronics calculations for the FTWR, ATWR and IFR. The neutronics calculations were 2-D discrete ordinates (S8) transport calculations using the DANT[69] code with material-dependent multi-group cross section libraries. The transport calculations were source-driven calculations for the FTWR and eigenvalue calculations for the ATWR and IFR. Material-dependent multi-group libraries based on the ENDF/B-V.2 nuclear data library processed using the MCC-2[70] and SDX[71] codes for a 34 group energy structure were created for each of the reactors. The reactors were modeled using R-Z geometry models.

The detailed composition of the spent IFR fuel is given in Table 135 in Appendix M.

Accelerator Transmutation of Waste

The accelerator transmutation of waste fuel cycle is identical to the FTWR fuel cycle. The FTWR is replaced with a sub-critical reactor driven by a spallation neutron source (ATWR). A single large proton accelerator will operate multiple ATWRs. The FTWR was based on preliminary design studies at Argonne National Laboratory of lead bismuth eutectic (LBE)[54] and sodium[62] cooled designs of the ATWR.

Reference ATWR Characteristics

The ATWR[4,72] is an 840 MW_{th} sodium-cooled, metal fueled, sub-critical reactor driven by an accelerator spallation neutron source being studied as part of the U.S. Department of Energy Advanced Accelerator Applications Program. The ATWR design consists of a central lead-bismuth eutectic target/buffer surrounded by 132 hexagonal fuel assemblies. The sub-critical reactor is an annulus with an inner radius of 37 cm, an outer radius of 105 cm, and a fuel height of 113 cm. The fuel is the TRU-40Zr

metal alloy clad with a steel similar to HT-9. Additional details of the ATWR design are provided in Ref. 72.

The ATWR design and fuel cycle were developed for SNF feed from an advanced light-water reactor (ALWR) operated to 50 GWd/MTU. The composition of the ALWR SNF is given in Table 101. For the purposes of this paper, the representative SNF given in Table 101 was used in this analysis. No other changes were made to the reactor design or fuel cycle. The ATWR operates on a 140 day cycle with two fuel zones operating on a 7 and 8 batch refueling scheme.

The BOC fuel loading for a single ATWR with the representative SNF feed is 2.44 MT of heavy metal, of which 2.39 MT are TRU and the rest a small quantity of uranium, mostly ^{234}U that has accumulated as a result of radioactive decay. The heavy metal loading for the ATWR given in Ref. 4 was 2.71 for the ALWR SNF feed. Other parameters were very similar for the two SNF feeds. The discharge TRU burnup calculated in this analysis was 31.0% compared with 29.2% for the ALWR feed. The burnup reactivity loss calculated in this analysis was 4.30% compared with 4.14% for the ALWR feed. The TRU charge enrichment was 98.4% in this analysis compared with 98.5% for the ALWR feed. Overall, the results suggest that differences in the SNF feed will have some impact on the design of the ATWR and/or the fuel cycle, but these would not be expected to be dramatic or impact the conclusions of this study.

ATWR Fuel Cycle Isotopic Data

The FTWR, ATWR and IFR fuel cycles were analyzed using the REBUS-3 fuel cycle analysis code, [73] in which the performance of the external cycle is explicitly modeled. The same techniques were used to produce the multigroup cross sections and perform the neutronics calculations for the FTWR, ATWR and IFR. The neutronics calculations were 2-D discrete ordinates (S8) transport calculations using the DANT[74] code with material-dependent multi-group cross section libraries. The transport calculations were source-driven calculations for the FTWR and eigenvalue calculations for the ATWR and IFR. Material-dependent multi-group libraries based on the ENDF/B-V.2 nuclear data library processed using the MCC-2[75] and SDX[76] codes for a 34 group energy structure were created for each of the reactors. The reactors were modeled using R-Z geometry models.

The detailed composition of the spent ATWR fuel is given in Table 136 in Appendix N.

Table 100 - Fuel Cycle Parameters

Design	OTC	MOX	FTWR	ATWR	IFR
Reactor Power Level (MW)	3000	3000	3000	840	840
Cycle Length (Effective Full Power Days)	276	435	564	140	310
Fuel Batches	3	3	5	7 / 8	7
BOC Neutron Multiplication Factor			0.925	0.970	1.021
EOC Neutron Multiplication Factor	1.000	1.000	0.836	0.927	1.000
BOC Heavy Metal Loading (MT)	75	75	24.32	2.44	13.89
BOC TRU Loading (MT)	0.35	3.88	23.27	2.39	3.78
Reactor Heavy Metal Discharge Burnup	3.3%	5.3%	29.0%	31.0%	12.7%
Charge TRU Enrichment	0%	5.60%	96.3%	98.4%	28.0%
Reactor Discharge TRU Burnup	N/A	25.4%	29.0%	31.0%	18.0%

Table 101 - Compositions of Transuranic Feed From Spent Nuclear Fuel

Isotope	YMP Inventory [35]	Representative SNF	ALWR SNF [4]
U235	0.004%	0.004%	0.002%
U236	0.002%	0.002%	0.002%
U238	0.419%	0.423%	0.325%
Np237	5.601%	4.313%	6.641%
Pu238	1.725%	1.236%	2.749%
Pu239	52.172%	53.901%	48.652%
Pu240	21.085%	21.231%	22.980%
Pu241	3.540%	3.870%	6.926%
Pu242	4.623%	4.677%	5.033%
Am241	9.431%	9.184%	4.654%
Am242M	0.019%	0.007%	0.019%
AM243	1.199%	1.021%	1.472%
Cm243	0.003%	0.002%	0.005%
Cm244	0.156%	0.116%	0.496%
Cm245	0.019%	0.013%	0.038%
Cm246	0.002%	0.001%	0.006%

Note: 0.005% of uranium and 99.9% of transuranics from spent nuclear fuel
YMP - Yucca Mountain Project average spent nuclear fuel;
Representative SNF - spent nuclear fuel used in this analysis;
ALWR SNF - advanced light-water reactor spent nuclear fuel.

Fuel Cycle Comparison

Energy Production and Mass Flow

The energy production and mass flows in the different fuel cycles and quantified in this section. For the FTWR, ATWR and IFR transmutation fuel cycles, values are given for the equilibrium conditions.

The capacity factor and thermal-to-net electrical conversion efficiency will have a significant effect on the performance and net cost of the transmutation system, if electricity is sold. The FTWR and ATWR will both require additional electricity (relative to LWRs and the IFR) for the systems required to operate the neutron source. The higher operating temperatures in the liquid metal cooled FTWR, ATWR and IFR should improve conversion efficiency relative to water-cooled reactors. The capacity factors initially would be greater for LWRs than for IFRs, which in turn would be greater than for FTWRs or ATWRs. Rather than introduce assumptions about these uncertain parameters, the analysis is based on effective full power operation and thermal energy generation. The results are summarized in Table 102.

The OTC generated 0.0903 GW_{th}-yr/MTU (33,000 MWd/MTU). The single recycle of Pu in MOX fuel produces an additional 0.025 GW_{th}-yr/MTU. The repeated recycle of the TRU in the FTWR and ATWR produce an additional 0.0298 GW_{th}-yr/MTU and 0.0315 GW_{th}-yr/MTU, respectively. Even though the FTWR and ATWR fission essentially the same mass of TRU, differences in neutron spectra and fuel cycles result in different equilibrium fuel compositions and fission rates for the various isotopes. As a result, the ATWR produces slightly more fission energy per gram than the FTWR, which produces small differences in a number of parameters normalized to total energy production. The repeated recycle of the TRU in the fertile-fuel IFR increases energy production by 0.075 GW_{th}-yr/MTU, which is roughly 2.5 times the increase in the FTWR or ATWR, because of the fast fission of ^{238}U and the subsequent fission of transuranics produced by neutron capture in ^{238}U.

The total energy production is the integral energy production resulting from one MTU during all phases of the fuel cycle. The total energy production includes the 0.0903 GW_{th}-yr/MTU from the initial irradiation in the LWR plus the additional energy produced by the transmutation of the TRU from the SNF. The IFR fuel cycle produces a total of 0.165 GW_{th}-yr/MTU, which is nearly double the total energy production of 0.0903 GW_{th}-yr/MTU for the OTC. A single recycle of Pu in MOX fuel and the repeated

recycle of TRU in the FTWR and ATWR increase the total energy production by roughly one third over the OTC to approximately 0.12 GW_{th}-yr/MTU for all three fuel cycles.

The OTC SNF has a TRU concentration of 11 kg/MTU. The TRU concentration in the waste from a transmutation fuel cycle is a function of the separation efficiency and the discharge TRU burnup in each pass through the transmutation reactor. The single recycle of Pu in MOX fuel would reduce the TRU concentration by nearly 3 kg/MTU, but 8 kg/MTU would remain. Of the original 11 kg/MTU of TRU, 37 g/MTU from the ATWR fuel cycle and 38 g/MTU from the FTWR fuel cycle will leak into the waste streams (the small difference results from the difference in discharge TRU burnup). The IFR fuel cycle waste streams contain a TRU concentration of 62 g/MTU. Because the IFR operates at about half the discharge TRU burnup of the FTWR and ATWR, a higher fraction of the TRU is recycled after each pass through the IFR, resulting in more TRU leaking into the waste stream. The mass flow of the major actinide groups is given in Table 103 and the totals in the different waste streams are summarized in Table 104.

The system TRU burnup is defined as the reduction in TRU concentration relative to the TRU concentration in the SNF feed. The single recycle of Pu in MOX fuel results in a system TRU burnup of 25%. If separations were perfect, repeated recycle of the TRU would result in a 100% system TRU burnup, regardless of reactor design. The IFR fuel cycle has a system TRU burnup of 99.4%, which is slightly less than the 99.7% system TRU burnup for the ATWR and FTWR fuel cycles. Improved separations efficiencies will improve the system TRU burnup for all designs, but the system TRU burnup of the fertile fuel will always lag because of a lower TRU discharge burnup.

The reference OTC scenario TRU discharge rate is 122 kg/GW_{th}-yr. This is reduced by 41% by a single recycle of Pu in MOX fuel as a result of the reduced TRU concentration and the increased energy production. Repeatedly recycling TRU from the SNF in a FTWR, ATWR or IFR fuel cycle reduces the TRU discharge rate by 99.7% or more. Despite the greater energy production in the IFR fuel cycle, the IFR fuel cycle TRU discharge rate of 374 g/GW_{th}-yr is higher than the TRU discharge rates of 316 g/GW_{th}-yr and 303 g/GW_{th}-yr for the FTWR or ATWR fuel cycles, respectively, because of the production of TRU in the fertile IFR fuel.

The average fission energy for actinides is approximately 1 MWd/g. This limits the maximum rate of TRU reduction to approximately 1 gram for each MWd of thermal energy, regardless of reactor design.

Utilization of a fertile fuel will increase the energy generated per unit reduction of the TRU inventory, because of the fast fission of ^{238}U and the subsequent fission of transuranics produced by neutron capture in ^{238}U. The non-fertile ATWR and FTWR both operate at the maximum rate, with a small difference resulting primarily from differences in the fission rates of the various isotopes. Transuranic reduction in the IFR or in a LWR using MOX fuel will produce 2.46 MWd/g or 3.33 MWd/g, respectively, which reduces the TRU inventory at significantly below the maximum rate. The IFR and the MOX LWR are operating at conversion rates of 0.6 and 0.7, respectively. Reduction of the conversion rate to 0.5 would reduce the energy generated to 2 MWd/g for transuranic reduction, which is probably achievable, but would still reduce the TRU inventory at half the rate of the non-fertile FTWR and ATWR. Further recycle in MOX fuel would lead to further increases in the total energy production and reductions in the sub-critical reactor energy production.

The inventory of discharged SNF is estimated to be over 47,000 MTU by the end of 2002. Over 14,000 GW_{th}-yr of operation will be required to destroy the TRU inventory in the accumulated inventory of discharged SNF. The current discharge rate for SNF is over 2000 MTU/yr. This would require over 60 GW_{th} of transmutation reactor capacity to stop the growth in the discharge SNF inventory. Operations using fertile fuel with a conversion rate of 0.5 would double these requirements.

A common way to express the efficiency of a transmutation system is the ratio of the LWR thermal power capacity to the required transmutation reactor thermal power capacity to transmute all TRU from LWR SNF. This "support ratio" would need to be adjusted for the relative capacity factors. The ATWR and FTWR will support LWRs producing three times the FTWR or ATWR thermal power. The IFR would support LWRs producing 1.2 times its thermal power. Reducing the conversion rate to 0.5 would increase the IFR support ratio to 1.5, which is still half that of the non-fertile ATWR and FTWR. The transmutation reactors would be a very large fraction of the nuclear generating capacity, about 25% for FTWR and ATWR systems and about 40-45% for the IFR system.

The feed rate is the rate SNF from the LWR is processed by the transmutation systems and is primarily a function of the TRU concentration in the SNF, the conversion rate, and system TRU burnup. There is only a small difference between the non-fertile FTWR and ATWR systems. The FTWR and ATWR fuel cycles would process the LWR SNF at a rate of 34 MTU/GW_{th}-yr and 32 MTU/GW_{th}-yr,

respectively. The fertile IFR would process SNF at the much lower rate of 13.3 MTU/GW_{th}-yr . Utilizing existing technology to recycle Pu once in MOX fuel would result in the highest processing rate, 40 MTU/GW_{th}-yr, allowing the SNF that has been accumulating to move into the transmutation system most rapidly, but a significant quantity of MA and spent MOX fuel would accumulate and would need to be sent to another transmutation system. For essentially total actinide destruction, the non-fertile FTWR and ATWR would process the SNF at the highest possible rates, but their operation would probably require the longest lead times for deployment and achievement of high-capacity operation.

The first core loading represents a significant logistics problem, because the initial startup of the transmutation systems would require a large quantity of SNF to be processed to produce fuel for at least the first full core loading and first reload. After recycled material from the previously irradiated fuel is available, a much smaller quantity of SNF will be required for makeup of the fissioned TRU. The equilibrium TRU loading can be used to estimate the quantity of SNF that will need to be processed for the first core loading. The actual value would be somewhat less than the equilibrium loading because the SNF TRU has a higher concentration of fissile isotopes than the recycled transmutation reactor fuel and there will not be any FP present from the fuel that was in the reactor during previous cycles. The FTWR has an equilibrium BOC TRU loading of 7.8 MT/GW_{th}, requiring 705 MTU/GW_{th} of SNF for the initial core loading. The equilibrium ATWR operates with a much lower TRU loading of 2.9 MT/GW_{th}, requiring 259 MTU/GW_{th} of SNF for the initial core loading. The equilibrium IFR operates at an intermediate TRU loading of 4.5 MT/GW_{th}, requiring 409 MTU/GW_{th} for the initial core loading. The MOX fuel can be interspersed with enriched uranium fuel and the entire first core of MOX fuel is not required if existing reactors are utilized.

If the MOX fuel is assumed to be loaded into existing reactors that would have otherwise produced SNF, the use of MOX fuel offsets the production of new sources of Pu. One MTU of SNF produces enough Pu for approximately 0.2 MT of MOX fuel. In other words, reprocessing one MTU of SNF offsets the production of 0.2 MTU of SNF. If the MOX fuel reduces the TRU inventory by 25% and the EU loading is reduced by 17%, the effective TRU reduction from a single MOX recycle is approximately 38%. Under these conditions, MOX recycle would reduce TRU inventories without increasing nuclear energy production.

The use of fertile fuel increases the required capacity of the transmutation system and the quantity of TRU in the waste streams. The use of MOX fuels make modest reductions in the TRU inventory and could offset new production of TRU. Non-fertile fuels transmute TRU at nearly the same rate regardless of the system. Differences in discharge burnup, electrical efficiencies, capacity factor, and ultimately cost will be distinguishing factors between these systems.

Table 102 - Energy Production and Mass Flow

Fuel Cycle	OTC	MOX	FTWR	ATWR	IFR
Reactor Energy Production (GW_{th}-yr/MTU)	0.0903	0.0250	0.0298	0.0315	0.0749
System Energy Production (GW_{th}-yr/MTU)	0.0903	0.1153	0.1202	0.1219	0.1653
System TRU Concentration (g/MTU)	11,005	8,264	38	37	62
System TRU Discharge Rate (g/GW_{th}-yr)	121,805	71,666	316	303	374
System TRU Burnup	N/A	24.9%	99.65%	99.67%	99.44%
SNF Feed Rate (MTU/GW_{th}-yr)	11.1	40.1	33.5	31.7	13.3
TRU Energy Generation (MWd/g)	N/A	3.33	0.96	0.99	2.46
Support Ratio (GW_{th} LWR/GW_{th})	N/A	3.64	3.05	2.88	1.21
First Core SNF Requirements (MTU/GW_{th})	N/A	118	705	259	409

Table 103 - Data for Actinide Mass Flow (MT/MTU)

Source	Component	Pu	TRU	MA	U
Uranium	Ore				5.77E+00
	Tails				8.32E-11
	Natural Uranium (NU)				5.77E+00
	Depleted Uranium (DU)				4.77E+00
	Enriched Uranium (EU)				1.00E+00
OTC	Reference SNF	1.04E-02	1.10E-02	6.46E-04	9.55E-01
MOX	Plutonium Feed	1.04E-02	1.04E-02		
	Irradiated EU Waste				9.55E-01
	HLW (MA & FP)	5.18E-07	6.46E-04	6.46E-04	4.77E-05
	DU Feed				4.60E+00
	Fresh MOX Fuel	1.04E-02	1.04E-02		4.60E+00
	Spent MOX Fuel	6.92E-03	7.72E-03	8.06E-04	1.67E-01
FTWR (HELE)	Transuranic Feed	9.45E-03	1.11E-02	1.63E-03	4.77E-05
	Irradiated EU Waste				9.55E-01
	Pyro A Waste	9.45E-06	1.11E-05	1.63E-06	4.77E-08
	Fresh Fuel	3.17E-02	3.84E-02	6.79E-03	1.46E-03
	Spent Fuel	2.19E-02	2.69E-02	5.04E-03	1.38E-03
	Pyro B Waste	2.19E-05	2.69E-05	5.04E-06	1.38E-06
ATWR	Transuranic Feed	9.45E-03	1.11E-02	1.63E-03	4.77E-05
	Irradiated EU Waste				9.55E-01
	Pyro A Waste	9.45E-06	1.11E-05	1.63E-06	4.77E-08
	Fresh Fuel	3.11E-02	3.74E-02	6.28E-03	5.95E-04
	Spent Fuel	2.12E-02	2.59E-02	4.61E-03	5.16E-04
	Pyro B Waste	2.12E-05	2.59E-05	4.61E-06	5.16E-07
IFR	Transuranic Feed	9.45E-03	1.11E-02	1.63E-03	4.77E-05
	Irradiated EU Waste				9.55E-01
	Pyro A Waste	9.45E-06	1.11E-05	1.63E-06	4.77E-08
	DU Feed				2.18E-02
	Fresh Fuel	5.45E-02	6.18E-02	7.31E-03	1.59E-01
	Spent Fuel	4.51E-02	5.07E-02	5.60E-03	1.42E-01
	Pyro B Waste	4.51E-05	5.07E-05	5.60E-06	1.42E-04

Table 104 - Actinide Mass Flow Summary (MT/MTU)

	Fuel Cycle	Pu	TRU	MA	U
HLW	OTC	1.04E+04	1.10E+04	6.46E+02	9.55E+05
	MOX	6.92E+03	8.37E+03	1.45E+03	1.67E+05
	FTWR (HELE)	3.13E+01	3.80E+01	6.67E+00	1.42E+00
	ATWR	3.07E+01	3.69E+01	6.24E+00	5.64E-01
	IFR	5.45E+01	6.18E+01	7.23E+00	1.42E+02
LLW	OTC				4.77E+00
	MOX				1.13E+00
	FTWR (HELE)				5.73E+00
	ATWR				5.73E+00
	IFR				5.71E+00
All Waste	OTC	1.04E+04	1.10E+04	6.46E+02	9.55E+05
	MOX	6.92E+03	8.37E+03	1.45E+03	1.67E+05
	FTWR (HELE)	3.13E+01	3.80E+01	6.67E+00	7.15E+00
	ATWR	3.07E+01	3.69E+01	6.24E+00	6.29E+00
	IFR	5.45E+01	6.18E+01	7.23E+00	1.48E+02

Toxicity

The time dependent toxicity of the unirradiated enriched uranium from which the LWR fuel is fabricated will be used as a benchmark of the HLW toxicity. The uranium ore mined for fuel fabrication will be used as a benchmark for the toxicity of all waste streams. The uranium ore is at equilibrium and would not vary over the one million year time frame if left in the ground. However, the uranium ore is split into the mill tails and natural uranium. The natural uranium is further divided into the EU and DU streams. Initially, nearly all of the toxicity is in the mill tails, which remains true for nearly 100,000 years. Slowly the daughter products will build to equilibrium levels and the toxicity will be determined by the ^{238}U concentration, the bulk of which is in the DU stream. The toxicity data is given in Table 105 and the totals in the different waste streams are summarized in Table 106.

Figure 84 shows the toxicity concentration in the HLW from the OTC SNF, from the single recycle of the Pu from the SNF in MOX fuel, and from repeatedly recycling TRU from the SNF in a FTWR, ATWR or IFR fuel cycle. The unirradiated EU is shown to illustrate the effect of irradiation and the separation and transmutation. The unirradiated EU will increase in toxicity by more than two orders of magnitude as its radioactive daughters build up, reaching a maximum at approximately 100,000 years, and then decline from the peak toxicity as the ^{234}U concentration falls from its enriched levels. The toxicity of the HLW from the OTC and from the single recycle of Pu in MOX fuel is reduced to the level of the unirradiated EU toxicity after about 100,000 years. The single recycle of Pu in MOX fuel has no significant effect on toxicity up to about 1,000 years and causes only a small reduction at later times. Recycling the TRU repeatedly in the FTWR, ATWR and IFR fuel cycles reduces the toxicity of the HLW below that of the unirradiated EU in about 6,000 to 8,000 years. Beyond 100,000 years, the separation of the irradiated enriched uranium from the SNF has a significant effect on the HLW toxicity because the recovered uranium is sent to a LLW facility.

In the short-term, the FTWR, ATWR and IFR transmutation systems increase the FP concentrations in the HLW, which increases the toxicity for a few hundred years. The medium-lived TRU isotopes and their daughters dominate the toxicity in the several hundred to 100,000 year timeframe. By reducing the TRU concentration dramatically, the transmutation systems reduce the toxicity by approximately two orders of magnitude relative to the untreated OTC SNF at 1,000 years. The MOX fuel

cycle destroys a large fraction of the long-lived Pu isotopes and increases many of the medium-lived MA isotopes, which tend to cancel each other in this time frame.

The HLW from the IFR fuel cycle has a long-term toxicity that is nearly double that of the HLW from the FTWR and ATWR fuel cycles because the lower system TRU burnup of the IFR fuel cycle results in a larger number of imperfect separations and hence a larger concentration of TRU in the HLW. The increased fissions in the IFR fuel cycle increase the short-term toxicity far more than in the FTWR and ATWR fuel cycles.

The previous discussion was about the toxicity sent to a repository as the result of one MTU irradiated in a LWR and then processed and irradiated according to the given fuel cycle. However, in the process, additional energy will be produced. A more relevant comparison might be the rate toxicity would be sent to the HLW repository as a function of total energy production for each fuel cycle. Figure 85 shows the HLW toxicity normalized to the total thermal energy generation. The differences in toxicity between the HLW from the IFR fuel cycle and the ATWR and FTWR fuel cycles are reduced because of the much larger energy production of the IFR. The rate of production of the short-term toxicity in the HLW is nearly the same for the FTWR, ATWR and IFR fuel cycles. Yet, the rate of production of the long term toxicity in the HLW from the IFR fuel cycle is still significantly higher than that from the ATWR and FTWR fuel cycles. The IFR HLW will have significantly higher levels of ^{238}U because of the fertile fuel and a greater concentration of TRU because of the lower system TRU burnup. The single MOX recycle shows a significant improvement over the OTC in terms of toxicity per unit thermal energy production.

Figure 86 shows the toxicity of all waste streams, including both the HLW and LLW streams. For comparison, the toxicity of the uranium ore is also shown. The toxicities of all waste streams from the FTWR, ATWR or IFR fuel cycles approaches the toxicity of uranium ore after about 500 years. For the FTWR, ATWR and IFR fuel cycles, once the FP have decayed, nearly all the toxicity will be in LLW facilities. The medium-lived TRU from the OTC and MOX fuel cycle produce a longer tail that increases the toxicity for tens of thousands of years. The toxicity of all waste streams from the OTC and MOX fuel cycle differ only slightly and approach the toxicity of uranium ore after about 100,000 years.

Complete transmutation of the TRU reduces the toxicity beyond a few hundred years in the HLW that will be sent to the repository. All fuel cycles analyzed only fission a very small fraction of the original

NU, the maximum is just over 1% in the IFR fuel cycle. Therefore, the long-term toxicity beyond 100,000 years is essentially unchanged. The FTWR, ATWR or IFR transmutation systems shift a large fraction of the long-term toxicity from the HLW repository to a LLW facility by separating the residual uranium in the LWR SNF.

Table 105 - Data for Toxicity (m^3 H_2O/MTU)

Source	Component	0	100	500	1,000	10,000	100,000	1,000,000
Uranium	Ore	9.1E+07	9.1E+07	9.1E+07	9.1E+07	9.0E+07	9.2E+07	9.1E+07
	Tails	9.1E+07	9.0E+07	9.0E+07	9.0E+07	8.4E+07	3.6E+07	9.0E+03
	Natural Uranium (NU)	1.2E+05	2.2E+05	2.9E+05	4.4E+05	6.8E+06	5.6E+07	9.1E+07
	Depleted Uranium (DU)	4.6E+04	1.3E+05	1.4E+05	1.5E+05	8.0E+05	1.1E+07	6.8E+07
	Enriched Uranium (EU)	6.9E+04	9.2E+04	1.5E+05	2.8E+05	6.0E+06	4.5E+07	2.3E+07
OTC	Reference SNF	4.6E+11	2.4E+10	7.8E+08	4.4E+08	1.0E+08	5.8E+07	2.8E+07
MOX	Plutonium Feed	1.5E+09	1.5E+09	7.6E+08	4.3E+08	9.6E+07	2.9E+07	8.1E+06
	Irradiated EU Waste	5.1E+04	7.0E+04	9.7E+04	1.6E+05	3.3E+06	2.6E+07	1.8E+07
	HLW (MA & FP)	4.6E+11	2.2E+10	2.6E+07	1.5E+07	4.9E+06	3.5E+06	2.2E+06
	DU Feed	1.7E+03	4.6E+03	5.0E+03	5.6E+03	2.9E+04	3.9E+05	2.4E+06
	Fresh MOX Fuel	1.5E+09	1.5E+09	7.6E+08	4.3E+08	9.6E+07	2.9E+07	1.1E+07
	Spent MOX Fuel	8.7E+10	4.6E+09	7.1E+08	3.9E+08	7.2E+07	3.5E+07	1.2E+07
FTWR	Transuranic Feed	8.0E+09	1.5E+09	7.6E+08	4.3E+08	1.0E+08	2.7E+07	9.1E+06
(HELE)	Irradiated EU Waste	5.7E+04	8.0E+04	1.1E+05	1.8E+05	3.9E+06	3.0E+07	1.8E+07
	Pyro A Waste	4.5E+11	2.2E+10	2.9E+06	1.3E+06	9.8E+05	7.8E+05	5.6E+05
	Fresh Fuel	3.0E+13	8.0E+09	2.9E+09	1.6E+09	8.5E+08	8.5E+08	8.5E+08
	Spent Fuel	8.8E+13	1.0E+10	2.2E+09	1.2E+09	6.3E+08	6.3E+08	6.3E+08
	Pyro B Waste	8.4E+13	3.9E+09	2.9E+06	1.6E+06	1.1E+06	1.0E+06	8.8E+05
ATWR	Transuranic Feed	8.0E+09	1.5E+09	7.6E+08	4.3E+08	1.0E+08	2.7E+07	9.1E+06
	Irradiated EU Waste	5.7E+04	8.0E+04	1.1E+05	1.8E+05	3.9E+06	3.0E+07	1.8E+07
	Pyro A Waste	4.5E+11	2.2E+10	2.9E+06	1.3E+06	9.8E+05	7.8E+05	5.6E+05
	Fresh Fuel	6.1E+12	7.7E+09	2.8E+09	1.6E+09	8.6E+08	8.6E+08	8.6E+08
	Spent Fuel	1.2E+14	9.9E+09	2.0E+09	1.1E+09	6.4E+08	6.4E+08	6.4E+08
	Pyro B Waste	1.2E+14	3.7E+09	2.8E+06	1.6E+06	1.1E+06	1.0E+06	9.0E+05
IFR	Transuranic Feed	8.0E+09	1.5E+09	7.6E+08	4.3E+08	1.0E+08	2.7E+07	9.1E+06
	Irradiated EU Waste	5.7E+04	8.0E+04	1.1E+05	1.8E+05	3.9E+06	3.0E+07	1.8E+07
	Pyro A Waste	4.5E+11	2.2E+10	2.9E+06	1.3E+06	9.8E+05	7.8E+05	5.6E+05
	DU Feed	3.7E+05	4.2E+03	2.1E+03	3.6E+03	8.4E+03	8.4E+03	8.4E+03
	Fresh Fuel	1.5E+13	9.7E+09	3.8E+09	2.2E+09	1.3E+09	1.3E+09	1.3E+09
	Spent Fuel	3.0E+14	1.8E+10	3.0E+09	1.8E+09	1.1E+09	1.1E+09	1.1E+09
	Pyro B Waste	2.9E+14	9.8E+09	4.9E+06	2.9E+06	2.2E+06	2.0E+06	1.7E+06

Table 106 - Toxicity Summary (m^3 H_2O/MTU)

	Fuel Cycle	0	100	500	1,000	10,000	100,000	1,000,000
HLW	OTC	4.6E+11	2.4E+10	7.8E+08	4.4E+08	1.0E+08	5.8E+07	2.8E+07
	MOX	5.5E+11	2.7E+10	7.4E+08	4.0E+08	7.7E+07	3.9E+07	1.4E+07
	FTWR (HELE)	8.4E+13	2.6E+10	5.8E+06	2.9E+06	2.1E+06	1.8E+06	1.4E+06
	ATWR	1.2E+14	2.6E+10	5.6E+06	2.9E+06	2.1E+06	1.8E+06	1.5E+06
	IFR	2.9E+14	3.2E+10	7.8E+06	4.3E+06	3.2E+06	2.8E+06	2.3E+06
LLW	OTC	9.1E+07	9.1E+07	9.0E+07	9.0E+07	8.4E+07	4.7E+07	6.8E+07
	MOX	9.1E+07	9.1E+07	9.1E+07	9.0E+07	8.8E+07	7.2E+07	8.3E+07
	FTWR (HELE)	9.1E+07	9.1E+07	9.1E+07	9.1E+07	8.8E+07	7.7E+07	8.6E+07
	ATWR	9.1E+07	9.1E+07	9.1E+07	9.1E+07	8.8E+07	7.7E+07	8.6E+07
	IFR	9.1E+07	9.1E+07	9.1E+07	9.1E+07	8.8E+07	7.7E+07	8.6E+07
All Waste	OTC	4.7E+11	2.4E+10	8.7E+08	5.3E+08	1.9E+08	1.0E+08	9.6E+07
	MOX	5.5E+11	2.7E+10	8.3E+08	4.9E+08	1.6E+08	1.1E+08	9.7E+07
	FTWR (HELE)	8.4E+13	2.6E+10	9.6E+07	9.3E+07	9.0E+07	7.9E+07	8.8E+07
	ATWR	1.2E+14	2.6E+10	9.6E+07	9.3E+07	9.0E+07	7.9E+07	8.8E+07
	IFR	2.9E+14	3.2E+10	9.8E+07	9.5E+07	9.2E+07	8.0E+07	8.9E+07

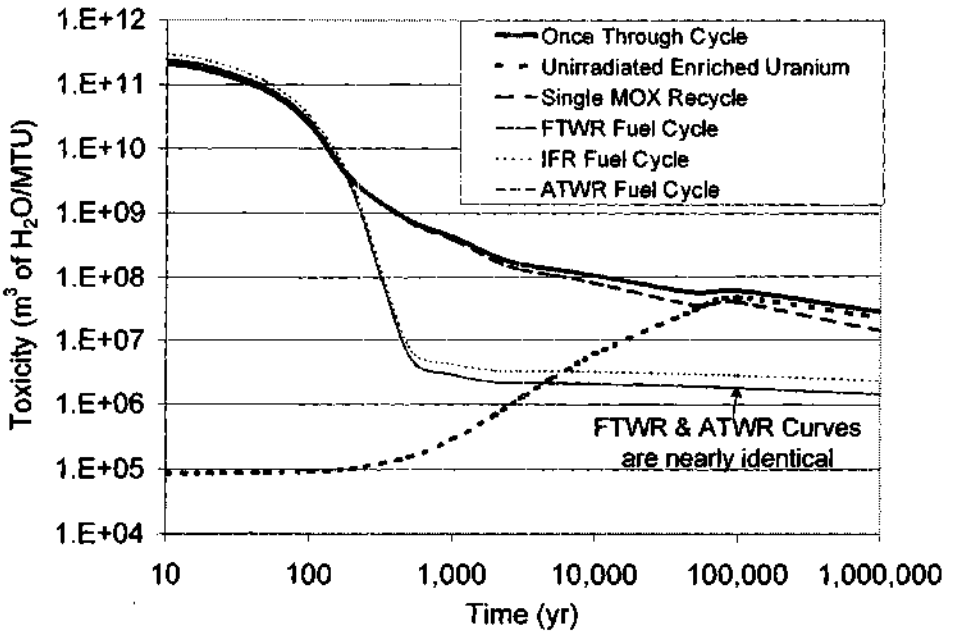

Figure 84 - Toxicity of Waste Sent to Repository per Unit Mass of LWR SNF

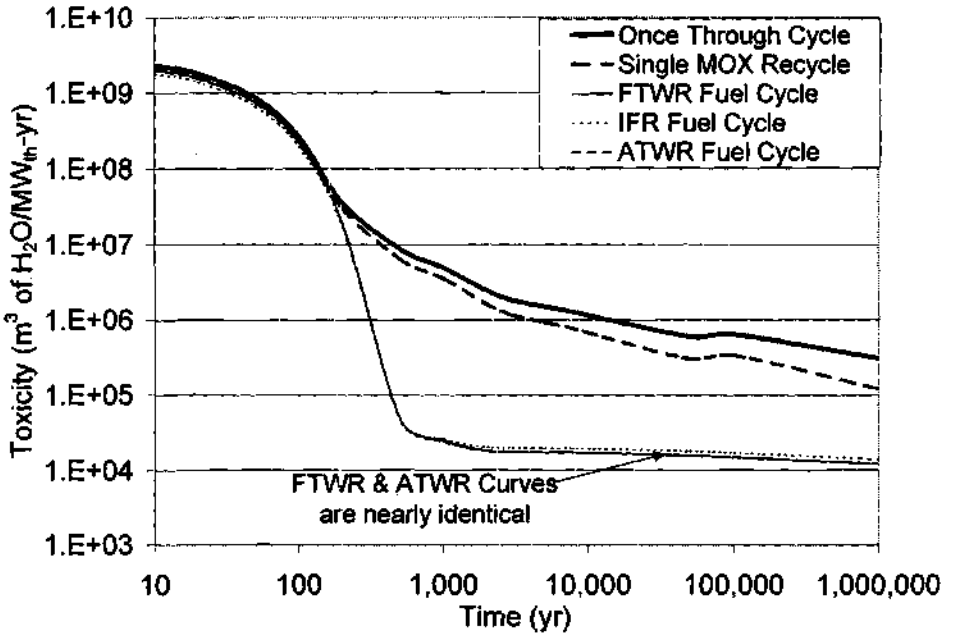

Figure 85 - Toxicity of Waste Sent to Repository per Unit Thermal Energy

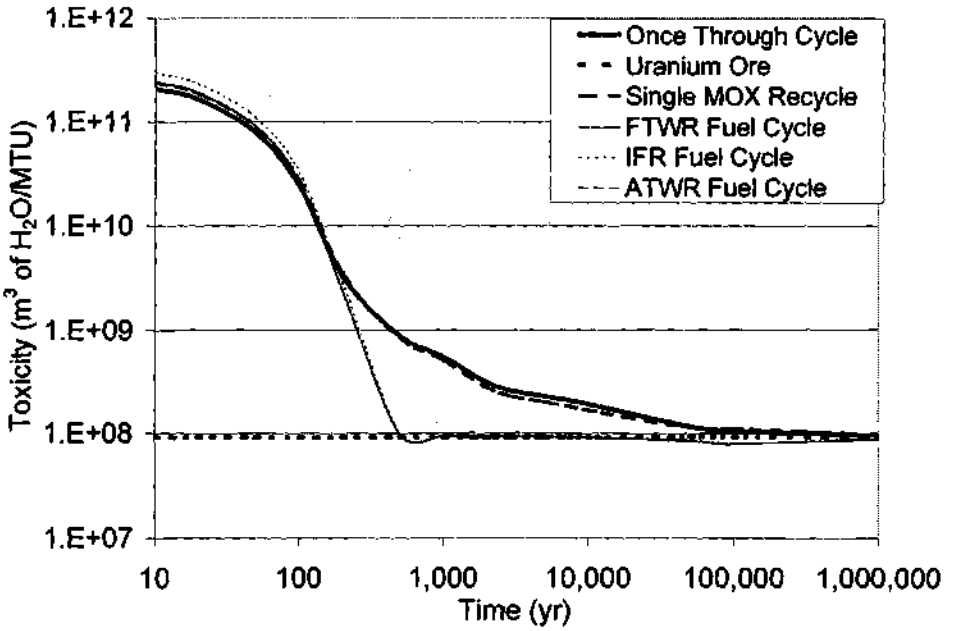

Figure 86 - Toxicity of All Waste Streams From 1 Ton Of Enriched Uranium

Repository Impacts

The repeated recycling of TRU in the FTWR, ATWR or IFR fuel cycles would have a dramatic impact on the design requirements for a HLW repository, relative to the requirements for a repository designed for intact LWR SNF. Transmutation would change the isotopic composition of the waste by converting actinides to fission products, most of which are relatively short-lived. This would change the radioactive source term, the heat source, and heat profile of the waste sent to the repository. We note that with the availability of separation and processing capability for repeated recycling in a transmutation reactor, it would be logical to prepare the waste in a vitrified or other form for improved performance relative to intact storage of SNF; however we do not consider this in our analysis.

The quantity of the six "repository" isotopes in the HLW of the different fuel cycles was evaluated. These repository isotopes contributed the largest fraction to predicted dose rates in the Yucca Mountain Viability Assessment[77] for scenarios involving waste dissolution and transportation via groundwater from the repository. The six repository isotopes include two long-lived fission products (LLFPs), ^{99}Tc and ^{129}I, and four actinides ^{237}Np, ^{234}U, ^{239}Pu, and ^{242}Pu. The individual repository isotopes include all parent isotopes that would decay to these isotopes on the time scale of the repository. For example, the repository isotope ^{234}U includes ^{238}Pu, but not ^{238}U as parent isotopes. The relative importance of these isotopes, and other isotopes not included, depends on many factors, including the waste form and assumptions about conditions in the repository and future climatic conditions. Therefore, large uncertainties exist about the actual dose rates that would occur, but significant reductions in these isotopes would be expected to translate into significant reductions in the predicted dose rates.

The fuel cycle performance was previously assessed in terms of TRU mass and all TRU isotopes were treated equally. In this section, only the actinide isotopes that are one of the four repository isotopes or included parents are considered. For example, neutron capture in ^{237}Np produces ^{238}Pu, which is a parent to and is included in the ^{234}U total, thereby reducing the ^{237}Np mass and increasing the ^{234}U mass. On the other hand, neutron capture in ^{239}Pu produces ^{240}Pu, which is not included as a repository isotope, and thus results in a net reduction in the repository isotopes without fission occurring. The different neutron spectra and fuel cycles result in different total concentrations of TRU as well as of the individual isotopes. Differences in the mass of repository isotopes are a combination of the system TRU burnup and variations

in the concentrations of individual isotopes. The repository isotope data is given in Table 107 and the totals in the different waste streams are summarized in Table 108.

Figure 87 shows the concentration of the repository isotopes in the HLW from the reference OTC SNF, from the single recycle of the Pu from the SNF in MOX fuel, and from repeatedly recycling TRU from the SNF in a FTWR, ATWR or IFR fuel cycle. As a benchmark, the ^{234}U concentration in the unirradiated EU is also included. The effect of the FTWR, ATWR and IFR fuel cycles is to convert actinides into FP, thus reducing the concentration of the TRU isotopes and increasing the concentration of the FP isotopes.

The OTC SNF contains 0.78 and 0.18 kg/MTU of ^{99}Tc and ^{129}I, respectively. The increased fissions with the MOX fuel cycle or the repeated recycles in a FTWR, ATWR or IFR fuel cycle will increase the concentration of LLFPs. The increase in the $^{99}Tc/^{129}I$ relative to the OTC SNF is 26%/33% in the MOX fuel cycle, 36%/44% in the FTWR fuel cycle, 35%/43% in the ATWR fuel cycle, and 87%/111% in the IFR fuel cycle.

The OTC SNF contains 1,900 g/MTU of ^{237}Np. By destroying the parent isotope ^{241}Pu, the production of additional ^{237}Np is forestalled, and one recycle of the Pu as MOX fuel cycle increases the ^{237}Np concentration in the HLW by approximately 2%. The FTWR, ATWR and IFR transmute nearly all the original ^{237}Np. The FTWR, ATWR, and IFR fuel cycles reduce the ^{237}Np concentration in the HLW to 6.3 g/MTU, 5.7 g/MTU, and 7.3 g/MTU, respectively. The combination of neutron spectrum and fuel cycle results in a lower fraction of ^{237}Np (^{237}Np, ^{241}Pu, ^{241}Am) in the HLW from the ATWR fuel cycle relative to the FTWR fuel cycle. The ^{237}Np concentration in the HLW is reduced by more than 99.6% in the FTWR, ATWR , and IFR fuel cycles, relative to the OTC SNF.

The original unirradiated EU has a concentration of 284 g/MTU. The OTC SNF contains 326 g/MTU of ^{234}U, which is a 14% increase relative to the original unirradiated EU. In the MOX, FTWR, ATWR and IFR fuel cycles, 46% of the repository isotope ^{234}U in the SNF is separated and sent to LLW facilities. The fraction of the ^{234}U that is not sent to a LLW facility is the parent TRU isotopes (e.g., ^{238}Pu) that have not yet decayed to ^{234}U and are separated with the other TRU. The fresh MOX fuel contains 152 g/MTU of ^{234}U, which is increased by 37% in the spent MOX fuel. The FTWR fuel cycle reduces the ^{234}U concentration in the HLW to 2.7 g/MTU, the ATWR fuel cycle to 2.1 g/MTU, and the IFR fuel cycle to 2.7

g/MTU. Excluding the ^{234}U, that is separated and sent to the LLW facility, the ATWR fuel cycle reduces the ^{234}U concentration in the TRU feed (136 g/MTU) by 98.5%, which is a slightly larger than the 98.0 % reduction for the FTWR and IFR fuel cycles. The larger reduction in the ^{234}U concentration in the ATWR fuel cycle relative to the FTWR fuel cycle exists despite the nearly identical total quantities of actinides in the HLW streams. The combination of neutron spectra and fuel cycle differences results in a lower fraction of ^{234}U (^{234}U, ^{238}Pu, ^{242}Cm, and ^{242m}Am) in the HLW from the ATWR fuel cycle relative to the FTWR fuel cycle. Nearly the same concentration of ^{234}U is in the HLW of the IFR as in the HLW of the FTWR despite, the much larger concentration of actinides in the HLW from the IFR fuel cycle.

The OTC SNF contains 6,100 g/MTU of ^{239}Pu. The single recycle of Pu in MOX fuel achieves a modest 48% reduction in the ^{239}Pu. The FTWR fuel cycle reduces the ^{239}Pu concentration in the HLW to 13.3 g/MTU, the ATWR fuel cycle to 12.1 g/MTU, and the IFR fuel cycle to 28.4 g/MTU. Because of the large ^{239}Pu source term resulting from the ^{238}U neutron capture in the fertile IFR fuel matrix, nearly three times as much ^{239}Pu will leak into the HLW streams from the IFR fuel cycle than the technologically equivalent FTWR or ATWR fuel cycles. The IFR still reduces the ^{239}Pu concentration by 99.5% compared with the 99.8% reduction in the FTWR and ATWR.

The OTC SNF contains 521 g/MTU of ^{242}Pu. Neutron capture in the MOX fuel shifts the Pu to higher isotopes, increasing the ^{242}Pu concentration by 62%. The FTWR fuel cycle reduces the ^{242}Pu concentration in the HLW to 3.7 g/MTU, the ATWR fuel cycle to 4.1 g/MTU, and the IFR fuel cycle to 4.4 g/MTU. The ^{242}Pu concentration in the HLW is reduced by more than 99% in the FTWR, ATWR , and IFR fuel cycles. While the combination of spectrum and fuel cycle resulted in a lower fraction of ^{234}U in the HLW from the ATWR fuel cycle relative to the FTWR fuel cycle, the opposite is true for ^{242}Pu. The combination of spectrum and fuel cycle results in a higher concentration of ^{242}Pu in the HLW from the ATWR fuel cycle relative to the FTWR fuel cycle.

Figure 88 compares the rate that the repository isotopes will be sent to the HLW repository per unit thermal energy production. The LLFPs ^{99}Tc and ^{129}I would be sent to the repository at rates of 9 g/MW_{th}-yr and 2 g/MW_{th}-yr, respectively. The small differences in rates for the LLFPs are a result of differences in fission yields and in-situ transmutation. The IFR, in general, appears to be the most effective at reducing the rates for the actinide repository isotopes, with the exception of a significantly higher rate for

^{239}Pu. Taken in aggregate, the OTC SNF would send the four actinide repository isotopes to the HLW repository at a rate of 97 g/MW_{th}-yr, the MOX fuel cycle at 53 g/MW_{th}-yr, the IFR fuel cycle at 0.26 g/MW_{th}-yr, the FTWR fuel cycle at 0.22 g/MW_{th}-yr, and the ATWR at 0.20 g/MW_{th}-yr. Normalized to total thermal output, the IFR fuel cycle has the lowest production rate for three of the four actinide repository isotopes, but produces the fourth at a much higher rate, when compared to the FTWR and ATWR fuel cycles. The significance of the differences between the FTWR, ATWR and IFR fuel cycles can only be determined by detailed analysis of the repository, including the final waste forms.

The heat source from the HLW is a major factor in the design of the repository. The decay heat will determine how the HLW is managed and the design of the containers used for shipping, storage, and disposal. The waste will be stored above ground for some period of time, and after emplacement the repository will remain open for an addition period of time. This time period will allow a large fraction of the FP to decay with the heat vented to the atmosphere. After the repository has been sealed, the waste will be well insulated and the temperature of the waste and surrounding repository will increase as a result of the heat load. This affects the behavior of the ground water as it moves through the repository, the dissolution rates of materials in contact with the ground water, and the quantity of material that can be placed in the repository. In order to evaluate the impact of the heat loading, two parameters were calculated. The first parameter was the instantaneous power from the decay heat of the HLW. The second parameter was the integral decay energy of the HLW after closure of the repository. The repository was assumed to be closed an average of 100 years after the waste was discharged from the reactor.

Figure 89 compares the decay heat production rates for the different fuel cycles. Over the first 100 years, there is very little difference because all systems are dominated by the FP, and the production of FP is roughly proportional to energy production. Beyond 100 years, the medium-lived TRU isotopes will dominate the heat source, and the HLW from both the OTC and MOX fuel cycle will still contain very large concentrations of these isotopes. Therefore, the heat sources from the HLW from the OTC and MOX fuel cycles will drop at a much slower rate than the heat sources from the HLW from the FTWR, ATWR and IFR fuel cycles, which have similar heat source time profiles. Thus, transmutation significantly reduces the repository heat removal requirement. The decay heat data is given in Table 109 and the totals in the different waste streams are summarized in Table 110.

Figure 90 shows the rate of production of the integral decay energy beyond 100 years, the assumed time to closure, for the different fuel cycles. The medium-lived actinides present the most significant heat load beyond 100 years. The HLW from the single recycle of Pu in MOX fuel reduces the energy deposited in the repository from 100 to 1,000 years by 23% relative to the OTC SNF. The energy deposited in the repository from 100 to 1,000 years after repeated recycle of the TRU in the FTWR, ATWR or IFR fuel cycles is reduced by 96% relative to the OTC SNF due to the highly reduced level of TRU in the HLW. Transmutation will allow for a much lower heat load design or a more tightly packed repository than with the OTC SNF. The integral decay energy data is given in Table 111 and the totals in the different waste streams are summarized in Table 112.

The repository for the HLW from the FTWR, ATWR or IFR fuel cycles will be loaded with significantly different waste than the OTC SNF. The waste will contain far lower concentrations of uranium and TRU and higher concentrations of FP for a given quantity of SNF. The initial heat load will be increased by the higher concentration of FP. Elimination of the TRU causes the heat load to fall rapidly beyond 100 years. Therefore, the heat deposited in the repository after closure will be dramatically reduced. The transmuted waste will be in a tailored waste form. All of these changes will almost certainly allow for a significant increase in the capacity of the repository without exceeding dose and heating limits.

Table 107 - Data for Repository Isotopes (MT/MTU)

Source	Component	Tc-99	I-129	Np-237	U-234	Pu-239	Pu-242
Uranium	Ore				3.09E-04		
	Tails				8.32E-11		
	Natural Uranium (NU)				3.09E-04		
	Depleted Uranium (DU)				2.47E-05		
	Enriched Uranium (EU)				2.84E-04		
OTC	Reference SNF	7.81E-04	1.81E-04	1.90E-03	3.26E-04	6.01E-03	5.21E-04
MOX	Plutonium Feed			1.42E-03	1.50E-04	5.89E-03	5.21E-04
	Irradiated EU Waste				1.61E-04		
	HLW (MA & FP)	7.81E-04	1.81E-04	4.83E-04	1.37E-05	1.13E-04	2.81E-07
	DU Feed				2.08E-06		
	Fresh MOX Fuel			1.42E-03	1.52E-04	5.89E-03	5.21E-04
	Spent MOX Fuel	2.03E-04	6.01E-05	1.45E-03	2.08E-04	3.00E-03	8.46E-04
FTWR (HELE)	Transuranic Feed			1.91E-03	1.36E-04	6.10E-03	5.21E-04
	Irradiated EU Waste				1.91E-04		
	Pyro A Waste	7.81E-04	1.81E-04	1.91E-06	1.36E-07	6.11E-06	5.21E-07
	Fresh Fuel			6.33E-03	2.71E-03	1.35E-02	3.74E-03
	Spent Fuel	2.77E-04	7.88E-05	4.34E-03	2.57E-03	7.14E-03	3.19E-03
	Pyro B Waste	2.77E-04	7.88E-05	4.34E-06	2.57E-06	7.14E-06	3.19E-06
ATWR	Transuranic Feed			1.91E-03	1.36E-04	6.10E-03	5.21E-04
	Irradiated EU Waste				1.91E-04		
	Pyro A Waste	7.81E-04	1.81E-04	1.91E-06	1.36E-07	6.11E-06	5.21E-07
	Fresh Fuel			5.75E-03	2.10E-03	1.24E-02	4.11E-03
	Spent Fuel	2.76E-04	7.76E-05	3.76E-03	1.96E-03	6.03E-03	3.57E-03
	Pyro B Waste	2.76E-04	7.76E-05	3.76E-06	1.96E-06	6.03E-06	3.57E-06
IFR	Transuranic Feed			1.91E-03	1.36E-04	6.10E-03	5.21E-04
	Irradiated EU Waste				1.91E-04		
	Pyro A Waste	7.81E-04	1.81E-04	1.91E-06	1.36E-07	6.11E-06	5.21E-07
	DU Feed				4.90E-06		
	Fresh Fuel			7.28E-03	2.74E-03	2.85E-02	4.37E-03
	Spent Fuel	6.77E-04	2.00E-04	5.35E-03	2.60E-03	2.23E-02	3.84E-03
	Pyro B Waste	6.77E-04	2.00E-04	5.35E-06	2.60E-06	2.23E-05	3.84E-06

Table 108 - Repository Isotopes Summary (MT/MTU)

	Fuel Cycle	Tc-99	I-129	Np-237	U-234	Pu-239	Pu-242
HLW	OTC	7.81E+02	1.81E+02	1.90E+03	3.26E+02	6.01E+03	5.21E+02
	MOX	9.84E+02	2.41E+02	1.94E+03	2.22E+02	3.11E+03	8.46E+02
	FTWR (HELE)	1.06E+03	2.59E+02	6.25E+00	2.71E+00	1.33E+01	3.72E+00
	ATWR	1.06E+03	2.58E+02	5.67E+00	2.09E+00	1.21E+01	4.09E+00
	IFR	1.46E+03	3.80E+02	7.26E+00	2.74E+00	2.84E+01	4.36E+00
LLW	OTC				2.47E-05		
	MOX				1.84E-04		
	FTWR (HELE)				2.16E-04		
	ATWR				2.16E-04		
	IFR				2.11E-04		
All Waste	OTC	7.81E+02	1.81E+02	1.90E+03	3.26E+02	6.01E+03	5.21E+02
	MOX	9.84E+02	2.41E+02	1.94E+03	2.22E+02	3.11E+03	8.46E+02
	FTWR (HELE)	1.06E+03	2.59E+02	6.25E+00	2.71E+00	1.33E+01	3.72E+00
	ATWR	1.46E+03	3.80E+02	7.26E+00	2.74E+00	2.84E+01	4.36E+00
	IFR	1.06E+03	2.58E+02	5.67E+00	2.09E+00	1.21E+01	4.09E+00

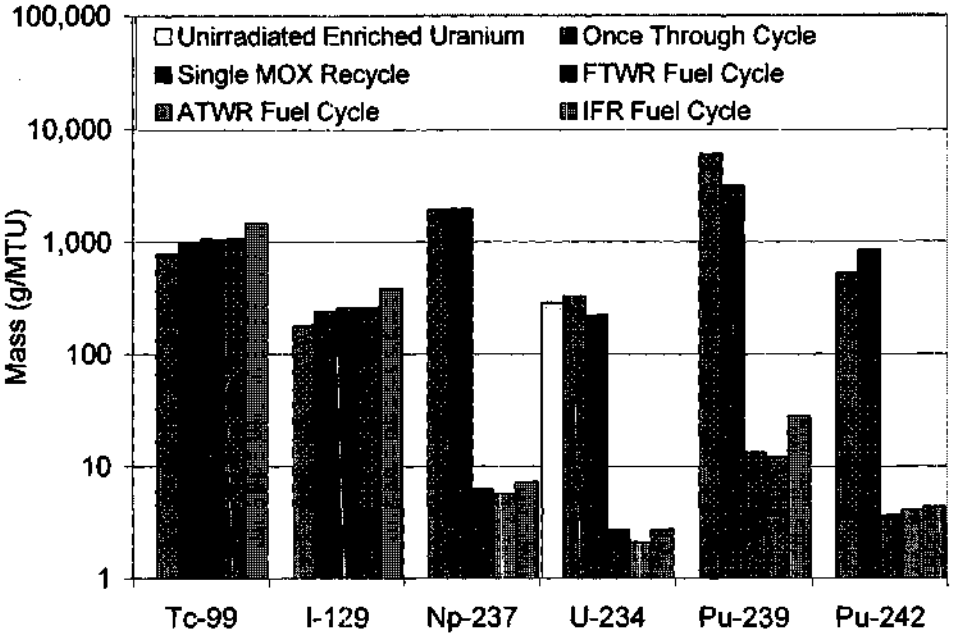

Figure 87 - Concentration of "Repository" Isotopes in HLW

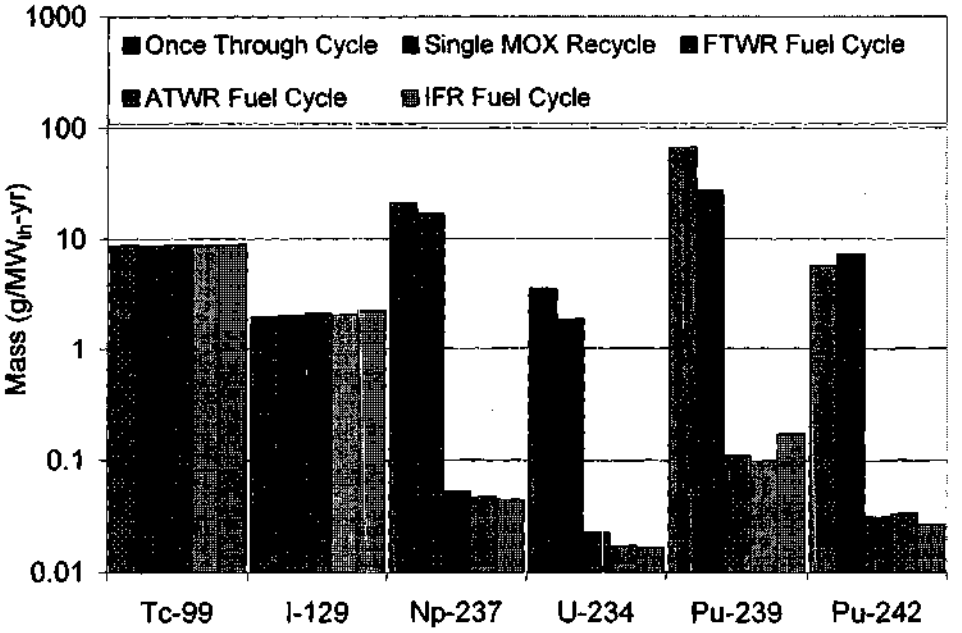

Figure 88 - Rate of Production of "Repository" Isotopes in HLW

Table 109 - Data for Decay Heat (W/MTU)

Source	Component	0	50	100	1,000	10,000	100,000	1,000,000
Uranium	Ore	5.7E-01	5.7E-01	5.7E-01	5.7E-01	5.7E-01	5.7E-01	5.7E-01
	Tails	4.6E-01	4.5E-01	4.5E-01	4.5E-01	4.2E-01	1.8E-01	4.5E-05
	Natural Uranium (NU)	1.1E-01	1.2E-01	1.2E-01	1.2E-01	1.5E-01	4.0E-01	5.7E-01
	Depleted Uranium (DU)	4.6E-02	5.4E-02	5.4E-02	5.4E-02	5.9E-02	1.2E-01	4.3E-01
	Enriched Uranium (EU)	6.1E-02	6.3E-02	6.3E-02	6.4E-02	9.3E-02	2.8E-01	1.4E-01
OTC	Reference SNF	5.5E+03	1.2E+03	3.2E+02	6.2E+01	1.5E+01	1.2E+00	4.2E-01
MOX	Plutonium Feed	1.2E+02	1.7E+02	2.1E+02	6.0E+01	1.4E+01	9.3E-01	2.4E-01
	Irradiated EU Waste	4.5E-02	4.7E-02	4.7E-02	4.7E-02	6.2E-02	1.7E-01	1.2E-01
	HLW (MA & FP)	5.3E+03	9.9E+02	1.1E+02	1.9E+00	5.4E-01	7.5E-02	7.1E-02
	DU Feed	1.6E-03	1.9E-03	1.9E-03	2.0E-03	2.1E-03	4.3E-03	1.5E-02
	Fresh MOX Fuel	1.2E+02	1.7E+02	2.1E+02	6.0E+01	1.4E+01	9.3E-01	2.5E-01
	Spent MOX Fuel	1.5E+03	6.8E+02	2.4E+02	5.4E+01	1.0E+01	7.1E-01	2.7E-01
FTWR (HELE)	Transuranic Feed	3.1E+02	2.6E+02	2.1E+02	6.1E+01	1.5E+01	9.8E-01	3.1E-01
	Irradiated EU Waste	5.0E-02	5.5E-02	5.3E-02	5.2E-02	7.0E-02	1.9E-01	1.2E-01
	Pyro A Waste	3.6E+03	9.1E+02	9.5E+01	7.8E-02	3.1E-02	1.1E-02	9.0E-04
	Fresh Fuel	3.6E+03	2.5E+03	1.3E+03	2.6E+02	6.2E+01	5.4E+00	1.6E+00
	Spent Fuel	1.3E+05	2.4E+03	1.0E+03	1.7E+02	3.9E+01	3.7E+00	1.0E+00
	Pyro B Waste	1.3E+05	2.4E+02	2.6E+01	1.8E-01	4.9E-02	9.5E-03	1.4E-03
ATWR	Transuranic Feed	3.1E+02	2.6E+02	2.1E+02	6.1E+01	1.5E+01	9.8E-01	3.1E-01
	Irradiated EU Waste	5.0E-02	5.5E-02	5.3E-02	5.2E-02	7.0E-02	1.9E-01	1.2E-01
	Pyro A Waste	3.6E+03	9.1E+02	9.5E+01	7.8E-02	3.1E-02	1.1E-02	9.0E-04
	Fresh Fuel	5.8E+03	3.3E+03	1.2E+03	2.3E+02	5.6E+01	4.1E+00	1.2E+00
	Spent Fuel	1.5E+05	3.4E+03	9.8E+02	1.6E+02	4.0E+01	3.0E+00	8.8E-01
	Pyro B Waste	1.2E+05	2.4E+02	2.6E+01	1.7E-01	5.0E-02	8.8E-03	1.2E-03
IFR	Transuranic Feed	3.1E+02	2.6E+02	2.1E+02	6.1E+01	1.5E+01	9.8E-01	3.1E-01
	Irradiated EU Waste	5.0E-02	5.5E-02	5.3E-02	5.2E-02	7.0E-02	1.9E-01	1.2E-01
	Pyro A Waste	3.6E+03	9.1E+02	9.5E+01	7.8E-02	3.1E-02	1.1E-02	9.0E-04
	DU Feed	7.3E-02	3.2E-03	1.9E-03	1.0E-03	1.4E-03	3.8E-03	2.2E-03
	Fresh Fuel	6.8E+03	3.2E+03	1.4E+03	3.2E+02	9.4E+01	6.5E+00	1.5E+00
	Spent Fuel	3.4E+05	3.7E+03	1.3E+03	2.6E+02	7.9E+01	5.5E+00	1.2E+00
	Pyro B Waste	3.2E+05	5.8E+02	6.4E+01	2.9E-01	1.0E-01	2.0E-02	2.0E-03

Table 110 - Decay Heat Summary (W/MTU)

	Fuel Cycle	0	50	100	1,000	10,000	100,000	1,000,000
HLW	OTC	5.5E+03	1.2E+03	3.2E+02	6.2E+01	1.5E+01	1.2E+00	4.2E-01
	MOX	6.8E+03	1.7E+03	3.5E+02	5.6E+01	1.1E+01	7.8E-01	3.4E-01
	FTWR (HELE)	1.3E+05	1.2E+03	1.2E+02	2.6E-01	8.0E-02	2.1E-02	2.3E-03
	ATWR	1.3E+05	1.1E+03	1.2E+02	2.5E-01	8.1E-02	2.0E-02	2.1E-03
	IFR	3.3E+05	1.5E+03	1.6E+02	3.6E-01	1.3E-01	3.1E-02	2.9E-03
LLW	OTC	5.1E-01	5.1E-01	5.1E-01	5.0E-01	4.8E-01	3.0E-01	4.3E-01
	MOX	5.5E-01	5.5E-01	5.5E-01	5.5E-01	5.4E-01	4.6E-01	5.3E-01
	FTWR (HELE)	5.6E-01	5.6E-01	5.6E-01	5.6E-01	5.5E-01	4.9E-01	5.5E-01
	ATWR	5.6E-01	5.6E-01	5.6E-01	5.6E-01	5.5E-01	4.9E-01	5.5E-01
	IFR	4.8E-01	5.6E-01	5.6E-01	5.5E-01	5.4E-01	4.8E-01	5.5E-01
All Waste	OTC	5.5E+03	1.2E+03	3.2E+02	6.3E+01	1.6E+01	1.5E+00	8.5E-01
	MOX	6.8E+03	1.7E+03	3.5E+02	5.7E+01	1.2E+01	1.2E+00	8.7E-01
	FTWR (HELE)	1.3E+05	1.2E+03	1.2E+02	8.1E-01	6.3E-01	5.1E-01	5.5E-01
	ATWR	1.3E+05	1.1E+03	1.2E+02	8.1E-01	6.3E-01	5.1E-01	5.5E-01
	IFR	3.3E+05	1.5E+03	1.6E+02	9.2E-01	6.8E-01	5.2E-01	5.5E-01

Table 111 - Data for Integral Decay Energy (J/MTU)

Source	Component	0	50	100	1,000	10,000	100,000	1,000,000
Uranium	Ore	0	1.7E+08	8.9E+08	1.8E+09	1.8E+10	1.6E+11	1.7E+12
	Tails	0	1.4E+08	7.1E+08	1.4E+09	1.4E+10	1.2E+11	9.0E+11
	Natural Uranium (NU)	0	3.7E+07	1.8E+08	3.7E+08	3.7E+09	4.2E+10	7.6E+11
	Depleted Uranium (DU)	0	1.7E+07	8.5E+07	1.7E+08	1.7E+09	1.8E+10	2.6E+11
	Enriched Uranium (EU)	0	2.0E+07	9.9E+07	2.0E+08	2.0E+09	2.4E+10	5.0E+11
OTC	Reference SNF	0	9.1E+11	1.9E+12	2.6E+12	5.9E+12	1.3E+13	2.5E+13
MOX	Plutonium Feed	0	4.6E+10	3.1E+11	6.6E+11	3.8E+12	1.1E+13	2.2E+13
	Irradiated EU Waste	0	1.5E+07	7.4E+07	1.5E+08	1.5E+09	1.7E+10	3.2E+11
	HLW (MA & FP)	0	8.7E+11	1.6E+12	1.9E+12	2.2E+12	2.4E+12	2.9E+12
	DU Feed	0	6.1E+05	3.1E+06	6.1E+06	6.2E+07	6.4E+08	9.3E+09
	Fresh MOX Fuel	0	4.6E+10	3.1E+11	6.6E+11	3.8E+12	1.1E+13	2.2E+13
	Spent MOX Fuel	0	3.6E+11	9.7E+11	1.4E+12	4.5E+12	1.0E+13	1.8E+13
FTWR	Transuranic Feed	0	9.4E+10	4.1E+11	7.6E+11	3.9E+12	1.1E+13	2.3E+13
(HELE)	Irradiated EU Waste	0	1.7E+07	8.6E+07	1.7E+08	1.6E+09	1.9E+10	3.6E+11
	Pyro A Waste	0	7.9E+11	1.5E+12	1.8E+12	1.9E+12	1.9E+12	1.9E+12
	Fresh Fuel	0	8.9E+11	3.5E+12	6.0E+12	2.1E+13	5.3E+13	9.8E+13
	Spent Fuel	0	1.3E+12	3.6E+12	5.5E+12	1.6E+13	3.6E+13	6.4E+13
	Pyro B Waste	0	4.6E+11	6.4E+11	7.1E+11	7.6E+11	7.8E+11	8.3E+11
ATWR	Transuranic Feed	0	9.4E+10	4.1E+11	7.6E+11	3.9E+12	1.1E+13	2.3E+13
	Irradiated EU Waste	0	1.7E+07	8.6E+07	1.7E+08	1.6E+09	1.9E+10	3.6E+11
	Pyro A Waste	0	7.9E+11	1.5E+12	1.8E+12	1.9E+12	1.9E+12	1.9E+12
	Fresh Fuel	0	1.2E+12	4.1E+12	6.3E+12	1.9E+13	4.7E+13	8.7E+13
	Spent Fuel	0	2.0E+12	4.8E+12	6.8E+12	1.7E+13	3.7E+13	6.4E+13
	Pyro B Waste	0	4.5E+11	6.2E+11	7.0E+11	7.5E+11	7.7E+11	8.2E+11
IFR	Transuranic Feed	0	9.4E+10	4.1E+11	7.6E+11	3.9E+12	1.1E+13	2.3E+13
	Irradiated EU Waste	0	1.7E+07	8.6E+07	1.7E+08	1.6E+09	1.9E+10	3.6E+11
	Pyro A Waste	0	7.9E+11	1.5E+12	1.8E+12	1.9E+12	1.9E+12	1.9E+12
	DU Feed	0	9.8E+05	4.5E+06	8.0E+06	4.0E+07	3.8E+08	7.2E+09
	Fresh Fuel	0	1.1E+12	4.3E+12	6.9E+12	2.4E+13	6.8E+13	1.4E+14
	Spent Fuel	0	2.4E+12	5.8E+12	8.3E+12	2.3E+13	5.9E+13	1.2E+14
	Pyro B Waste	0	1.1E+12	1.6E+12	1.8E+12	1.8E+12	1.9E+12	2.0E+12

Table 112 - Integral Decay Energy Summary (J/MTU)

Source	Component	0	50	100	1,000	10,000	100,000	1,000,000
HLW	OTC	0	9.1E+11	1.9E+12	2.6E+12	5.9E+12	1.3E+13	2.5E+13
	MOX	0	1.2E+12	2.6E+12	3.3E+12	6.6E+12	1.3E+13	2.1E+13
	FTWR (HELE)	0	1.2E+12	2.1E+12	2.5E+12	2.6E+12	2.7E+12	2.8E+12
	ATWR	0	1.2E+12	2.1E+12	2.5E+12	2.6E+12	2.7E+12	2.8E+12
	IFR	0	1.9E+12	3.0E+12	3.5E+12	3.7E+12	3.8E+12	4.0E+12
LLW	OTC	0	1.5E+08	7.9E+08	1.6E+09	1.6E+10	1.3E+11	1.2E+12
	MOX	0	1.7E+08	8.6E+08	1.7E+09	1.7E+10	1.5E+11	1.5E+12
	FTWR (HELE)	0	1.7E+08	8.8E+08	1.8E+09	1.7E+10	1.5E+11	1.5E+12
	ATWR	0	1.7E+08	8.8E+08	1.8E+09	1.7E+10	1.5E+11	1.5E+12
	IFR	0	1.7E+08	8.7E+08	1.7E+09	1.7E+10	1.5E+11	1.5E+12
All Waste	OTC	0	9.1E+11	1.9E+12	2.6E+12	5.9E+12	1.3E+13	2.7E+13
	MOX	0	1.2E+12	2.6E+12	3.3E+12	6.7E+12	1.3E+13	2.2E+13
	FTWR (HELE)	0	1.2E+12	2.1E+12	2.5E+12	2.7E+12	2.8E+12	4.3E+12
	ATWR	0	1.9E+12	3.0E+12	3.5E+12	3.8E+12	3.9E+12	5.5E+12
	IFR	0	1.2E+12	2.1E+12	2.5E+12	2.7E+12	2.8E+12	4.3E+12

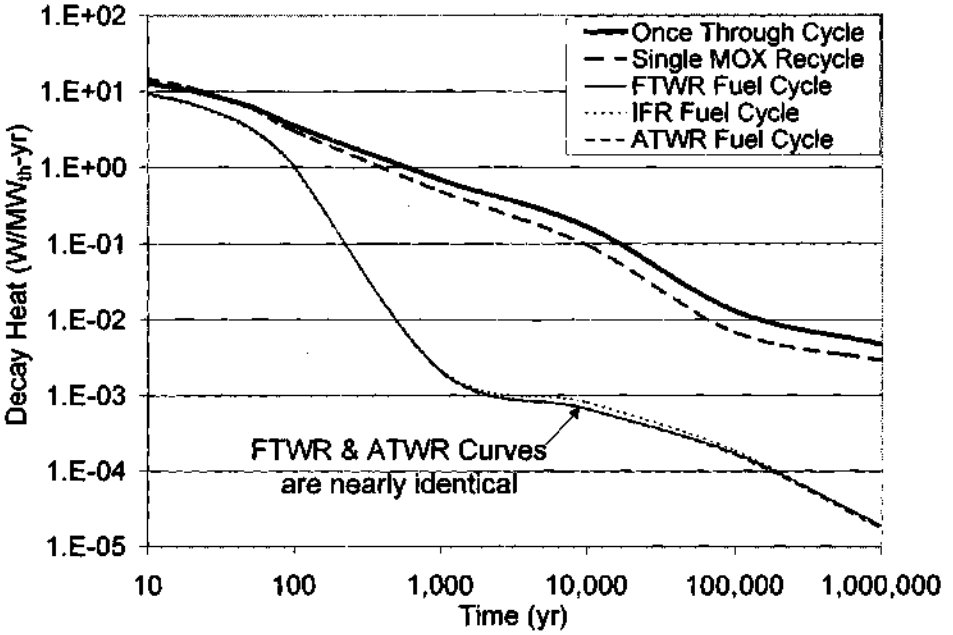

Figure 89 - Rate of Production of Decay Heat

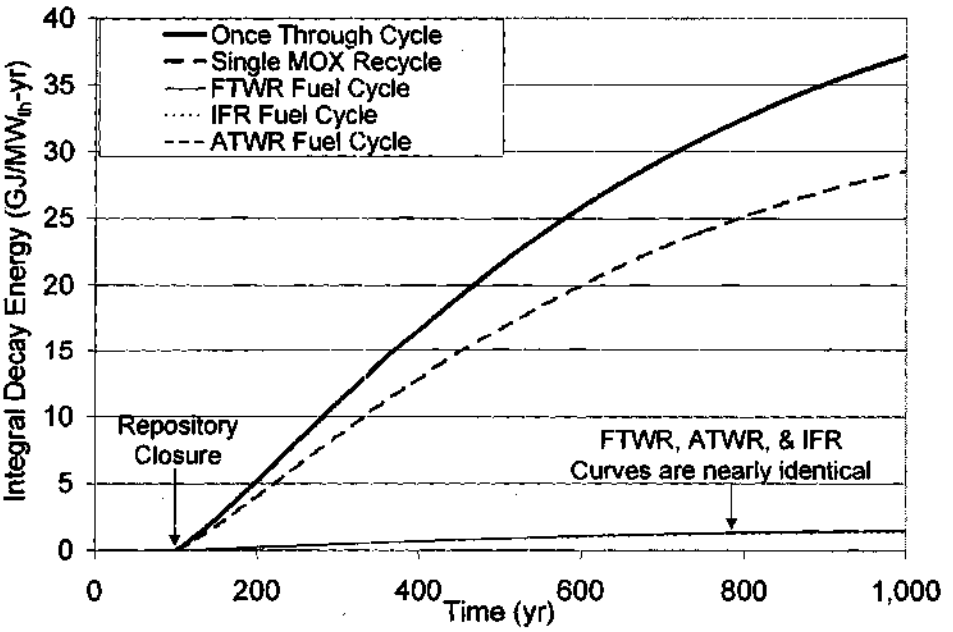

Figure 90 - Rate of Accumulation of Integral Decay Energy (After Repository Closure at 100 years)

Proliferation Resistance of HLW Repository Waste

One concern that has been raised about the disposal of the intact SNF is that the large quantity of TRU will present a proliferation risk after the radiation barrier has fallen to levels where the SNF is no longer self-protecting. Repeatedly recycling the TRU in the FTWR, ATWR or IFR fuel cycle would result in a far more dilute TRU waste with a much higher concentration of FP, although the very existence of separation systems will raise a different type of proliferation concern. Several parameters were calculated to evaluate the relative proliferation risk of the SNF from the OTC, spent MOX fuel from the single recycle of Pu in MOX fuel, and the HLW from the repeated recycle of TRU in a FTWR, ATWR or IFR fuel cycle. These parameters are related to technical and physical barriers to proliferation and are based on the analysis of ref 78.

The technical barrier parameters provide a measure of the relative difficulty of achieving a significant nuclear yield from an explosive device. The first parameter is the bare critical mass (BCM). The BCM is the minimum unreflected quantity required to produce a critical nuclear device. A critical configuration can be created from nearly all TRU isotopes. The BCM was calculated in two ways: 1) assuming separation of pure Pu; and 2) assuming separation of all TRU en masse. The BCM is time dependent because short-lived isotopes decay, changing the isotopic composition of the remaining Pu and TRU. Other technical parameters are the decay heat (DH) and spontaneous neutron source (SNS). The higher the levels of DH and SNS of the explosive device, the more technically challenging it is to produce a significant nuclear yield. These quantities are a function of the BCM and isotopic composition of the material.

The physical barrier parameters provide a measure of the relative difficulty of acquiring sufficient material in a form pure enough to produce a nuclear explosive. The two physical barrier parameters analyzed are related to the quantity of waste containing one BCM and the radiological hazard associated with that quantity of waste. The mass of radioactive waste (MRW) containing one BCM provides a measure of the relative amounts of radioactive waste, actinides and FP, that would need to be handled and processed to recover sufficient material to produce an explosive device. The MRW does not account for the additional dilution and tailoring of the waste from the transmutation systems that would increase the barrier

to proliferation. The unshielded dose rate at 1 meter (UDR) provides a measure of the relative radiological hazard of separating sufficient material to produce an explosive device.

Figure 91 shows the *bare critical mass* (BCM) of the Pu and TRU in the HLW from the OTC SNF, from the single recycle of the Pu from the SNF in MOX fuel, and from repeatedly recycling TRU from the SNF in a FTWR, ATWR or IFR fuel cycle. For reference, the BCM (10.7 kg) for weapons-grade plutonium (WGPu) is also shown. Transmutation increases the BCM by increasing the concentrations of the ^{242}Pu, which in pure form has a BCM of 92 kg, and ^{240}Pu, which in pure form has a BCM of 36 kg, relative to the other Pu isotopes, which have much smaller BCMs in pure form. Initially, the OTC SNF Pu has a BCM 40% larger than the BCM of WGPu, and the Pu in the spent MOX fuel has a BCM about 20% higher than the BCM of the OTC SNF Pu. Initially, the BCM of the Pu in the HLW from the FTWR, ATWR and IFR fuel cycles is approximately 50% higher than the BCM of the OTC SNF Pu. The BCMs remain fairly constant for more than 10,000 years, then slowly increase as the ^{239}Pu decays with a 24,110 year half-life. At one million years, ^{242}Pu, with a 373,300 yr half-life, is the only Pu isotope present in significant quantities; the small differences in the BCM at this time are from statistical sampling in the MCNP Monte Carlo code and from convergence of the radius of the critical sphere.

At one million years, ^{242}Pu and ^{237}Np, with a 2,144,000 yr half-life, are the only TRU isotopes present in significant quantities. The TRU shows similar time behavior; with small increases in the BCM until a significant fraction of the ^{239}Pu has decayed.

Figure 92 shows the *decay heat* (DH) of one BCM of the Pu and one BCM of the TRU in the HLW from the OTC SNF, from the single recycle of the Pu from the SNF in MOX fuel, and from repeatedly recycling TRU from the SNF in a FTWR, ATWR or IFR fuel cycle. For reference, the DH of one BCM of WGPu (24.6 W) is also shown. Transmutation increases the DH by increasing the concentrations of the relatively short-lived alpha emitting isotopes ^{238}Pu and ^{240}Pu. Initially, one BCM of Pu from the OTC SNF generates eight times more heat then one BCM of ^{239}Pu. One BCM of the Pu in the spent MOX fuel has a DH that is twice that of the OTC SNF Pu. The DH of one BCM of Pu in the HLW from the IFR fuel cycle is increased 3 times, from the FTWR fuel cycle is increased 6 times, and from the ATWR fuel cycle is increased 7 times, relative to the OTC SNF Pu. The increased DH from one BCM of Pu relative to the DH from one BCM of Pu from the OTC Pu tends to diminish with time and has fallen to

roughly double that of one BCM of Pu from the OTC SNF by 1,000 years for the Pu in the spent MOX fuel, and the Pu in the HLW from the FTWR, ATWR and IFR fuel cycles. The short-lived Pu isotopes that are producing the heat decay away and reduce the DH. Even so, the DH of the Pu remains significantly higher than that of WGPu for tens of thousands of years.

Even though the MA have a small effect on the BCM, initially, they roughly double the DH of one BCM of TRU relative to the DH of one BCM of Pu from the same fuel cycle. The increased DH of the TRU relative to Pu falls significantly with time, and the DH of the TRU is roughly equal to that of Pu at 10,000 years. Beyond about 70,000 years the DH of one BCM of TRU fall below the DH of one BCM of WGPu.

Figure 93 shows the *spontaneous neutron source* (SNS) of one BCM of the Pu and TRU in the HLW from the OTC SNF, from the single recycle of the Pu from the SNF in MOX fuel, and from repeatedly recycling TRU from the SNF in a FTWR, ATWR or IFR fuel cycle. For reference, the SNS of one BCM of WGPu (6.0×10^5 n/s) is also shown. Transmutation increases the SNS by increasing the even mass Pu isotopes, which have SNS that are orders of magnitude greater than ^{239}Pu and ^{241}Pu. The OTC Pu has a SNS an orders of magnitude higher than WGPu. The Pu from the spent MOX fuel, and the Pu in the HLW from the FTWR, ATWR and IFR fuel cycles increases the SNS for one BCM relative to the SNF from one BCM of Pu from the OTC SNF. The SNS of the TRU remains significantly above WGPu for all fuel cycles, with the TRU in the ATWR HLW being significantly higher than the other fuel cycles. The variation in the concentration in the very small concentrations of a few isotopes with very high spontaneous fission rates result in the different SNS from the TRU in the different fuel cycles.

Figure 94 shows the *mass of radioactive waste* (MRW) containing one BCM of the Pu and one BCM of the TRU from the OTC SNF, from the single recycle of the Pu from the SNF in MOX fuel, and from repeatedly recycling TRU from the SNF in a FTWR, ATWR or IFR fuel cycle. A relatively small MRW, less than 2 MT, of OTC SNF would have to be processed to recover one BCM of Pu. By concentrating the Pu in the MOX fuel, the MRW of spent MOX fuel is reduced to less than one third that of the OTC SNF. The IFR fuel cycle triples the MRW and the ATWR and FTWR fuel cycles increase the MRW by roughly a factor of eight over the OTC SNF. The actual mass that will need to be processed will be significantly larger than the MRW from the FTWR, ATWR and IFR fuel cycles because the HLW will

be further diluted in the final waste form. Over time, the MRW rises as significant fractions of the Pu decay, and at one million years, the MRW is over 1,000 MT for all but the spent MOX fuel, which is over 100 MT. Inclusion of the MA has little effect on the MRW until well beyond 10,000 years, but has a large effect at one million years, where the MRW for one BCM of TRU is roughly an order of magnitude less than for one BCM of the Pu.

Figure 95 shows the radiation barrier as measured by the *unshielded dose rate* (UDR) from the HLW containing one BCM of the Pu and one BCM of the TRU from the OTC SNF, from the single recycle of the Pu from the SNF in MOX fuel, and from repeatedly recycling TRU from the SNF in a FTWR, ATWR or IFR fuel cycle. The repeated recycle of the TRU in the FTWR, ATWR and IFR fuel cycles produce HLW streams that will present a significantly larger radiation barrier than the OTC SNF or spent MOX fuel for nearly one million years because the Pu and TRU are distributed in a very large quantity of FP. The radiation barrier falls significantly over time for all fuel cycles. The minimum radiation barrier of the OTC SNF and spent MOX fuel occurs in the 1,000 to 10,000 year time frame, when many hours would be required to receive a lethal dose, 100's of REM, even neglecting self-shielding and any other shielding that might be provided.

Figure 96 shows the *BCM Production Rate* (BCM/MW_{th}-yr) of the Pu and TRU in the HLW from the OTC SNF, from the single recycle of the Pu from the SNF in MOX fuel, and from repeatedly recycling TRU from the SNF in a FTWR, ATWR or IFR fuel cycle. The BCM production rate is the rate based on thermal energy production from the one BCM quantity of Pu that will be discharged to the waste stream. More than 7 BCM/GW_{th}-yr would be discharged in the OTC SNF. By increasing the BCM, reducing the mass of Pu, and producing more energy, the MOX fuel cycle would reduce by roughly half the rate of production of BCM quantities of Pu. The nearly complete fission of the TRU in the FTWR, ATWR and IFR fuel cycles reduce the BCM production rates to a very low level compared to the OTC SNF. Inclusion of the MA has a significant effect only at long times after most of the Pu has decayed.

The Pu or TRU from any of the fuel cycles can theoretically be used to produce a nuclear explosive. The Pu from the OTC SNF is significantly degraded relative to WGPu. The proliferation effects of the MOX fuel are mixed relative to the OTC; there is a higher concentration of lower quality material in the spent MOX fuel. Transmutation in a FTWR, ATWR or IFR will result in a very small quantity of even

lower quality material that will be diluted in a large concentration of FP. The HLW from the FTWR, ATWR and IFR fuel cycles would provide a very significant barrier to the proliferation of the repository waste at any time in the future.

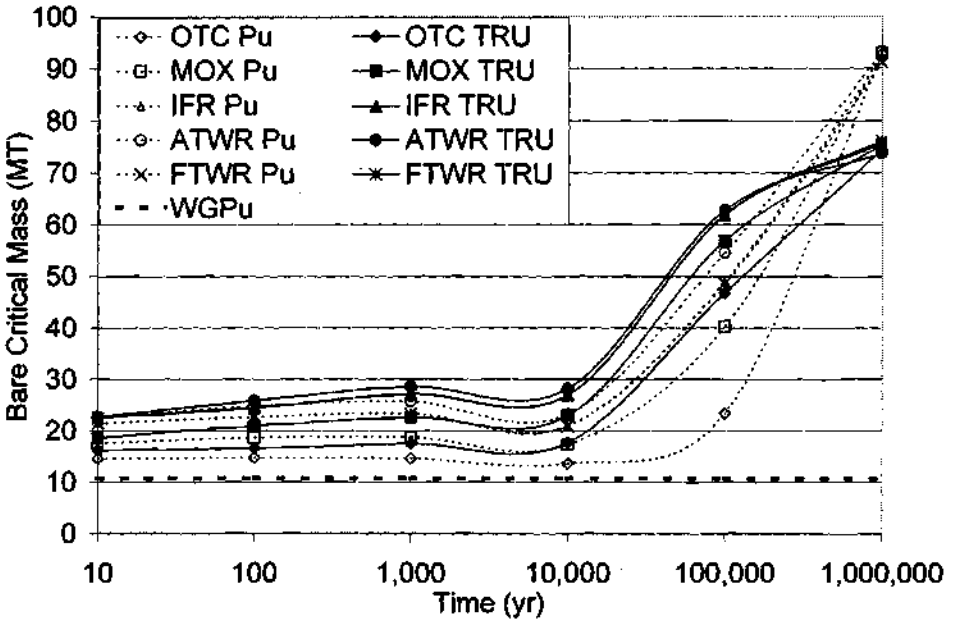

Figure 91 - Bare Critical Mass
(dashed lines - plutonium only; solid lines - all transuranics)

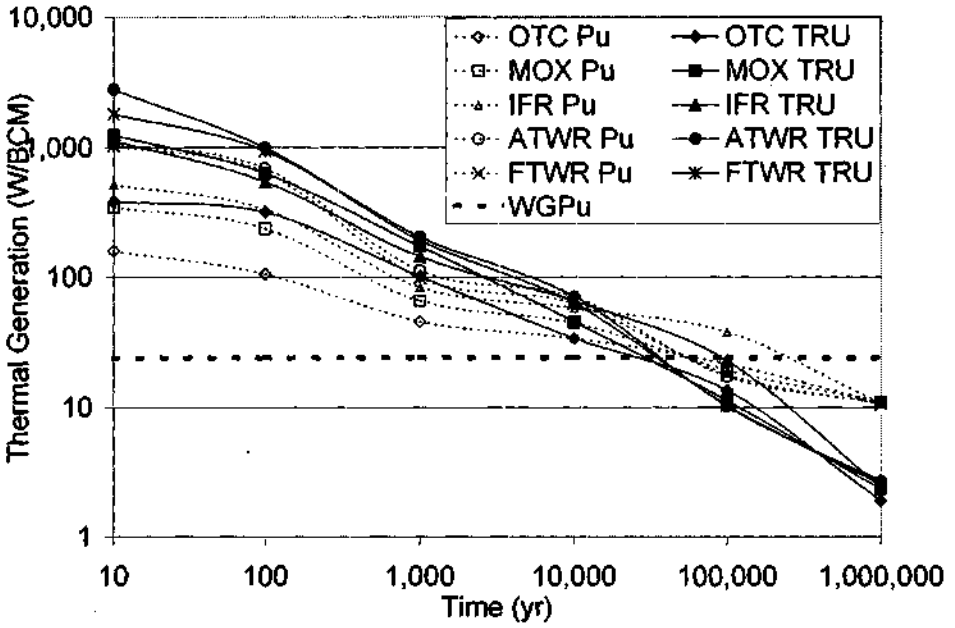

Figure 92 - Decay Heat From One Bare Critical Mass
(dashed lines - plutonium only; solid lines - all transuranics)

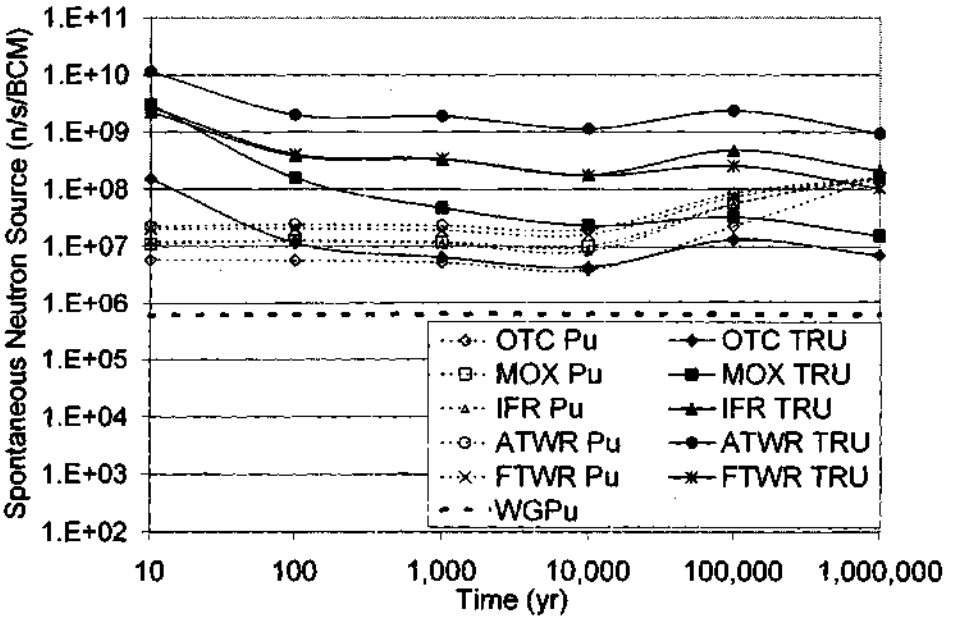

Figure 93 - Spontaneous Neutron Source From One Bare Critical Mass
(dashed lines - plutonium only; solid lines - all transuranics)

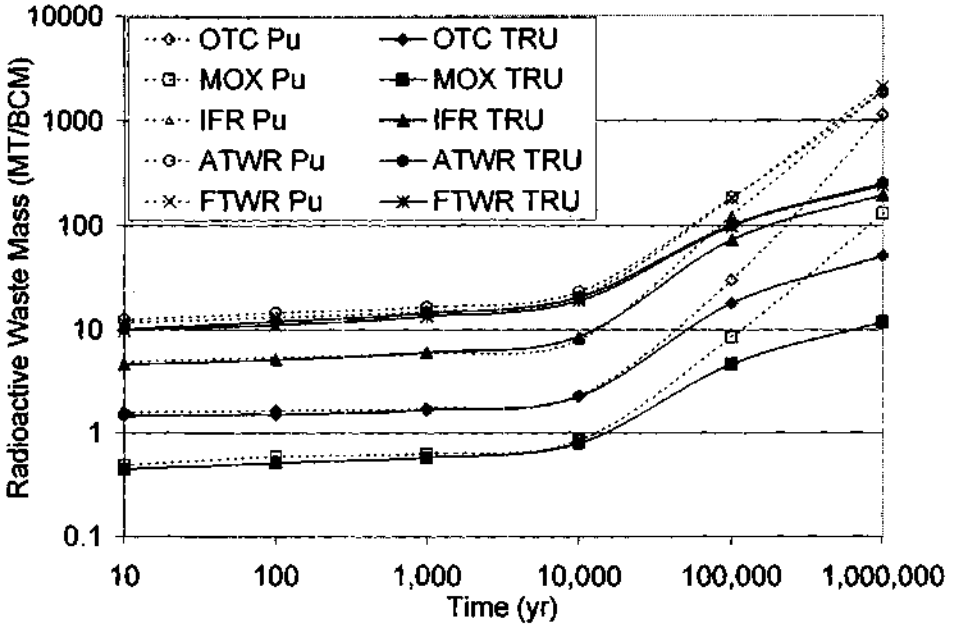

Figure 94 - Mass of Radioactive Waste Containing One Bare Critical Mass
(dashed lines - plutonium only; solid lines - all transuranics)

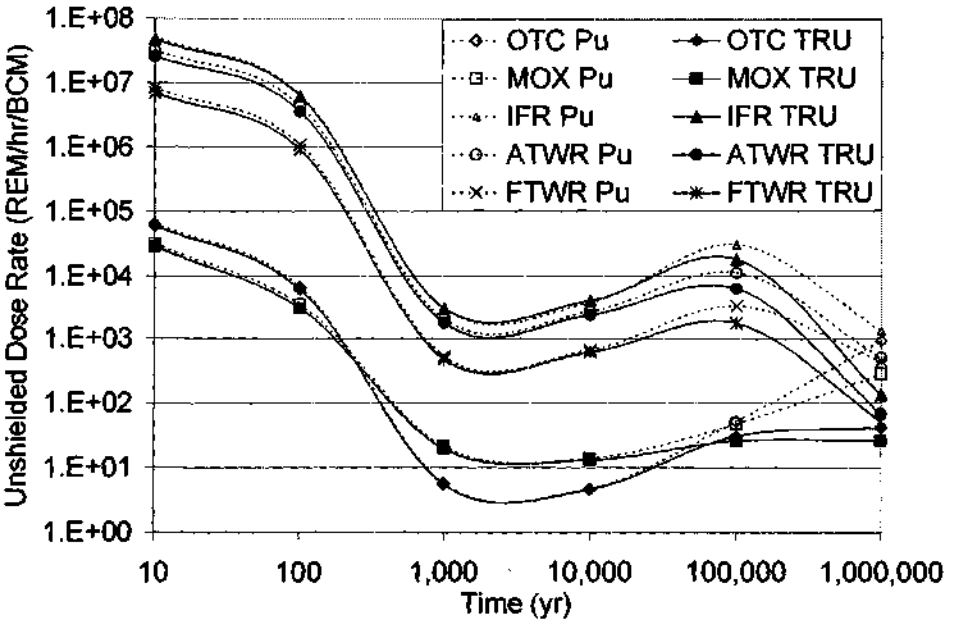

Figure 95 - Radiation Barrier of Waste Containing One Bare Critical Mass
(dashed lines - plutonium only; solid lines - all transuranics)

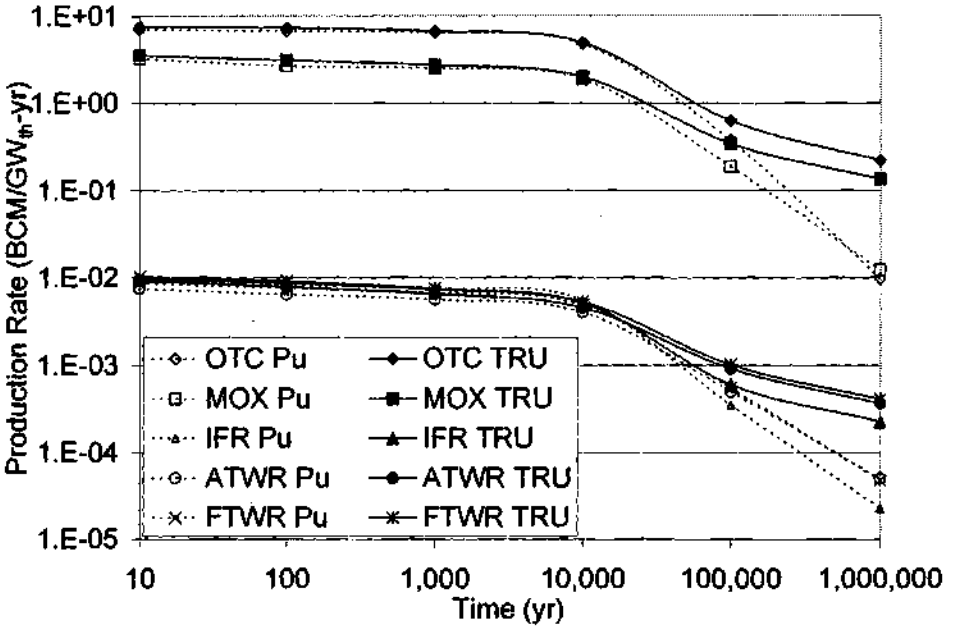

Figure 96 - Bare Critical Mass Production Rate

CHAPTER IX

CONCLUSIONS

Design concepts were presented for two sub-critical fast transmutation reactors driven by a tokamak fusion neutron source. The design concepts are for metal fueled, liquid metal cooled annular reactors that surround the toroidal plasma chamber on the outboard. Detailed fuel cycle analyses were performed to evaluate the impacts of further transmutation of spent nuclear fuel (SNF) on mass flows into high-level waste (HLW) and low-level waste (LLW) repositories, on the potential radiological hazard of the repository wastes, on the capacity of the HLW repositories, and on the proliferation-resistance of the material stored in HLW repositories. A SNF composition representative of the current inventory of SNF discharged from LWRs in the once-through fuel cycle (OTC) was taken as the base case against which the impact of further transmutation was compared.

Fusion Transmutation of Waste Reactor (FTWR) design concepts utilize nuclear and processing technologies that exist or are being developed. The FTWR designs satisfy a broad set of design constraints, including tritium self-sufficiency, thermo-mechanical limits, radiation damage limits, etc. FTWR designs can be developed for solid-fueld, non-feritle, sub-critical reactors located in the outboard blanket of a DT tokamak fusion reactor and more detailed analysis would not be expected to result in significant changes to the designs that were developed.

The geometry of the FTWR is significantly different than that of an accelerator-driven sub-critical reactor, but the transmutation performance will be similar. The FTWR may be significantly more sub-critical (k=0.95 versus 0.97) and operate for a much longer time between refuelings (560 days versus 140 days) because of the need to limit the size of the accelerator. Both are significant advantages of the FTWR.

The nuclear characteristics of the FTWR appear to be very favorable. Utililizing only transuranics from the light-water reactors (LWRs) as makeup and repeatedly recycling all actinides (including uranium

produced by decay), the sub-critical reactor will be stable and will remain sub-critical for a wide variety of off-normal conditions.

The sub-critical FTWR would be stable with relatively large positive reactivity coefficients, a condition that is unstable in critical reactors. The standard linear stability model for critical systems was extended for evaluation of the linear stability of sub-critical systems, and the FTWR was shown to be stable to power excursions even when substantial positive fuel and coolant temperature coefficients exist. For a sub-critical multiplication factor (k_{sub}) of 0.95 and a zero fuel temperature coefficient (FTC), the LiPb cooled FTWR is stable with a coolant temperature coefficient (CTC) less than 12.0 pcm/K, and with a zero CTC, the FTWR is stable with a FTC less than 5.4 pcm/K. Over the range studied, the line of marginal stability appeared to be a linear function of CTC and FTC and shifts to increasingly positive reactivity coefficients with increasing levels of sub-criticality. Similar thermal properties of the PbBi cooled FTWR resulted in similar behavior.

The large absorption cross section of ^{6}Li will produce a positive CTC, if its concentration is too high in the reactor coolant. Even though the LiPb cooled FTWR would be stable, it may experience power excursions unless actively controlled. By limiting the ^{6}Li enrichment in the reactor coolant, a LiPb cooled FTWR was designed that has a –0.25 pcm/K CTC at the beginning of cycle and a slightly positive 0.13 pcm/K CTC at the end of cycle. Thermal expansion is a large reactivity effect in fast reactors, but was not evaluated. Thermal expansion would be expected to make the total CTC negative. With improved techniques to evaluate the reactivity coefficients and possible small design changes, a LiPb cooled FTWR that has all negative reactivity coefficients at all times should be easily designed. The PbBi cooled design has all negative reactivity coefficients.

The geometry of the FTWR is a high neutron leakage design containing a large mass of transuranics that can theoretically form a critical configuration. Off-normal conditions were evaluated where the fuel is assumed to remain undamaged. These included flooding the plasma chamber, voiding the fuel, draining the outer reflector/breeder region, and combinations of these conditions. The basic assumptions for the analysis of off-normal conditions are that the source will be turned off and control rods will be inserted into the reactor. The maximum eigenvalue (k) under these conditions for the LiPb cooled design was 0.95. The PbBi cooled design the FTWR would be critical (k=1.001) with the plasma chamber

flooded. A conservative design for the number of control rods was used in this analysis. By increasing this number and/or by increasing the ^{10}B enrichment or using a more effective control rod material, the PbBi design should remain sub-critical under these conditions.

Fuel damage and fuel melting accidents will probably result in more limiting criticality safety accidents. These accidents are far beyond the capabilities of this analysis. The dissolution, fuel sweep out, and rearrangement of the fuel involve very complex phenomena. These issues were addressed in some detail for heavy metal cooled reactors in Wider[60] and Maschek[61]. Their results suggest that the FTWR should be able to be designed for this type of accident without significant modification.

Relative to the OTC, the impacts on waste management of a fuel cycle based on a single recycle of the plutonium from the SNF as MOX fuel in a LWR and of fuel cycles based on repeated recycling of the transuranics from the SNF as metal fuel in liquid metal cooled fast reactors were evaluated. Fuel cycles corresponding to three fast transmutation reactor concepts were evaluated: 1) a sub-critical reactor with a 'non-fertile' transuranics metal fuel and PbLi eutectic coolant, driven by a tokamak DT fusion neutron source (FTWR); 2) a sub-critical reactor with a 'non-fertile' transuranics metal fuel and Na coolant, driven by an accelerator spallation neutron source (Accelerator Transmutation of Waster Reactor - ATWR); and 3) a critical reactor with a 'fertile' transuranics plus uranium metal fuel and Na coolant (the Integral Fast Reactor - IFR).

Transmutation fuel cycles would reduce the transuranic inventory in the HLW, by fissioning the transuranics into fission products, most of which are relatively short-lived. A single recycle of the plutonium in SNF as MOX fuel in a LWR would reduce the HLW transuranic inventory by 25%, and repeated recycling in any of the fast transmutation reactors would eventually reduce the HLW transuranic inventory by > 99%. The ATWR and FTWR would be capable of a net transuranic destruction rate that is 2-3 times larger than for the IFR, because of the production of transuranics in the fertile fuel in the IFR. Therefore, on a per unit energy basis, the critical IFR will ultimately achieve similar levels of transuranic destruction, but, if a fertile matrix is used, the critical IFR will support one half to one third of the LWRs that the sub-critical reactors utilizing non-fertile matrices will support.

Toxicity is a simple measure commonly used to evaluate the impact of transmutation. The toxicity of the HLW is often compared with the toxicity of the uranium ore required to produce the LWR fuel. This

comparison neglects that only a very small fraction of the uranium is fissioned (< 1%). Therefore, the maximum the toxicity can be reduced is less than 1% for the aggregate of all waste streams. The toxicity beyond 100,000 years is dominated by the radioactive daughter products of uranium for all scenarios analyzed.

Destruction of the transuranics by repeated recycling in fast transmutation reactors reduces the toxicity of the repository wastes after the first 100 years or so, during which many of the additional short-lived fission products that were produced have decayed. The toxicity of all waste streams from the fast transmutation reactors approaches the toxicity of the original uranium ore in about 500 years. On the other hand, a single recycle of the plutonium from SNF as MOX fuel only slightly reduces the toxicity from all waste streams for LWR operation, and the toxicities of both the OTC and MOX fuel cycles remain above the toxicity of uranium ore for almost 100,000 years.

The decay heat source from the HLW is a major determinant in the design of a HLW repository. Repeated recycling of transuranics in fast transmutation reactors results in a HLW decay heat source is about two orders of magnitude lower than for the OTC SNF after the repository is closed. This should allow a significant increase in the capacity of the repository. A single recycle of the plutonium from SNF as MOX fuel, on the other hand, only achieves a small reduction in decay heat source and would not significantly impact the HLW repository capacity.

The transuranics in the SNF that would be stored intact in a HLW repository in the present OTC scenario could conceivably be a proliferation risk after the radiation has decreased to levels where the SNF is no longer 'self-protecting'. Repeatedly recycling the transuranics from the SNF in fast transmutation reactors not only destroys a large fraction of the transuranics but also increases the inventory of highly radioactive fission products in the waste that is deposited in the HLW repository. The bare critical mass of plutonium in the HLW going to the repository in the ATWR, FTWR or IFR fuel cycles is about 50% greater than the bare critical mass of the plutonium in the OTC SNF. Furthermore, because the transuranics are more dilute in the HLW from the fast transmutation reactors, the mass of HLW that must be processed to obtain a bare critical mass of plutonium is about 3 times greater for the HLW from the IFR fuel cycle, and about 8 times greater for the HLW from the ATWR and FTWR fuel cycles, than from the intact OTC SNF. On the other hand, while the bare critical mass of the plutonium in the HLW from once-recycled

MOX fuel is about 20% greater than the bare critical mass of plutonium from the OTC SNF, the mass of spent MOX fuel that must be processed to obtain this bare critical mass is less than one-third the mass of OTC SNF that must be processed to obtain a bare critical mass, because the plutonium is concentrated in making the MOX fuel.

The overall conclusion is that the repeated recycling of the transuranics from spent nuclear fuel would significantly increase the capacity of HLW repositories per unit of nuclear energy produced, significantly increase the nuclear energy production per unit mass of uranium ore mined, significantly reduce the time period of increased toxicity of combined HLW and LLW streams, and significantly enhance the proliferation-resistance of the material stored in HLW repositories.

CHAPTER X

FUTURE WORK

There are several areas that should be explored further. The design of the FTWR and related fuel cycle is not fully optimized. Improvements in the measures of the waste management and reactor performance need to be made. In particular, no measure of cost was evaluated. A limited set of design concepts and fuel cycles were evaluated. Additional neutron source designs and fuel cycles should be compared. The future work should focus on optimizing the FTWR design, developing better comparison techniques, and comparing the broadest range of options.

The first step is to better understand and define the goals of the transmutation systems. This includes more detailed figures of merit related to the performance of the repository and a costing model for the entire nuclear fuel cycle. Without more in-depth analysis of the design goals for the transmutation systems, real improvement in the nuclear fuel cycle is hard to guarantee.

For both the solid and liquid breeder design the ^{6}Li enrichment required to achieve tritium self-sufficiency seems to high for practical applications. The first step in optimizing the design of the FTWR is to develop a model that can determine the reactivity feedback associated with thermal expansion. A significant negative feedback from thermal expansion will allow for a large concentration of ^{6}Li in the reactor coolant and a greatly reduced ^{6}Li concentration in the remainder of the coolant. In addition, no attempt was made to used neutron moderation to exploit the large ^{6}Li resonance, which would help reduce the very high ^{6}Li enrichment and concentration required in the solid breeder design as well as for the liquid breeder design.

Neutron moderation and other techniques need to be evaluated to minimize the shield thickness and to reduce the required long-lived fission product loading. The FTWR is a very large neutronically unconnected reactor that offers the potential for very unique and novel designs for transmutation of the transuranics and long-lived fission products. Reducing transuranic loadings and increasing discharge

burnups will have a significant benefit on the waste management performance. More creative designs and fuel cycles may achieve a significant improvement in the performance of the FTWR.

The designs analyzed were based on liquid metal coolants. Other coolants studied in fusion and reactor applications should be evaluated to determine if there is significant improvement that can be made by operating with a different coolant system.

Other fuel cycles for the FTWR should be evaluated such as an initial recycle(s) of the plutonium back to the LWRs before the residual plutonium and minor actinides are transmuted in the FTWR. There is most likely some optimum balance between the performance of the FTWRs and LWRs that would be a significant improvement over either concept.

Other complete transmutation systems, besides the ATWR and IFR should be evaluated and compared with the performance of the FTWR. There are a number of other systems that are at very stages of development, which may perform significantly better than any of the systems analyzed.

APPENDIX A

TOXICITY INDICES

Table 113 - Toxicity Indices (m^3 of H_2O/Mole) for Actinide Isotopes

Note: Starting with one mole of given isotope and includes all daughters.

	Time (yr)					
Isotope	0	100	1,000	10,000	100,000	1,000,000
he 4						
tl206	4.5E+10					
tl207	4.9E+12					
tl208	1.2E+13					
tl209	8.6E+12					
pb206						
pb207						
pb208						
pb209	3.2E+11					
pb210	1.6E+11	8.2E+09	5.8E-03			
pb211	1.3E+13					
pb212	1.5E+13					
pb214	1.4E+13	8.2E+09	5.8E-03			
bi208	3.2E+05	3.2E+05	3.2E+05	3.2E+05	2.7E+05	4.9E+04
bi209						
bi210m	4.0E+06	4.0E+06	4.0E+06	4.0E+06	3.9E+06	3.2E+06
bi210	6.5E+11					
bi211	1.3E+13					
bi212	7.8E+12					
bi213	8.3E+12					
bi214	1.6E+13	8.2E+09	5.8E-03			
po210	1.4E+12					
po211m	1.5E+19					
po211	7.3E+12					
po212	9.5E+12					
po213	9.0E+12					
po214	9.8E+12	8.2E+09	5.8E-03			
po215	2.1E+13					
po216	1.1E+13					
po218	1.5E+13	8.2E+09	5.8E-03			
at217	5.8E+14					
rn218	1.1E+22	8.2E+09	5.8E-03			
rn219	9.5E+19					
rn220	2.0E+11					
rn222	3.4E+07	8.2E+09	5.8E-03			
fr221	4.8E+13					
fr223	2.9E+13					
ra222	9.9E+18	8.2E+09	5.8E-03			
ra223	1.6E+13					
ra224	1.8E+13					

	Time (yr)					
Isotope	0	100	1,000	10,000	100,000	1,000,000
ra225	1.8E+13					
ra226	7.5E+09	9.5E+09	6.5E+09	1.3E+08	1.5E-09	
ra228	2.1E+12	1.2E+07				
ac225	2.6E+12					
ac227	8.2E+09	2.4E+10	8.6E-03			
ac228	5.7E+12	2.4E-05				
th226	2.0E+17	8.2E+09	5.8E-03			
th227	3.5E+11					
th228	2.7E+10	2.4E-05				
th229	1.1E+08	2.1E+08	2.0E+08	8.9E+07	3.2E+04	1.3E-30
th230	2.4E+06	1.1E+07	7.7E+07	2.0E+08	8.8E+07	2.2E+04
th231	6.1E+11	3.8E+08	3.9E+08	3.2E+08	4.8E+07	2.6E-01
th232	1.3E+01	8.8E+02	8.8E+02	8.8E+02	8.8E+02	8.8E+02
th233	4.2E+12	1.7E+05	9.6E+05	6.1E+06	7.2E+06	1.4E+05
th234	2.7E+11	5.0E+04	1.7E+05	4.5E+06	3.4E+07	5.7E+06
pa231	1.2E+07	3.8E+08	3.9E+08	3.2E+08	4.8E+07	2.6E-01
pa232	1.7E+12	1.4E+09	1.9E+05	1.8E+00	1.8E+00	1.8E+00
pa233	4.8E+10	1.7E+05	9.6E+05	6.1E+06	7.2E+06	1.4E+05
pa234m	8.0E+12	5.0E+04	1.7E+05	4.5E+06	3.4E+07	5.7E+06
pa234	4.7E+12	5.0E+04	1.7E+05	4.5E+06	3.4E+07	5.7E+06
pa235	7.8E+09	4.7E+01	4.1E+02	3.6E+03	1.6E+04	1.9E+04
u230	1.3E+12	8.2E+09	5.8E-03			
u231	1.0E+15	3.8E+08	3.9E+08	3.2E+08	4.8E+07	2.6E-01
u232	1.7E+08	1.4E+09	1.9E+05	8.8E-35		
u233	7.5E+04	1.7E+05	9.6E+05	6.1E+06	7.2E+06	1.4E+05
u234	4.9E+04	5.0E+04	1.7E+05	4.5E+06	3.4E+07	5.7E+06
u235	1.7E+01	4.7E+01	4.1E+02	3.6E+03	1.6E+04	1.9E+04
u236	5.1E+02	5.1E+02	5.1E+02	5.1E+02	5.1E+02	5.2E+02
u237	1.9E+11	5.7E+04	5.8E+04	6.9E+04	3.1E+05	6.5E+05
u238	2.0E+00	6.0E+00	6.0E+00	9.0E+00	3.3E+02	3.3E+03
u239	4.0E+12	3.0E+06	2.9E+06	2.2E+06	1.8E+05	1.9E+04
u240	7.4E+12	1.1E+07	9.8E+06	3.8E+06	7.9E+02	5.2E+02
u241	1.1E+13	1.8E+08	4.3E+07	6.8E+04	3.0E+05	6.5E+05
np235	1.1E+13	5.4E+03	5.9E+03	8.1E+03	1.7E+04	1.9E+04
np236m	4.6E+13	7.1E+08	9.4E+04	2.7E+02	2.7E+02	2.7E+02
np236	6.2E+04	2.0E+05	2.7E+05	2.6E+05	1.5E+05	1.1E+03
np237	5.6E+04	5.7E+04	5.8E+04	6.9E+04	3.1E+05	6.5E+05
np238	1.2E+12	3.7E+08	4.4E+05	4.5E+06	3.4E+07	5.7E+06
np239	5.6E+11	3.0E+06	2.9E+06	2.2E+06	1.8E+05	1.9E+04
np240m	6.5E+12	1.1E+07	9.8E+06	3.8E+06	7.9E+02	5.2E+02
np240	1.5E+12	1.1E+07	9.8E+06	3.8E+06	7.9E+02	5.2E+02
np241	1.4E+10	1.8E+08	4.3E+07	6.8E+04	3.0E+05	6.5E+05
pu236	4.1E+09	1.5E+09	2.0E+05	8.8E-35		
pu237	9.6E+13	5.7E+04	5.8E+04	6.9E+04	3.1E+05	6.5E+05
pu238	8.2E+08	3.7E+08	4.4E+05	4.5E+06	3.4E+07	5.7E+06
pu239	3.0E+06	3.0E+06	2.9E+06	2.2E+06	1.8E+05	1.9E+04
pu240	1.1E+07	1.1E+07	9.8E+06	3.8E+06	7.9E+02	5.2E+02
pu241	1.3E+08	1.8E+08	4.3E+07	6.8E+04	3.0E+05	6.5E+05
pu242	1.9E+05	1.9E+05	1.9E+05	1.9E+05	1.6E+05	3.2E+04
pu243	2.1E+12	1.3E+07	1.2E+07	6.5E+06	2.5E+05	1.9E+04
pu244	1.1E+03	1.3E+03	1.4E+03	1.9E+03	2.2E+03	2.2E+03

Isotope	Time (yr)					
	0	100	1,000	10,000	100,000	1,000,000
pu245	5.0E+12	1.2E+07	1.8E+07	9.7E+06	2.8E+05	6.6E+05
pu246	4.0E+12	1.9E+07	1.6E+07	4.5E+06	1.6E+05	3.3E+04
am239	8.8E+15	3.0E+06	2.9E+06	2.2E+06	1.8E+05	1.9E+04
am240	2.1E+15	1.1E+07	9.8E+06	3.8E+06	7.9E+02	5.2E+02
am241	2.1E+08	1.8E+08	4.2E+07	6.8E+04	3.0E+05	6.5E+05
am242m	6.3E+08	6.4E+08	1.4E+07	3.6E+06	2.9E+07	4.7E+06
am242	2.0E+12	3.1E+08	4.0E+05	3.7E+06	2.9E+07	4.7E+06
am243	1.2E+07	1.3E+07	1.2E+07	6.5E+06	2.5E+05	1.9E+04
am244m	7.2E+09	7.2E+07	9.8E+06	3.8E+06	7.9E+02	5.2E+02
am244	6.2E+10	7.2E+07	9.8E+06	3.8E+06	7.9E+02	5.2E+02
am245	1.5E+12	1.2E+07	1.8E+07	9.7E+06	2.8E+05	6.6E+05
am246	4.8E+09	1.9E+07	1.6E+07	4.5E+06	1.6E+05	3.3E+04
cm241	1.3E+14	1.7E+08	4.1E+07	6.9E+04	3.1E+05	6.7E+05
cm242	4.0E+10	3.7E+08	4.5E+05	4.4E+06	3.4E+07	5.7E+06
cm243	2.5E+09	2.2E+08	2.9E+06	2.2E+06	1.8E+05	1.9E+04
cm244	2.8E+09	7.2E+07	9.8E+06	3.8E+06	7.9E+02	5.2E+02
cm245	1.1E+07	1.2E+07	1.8E+07	9.7E+06	2.8E+05	6.6E+05
cm246	1.9E+07	1.9E+07	1.6E+07	4.5E+06	1.6E+05	3.3E+04
cm247	5.6E+03	5.7E+03	6.2E+03	9.6E+03	1.6E+04	1.6E+04
cm248	2.6E+06	2.6E+06	2.6E+06	2.6E+06	2.2E+06	3.4E+05
cm249	1.5E+12	2.1E+08	4.9E+07	1.0E+07	2.8E+05	6.6E+05
cm250	3.4E+08	3.4E+08	3.3E+08	2.3E+08	6.5E+06	1.3E+04
cm251	1.1E+10	9.2E+07	4.6E+07	5.3E+04	1.6E+04	1.6E+04
bk249	6.8E+08	2.1E+08	4.9E+07	1.0E+07	2.8E+05	6.6E+05
bk250	4.9E+12	3.2E+07	1.6E+07	4.5E+06	1.6E+05	3.2E+04
bk251	3.3E+09	9.2E+07	4.6E+07	5.3E+04	1.6E+04	1.6E+04
cf249	2.6E+08	2.1E+08	4.9E+07	1.0E+07	2.8E+05	6.6E+05
cf250	2.7E+09	3.2E+07	1.6E+07	4.5E+06	1.6E+05	3.2E+04
cf251	1.0E+08	9.2E+07	4.6E+07	5.3E+04	1.6E+04	1.6E+04
cf252	6.8E+09	2.6E+06	2.5E+06	2.5E+06	2.1E+06	3.3E+05
cf253	7.3E+10	2.4E+08	5.6E+07	1.1E+07	3.2E+05	7.4E+05
cf254	2.2E+13	1.1E+06	1.0E+06	7.2E+05	2.0E+04	4.1E+01
cf255	2.1E+09	9.2E+07	4.6E+07	5.4E+04	1.6E+04	1.6E+04
es253	3.2E+11	2.3E+08	5.3E+07	1.1E+07	3.0E+05	7.0E+05
es254m	4.0E+12	3.2E+07	1.6E+07	4.5E+06	1.6E+05	3.2E+04
es254	4.7E+10	3.3E+07	1.6E+07	4.5E+06	1.6E+05	3.2E+04
es255	1.1E+11	9.2E+07	4.6E+07	5.4E+04	1.6E+04	1.6E+04

Table 114 - Toxicity Indices (m^3 of H_2O/Mole) for Fission Product Isotopes

Note: Starting with one mole of given isotope and includes all daughters.

	Time (yr)					
Isotope	0	100	1,000	10,000	100,000	1,000,000
H 3	9.7E+06	3.5E+04	3.7E-18			
Li 6						
Li 7						
Be 9						
Be 10	7.5E+04	7.5E+04	7.5E+04	7.4E+04	7.1E+04	4.8E+04
C 14	7.8E+04	7.7E+04	6.9E+04	2.3E+04	4.3E-01	
Ni 66	1.9E+13					
Cu 66	3.7E+10					
Zn 66						
Cu 67	1.7E+13					
Zn 67						
Zn 68						
Zn 69	1.7E+12					
Zn 69m	3.8E+12					
Ga 69						
Zn 70						
Ga 70	8.9E+09					
Ge 70						
Zn 71	7.7E+10					
Zn 71m	2.6E+14					
Ga 71						
Ge 71	5.7E+09					
Ge 71m	5.5E+14					
Co 72	9.1E+13					
Ni 72	3.0E+12					
Cu 72	1.7E+12					
Zn 72	2.3E+13					
Ga 72	5.6E+12					
Ge 72						
Co 73	8.8E+13					
Ni 73	2.3E+13					
Cu 73	2.2E+12					
Zn 73	4.8E+11					
Ga 73	2.2E+14					
Ge 73						
Ge 73m	2.3E+13					
Co 74	1.2E+14					
Ni 74	1.3E+13					
Cu 74	1.7E+13					
Zn 74	1.2E+11					
Ga 74	2.3E+10					
Ge 74						
Co 75	1.4E+14					
Ni 75	4.9E+13					
Cu 75	1.2E+13					
Zn 75	1.1E+12					
Ga 75	9.0E+10					
Ge 75	2.3E+09					

	Time (yr)					
Isotope	0	100	1,000	10,000	100,000	1,000,000
Ge 75m	2.4E+11					
As 75						
Ni 76	3.7E+13					
Cu 76	4.3E+13					
Zn 76	2.0E+12					
Ga 76	3.5E+11					
Ge 76						
As 76	6.0E+12					
Se 76						
Ni 77	1.1E+14					
Cu 77	3.7E+13					
Zn 77	5.4E+12					
Ga 77	8.6E+11					
Ge 77	9.3E+13					
Ge 77m	2.1E+11					
As 77	2.7E+13					
Se 77						
Se 77m	6.5E+11					
Ni 78	8.6E+13					
Cu 78	9.6E+13					
Zn 78	7.7E+12					
Ga 78	2.2E+12					
Ge 78	2.1E+09					
As 78	2.6E+13					
Se 78						
Cu 79	8.4E+13	2.6E+05	2.6E+05	2.5E+05	2.1E+05	3.1E+04
Zn 79	1.1E+13	3.4E+05	3.4E+05	3.3E+05	2.7E+05	4.1E+04
Ga 79	3.8E+12	3.4E+05	3.4E+05	3.4E+05	2.8E+05	4.2E+04
Ge 79	5.9E+11	3.6E+05	3.6E+05	3.5E+05	2.9E+05	4.4E+04
As 79	2.1E+10	3.6E+05	3.6E+05	3.5E+05	2.9E+05	4.4E+04
Se 79	3.6E+05	3.6E+05	3.6E+05	3.5E+05	2.9E+05	4.4E+04
Se 79m	4.8E+10	3.6E+05	3.6E+05	3.5E+05	2.9E+05	4.4E+04
Br 79						
Br 79m	2.3E+12					
Kr 79	3.0E+13					
Cu 80	1.3E+14	5.7E+04	5.6E+04	5.5E+04	4.6E+04	6.9E+03
Zn 80	2.1E+13	6.7E+03	6.7E+03	6.6E+03	5.4E+03	8.2E+02
Ga 80	6.8E+12	3.0E+03	3.0E+03	2.9E+03	2.4E+03	3.6E+02
Ge 80	3.8E+11					
As 80	7.4E+11					
Se 80						
Br 80	1.1E+10					
Br 80m	2.4E+14					
Kr 80						
Cu 81	1.5E+14	3.6E+03	3.6E+03	3.6E+03	2.9E+03	4.4E+02
Zn 81	9.2E+13	1.7E+02	1.7E+02	1.7E+02	1.4E+02	2.1E+01
Ga 81	9.2E+12					
Ge 81	1.5E+12					
As 81	3.4E+11					
Se 81	1.0E+10					
Se 81m	3.3E+09					

	Time (yr)					
Isotope	0	100	1,000	10,000	100,000	1,000,000
Br 81						
Kr 81	5.6E+05	5.6E+05	5.6E+05	5.4E+05	4.0E+05	2.2E+04
Kr 81m	8.7E+11	5.6E+05	5.6E+05	5.4E+05	4.0E+05	2.2E+04
Zn 82	8.9E+13					
Ga 82	1.9E+13					
Ge 82	2.5E+12					
As 82	5.9E+11					
As 82m	8.3E+11					
Se 82						
Br 82	2.2E+12					
Br 82m	3.1E+10					
Kr 82						
Zn 83	1.4E+14					
Ga 83	3.6E+13					
Ge 83	5.9E+12					
As 83	8.4E+11					
Se 83	8.4E+09					
Se 83m	1.6E+11					
Br 83	4.4E+14					
Kr 83						
Kr 83m	1.7E+09					
Ga 84	1.2E+14					
Ge 84	9.4E+12					
As 84	2.1E+12					
Se 84	5.9E+10					
Br 84	5.9E+09					
Br 84m	3.1E+10					
Kr 84						
Ga 85	1.3E+14	1.4E+00	7.4E-26			
Ge 85	4.5E+13	2.5E+00	1.4E-25			
As 85	5.6E+12	3.2E+00	1.7E-25			
Se 85	3.6E+11	1.1E+01	5.8E-25			
Se 85m	5.9E+11	1.1E+01	5.8E-25			
Br 85	6.6E+10	1.1E+01	5.8E-25			
Kr 85	3.3E+04	5.2E+01	2.8E-24			
Kr 85m	7.0E+08	1.1E+01	5.8E-25			
Rb 85						
Ge 86	4.6E+13	1.7E+00	9.2E-26			
As 86	1.3E+13	1.3E+00	7.0E-26			
Se 86	7.4E+11					
Br 86	2.1E+11					
Br 86m	2.5E+12					
Kr 86						
Rb 86	3.5E+11					
Rb 86m	1.9E+11					
Sr 86						
Ge 87	8.4E+13	2.3E-01	3.5E-02	3.5E-02	3.5E-02	3.5E-02
As 87	3.8E+13	4.1E-02	4.1E-02	4.1E-02	4.1E-02	4.1E-02
Se 87	2.0E+12	7.3E-02	7.3E-02	7.3E-02	7.3E-02	7.3E-02
Br 87	2.0E+11	7.3E-02	7.3E-02	7.3E-02	7.3E-02	7.3E-02
Kr 87	2.5E+09	7.5E-02	7.5E-02	7.5E-02	7.5E-02	7.5E-02

	Time (yr)					
Isotope	0	100	1,000	10,000	100,000	1,000,000
Rb 87	7.5E-02	7.5E-02	7.5E-02	7.5E-02	7.5E-02	7.5E-02
Sr 87						
Sr 87m	3.7E+14	2.2E-04	2.2E-04	2.2E-04	2.2E-04	2.2E-04
Ge 88	8.8E+13	2.3E-02	2.3E-02	2.3E-02	2.3E-02	2.3E-02
As 88	8.4E+13	1.9E-02	1.9E-02	1.9E-02	1.9E-02	1.9E-02
Se 88	7.5E+12	5.1E-03	5.1E-03	5.1E-03	5.1E-03	5.1E-03
Br 88	6.8E+11	4.8E-03	4.8E-03	4.8E-03	4.8E-03	4.8E-03
Kr 88	1.1E+09					
Rb 88	1.1E+10					
Sr 88						
As 89	9.3E+13	1.9E-03	1.9E-03	1.9E-03	1.9E-03	1.9E-03
Se 89	2.8E+13	2.4E-04	2.4E-04	2.4E-04	2.4E-04	2.4E-04
Br 89	2.6E+12					
Kr 89	5.9E+10					
Rb 89	1.2E+10					
Sr 89	8.6E+11					
Y 89						
Y 89m	7.0E+11					
As 90	1.2E+14	1.9E+09	4.5E-01	5.8E-05	5.8E-05	5.8E-05
Se 90	2.6E+13	2.5E+09	5.9E-01			
Br 90	5.9E+12	2.8E+09	6.7E-01			
Kr 90	3.5E+11	3.7E+09	8.7E-01			
Rb 90	7.4E+10	3.7E+09	8.7E-01			
Rb 90m	4.4E+10	3.7E+09	8.7E-01			
Sr 90	4.2E+10	3.7E+09	8.7E-01			
Y 90	2.5E+12					
Y 90m	3.3E+14					
Zr 90						
Zr 90m	1.4E+13					
Se 91	4.2E+13	9.1E+08	2.2E-01			
Br 91	1.9E+13	4.0E+08	9.5E-02			
Kr 91	1.3E+12					
Rb 91	1.9E+11	3.7E+03	8.7E-07			
Sr 91	6.6E+12					
Y 91	7.4E+10					
Y 91m	1.3E+12					
Zr 91						
Nb 91	1.8E+08	1.6E+08	6.3E+07	6.6E+03	9.8E-37	
Se 92	6.7E+13	5.3E+07	1.3E-02			
Br 92	3.1E+13					
Kr 92	6.1E+12					
Rb 92	2.5E+12					
Sr 92	1.9E+13					
Y 92	1.5E+13					
Zr 92						
Nb 92	3.4E+03	3.4E+03	3.4E+03	3.4E+03	3.4E+03	3.3E+03
Se 93	1.2E+14	2.9E+02	2.9E+02	2.9E+02	2.8E+02	1.8E+02
Br 93	6.4E+13	3.2E+02	3.3E+02	3.3E+02	3.1E+02	2.1E+02
Kr 93	8.8E+12	5.5E+02	5.5E+02	5.5E+02	5.3E+02	3.5E+02
Rb 93	2.0E+12	5.6E+02	5.7E+02	5.6E+02	5.4E+02	3.6E+02
Sr 93	2.5E+10	5.7E+02	5.7E+02	5.7E+02	5.5E+02	3.6E+02

	Time (yr)					
Isotope	0	100	1,000	10,000	100,000	1,000,000
Y 93	1.0E+13	8.7E+02	8.8E+02	8.7E+02	8.4E+02	5.6E+02
Zr 93	2.9E+02	8.7E+02	8.8E+02	8.7E+02	8.4E+02	5.6E+02
Nb 93						
Nb 93m	5.5E+07	7.5E+05	1.2E-11			
Br 94	1.0E+14	2.2E+02	2.3E+02	2.3E+02	2.2E+02	1.4E+02
Kr 94	5.4E+13	8.6E+01	8.7E+01	8.7E+01	8.3E+01	5.5E+01
Rb 94	4.2E+12	5.8E+01	5.8E+01	5.8E+01	5.6E+01	3.7E+01
Sr 94	1.5E+11					
Y 94	1.0E+10					
Zr 94						
Nb 94	5.9E+06	5.9E+06	5.7E+06	4.2E+06	1.9E+05	8.7E-09
Nb 94m	3.0E+10	5.8E+06	5.7E+06	4.2E+06	1.9E+05	8.6E-09
Br 95	1.1E+14	2.7E+01	2.8E+01	2.8E+01	2.6E+01	1.8E+01
Kr 95	1.5E+13	5.5E+00	5.5E+00	5.5E+00	5.3E+00	3.5E+00
Rb 95	2.9E+13					
Sr 95	4.5E+11					
Y 95	1.8E+10					
Zr 95	3.4E+10					
Nb 95	3.7E+10					
Nb 95m	1.2E+13					
Mo 95						
Br 96	1.3E+14	1.2E+00	1.2E+00	1.2E+00	1.2E+00	7.7E-01
Kr 96	3.9E+13					
Rb 96	5.7E+13					
Sr 96	1.1E+13					
Y 96	1.9E+12					
Zr 96						
Nb 96	4.5E+13					
Mo 96						
Kr 97	1.1E+14					
Rb 97	6.6E+13					
Sr 97	2.7E+13					
Y 97	3.2E+12					
Zr 97	9.3E+12					
Nb 97	2.9E+12					
Nb 97m	1.9E+11					
Mo 97						
Kr 98	7.1E+13					
Rb 98	9.9E+13					
Sr 98	1.7E+13					
Y 98	1.8E+13					
Zr 98	3.7E+11					
Nb 98	4.0E+12					
Nb 98m	3.7E+09					
Mo 98						
Tc 98	2.8E+04	2.8E+04	2.8E+04	2.8E+04	2.8E+04	2.4E+04
Rb 99	1.9E+14	7.1E+03	7.1E+03	6.9E+03	5.1E+03	2.7E+02
Sr 99	4.2E+13	8.3E+03	8.3E+03	8.1E+03	6.0E+03	3.1E+02
Y 99	7.7E+12	8.3E+03	8.3E+03	8.1E+03	6.0E+03	3.1E+02
Zr 99	5.4E+12	8.5E+03	8.4E+03	8.2E+03	6.1E+03	3.2E+02
Nb 99	7.5E+11	8.5E+03	8.4E+03	8.2E+03	6.1E+03	3.2E+02

	Time (yr)					
Isotope	0	100	1,000	10,000	100,000	1,000,000
Nb 99m	7.2E+10	8.5E+03	8.4E+03	8.2E+03	6.1E+03	3.2E+02
Mo 99	1.2E+12	8.5E+03	8.4E+03	8.2E+03	6.1E+03	3.2E+02
Tc 99	8.5E+03	8.5E+03	8.4E+03	8.2E+03	6.1E+03	3.2E+02
Tc 99m	1.7E+11	8.5E+03	8.4E+03	8.2E+03	6.1E+03	3.2E+02
Ru 99						
Rb100	1.2E+14	5.4E+02	5.4E+02	5.2E+02	3.9E+02	2.0E+01
Sr100	5.6E+13	1.3E+02	1.3E+02	1.3E+02	9.7E+01	5.0E+00
Y100	1.5E+13	7.2E+01	7.2E+01	7.0E+01	5.2E+01	2.7E+00
Zr100	1.6E+12					
Nb100	7.5E+12					
Nb100m	3.8E+12					
Mo100						
Tc100	7.1E+11					
Ru100						
Rb101	1.2E+14	3.9E+01	3.9E+01	3.8E+01	2.8E+01	1.5E+00
Sr101	5.8E+13	1.8E+00	1.8E+00	1.7E+00	1.3E+00	6.7E-02
Y101	2.3E+13					
Zr101	5.6E+12					
Nb101	1.6E+12					
Mo101	1.3E+10					
Tc101	1.3E+10					
Ru101						
Sr102	3.9E+13					
Y102	1.3E+13					
Zr102	3.9E+12					
Nb102	8.7E+12					
Mo102	1.7E+10					
Tc102	2.1E+12					
Tc102m	4.3E+10					
Ru102						
Rh102	4.1E+10	1.7E+00				
Pd102						
Sr103	9.4E+13					
Y103	4.3E+13					
Zr103	8.7E+12					
Nb103	7.5E+12					
Mo103	1.7E+11					
Tc103	2.1E+11					
Ru103	4.2E+10					
Rh103						
Rh103m	3.4E+11					
Sr104	6.9E+13					
Y104	8.8E+13					
Zr104	4.4E+12					
Nb104	2.4E+12					
Mo104	1.9E+11					
Tc104	1.0E+10					
Ru104						
Rh104	2.7E+11					
Rh104m	4.3E+10					
Pd104						

	Time (yr)					
Isotope	0	100	1,000	10,000	100,000	1,000,000
Y105	7.7E+13					
Zr105	2.3E+13					
Nb105	3.8E+12					
Mo105	3.2E+11					
Tc105	2.5E+10					
Ru105	7.1E+12					
Rh105	8.9E+11					
Rh105m	2.5E+11					
Pd105						
Y106	1.3E+14	7.1E-20				
Zr106	1.2E+13	8.5E-20				
Nb106	1.1E+13	8.6E-20				
Mo106	1.3E+12	9.1E-20				
Tc106	3.1E+11	9.1E-20				
Ru106	3.5E+10	9.1E-20				
Rh106	3.8E+11					
Rh106m	4.8E+14					
Pd106						
Ag106	2.6E+15					
Y107	1.2E+14	1.2E+04	1.2E+04	1.2E+04	1.2E+04	1.1E+04
Zr107	4.6E+13	1.6E+04	1.6E+04	1.6E+04	1.6E+04	1.5E+04
Nb107	1.5E+13	1.7E+04	1.7E+04	1.7E+04	1.7E+04	1.5E+04
Mo107	3.2E+12	1.8E+04	1.8E+04	1.8E+04	1.8E+04	1.7E+04
Tc107	5.3E+11	1.8E+04	1.8E+04	1.8E+04	1.8E+04	1.7E+04
Ru107	5.0E+10	1.8E+04	1.8E+04	1.8E+04	1.8E+04	1.7E+04
Rh107	8.7E+09	1.8E+04	1.8E+04	1.8E+04	1.8E+04	1.7E+04
Pd107	1.8E+04	1.8E+04	1.8E+04	1.8E+04	1.8E+04	1.7E+04
Pd107m	5.3E+11	1.8E+04	1.8E+04	1.8E+04	1.8E+04	1.7E+04
Ag107						
Zr108	3.0E+13	2.3E+03	2.3E+03	2.3E+03	2.3E+03	2.1E+03
Nb108	4.7E+13	1.2E+03	1.2E+03	1.2E+03	1.2E+03	1.1E+03
Mo108	7.5E+12					
Tc108	2.2E+12					
Ru108	4.1E+10					
Rh108	6.7E+11					
Rh108m	3.1E+10					
Pd108						
Ag108	7.9E+10					
Ag108m	9.4E+08	5.4E+08	4.0E+06	1.9E-15		
Cd108						
Zr109	8.7E+13	8.8E+01	8.8E+01	8.8E+01	8.7E+01	7.9E+01
Nb109	3.6E+13					
Mo109	8.0E+12					
Tc109	8.1E+12					
Ru109	3.2E+11					
Rh109	1.4E+11					
Rh109m	2.3E+11					
Pd109	3.3E+12					
Pd109m	4.0E+10					
Ag109						
Ag109m	2.9E+11					

	Time (yr)					
Isotope	0	100	1,000	10,000	100,000	1,000,000
Cd109	7.1E+09	1.2E-14				
Nb110	8.7E+13					
Mo110	4.1E+12					
Tc110	1.4E+13					
Ru110	7.5E+11					
Rh110	3.6E+12					
Rh110m	4.0E+11					
Pd110						
Ag110	4.6E+11					
Ag110m	1.7E+10					
Cd110						
Nb111	6.6E+13					
Mo111	2.4E+13					
Tc111	5.7E+12					
Ru111	7.1E+12					
Rh111	1.0E+12					
Pd111	8.0E+09					
Pd111m	1.9E+14					
Ag111	4.4E+11					
Ag111m	1.7E+11					
Cd111						
Cd111m	3.9E+09					
Nb112	1.3E+14					
Mo112	1.2E+13					
Tc112	2.6E+13					
Ru112	3.1E+12					
Rh112	7.5E+12					
Pd112	5.0E+13					
Ag112	3.3E+14					
Cd112						
Mo113	4.9E+13	9.1E+05	3.4E-11	3.4E-11	3.4E-11	3.4E-11
Tc113	1.7E+13	9.4E+05	3.5E-11	3.5E-11	3.5E-11	3.5E-11
Ru113	3.8E+12	1.0E+06	3.8E-11	3.8E-11	3.8E-11	3.8E-11
Rh113	1.3E+13	1.0E+06	3.8E-11	3.8E-11	3.8E-11	3.8E-11
Pd113	1.2E+11	1.0E+06	3.8E-11	3.8E-11	3.8E-11	3.8E-11
Ag113	2.0E+14	1.1E+06	3.8E-11	3.8E-11	3.8E-11	3.8E-11
Ag113m	1.6E+11	8.4E+05	3.8E-11	3.8E-11	3.8E-11	3.8E-11
Cd113	3.9E-11	3.9E-11	3.9E-11	3.9E-11	3.9E-11	3.9E-11
Cd113m	8.5E+09	6.2E+07	3.8E-12	5.4E-14	5.4E-14	5.4E-14
In113						
In113m	1.9E+12					
Mo114	3.0E+13	6.7E+04	2.5E-12	2.5E-12	2.5E-12	2.5E-12
Tc114	5.6E+13	6.7E+04	2.5E-12	2.5E-12	2.5E-12	2.5E-12
Ru114	1.4E+12	1.1E+03	4.0E-14	4.0E-14	4.0E-14	4.0E-14
Rh114	6.6E+12	7.3E-16	7.3E-16	7.3E-16	7.3E-16	7.3E-16
Pd114	7.7E+10					
Ag114	2.5E+12					
Cd114						
In114	1.6E+11					
In114m	1.3E+11					
Sn114						

	Time (yr)					
Isotope	0	100	1,000	10,000	100,000	1,000,000
Mo115	9.0E+13	1.3E+02	7.3E-06	7.3E-06	7.3E-06	7.3E-06
Tc115	4.2E+13	1.3E+02	7.3E-06	7.3E-06	7.3E-06	7.3E-06
Ru115	1.3E+13	8.5E-06	8.5E-06	8.5E-06	8.5E-06	8.5E-06
Rh115	1.4E+12	8.5E-06	8.5E-06	8.5E-06	8.5E-06	8.5E-06
Pd115	3.0E+11	8.6E-06	8.6E-06	8.6E-06	8.6E-06	8.6E-06
Ag115	9.4E+09	8.6E-06	8.6E-06	8.6E-06	8.6E-06	8.6E-06
Ag115m	6.3E+11	8.6E-06	8.6E-06	8.6E-06	8.6E-06	8.6E-06
Cd115	2.0E+12	8.6E-06	8.6E-06	8.6E-06	8.6E-06	8.6E-06
Cd115m	9.8E+10	9.0E-06	9.0E-06	9.0E-06	9.0E-06	9.0E-06
In115	9.0E-06	9.0E-06	9.0E-06	9.0E-06	9.0E-06	9.0E-06
In115m	1.8E+12	8.6E-06	8.6E-06	8.6E-06	8.6E-06	8.6E-06
Sn115						
Tc116	9.8E+13	1.2E-06	1.2E-06	1.2E-06	1.2E-06	1.2E-06
Ru116	6.6E+12	1.4E-07	1.4E-07	1.4E-07	1.4E-07	1.4E-07
Rh116	1.2E+13	4.6E-08	4.6E-08	4.6E-08	4.6E-08	4.6E-08
Pd116	8.9E+11					
Ag116	7.0E+10					
Ag116m	1.1E+12					
Cd116						
In116	8.0E+11					
In116m	3.5E+09					
Sn116						
Tc117	7.4E+13	3.0E-08	3.0E-08	3.0E-08	3.0E-08	3.0E-08
Ru117	3.3E+13	9.5E-10	9.5E-10	9.5E-10	9.5E-10	9.5E-10
Rh117	9.3E+12					
Pd117	2.3E+12					
Ag117	1.6E+11					
Ag117m	2.1E+12					
Cd117	4.2E+14					
Cd117m	3.1E+14					
In117	4.3E+09					
In117m	1.6E+09					
Sn117						
Sn117m	3.2E+12					
Tc118	1.4E+14					
Ru118	1.7E+13					
Rh118	3.6E+13					
Pd118	3.6E+12					
Ag118	3.0E+12					
Ag118m	5.6E+12					
Cd118	3.7E+09					
In118	2.3E+12					
In118m	4.2E+10					
Sn118						
Ru119	5.8E+13	1.2E-29				
Rh119	2.4E+13	1.2E-29				
Pd119	6.4E+12	1.3E-29				
Ag119	5.4E+12	1.3E-29				
Cd119	7.0E+10	5.1E-30				
Cd119m	8.6E+10	4.2E-29				
In119	7.8E+10	4.2E-29				

	Time (yr)					
Isotope	0	100	1,000	10,000	100,000	1,000,000
In119m	1.1E+10	1.0E-30				
Sn119						
Sn119m	1.5E+11	4.5E-27				
Ru120	3.2E+13	7.8E-31				
Rh120	6.5E+13	7.8E-31				
Pd120	2.9E+12					
Ag120	9.7E+12					
Cd120	2.2E+11					
In120	3.7E+12					
In120m	2.4E+11					
Sn120						
Rh121	4.5E+13	1.3E+06	1.5E+01			
Pd121	1.8E+13	1.5E+06	1.8E+01			
Ag121	1.4E+13	1.5E+06	1.8E+01			
Cd121	8.4E+11	1.5E+06	1.8E+01			
In121	4.9E+11	1.2E+08	1.5E+03			
In121m	4.9E+10	1.5E+06	1.8E+01			
Sn121	3.9E+13					
Sn121m	2.2E+09	1.1E+09	1.3E+04			
Sb121						
Rh122	1.1E+14	1.3E+05	1.6E+00			
Pd122	8.0E+12	9.2E+03	1.1E-01			
Ag122	2.4E+13	2.8E+03	3.3E-02			
Cd122	2.2E+12					
In122	7.5E+12					
In122m	1.1E+12					
Sn122						
Sb122	1.6E+12					
Sb122m	4.5E+10					
Te122						
Rh123	8.4E+13	1.1E+03	1.3E-02			
Pd123	3.8E+13					
Ag123	2.9E+13					
Cd123	1.3E+12					
In123	1.9E+12					
In123m	2.4E+11					
Sn123	3.4E+11					
Sn123m	4.7E+09					
Sb123						
Te123	9.6E-03	9.6E-03	9.6E-03	9.6E-03	9.6E-03	9.6E-03
Te123m	3.6E+11	9.6E-03	9.6E-03	9.6E-03	9.6E-03	9.6E-03
Pd124	2.2E+13					
Ag124	4.5E+13					
Cd124	1.3E+13					
In124	3.6E+12					
Sn124						
Sb124	1.1E+11					
Sb124m	1.2E+11					
Te124						
Pd125	6.8E+13	1.4E-02				
Ag125	3.4E+13	1.4E-02				

	Time (yr)					
Isotope	0	100	1,000	10,000	100,000	1,000,000
Cd125	7.3E+12	1.5E-02				
In125	4.8E+12	1.5E-02				
In125m	9.3E+11	1.5E-02				
Sn125	6.8E+11	1.5E-02				
Sn125m	2.0E+10	1.5E-02				
Sb125	1.3E+09	1.5E-02				
Te125						
Te125m	2.3E+10					
Pd126	4.5E+13	1.4E-03				
Ag126	8.1E+13	7.1E-04				
Cd126	2.2E+13					
In126	7.8E+12	1.4E+06	1.4E+06	1.3E+06	6.8E+05	1.3E+03
Sn126	1.2E+06	1.4E+06	1.4E+06	1.3E+06	6.8E+05	1.3E+03
Sb126	3.5E+12					
Sb126m	9.9E+09					
Te126						
Xe126						
Ag127	6.4E+13	8.1E+03	8.1E+03	7.6E+03	4.1E+03	8.0E+00
Cd127	2.0E+13	9.0E+03	9.0E+03	8.4E+03	4.5E+03	8.8E+00
In127	9.8E+12	9.0E+03	8.9E+03	8.4E+03	4.5E+03	8.8E+00
In127m	3.0E+12	8.8E+03	8.8E+03	8.2E+03	4.4E+03	8.6E+00
Sn127	5.0E+14					
Sn127m	4.6E+10					
Sb127	1.1E+13					
Te127	1.7E+12					
Te127m	2.4E+10					
I127						
Xe127	1.2E+12					
Ag128	1.2E+14	6.3E+02	6.3E+02	5.9E+02	3.2E+02	6.2E-01
Cd128	1.1E+13	9.9E+00	9.8E+00	9.2E+00	4.9E+00	9.6E-03
In128	1.3E+13					
Sn128	3.2E+09					
Sb128	1.2E+14					
Sb128m	1.8E+10					
Te128						
I128	7.5E+09					
Xe128						
Cd129	3.8E+13	3.8E+05	3.8E+05	3.8E+05	3.8E+05	3.6E+05
In129	1.9E+13	3.8E+05	3.8E+05	3.8E+05	3.8E+05	3.6E+05
Sn129	8.7E+10	3.8E+05	3.8E+05	3.8E+05	3.8E+05	3.6E+05
Sn129m	2.8E+10	3.8E+05	3.8E+05	3.8E+05	3.8E+05	3.6E+05
Sb129	2.4E+14	3.8E+05	3.8E+05	3.8E+05	3.8E+05	3.6E+05
Te129	3.4E+12	3.8E+05	3.8E+05	3.8E+05	3.8E+05	3.6E+05
Te129m	1.9E+11	3.8E+05	3.8E+05	3.8E+05	3.8E+05	3.6E+05
I129	3.8E+05	3.8E+05	3.8E+05	3.8E+05	3.8E+05	3.6E+05
Xe129						
Xe129m	4.9E+12					
Cd130	2.4E+13	7.1E+03	7.1E+03	7.1E+03	7.1E+03	6.8E+03
In130	3.5E+13	3.5E+03	3.5E+03	3.5E+03	3.4E+03	3.3E+03
Sn130	5.1E+10					
Sb130	4.8E+09					

	Time (yr)					
Isotope	0	100	1,000	10,000	100,000	1,000,000
Sb130m	3.0E+10					
Te130						
I130	8.5E+13					
I130m	2.1E+10					
Xe130						
Cd131	1.1E+14	1.7E+02	1.7E+02	1.7E+02	1.7E+02	1.6E+02
In131	4.2E+13					
Sn131	2.9E+11					
Sb131	8.2E+09					
Te131	7.5E+09					
Te131m	2.6E+12					
I131	5.4E+13					
Xe131						
Xe131m	1.1E+07					
Cd132	8.3E+13					
In132	6.1E+13					
Sn132	2.8E+11					
Sb132	4.5E+10					
Sb132m	6.7E+10					
Te132	2.0E+12					
I132	1.7E+14					
Xe132						
Cs132	6.7E+12					
Ba132						
In133	1.0E+14					
Sn133	7.8E+12					
Sb133	7.5E+10					
Te133	1.5E+10					
Te133m	3.4E+09					
I133	1.5E+14					
I133m	1.3E+12					
Xe133	2.5E+07					
Xe133m	6.0E+07					
Cs133						
Ba133	1.1E+10	1.6E+07	2.7E-19			
In134	1.4E+14					
Sn134	1.1E+13					
Sb134	1.3E+13					
Sb134m	1.1E+12					
Te134	4.5E+09					
I134	1.8E+14					
I134m	5.1E+10					
Xe134						
Xe134m	3.9E+13					
Cs134	1.9E+10	4.8E-05				
Cs134m	1.1E+12	4.8E-05				
Ba134						
Sn135	2.7E+13	1.1E+03	1.1E+03	1.1E+03	1.1E+03	8.4E+02
Sb135	6.6E+12	1.2E+03	1.2E+03	1.2E+03	1.2E+03	9.2E+02
Te135	5.9E+11	1.6E+03	1.6E+03	1.6E+03	1.5E+03	1.2E+03
I135	1.2E+14	1.6E+03	1.6E+03	1.6E+03	1.5E+03	1.2E+03

	Time (yr)					
Isotope	0	100	1,000	10,000	100,000	1,000,000
Xe135	3.4E+08	1.6E+03	1.6E+03	1.6E+03	1.5E+03	1.2E+03
Xe135m	1.2E+10	1.6E+03	1.6E+03	1.6E+03	1.5E+03	1.2E+03
Cs135	1.6E+03	1.6E+03	1.6E+03	1.6E+03	1.5E+03	1.2E+03
Cs135m	3.6E+09	1.6E+03	1.6E+03	1.6E+03	1.5E+03	1.2E+03
Ba135						
Ba135m	3.6E+13					
Sn136	1.6E+13	5.1E+02	5.1E+02	5.1E+02	5.0E+02	3.8E+02
Sb136	1.4E+13	3.7E+02	3.7E+02	3.7E+02	3.6E+02	2.7E+02
Te136	6.5E+11	1.4E+01	1.4E+01	1.4E+01	1.4E+01	1.0E+01
I136	1.4E+11					
I136m	2.4E+11					
Xe136						
Cs136	1.7E+11					
Ba136						
Ba136m	3.7E+13					
Sb137	2.4E+13	4.3E+07	2.8E+00	2.8E+00	2.7E+00	2.1E+00
Te137	3.2E+12	5.4E+07	5.0E-02			
I137	4.6E+11	5.5E+07	5.1E-02			
Xe137	4.9E+10	5.9E+07	5.5E-02			
Cs137	6.0E+08	5.9E+07	5.5E-02			
Ba137						
Ba137m	7.4E+10					
Sb138	6.5E+13	1.7E+07	1.6E-02			
Te138	8.1E+12	6.4E+06	6.0E-03			
I138	1.7E+12	3.2E+06	2.9E-03			
Xe138	1.3E+10					
Cs138	5.8E+09					
Cs138m	6.5E+10					
Ba138						
La138	1.1E+00	1.1E+00	1.1E+00	1.1E+00	1.1E+00	1.1E+00
Sb139	5.2E+13	2.8E+06	2.6E-03			
Te139	2.0E+13	2.0E+05	1.9E-04			
I139	4.9E+12					
Xe139	2.8E+11					
Cs139	2.0E+10					
Ba139	2.2E+09					
La139						
Ce139	3.2E+11					
Pr139	2.4E+14					
Te140	1.3E+13					
I140	1.3E+13					
Xe140	8.3E+11					
Cs140	1.8E+11					
Ba140	5.1E+11					
La140	3.9E+12					
Ce140						
Pr140	5.6E+10					
Te141	4.1E+13					
I141	2.5E+13					
Xe141	6.5E+12					
Cs141	4.5E+11					

	Time (yr)					
Isotope	0	100	1,000	10,000	100,000	1,000,000
Ba141	1.0E+10					
La141	2.7E+14					
Ce141	4.5E+10					
Pr141						
Nd141	1.3E+15					
Te142	1.9E+13	8.1E+01	8.1E+01	8.1E+01	8.1E+01	8.1E+01
I142	5.6E+13	9.5E+01	9.5E+01	9.5E+01	9.5E+01	9.5E+01
Xe142	9.3E+12	1.1E+02	1.1E+02	1.1E+02	1.1E+02	1.1E+02
Cs142	6.6E+12	1.1E+02	1.1E+02	1.1E+02	1.1E+02	1.1E+02
Ba142	1.8E+10	1.1E+02	1.1E+02	1.1E+02	1.1E+02	1.1E+02
La142	2.1E+09	1.1E+02	1.1E+02	1.1E+02	1.1E+02	1.1E+02
Ce142	1.1E+02	1.1E+02	1.1E+02	1.1E+02	1.1E+02	1.1E+02
Pr142	5.5E+12	1.9E-02	1.9E-02	1.9E-02	1.9E-02	1.9E-02
Pr142m	1.3E+10	1.9E-02	1.9E-02	1.9E-02	1.9E-02	1.9E-02
Nd142						
I143	2.8E+13	2.3E+01	2.3E+01	2.3E+01	2.3E+01	2.3E+01
Xe143	1.2E+13	3.2E+00	3.2E+00	3.2E+00	3.2E+00	3.2E+00
Cs143	6.3E+12	1.8E+00	1.8E+00	1.8E+00	1.8E+00	1.8E+00
Ba143	7.8E+11					
La143	1.3E+10					
Ce143	2.4E+12					
Pr143	1.9E+15					
Nd143						
I144	7.7E+13	4.9E-01	4.9E-01	4.9E-01	4.9E-01	4.9E-01
Xe144	1.0E+13	1.3E-02	1.3E-02	1.3E-02	1.3E-02	1.3E-02
Cs144	1.1E+13	2.4E-06	2.4E-06	2.4E-06	2.4E-06	2.4E-06
Ba144	9.9E+11	2.4E-06	2.4E-06	2.4E-06	2.4E-06	2.4E-06
La144	2.8E+11	2.4E-06	2.4E-06	2.4E-06	2.4E-06	2.4E-06
Ce144	4.6E+10	2.4E-06	2.4E-06	2.4E-06	2.4E-06	2.4E-06
Pr144	1.1E+10	2.4E-06	2.4E-06	2.4E-06	2.4E-06	2.4E-06
Pr144m	2.6E+10	2.4E-06	2.4E-06	2.4E-06	2.4E-06	2.4E-06
Nd144	2.4E-06	2.4E-06	2.4E-06	2.4E-06	2.4E-06	2.4E-06
I145	5.8E+13	3.2E-03	3.2E-03	3.2E-03	3.2E-03	3.2E-03
Xe145	1.3E+13	4.8E-07	4.8E-07	4.8E-07	4.8E-07	4.8E-07
Cs145	1.9E+13	3.6E-07	3.6E-07	3.6E-07	3.6E-07	3.6E-07
Ba145	2.6E+12					
La145	4.6E+11					
Ce145	6.3E+10					
Pr145	1.8E+14					
Nd145						
Pm145	6.7E+09	1.3E+08	6.6E-08			
Sm145	1.3E+11	1.4E+08	7.0E-08			
Xe146	2.0E+13	2.3E-08	2.3E-08	2.3E-08	2.3E-08	2.3E-08
Cs146	3.3E+13					
Ba146	5.1E+12					
La146	1.8E+12					
Ce146	1.4E+10					
Pr146	7.8E+09					
Nd146						
Pm146	2.2E+10	1.2E+05	3.9E+04	3.9E+04	3.9E+04	3.9E+04
Sm146	1.2E+05	1.2E+05	1.2E+05	1.2E+05	1.2E+05	1.2E+05

	Time (yr)					
Isotope	0	100	1,000	10,000	100,000	1,000,000
Xe147	5.7E+13	4.1E-02	3.9E-02	3.9E-02	3.9E-02	3.9E-02
Cs147	2.1E+13	4.4E-02	4.3E-02	4.3E-02	4.3E-02	4.3E-02
Ba147	1.6E+13	5.9E-02	5.7E-02	5.7E-02	5.7E-02	5.7E-02
La147	2.6E+12	5.9E-02	5.7E-02	5.7E-02	5.7E-02	5.7E-02
Ce147	2.0E+11	5.9E-02	5.7E-02	5.7E-02	5.7E-02	5.7E-02
Pr147	1.4E+10	5.9E-02	5.7E-02	5.7E-02	5.7E-02	5.7E-02
Nd147	2.0E+11	5.9E-02	5.7E-02	5.7E-02	5.7E-02	5.7E-02
Pm147	6.8E+08	5.9E-02	5.6E-02	5.6E-02	5.6E-02	5.6E-02
Sm147	5.6E-02	5.6E-02	5.6E-02	5.6E-02	5.6E-02	5.6E-02
Cs148	5.5E+13	1.5E-02	1.4E-02	1.4E-02	1.4E-02	1.4E-02
Ba148	1.9E+13	1.1E-04	1.1E-04	1.1E-04	1.1E-04	1.1E-04
La148	1.1E+13	7.9E-05	7.6E-05	7.6E-05	7.6E-05	7.6E-05
Ce148	2.0E+11					
Pr148	8.3E+10					
Nd148						
Pm148	8.1E+12	1.5E-03	1.5E-03	1.5E-03	1.5E-03	1.5E-03
Pm148m	1.1E+12	1.5E-03	1.5E-03	1.5E-03	1.5E-03	1.5E-03
Sm148	1.5E-03	1.5E-03	1.5E-03	1.5E-03	1.5E-03	1.5E-03
Cs149	4.6E+13	8.3E-04	8.3E-04	8.3E-04	8.3E-04	8.3E-04
Ba149	1.6E+13	1.2E-03	1.2E-03	1.2E-03	1.2E-03	1.2E-03
La149	4.7E+12	1.2E-03	1.2E-03	1.2E-03	1.2E-03	1.2E-03
Ce149	2.2E+12	1.2E-03	1.2E-03	1.2E-03	1.2E-03	1.2E-03
Pr149	8.3E+10	1.2E-03	1.2E-03	1.2E-03	1.2E-03	1.2E-03
Nd149	6.1E+12	1.2E-03	1.2E-03	1.2E-03	1.2E-03	1.2E-03
Pm149	1.5E+12	1.2E-03	1.2E-03	1.2E-03	1.2E-03	1.2E-03
Sm149	1.2E-03	1.2E-03	1.2E-03	1.2E-03	1.2E-03	1.2E-03
Eu149	4.7E+11	1.2E-03	1.2E-03	1.2E-03	1.2E-03	1.2E-03
Cs150	9.1E+13	1.9E-04	1.9E-04	1.9E-04	1.9E-04	1.9E-04
Ba150	1.2E+13	1.4E-05	1.4E-05	1.4E-05	1.4E-05	1.4E-05
La150	1.9E+13	1.1E-05	1.1E-05	1.1E-05	1.1E-05	1.1E-05
Ce150	2.8E+12					
Pr150	1.8E+12					
Nd150						
Pm150	3.9E+14					
Sm150						
Eu150	3.3E+09	4.8E+08	1.3E+01			
Ba151	3.4E+13	4.1E+06	4.0E+03	4.2E-07	4.2E-07	4.2E-07
La151	1.6E+13	4.3E+06	4.2E+03	3.3E-27		
Ce151	1.1E+13	4.6E+06	4.5E+03	3.5E-27		
Pr151	6.0E+11	4.6E+06	4.5E+03	3.5E-27		
Nd151	1.5E+10	4.6E+06	4.5E+03	3.5E-27		
Pm151	3.7E+13	4.6E+06	4.5E+03	3.5E-27		
Sm151	9.9E+06	4.6E+06	4.5E+03	3.5E-27		
Eu151						
Ba152	2.7E+13	5.1E+05	5.0E+02	3.9E-28		
La152	4.0E+13	2.8E+05	2.7E+02	2.1E-28		
Ce152	1.5E+12					
Pr152	1.7E+12					
Nd152	1.7E+10					
Pm152	4.6E+10					
Pm152m	2.5E+10					

	Time (yr)					
Isotope	0	100	1,000	10,000	100,000	1,000,000
Sm152						
Eu152	3.4E+08	1.9E+06	3.1E-02	3.1E-02	3.1E-02	3.1E-02
Eu152m	5.6E+12	8.0E-02	8.0E-02	8.0E-02	8.0E-02	8.0E-02
Gd152	1.1E-01	1.1E-01	1.1E-01	1.1E-01	1.1E-01	1.1E-01
La153	3.5E+13					
Ce153	7.7E+12					
Pr153	2.5E+12					
Nd153	1.7E+11					
Pm153	3.5E+10					
Sm153	8.5E+11					
Eu153						
Gd153	2.7E+09					
La154	7.6E+13					
Ce154	5.6E+12					
Pr154	1.1E+13					
Nd154	2.8E+11					
Pm154	1.1E+11					
Pm154m	7.0E+10					
Sm154						
Eu154	2.1E+09	6.5E+05	1.9E-26			
Gd154						
La155	7.3E+13	1.1E+02				
Ce155	2.1E+13	1.4E+02				
Pr155	1.0E+13	1.4E+02				
Nd155	6.2E+11	1.4E+02				
Pm155	2.4E+11	1.4E+02				
Sm155	8.4E+09	1.4E+02				
Eu155	3.8E+08	1.4E+02				
Gd155						
Gd155m	3.6E+14					
Ce156	1.9E+13	7.9E+00				
Pr156	3.0E+13	3.8E+00				
Nd156	5.8E+11					
Pm156	8.6E+11					
Sm156	1.1E+14					
Eu156	2.9E+12					
Gd156						
Ce157	5.3E+13	1.7E-01				
Pr157	3.0E+13					
Nd157	4.6E+12					
Pm157	1.8E+11					
Sm157	2.3E+10					
Eu157	6.9E+13					
Gd157						
Pr158	6.7E+13					
Nd158	4.2E+12					
Pm158	3.0E+12					
Sm158	3.4E+10					
Eu158	4.1E+09					
Gd158						
Pr159	6.3E+13					

	Time (yr)					
Isotope	0	100	1,000	10,000	100,000	1,000,000
Nd159	1.8E+13					
Pm159	3.8E+12					
Sm159	7.0E+10					
Eu159	1.0E+10					
Gd159	2.1E+12					
Tb159						
Nd160	1.4E+13					
Pm160	1.6E+13					
Sm160	1.6E+11					
Eu160	2.6E+11					
Gd160						
Tb160	4.5E+10					
Dy160						
Nd161	3.6E+13					
Pm161	1.4E+13					
Sm161	2.4E+12					
Eu161	2.7E+11					
Gd161	5.1E+10					
Tb161	6.3E+12					
Dy161						
Pm162	3.5E+13					
Sm162	2.2E+12					
Eu162	7.0E+10					
Gd162	2.2E+10					
Tb162	2.4E+10					
Tb162m	4.7E+14					
Dy162						
Sm163	8.9E+12					
Eu163	1.5E+12					
Gd163	1.2E+11					
Tb163	9.7E+09					
Tb163m	2.7E+10					
Dy163						
Sm164	8.2E+12					
Eu164	7.4E+12					
Gd164	8.7E+09					
Tb164	6.3E+10					
Dy164						
Sm165	2.5E+13					
Eu165	8.3E+12					
Gd165	2.7E+11					
Tb165	8.9E+10					
Dy165	3.4E+12					
Dy165m	1.5E+11					
Ho165						
Dy166	9.6E+11					
Ho166	3.9E+12					
Ho166m	9.9E+07	9.4E+07	5.6E+07	3.1E+05	8.1E-18	
Er166						
Er167						
Er167m	5.0E+12					

	Time (yr)					
Isotope	0	100	1,000	10,000	100,000	1,000,000
Er168						
Yb168						
Er169	1.5E+11					
Tm169						
Yb169	1.4E+12					
Er170						
Tm170	2.0E+10					
Tm170m	2.8E+18					
Yb170						
Er171	4.2E+12	7.8E-08				
Tm171	3.7E+08	7.8E-08				
Yb171						
Er172	2.1E+13					
Tm172	1.6E+13					
Yb172						

APPENDIX B

DECAY HEAT

Table 115 - Decay Heat (W/mole) for Actinide Isotopes

Note: Starting with one mole of given isotope and includes all daughters.

	Time (yr)					
Isotope	0	10	100	1,000	100,000	1,000,000
He 4						
Tl206	1.4E+08					
Tl207	1.2E+08					
Tl208	1.4E+09					
Tl209	1.4E+09					
Pb206						
Pb207						
Pb208						
Pb209	1.1E+06					
Pb210	3.8E+00	4.1E+02	2.5E+01	1.8E-11		
Pb211	1.6E+07					
Pb212	5.6E+05					
Pb214	2.3E+07	4.1E+02	2.5E+01	1.8E-11		
Bi208	1.5E-02	1.5E-02	1.5E-02	1.5E-02	1.3E-02	2.3E-03
Bi209						
Bi210m	3.8E-03	4.1E-03	4.1E-03	4.1E-03	4.0E-03	3.3E-03
Bi210	6.0E+04	3.6E-04				
Bi211	3.5E+09					
Bi212	5.2E+07					
Bi213	1.8E+07					
Bi214	1.2E+08	4.1E+02	2.5E+01	1.8E-11		
Po210	3.0E+04	3.4E-04				
Po211m	2.0E+10					
Po211	9.9E+11					
Po212	2.0E+18					
Po213	1.4E+17					
Po214	3.2E+15	4.1E+02	2.5E+01	1.8E-11		
Po215	2.8E+14					
Po216	3.2E+12					
Po218	2.2E+09	4.1E+02	2.5E+01	1.8E-11		
At217	1.5E+13					
Rn218	1.4E+13	4.1E+02	2.5E+01	1.8E-11		
Rn219	1.2E+11					
Rn220	7.7E+09					
Rn222	1.1E+06	4.1E+02	2.5E+01	1.8E-11		
Fr221	1.5E+09					
Fr223	2.1E+07					
Ra222	1.2E+10	4.1E+02	2.5E+01	1.8E-11		
Ra223	4.1E+05					
Ra224	1.2E+06					

	Time (yr)					
Isotope	0	10	100	1,000	100,000	1,000,000
Ra225	6.4E+03					
Ra226	6.5E+00	3.8E+01	4.2E+01	2.8E+01	6.7E-18	
Ra228	3.5E+00	5.4E+03	7.8E-02			
Ac225	4.6E+05					
Ac227	8.0E+00	2.5E+03	1.4E+02	5.0E-11		
Ac228	4.0E+06	1.0E+03	7.1E-12			
Th226	2.3E+08	4.1E+02	2.5E+01	1.8E-11		
Th227	2.6E+05					
Th228	6.1E+03	1.0E+03	7.1E-12			
Th229	1.4E+00	9.2E+00	9.1E+00	8.4E+00	1.4E-03	1.9E-38
Th230	1.3E-01	1.4E-01	1.7E-01	4.6E-01	4.3E-01	1.1E-04
Th231	1.3E+05	9.4E-01	2.5E+00	2.5E+00	3.1E-01	1.7E-09
Th232	6.2E-07	3.7E-06	6.1E-06	6.1E-06	6.1E-06	6.1E-06
Th233	2.3E+07	6.6E-02	7.0E-02	1.0E-01	3.5E-01	7.0E-03
Th234	2.2E+03	4.2E-02	4.2E-02	4.3E-02	2.0E-01	3.0E-02
Pa231	3.3E-01	9.4E-01	2.5E+00	2.5E+00	3.1E-01	1.7E-09
Pa232	6.5E+05	1.1E+03	4.7E+02	6.1E-02	1.2E-08	1.2E-08
Pa233	1.2E+04	6.6E-02	6.9E-02	1.0E-01	3.5E-01	7.0E-03
Pa234m	7.9E+08	4.2E-02	4.2E-02	4.3E-02	2.0E-01	3.0E-02
Pa234	6.9E+06	4.2E-02	4.2E-02	4.3E-02	2.0E-01	3.0E-02
Pa235	2.2E+07	1.5E-05	1.5E-05	1.7E-05	1.2E-04	1.3E-04
U230	2.2E+05	4.1E+02	2.5E+01	1.8E-11		
U231	1.7E+04	9.4E-01	2.5E+00	2.5E+00	3.1E-01	1.7E-09
U232	1.6E+02	1.1E+03	4.7E+02	6.1E-02		
U233	6.6E-02	6.6E-02	6.9E-02	1.0E-01	3.5E-01	7.0E-03
U234	4.2E-02	4.2E-02	4.2E-02	4.3E-02	2.0E-01	3.0E-02
U235	1.4E-05	1.5E-05	1.5E-05	1.7E-05	1.2E-04	1.3E-04
U236	4.1E-04	4.1E-04	4.1E-04	4.1E-04	4.1E-04	4.0E-04
U237	3.8E+04	5.2E-03	5.2E-03	5.2E-03	1.7E-02	3.4E-02
U238	2.0E-06	2.5E-06	2.5E-06	2.5E-06	4.6E-06	2.1E-05
U239	2.2E+07	4.6E-01	4.6E-01	4.5E-01	2.6E-02	1.3E-04
U240	2.0E+05	1.7E+00	1.7E+00	1.5E+00	4.6E-04	4.0E-04
U241	2.7E+10	1.1E+01	2.4E+01	5.8E+00	1.7E-02	3.4E-02
Np235	2.0E+01	3.3E-02	4.9E-05	5.2E-05	1.2E-04	1.3E-04
Np236m	1.1E+05	6.4E+02	2.3E+02	3.1E-02	2.1E-04	2.1E-04
Np236	6.4E-03	1.8E-02	5.7E-02	8.1E-02	4.5E-02	5.6E-04
Np237	4.8E-03	5.2E-03	5.2E-03	5.2E-03	1.7E-02	3.4E-02
Np238	3.1E+05	1.3E+02	6.1E+01	9.2E-02	2.0E-01	3.0E-02
Np239	1.4E+05	4.6E-01	4.6E-01	4.5E-01	2.6E-02	1.3E-04
Np240m	1.5E+08	1.7E+00	1.7E+00	1.5E+00	4.6E-04	4.0E-04
Np240	2.9E+07	1.7E+00	1.7E+00	1.5E+00	4.6E-04	4.0E-04
Np241	3.8E+07	1.1E+01	2.4E+01	5.8E+00	1.7E-02	3.4E-02
Pu236	4.3E+03	1.3E+03	4.9E+02	6.4E-02		
Pu237	1.1E+03	5.2E-03	5.2E-03	5.2E-03	1.7E-02	3.4E-02
Pu238	1.4E+02	1.3E+02	6.1E+01	9.2E-02	2.0E-01	3.0E-02
Pu239	4.6E-01	4.6E-01	4.6E-01	4.5E-01	2.6E-02	1.3E-04
Pu240	1.7E+00	1.7E+00	1.7E+00	1.5E+00	4.6E-04	4.0E-04
Pu241	7.9E-01	1.1E+01	2.4E+01	5.8E+00	1.7E-02	3.4E-02
Pu242	2.8E-02	2.8E-02	2.8E-02	2.8E-02	2.4E-02	4.4E-03
Pu243	7.3E+05	1.7E+00	1.7E+00	1.6E+00	3.8E-02	1.3E-04
Pu244	1.3E-04	1.6E-04	1.6E-04	1.7E-04	3.0E-04	3.0E-04

	Time (yr)					
Isotope	0	10	100	1,000	100,000	1,000,000
Pu245	1.3E+06	1.4E+00	1.6E+00	2.3E+00	1.7E-02	3.4E-02
Pu246	1.8E+04	2.5E+00	2.4E+00	2.1E+00	2.4E-02	4.5E-03
Am239	5.8E+05	4.6E-01	4.6E-01	4.5E-01	2.6E-02	1.3E-04
Am240	4.0E+05	1.7E+00	1.7E+00	1.5E+00	4.6E-04	4.0E-04
Am241	2.8E+01	2.7E+01	2.4E+01	5.6E+00	1.7E-02	3.4E-02
Am242m	1.0E+00	8.1E+01	7.8E+01	1.9E+00	1.7E-01	2.6E-02
Am242	2.3E+05	1.0E+02	5.1E+01	8.2E-02	1.7E-01	2.6E-02
Am243	1.6E+00	1.7E+00	1.7E+00	1.6E+00	3.8E-02	1.3E-04
Am244m	2.2E+07	4.7E+02	1.7E+01	1.5E+00	4.6E-04	4.0E-04
Am244	2.1E+06	4.7E+02	1.7E+01	1.5E+00	4.6E-04	4.0E-04
Am245	2.9E+06	1.4E+00	1.6E+00	2.3E+00	1.7E-02	3.4E-02
Am246	3.9E+07	2.5E+00	2.4E+00	2.1E+00	2.4E-02	4.5E-03
Cm241	1.6E+04	2.7E+01	2.3E+01	5.5E+00	1.7E-02	3.4E-02
Cm242	2.9E+04	1.3E+02	6.2E+01	9.3E-02	2.0E-01	3.0E-02
Cm243	4.6E+02	3.6E+02	4.1E+01	4.5E-01	2.6E-02	1.3E-04
Cm244	6.9E+02	4.7E+02	1.7E+01	1.5E+00	4.6E-04	4.0E-04
Cm245	1.4E+00	1.4E+00	1.6E+00	2.3E+00	1.7E-02	3.4E-02
Cm246	2.5E+00	2.5E+00	2.4E+00	2.1E+00	2.4E-02	4.5E-03
Cm247	7.1E-04	7.4E-04	7.4E-04	8.1E-04	2.1E-03	2.1E-03
Cm248	1.3E-01	1.3E-01	1.3E-01	1.3E-01	1.1E-01	1.8E-02
Cm249	5.1E+06	3.7E+01	3.2E+01	7.1E+00	1.7E-02	3.4E-02
Cm250	1.5E+01	1.5E+01	1.5E+01	1.5E+01	3.0E-01	1.8E-03
Cm251	3.7E+07	1.4E+01	1.3E+01	6.6E+00	2.1E-03	2.1E-03
Bk249	8.0E+01	3.7E+01	3.2E+01	7.1E+00	1.7E-02	3.4E-02
Bk250	6.9E+06	6.0E+02	7.5E+00	2.2E+00	2.4E-02	4.5E-03
Bk251	2.2E+07	1.4E+01	1.3E+01	6.6E+00	2.1E-03	2.1E-03
Cf249	3.8E+01	3.7E+01	3.2E+01	7.1E+00	1.7E-02	3.4E-02
Cf250	1.0E+03	6.0E+02	7.5E+00	2.2E+00	2.4E-02	4.5E-03
Cf251	1.4E+01	1.4E+01	1.3E+01	6.6E+00	2.1E-03	2.1E-03
Cf252	9.8E+03	7.1E+02	1.3E-01	1.3E-01	1.1E-01	1.7E-02
Cf253	4.2E+03	1.7E+02	1.5E+02	3.3E+01	7.8E-02	1.6E-01
Cf254	2.6E+06	4.7E-02	4.7E-02	4.5E-02	9.2E-04	5.7E-06
Cf255	1.2E+06	1.4E+01	1.3E+01	6.6E+00	2.1E-03	2.1E-03
Es253	2.6E+05	3.7E+01	3.2E+01	7.1E+00	1.7E-02	3.4E-02
Es254m	3.9E+06	6.0E+02	7.5E+00	2.1E+00	2.4E-02	4.5E-03
Es254	1.8E+04	6.4E+02	7.8E+00	2.2E+00	2.4E-02	4.5E-03
Es255	1.5E+05	1.4E+01	1.3E+01	6.6E+00	2.1E-03	2.1E-03

Table 116 - Decay Heat (W/mole) for Fission Product Isotopes

Note: Starting with one mole of given isotope and includes all daughters.

	Time (yr)					
Isotope	0	10	100	1,000	100,000	1,000,000
H 3	9.8E-01	5.6E-01	3.5E-03	3.8E-25		
Li 6						
Li 7						
Be 9						
Be 10	2.7E-04	2.7E-04	2.7E-04	2.7E-04	2.6E-04	1.7E-04
C 14	1.8E-02	1.8E-02	1.8E-02	1.6E-02	1.0E-07	
Ni 66	2.2E+04					
Cu 66	2.5E+08					
Zn 66						
Cu 67	8.1E+04					
Zn 67						
Zn 68						
Zn 69	6.4E+06					
Zn 69m	5.9E+05					
Ga 69						
Zn 70						
Ga 70	3.4E+07					
Ge 70						
Zn 71	6.2E+08					
Zn 71m	9.8E+06					
Ga 71						
Ge 71	6.1E+02					
Ge 71m	5.9E+11					
Co 72	5.1E+12					
Ni 72	4.9E+10					
Cu 72	5.2E+10					
Zn 72	1.0E+05					
Ga 72	4.2E+06					
Ge 72						
Co 73	4.1E+12					
Ni 73	6.7E+11					
Cu 73	3.6E+10					
Zn 73	7.7E+09					
Ga 73	3.0E+06					
Ge 73						
Ge 73m	8.8E+09					
Co 74	7.8E+12					
Ni 74	2.9E+11					
Cu 74	5.9E+11					
Zn 74	1.0E+09					
Ga 74	5.5E+08					
Ge 74						
Co 75	7.6E+12					
Ni 75	1.8E+12					
Cu 75	2.7E+11					
Zn 75	2.5E+10					
Ga 75	8.8E+08					
Ge 75	6.1E+06					

	Time (yr)					
Isotope	0	10	100	1,000	100,000	1,000,000
Ge 75m	1.9E+08					
As 75						
Ni 76	1.1E+12					
Cu 76	1.7E+12					
Zn 76	2.6E+10					
Ga 76	9.7E+09					
Ge 76						
As 76	1.1E+06					
Se 76						
Ni 77	4.9E+12					
Cu 77	1.1E+12					
Zn 77	1.4E+11					
Ga 77	1.4E+10					
Ge 77	2.8E+06					
Ge 77m	1.3E+09					
As 77	1.1E+05					
Se 77						
Se 77m	6.1E+08					
Ni 78	3.0E+12					
Cu 78	4.5E+12					
Zn 78	1.7E+11					
Ga 78	6.7E+10					
Ge 78	6.4E+06					
As 78	3.2E+07					
Se 78						
Cu 79	2.9E+12	2.4E-04	2.4E-04	2.4E-04	2.0E-04	3.0E-05
Zn 79	4.0E+11	3.2E-04	3.2E-04	3.2E-04	2.6E-04	3.9E-05
Ga 79	9.4E+10	3.2E-04	3.2E-04	3.2E-04	2.6E-04	3.9E-05
Ge 79	7.2E+09	3.4E-04	3.4E-04	3.4E-04	2.8E-04	4.2E-05
As 79	1.1E+08	3.4E-04	3.4E-04	3.4E-04	2.8E-04	4.2E-05
Se 79	3.4E-04	3.4E-04	3.4E-04	3.4E-04	2.8E-04	4.2E-05
Se 79m	2.7E+07	3.4E-04	3.4E-04	3.4E-04	2.8E-04	4.2E-05
Br 79						
Br 79m	2.8E+09					
Kr 79	1.5E+05					
Cu 80	6.7E+12	5.3E-05	5.3E-05	5.3E-05	4.3E-05	6.5E-06
Zn 80	5.0E+11	6.3E-06	6.3E-06	6.3E-06	5.1E-06	7.7E-07
Ga 80	2.7E+11	2.8E-06	2.8E-06	2.8E-06	2.3E-06	3.4E-07
Ge 80	3.4E+09					
As 80	1.3E+10					
Se 80						
Br 80	5.1E+07					
Br 80m	3.6E+05					
Kr 80						
Cu 81	7.9E+12	3.4E-06	3.4E-06	3.4E-06	2.8E-06	4.2E-07
Zn 81	3.7E+12	1.6E-07	1.6E-07	1.6E-07	1.3E-07	2.0E-08
Ga 81	2.6E+11					
Ge 81	2.9E+10					
As 81	3.6E+09					
Se 81	3.7E+07					
Se 81m	2.0E+06					

	Time (yr)					
Isotope	0	10	100	1,000	100,000	1,000,000
Br 81						
Kr 81	2.2E-04	2.2E-04	2.2E-04	2.2E-04	1.6E-04	8.4E-06
Kr 81m	9.6E+08	2.2E-04	2.2E-04	2.2E-04	1.6E-04	8.4E-06
Zn 82	3.5E+12					
Ga 82	9.0E+11					
Ge 82	3.2E+10					
As 82	1.4E+10					
As 82m	2.3E+10					
Se 82						
Br 82	1.5E+06					
Br 82m	1.4E+07					
Kr 82						
Zn 83	6.6E+12					
Ga 83	1.7E+12					
Ge 83	1.8E+11					
As 83	2.0E+10					
Se 83	1.5E+08					
Se 83m	2.1E+09					
Br 83	2.6E+06					
Kr 83						
Kr 83m	3.9E+05					
Ga 84	6.2E+12					
Ge 84	2.8E+11					
As 84	6.6E+10					
Se 84	3.4E+08					
Br 84	1.1E+08					
Br 84m	6.8E+08					
Kr 84						
Ga 85	7.1E+12	7.1E-01	2.1E-03	1.1E-28		
Ge 85	1.7E+12	1.3E+00	3.8E-03	2.0E-28		
As 85	2.1E+11	1.6E+00	4.8E-03	2.5E-28		
Se 85	8.4E+09	5.5E+00	1.6E-02	8.7E-28		
Se 85m	1.2E+10	5.5E+00	1.6E-02	8.7E-28		
Br 85	4.3E+08	5.5E+00	1.6E-02	8.7E-28		
Kr 85	5.0E+01	2.6E+01	7.8E-02	4.1E-27		
Kr 85m	1.7E+06	5.5E+00	1.6E-02	8.7E-28		
Rb 85						
Ge 86	1.7E+12	8.7E-01	2.6E-03	1.4E-28		
As 86	5.3E+11	6.7E-01	2.0E-03	1.1E-28		
Se 86	1.6E+10					
Br 86	6.5E+09					
Br 86m	7.1E+10					
Kr 86						
Rb 86	3.2E+04					
Rb 86m	6.1E+08					
Sr 86						
Ge 87	3.6E+12	1.0E-01	3.0E-04	1.7E-09	1.7E-09	1.7E-09
As 87	1.6E+12	2.0E-09	2.0E-09	2.0E-09	2.0E-09	2.0E-09
Se 87	5.6E+10	3.5E-09	3.5E-09	3.5E-09	3.5E-09	3.5E-09
Br 87	6.0E+09	3.5E-09	3.5E-09	3.5E-09	3.5E-09	3.5E-09
Kr 87	3.1E+07	3.6E-09	3.6E-09	3.6E-09	3.6E-09	3.6E-09

	Time (yr)					
Isotope	0	10	100	1,000	100,000	1,000,000
Rb 87	3.6E-09	3.6E-09	3.6E-09	3.6E-09	3.6E-09	3.6E-09
Sr 87						
Sr 87m	2.6E+06	1.1E-11	1.1E-11	1.1E-11	1.1E-11	1.1E-11
Ge 88	3.7E+12	1.1E-09	1.1E-09	1.1E-09	1.1E-09	1.1E-09
As 88	4.0E+12	9.0E-10	9.0E-10	9.0E-10	9.0E-10	9.0E-10
Se 88	1.9E+11	2.5E-10	2.5E-10	2.5E-10	2.5E-10	2.5E-10
Br 88	2.4E+10	2.3E-10	2.3E-10	2.3E-10	2.3E-10	2.3E-10
Kr 88	1.5E+07					
Rb 88	1.7E+08					
Sr 88						
As 89	4.5E+12	9.0E-11	9.0E-11	9.0E-11	9.0E-11	9.0E-11
Se 89	8.2E+11	1.2E-11	1.2E-11	1.2E-11	1.2E-11	1.2E-11
Br 89	8.4E+10	1.4E-18				
Kr 89	1.1E+09	1.6E-18				
Rb 89	2.3E+08	1.6E-18				
Sr 89	8.9E+03	1.6E-18				
Y 89						
Y 89m	3.8E+09					
As 90	6.7E+12	3.4E+01	3.8E+00	8.9E-10	2.8E-12	2.8E-12
Se 90	8.8E+11	4.6E+01	5.0E+00	1.2E-09		
Br 90	2.1E+11	5.1E+01	5.6E+00	1.3E-09		
Kr 90	5.3E+09	6.7E+01	7.3E+00	1.7E-09		
Rb 90	1.8E+09	6.7E+01	7.3E+00	1.7E-09		
Rb 90m	1.2E+09	6.7E+01	7.3E+00	1.7E-09		
Sr 90	1.5E+01	6.7E+01	7.3E+00	1.7E-09		
Y 90	2.7E+05					
Y 90m	4.0E+06					
Zr 90						
Zr 90m	1.9E+11					
Se 91	1.8E+12	1.7E+01	1.8E+00	4.3E-10		
Br 91	6.3E+11	7.3E+00	7.9E-01	1.9E-10		
Kr 91	3.0E+10	1.3E-15				
Rb 91	4.5E+09	6.7E-05	7.3E-06	1.7E-15		
Sr 91	2.6E+06	1.3E-15				
Y 91	8.0E+03	1.3E-15				
Y 91m	1.3E+07	1.3E-15				
Zr 91						
Nb 91	5.3E-02	5.3E-02	4.8E-02	1.9E-02		
Se 92	2.6E+12	9.6E-01	1.1E-01	2.5E-11		
Br 92	1.4E+12	3.9E-16				
Kr 92	1.3E+11	5.7E-19				
Rb 92	6.0E+10	1.4E-19				
Sr 92	1.0E+07					
Y 92	8.9E+06					
Zr 92						
Nb 92	9.2E-05	9.2E-05	9.2E-05	9.2E-05	9.2E-05	9.0E-05
Se 93	5.8E+12	1.3E-05	2.2E-05	2.2E-05	2.1E-05	1.4E-05
Br 93	2.9E+12	1.5E-05	2.5E-05	2.5E-05	2.4E-05	1.6E-05
Kr 93	2.7E+11	2.6E-05	4.2E-05	4.2E-05	4.0E-05	2.7E-05
Rb 93	4.8E+10	2.6E-05	4.3E-05	4.3E-05	4.1E-05	2.7E-05
Sr 93	4.6E+08	2.6E-05	4.3E-05	4.4E-05	4.2E-05	2.8E-05

	Time (yr)					
Isotope	0	10	100	1,000	100,000	1,000,000
Y 93	2.3E+06	4.0E-05	6.6E-05	6.7E-05	6.4E-05	4.2E-05
Zr 93	2.6E-05	4.0E-05	6.6E-05	6.7E-05	6.4E-05	4.2E-05
Nb 93						
Nb 93m	3.8E+00	2.5E+00	5.2E-02	8.2E-19		
Br 94	5.4E+12	1.0E-05	1.7E-05	1.7E-05	1.6E-05	1.1E-05
Kr 94	1.4E+12	4.0E-06	6.6E-06	6.6E-06	6.3E-06	4.2E-06
Rb 94	1.7E+11	2.7E-06	4.4E-06	4.4E-06	4.2E-06	2.8E-06
Sr 94	2.0E+09					
Y 94	1.5E+08					
Zr 94						
Nb 94	1.8E-01	1.8E-01	1.8E-01	1.7E-01	5.9E-03	2.7E-16
Nb 94m	8.3E+06	1.8E-01	1.8E-01	1.7E-01	5.9E-03	2.6E-16
Br 95	4.7E+12	1.3E-06	2.1E-06	2.1E-06	2.0E-06	1.3E-06
Kr 95	5.5E+11	2.6E-07	4.2E-07	4.2E-07	4.0E-07	2.7E-07
Rb 95	1.1E+12	1.9E-13				
Sr 95	1.0E+10	2.1E-13				
Y 95	2.8E+08	2.1E-13				
Zr 95	1.0E+04	2.1E-13				
Nb 95	1.8E+04	6.4E-28				
Nb 95m	5.1E+04	6.7E-28				
Mo 95						
Br 96	7.1E+12	5.6E-08	9.1E-08	9.2E-08	8.8E-08	5.8E-08
Kr 96	1.1E+12	4.1E-14				
Rb 96	2.6E+12	2.8E-14				
Sr 96	2.0E+11	2.3E-18				
Y 96	5.0E+10					
Zr 96						
Nb 96	2.2E+06					
Mo 96						
Kr 97	4.6E+12	2.4E-15				
Rb 97	3.3E+12	6.2E-19				
Sr 97	7.4E+11					
Y 97	7.6E+10					
Zr 97	9.7E+05					
Nb 97	1.8E+07					
Nb 97m	8.3E+08					
Mo 97						
Kr 98	2.3E+12					
Rb 98	4.0E+12					
Sr 98	3.3E+11					
Y 98	5.4E+11					
Zr 98	2.2E+09					
Nb 98	6.2E+10					
Nb 98m	7.5E+07					
Mo 98						
Tc 98	7.7E-04	7.7E-04	7.7E-04	7.7E-04	7.5E-04	6.5E-04
Rb 99	7.3E+12	7.1E-04	7.1E-04	7.1E-04	5.1E-04	2.7E-05
Sr 99	1.3E+12	8.4E-04	8.4E-04	8.3E-04	6.0E-04	3.1E-05
Y 99	1.8E+11	8.4E-04	8.4E-04	8.3E-04	6.0E-04	3.1E-05
Zr 99	8.3E+10	8.5E-04	8.5E-04	8.5E-04	6.1E-04	3.2E-05
Nb 99	9.0E+09	8.5E-04	8.5E-04	8.5E-04	6.1E-04	3.2E-05

	Time (yr)					
Isotope	0	10	100	1,000	100,000	1,000,000
Nb 99m	1.1E+09	8.5E-04	8.5E-04	8.5E-04	6.1E-04	3.2E-05
Mo 99	1.9E+05	8.5E-04	8.5E-04	8.5E-04	6.1E-04	3.2E-05
Tc 99	8.5E-04	8.5E-04	8.5E-04	8.5E-04	6.1E-04	3.2E-05
Tc 99m	4.9E+05	8.5E-04	8.5E-04	8.5E-04	6.1E-04	3.2E-05
Ru 99						
Rb100	6.1E+12	5.4E-05	5.4E-05	5.4E-05	3.9E-05	2.0E-06
Sr100	1.3E+12	1.3E-05	1.3E-05	1.3E-05	9.7E-06	5.0E-07
Y100	5.3E+11	7.2E-06	7.2E-06	7.2E-06	5.2E-06	2.7E-07
Zr100	1.7E+10					
Nb100	1.4E+11					
Nb100m	8.8E+10					
Mo100						
Tc100	5.9E+09					
Ru100						
Rb101	5.3E+12	3.9E-06	3.9E-06	3.9E-06	2.8E-06	1.5E-07
Sr101	2.1E+12	1.8E-07	1.8E-07	1.8E-07	1.3E-07	6.7E-09
Y101	5.7E+11					
Zr101	1.1E+11					
Nb101	2.3E+10					
Mo101	1.6E+08					
Tc101	6.4E+07					
Ru101						
Sr102	1.1E+12					
Y102	5.2E+11					
Zr102	4.6E+10					
Nb102	2.2E+11					
Mo102	3.9E+07					
Tc102	3.3E+10					
Tc102m	8.5E+08					
Ru102						
Rh102	1.6E+03	1.5E+02	6.6E-08			
Pd102						
Sr103	3.8E+12	9.3E-25				
Y103	1.3E+12	1.0E-24				
Zr103	2.0E+11	1.2E-24				
Nb103	1.4E+11	1.2E-24				
Mo103	2.3E+09	1.2E-24				
Tc103	1.6E+09	1.2E-24				
Ru103	1.1E+04	1.2E-24				
Rh103						
Rh103m	7.6E+05					
Sr104	2.2E+12	2.3E-25				
Y104	3.8E+12	1.1E-25				
Zr104	6.9E+10	9.5E-27				
Nb104	8.2E+10	8.2E-27				
Mo104	1.4E+09					
Tc104	2.3E+08					
Ru104						
Rh104	1.6E+09					
Rh104m	3.3E+07					
Pd104						

	Time (yr)					
Isotope	0	10	100	1,000	100,000	1,000,000
Y105	2.7E+12	2.0E-27				
Zr105	6.0E+11	1.2E-28				
Nb105	8.9E+10					
Mo105	6.0E+09					
Tc105	2.9E+08					
Ru105	4.8E+06					
Rh105	1.2E+05					
Rh105m	1.9E+08					
Pd105						
Y106	6.1E+12	2.9E+00	6.9E-27			
Zr106	2.4E+11	3.5E+00	8.2E-27			
Nb106	3.9E+11	3.5E+00	8.3E-27			
Mo106	1.6E+10	3.7E+00	8.8E-27			
Tc106	8.6E+09	3.7E+00	8.8E-27			
Ru106	2.1E+01	3.7E+00	8.8E-27			
Rh106	3.6E+09					
Rh106m	2.7E+07					
Pd106						
Ag106	2.8E+07					
Y107	4.8E+12	1.2E+00	2.0E-06	2.0E-06	2.0E-06	1.8E-06
Zr107	1.4E+12	4.5E-01	2.7E-06	2.7E-06	2.6E-06	2.4E-06
Nb107	4.1E+11	3.3E-01	2.8E-06	2.8E-06	2.7E-06	2.5E-06
Mo107	7.1E+10	3.0E-06	3.0E-06	3.0E-06	3.0E-06	2.7E-06
Tc107	8.2E+09	3.0E-06	3.0E-06	3.0E-06	3.0E-06	2.7E-06
Ru107	4.9E+08	3.0E-06	3.0E-06	3.0E-06	3.0E-06	2.7E-06
Rh107	3.9E+07	3.0E-06	3.0E-06	3.0E-06	3.0E-06	2.7E-06
Pd107	3.0E-06	3.0E-06	3.0E-06	3.0E-06	3.0E-06	2.7E-06
Pd107m	6.7E+08	3.0E-06	3.0E-06	3.0E-06	3.0E-06	2.7E-06
Ag107						
Zr108	7.0E+11	2.3E-02	3.8E-07	3.8E-07	3.7E-07	3.4E-07
Nb108	1.9E+12	2.0E-07	2.0E-07	2.0E-07	1.9E-07	1.8E-07
Mo108	1.2E+11					
Tc108	6.8E+10					
Ru108	1.4E+08					
Rh108	1.1E+10					
Rh108m	6.5E+08					
Pd108						
Ag108	3.0E+08					
Ag108m	2.7E+01	2.7E+01	1.6E+01	1.2E-01		
Cd108						
Zr109	3.2E+12	1.5E-08	1.5E-08	1.5E-08	1.4E-08	1.3E-08
Nb109	1.2E+12					
Mo109	2.2E+11					
Tc109	1.6E+11					
Ru109	4.4E+09					
Rh109	1.0E+09					
Rh109m	6.7E+07					
Pd109	4.9E+05					
Pd109m	4.4E+07					
Ag109						
Ag109m	1.4E+08					

	Time (yr)					
Isotope	0	10	100	1,000	100,000	1,000,000
Cd109	3.3E+01	7.3E-01	3.0E-22			
Nb110	4.0E+12					
Mo110	8.1E+10					
Tc110	4.2E+11					
Ru110	5.6E+09					
Rh110	6.3E+10					
Rh110m	8.8E+09					
Pd110						
Ag110	3.3E+09					
Ag110m	8.7E+03	3.5E-01	8.6E-41			
Cd110						
Nb111	2.4E+12					
Mo111	7.9E+11					
Tc111	1.4E+11					
Ru111	1.2E+11					
Rh111	1.2E+10					
Pd111	4.2E+07					
Pd111m	1.8E+06					
Ag111	4.0E+04					
Ag111m	6.4E+07					
Cd111						
Cd111m	8.9E+06					
Nb112	6.5E+12					
Mo112	2.7E+11					
Tc112	9.5E+11					
Ru112	3.4E+10					
Rh112	1.6E+11					
Pd112	8.5E+04					
Ag112	1.2E+07					
Cd112						
Mo113	1.8E+12	2.5E-01	3.0E-03	1.8E-14	1.8E-14	1.8E-14
Tc113	4.7E+11	2.6E-01	3.1E-03	1.9E-14	1.9E-14	1.9E-14
Ru113	8.2E+10	2.8E-01	3.3E-03	2.1E-14	2.1E-14	2.1E-14
Rh113	1.9E+11	2.8E-01	3.3E-03	2.1E-14	2.1E-14	2.1E-14
Pd113	1.2E+09	2.8E-01	3.3E-03	2.1E-14	2.1E-14	2.1E-14
Ag113	2.9E+06	2.9E-01	3.4E-03	2.1E-14	2.1E-14	2.1E-14
Ag113m	2.5E+08	2.3E-01	2.8E-03	2.1E-14	2.1E-14	2.1E-14
Cd113	2.1E-14	2.1E-14	2.1E-14	2.1E-14	2.1E-14	2.1E-14
Cd113m	2.8E+01	1.7E+01	2.0E-01	2.9E-17	2.9E-17	2.9E-17
In113						
In113m	4.3E+06					
Mo114	8.0E+11	1.8E-02	2.2E-04	1.4E-15	1.4E-15	1.4E-15
Tc114	2.3E+12	1.8E-02	2.2E-04	1.4E-15	1.4E-15	1.4E-15
Ru114	1.9E+10	2.9E-04	3.4E-06	2.2E-17	2.2E-17	2.2E-17
Rh114	1.8E+11	3.9E-19	3.9E-19	3.9E-19	3.9E-19	3.9E-19
Pd114	2.6E+08					
Ag114	3.3E+10					
Cd114						
In114	7.2E+08					
In114m	3.7E+03	9.5E-19				
Sn114						

	Time (yr)					
Isotope	0	10	100	1,000	100,000	1,000,000
Mo115	3.5E+12	3.5E-05	4.2E-07	5.9E-13	5.9E-13	5.9E-13
Tc115	1.3E+12	3.5E-05	4.2E-07	5.9E-13	5.9E-13	5.9E-13
Ru115	3.3E+11	6.9E-13	6.9E-13	6.9E-13	6.9E-13	6.9E-13
Rh115	2.5E+10	7.0E-13	7.0E-13	7.0E-13	7.0E-13	7.0E-13
Pd115	4.6E+09	7.0E-13	7.0E-13	7.0E-13	7.0E-13	7.0E-13
Ag115	8.8E+07	7.0E-13	7.0E-13	7.0E-13	7.0E-13	7.0E-13
Ag115m	6.7E+09	7.0E-13	7.0E-13	7.0E-13	7.0E-13	7.0E-13
Cd115	1.8E+05	7.0E-13	7.0E-13	7.0E-13	7.0E-13	7.0E-13
Cd115m	1.1E+04	7.4E-13	7.4E-13	7.4E-13	7.4E-13	7.4E-13
In115	7.4E-13	7.4E-13	7.4E-13	7.4E-13	7.4E-13	7.4E-13
In115m	1.4E+06	7.0E-13	7.0E-13	7.0E-13	7.0E-13	7.0E-13
Sn115						
Tc116	4.2E+12	9.5E-14	9.5E-14	9.5E-14	9.5E-14	9.5E-14
Ru116	1.1E+11	1.1E-14	1.1E-14	1.1E-14	1.1E-14	1.1E-14
Rh116	3.7E+11	3.8E-15	3.8E-15	3.8E-15	3.8E-15	3.8E-15
Pd116	6.7E+09					
Ag116	1.6E+09					
Ag116m	2.6E+10					
Cd116						
In116	6.6E+09					
In116m	5.7E+07					
Sn116						
Tc117	2.5E+12	2.5E-15	2.5E-15	2.5E-15	2.5E-15	2.5E-15
Ru117	9.2E+11	7.7E-17	7.7E-17	7.7E-17	7.7E-17	7.7E-17
Rh117	2.0E+11					
Pd117	4.0E+10					
Ag117	2.3E+09					
Ag117m	2.9E+10					
Cd117	1.1E+07					
Cd117m	1.2E+07					
In117	2.4E+07					
In117m	5.0E+06					
Sn117						
Sn117m	1.8E+04					
Tc118	6.3E+12					
Ru118	3.3E+11					
Rh118	1.2E+12					
Pd118	3.8E+10					
Ag118	7.3E+10					
Ag118m	9.2E+10					
Cd118	5.9E+06					
In118	2.5E+10					
In118m	8.2E+08					
Sn118						
Ru119	1.8E+12	1.1E-04	1.8E-38			
Rh119	5.9E+11	1.1E-04	1.9E-38			
Pd119	1.3E+11	1.2E-04	2.0E-38			
Ag119	1.1E+11	1.2E-04	2.0E-38			
Cd119	1.0E+09	4.7E-05	7.9E-39			
Cd119m	1.6E+09	3.8E-04	6.5E-38			
In119	6.4E+08	3.8E-04	6.5E-38			

	Time (yr)					
Isotope	0	10	100	1,000	100,000	1,000,000
In119m	6.9E+07	9.5E-06	1.6E-39			
Sn119						
Sn119m	2.3E+02	4.1E-02	6.9E-36			
Ru120	8.3E+11	7.1E-06	1.2E-39			
Rh120	2.4E+12	7.1E-06	1.2E-39			
Pd120	3.7E+10					
Ag120	3.0E+11					
Cd120	9.7E+08					
In120	6.0E+10					
In120m	5.7E+09					
Sn120						
Rh121	1.2E+12	5.1E-03	1.6E-03	2.0E-08		
Pd121	4.1E+11	5.9E-03	1.9E-03	2.3E-08		
Ag121	3.1E+11	5.9E-03	1.9E-03	2.3E-08		
Cd121	1.6E+10	5.9E-03	1.9E-03	2.3E-08		
In121	5.5E+09	4.9E-01	1.6E-01	1.9E-06		
In121m	4.6E+08	5.9E-03	1.9E-03	2.3E-08		
Sn121	7.9E+04					
Sn121m	1.5E+00	4.4E+00	1.4E+00	1.7E-05		
Sb121						
Rh122	4.1E+12	5.2E-04	1.7E-04	2.0E-09		
Pd122	1.2E+11	3.7E-05	1.2E-05	1.4E-10		
Ag122	7.8E+11	1.1E-05	3.5E-06	4.2E-11		
Cd122	1.6E+10					
In122	1.6E+11					
In122m	2.6E+10					
Sn122						
Sb122	2.9E+05					
Sb122m	4.2E+07					
Te122						
Rh123	2.6E+12	4.6E-06	1.4E-06	1.7E-11		
Pd123	9.7E+11	2.3E-07				
Ag123	7.7E+11	2.3E-07				
Cd123	2.2E+10	2.4E-07				
In123	2.8E+10	3.1E-07				
In123m	2.9E+09					
Sn123	3.2E+03	9.7E-06				
Sn123m	1.7E+07					
Sb123						
Te123	2.9E-12	2.9E-12	2.9E-12	2.9E-12	2.9E-12	2.9E-12
Te123m	1.6E+03	1.0E-06	2.9E-12	2.9E-12	2.9E-12	2.9E-12
Pd124	4.0E+11	1.2E-08				
Ag124	1.5E+12	5.5E-09				
Cd124	1.3E+11					
In124	9.8E+10					
Sn124						
Sb124	2.9E+04	1.6E-14				
Sb124m	4.0E+08	1.2E-14				
Te124						
Pd125	1.9E+12	3.2E+01	3.8E-09			
Ag125	8.9E+11	3.3E+01	3.9E-09			

	Time (yr)					
Isotope	0	10	100	1,000	100,000	1,000,000
Cd125	1.5E+11	3.5E+01	4.1E-09			
In125	8.9E+10	3.5E+01	4.1E-09			
In125m	1.5E+10	3.5E+01	4.1E-09			
Sn125	9.0E+04	3.5E+01	4.2E-09			
Sn125m	1.4E+08	3.5E+01	4.1E-09			
Sb125	4.1E+02	3.5E+01	4.1E-09			
Te125						
Te125m	1.9E+03	2.1E-16				
Pd126	9.7E+11	3.2E+00	3.8E-10			
Ag126	3.1E+12	1.6E+00	1.9E-10			
Cd126	2.9E+11					
In126	2.9E+11	6.1E-02	6.1E-02	6.1E-02	3.1E-02	6.0E-05
Sn126	5.6E-03	6.1E-02	6.1E-02	6.1E-02	3.1E-02	6.0E-05
Sb126	2.0E+05					
Sb126m	1.3E+08					
Te126						
Xe126						
Ag127	2.0E+12	3.7E-04	3.7E-04	3.6E-04	1.8E-04	3.6E-07
Cd127	4.8E+11	4.1E-04	4.1E-04	4.0E-04	2.0E-04	4.0E-07
In127	2.3E+11	4.0E-04	4.0E-04	4.0E-04	2.0E-04	3.9E-07
In127m	7.0E+10	4.0E-04	4.0E-04	4.0E-04	2.0E-04	3.9E-07
Sn127	2.1E+07	3.3E-08				
Sn127m	4.8E+08	3.3E-08				
Sb127	2.0E+05	3.3E-08				
Te127	4.6E+05					
Te127m	6.4E+02	1.8E-07				
I127						
Xe127	6.6E+03	4.1E-27				
Ag128	4.9E+12	2.8E-05	2.8E-05	2.8E-05	1.4E-05	2.8E-08
Cd128	1.8E+11	4.4E-07	4.4E-07	4.4E-07	2.2E-07	4.3E-10
In128	4.3E+11	1.4E-11				
Sn128	1.6E+07					
Sb128	7.4E+06					
Sb128m	3.1E+08					
Te128						
I128	3.7E+07					
Xe128						
Cd129	1.0E+12	1.1E-05	1.1E-05	1.1E-05	1.1E-05	1.0E-05
In129	5.3E+11	1.1E-05	1.1E-05	1.1E-05	1.1E-05	1.0E-05
Sn129	1.4E+09	1.1E-05	1.1E-05	1.1E-05	1.1E-05	1.0E-05
Sn129m	4.8E+08	1.1E-05	1.1E-05	1.1E-05	1.1E-05	1.0E-05
Sb129	7.4E+06	1.1E-05	1.1E-05	1.1E-05	1.1E-05	1.0E-05
Te129	9.6E+06	1.1E-05	1.1E-05	1.1E-05	1.1E-05	1.0E-05
Te129m	7.1E+03	1.1E-05	1.1E-05	1.1E-05	1.1E-05	1.0E-05
I129	1.1E-05	1.1E-05	1.1E-05	1.1E-05	1.1E-05	1.0E-05
Xe129						
Xe129m	2.0E+04					
Cd130	4.9E+11	2.0E-07	2.0E-07	2.0E-07	2.0E-07	1.9E-07
In130	1.3E+12	9.7E-08	9.7E-08	9.7E-08	9.7E-08	9.3E-08
Sn130	4.3E+08					
Sb130	1.1E+08					

Isotope	Time (yr)					
	0	10	100	1,000	100,000	1,000,000
Sb130m	6.5E+08					
Te130						
I130	3.7E+06					
I130m	3.6E+07					
Xe130						
Cd131	4.3E+12	4.7E-09	4.7E-09	4.7E-09	4.7E-09	4.5E-09
In131	1.2E+12					
Sn131	5.6E+09					
Sb131	1.1E+08					
Te131	5.1E+07					
Te131m	1.0E+06					
I131	5.5E+04					
Xe131						
Xe131m	1.1E+04					
Cd132	2.7E+12					
In132	3.3E+12					
Sn132	3.4E+09					
Sb132	1.0E+09					
Sb132m	1.5E+09					
Te132	7.9E+04					
I132	2.3E+07					
Xe132						
Cs132	8.7E+04					
Ba132						
In133	4.4E+12					
Sn133	2.2E+11					
Sb133	1.2E+09					
Te133	1.7E+08					
Te133m	4.1E+07					
I133	9.1E+05					
I133m	1.2E+10					
Xe133	2.7E+04					
Xe133m	8.0E+04					
Cs133						
Ba133	9.2E+01	4.8E+01	1.3E-01	2.2E-27		
In134	7.4E+12					
Sn134	2.3E+11					
Sb134	4.0E+11					
Sb134m	3.3E+10					
Te134	2.9E+07					
I134	6.8E+07					
I134m	9.8E+07					
Xe134						
Xe134m	4.5E+11					
Cs134	1.8E+03	6.1E+01	4.4E-12			
Cs134m	8.4E+05	6.1E+01	4.4E-12			
Ba134						
Sn135	8.1E+11	3.8E-05	3.8E-05	3.8E-05	3.7E-05	2.8E-05
Sb135	1.6E+11	4.1E-05	4.1E-05	4.1E-05	4.0E-05	3.1E-05
Te135	1.3E+10	5.2E-05	5.2E-05	5.2E-05	5.0E-05	3.8E-05
I135	5.5E+06	5.2E-05	5.2E-05	5.2E-05	5.0E-05	3.8E-05

	Time (yr)					
Isotope	0	10	100	1,000	100,000	1,000,000
Xe135	1.2E+06	5.2E-05	5.2E-05	5.2E-05	5.0E-05	3.8E-05
Xe135m	3.8E+07	5.2E-05	5.2E-05	5.2E-05	5.0E-05	3.8E-05
Cs135	5.2E-05	5.2E-05	5.2E-05	5.2E-05	5.0E-05	3.8E-05
Cs135m	3.4E+07	5.2E-05	5.2E-05	5.2E-05	5.0E-05	3.8E-05
Ba135						
Ba135m	1.7E+05					
Sn136	3.9E+11	1.7E-05	1.7E-05	1.7E-05	1.7E-05	1.3E-05
Sb136	4.6E+11	1.2E-05	1.2E-05	1.2E-05	1.2E-05	9.1E-06
Te136	1.3E+10	4.7E-07	4.7E-07	4.7E-07	4.5E-07	3.5E-07
I136	3.5E+09					
I136m	6.9E+09					
Xe136						
Cs136	1.2E+05					
Ba136						
Ba136m	4.4E+11					
Sb137	7.1E+11	3.3E+01	4.2E+00	9.7E-08	9.1E-08	6.9E-08
Te137	7.2E+10	4.2E+01	5.2E+00	4.8E-09		
I137	9.0E+09	4.3E+01	5.3E+00	4.9E-09		
Xe137	5.5E+08	4.6E+01	5.7E+00	5.3E-09		
Cs137	1.3E+01	4.6E+01	5.7E+00	5.3E-09		
Ba137						
Ba137m	2.9E+08					
Sb138	2.6E+12	1.3E+01	1.6E+00	1.5E-09		
Te138	1.5E+11	5.0E+00	6.2E-01	5.8E-10		
I138	4.9E+10	2.5E+00	3.1E-01	2.8E-10		
Xe138	1.4E+08					
Cs138	1.3E+08					
Cs138m	3.8E+08					
Ba138						
La138	2.6E-08	2.6E-08	2.6E-08	2.6E-08	2.6E-08	2.6E-08
Sb139	1.8E+12	2.2E+00	2.7E-01	2.5E-10		
Te139	5.5E+11	1.5E-01	1.9E-02	1.8E-11		
I139	1.1E+11					
Xe139	4.5E+09					
Cs139	2.4E+08					
Ba139	1.2E+07					
La139						
Ce139	1.4E+03	1.4E-05				
Pr139	9.2E+05	1.4E-05				
Te140	2.8E+11					
I140	4.0E+11					
Xe140	1.2E+10					
Cs140	4.2E+09					
Ba140	3.0E+04					
La140	1.3E+06					
Ce140						
Pr140	3.6E+08					
Te141	1.3E+12	4.7E-31				
I141	6.3E+11	5.3E-31				
Xe141	1.4E+11	8.7E-31				
Cs141	7.4E+09	8.7E-31				

	Time (yr)					
Isotope	0	10	100	1,000	100,000	1,000,000
Ba141	1.1E+08	8.7E-31				
La141	4.7E+06	8.7E-31				
Ce141	5.9E+03	8.6E-31				
Pr141						
Nd141	6.7E+05					
Te142	4.5E+11	2.0E-31				
I142	2.0E+12	1.4E-31				
Xe142	1.6E+11	4.4E-33				
Cs142	1.7E+11	8.4E-34				
Ba142	1.5E+08					
La142	4.0E+07					
Ce142						
Pr142	8.4E+05					
Pr142m	1.2E+05					
Nd142						
I143	7.9E+11	8.0E-34				
Xe143	2.9E+11	1.0E-35				
Cs143	1.2E+11					
Ba143	1.1E+10					
La143	1.1E+08					
Ce143	4.0E+05					
Pr143	1.8E+04					
Nd143						
I144	2.8E+12	4.1E-01	1.6E-12	1.6E-12	1.6E-12	1.6E-12
Xe144	1.5E+11	4.9E-01	1.9E-12	1.9E-12	1.9E-12	1.9E-12
Cs144	3.3E+11	4.9E-01	1.9E-12	1.9E-12	1.9E-12	1.9E-12
Ba144	9.7E+09	5.1E-01	1.9E-12	1.9E-12	1.9E-12	1.9E-12
La144	6.0E+09	5.1E-01	1.9E-12	1.9E-12	1.9E-12	1.9E-12
Ce144	3.0E+02	5.1E-01	1.9E-12	1.9E-12	1.9E-12	1.9E-12
Pr144	8.0E+07	1.9E-12	1.9E-12	1.9E-12	1.9E-12	1.9E-12
Pr144m	9.0E+06	1.9E-12	1.9E-12	1.9E-12	1.9E-12	1.9E-12
Nd144	1.9E-12	1.9E-12	1.9E-12	1.9E-12	1.9E-12	1.9E-12
I145	1.7E+12	1.9E-01	7.4E-13	7.4E-13	7.4E-13	7.4E-13
Xe145	3.1E+11	1.0E-01	3.8E-13	3.8E-13	3.8E-13	3.8E-13
Cs145	4.3E+11	7.4E-02	2.8E-13	2.8E-13	2.8E-13	2.8E-13
Ba145	4.9E+10					
La145	6.4E+09					
Ce145	5.7E+08					
Pr145	2.2E+06					
Nd145						
Pm145	5.3E+00	3.6E+00	1.1E-01	5.2E-17		
Sm145	2.1E+02	3.9E+00	1.1E-01	5.5E-17		
Xe146	3.7E+11	4.8E-03	1.8E-14	1.8E-14	1.8E-14	1.8E-14
Cs146	1.0E+12					
Ba146	6.8E+10					
La146	4.5E+10					
Ce146	4.7E+07					
Pr146	1.1E+08					
Nd146						
Pm146	3.2E+02	9.2E+01	1.2E-03	1.8E-05	1.8E-05	1.8E-05
Sm146	5.2E-05	5.2E-05	5.2E-05	5.2E-05	5.2E-05	5.2E-05

	Time (yr)					
Isotope	0	10	100	1,000	100,000	1,000,000
Xe147	1.6E+12	2.5E+00	3.2E-08	3.2E-08	3.2E-08	3.2E-08
Cs147	4.8E+11	2.7E+00	3.5E-08	3.5E-08	3.5E-08	3.5E-08
Ba147	3.0E+11	3.6E+00	4.7E-08	4.7E-08	4.7E-08	4.7E-08
La147	3.9E+10	3.6E+00	4.7E-08	4.7E-08	4.7E-08	4.7E-08
Ce147	2.3E+09	3.6E+00	4.7E-08	4.7E-08	4.7E-08	4.7E-08
Pr147	1.3E+08	3.6E+00	4.7E-08	4.7E-08	4.7E-08	4.7E-08
Nd147	2.9E+04	3.6E+00	4.7E-08	4.7E-08	4.7E-08	4.7E-08
Pm147	5.0E+01	3.6E+00	4.6E-08	4.6E-08	4.6E-08	4.6E-08
Sm147	4.6E-08	4.6E-08	4.6E-08	4.6E-08	4.6E-08	4.6E-08
Cs148	1.8E+12	9.1E-01	1.2E-08	1.2E-08	1.2E-08	1.2E-08
Ba148	2.4E+11	6.9E-03	9.0E-11	9.0E-11	9.0E-11	9.0E-11
La148	2.1E+11	4.8E-03	6.2E-11	6.2E-11	6.2E-11	6.2E-11
Ce148	1.2E+09					
Pr148	1.4E+09					
Nd148						
Pm148	1.9E+05	5.3E-13	5.3E-13	5.3E-13	5.3E-13	5.3E-13
Pm148m	4.0E+04	5.3E-13	5.3E-13	5.3E-13	5.3E-13	5.3E-13
Sm148	5.3E-13	5.3E-13	5.3E-13	5.3E-13	5.3E-13	5.3E-13
Cs149	1.4E+12	2.3E-03	3.0E-11	2.9E-11	2.9E-11	2.9E-11
Ba149	3.4E+11					
La149	8.0E+10					
Ce149	2.9E+10					
Pr149	7.7E+08					
Nd149	9.4E+06					
Pm149	1.3E+05					
Sm149						
Eu149	7.1E+02	1.1E-09				
Cs150	3.3E+12					
Ba150	2.1E+11					
La150	5.1E+11					
Ce150	1.9E+10					
Pr150	3.3E+10					
Nd150						
Pm150	1.6E+07					
Sm150						
Eu150	9.2E+01	7.6E+01	1.3E+01	3.6E-07		
Ba151	8.9E+11	3.9E-01	2.0E-01	1.9E-04		
La151	3.6E+11	4.0E-01	2.0E-01	2.0E-04		
Ce151	1.5E+11	4.3E-01	2.2E-01	2.1E-04		
Pr151	6.9E+09	4.3E-01	2.2E-01	2.1E-04		
Nd151	1.3E+08	4.3E-01	2.2E-01	2.1E-04		
Pm151	4.0E+05	4.3E-01	2.2E-01	2.1E-04		
Sm151	4.7E-01	4.3E-01	2.2E-01	2.1E-04		
Eu151						
Ba152	6.3E+11	4.8E-02	2.4E-02	2.3E-05		
La152	1.2E+12	2.6E-02	1.3E-02	1.3E-05		
Ce152	1.7E+10					
Pr152	3.6E+10					
Nd152	4.8E+07					
Pm152	4.2E+08					
Pm152m	3.5E+08					

	Time (yr)					
Isotope	0	10	100	1,000	100,000	1,000,000
Sm152						
Eu152	2.1E+02	1.2E+02	1.1E+00	1.2E-11	1.2E-11	1.2E-11
Eu152m	1.6E+06	3.1E-11	3.1E-11	3.1E-11	3.1E-11	3.1E-11
Gd152	4.3E-11	4.3E-11	4.3E-11	4.3E-11	4.3E-11	4.3E-11
La153	9.7E+11					
Ce153	1.3E+11					
Pr153	4.1E+10					
Nd153	1.8E+09					
Pm153	1.6E+08					
Sm153	1.3E+05					
Eu153						
Gd153	4.8E+02	1.3E-02				
La154	2.6E+12					
Ce154	8.8E+10					
Pr154	2.7E+11					
Nd154	2.0E+09					
Pm154	1.8E+09					
Pm154m	1.2E+09					
Sm154						
Eu154	3.8E+02	1.7E+02	1.2E-01	3.4E-33		
Gd154						
La155	2.4E+12	1.1E+01	1.8E-05			
Ce155	4.6E+11	1.3E+01	2.1E-05			
Pr155	2.1E+11	1.3E+01	2.2E-05			
Nd155	8.1E+09	1.4E+01	2.2E-05			
Pm155	2.3E+09	1.4E+01	2.2E-05			
Sm155	3.3E+07	1.4E+01	2.2E-05			
Eu155	5.9E+01	1.4E+01	2.2E-05			
Gd155						
Gd155m	2.6E+11					
Ce156	3.7E+11	7.5E-01	1.2E-06			
Pr156	8.6E+11	3.7E-01	6.0E-07			
Nd156	6.4E+09					
Pm156	1.6E+10					
Sm156	6.5E+05					
Eu156	8.6E+04					
Gd156						
Ce157	1.4E+12	1.6E-02	2.7E-08			
Pr157	7.6E+11					
Nd157	7.6E+10					
Pm157	2.5E+09					
Sm157	1.8E+08					
Eu157	8.1E+05					
Gd157						
Pr158	2.3E+12					
Nd158	6.2E+10					
Pm158	6.6E+10					
Sm158	2.0E+08					
Eu158	5.0E+07					
Gd158						
Pr159	1.9E+12					

	Time (yr)					
Isotope	0	10	100	1,000	100,000	1,000,000
Nd159	3.9E+11					
Pm159	6.6E+10					
Sm159	8.1E+08					
Eu159	7.9E+07					
Gd159	3.6E+05					
Tb159						
Nd160	2.8E+11					
Pm160	4.1E+11					
Sm160	1.4E+09					
Eu160	4.7E+09					
Gd160						
Tb160	1.6E+04	9.8E-12				
Dy160						
Nd161	8.7E+11					
Pm161	3.2E+11					
Sm161	3.7E+10					
Eu161	3.2E+09					
Gd161	3.0E+08					
Tb161	2.6E+04					
Dy161						
Pm162	9.7E+11					
Sm162	2.9E+10					
Eu162	1.4E+09					
Gd162	1.1E+08					
Tb162	2.4E+08					
Tb162m	1.5E+07					
Dy162						
Sm163	1.6E+11					
Eu163	2.3E+10					
Gd163	1.3E+09					
Tb163	6.4E+07					
Tb163m	1.2E+08					
Dy163						
Sm164	1.4E+11					
Eu164	1.6E+11					
Gd164	7.0E+07					
Tb164	1.1E+09					
Dy164						
Sm165	5.4E+11					
Eu165	1.6E+11					
Gd165	3.3E+09					
Tb165	9.0E+08					
Dy165	3.8E+06					
Dy165m	1.1E+08					
Ho165						
Dy166	4.7E+04					
Ho166	5.0E+05					
Ho166m	3.1E+00	3.1E+00	3.0E+00	1.8E+00	2.6E-25	
Er166						
Er167						
Er167m	6.0E+09					

	Time (yr)					
Isotope	0	10	100	1,000	100,000	1,000,000
Er168						
Yb168						
Er169	8.5E+03					
Tm169						
Yb169	1.0E+04	4.8E-31				
Er170						
Tm170	2.0E+03	5.7E-06				
Tm170m		5.7E-06				
Yb170						
Er171	2.0E+06	7.8E-01	6.0E-15			
Tm171	2.9E+01	7.8E-01	6.0E-15			
Yb171						
Er172	2.4E+05					
Tm172	2.9E+05					
Yb172						

APPENDIX C

INTEGRAL DECAY ENERGY

Table 117 - Integral Decay Energy (J/mole) for Actinide Isotopes

Note: Starting with one mole of given isotope and includes all daughters.

	Time (yr)					
Isotope	0	10	100	1,000	100,000	1,000,000
He 4						
Tl206						
Tl207						
Tl208						
Tl209						
Pb206						
Pb207						
Pb208						
Pb209						
Pb210		1.3E+11	5.2E+11	5.4E+11	5.4E+11	5.4E+11
Pb211						
Pb212						
Pb214		6.6E+13	6.6E+13	6.6E+13	6.6E+13	6.6E+13
Bi208		4.8E+06	4.8E+07	4.8E+08	4.4E+10	2.2E+11
Bi209						
Bi210m		1.3E+06	1.3E+07	1.3E+08	1.3E+10	1.2E+11
Bi210		7.9E+11	7.9E+11	7.9E+11	7.9E+11	7.9E+11
Bi211						
Bi212						
Bi213						
Bi214		3.1E+14	3.1E+14	3.1E+14	3.1E+14	3.1E+14
Po210		5.2E+11	5.2E+11	5.2E+11	5.2E+11	5.2E+11
Po211m						
Po211						
Po212						
Po213						
Po214		3.4E+21	3.4E+21	3.4E+21	3.4E+21	3.4E+21
Po215						
Po216						
Po218		4.5E+15	4.5E+15	4.5E+15	4.5E+15	4.5E+15
At217						
Rn218		1.8E+19	1.8E+19	1.8E+19	1.8E+19	1.8E+19
Rn219						
Rn220						
Rn222		4.7E+12	5.1E+12	5.1E+12	5.1E+12	5.1E+12
Fr221						
Fr223		2.7E+13	2.7E+13	2.7E+13	2.7E+13	2.7E+13
Ra222		2.2E+16	2.2E+16	2.2E+16	2.2E+16	2.2E+16
Ra223		6.2E+11	6.2E+11	6.2E+11	6.2E+11	6.2E+11
Ra224		5.7E+11	5.7E+11	5.7E+11	5.7E+11	5.7E+11

	Time (yr)					
Isotope	0	10	100	1,000	100,000	1,000,000
Ra225		1.9E+10	1.9E+10	1.9E+10	1.9E+10	1.9E+10
Ra226		1.1E+10	1.3E+11	1.1E+12	3.2E+12	3.2E+12
Ra228		1.8E+12	3.3E+12	3.3E+12	3.3E+12	3.3E+12
Ac225		6.1E+11	6.1E+11	6.1E+11	6.1E+11	6.1E+11
Ac227		8.2E+11	3.1E+12	3.2E+12	3.2E+12	3.2E+12
Ac228		2.7E+13	2.7E+13	2.7E+13	2.7E+13	2.7E+13
Th226		5.6E+14	5.6E+14	5.6E+14	5.6E+14	5.6E+14
Th227		7.3E+11	7.3E+11	7.3E+11	7.3E+11	7.3E+11
Th228		2.7E+12	2.8E+12	2.8E+12	2.8E+12	2.8E+12
Th229		2.7E+09	2.9E+10	2.8E+11	3.3E+12	3.3E+12
Th230		4.3E+07	4.8E+08	8.7E+09	2.1E+12	3.6E+12
Th231		3.3E+11	3.4E+11	4.1E+11	3.7E+12	4.1E+12
Th232		6.3E+02	1.7E+04	1.9E+05	1.9E+07	1.9E+08
Th233		4.3E+13	4.3E+13	4.3E+13	4.4E+13	4.6E+13
Th234		9.0E+09	9.1E+09	1.0E+10	3.6E+11	2.9E+12
Pa231		2.0E+08	5.8E+09	7.7E+10	3.4E+12	3.8E+12
Pa232		3.1E+12	5.2E+12	6.7E+12	6.7E+12	6.7E+12
Pa233		4.2E+10	4.2E+10	4.4E+10	1.1E+12	3.6E+12
Pa234m		1.1E+15	1.1E+15	1.1E+15	1.1E+15	1.1E+15
Pa234		1.1E+13	1.1E+13	1.1E+13	1.2E+13	1.4E+13
Pa235		2.4E+13	2.4E+13	2.4E+13	2.4E+13	2.4E+13
U230		1.3E+12	1.6E+12	1.7E+12	1.7E+12	1.7E+12
U231		4.9E+10	5.5E+10	1.3E+11	3.4E+12	3.9E+12
U232		2.7E+11	2.4E+12	3.9E+12	3.9E+12	3.9E+12
U233		2.1E+07	2.1E+08	2.6E+09	1.0E+12	3.5E+12
U234		1.3E+07	1.3E+08	1.3E+09	3.5E+11	2.9E+12
U235		4.6E+03	4.6E+04	5.0E+05	2.1E+08	3.8E+09
U236		1.3E+05	1.3E+06	1.3E+07	1.3E+09	1.3E+10
U237		7.5E+10	7.5E+10	7.5E+10	1.1E+11	8.1E+11
U238		7.7E+02	7.7E+03	7.7E+04	1.1E+07	3.2E+08
U239		3.9E+13	3.9E+13	3.9E+13	3.9E+13	4.0E+13
U240		5.4E+11	5.4E+11	5.9E+11	1.1E+12	1.1E+12
U241		3.7E+16	3.7E+16	3.7E+16	3.7E+16	3.7E+16
Np235		9.6E+08	9.6E+08	9.6E+08	1.2E+09	4.9E+09
Np236m		1.1E+12	2.2E+12	2.9E+12	2.9E+12	2.9E+12
Np236		4.1E+06	1.2E+08	2.1E+09	1.9E+11	4.8E+11
Np237		1.6E+06	1.6E+07	1.6E+08	3.2E+10	7.3E+11
Np238		1.3E+12	1.5E+12	1.8E+12	2.2E+12	4.7E+12
Np239		3.5E+11	3.5E+11	3.6E+11	8.3E+11	9.7E+11
Np240m		2.5E+14	2.5E+14	2.5E+14	2.5E+14	2.5E+14
Np240		5.5E+13	5.5E+13	5.5E+13	5.6E+13	5.6E+13
Np241		7.2E+13	7.2E+13	7.2E+13	7.3E+13	7.3E+13
Pu236		6.9E+11	2.9E+12	4.5E+12	4.5E+12	4.5E+12
Pu237		6.4E+09	6.4E+09	6.5E+09	3.8E+10	7.4E+11
Pu238		4.1E+10	2.9E+11	5.6E+11	9.2E+11	3.5E+12
Pu239		1.5E+08	1.5E+09	1.4E+10	4.8E+11	6.2E+11
Pu240		5.4E+08	5.3E+09	5.1E+10	5.6E+11	5.8E+11
Pu241		1.9E+09	6.3E+10	4.3E+11	6.9E+11	1.4E+12
Pu242		8.9E+06	8.9E+07	8.9E+08	8.2E+10	4.1E+11
Pu243		1.8E+12	1.8E+12	1.8E+12	2.9E+12	3.1E+12
Pu244		5.0E+04	5.0E+05	5.2E+06	8.4E+08	9.3E+09

	Time (yr)					
Isotope	0	10	100	1,000	100,000	1,000,000
Pu245		3.0E+12	3.0E+12	3.0E+12	4.4E+12	5.0E+12
Pu246		6.6E+10	7.3E+10	1.4E+11	9.8E+11	1.3E+12
Am239		1.3E+12	1.3E+12	1.3E+12	1.8E+12	1.9E+12
Am240		1.0E+12	1.0E+12	1.1E+12	1.6E+12	1.6E+12
Am241		8.6E+09	8.0E+10	4.3E+11	6.9E+11	1.4E+12
Am242m		2.2E+10	2.5E+11	8.4E+11	1.3E+12	3.4E+12
Am242		2.0E+12	2.2E+12	2.5E+12	2.8E+12	5.0E+12
Am243		5.3E+08	5.3E+09	5.1E+10	1.2E+12	1.4E+12
Am244m		6.8E+13	6.8E+13	6.8E+13	6.9E+13	6.9E+13
Am244		8.3E+12	8.7E+12	8.9E+12	9.4E+12	9.4E+12
Am245		6.3E+12	6.3E+12	6.4E+12	7.7E+12	8.3E+12
Am246		7.5E+13	7.5E+13	7.5E+13	7.6E+13	7.6E+13
Cm241		9.1E+10	1.6E+11	5.1E+11	7.7E+11	1.5E+12
Cm242		7.0E+11	9.5E+11	1.2E+12	1.6E+12	4.1E+12
Cm243		1.3E+11	5.4E+11	8.0E+11	1.3E+12	1.4E+12
Cm244		1.8E+11	5.6E+11	7.4E+11	1.3E+12	1.3E+12
Cm245		4.4E+08	4.6E+09	5.9E+10	1.4E+12	2.1E+12
Cm246		7.8E+08	7.8E+09	7.3E+10	9.2E+11	1.2E+12
Cm247		2.3E+05	2.3E+06	2.4E+07	5.0E+09	6.6E+10
Cm248		4.2E+07	4.2E+08	4.2E+09	3.8E+11	1.8E+12
Cm249		1.4E+13	1.4E+13	1.5E+13	1.7E+13	1.7E+13
Cm250		4.8E+09	4.8E+10	4.7E+11	1.2E+13	1.4E+13
Cm251		7.9E+13	8.0E+13	8.0E+13	8.0E+13	8.0E+13
Bk249		1.4E+10	1.1E+11	5.8E+11	2.4E+12	3.1E+12
Bk250		2.5E+13	2.5E+13	2.5E+13	2.6E+13	2.6E+13
Bk251		4.8E+13	4.8E+13	4.8E+13	4.8E+13	4.8E+13
Cf249		1.2E+10	1.1E+11	5.7E+11	2.4E+12	3.1E+12
Cf250		2.5E+11	6.1E+11	7.3E+11	1.6E+12	1.9E+12
Cf251		4.5E+09	4.3E+10	3.1E+11	6.0E+11	6.6E+11
Cf252		1.1E+12	1.2E+12	1.2E+12	1.5E+12	2.9E+12
Cf253		1.0E+11	5.5E+11	2.7E+12	1.1E+13	1.4E+13
Cf254		1.9E+13	1.9E+13	1.9E+13	1.9E+13	1.9E+13
Cf255		4.7E+12	4.7E+12	5.0E+12	5.3E+12	5.3E+12
Es253		9.7E+11	1.1E+12	1.5E+12	3.3E+12	4.0E+12
Es254m		1.5E+13	1.6E+13	1.6E+13	1.7E+13	1.7E+13
Es254		1.0E+12	1.4E+12	1.5E+12	2.4E+12	2.7E+12
Es255		7.4E+11	7.8E+11	1.1E+12	1.3E+12	1.4E+12

Table 118 - Integral Decay Energy (J/mole) for Fission Product Isotopes

Note: Starting with one mole of given isotope and includes all daughters.

	Time (yr)					
Isotope	0	10	100	1,000	100,000	1,000,000
H 3		2.4E+08	5.5E+08	5.5E+08	5.5E+08	5.5E+08
Li 6						
Li 7						
Be 9						
Be 10		8.5E+04	8.5E+05	8.5E+06	8.3E+08	6.9E+09
C 14		5.8E+06	5.7E+07	5.4E+08	4.8E+09	4.8E+09
Ni 66						
Cu 66						
Zn 66						
Cu 67		2.6E+10	2.6E+10	2.6E+10	2.6E+10	2.6E+10
Zn 67						
Zn 68						
Zn 69						
Zn 69m						
Ga 69						
Zn 70						
Ga 70						
Ge 70						
Zn 71						
Zn 71m						
Ga 71						
Ge 71		8.7E+08	8.7E+08	8.7E+08	8.7E+08	8.7E+08
Ge 71m		4.4E+17	4.4E+17	4.4E+17	4.4E+17	4.4E+17
Co 72						
Ni 72						
Cu 72						
Zn 72						
Ga 72						
Ge 72						
Co 73						
Ni 73						
Cu 73						
Zn 73						
Ga 73						
Ge 73						
Ge 73m						
Co 74						
Ni 74						
Cu 74						
Zn 74						
Ga 74						
Ge 74						
Co 75						
Ni 75						
Cu 75						
Zn 75						
Ga 75						
Ge 75						

	Time (yr)					
Isotope	0	10	100	1,000	100,000	1,000,000
Ge 75m						
As 75						
Ni 76						
Cu 76						
Zn 76						
Ga 76						
Ge 76						
As 76						
Se 76						
Ni 77						
Cu 77						
Zn 77						
Ga 77						
Ge 77						
Ge 77m						
As 77						
Se 77						
Se 77m						
Ni 78						
Cu 78						
Zn 78						
Ga 78						
Ge 78						
As 78						
Se 78						
Cu 79		2.5E+18	2.5E+18	2.5E+18	2.5E+18	2.5E+18
Zn 79		3.6E+17	3.6E+17	3.6E+17	3.6E+17	3.6E+17
Ga 79		8.9E+16	8.9E+16	8.9E+16	8.9E+16	8.9E+16
Ge 79		7.4E+15	7.4E+15	7.4E+15	7.4E+15	7.4E+15
As 79		1.3E+14	1.3E+14	1.3E+14	1.3E+14	1.3E+14
Se 79		1.1E+05	1.1E+06	1.1E+07	9.7E+08	4.5E+09
Se 79m		3.4E+13	3.4E+13	3.4E+13	3.4E+13	3.4E+13
Br 79						
Br 79m						
Kr 79						
Cu 80		5.4E+18	5.4E+18	5.4E+18	5.4E+18	5.4E+18
Zn 80		4.0E+17	4.0E+17	4.0E+17	4.0E+17	4.0E+17
Ga 80		2.2E+17	2.2E+17	2.2E+17	2.2E+17	2.2E+17
Ge 80						
As 80						
Se 80						
Br 80						
Br 80m						
Kr 80						
Cu 81		5.9E+18	5.9E+18	5.9E+18	5.9E+18	5.9E+18
Zn 81		2.6E+18	2.6E+18	2.6E+18	2.6E+18	2.6E+18
Ga 81						
Ge 81						
As 81						
Se 81						
Se 81m						

	Time (yr)					
Isotope	0	10	100	1,000	100,000	1,000,000
Br 81						
Kr 81		6.9E+04	6.9E+05	6.9E+06	5.9E+08	2.0E+09
Kr 81m		1.0E+15	1.0E+15	1.0E+15	1.0E+15	1.0E+15
Zn 82						
Ga 82						
Ge 82						
As 82						
As 82m						
Se 82						
Br 82						
Br 82m						
Kr 82						
Zn 83						
Ga 83						
Ge 83						
As 83						
Se 83						
Se 83m						
Br 83						
Kr 83						
Kr 83m						
Ga 84						
Ge 84						
As 84						
Se 84						
Br 84						
Br 84m						
Kr 84						
Ga 85		7.6E+18	7.6E+18	7.6E+18	7.6E+18	7.6E+18
Ge 85		2.0E+18	2.0E+18	2.0E+18	2.0E+18	2.0E+18
As 85		2.6E+17	2.6E+17	2.6E+17	2.6E+17	2.6E+17
Se 85		1.3E+16	1.3E+16	1.3E+16	1.3E+16	1.3E+16
Se 85m		1.9E+16	1.9E+16	1.9E+16	1.9E+16	1.9E+16
Br 85		7.7E+14	7.7E+14	7.7E+14	7.7E+14	7.7E+14
Kr 85		1.2E+10	2.4E+10	2.4E+10	2.4E+10	2.4E+10
Kr 85m		4.5E+12	4.5E+12	4.5E+12	4.5E+12	4.5E+12
Rb 85						
Ge 86		1.9E+18	1.9E+18	1.9E+18	1.9E+18	1.9E+18
As 86		6.3E+17	6.3E+17	6.3E+17	6.3E+17	6.3E+17
Se 86						
Br 86						
Br 86m						
Kr 86						
Rb 86		7.3E+10	7.3E+10	7.3E+10	7.3E+10	7.3E+10
Rb 86m		8.2E+14	8.2E+14	8.2E+14	8.2E+14	8.2E+14
Sr 86						
Ge 87		3.7E+18	3.7E+18	3.7E+18	3.7E+18	3.7E+18
As 87		1.1E+18	1.1E+18	1.1E+18	1.1E+18	1.1E+18
Se 87		4.0E+16	4.0E+16	4.0E+16	4.0E+16	4.0E+16
Br 87		4.5E+15	4.5E+15	4.5E+15	4.5E+15	4.5E+15
Kr 87		2.7E+13	2.7E+13	2.7E+13	2.7E+13	2.7E+13

	Time (yr)					
Isotope	0	10	100	1,000	100,000	1,000,000
Rb 87		1.1E+00	1.1E+01	1.1E+02	1.1E+04	1.1E+05
Sr 87						
Sr 87m		2.0E+12	2.0E+12	2.0E+12	2.0E+12	2.0E+12
Ge 88		2.4E+18	2.4E+18	2.4E+18	2.4E+18	2.4E+18
As 88		2.6E+18	2.6E+18	2.6E+18	2.6E+18	2.6E+18
Se 88		1.2E+17	1.2E+17	1.2E+17	1.2E+17	1.2E+17
Br 88		1.6E+16	1.6E+16	1.6E+16	1.6E+16	1.6E+16
Kr 88						
Rb 88						
Sr 88						
As 89		5.6E+18	5.6E+18	5.6E+18	5.6E+18	5.6E+18
Se 89		1.1E+18	1.1E+18	1.1E+18	1.1E+18	1.1E+18
Br 89		1.2E+17	1.2E+17	1.2E+17	1.2E+17	1.2E+17
Kr 89		2.1E+15	2.1E+15	2.1E+15	2.1E+15	2.1E+15
Rb 89		4.7E+14	4.7E+14	4.7E+14	4.7E+14	4.7E+14
Sr 89		5.6E+10	5.6E+10	5.6E+10	5.6E+10	5.6E+10
Y 89						
Y 89m						
As 90		8.4E+18	8.4E+18	8.4E+18	8.4E+18	8.4E+18
Se 90		1.2E+18	1.2E+18	1.2E+18	1.2E+18	1.2E+18
Br 90		3.0E+17	3.0E+17	3.0E+17	3.0E+17	3.0E+17
Kr 90		9.4E+15	9.4E+15	9.4E+15	9.4E+15	9.4E+15
Rb 90		3.4E+15	3.4E+15	3.4E+15	3.4E+15	3.4E+15
Rb 90m		2.4E+15	2.4E+15	2.4E+15	2.4E+15	2.4E+15
Sr 90		2.2E+10	9.8E+10	1.1E+11	1.1E+11	1.1E+11
Y 90		9.0E+10	9.0E+10	9.0E+10	9.0E+10	9.0E+10
Y 90m		1.3E+12	1.3E+12	1.3E+12	1.3E+12	1.3E+12
Zr 90						
Zr 90m						
Se 91		2.3E+18	2.3E+18	2.3E+18	2.3E+18	2.3E+18
Br 91		8.8E+17	8.8E+17	8.8E+17	8.8E+17	8.8E+17
Kr 91		4.8E+16	4.8E+16	4.8E+16	4.8E+16	4.8E+16
Rb 91		8.0E+15	8.0E+15	8.0E+15	8.0E+15	8.0E+15
Sr 91		8.2E+12	8.2E+12	8.2E+12	8.2E+12	8.2E+12
Y 91		5.9E+10	5.9E+10	5.9E+10	5.9E+10	5.9E+10
Y 91m		3.4E+13	3.4E+13	3.4E+13	3.4E+13	3.4E+13
Zr 91						
Nb 91		1.7E+07	1.6E+08	1.1E+09	1.7E+09	1.7E+09
Se 92		3.3E+18	3.3E+18	3.3E+18	3.3E+18	3.3E+18
Br 92		1.8E+18	1.8E+18	1.8E+18	1.8E+18	1.8E+18
Kr 92		1.4E+17	1.4E+17	1.4E+17	1.4E+17	1.4E+17
Rb 92		6.5E+16	6.5E+16	6.5E+16	6.5E+16	6.5E+16
Sr 92						
Y 92						
Zr 92						
Nb 92		2.9E+04	2.9E+05	2.9E+06	2.9E+08	2.9E+09
Se 93		6.5E+18	6.5E+18	6.5E+18	6.5E+18	6.5E+18
Br 93		2.8E+18	2.8E+18	2.8E+18	2.8E+18	2.8E+18
Kr 93		2.4E+17	2.4E+17	2.4E+17	2.4E+17	2.4E+17
Rb 93		4.2E+16	4.2E+16	4.2E+16	4.2E+16	4.2E+16
Sr 93		4.7E+14	4.7E+14	4.7E+14	4.7E+14	4.7E+14

	Time (yr)					
Isotope	0	10	100	1,000	100,000	1,000,000
Y 93		2.9E+12	2.9E+12	2.9E+12	2.9E+12	2.9E+12
Zr 93		1.1E+04	1.8E+05	2.1E+06	2.1E+08	1.7E+09
Nb 93						
Nb 93m		9.8E+08	2.8E+09	2.8E+09	2.8E+09	2.8E+09
Br 94		4.1E+18	4.1E+18	4.1E+18	4.1E+18	4.1E+18
Kr 94		1.1E+18	1.1E+18	1.1E+18	1.1E+18	1.1E+18
Rb 94		1.4E+17	1.4E+17	1.4E+17	1.4E+17	1.4E+17
Sr 94						
Y 94						
Zr 94						
Nb 94		5.6E+07	5.6E+08	5.6E+09	1.6E+11	1.7E+11
Nb 94m		1.5E+13	1.5E+13	1.5E+13	1.5E+13	1.5E+13
Br 95		6.4E+18	6.4E+18	6.4E+18	6.4E+18	6.4E+18
Kr 95		8.4E+17	8.4E+17	8.4E+17	8.4E+17	8.4E+17
Rb 95		1.6E+18	1.6E+18	1.6E+18	1.6E+18	1.6E+18
Sr 95		1.9E+16	1.9E+16	1.9E+16	1.9E+16	1.9E+16
Y 95		6.8E+14	6.8E+14	6.8E+14	6.8E+14	6.8E+14
Zr 95		1.1E+11	1.1E+11	1.1E+11	1.1E+11	1.1E+11
Nb 95		7.8E+10	7.8E+10	7.8E+10	7.8E+10	7.8E+10
Nb 95m		2.0E+11	2.0E+11	2.0E+11	2.0E+11	2.0E+11
Mo 95						
Br 96		9.3E+18	9.3E+18	9.3E+18	9.3E+18	9.3E+18
Kr 96		1.5E+18	1.5E+18	1.5E+18	1.5E+18	1.5E+18
Rb 96		3.4E+18	3.4E+18	3.4E+18	3.4E+18	3.4E+18
Sr 96		2.0E+17	2.0E+17	2.0E+17	2.0E+17	2.0E+17
Y 96						
Zr 96						
Nb 96						
Mo 96						
Kr 97		5.3E+18	5.3E+18	5.3E+18	5.3E+18	5.3E+18
Rb 97		3.0E+18	3.0E+18	3.0E+18	3.0E+18	3.0E+18
Sr 97						
Y 97						
Zr 97						
Nb 97						
Nb 97m						
Mo 97						
Kr 98						
Rb 98						
Sr 98						
Y 98						
Zr 98						
Nb 98						
Nb 98m						
Mo 98						
Tc 98		2.4E+05	2.4E+06	2.4E+07	2.4E+09	2.2E+10
Rb 99		6.2E+18	6.2E+18	6.2E+18	6.2E+18	6.2E+18
Sr 99		1.2E+18	1.2E+18	1.2E+18	1.2E+18	1.2E+18
Y 99		1.7E+17	1.7E+17	1.7E+17	1.7E+17	1.7E+17
Zr 99		8.1E+16	8.1E+16	8.1E+16	8.1E+16	8.1E+16
Nb 99		9.5E+15	9.5E+15	9.5E+15	9.5E+15	9.5E+15

	Time (yr)					
Isotope	0	10	100	1,000	100,000	1,000,000
Nb 99m		1.3E+15	1.3E+15	1.3E+15	1.3E+15	1.3E+15
Mo 99		3.1E+11	3.1E+11	3.1E+11	3.1E+11	3.2E+11
Tc 99		2.7E+05	2.7E+06	2.7E+07	2.3E+09	7.9E+09
Tc 99m		7.6E+11	7.6E+11	7.6E+11	7.7E+11	7.7E+11
Ru 99						
Rb100		4.9E+18	4.9E+18	4.9E+18	4.9E+18	4.9E+18
Sr100		1.0E+18	1.0E+18	1.0E+18	1.0E+18	1.0E+18
Y100		4.3E+17	4.3E+17	4.3E+17	4.3E+17	4.3E+17
Zr100						
Nb100						
Nb100m						
Mo100						
Tc100						
Ru100						
Rb101		4.0E+18	4.0E+18	4.0E+18	4.0E+18	4.0E+18
Sr101		1.5E+18	1.5E+18	1.5E+18	1.5E+18	1.5E+18
Y101						
Zr101						
Nb101						
Mo101						
Tc101						
Ru101						
Sr102						
Y102						
Zr102						
Nb102						
Mo102						
Tc102						
Tc102m						
Ru102						
Rh102		1.9E+11	2.1E+11	2.1E+11	2.1E+11	2.1E+11
Pd102						
Sr103		4.5E+18	4.5E+18	4.5E+18	4.5E+18	4.5E+18
Y103		1.6E+18	1.6E+18	1.6E+18	1.6E+18	1.6E+18
Zr103		2.8E+17	2.8E+17	2.8E+17	2.8E+17	2.8E+17
Nb103		1.9E+17	1.9E+17	1.9E+17	1.9E+17	1.9E+17
Mo103		3.8E+15	3.8E+15	3.8E+15	3.8E+15	3.8E+15
Tc103		2.7E+15	2.7E+15	2.7E+15	2.7E+15	2.7E+15
Ru103		5.5E+10	5.5E+10	5.5E+10	5.5E+10	5.5E+10
Rh103						
Rh103m						
Sr104		2.6E+18	2.6E+18	2.6E+18	2.6E+18	2.6E+18
Y104		4.2E+18	4.2E+18	4.2E+18	4.2E+18	4.2E+18
Zr104		8.1E+16	8.1E+16	8.1E+16	8.1E+16	8.1E+16
Nb104		9.5E+16	9.5E+16	9.5E+16	9.5E+16	9.5E+16
Mo104						
Tc104						
Ru104						
Rh104						
Rh104m						
Pd104						

	Time (yr)					
Isotope	0	10	100	1,000	100,000	1,000,000
Y105		2.6E+18	2.6E+18	2.6E+18	2.6E+18	2.6E+18
Zr105		5.7E+17	5.7E+17	5.7E+17	5.7E+17	5.7E+17
Nb105						
Mo105						
Tc105						
Ru105						
Rh105						
Rh105m						
Pd105						
Y106		8.6E+18	8.6E+18	8.6E+18	8.6E+18	8.6E+18
Zr106		4.0E+17	4.0E+17	4.0E+17	4.0E+17	4.0E+17
Nb106		6.4E+17	6.4E+17	6.4E+17	6.4E+17	6.4E+17
Mo106		3.1E+16	3.1E+16	3.1E+16	3.1E+16	3.1E+16
Tc106		1.8E+16	1.8E+16	1.8E+16	1.8E+16	1.8E+16
Ru106		9.1E+10	9.2E+10	9.2E+10	9.2E+10	9.2E+10
Rh106						
Rh106m						
Pd106						
Ag106						
Y107		6.7E+18	6.7E+18	6.7E+18	6.7E+18	6.7E+18
Zr107		2.0E+18	2.0E+18	2.0E+18	2.0E+18	2.0E+18
Nb107		5.9E+17	5.9E+17	5.9E+17	5.9E+17	5.9E+17
Mo107		5.9E+16	5.9E+16	5.9E+16	5.9E+16	5.9E+16
Tc107		7.2E+15	7.2E+15	7.2E+15	7.2E+15	7.2E+15
Ru107		4.7E+14	4.7E+14	4.7E+14	4.7E+14	4.7E+14
Rh107		4.0E+13	4.0E+13	4.0E+13	4.0E+13	4.0E+13
Pd107		9.6E+02	9.6E+03	9.6E+04	9.5E+06	9.1E+07
Pd107m		6.4E+14	6.4E+14	6.4E+14	6.4E+14	6.4E+14
Ag107						
Zr108		8.8E+17	8.8E+17	8.8E+17	8.8E+17	8.8E+17
Nb108		1.3E+18	1.3E+18	1.3E+18	1.3E+18	1.3E+18
Mo108						
Tc108						
Ru108						
Rh108						
Rh108m						
Pd108						
Ag108						
Ag108m		8.7E+09	6.9E+10	1.6E+11	1.6E+11	1.6E+11
Cd108						
Zr109		2.1E+18	2.1E+18	2.1E+18	2.1E+18	2.1E+18
Nb109						
Mo109						
Tc109						
Ru109						
Rh109						
Rh109m						
Pd109						
Pd109m						
Ag109						
Ag109m						

	Time (yr)					
Isotope	0	10	100	1,000	100,000	1,000,000
Cd109		7.7E+09	7.7E+09	7.7E+09	7.7E+09	7.7E+09
Nb110						
Mo110						
Tc110						
Ru110						
Rh110						
Rh110m						
Pd110						
Ag110						
Ag110m		2.7E+11	2.7E+11	2.7E+11	2.7E+11	2.7E+11
Cd110						
Nb111		1.4E+18	1.4E+18	1.4E+18	1.4E+18	1.4E+18
Mo111		4.9E+17	4.9E+17	4.9E+17	4.9E+17	4.9E+17
Tc111		8.7E+16	8.7E+16	8.7E+16	8.7E+16	8.7E+16
Ru111		7.6E+16	7.6E+16	7.6E+16	7.6E+16	7.6E+16
Rh111		8.1E+15	8.1E+15	8.1E+15	8.1E+15	8.1E+15
Pd111		3.2E+13	3.2E+13	3.2E+13	3.2E+13	3.2E+13
Pd111m		1.5E+12	1.5E+12	1.5E+12	1.5E+12	1.5E+12
Ag111		3.7E+10	3.7E+10	3.7E+10	3.7E+10	3.7E+10
Ag111m		4.9E+13	4.9E+13	4.9E+13	4.9E+13	4.9E+13
Cd111						
Cd111m						
Nb112		3.7E+18	3.7E+18	3.7E+18	3.7E+18	3.7E+18
Mo112		1.6E+17	1.6E+17	1.6E+17	1.6E+17	1.6E+17
Tc112		5.6E+17	5.6E+17	5.6E+17	5.6E+17	5.6E+17
Ru112						
Rh112						
Pd112						
Ag112						
Cd112						
Mo113		2.0E+18	2.0E+18	2.0E+18	2.0E+18	2.0E+18
Tc113		5.3E+17	5.3E+17	5.3E+17	5.3E+17	5.3E+17
Ru113		9.9E+16	9.9E+16	9.9E+16	9.9E+16	9.9E+16
Rh113		2.2E+17	2.2E+17	2.2E+17	2.2E+17	2.2E+17
Pd113		1.8E+15	1.8E+15	1.8E+15	1.8E+15	1.8E+15
Ag113		5.8E+12	5.8E+12	5.8E+12	5.8E+12	5.8E+12
Ag113m		3.8E+14	3.8E+14	3.8E+14	3.8E+14	3.8E+14
Cd113		6.6E-06	6.6E-05	6.6E-04	6.6E-02	6.6E-01
Cd113m		6.9E+09	1.8E+10	1.8E+10	1.8E+10	1.8E+10
In113						
In113m						
Mo114		8.2E+17	8.2E+17	8.2E+17	8.2E+17	8.2E+17
Tc114		2.2E+18	2.2E+18	2.2E+18	2.2E+18	2.2E+18
Ru114		1.9E+16	1.9E+16	1.9E+16	1.9E+16	1.9E+16
Rh114		8.2E+16	8.2E+16	8.2E+16	8.2E+16	8.2E+16
Pd114						
Ag114						
Cd114						
In114						
In114m		3.1E+10	3.1E+10	3.1E+10	3.1E+10	3.1E+10
Sn114						

	Time (yr)					
Isotope	0	10	100	1,000	100,000	1,000,000
Mo115		3.9E+18	3.9E+18	3.9E+18	3.9E+18	3.9E+18
Tc115		1.5E+18	1.5E+18	1.5E+18	1.5E+18	1.5E+18
Ru115		4.0E+17	4.0E+17	4.0E+17	4.0E+17	4.0E+17
Rh115		3.3E+16	3.3E+16	3.3E+16	3.3E+16	3.3E+16
Pd115		6.6E+15	6.6E+15	6.6E+15	6.6E+15	6.6E+15
Ag115		1.6E+14	1.6E+14	1.6E+14	1.6E+14	1.6E+14
Ag115m		4.2E+15	4.2E+15	4.2E+15	4.2E+15	4.2E+15
Cd115		1.4E+11	1.4E+11	1.4E+11	1.4E+11	1.4E+11
Cd115m		6.1E+10	6.1E+10	6.1E+10	6.1E+10	6.1E+10
In115		2.3E-04	2.3E-03	2.3E-02	2.3E+00	2.3E+01
In115m		1.0E+12	1.0E+12	1.0E+12	1.0E+12	1.0E+12
Sn115						
Tc116		4.3E+18	4.3E+18	4.3E+18	4.3E+18	4.3E+18
Ru116		1.2E+17	1.2E+17	1.2E+17	1.2E+17	1.2E+17
Rh116		3.7E+17	3.7E+17	3.7E+17	3.7E+17	3.7E+17
Pd116						
Ag116						
Ag116m						
Cd116						
In116						
In116m						
Sn116						
Tc117		2.3E+18	2.3E+18	2.3E+18	2.3E+18	2.3E+18
Ru117		8.0E+17	8.0E+17	8.0E+17	8.0E+17	8.0E+17
Rh117		1.5E+17	1.5E+17	1.5E+17	1.5E+17	1.5E+17
Pd117		3.2E+16	3.2E+16	3.2E+16	3.2E+16	3.2E+16
Ag117		2.0E+15	2.0E+15	2.0E+15	2.0E+15	2.0E+15
Ag117m		2.3E+16	2.3E+16	2.3E+16	2.3E+16	2.3E+16
Cd117		1.1E+13	1.1E+13	1.1E+13	1.1E+13	1.1E+13
Cd117m		1.3E+13	1.3E+13	1.3E+13	1.3E+13	1.3E+13
In117		2.4E+13	2.4E+13	2.4E+13	2.4E+13	2.4E+13
In117m		5.1E+12	5.1E+12	5.1E+12	5.1E+12	5.1E+12
Sn117						
Sn117m		3.0E+10	3.0E+10	3.0E+10	3.0E+10	3.0E+10
Tc118		4.2E+18	4.2E+18	4.2E+18	4.2E+18	4.2E+18
Ru118		2.3E+17	2.3E+17	2.3E+17	2.3E+17	2.3E+17
Rh118		8.1E+17	8.1E+17	8.1E+17	8.1E+17	8.1E+17
Pd118						
Ag118						
Ag118m						
Cd118						
In118						
In118m						
Sn118						
Ru119		1.9E+18	1.9E+18	1.9E+18	1.9E+18	1.9E+18
Rh119		6.6E+17	6.6E+17	6.6E+17	6.6E+17	6.6E+17
Pd119		1.5E+17	1.5E+17	1.5E+17	1.5E+17	1.5E+17
Ag119		1.2E+17	1.2E+17	1.2E+17	1.2E+17	1.2E+17
Cd119		1.4E+15	1.4E+15	1.4E+15	1.4E+15	1.4E+15
Cd119m		2.3E+15	2.3E+15	2.3E+15	2.3E+15	2.3E+15
In119		9.9E+14	9.9E+14	9.9E+14	9.9E+14	9.9E+14

	Time (yr)					
Isotope	0	10	100	1,000	100,000	1,000,000
In119m		9.9E+13	9.9E+13	9.9E+13	9.9E+13	9.9E+13
Sn119						
Sn119m		8.4E+09	8.4E+09	8.4E+09	8.4E+09	8.4E+09
Ru120		8.3E+17	8.3E+17	8.3E+17	8.3E+17	8.3E+17
Rh120		2.3E+18	2.3E+18	2.3E+18	2.3E+18	2.3E+18
Pd120						
Ag120						
Cd120						
In120						
In120m						
Sn120						
Rh121		1.2E+18	1.2E+18	1.2E+18	1.2E+18	1.2E+18
Pd121		4.1E+17	4.1E+17	4.1E+17	4.1E+17	4.1E+17
Ag121		3.1E+17	3.1E+17	3.1E+17	3.1E+17	3.1E+17
Cd121		1.7E+16	1.7E+16	1.7E+16	1.7E+16	1.7E+16
In121		7.6E+15	7.6E+15	7.6E+15	7.6E+15	7.6E+15
In121m		5.8E+14	5.8E+14	5.8E+14	5.8E+14	5.8E+14
Sn121						
Sn121m		1.4E+09	8.8E+09	1.2E+10	1.2E+10	1.2E+10
Sb121						
Rh122		3.5E+18	3.5E+18	3.5E+18	3.5E+18	3.5E+18
Pd122		1.1E+17	1.1E+17	1.1E+17	1.1E+17	1.1E+17
Ag122		6.3E+17	6.3E+17	6.3E+17	6.3E+17	6.3E+17
Cd122						
In122						
In122m						
Sn122						
Sb122		9.7E+10	9.7E+10	9.7E+10	9.7E+10	9.7E+10
Sb122m		1.4E+13	1.4E+13	1.4E+13	1.4E+13	1.4E+13
Te122						
Rh123		3.1E+18	3.1E+18	3.1E+18	3.1E+18	3.1E+18
Pd123		1.2E+18	1.2E+18	1.2E+18	1.2E+18	1.2E+18
Ag123		9.8E+17	9.8E+17	9.8E+17	9.8E+17	9.8E+17
Cd123		3.3E+16	3.3E+16	3.3E+16	3.3E+16	3.3E+16
In123		4.1E+16	4.1E+16	4.1E+16	4.1E+16	4.1E+16
In123m						
Sn123		5.1E+10	5.1E+10	5.1E+10	5.1E+10	5.1E+10
Sn123m						
Sb123						
Te123		9.1E-04	9.1E-03	9.1E-02	9.1E+00	9.1E+01
Te123m		2.4E+10	2.4E+10	2.4E+10	2.4E+10	2.4E+10
Pd124		4.6E+17	4.6E+17	4.6E+17	4.6E+17	4.6E+17
Ag124		1.6E+18	1.6E+18	1.6E+18	1.6E+18	1.6E+18
Cd124						
In124						
Sn124						
Sb124		2.2E+11	2.2E+11	2.2E+11	2.2E+11	2.2E+11
Sb124m		9.0E+14	9.0E+14	9.0E+14	9.0E+14	9.0E+14
Te124						
Pd125		2.7E+18	2.7E+18	2.7E+18	2.7E+18	2.7E+18
Ag125		1.3E+18	1.3E+18	1.3E+18	1.3E+18	1.3E+18

	Time (yr)					
Isotope	0	10	100	1,000	100,000	1,000,000
Cd125		2.3E+17	2.3E+17	2.3E+17	2.3E+17	2.3E+17
In125		1.4E+17	1.4E+17	1.4E+17	1.4E+17	1.4E+17
In125m		2.7E+16	2.7E+16	2.7E+16	2.7E+16	2.7E+16
Sn125		5.5E+11	5.5E+11	5.5E+11	5.5E+11	5.5E+11
Sn125m		3.3E+14	3.3E+14	3.3E+14	3.3E+14	3.3E+14
Sb125		5.0E+10	5.4E+10	5.4E+10	5.4E+10	5.4E+10
Te125						
Te125m		1.4E+10	1.4E+10	1.4E+10	1.4E+10	1.4E+10
Pd126		1.3E+18	1.3E+18	1.3E+18	1.3E+18	1.3E+18
Ag126		3.8E+18	3.8E+18	3.8E+18	3.8E+18	3.8E+18
Cd126						
In126		3.1E+17	3.1E+17	3.1E+17	3.1E+17	3.1E+17
Sn126		1.8E+07	1.9E+08	1.9E+09	1.4E+11	2.8E+11
Sb126		3.0E+11	3.0E+11	3.0E+11	3.0E+11	3.0E+11
Sb126m		1.4E+14	1.4E+14	1.4E+14	1.4E+14	1.4E+14
Te126						
Xe126						
Ag127		2.5E+18	2.5E+18	2.5E+18	2.5E+18	2.5E+18
Cd127		6.5E+17	6.5E+17	6.5E+17	6.5E+17	6.5E+17
In127		3.2E+17	3.2E+17	3.2E+17	3.2E+17	3.2E+17
In127m		1.0E+17	1.0E+17	1.0E+17	1.0E+17	1.0E+17
Sn127		5.1E+13	5.1E+13	5.1E+13	5.1E+13	5.1E+13
Sn127m		9.3E+14	9.3E+14	9.3E+14	9.3E+14	9.3E+14
Sb127		7.3E+11	7.3E+11	7.3E+11	7.3E+11	7.3E+11
Te127						
Te127m		1.5E+10	1.5E+10	1.5E+10	1.5E+10	1.5E+10
I127						
Xe127		3.0E+10	3.0E+10	3.0E+10	3.0E+10	3.0E+10
Ag128		5.5E+18	5.5E+18	5.5E+18	5.5E+18	5.5E+18
Cd128		2.0E+17	2.0E+17	2.0E+17	2.0E+17	2.0E+17
In128		4.4E+17	4.4E+17	4.4E+17	4.4E+17	4.4E+17
Sn128						
Sb128						
Sb128m						
Te128						
I128						
Xe128						
Cd129		1.2E+18	1.2E+18	1.2E+18	1.2E+18	1.2E+18
In129		6.3E+17	6.3E+17	6.3E+17	6.3E+17	6.3E+17
Sn129		2.1E+15	2.1E+15	2.1E+15	2.1E+15	2.1E+15
Sn129m		7.8E+14	7.8E+14	7.8E+14	7.8E+14	7.8E+14
Sb129		1.5E+13	1.5E+13	1.5E+13	1.5E+13	1.5E+13
Te129		1.1E+13	1.1E+13	1.1E+13	1.1E+13	1.1E+13
Te129m		3.3E+10	3.3E+10	3.3E+10	3.3E+10	3.4E+10
I129		3.4E+03	3.4E+04	3.4E+05	3.4E+07	3.3E+08
Xe129						
Xe129m		2.2E+10	2.2E+10	2.2E+10	2.2E+10	2.2E+10
Cd130		5.1E+17	5.1E+17	5.1E+17	5.1E+17	5.1E+17
In130		1.2E+18	1.2E+18	1.2E+18	1.2E+18	1.2E+18
Sn130						
Sb130						

	Time (yr)					
Isotope	0	10	100	1,000	100,000	1,000,000
Sb130m						
Te130						
I130						
I130m						
Xe130						
Cd131		3.7E+18	3.7E+18	3.7E+18	3.7E+18	3.7E+18
In131		8.5E+17	8.5E+17	8.5E+17	8.5E+17	8.5E+17
Sn131		4.6E+15	4.6E+15	4.6E+15	4.6E+15	4.6E+15
Sb131		1.1E+14	1.1E+14	1.1E+14	1.1E+14	1.1E+14
Te131		4.8E+13	4.8E+13	4.8E+13	4.8E+13	4.8E+13
Te131m		1.1E+12	1.1E+12	1.1E+12	1.1E+12	1.1E+12
I131		6.6E+10	6.6E+10	6.6E+10	6.6E+10	6.6E+10
Xe131						
Xe131m		1.6E+10	1.6E+10	1.6E+10	1.6E+10	1.6E+10
Cd132		1.9E+18	1.9E+18	1.9E+18	1.9E+18	1.9E+18
In132		2.2E+18	2.2E+18	2.2E+18	2.2E+18	2.2E+18
Sn132		1.2E+15	1.2E+15	1.2E+15	1.2E+15	1.2E+15
Sb132		3.8E+14	3.8E+14	3.8E+14	3.8E+14	3.8E+14
Sb132m		5.7E+14	5.7E+14	5.7E+14	5.7E+14	5.7E+14
Te132		3.3E+10	3.3E+10	3.3E+10	3.3E+10	3.3E+10
I132						
Xe132						
Cs132		7.0E+10	7.0E+10	7.0E+10	7.0E+10	7.0E+10
Ba132						
In133		2.1E+18	2.1E+18	2.1E+18	2.1E+18	2.1E+18
Sn133		1.1E+17	1.1E+17	1.1E+17	1.1E+17	1.1E+17
Sb133		6.4E+14	6.4E+14	6.4E+14	6.4E+14	6.4E+14
Te133		9.3E+13	9.3E+13	9.3E+13	9.3E+13	9.3E+13
Te133m		2.4E+13	2.4E+13	2.4E+13	2.4E+13	2.4E+13
I133		5.6E+11	5.6E+11	5.6E+11	5.6E+11	5.6E+11
I133m		6.2E+15	6.2E+15	6.2E+15	6.2E+15	6.2E+15
Xe133		1.8E+10	1.8E+10	1.8E+10	1.8E+10	1.8E+10
Xe133m		5.2E+10	5.2E+10	5.2E+10	5.2E+10	5.2E+10
Cs133						
Ba133		2.1E+10	4.4E+10	4.4E+10	4.4E+10	4.4E+10
In134		3.4E+18	3.4E+18	3.4E+18	3.4E+18	3.4E+18
Sn134		1.1E+17	1.1E+17	1.1E+17	1.1E+17	1.1E+17
Sb134		1.7E+17	1.7E+17	1.7E+17	1.7E+17	1.7E+17
Sb134m		1.5E+16	1.5E+16	1.5E+16	1.5E+16	1.5E+16
Te134						
I134						
I134m						
Xe134						
Xe134m						
Cs134		1.6E+11	1.7E+11	1.7E+11	1.7E+11	1.7E+11
Cs134m		4.2E+12	4.2E+12	4.2E+12	4.2E+12	4.2E+12
Ba134						
Sn135		6.8E+17	6.8E+17	6.8E+17	6.8E+17	6.8E+17
Sb135		1.4E+17	1.4E+17	1.4E+17	1.4E+17	1.4E+17
Te135		1.2E+16	1.2E+16	1.2E+16	1.2E+16	1.2E+16
I135		6.9E+12	6.9E+12	6.9E+12	6.9E+12	6.9E+12

	Time (yr)					
Isotope	0	10	100	1,000	100,000	1,000,000
Xe135		1.5E+12	1.5E+12	1.5E+12	1.5E+12	1.5E+12
Xe135m		4.4E+13	4.4E+13	4.4E+13	4.4E+13	4.4E+13
Cs135		1.6E+04	1.6E+05	1.6E+06	1.6E+08	1.4E+09
Cs135m		4.0E+13	4.0E+13	4.0E+13	4.0E+13	4.0E+13
Ba135						
Ba135m						
Sn136		3.2E+17	3.2E+17	3.2E+17	3.2E+17	3.2E+17
Sb136		3.8E+17	3.8E+17	3.8E+17	3.8E+17	3.8E+17
Te136		1.1E+16	1.1E+16	1.1E+16	1.1E+16	1.1E+16
I136						
I136m						
Xe136						
Cs136		2.0E+11	2.0E+11	2.0E+11	2.0E+11	2.0E+11
Ba136						
Ba136m						
Sb137		9.5E+17	9.5E+17	9.5E+17	9.5E+17	9.5E+17
Te137		1.1E+17	1.1E+17	1.1E+17	1.1E+17	1.1E+17
I137		1.5E+16	1.5E+16	1.5E+16	1.5E+16	1.5E+16
Xe137		1.1E+15	1.1E+15	1.1E+15	1.1E+15	1.1E+15
Cs137		1.5E+10	7.0E+10	7.8E+10	7.8E+10	7.8E+10
Ba137						
Ba137m						
Sb138		3.2E+18	3.2E+18	3.2E+18	3.2E+18	3.2E+18
Te138		1.9E+17	1.9E+17	1.9E+17	1.9E+17	1.9E+17
I138		6.5E+16	6.5E+16	6.5E+16	6.5E+16	6.5E+16
Xe138						
Cs138						
Cs138m						
Ba138						
La138		8.0E+00	8.0E+01	8.0E+02	8.0E+04	8.0E+05
Sb139		2.1E+18	2.1E+18	2.1E+18	2.1E+18	2.1E+18
Te139		6.0E+17	6.0E+17	6.0E+17	6.0E+17	6.0E+17
I139						
Xe139						
Cs139						
Ba139						
La139						
Ce139		2.4E+10	2.4E+10	2.4E+10	2.4E+10	2.4E+10
Pr139		3.5E+12	3.5E+12	3.5E+12	3.5E+12	3.5E+12
Te140		2.6E+17	2.6E+17	2.6E+17	2.6E+17	2.6E+17
I140		3.7E+17	3.7E+17	3.7E+17	3.7E+17	3.7E+17
Xe140		1.3E+16	1.3E+16	1.3E+16	1.3E+16	1.3E+16
Cs140		4.4E+15	4.4E+15	4.4E+15	4.4E+15	4.4E+15
Ba140		5.3E+10	5.3E+10	5.3E+10	5.3E+10	5.3E+10
La140						
Ce140						
Pr140						
Te141		1.5E+18	1.5E+18	1.5E+18	1.5E+18	1.5E+18
I141		7.4E+17	7.4E+17	7.4E+17	7.4E+17	7.4E+17
Xe141		1.8E+17	1.8E+17	1.8E+17	1.8E+17	1.8E+17
Cs141		1.1E+16	1.1E+16	1.1E+16	1.1E+16	1.1E+16

	Time (yr)					
Isotope	0	10	100	1,000	100,000	1,000,000
Ba141		1.9E+14	1.9E+14	1.9E+14	1.9E+14	1.9E+14
La141		1.0E+13	1.0E+13	1.0E+13	1.0E+13	1.0E+13
Ce141		2.4E+10	2.4E+10	2.4E+10	2.4E+10	2.4E+10
Pr141						
Nd141						
Te142		5.2E+17	5.2E+17	5.2E+17	5.2E+17	5.2E+17
I142		2.2E+18	2.2E+18	2.2E+18	2.2E+18	2.2E+18
Xe142		1.7E+17	1.7E+17	1.7E+17	1.7E+17	1.7E+17
Cs142		1.7E+17	1.7E+17	1.7E+17	1.7E+17	1.7E+17
Ba142						
La142						
Ce142						
Pr142						
Pr142m						
Nd142						
I143		7.4E+17	7.4E+17	7.4E+17	7.4E+17	7.4E+17
Xe143		2.6E+17	2.6E+17	2.6E+17	2.6E+17	2.6E+17
Cs143		1.1E+17	1.1E+17	1.1E+17	1.1E+17	1.1E+17
Ba143		1.1E+16	1.1E+16	1.1E+16	1.1E+16	1.1E+16
La143		1.3E+14	1.3E+14	1.3E+14	1.3E+14	1.3E+14
Ce143		5.8E+11	5.8E+11	5.8E+11	5.8E+11	5.8E+11
Pr143		3.0E+10	3.0E+10	3.0E+10	3.0E+10	3.0E+10
Nd143						
I144		4.1E+18	4.1E+18	4.1E+18	4.1E+18	4.1E+18
Xe144		2.6E+17	2.6E+17	2.6E+17	2.6E+17	2.6E+17
Cs144		5.4E+17	5.4E+17	5.4E+17	5.4E+17	5.4E+17
Ba144		2.0E+16	2.0E+16	2.0E+16	2.0E+16	2.0E+16
La144		1.2E+16	1.2E+16	1.2E+16	1.2E+16	1.2E+16
Ce144		7.7E+10	7.7E+10	7.7E+10	7.7E+10	7.7E+10
Pr144		5.6E+13	5.6E+13	5.6E+13	5.6E+13	5.6E+13
Pr144m		6.6E+12	6.6E+12	6.6E+12	6.6E+12	6.6E+12
Nd144		6.1E-04	6.1E-03	6.1E-02	6.1E+00	6.1E+01
I145		2.5E+18	2.5E+18	2.5E+18	2.5E+18	2.5E+18
Xe145		4.7E+17	4.7E+17	4.7E+17	4.7E+17	4.7E+17
Cs145		6.3E+17	6.3E+17	6.3E+17	6.3E+17	6.3E+17
Ba145						
La145						
Ce145						
Pr145						
Nd145						
Pm145		1.4E+09	4.2E+09	4.2E+09	4.2E+09	4.2E+09
Sm145		1.1E+10	1.4E+10	1.4E+10	1.4E+10	1.4E+10
Xe146		4.8E+17	4.8E+17	4.8E+17	4.8E+17	4.8E+17
Cs146						
Ba146						
La146						
Ce146						
Pr146						
Nd146						
Pm146		5.8E+10	8.1E+10	8.1E+10	8.1E+10	8.2E+10
Sm146		1.7E+04	1.7E+05	1.7E+06	1.7E+08	1.6E+09

	Time (yr)					
Isotope	0	10	100	1,000	100,000	1,000,000
Xe147		2.0E+18	2.0E+18	2.0E+18	2.0E+18	2.0E+18
Cs147		6.5E+17	6.5E+17	6.5E+17	6.5E+17	6.5E+17
Ba147		4.2E+17	4.2E+17	4.2E+17	4.2E+17	4.2E+17
La147		5.9E+16	5.9E+16	5.9E+16	5.9E+16	5.9E+16
Ce147		4.1E+15	4.1E+15	4.1E+15	4.1E+15	4.1E+15
Pr147		2.8E+14	2.8E+14	2.8E+14	2.8E+14	2.8E+14
Nd147		1.4E+11	1.4E+11	1.4E+11	1.4E+11	1.4E+11
Pm147		5.6E+09	6.0E+09	6.0E+09	6.0E+09	6.0E+09
Sm147		1.5E+01	1.5E+02	1.5E+03	1.5E+05	1.5E+06
Cs148		2.2E+18	2.2E+18	2.2E+18	2.2E+18	2.2E+18
Ba148		2.6E+17	2.6E+17	2.6E+17	2.6E+17	2.6E+17
La148		2.3E+17	2.3E+17	2.3E+17	2.3E+17	2.3E+17
Ce148						
Pr148						
Nd148						
Pm148		1.5E+11	1.5E+11	1.5E+11	1.5E+11	1.5E+11
Pm148m		2.1E+11	2.1E+11	2.1E+11	2.1E+11	2.1E+11
Sm148		1.7E-04	1.7E-03	1.7E-02	1.7E+00	1.7E+01
Cs149		1.4E+18	1.4E+18	1.4E+18	1.4E+18	1.4E+18
Ba149						
La149						
Ce149						
Pr149						
Nd149						
Pm149						
Sm149						
Eu149		8.3E+09	8.3E+09	8.3E+09	8.3E+09	8.3E+09
Cs150						
Ba150						
La150						
Ce150						
Pr150						
Nd150						
Pm150						
Sm150						
Eu150		2.6E+10	1.3E+11	1.5E+11	1.5E+11	1.5E+11
Ba151		9.9E+17	9.9E+17	9.9E+17	9.9E+17	9.9E+17
La151		4.1E+17	4.1E+17	4.1E+17	4.1E+17	4.1E+17
Ce151		1.8E+17	1.8E+17	1.8E+17	1.8E+17	1.8E+17
Pr151		9.2E+15	9.2E+15	9.2E+15	9.2E+15	9.2E+15
Nd151		2.2E+14	2.2E+14	2.2E+14	2.2E+14	2.2E+14
Pm151		9.3E+11	9.3E+11	9.3E+11	9.3E+11	9.3E+11
Sm151		1.4E+08	1.0E+09	1.9E+09	1.9E+09	1.9E+09
Eu151						
Ba152		6.6E+17	6.6E+17	6.6E+17	6.6E+17	6.6E+17
La152		1.2E+18	1.2E+18	1.2E+18	1.2E+18	1.2E+18
Ce152						
Pr152						
Nd152						
Pm152						
Pm152m						

	Time (yr)					
Isotope	0	10	100	1,000	100,000	1,000,000
Sm152						
Eu152		5.0E+10	1.2E+11	1.2E+11	1.2E+11	1.2E+11
Eu152m		1.3E+12	1.3E+12	1.3E+12	1.3E+12	1.3E+12
Gd152		1.4E-02	1.4E-01	1.4E+00	1.4E+02	1.4E+03
La153						
Ce153						
Pr153						
Nd153						
Pm153						
Sm153						
Eu153						
Gd153		1.4E+10	1.4E+10	1.4E+10	1.4E+10	1.4E+10
La154						
Ce154						
Pr154						
Nd154						
Pm154						
Pm154m						
Sm154						
Eu154		8.2E+10	1.5E+11	1.5E+11	1.5E+11	1.5E+11
Gd154						
La155		3.1E+18	3.1E+18	3.1E+18	3.1E+18	3.1E+18
Ce155		6.3E+17	6.3E+17	6.3E+17	6.3E+17	6.3E+17
Pr155		3.0E+17	3.0E+17	3.0E+17	3.0E+17	3.0E+17
Nd155		1.4E+16	1.4E+16	1.4E+16	1.4E+16	1.4E+16
Pm155		4.1E+15	4.1E+15	4.1E+15	4.1E+15	4.1E+15
Sm155		7.9E+13	7.9E+13	7.9E+13	7.9E+13	7.9E+13
Eu155		9.8E+09	1.3E+10	1.3E+10	1.3E+10	1.3E+10
Gd155						
Gd155m						
Ce156		4.6E+17	4.6E+17	4.6E+17	4.6E+17	4.6E+17
Pr156		9.9E+17	9.9E+17	9.9E+17	9.9E+17	9.9E+17
Nd156		7.3E+15	7.3E+15	7.3E+15	7.3E+15	7.3E+15
Pm156		1.8E+16	1.8E+16	1.8E+16	1.8E+16	1.8E+16
Sm156		1.1E+12	1.1E+12	1.1E+12	1.1E+12	1.1E+12
Eu156		1.6E+11	1.6E+11	1.6E+11	1.6E+11	1.6E+11
Gd156						
Ce157		1.5E+18	1.5E+18	1.5E+18	1.5E+18	1.5E+18
Pr157		6.7E+17	6.7E+17	6.7E+17	6.7E+17	6.7E+17
Nd157						
Pm157						
Sm157						
Eu157						
Gd157						
Pr158						
Nd158						
Pm158						
Sm158						
Eu158						
Gd158						
Pr159						

Isotope	Time (yr)					
	0	10	100	1,000	100,000	1,000,000
Nd159						
Pm159						
Sm159						
Eu159						
Gd159						
Tb159						
Nd160						
Pm160						
Sm160						
Eu160						
Gd160						
Tb160		1.4E+11	1.4E+11	1.4E+11	1.4E+11	1.4E+11
Dy160						
Nd161		5.1E+17	5.1E+17	5.1E+17	5.1E+17	5.1E+17
Pm161		1.9E+17	1.9E+17	1.9E+17	1.9E+17	1.9E+17
Sm161		2.3E+16	2.3E+16	2.3E+16	2.3E+16	2.3E+16
Eu161		2.1E+15	2.1E+15	2.1E+15	2.1E+15	2.1E+15
Gd161		2.0E+14	2.0E+14	2.0E+14	2.0E+14	2.0E+14
Tb161		2.2E+10	2.2E+10	2.2E+10	2.2E+10	2.2E+10
Dy161						
Pm162		5.3E+17	5.3E+17	5.3E+17	5.3E+17	5.3E+17
Sm162						
Eu162						
Gd162						
Tb162						
Tb162m						
Dy162						
Sm163						
Eu163						
Gd163						
Tb163						
Tb163m						
Dy163						
Sm164						
Eu164						
Gd164						
Tb164						
Dy164						
Sm165						
Eu165						
Gd165						
Tb165						
Dy165						
Dy165m						
Ho165						
Dy166		2.0E+10	2.0E+10	2.0E+10	2.0E+10	2.0E+10
Ho166						
Ho166m		9.9E+08	9.6E+09	7.5E+10	1.7E+11	1.7E+11
Er166						
Er167						
Er167m						

	Time (yr)					
Isotope	0	10	100	1,000	100,000	1,000,000
Er168						
Yb168						
Er169		9.9E+09	9.9E+09	9.9E+09	9.9E+09	9.9E+09
Tm169						
Yb169		4.2E+10	4.2E+10	4.2E+10	4.2E+10	4.2E+10
Er170						
Tm170		3.2E+10	3.2E+10	3.2E+10	3.2E+10	3.2E+10
Tm170m		4.5E+09	4.5E+09	4.5E+09	4.5E+09	4.5E+09
Yb170						
Er171		5.4E+12	5.4E+12	5.4E+12	5.4E+12	5.4E+12
Tm171		2.4E+09	2.5E+09	2.5E+09	2.5E+09	2.5E+09
Yb171						
Er172		8.0E+10	8.0E+10	8.0E+10	8.0E+10	8.0E+10
Tm172		9.7E+10	9.7E+10	9.7E+10	9.7E+10	9.7E+10
Yb172						

APPENDIX D

UNSHIELDED PHOTON DOSE RATE

Table 119 - Unshielded Photon Dose Rate (REM/hr/mole) for Actinide Isotopes

Note: Starting with one mole of given isotope and includes all daughters.

	Time (yr)					
Isotope	0	10	100	1,000	100,000	1,000,000
He 4						
Tl206						
Tl207	4.7E+08					
Tl208	9.9E+10					
Tl209	1.0E+11					
Pb206						
Pb207						
Pb208						
Pb209	1.4E+06					
Pb210	2.0E-12	7.7E+01	4.7E+00	3.3E-12		
Pb211	2.2E+08					
Pb212	2.6E+07					
Pb214	1.2E+09	7.7E+01	4.7E+00	3.3E-12		
Bi208						
Bi209						
Bi210m	7.9E-10	7.9E-10	7.9E-10	7.9E-10	7.8E-10	6.3E-10
Bi210	1.7E+05	6.2E-08				
Bi211	2.8E+09					
Bi212	3.7E+08					
Bi213	3.8E+08					
Bi214	8.0E+09	7.7E+01	4.7E+00	3.3E-12		
Po210	5.2E+00	6.0E-08				
Po211m	3.0E+03					
Po211	1.1E+11					
Po212	2.5E+11					
Po213	5.3E+13					
Po214	3.7E+12	7.7E+01	4.7E+00	3.3E-12		
Po215	7.3E+11					
Po216	5.2E+05					
Po218	4.0E+02	7.7E+01	4.7E+00	3.3E-12		
At217	7.0E+10					
Rn218	2.1E+06	7.7E+01	4.7E+00	3.3E-12		
Rn219	1.1E+11					
Rn220	5.1E+07					
Rn222	8.9E+03	7.7E+01	4.7E+00	3.3E-12		
Fr221	8.1E+08					
Fr223	1.9E+08					
Ra222	2.0E+03	7.7E+01	4.7E+00	3.3E-12		
Ra223	7.3E+05					
Ra224	2.5E+05					

	Time (yr)					
Isotope	0	10	100	1,000	100,000	1,000,000
Ra225	1.5E+03					
Ra226	1.0E+00	2.3E+02	2.2E+02	1.5E+02	3.5E-17	
Ra228		3.1E+04	4.9E-01			
Ac225	9.0E+04					
Ac227	1.0E+00	3.1E+03	1.8E+02	6.3E-11		
Ac228	2.9E+08	4.0E+03	2.7E-11			
Th226	4.0E+01	7.7E+01	4.7E+00	3.3E-12		
Th227	4.8E+05					
Th228	1.3E+02	4.0E+03	2.7E-11			
Th229	1.4E+00	8.0E+00	8.0E+00	7.3E+00	1.2E-03	1.1E-38
Th230	3.9E-04	2.1E-02	2.1E-01	1.7E+00	2.0E+00	5.1E-04
Th231	1.3E+05	1.0E+00	3.0E+00	3.0E+00	3.7E-01	2.0E-09
Th232	1.1E-09	2.2E-05	3.5E-05	3.5E-05	3.5E-05	3.5E-05
Th233		6.8E-04	3.8E-03	3.4E-02	2.7E-01	5.4E-03
Th234	1.3E+03	5.6E-05	8.5E-05	2.6E-03	7.8E-01	1.3E-01
Pa231	2.7E-01	1.0E+00	3.0E+00	3.0E+00	3.7E-01	2.0E-09
Pa232	5.6E+07	3.7E+03	1.6E+03	2.0E-01	7.0E-08	7.0E-08
Pa233	5.8E+05	6.8E-04	3.8E-03	3.4E-02	2.7E-01	5.4E-03
Pa234m	5.6E+09	5.6E-05	8.5E-05	2.6E-03	7.8E-01	1.3E-01
Pa234	5.6E+08	5.6E-05	8.5E-05	2.6E-03	7.8E-01	1.3E-01
Pa235	7.7E+07	5.4E-05	5.4E-05	5.7E-05	1.8E-04	2.0E-04
U230	4.2E-02	7.7E+01	4.7E+00	3.3E-12		
U231	4.0E+05	1.0E+00	3.0E+00	3.0E+00	3.7E-01	2.0E-09
U232	4.7E-01	3.7E+03	1.6E+03	2.0E-01		
U233	3.3E-04	6.8E-04	3.8E-03	3.4E-02	2.7E-01	5.4E-03
U234	5.6E-05	5.6E-05	8.5E-05	2.6E-03	7.8E-01	1.3E-01
U235	5.4E-05	5.4E-05	5.4E-05	5.7E-05	1.8E-04	2.0E-04
U236	2.6E-07	2.6E-07	2.6E-07	2.6E-07	3.6E-07	1.3E-06
U237	1.3E+06	2.1E-02	2.1E-02	2.1E-02	2.9E-02	3.8E-02
U238	3.0E-10	3.0E-06	3.0E-06	3.0E-06	1.0E-05	7.8E-05
U239	1.1E+08	4.3E-04	4.3E-04	4.2E-04	1.8E-04	2.0E-04
U240	4.7E+04	3.7E-04	3.6E-04	3.3E-04	3.6E-07	1.3E-06
U241		3.4E-02	2.6E-02	2.2E-02	2.9E-02	3.8E-02
Np235	1.3E+02	2.2E-01	9.6E-05	9.9E-05	1.9E-04	2.0E-04
Np236m	1.8E+06	1.5E+03	7.8E+02	1.0E-01	1.9E-07	6.6E-07
Np236	1.6E-01	1.7E-01	3.0E-01	3.8E-01	2.1E-01	9.3E-04
Np237	6.9E-04	2.1E-02	2.1E-02	2.1E-02	2.9E-02	3.8E-02
Np238	1.9E+07	1.6E-02	8.1E-03	2.1E-03	7.8E-01	1.3E-01
Np239	6.5E+06	4.3E-04	4.3E-04	4.2E-04	1.8E-04	2.0E-04
Np240m	5.8E+09	3.7E-04	3.6E-04	3.3E-04	3.6E-07	1.3E-06
Np240	2.4E+09	3.7E-04	3.6E-04	3.3E-04	3.6E-07	1.3E-06
Np241		3.4E-02	2.6E-02	2.2E-02	2.9E-02	3.8E-02
Pu236	1.6E+00	3.0E+03	1.6E+03	2.1E-01		
Pu237	8.1E-07	2.1E-02	2.1E-02	2.1E-02	2.9E-02	3.8E-02
Pu238	1.8E-02	1.6E-02	8.1E-03	2.1E-03	7.8E-01	1.3E-01
Pu239	4.3E-04	4.3E-04	4.3E-04	4.2E-04	1.8E-04	2.0E-04
Pu240	3.7E-04	3.7E-04	3.6E-04	3.3E-04	3.6E-07	1.3E-06
Pu241	4.0E-09	3.4E-02	2.6E-02	2.2E-02	2.9E-02	3.8E-02
Pu242	4.2E-05	4.2E-05	4.2E-05	4.2E-05	3.6E-05	5.8E-05
Pu243	2.1E+06	5.7E+00	5.6E+00	5.2E+00	6.4E-04	2.0E-04
Pu244	3.7E-05	1.0E-03	1.0E-03	1.0E-03	1.0E-03	1.0E-03

	Time (yr)					
Isotope	0	10	100	1,000	100,000	1,000,000
Pu245	8.7E+05	2.1E+00	2.1E+00	1.9E+00	2.9E-02	3.8E-02
Pu246		1.4E-01	1.3E-01	1.2E-01	3.7E-05	5.8E-05
Am239	4.2E+07	4.5E-04	4.3E-04	4.2E-04	1.8E-04	2.0E-04
Am240	3.6E+07	3.7E-04	3.6E-04	3.3E-04	7.6E-07	1.3E-06
Am241	2.6E-02	2.6E-02	2.5E-02	2.2E-02	2.9E-02	3.8E-02
Am242m	2.3E-01	2.7E+01	1.7E+01	2.1E-01	6.4E-01	1.1E-01
Am242	1.9E+06	1.4E-02	6.8E-03	1.8E-03	6.4E-01	1.1E-01
Am243	3.2E-02	5.7E+00	5.6E+00	5.2E+00	6.4E-04	2.0E-04
Am244m	8.1E+07	1.3E-01	4.3E-03	3.3E-04	7.4E-07	1.6E-06
Am244	8.6E+04	1.3E-01	4.3E-03	3.3E-04	3.6E-07	1.3E-06
Am245	4.4E+06	2.1E+00	2.1E+00	1.9E+00	2.9E-02	3.8E-02
Am246	2.8E+07	1.4E-01	1.3E-01	1.2E-01	3.7E-05	5.8E-05
Cm241	2.7E-04	2.6E-02	2.5E-02	2.2E-02	2.9E-02	3.8E-02
Cm242	4.2E+00	1.6E-02	8.1E-03	2.1E-03	7.8E-01	1.3E-01
Cm243	1.1E+03	8.7E+02	9.8E+01	1.3E-02	1.8E-04	2.0E-04
Cm244	1.8E-01	1.3E-01	4.3E-03	3.3E-04	3.6E-07	1.3E-06
Cm245	2.1E+00	2.1E+00	2.1E+00	1.9E+00	2.9E-02	3.8E-02
Cm246	1.4E-01	1.4E-01	1.3E-01	1.2E-01	3.7E-05	5.8E-05
Cm247	5.3E-03	5.4E-03	5.4E-03	5.6E-03	7.9E-03	7.7E-03
Cm248	6.0E-01	6.0E-01	6.0E-01	6.0E-01	4.9E-01	7.9E-02
Cm249	4.6E+07	2.4E+02	2.1E+02	3.6E+01	2.9E-02	3.8E-02
Cm250	8.6E+01	8.8E+01	8.7E+01	8.4E+01	1.6E+00	2.2E-05
Cm251		3.4E+01	3.2E+01	1.6E+01	7.9E-03	7.7E-03
Bk249	6.8E-02	2.4E+02	2.1E+02	3.6E+01	2.9E-02	3.8E-02
Bk250	4.9E+08	8.5E+01	8.6E-01	1.2E-01	3.7E-05	5.8E-05
Bk251		3.4E+01	3.2E+01	1.6E+01	7.9E-03	7.7E-03
Cf249	2.5E+02	2.4E+02	2.1E+02	3.6E+01	2.9E-02	3.8E-02
Cf250	1.4E+02	8.5E+01	8.6E-01	1.2E-01	3.7E-05	5.8E-05
Cf251	3.4E+01	3.4E+01	3.2E+01	1.6E+01	7.9E-03	7.7E-03
Cf252	2.9E+04	2.1E+03	5.8E-01	5.8E-01	4.7E-01	7.6E-02
Cf253	6.3E+02	1.1E+03	9.5E+02	1.7E+02	1.3E-01	1.8E-01
Cf254	1.5E+07	2.7E-01	2.7E-01	2.6E-01	5.1E-03	6.9E-08
Cf255		3.4E+01	3.2E+01	1.6E+01	8.0E-03	7.7E-03
Es253	3.9E+00	2.4E+02	2.1E+02	3.6E+01	2.9E-02	3.8E-02
Es254m	7.3E+05	8.6E+01	8.6E-01	1.2E-01	4.1E-05	5.8E-05
Es254	3.2E-03	1.1E+02	9.0E-01	1.2E-01	3.7E-05	5.8E-05
Es255	9.6E+02	3.4E+01	3.2E+01	1.6E+01	7.9E-03	7.7E-03

Table 120 - Unshielded Photon Dose Rate (REM/hr/mole) for Fission Product Isotopes

Note: Starting with one mole of given isotope and includes all daughters.

	Time (yr)					
Isotope	0	10	100	1,000	100,000	1,000,000
H 3						
Li 6						
Li 7						
Be 9						
Be 10	5.7E-05	5.7E-05	5.7E-05	5.7E-05	5.4E-05	3.7E-05
C 14						
Ni 66	4.4E-05					
Cu 66	2.9E+09					
Zn 66						
Cu 67	1.3E+05					
Zn 67						
Zn 68						
Zn 69	5.2E+06					
Zn 69m	6.2E+07					
Ga 69						
Zn 70						
Ga 70	1.1E+08					
Ge 70						
Zn 71	2.3E+09					
Zn 71m	5.6E+06					
Ga 71						
Ge 71						
Ge 71m						
Co 72						
Ni 72						
Cu 72						
Zn 72	8.4E+01					
Ga 72	3.3E+08					
Ge 72						
Co 73						
Ni 73						
Cu 73						
Zn 73						
Ga 73						
Ge 73						
Ge 73m						
Co 74						
Ni 74						
Cu 74						
Zn 74	4.1E+09					
Ga 74	3.9E+10					
Ge 74						
Co 75						
Ni 75						
Cu 75						
Zn 75						
Ga 75						
Ge 75	7.7E+06					

	Time (yr)					
Isotope	0	10	100	1,000	100,000	1,000,000
Ge 75m						
As 75						
Ni 76						
Cu 76						
Zn 76						
Ga 76	5.2E+11					
Ge 76						
As 76	3.6E+07					
Se 76						
Ni 77						
Cu 77						
Zn 77						
Ga 77						
Ge 77	2.0E+08					
Ge 77m	6.3E+09					
As 77	5.2E+05					
Se 77						
Se 77m						
Ni 78						
Cu 78						
Zn 78						
Ga 78						
Ge 78	1.3E+06					
As 78	1.7E+09					
Se 78						
Cu 79						
Zn 79						
Ga 79						
Ge 79	4.7E+10					
As 79	3.8E+08					
Se 79						
Se 79m						
Br 79						
Br 79m						
Kr 79	7.0E+04					
Cu 80						
Zn 80						
Ga 80						
Ge 80						
As 80	1.2E+11					
Se 80						
Br 80	4.4E+09					
Br 80m						
Kr 80						
Cu 81						
Zn 81						
Ga 81						
Ge 81						
As 81						
Se 81						
Se 81m						

	Time (yr)					
Isotope	0	10	100	1,000	100,000	1,000,000
Br 81						
Kr 81						
Kr 81m						
Zn 82						
Ga 82						
Ge 82						
As 82	2.7E+11					
As 82m	1.8E+12					
Se 82						
Br 82	1.4E+08					
Br 82m	4.0E+07					
Kr 82						
Zn 83						
Ga 83						
Ge 83						
As 83						
Se 83	7.3E+07					
Se 83m	8.8E+09					
Br 83	8.5E+06					
Kr 83						
Kr 83m						
Ga 84						
Ge 84						
As 84						
Se 84						
Br 84	5.6E+09					
Br 84m						
Kr 84						
Ga 85		1.0E+00	3.0E-03	1.6E-28		
Ge 85		1.9E+00	5.5E-03	2.9E-28		
As 85		2.3E+00	6.9E-03	3.7E-28		
Se 85		8.0E+00	2.4E-02	1.3E-27		
Se 85m		8.0E+00	2.4E-02	1.3E-27		
Br 85	2.6E+09	8.0E+00	2.4E-02	1.3E-27		
Kr 85	7.2E+01	3.8E+01	1.1E-01	6.0E-27		
Kr 85m	2.3E+07	7.9E+00	2.4E-02	1.2E-27		
Rb 85						
Ge 86		1.3E+00	3.7E-03	2.0E-28		
As 86		9.6E-01	2.8E-03	1.5E-28		
Se 86						
Br 86						
Br 86m						
Kr 86						
Rb 86	4.6E+05					
Rb 86m						
Sr 86						
Ge 87		1.4E-01	4.3E-04	8.3E-13	8.3E-13	8.3E-13
As 87		9.8E-13	9.8E-13	9.8E-13	9.8E-13	9.8E-13
Se 87		1.7E-12	1.7E-12	1.7E-12	1.7E-12	1.7E-12
Br 87		1.7E-12	1.7E-12	1.7E-12	1.7E-12	1.7E-12
Kr 87	1.2E+09	1.8E-12	1.8E-12	1.8E-12	1.8E-12	1.8E-12

	Time (yr)					
Isotope	0	10	100	1,000	100,000	1,000,000
Rb 87	1.8E-12	1.8E-12	1.8E-12	1.8E-12	1.8E-12	1.8E-12
Sr 87						
Sr 87m	2.7E+08	5.4E-15	5.4E-15	5.4E-15	5.4E-15	5.4E-15
Ge 88		5.6E-13	5.6E-13	5.6E-13	5.6E-13	5.6E-13
As 88		4.5E-13	4.5E-13	4.5E-13	4.5E-13	4.5E-13
Se 88		1.2E-13	1.2E-13	1.2E-13	1.2E-13	1.2E-13
Br 88	9.6E+11	1.1E-13	1.1E-13	1.1E-13	1.1E-13	1.1E-13
Kr 88	1.0E+09					
Rb 88	4.6E+09					
Sr 88						
As 89		4.5E-14	4.5E-14	4.5E-14	4.5E-14	4.5E-14
Se 89		5.7E-15	5.7E-15	5.7E-15	5.7E-15	5.7E-15
Br 89		3.2E-18				
Kr 89	6.0E+10	3.7E-18				
Rb 89	1.4E+10	3.7E-18				
Sr 89	2.1E+04	3.7E-18				
Y 89						
Y 89m	3.9E+11					
As 90		1.2E+02	1.3E+01	3.2E-09	1.4E-15	1.4E-15
Se 90		1.6E+02	1.8E+01	4.2E-09		
Br 90		1.8E+02	2.0E+01	4.7E-09		
Kr 90	2.6E+11	2.4E+02	2.6E+01	6.1E-09		
Rb 90	7.6E+10	2.4E+02	2.6E+01	6.1E-09		
Rb 90m	7.2E+10	2.4E+02	2.6E+01	6.1E-09		
Sr 90	3.5E+00	2.4E+02	2.6E+01	6.1E-09		
Y 90	1.2E+06					
Y 90m	3.4E-03					
Zr 90						
Zr 90m						
Se 91		5.9E+01	6.4E+00	1.5E-09		
Br 91		2.6E+01	2.8E+00	6.7E-10		
Kr 91		3.9E-15				
Rb 91		2.4E-04	2.6E-05	6.1E-15		
Sr 91	1.4E+08	3.9E-15				
Y 91	2.4E+04	3.9E-15				
Y 91m	1.3E+09	3.9E-15				
Zr 91						
Nb 91						
Se 92		3.4E+00	3.7E-01	8.8E-11		
Br 92		1.2E-15				
Kr 92	3.6E+12	1.7E-18				
Rb 92	1.1E+12	4.1E-19				
Sr 92	8.0E+08					
Y 92	1.8E+08					
Zr 92						
Nb 92						
Se 93		1.4E-16				
Br 93		6.9E-19				
Kr 93		4.6E-21				
Rb 93						
Sr 93						

	Time (yr)					
Isotope	0	10	100	1,000	100,000	1,000,000
Y 93	2.8E+07					
Zr 93						
Nb 93						
Nb 93m						
Br 94						
Kr 94						
Rb 94	4.0E+12					
Sr 94						
Y 94	7.0E+09					
Zr 94						
Nb 94	1.8E+01	1.8E+01	1.8E+01	1.7E+01	5.9E-01	2.7E-14
Nb 94m	8.3E+07	1.8E+01	1.8E+01	1.7E+01	5.9E-01	2.7E-14
Br 95		1.3E-11				
Kr 95		1.8E-11				
Rb 95		2.0E-11				
Sr 95		2.2E-11				
Y 95		2.2E-11				
Zr 95	9.8E+05	2.1E-11				
Nb 95	1.9E+06	6.6E-26				
Nb 95m	1.6E+06	7.0E-26				
Mo 95						
Br 96		7.2E-12				
Kr 96		4.2E-12				
Rb 96		2.9E-12				
Sr 96		2.4E-16				
Y 96	3.9E+11					
Zr 96						
Nb 96	2.1E+08					
Mo 96						
Kr 97		2.4E-13				
Rb 97		6.2E-17				
Sr 97						
Y 97						
Zr 97	2.2E+07					
Nb 97	1.1E+09					
Nb 97m	8.9E+10					
Mo 97						
Kr 98						
Rb 98						
Sr 98						
Y 98						
Zr 98						
Nb 98	7.0E+11					
Nb 98m	5.3E+09					
Mo 98						
Tc 98	7.9E-02	7.9E-02	7.9E-02	7.9E-02	7.7E-02	6.7E-02
Rb 99		1.7E-06	1.7E-06	1.7E-06	1.2E-06	6.3E-08
Sr 99		2.0E-06	2.0E-06	2.0E-06	1.4E-06	7.5E-08
Y 99		2.0E-06	2.0E-06	2.0E-06	1.4E-06	7.5E-08
Zr 99		2.0E-06	2.0E-06	2.0E-06	1.5E-06	7.6E-08
Nb 99	5.0E+10	2.0E-06	2.0E-06	2.0E-06	1.5E-06	7.6E-08

	Time (yr)					
Isotope	0	10	100	1,000	100,000	1,000,000
Nb 99m	3.4E+10	2.0E-06	2.0E-06	2.0E-06	1.5E-06	7.6E-08
Mo 99	4.2E+06	2.0E-06	2.0E-06	2.0E-06	1.5E-06	7.6E-08
Tc 99	2.0E-06	2.0E-06	2.0E-06	2.0E-06	1.5E-06	7.6E-08
Tc 99m		2.0E-06	2.0E-06	2.0E-06	1.5E-06	7.6E-08
Ru 99						
Rb100		1.3E-07	1.3E-07	1.3E-07	9.3E-08	4.8E-09
Sr100		3.2E-08	3.2E-08	3.2E-08	2.3E-08	1.2E-09
Y100		1.7E-08	1.7E-08	1.7E-08	1.2E-08	6.5E-10
Zr100						
Nb100						
Nb100m						
Mo100						
Tc100	7.6E+10					
Ru100						
Rb101		9.4E-09	9.4E-09	9.4E-09	6.8E-09	3.5E-10
Sr101		4.2E-10	4.2E-10	4.2E-10	3.1E-10	1.6E-11
Y101						
Zr101	2.6E+12					
Nb101						
Mo101	9.6E+09					
Tc101	3.2E+09					
Ru101						
Sr102						
Y102						
Zr102						
Nb102						
Mo102						
Tc102	8.5E+11					
Tc102m	5.8E+10					
Ru102						
Rh102						
Pd102						
Sr103		8.3E-23				
Y103		9.1E-23				
Zr103		1.0E-22				
Nb103		1.0E-22				
Mo103		1.0E-22				
Tc103		1.0E-22				
Ru103	1.1E+06	1.0E-22				
Rh103						
Rh103m						
Sr104		2.1E-23				
Y104		9.9E-24				
Zr104		8.5E-25				
Nb104		7.4E-25				
Mo104						
Tc104	1.2E+10					
Ru104						
Rh104	9.0E+09					
Rh104m	3.9E+08					
Pd104						

	Time (yr)					
Isotope	0	10	100	1,000	100,000	1,000,000
Y105		1.8E-25				
Zr105		1.0E-26				
Nb105						
Mo105						
Tc105						
Ru105	3.7E+08					
Rh105	5.1E+06					
Rh105m						
Pd105						
Y106		5.6E+01	1.3E-25			
Zr106		6.7E+01	1.6E-25			
Nb106		6.8E+01	1.6E-25			
Mo106		7.2E+01	1.7E-25			
Tc106		7.2E+01	1.7E-25			
Ru106		7.2E+01	1.7E-25			
Rh106	7.0E+10					
Rh106m	2.5E+09					
Pd106						
Ag106						
Y107		2.4E+01	5.6E-26			
Zr107		8.6E+00	2.0E-26			
Nb107		6.3E+00	1.5E-26			
Mo107						
Tc107						
Ru107	8.5E+09					
Rh107	2.3E+09					
Pd107						
Pd107m						
Ag107						
Zr108		4.4E-01	1.0E-27			
Nb108						
Mo108						
Tc108						
Ru108						
Rh108	2.8E+11					
Rh108m	4.4E+10					
Pd108						
Ag108	1.6E+09					
Ag108m	3.0E+03	2.8E+03	1.7E+03	1.3E+01		
Cd108						
Zr109						
Nb109						
Mo109						
Tc109						
Ru109						
Rh109						
Rh109m						
Pd109	6.2E+05					
Pd109m						
Ag109						
Ag109m						

	Time (yr)					
Isotope	0	10	100	1,000	100,000	1,000,000
Cd109						
Nb110						
Mo110						
Tc110						
Ru110						
Rh110	1.1E+11					
Rh110m	6.3E+10					
Pd110						
Ag110	2.6E+10					
Ag110m	8.8E+05	3.5E+01	8.6E-39			
Cd110						
Nb111						
Mo111						
Tc111						
Ru111						
Rh111						
Pd111						
Pd111m						
Ag111	3.4E+05					
Ag111m						
Cd111						
Cd111m						
Nb112						
Mo112						
Tc112						
Ru112						
Rh112						
Pd112						
Ag112	3.8E+08					
Cd112						
Mo113		5.9E-02	7.0E-04	1.3E-16	1.3E-16	1.3E-16
Tc113		6.1E-02	7.3E-04	1.4E-16	1.4E-16	1.4E-16
Ru113		6.5E-02	7.8E-04	1.5E-16	1.5E-16	1.5E-16
Rh113		6.5E-02	7.8E-04	1.5E-16	1.5E-16	1.5E-16
Pd113		6.5E-02	7.8E-04	1.5E-16	1.5E-16	1.5E-16
Ag113		6.8E-02	8.2E-04	1.5E-16	1.5E-16	1.5E-16
Ag113m		5.4E-02	6.5E-04	1.5E-16	1.5E-16	1.5E-16
Cd113	1.5E-16	1.5E-16	1.5E-16	1.5E-16	1.5E-16	1.5E-16
Cd113m	6.5E+00	4.0E+00	4.8E-02	2.2E-19	2.1E-19	2.1E-19
In113						
In113m						
Mo114		4.3E-03	5.2E-05	9.9E-18	9.9E-18	9.9E-18
Tc114		4.3E-03	5.2E-05	9.9E-18	9.9E-18	9.9E-18
Ru114		6.8E-05	8.2E-07	1.6E-19	1.6E-19	1.6E-19
Rh114		2.9E-21	2.9E-21	2.9E-21	2.9E-21	2.9E-21
Pd114						
Ag114	4.7E+11					
Cd114						
In114	2.6E+09					
In114m	9.6E+04	8.5E-18				
Sn114						

	Time (yr)					
Isotope	0	10	100	1,000	100,000	1,000,000
Mo115		8.3E-06	9.9E-08	7.1E-14	7.1E-14	7.1E-14
Tc115		8.3E-06	9.9E-08	7.1E-14	7.1E-14	7.1E-14
Ru115		8.3E-14	8.3E-14	8.3E-14	8.3E-14	8.3E-14
Rh115		8.3E-14	8.3E-14	8.3E-14	8.3E-14	8.3E-14
Pd115		8.4E-14	8.4E-14	8.4E-14	8.4E-14	8.4E-14
Ag115	3.9E+09	8.4E-14	8.4E-14	8.4E-14	8.4E-14	8.4E-14
Ag115m		8.3E-14	8.3E-14	8.3E-14	8.3E-14	8.3E-14
Cd115	9.0E+06	8.3E-14	8.3E-14	8.3E-14	8.3E-14	8.3E-14
Cd115m	6.2E+04	8.8E-14	8.8E-14	8.8E-14	8.8E-14	8.8E-14
In115	8.8E-14	8.8E-14	8.8E-14	8.8E-14	8.8E-14	8.8E-14
In115m	8.2E+07	8.3E-14	8.3E-14	8.3E-14	8.3E-14	8.3E-14
Sn115						
Tc116		1.1E-14	1.1E-14	1.1E-14	1.1E-14	1.1E-14
Ru116		1.3E-15	1.3E-15	1.3E-15	1.3E-15	1.3E-15
Rh116		4.5E-16	4.5E-16	4.5E-16	4.5E-16	4.5E-16
Pd116						
Ag116	5.0E+10					
Ag116m	1.1E+12					
Cd116						
In116	4.9E+10					
In116m	4.8E+09					
Sn116						
Tc117		2.9E-16	2.9E-16	2.9E-16	2.9E-16	2.9E-16
Ru117		9.2E-18	9.2E-18	9.2E-18	9.2E-18	9.2E-18
Rh117						
Pd117						
Ag117						
Ag117m						
Cd117						
Cd117m						
In117						
In117m						
Sn117						
Sn117m						
Tc118						
Ru118						
Rh118						
Pd118						
Ag118	1.8E+12					
Ag118m	9.7E+11					
Cd118						
In118	5.9E+11					
In118m	6.7E+10					
Sn118						
Ru119						
Rh119						
Pd119						
Ag119						
Cd119						
Cd119m						
In119						

	Time (yr)					
Isotope	0	10	100	1,000	100,000	1,000,000
In119m						
Sn119						
Sn119m						
Ru120						
Rh120						
Pd120						
Ag120	1.6E+12					
Cd120	1.6E+09					
In120	6.6E+12					
In120m	5.0E+10					
Sn120						
Rh121						
Pd121						
Ag121						
Cd121						
In121						
In121m						
Sn121						
Sn121m						
Sb121						
Rh122						
Pd122						
Ag122						
Cd122						
In122	1.3E+13					
In122m	4.2E+11					
Sn122						
Sb122	1.4E+07					
Sb122m						
Te122						
Rh123		6.1E-07				
Pd123		7.4E-07				
Ag123		7.4E-07				
Cd123		7.8E-07				
In123	1.1E+12	1.0E-06				
In123m						
Sn123	1.0E+04	3.2E-05				
Sn123m	2.1E+07					
Sb123						
Te123						
Te123m						
Pd124		3.7E-08				
Ag124		1.8E-08				
Cd124						
In124						
Sn124						
Sb124	2.3E+06	1.2E-12				
Sb124m	2.8E+10	9.3E-13				
Te124						
Pd125		2.5E+03	3.0E-07			
Ag125		2.6E+03	3.0E-07			

	Time (yr)					
Isotope	0	10	100	1,000	100,000	1,000,000
Cd125		2.7E+03	3.2E-07			
In125		2.7E+03	3.2E-07			
In125m		2.7E+03	3.2E-07			
Sn125	2.7E+06	2.7E+03	3.3E-07			
Sn125m	5.5E+09	2.7E+03	3.2E-07			
Sb125	3.5E+04	2.7E+03	3.2E-07			
Te125						
Te125m						
Pd126		2.5E+02	3.0E-08			
Ag126		1.3E+02	1.5E-08			
Cd126						
In126		4.6E+00	4.6E+00	4.6E+00	2.3E+00	4.5E-03
Sn126	3.3E-05	4.6E+00	4.6E+00	4.6E+00	2.3E+00	4.5E-03
Sb126	2.0E+07					
Sb126m	1.0E+10					
Te126						
Xe126						
Ag127		2.8E-02	2.8E-02	2.7E-02	1.4E-02	2.7E-05
Cd127		3.1E-02	3.1E-02	3.0E-02	1.5E-02	3.0E-05
In127		3.0E-02	3.0E-02	3.0E-02	1.5E-02	3.0E-05
In127m		3.0E-02	3.0E-02	3.0E-02	1.5E-02	2.9E-05
Sn127	1.6E+09	6.5E-08				
Sn127m		6.5E-08				
Sb127	1.5E+07	6.5E-08				
Te127	1.3E+06					
Te127m	2.5E+00	3.6E-07				
I127						
Xe127	5.4E+05	3.4E-25				
Ag128		2.1E-03	2.1E-03	2.1E-03	1.1E-03	2.1E-06
Cd128		3.4E-05	3.3E-05	3.3E-05	1.7E-05	3.3E-08
In128		2.8E-11				
Sn128						
Sb128	7.0E+08					
Sb128m	2.4E+10					
Te128						
I128	5.2E+08					
Xe128						
Cd129		6.2E-29				
In129		6.2E-29				
Sn129		6.2E-29				
Sn129m		6.2E-29				
Sb129	6.3E+08	6.2E-29				
Te129	1.1E+08					
Te129m	7.8E+04	3.4E-28				
I129						
Xe129						
Xe129m						
Cd130		1.2E-30				
In130	5.2E+13	5.6E-31				
Sn130	2.5E+10					
Sb130	9.5E+09					

	Time (yr)					
Isotope	0	10	100	1,000	100,000	1,000,000
Sb130m	5.0E+10					
Te130						
I130	3.5E+08					
I130m	1.5E+09					
Xe130						
Cd131		2.7E-32				
In131						
Sn131						
Sb131	8.7E+09					
Te131	1.5E+09					
Te131m	9.0E+07					
I131	4.5E+06					
Xe131						
Xe131m						
Cd132						
In132						
Sn132	2.2E+11					
Sb132	7.0E+10					
Sb132m	1.0E+11					
Te132	6.0E+06					
I132	2.0E+09					
Xe132						
Cs132	9.1E+06					
Ba132						
In133						
Sn133						
Sb133						
Te133	9.0E+09					
Te133m	4.7E+09					
I133	5.9E+07					
I133m	1.2E+12					
Xe133	6.6E+02					
Xe133m	1.1E+06					
Cs133						
Ba133	8.4E+03	4.3E+03	1.2E+01	2.0E-25		
In134						
Sn134						
Sb134	1.9E+13					
Sb134m						
Te134	2.5E+09					
I134	5.8E+09					
I134m	9.5E+09					
Xe134						
Xe134m	4.7E+13					
Cs134	1.7E+05	6.0E+03	4.4E-10			
Cs134m		6.0E+03	4.4E-10			
Ba134						
Sn135						
Sb135						
Te135	3.6E+11					
I135	4.1E+08					

	Time (yr)					
Isotope	0	10	100	1,000	100,000	1,000,000
Xe135	6.3E+07					
Xe135m	3.4E+09					
Cs135						
Cs135m	3.7E+09					
Ba135						
Ba135m	3.5E+06					
Sn136						
Sb136						
Te136						
I136	1.7E+11					
I136m	2.9E+11					
Xe136						
Cs136	1.3E+07					
Ba136						
Ba136m						
Sb137		2.5E+03	3.2E+02	2.9E-07		
Te137		3.2E+03	4.0E+02	3.7E-07		
I137		3.2E+03	4.0E+02	3.8E-07		
Xe137	9.9E+09	3.5E+03	4.3E+02	4.0E-07		
Cs137	3.6E+00	3.5E+03	4.3E+02	4.0E-07		
Ba137						
Ba137m	2.9E+10					
Sb138		9.9E+02	1.2E+02	1.1E-07		
Te138		3.8E+02	4.7E+01	4.4E-08		
I138	1.4E+12	1.9E+02	2.3E+01	2.2E-08		
Xe138	8.2E+09					
Cs138	7.3E+09					
Cs138m	1.7E+10					
Ba138						
La138	5.8E-07	5.8E-07	5.8E-07	5.8E-07	5.8E-07	5.8E-07
Sb139		1.6E+02	2.1E+01	1.9E-08		
Te139		1.2E+01	1.5E+00	1.4E-09		
I139						
Xe139	1.7E+11					
Cs139	4.8E+09					
Ba139	5.1E+07					
La139						
Ce139						
Pr139						
Te140						
I140						
Xe140						
Cs140						
Ba140	9.3E+05					
La140	9.7E+07					
Ce140						
Pr140						
Te141		3.4E-32				
I141		3.8E-32				
Xe141		6.3E-32				
Cs141		6.3E-32				

	Time (yr)					
Isotope	0	10	100	1,000	100,000	1,000,000
Ba141	5.0E+09	6.3E-32				
La141	3.7E+07	6.3E-32				
Ce141	4.3E+02	6.3E-32				
Pr141						
Nd141						
Te142		1.6E-14	1.6E-14	1.6E-14	1.6E-14	1.6E-14
I142		1.9E-14	1.9E-14	1.9E-14	1.9E-14	1.9E-14
Xe142		2.3E-14	2.3E-14	2.3E-14	2.3E-14	2.3E-14
Cs142		2.3E-14	2.3E-14	2.3E-14	2.3E-14	2.3E-14
Ba142	1.1E+10	2.3E-14	2.3E-14	2.3E-14	2.3E-14	2.3E-14
La142	2.8E+09	2.3E-14	2.3E-14	2.3E-14	2.3E-14	2.3E-14
Ce142	2.3E-14	2.3E-14	2.3E-14	2.3E-14	2.3E-14	2.3E-14
Pr142	7.9E+06	3.7E-18	3.7E-18	3.7E-18	3.7E-18	3.7E-18
Pr142m		3.7E-18	3.7E-18	3.7E-18	3.7E-18	3.7E-18
Nd142						
I143		4.6E-15	4.6E-15	4.6E-15	4.6E-15	4.6E-15
Xe143		6.3E-16	6.3E-16	6.3E-16	6.3E-16	6.3E-16
Cs143		3.7E-16	3.7E-16	3.7E-16	3.7E-16	3.7E-16
Ba143						
La143						
Ce143	1.7E+07					
Pr143	1.5E+04					
Nd143						
I144		3.0E+00	1.0E-16	1.0E-16	1.0E-16	1.0E-16
Xe144		3.5E+00	3.8E-18	3.8E-18	3.8E-18	3.8E-18
Cs144		3.5E+00	1.1E-18	1.1E-18	1.1E-18	1.1E-18
Ba144		3.6E+00	1.1E-18	1.1E-18	1.1E-18	1.1E-18
La144		3.6E+00	1.1E-18	1.1E-18	1.1E-18	1.1E-18
Ce144	1.0E+00	3.6E+00	1.1E-18	1.1E-18	1.1E-18	1.1E-18
Pr144	6.2E+08	1.1E-18	1.1E-18	1.1E-18	1.1E-18	1.1E-18
Pr144m	1.5E+07	1.1E-18	1.1E-18	1.1E-18	1.1E-18	1.1E-18
Nd144	1.1E-18	1.1E-18	1.1E-18	1.1E-18	1.1E-18	1.1E-18
I145		1.4E+00	1.1E-18	1.1E-18	1.1E-18	1.1E-18
Xe145		7.1E-01	2.2E-19	2.2E-19	2.2E-19	2.2E-19
Cs145		5.3E-01	1.7E-19	1.7E-19	1.7E-19	1.7E-19
Ba145						
La145						
Ce145	3.3E+10					
Pr145	1.0E+07					
Nd145						
Pm145	3.8E-13	2.5E-13	7.5E-15	3.7E-30		
Sm145	3.4E+00	2.0E-03	7.9E-15	3.9E-30		
Xe146		3.4E-02	1.1E-20	1.1E-20	1.1E-20	1.1E-20
Cs146						
Ba146						
La146						
Ce146	1.6E+09					
Pr146						
Nd146						
Pm146	1.2E+04	3.4E+03	4.3E-02	7.8E-12	7.8E-12	7.8E-12
Sm146	2.3E-11	2.3E-11	2.3E-11	2.3E-11	2.3E-11	2.3E-11

	Time (yr)					
Isotope	0	10	100	1,000	100,000	1,000,000
Xe147		1.4E-14	1.6E-14	1.6E-14	1.6E-14	1.6E-14
Cs147		1.6E-14	1.7E-14	1.7E-14	1.7E-14	1.7E-14
Ba147		2.1E-14	2.3E-14	2.3E-14	2.3E-14	2.3E-14
La147		2.1E-14	2.3E-14	2.3E-14	2.3E-14	2.3E-14
Ce147		2.1E-14	2.3E-14	2.3E-14	2.3E-14	2.3E-14
Pr147		2.1E-14	2.3E-14	2.3E-14	2.3E-14	2.3E-14
Nd147	7.6E+05	2.1E-14	2.3E-14	2.3E-14	2.3E-14	2.3E-14
Pm147		2.1E-14	2.2E-14	2.2E-14	2.2E-14	2.2E-14
Sm147	2.2E-14	2.2E-14	2.2E-14	2.2E-14	2.2E-14	2.2E-14
Cs148		5.3E-15	5.7E-15	5.7E-15	5.7E-15	5.7E-15
Ba148		4.0E-17	4.4E-17	4.4E-17	4.4E-17	4.4E-17
La148		2.8E-17	3.0E-17	3.0E-17	3.0E-17	3.0E-17
Ce148						
Pr148	6.5E+10					
Nd148						
Pm148	8.1E+06	3.0E-19	3.0E-19	3.0E-19	3.0E-19	3.0E-19
Pm148m	4.0E+06	3.1E-19	3.0E-19	3.0E-19	3.0E-19	3.0E-19
Sm148	3.0E-19	3.0E-19	3.0E-19	3.0E-19	3.0E-19	3.0E-19
Cs149		1.3E-17	1.4E-17	1.4E-17	1.4E-17	1.4E-17
Ba149		2.4E-19	2.4E-19	2.4E-19	2.4E-19	2.4E-19
La149		2.4E-19	2.4E-19	2.4E-19	2.4E-19	2.4E-19
Ce149		2.4E-19	2.4E-19	2.4E-19	2.4E-19	2.4E-19
Pr149	3.1E+09	2.4E-19	2.4E-19	2.4E-19	2.4E-19	2.4E-19
Nd149	4.2E+08	2.4E-19	2.4E-19	2.4E-19	2.4E-19	2.4E-19
Pm149	6.0E+05	2.4E-19	2.4E-19	2.4E-19	2.4E-19	2.4E-19
Sm149	2.4E-19	2.4E-19	2.4E-19	2.4E-19	2.4E-19	2.4E-19
Eu149		2.4E-19	2.4E-19	2.4E-19	2.4E-19	2.4E-19
Cs150		3.8E-20	3.8E-20	3.8E-20	3.8E-20	3.8E-20
Ba150		2.8E-21	2.8E-21	2.8E-21	2.8E-21	2.8E-21
La150		2.2E-21	2.2E-21	2.2E-21	2.2E-21	2.2E-21
Ce150						
Pr150						
Nd150						
Pm150	1.1E+09					
Sm150						
Eu150						
Ba151		8.4E-23	8.4E-23	8.4E-23	8.4E-23	8.4E-23
La151						
Ce151						
Pr151						
Nd151	1.5E+08					
Pm151	1.6E+05					
Sm151						
Eu151						
Ba152						
La152						
Ce152						
Pr152						
Nd152						
Pm152						
Pm152m						

	Time (yr)					
Isotope	0	10	100	1,000	100,000	1,000,000
Sm152						
Eu152	1.7E+04	1.0E+04	9.3E+01	6.6E-18	6.1E-18	6.1E-18
Eu152m	5.8E+07	1.6E-17	1.6E-17	1.6E-17	1.6E-17	1.6E-17
Gd152	2.2E-17	2.2E-17	2.2E-17	2.2E-17	2.2E-17	2.2E-17
La153						
Ce153						
Pr153						
Nd153						
Pm153	3.5E+08					
Sm153	9.2E+04					
Eu153						
Gd153						
La154						
Ce154						
Pr154						
Nd154						
Pm154						
Pm154m						
Sm154						
Eu154	2.9E+04	1.3E+04	9.0E+00	2.6E-31		
Gd154						
La155		6.3E-06	1.0E-11			
Ce155		7.5E-06	1.2E-11			
Pr155		7.7E-06	1.3E-11			
Nd155		7.8E-06	1.3E-11			
Pm155		7.8E-06	1.3E-11			
Sm155	5.9E+07	7.8E-06	1.3E-11			
Eu155	3.4E-05	7.8E-06	1.3E-11			
Gd155						
Gd155m						
Ce156		4.4E-07	7.1E-13			
Pr156		2.1E-07	3.4E-13			
Nd156						
Pm156						
Sm156	1.0E+05					
Eu156	6.2E+06					
Gd156						
Ce157		9.4E-09	1.5E-14			
Pr157						
Nd157						
Pm157						
Sm157						
Eu157	5.7E+05					
Gd157						
Pr158						
Nd158						
Pm158						
Sm158						
Eu158						
Gd158						
Pr159						

	Time (yr)					
Isotope	0	10	100	1,000	100,000	1,000,000
Nd159						
Pm159						
Sm159						
Eu159	2.3E+08					
Gd159	2.4E+05					
Tb159						
Nd160						
Pm160						
Sm160						
Eu160						
Gd160						
Tb160	1.2E+06	7.4E-10				
Dy160						
Nd161						
Pm161						
Sm161						
Eu161						
Gd161	3.8E+08					
Tb161	2.3E+03					
Dy161						
Pm162						
Sm162						
Eu162						
Gd162	3.8E+07					
Tb162	1.1E+08					
Tb162m						
Dy162						
Sm163						
Eu163						
Gd163						
Tb163						
Tb163m						
Dy163						
Sm164						
Eu164						
Gd164						
Tb164	9.2E+08					
Dy164						
Sm165						
Eu165						
Gd165						
Tb165						
Dy165	5.6E+06					
Dy165m	1.1E+05					
Ho165						
Dy166	1.1E+03					
Ho166	2.4E+06					
Ho166m	3.1E+02	3.1E+02	2.9E+02	1.7E+02	2.5E-23	
Er166						
Er167						
Er167m						

	Time (yr)					
Isotope	0	10	100	1,000	100,000	1,000,000
Er168						
Yb168						
Er169	1.2E+02					
Tm169						
Yb169	1.1E+05	4.9E-30				
Er170						
Tm170	1.6E+03	4.6E-06				
Tm170m		4.6E-06				
Yb170						
Er171	9.9E+07					
Tm171						
Yb171						
Er172	8.4E+02					
Tm172	3.8E+05					
Yb172						

APPENDIX E

UNSHIELDED SPONTANEOUS NEUTRON DOSE RATE

Table 121 - Unshielded Spontaneous Neutron Dose Rate (REM/hr/mole) for Actinide Isotopes

Note: Starting with one mole of given isotope and includes all daughters.

	Time (yr)					
Isotope	0	10	100	1,000	100,000	1,000,000
He 4						
Tl206						
Tl207						
Tl208						
Tl209						
Pb206						
Pb207						
Pb208						
Pb209						
Pb210						
Pb211						
Pb212						
Pb214						
Bi208						
Bi209						
Bi210m						
Bi210						
Bi211						
Bi212						
Bi213						
Bi214						
Po210						
Po211m						
Po211						
Po212						
Po213						
Po214						
Po215						
Po216						
Po218						
At217						
Rn218						
Rn219						
Rn220						
Rn222						
Fr221						
Fr223						
Ra222						
Ra223						
Ra224						
Ra225						
Ra226						

	Time (yr)					
Isotope	0	10	100	1,000	100,000	1,000,000
Ra228						
Ac225						
Ac227						
Ac228						
Th226						
Th227						
Th228						
Th229						
Th230	5.7E-11	5.7E-11	5.7E-11	5.7E-11	2.3E-11	5.8E-15
Th231		8.4E-10	8.4E-10	8.2E-10	1.0E-10	5.4E-19
Th232						
Th233						
Th234		1.6E-09	1.6E-09	1.6E-09	1.2E-09	9.6E-11
Pa231	8.4E-10	8.4E-10	8.4E-10	8.2E-10	1.0E-10	5.4E-19
Pa232		2.2E-07	9.1E-08	1.2E-11		
Pa233						
Pa234m		1.6E-09	1.6E-09	1.6E-09	1.2E-09	9.6E-11
Pa234		1.6E-09	1.6E-09	1.6E-09	1.2E-09	9.6E-11
Pa235		2.3E-12	2.3E-12	2.3E-12	2.4E-12	2.4E-12
U230						
U231		8.4E-10	8.4E-10	8.2E-10	1.0E-10	5.4E-19
U232	2.5E-07	2.2E-07	9.1E-08	1.2E-11		
U233						
U234	1.6E-09	1.6E-09	1.6E-09	1.6E-09	1.2E-09	9.6E-11
U235	2.3E-12	2.3E-12	2.3E-12	2.3E-12	2.4E-12	2.4E-12
U236	9.1E-10	9.1E-10	9.1E-10	9.1E-10	9.0E-10	8.8E-10
U237	4.0E-13					
U238	3.3E-09	3.3E-09	3.3E-09	3.3E-09	3.3E-09	3.3E-09
U239	3.1E-12	5.5E-09	5.4E-09	5.3E-09	3.1E-10	2.4E-12
U240		2.5E-04	2.5E-04	2.3E-04	7.4E-09	8.8E-10
U241		1.1E-07	2.4E-07	5.8E-08		
Np235		2.3E-12	2.3E-12	2.3E-12	2.4E-12	2.4E-12
Np236m		3.8E-04	4.6E-08	4.8E-10	4.7E-10	4.6E-10
Np236	3.8E-11	1.8E-08	2.0E-08	1.9E-08	1.1E-08	8.5E-10
Np237						
Np238	1.3E-11	6.1E-04	3.0E-04	2.5E-07	1.2E-09	9.6E-11
Np239	4.4E-10	5.5E-09	5.4E-09	5.3E-09	3.1E-10	2.4E-12
Np240m		2.5E-04	2.5E-04	2.3E-04	7.4E-09	8.8E-10
Np240		2.5E-04	2.5E-04	2.3E-04	7.4E-09	8.8E-10
Np241		1.1E-07	2.4E-07	5.8E-08		
Pu236	8.7E-03	8.0E-04	9.5E-08	1.2E-11		
Pu237						
Pu238	6.6E-04	6.1E-04	3.0E-04	2.5E-07	1.2E-09	9.6E-11
Pu239	5.5E-09	5.5E-09	5.4E-09	5.3E-09	3.1E-10	2.4E-12
Pu240	2.5E-04	2.5E-04	2.5E-04	2.3E-04	7.4E-09	8.8E-10
Pu241	1.2E-08	1.1E-07	2.4E-07	5.8E-08		
Pu242	4.2E-04	4.2E-04	4.2E-04	4.2E-04	3.5E-04	6.6E-05
Pu243	1.6E-08	1.7E-07	1.7E-07	1.5E-07	4.6E-10	2.4E-12
Pu244	4.6E-04	4.6E-04	4.6E-04	4.6E-04	4.6E-04	4.6E-04
Pu245		9.6E-06	9.5E-06	8.8E-06	2.8E-09	
Pu246		2.2E+00	2.2E+00	1.9E+00	3.6E-04	6.7E-05

	Time (yr)					
Isotope	0	10	100	1,000	100,000	1,000,000
Am239		5.5E-09	5.4E-09	5.3E-09	3.1E-10	2.4E-12
Am240		2.5E-04	2.5E-04	2.3E-04	7.4E-09	8.8E-10
Am241	2.8E-07	2.7E-07	2.4E-07	5.6E-08		
Am242m	3.9E-05	1.2E-02	8.0E-03	1.7E-04	6.0E-05	1.1E-05
Am242	3.3E-03	5.8E-04	3.2E-04	7.3E-05	6.1E-05	1.1E-05
Am243	1.7E-07	1.7E-07	1.7E-07	1.5E-07	4.6E-10	2.4E-12
Am244m		1.9E+00	6.0E-02	2.3E-04	1.7E-07	1.7E-07
Am244	4.5E-07	1.9E+00	6.0E-02	2.3E-04	7.4E-09	8.8E-10
Am245		9.6E-06	9.5E-06	8.8E-06	2.8E-09	
Am246		2.2E+00	2.2E+00	1.9E+00	3.6E-04	6.7E-05
Cm241		2.7E-07	2.3E-07	5.5E-08		
Cm242	4.9E+00	6.1E-04	3.0E-04	2.5E-07	1.2E-09	9.6E-11
Cm243	3.0E-04	2.3E-04	2.6E-05	5.7E-09	3.1E-10	2.4E-12
Cm244	2.8E+00	1.9E+00	6.0E-02	2.3E-04	7.4E-09	8.8E-10
Cm245	9.6E-06	9.6E-06	9.5E-06	8.8E-06	2.8E-09	
Cm246	2.2E+00	2.2E+00	2.2E+00	1.9E+00	3.6E-04	6.7E-05
Cm247		7.3E-14	7.3E-13	7.0E-12	8.5E-11	8.3E-11
Cm248	1.0E+01	1.0E+01	1.0E+01	1.0E+01	8.3E+00	1.3E+00
Cm249		6.9E-04	5.7E-04	1.0E-04	2.9E-09	
Cm250	1.6E+03	1.6E+03	1.5E+03	1.5E+03	2.9E+01	2.7E-05
Cm251		2.8E-16	2.7E-14	2.2E-12	8.5E-11	8.3E-11
Bk249	2.6E-02	6.9E-04	5.7E-04	1.0E-04	2.9E-09	
Bk250		1.6E+03	1.6E+01	1.9E+00	3.6E-04	6.7E-05
Bk251		2.8E-16	2.7E-14	2.2E-12	8.5E-11	8.3E-11
Cf249	6.9E-04	6.8E-04	5.7E-04	1.0E-04	2.9E-09	
Cf250	2.8E+03	1.6E+03	1.6E+01	1.9E+00	3.6E-04	6.7E-05
Cf251		2.8E-16	2.7E-14	2.2E-12	8.5E-11	8.3E-11
Cf252	5.9E+05	4.3E+04	9.9E+00	9.9E+00	8.1E+00	1.3E+00
Cf253		3.2E-03	2.6E-03	4.8E-04	1.3E-08	
Cf254	3.1E+08	4.8E+00	4.8E+00	4.6E+00	8.9E-02	8.4E-08
Cf255		2.7E-16	2.7E-14	2.2E-12	8.5E-11	8.3E-11
Es253	7.8E+01	6.9E-04	5.7E-04	1.0E-04	2.9E-09	
Es254m	1.2E+07	1.6E+03	1.6E+01	1.9E+00	4.3E-04	6.7E-05
Es254		1.7E+03	1.7E+01	1.9E+00	3.6E-04	6.7E-05
Es255	2.1E+04	2.7E-16	2.7E-14	2.2E-12	8.5E-11	8.3E-11

APPENDIX F

UNSHIELDED α,N NEUTRON DOSE RATE

Table 122 - Unshielded α,n Neutron Dose Rate (REM/hr/mole) for Actinide Isotopes

Note: Starting with one mole of given isotope and includes all daughters.

	Time (yr)					
Isotope	0	10	100	"1,000"	"100,000"	"1,000,000"
He 4						
Tl206						
Tl207						
Tl208						
Tl209						
Pb206						
Pb207						
Pb208						
Pb209						
Pb210	4.1E-11	9.5E-03	5.7E-04	4.1E-16		
Pb211						
Pb212						
Pb214		9.5E-03	5.7E-04	4.1E-16		
Bi208						
Bi209						
Bi210m	7.3E-08	7.3E-08	7.3E-08	7.3E-08	7.2E-08	5.8E-08
Bi210	1.7E-05	8.9E-09				
Bi211	1.5E+05					
Bi212	1.4E+03					
Bi213	1.0E+02					
Bi214	2.8E+00	9.5E-03	5.7E-04	4.1E-16		
Po210	7.6E-01	8.6E-09				
Po211m	1.0E+06					
Po211	5.3E+07					
Po212	1.4E+14					
Po213	8.8E+12					
Po214	1.8E+11	9.5E-03	5.7E-04	4.1E-16		
Po215	1.5E+10					
Po216	1.4E+08					
Po218	7.6E+04	9.5E-03	5.7E-04	4.1E-16		
At217	7.3E+08					
Rn218	6.9E+08	9.5E-03	5.7E-04	4.1E-16		
Rn219	5.4E+06					
Rn220	3.0E+05					
Rn222	3.1E+01	9.5E-03	5.7E-04	4.1E-16		
Fr221	5.8E+04					
Fr223	4.5E-01					
Ra222	4.9E+05	9.5E-03	5.7E-04	4.1E-16		
Ra223	1.2E+01					
Ra224	3.7E+01					

	Time (yr)					
Isotope	0	10	100	"1,000"	"100,000"	"1,000,000"
Ra225						
Ra226	1.2E-04	1.2E-03	1.3E-03	8.9E-04	2.1E-22	
Ra228		2.0E-01	2.9E-06			
Ac225	1.4E+01					
Ac227	1.3E-04	9.8E-02	5.6E-03	2.0E-15		
Ac228	9.4E-06	4.0E-02	2.8E-16			
Th226	9.1E+03	9.5E-03	5.7E-04	4.1E-16		
Th227	8.5E+00					
Th228	1.6E-01	4.0E-02	2.8E-16			
Th229	2.9E-05	3.9E-04	3.9E-04	3.6E-04	5.9E-08	
Th230	2.3E-06	2.4E-06	3.5E-06	1.2E-05	1.3E-05	3.3E-09
Th231		3.1E-05	9.3E-05	9.5E-05	1.2E-05	6.3E-14
Th232	6.0E-12	1.2E-10	2.1E-10	2.1E-10	2.1E-10	2.1E-10
Th233		1.3E-06	1.4E-06	2.9E-06	1.4E-05	2.8E-07
Th234		7.7E-07	7.7E-07	7.9E-07	5.6E-06	8.7E-07
Pa231	7.0E-06	3.1E-05	9.3E-05	9.5E-05	1.2E-05	6.3E-14
Pa232		4.1E-02	1.7E-02	2.3E-06	4.2E-13	4.2E-13
Pa233		1.3E-06	1.4E-06	2.9E-06	1.4E-05	2.8E-07
Pa234m		7.7E-07	7.7E-07	7.9E-07	5.6E-06	8.7E-07
Pa234		7.7E-07	7.7E-07	7.9E-07	5.6E-06	8.7E-07
Pa235		2.0E-10	2.0E-10	2.9E-10	4.2E-09	4.7E-09
U230	7.4E+00	9.5E-03	5.8E-04	4.1E-16		
U231	1.5E-03	3.1E-05	9.3E-05	9.5E-05	1.2E-05	6.3E-14
U232	4.2E-03	4.1E-02	1.7E-02	2.3E-06		
U233	1.3E-06	1.3E-06	1.4E-06	2.9E-06	1.4E-05	2.8E-07
U234	7.7E-07	7.7E-07	7.7E-07	7.9E-07	5.6E-06	8.7E-07
U235	2.0E-10	2.0E-10	2.0E-10	2.9E-10	4.2E-09	4.7E-09
U236	6.3E-09	6.3E-09	6.3E-09	6.3E-09	6.3E-09	6.1E-09
U237		8.4E-08	8.4E-08	8.4E-08	5.6E-07	1.2E-06
U238	2.4E-11	2.4E-11	2.4E-11	2.4E-11	8.2E-11	5.5E-10
U239		1.1E-05	1.1E-05	1.0E-05	6.0E-07	4.7E-09
U240		3.9E-05	3.9E-05	3.5E-05	7.3E-09	6.1E-09
U241		2.9E-04	6.6E-04	1.6E-04	5.6E-07	1.2E-06
Np235	3.0E-06	5.5E-09	1.5E-09	1.6E-09	4.3E-09	4.7E-09
Np236m		2.2E-02	8.6E-03	1.1E-06	3.3E-09	3.2E-09
Np236		3.7E-07	1.8E-06	2.7E-06	1.5E-06	1.2E-08
Np237	8.4E-08	8.4E-08	8.4E-08	8.4E-08	5.6E-07	1.2E-06
Np238		3.4E-03	1.7E-03	2.1E-06	5.6E-06	8.7E-07
Np239		1.1E-05	1.1E-05	1.0E-05	6.0E-07	4.7E-09
Np240m		3.9E-05	3.9E-05	3.5E-05	7.3E-09	6.1E-09
Np240		3.9E-05	3.9E-05	3.5E-05	7.3E-09	6.1E-09
Np241		2.9E-04	6.6E-04	1.6E-04	5.6E-07	1.2E-06
Pu236	1.3E-01	4.6E-02	1.8E-02	2.4E-06		
Pu237	1.0E-04	8.4E-08	8.4E-08	8.5E-08	5.7E-07	1.2E-06
Pu238	3.7E-03	3.4E-03	1.7E-03	2.1E-06	5.6E-06	8.7E-07
Pu239	1.1E-05	1.1E-05	1.1E-05	1.0E-05	6.0E-07	4.7E-09
Pu240	3.9E-05	3.9E-05	3.9E-05	3.5E-05	7.3E-09	6.1E-09
Pu241	3.5E-07	2.9E-04	6.6E-04	1.6E-04	5.6E-07	1.2E-06
Pu242	5.6E-07	5.6E-07	5.6E-07	5.6E-07	4.7E-07	8.9E-08
Pu243		3.8E-05	3.8E-05	3.6E-05	8.7E-07	4.7E-09
Pu244	2.0E-09	2.0E-09	2.0E-09	2.3E-09	5.2E-09	5.2E-09

	Time (yr)					
Isotope	0	10	100	"1,000"	"100,000"	"1,000,000"
Pu245		3.7E-05	4.1E-05	6.2E-05	5.3E-07	1.2E-06
Pu246		6.4E-05	6.3E-05	5.5E-05	4.8E-07	9.0E-08
Am239	2.9E-02	1.1E-05	1.1E-05	1.0E-05	6.0E-07	4.7E-09
Am240	9.9E-05	3.9E-05	3.9E-05	3.5E-05	7.3E-09	6.1E-09
Am241	7.5E-04	7.4E-04	6.4E-04	1.5E-04	5.6E-07	1.2E-06
Am242m	8.6E-06	2.8E-03	2.5E-03	5.6E-05	4.7E-06	7.4E-07
Am242		2.8E-03	1.4E-03	1.9E-06	4.7E-06	7.4E-07
Am243	3.8E-05	3.8E-05	3.8E-05	3.6E-05	8.7E-07	4.7E-09
Am244m		1.5E-02	5.2E-04	3.6E-05	7.3E-09	6.1E-09
Am244		1.5E-02	5.2E-04	3.6E-05	7.3E-09	6.1E-09
Am245		3.7E-05	4.1E-05	6.2E-05	5.3E-07	1.2E-06
Am246		6.4E-05	6.3E-05	5.5E-05	4.8E-07	9.0E-08
Cm241	4.7E-02	7.3E-04	6.3E-04	1.5E-04	5.6E-07	1.2E-06
Cm242	1.1E+00	3.4E-03	1.7E-03	2.1E-06	5.6E-06	8.7E-07
Cm243	1.4E-02	1.1E-02	1.3E-03	1.0E-05	6.0E-07	4.7E-09
Cm244	2.2E-02	1.5E-02	5.2E-04	3.6E-05	7.3E-09	6.1E-09
Cm245	3.7E-05	3.7E-05	4.1E-05	6.2E-05	5.3E-07	1.2E-06
Cm246	6.4E-05	6.4E-05	6.3E-05	5.5E-05	4.8E-07	9.0E-08
Cm247	1.4E-08	1.4E-08	1.4E-08	1.5E-08	4.6E-08	4.6E-08
Cm248	6.5E-07	6.5E-07	6.5E-07	6.5E-07	5.3E-07	8.9E-08
Cm249		1.2E-03	9.8E-04	2.1E-04	5.3E-07	1.3E-06
Cm250	3.8E-06	5.3E-06	7.5E-06	8.0E-06	4.5E-07	3.7E-08
Cm251		4.5E-04	4.2E-04	2.1E-04	4.6E-08	4.6E-08
Bk249	4.9E-06	1.2E-03	9.8E-04	2.1E-04	5.3E-07	1.3E-06
Bk250		2.0E-02	2.4E-04	5.6E-05	4.7E-07	9.0E-08
Bk251		4.5E-04	4.2E-04	2.1E-04	4.6E-08	4.6E-08
Cf249	1.2E-03	1.2E-03	9.8E-04	2.1E-04	5.3E-07	1.3E-06
Cf250	3.5E-02	2.0E-02	2.4E-04	5.6E-05	4.7E-07	9.0E-08
Cf251	4.5E-04	4.5E-04	4.2E-04	2.1E-04	4.6E-08	4.6E-08
Cf252	1.8E-01	1.3E-02	6.3E-07	6.3E-07	5.2E-07	8.6E-08
Cf253	2.9E-02	5.4E-03	4.5E-03	9.9E-04	2.5E-06	5.8E-06
Cf254	7.6E-03	1.6E-08	2.3E-08	2.5E-08	1.4E-09	1.1E-10
Cf255		4.5E-04	4.2E-04	2.1E-04	4.6E-08	4.6E-08
Es253	1.1E+01	1.2E-03	9.8E-04	2.1E-04	5.3E-07	1.3E-06
Es254m	1.2E+02	2.0E-02	2.4E-04	5.5E-05	4.7E-07	9.0E-08
Es254	7.0E-01	2.2E-02	2.5E-04	5.6E-05	4.7E-07	9.0E-08
Es255	7.5E+00	4.5E-04	4.2E-04	2.1E-04	4.6E-08	4.6E-08

APPENDIX G

SPONTANEOUS NEUTRON EMISSION RATE

Table 123 - Spontaneous Neutron Emission Rate (n/s/mole) for Actinide Isotopes

Note: Starting with one mole of given isotope and includes all daughters.

	Time (yr)					
Isotope	0	10	100	"1,000"	"100,000"	"1,000,000"
He 4						
Tl206						
Tl207						
Tl208						
Tl209						
Pb206						
Pb207						
Pb208						
Pb209						
Pb210						
Pb211						
Pb212						
Pb214						
Bi208						
Bi209						
Bi210m						
Bi210						
Bi211						
Bi212						
Bi213						
Bi214						
Po210						
Po211m						
Po211						
Po212						
Po213						
Po214						
Po215						
Po216						
Po218						
At217						
Rn218						
Rn219						
Rn220						
Rn222						
Fr221						
Fr223						
Ra222						
Ra223						
Ra224						

	Time (yr)					
Isotope	0	10	100	"1,000"	"100,000"	"1,000,000"
Ra225						
Ra226						
Ra228						
Ac225						
Ac227						
Ac228						
Th226						
Th227						
Th228						
Th229						
Th230	5.7E-02	5.7E-02	5.7E-02	5.6E-02	2.3E-02	5.8E-06
Th231		8.3E-01	8.3E-01	8.1E-01	1.0E-01	5.4E-10
Th232						
Th233						
Th234		1.6E+00	1.6E+00	1.6E+00	1.2E+00	9.5E-02
Pa231	8.3E-01	8.3E-01	8.3E-01	8.1E-01	1.0E-01	5.4E-10
Pa232		2.2E+02	9.0E+01	1.2E-02		
Pa233						
Pa234m		1.6E+00	1.6E+00	1.6E+00	1.2E+00	9.5E-02
Pa234		1.6E+00	1.6E+00	1.6E+00	1.2E+00	9.5E-02
Pa235		2.3E-03	2.3E-03	2.3E-03	2.3E-03	2.3E-03
U230						
U231		8.3E-01	8.3E-01	8.1E-01	1.0E-01	5.4E-10
U232	2.4E+02	2.2E+02	9.0E+01	1.2E-02		
U233						
U234	1.6E+00	1.6E+00	1.6E+00	1.6E+00	1.2E+00	9.5E-02
U235	2.3E-03	2.3E-03	2.3E-03	2.3E-03	2.3E-03	2.3E-03
U236	9.0E-01	9.0E-01	9.0E-01	9.0E-01	9.0E-01	8.7E-01
U237	3.9E-04					
U238	3.2E+00	3.2E+00	3.2E+00	3.2E+00	3.2E+00	3.2E+00
U239	3.0E-03	5.4E+00	5.4E+00	5.3E+00	3.1E-01	2.3E-03
U240		2.5E+05	2.5E+05	2.2E+05	7.3E+00	8.7E-01
U241		1.1E+02	2.4E+02	5.7E+01		
Np235		2.3E-03	2.3E-03	2.3E-03	2.3E-03	2.3E-03
Np236m		3.8E+05	4.6E+01	4.7E-01	4.7E-01	4.5E-01
Np236	3.7E-02	1.8E+01	1.9E+01	1.9E+01	1.1E+01	8.4E-01
Np237						
Np238	1.3E-02	6.0E+05	3.0E+05	2.4E+02	1.2E+00	9.5E-02
Np239	4.3E-01	5.4E+00	5.4E+00	5.3E+00	3.1E-01	2.3E-03
Np240m		2.5E+05	2.5E+05	2.2E+05	7.3E+00	8.7E-01
Np240		2.5E+05	2.5E+05	2.2E+05	7.3E+00	8.7E-01
Np241		1.1E+02	2.4E+02	5.7E+01		
Pu236	8.6E+06	7.9E+05	9.4E+01	1.2E-02		
Pu237						
Pu238	6.5E+05	6.0E+05	3.0E+05	2.4E+02	1.2E+00	9.5E-02
Pu239	5.4E+00	5.4E+00	5.4E+00	5.3E+00	3.1E-01	2.3E-03
Pu240	2.5E+05	2.5E+05	2.5E+05	2.2E+05	7.3E+00	8.7E-01
Pu241	1.2E+01	1.1E+02	2.4E+02	5.7E+01		
Pu242	4.2E+05	4.2E+05	4.2E+05	4.2E+05	3.5E+05	6.5E+04
Pu243	1.6E+01	1.7E+02	1.7E+02	1.5E+02	4.6E-01	2.3E-03
Pu244	4.6E+05	4.6E+05	4.6E+05	4.6E+05	4.6E+05	4.5E+05

	Time (yr)					
Isotope	0	10	100	"1,000"	"100,000"	"1,000,000"
Pu245		9.5E+03	9.4E+03	8.8E+03	2.7E+00	3.6E-32
Pu246		2.2E+09	2.2E+09	1.9E+09	3.5E+05	6.6E+04
Am239		5.4E+00	5.4E+00	5.3E+00	3.1E-01	2.3E-03
Am240		2.5E+05	2.5E+05	2.2E+05	7.3E+00	8.7E-01
Am241	2.7E+02	2.7E+02	2.3E+02	5.5E+01		
Am242m	3.9E+04	1.2E+07	7.9E+06	1.7E+05	6.0E+04	1.1E+04
Am242	3.3E+06	5.8E+05	3.2E+05	7.2E+04	6.0E+04	1.1E+04
Am243	1.7E+02	1.7E+02	1.7E+02	1.5E+02	4.6E-01	2.3E-03
Am244m		1.9E+09	5.9E+07	2.2E+05	1.7E+02	1.6E+02
Am244	4.5E+02	1.9E+09	5.9E+07	2.2E+05	7.3E+00	8.7E-01
Am245		9.5E+03	9.4E+03	8.8E+03	2.7E+00	3.6E-32
Am246		2.2E+09	2.2E+09	1.9E+09	3.5E+05	6.6E+04
Cm241		2.7E+02	2.3E+02	5.5E+01		
Cm242	4.9E+09	6.1E+05	3.0E+05	2.4E+02	1.2E+00	9.5E-02
Cm243	3.0E+05	2.3E+05	2.6E+04	5.6E+00	3.1E-01	2.3E-03
Cm244	2.7E+09	1.9E+09	5.9E+07	2.2E+05	7.3E+00	8.7E-01
Cm245	9.5E+03	9.5E+03	9.4E+03	8.8E+03	2.7E+00	3.6E-32
Cm246	2.2E+09	2.2E+09	2.2E+09	1.9E+09	3.5E+05	6.6E+04
Cm247		7.3E-05	7.2E-04	6.9E-03	8.4E-02	8.2E-02
Cm248	1.0E+10	1.0E+10	1.0E+10	1.0E+10	8.3E+09	1.3E+09
Cm249		6.8E+05	5.6E+05	1.0E+05	2.9E+00	3.7E-32
Cm250	1.5E+12	1.5E+12	1.5E+12	1.5E+12	2.9E+10	2.7E+04
Cm251		2.8E-07	2.7E-05	2.1E-03	8.4E-02	8.2E-02
Bk249	2.6E+07	6.8E+05	5.6E+05	1.0E+05	2.9E+00	3.7E-32
Bk250		1.6E+12	1.6E+10	1.9E+09	3.5E+05	6.6E+04
Bk251		2.8E-07	2.7E-05	2.1E-03	8.4E-02	8.2E-02
Cf249	6.8E+05	6.7E+05	5.6E+05	1.0E+05	2.9E+00	3.7E-32
Cf250	2.8E+12	1.6E+12	1.6E+10	1.9E+09	3.5E+05	6.6E+04
Cf251		2.8E-07	2.7E-05	2.1E-03	8.4E-02	8.2E-02
Cf252	5.8E+14	4.2E+13	9.8E+09	9.8E+09	8.0E+09	1.3E+09
Cf253		3.2E+06	2.6E+06	4.8E+05	1.3E+01	1.7E-31
Cf254	3.1E+17	4.8E+09	4.7E+09	4.6E+09	8.9E+07	8.4E+01
Cf255		2.7E-07	2.7E-05	2.1E-03	8.5E-02	8.2E-02
Es253	7.8E+10	6.8E+05	5.6E+05	1.0E+05	2.9E+00	3.7E-32
Es254m	1.2E+16	1.6E+12	1.6E+10	1.9E+09	4.2E+05	6.6E+04
Es254		1.7E+12	1.7E+10	1.9E+09	3.5E+05	6.6E+04
Es255	2.1E+13	2.7E-07	2.7E-05	2.1E-03	8.4E-02	8.2E-02

APPENDIX H

REFERENCE CASE ONCE-THROUGH CYCLE DATA

Table 124 - Reference SNF Transmutation Reactor Feed Composition (Moles per MTU SNF)

Isotope	UREX Feed (LWR SNF)	UREX Waste	Pyro-A Feed	Pyro-A Waste	Tranmsuter Feed
Th230	5.82E-05	5.82E-05			
Th232	1.31E-05	1.31E-05			
Pa231	2.21E-06	2.21E-06			
U232	3.42E-06	3.42E-06	1.71E-10	1.71E-13	1.71E-10
U233	2.53E-05	2.53E-05	1.27E-09	1.27E-12	1.26E-09
U234	8.18E-01	8.18E-01	4.09E-05	4.09E-08	4.08E-05
U235	3.63E+01	3.63E+01	1.82E-03	1.82E-06	1.82E-03
U236	1.66E+01	1.66E+01	8.32E-04	8.32E-07	8.31E-04
U238	3.96E+03	3.96E+03	1.98E-01	1.98E-04	1.98E-01
Np236	3.20E-06		3.20E-06	3.20E-09	3.20E-06
Np237	2.03E+00		2.03E+00	2.03E-03	2.03E+00
Pu238	5.80E-01		5.80E-01	5.80E-04	5.79E-01
Pu239	2.51E+01		2.51E+01	2.51E-02	2.51E+01
Pu240	9.86E+00		9.86E+00	9.86E-03	9.86E+00
Pu241	1.79E+00		1.79E+00	1.79E-03	1.79E+00
Pu242	2.15E+00		2.15E+00	2.15E-03	2.15E+00
Pu244	7.29E-05		7.29E-05	7.29E-08	7.28E-05
Am241	4.24E+00		4.24E+00	4.24E-03	4.24E+00
Am242m	3.07E-03		3.07E-03	3.07E-06	3.07E-03
Am243	4.69E-01		4.69E-01	4.69E-04	4.69E-01
Cm242	8.05E-06		8.05E-06	8.05E-09	8.04E-06
Cm243	8.13E-04		8.13E-04	8.13E-07	8.13E-04
Cm244	5.28E-02		5.28E-02	5.28E-05	5.27E-02
Cm245	5.69E-03		5.69E-03	5.69E-06	5.68E-03
Cm246	4.50E-04		4.50E-04	4.50E-07	4.50E-04
Cm247	4.54E-06		4.54E-06	4.54E-09	4.54E-06
H 3	1.68E-02		1.68E-02	1.68E-02	
Li 6	3.30E-05		3.30E-05	3.30E-05	
Li 7	1.46E-06		1.46E-06	1.46E-06	
Be 9	2.18E-06		2.18E-06	2.18E-06	
Be 10	1.31E-05		1.31E-05	1.31E-05	
C 14	1.89E-06		1.89E-06	1.89E-06	
Zn 70	1.21E-07		1.21E-07	1.21E-07	
Ga 71	1.15E-06		1.15E-06	1.15E-06	
Ge 72	6.94E-05		6.94E-05	6.94E-05	
Ge 73	2.02E-04		2.02E-04	2.02E-04	
Ge 74	1.72E-04		1.72E-04	1.72E-04	
As 75	1.51E-03		1.51E-03	1.51E-03	
Ge 76	4.53E-03		4.53E-03	4.53E-03	

Isotope	UREX Feed (LWR SNF)	UREX Waste	Pyro-A Feed	Pyro-A Waste	Tranmsuter Feed
Se 76	4.75E-05		4.75E-05	4.75E-05	
Se 77	1.01E-02		1.01E-02	1.01E-02	
Se 78	3.30E-02		3.30E-02	3.30E-02	
Se 79	6.16E-02		6.16E-02	6.16E-02	
Br 79	1.86E-07		1.86E-07	1.86E-07	
Se 80	1.68E-01		1.68E-01	1.68E-01	
Kr 80	7.22E-07		7.22E-07	7.22E-07	
Br 81	2.45E-01		2.45E-01	2.45E-01	
Kr 81	5.31E-08		5.31E-08	5.31E-08	
Se 82	3.93E-01		3.93E-01	3.93E-01	
Kr 82	7.78E-03		7.78E-03	7.78E-03	
Kr 83	4.98E-01		4.98E-01	4.98E-01	
Kr 84	1.35E+00		1.35E+00	1.35E+00	
Kr 85	2.65E-01		2.65E-01	2.65E-01	
Rb 85	1.07E+00		1.07E+00	1.07E+00	
Kr 86	2.12E+00		2.12E+00	2.12E+00	
Sr 86	4.05E-03		4.05E-03	4.05E-03	
Rb 87	2.74E+00		2.74E+00	2.74E+00	
Sr 87	2.05E-05		2.05E-05	2.05E-05	
Sr 88	3.86E+00		3.86E+00	3.86E+00	
Y 89	4.76E+00		4.76E+00	4.76E+00	
Sr 90	5.96E+00		5.96E+00	5.96E+00	
Y 90	1.62E-03		1.62E-03	1.62E-03	
Zr 90	2.19E-01		2.19E-01	2.19E-01	
Zr 91	5.97E+00		5.97E+00	5.97E+00	
Zr 92	6.87E+00		6.87E+00	6.87E+00	
Zr 93	5.02E+00		5.02E+00	5.02E+00	
Nb 93	2.35E-07		2.35E-07	2.35E-07	
Nb 93m	3.05E-06		3.05E-06	3.05E-06	
Zr 94	8.10E+00		8.10E+00	8.10E+00	
Nb 94	5.11E-06		5.11E-06	5.11E-06	
Mo 95	6.70E+00		6.70E+00	6.70E+00	
Zr 96	8.36E+00		8.36E+00	8.36E+00	
Mo 96	3.74E-01		3.74E-01	3.74E-01	
Mo 97	7.83E+00		7.83E+00	7.83E+00	
Mo 98	8.43E+00		8.43E+00	8.43E+00	
Tc 98	7.28E-05		7.28E-05	7.28E-05	
Tc 99	7.89E+00		7.89E+00	7.89E+00	
Ru 99	3.08E-04		3.08E-04	3.08E-04	
Mo100	9.37E+00		9.37E+00	9.37E+00	
Ru100	1.04E+00		1.04E+00	1.04E+00	
Ru101	7.63E+00		7.63E+00	7.63E+00	
Ru102	7.68E+00		7.68E+00	7.68E+00	
Rh102	1.27E-05		1.27E-05	1.27E-05	
Rh103	4.26E+00		4.26E+00	4.26E+00	
Ru104	5.33E+00		5.33E+00	5.33E+00	
Pd104	2.01E+00		2.01E+00	2.01E+00	
Pd105	3.71E+00		3.71E+00	3.71E+00	

Isotope	UREX Feed (LWR SNF)	UREX Waste	Pyro-A Feed	Pyro-A Waste	Tranmsuter Feed
Ru106	1.68E+00		1.68E+00	1.68E+00	
Pd106	1.90E+00		1.90E+00	1.90E+00	
Pd107	2.14E+00		2.14E+00	2.14E+00	
Ag107	2.22E-07		2.22E-07	2.22E-07	
Pd108	1.38E+00		1.38E+00	1.38E+00	
Ag108m	2.04E-06		2.04E-06	2.04E-06	
Cd108	2.08E-06		2.08E-06	2.08E-06	
Ag109	8.38E-01		8.38E-01	8.38E-01	
Pd110	4.05E-01		4.05E-01	4.05E-01	
Cd110	3.60E-01		3.60E-01	3.60E-01	
Cd111	2.05E-01		2.05E-01	2.05E-01	
Cd112	1.06E-01		1.06E-01	1.06E-01	
Cd113	9.50E-04		9.50E-04	9.50E-04	
Cd113m	1.17E-03		1.17E-03	1.17E-03	
In113	5.57E-05		5.57E-05	5.57E-05	
Cd114	1.08E-01		1.08E-01	1.08E-01	
Sn114	2.85E-06		2.85E-06	2.85E-06	
In115	1.34E-02		1.34E-02	1.34E-02	
Sn115	1.55E-03		1.55E-03	1.55E-03	
Cd116	4.35E-02		4.35E-02	4.35E-02	
Sn116	1.90E-02		1.90E-02	1.90E-02	
Sn117	4.07E-02		4.07E-02	4.07E-02	
Sn118	3.25E-02		3.25E-02	3.25E-02	
Sn119	3.36E-02		3.36E-02	3.36E-02	
Sn120	3.28E-02		3.28E-02	3.28E-02	
Sn121m	3.63E-04		3.63E-04	3.63E-04	
Sb121	3.24E-02		3.24E-02	3.24E-02	
Sn122	4.17E-02		4.17E-02	4.17E-02	
Te122	2.16E-03		2.16E-03	2.16E-03	
Sb123	3.69E-02		3.69E-02	3.69E-02	
Te123	1.83E-05		1.83E-05	1.83E-05	
Sn124	6.86E-02		6.86E-02	6.86E-02	
Te124	1.57E-03		1.57E-03	1.57E-03	
Sb125	6.32E-02		6.32E-02	6.32E-02	
Te125	1.94E-02		1.94E-02	1.94E-02	
Te125m	7.70E-04		7.70E-04	7.70E-04	
Sn126	1.55E-01		1.55E-01	1.55E-01	
Te126	2.85E-03		2.85E-03	2.85E-03	
I127	3.24E-01		3.24E-01	3.24E-01	
Te128	7.10E-01		7.10E-01	7.10E-01	
Xe128	2.01E-02		2.01E-02	2.01E-02	
I129	1.40E+00		1.40E+00	1.40E+00	
Xe129	1.13E-04		1.13E-04	1.13E-04	
Te130	2.80E+00		2.80E+00	2.80E+00	
Xe130	5.39E-02		5.39E-02	5.39E-02	
Xe131	3.14E+00		3.14E+00	3.14E+00	
Xe132	8.31E+00		8.31E+00	8.31E+00	
Ba132	1.82E-06		1.82E-06	1.82E-06	

Isotope	UREX Feed (LWR SNF)	UREX Waste	Pyro-A Feed	Pyro-A Waste	Tranmsuter Feed
Cs133	8.51E+00		8.51E+00	8.51E+00	
Xe134	1.13E+01		1.13E+01	1.13E+01	
Cs134	8.91E-01		8.91E-01	8.91E-01	
Ba134	2.71E-01		2.71E-01	2.71E-01	
Cs135	2.52E+00		2.52E+00	2.52E+00	
Ba135	2.07E-03		2.07E-03	2.07E-03	
Xe136	1.70E+01		1.70E+01	1.70E+01	
Ba136	1.20E-01		1.20E-01	1.20E-01	
Cs137	9.10E+00		9.10E+00	9.10E+00	
Ba137	2.80E-01		2.80E-01	2.80E-01	
Ba137m	1.40E-06		1.40E-06	1.40E-06	
Ba138	9.30E+00		9.30E+00	9.30E+00	
La138	6.19E-05		6.19E-05	5.88E-05	3.10E-06
La139	8.70E+00		8.70E+00	8.27E+00	4.35E-01
Ce140	8.93E+00		8.93E+00	8.49E+00	4.47E-01
Pr141	7.49E+00		7.49E+00	7.11E+00	3.74E-01
Ce142	7.94E+00		7.94E+00	7.54E+00	3.97E-01
Nd142	1.30E-01		1.30E-01	1.23E-01	6.49E-03
Nd143	5.57E+00		5.57E+00	5.29E+00	2.78E-01
Ce144	2.64E+00		2.64E+00	2.51E+00	1.32E-01
Nd144	6.25E+00		6.25E+00	5.94E+00	3.12E-01
Nd145	4.61E+00		4.61E+00	4.38E+00	2.31E-01
Pm145	1.70E-07		1.70E-07	1.62E-07	8.50E-09
Nd146	4.73E+00		4.73E+00	4.49E+00	2.36E-01
Pm146	6.06E-05		6.06E-05	5.76E-05	3.03E-06
Sm146	3.99E-05		3.99E-05	3.79E-05	1.99E-06
Pm147	1.21E+00		1.21E+00	1.15E+00	6.06E-02
Sm147	4.37E-01		4.37E-01	4.15E-01	2.19E-02
Nd148	2.48E+00		2.48E+00	2.36E+00	1.24E-01
Sm148	7.70E-01		7.70E-01	7.32E-01	3.85E-02
Sm149	1.87E-02		1.87E-02	1.78E-02	9.36E-04
Nd150	1.20E+00		1.20E+00	1.14E+00	5.99E-02
Sm150	2.08E+00		2.08E+00	1.97E+00	1.04E-01
Sm151	1.13E-01		1.13E-01	1.08E-01	5.67E-03
Eu151	1.09E-04		1.09E-04	1.04E-04	5.45E-06
Sm152	8.57E-01		8.57E-01	8.14E-01	4.28E-02
Eu152	2.52E-04		2.52E-04	2.39E-04	1.26E-05
Gd152	3.36E-04		3.36E-04	3.19E-04	1.68E-05
Eu153	7.79E-01		7.79E-01	7.40E-01	3.90E-02
Sm154	2.44E-01		2.44E-01	2.32E-01	1.22E-02
Eu154	1.63E-01		1.63E-01	1.55E-01	8.15E-03
Gd154	1.07E-02		1.07E-02	1.01E-02	5.33E-04
Eu155	3.63E-02		3.63E-02	3.45E-02	1.81E-03
Gd155	2.74E-04		2.74E-04	2.60E-04	1.37E-05
Gd156	4.52E-01		4.52E-01	4.29E-01	2.26E-02
Gd157	7.76E-04		7.76E-04	7.37E-04	3.88E-05
Gd158	1.18E-01		1.18E-01	1.12E-01	5.90E-03
Tb159	1.50E-02		1.50E-02	1.42E-02	7.48E-04

Isotope	UREX Feed (LWR SNF)	UREX Waste	Pyro-A Feed	Pyro-A Waste	Tranmsuter Feed
Gd160	6.54E-03		6.54E-03	6.22E-03	3.27E-04
Dy160	1.13E-03		1.13E-03	1.07E-03	5.65E-05
Dy161	2.20E-03		2.20E-03	2.09E-03	1.10E-04
Dy162	1.68E-03		1.68E-03	1.60E-03	8.41E-05
Dy163	1.34E-03		1.34E-03	1.27E-03	6.70E-05
Dy164	3.06E-04		3.06E-04	2.91E-04	1.53E-05
Ho165	3.96E-04		3.96E-04	3.76E-04	1.98E-05
Ho166m	1.37E-06		1.37E-06	1.30E-06	6.84E-08
Er166	8.74E-05		8.74E-05	8.31E-05	4.37E-06
Er167	1.71E-06		1.71E-06	1.62E-06	8.55E-08
Er168	2.09E-06		2.09E-06	1.98E-06	1.04E-07
Tm169	1.89E-08		1.89E-08	1.89E-08	
Er170	2.09E-08		2.09E-08	1.98E-08	1.04E-09
Yb171	7.73E-09		7.73E-09	7.73E-09	
Yb172	1.76E-08		1.76E-08	1.76E-08	

APPENDIX I

ONCE-THROUGH CYCLE RESULTS

Table 125 - Composition of discharge LWR SNF (Moles per MTU SNF)

	Burnup (GWd-th/MTU)				
Isotope	Base Case (33 GWd + 25 years storge)	42	46	50	55
Th230	2.69E-05	4.32E-06	4.82E-06	5.33E-06	6.00E-06
Th232	6.04E-06	8.99E-07	1.07E-06	1.25E-06	1.50E-06
Pa231	1.02E-06	9.89E-07	1.16E-06	1.34E-06	1.60E-06
U232	1.58E-06	1.58E-06	2.02E-06	2.52E-06	3.24E-06
U233	1.17E-05	6.29E-06	7.01E-06	7.73E-06	8.72E-06
U234	3.78E-01	3.67E-01	3.80E-01	3.93E-01	4.12E-01
U235	1.68E+01	1.75E+01	1.74E+01	1.73E+01	1.73E+01
U236	7.69E+00	9.85E+00	1.07E+01	1.16E+01	1.28E+01
U238	1.83E+03	1.81E+03	1.80E+03	1.79E+03	1.77E+03
Np236	1.48E-06	2.63E-06	3.27E-06	4.00E-06	5.03E-06
Np237	9.37E-01	1.23E+00	1.38E+00	1.54E+00	1.73E+00
Pu236	0.00E+00	1.80E-06	2.13E-06	2.48E-06	2.93E-06
Pu238	2.68E-01	5.17E-01	6.21E-01	7.33E-01	8.84E-01
Pu239	1.16E+01	1.25E+01	1.28E+01	1.31E+01	1.35E+01
Pu240	4.56E+00	5.10E+00	5.33E+00	5.55E+00	5.79E+00
Pu241	8.26E-01	3.10E+00	3.29E+00	3.46E+00	3.65E+00
Pu242	9.95E-01	1.33E+00	1.48E+00	1.64E+00	1.82E+00
Pu244	3.37E-05	5.17E-05	6.14E-05	7.17E-05	8.43E-05
Am241	1.96E+00	2.75E-01	3.12E-01	3.50E-01	3.99E-01
Am242m	1.42E-03	2.30E-03	2.61E-03	2.92E-03	3.32E-03
Am243	2.17E-01	3.37E-01	3.99E-01	4.63E-01	5.42E-01
Cm242	3.72E-06	6.47E-03	6.41E-03	6.25E-03	5.91E-03
Cm243	3.76E-04	1.15E-03	1.40E-03	1.66E-03	1.99E-03
Cm244	2.44E-02	1.16E-01	1.48E-01	1.84E-01	2.32E-01
Cm245	2.63E-03	5.97E-03	8.18E-03	1.08E-02	1.47E-02
Cm246	2.08E-04	5.50E-04	8.05E-04	1.13E-03	1.64E-03
Cm247	2.10E-06	6.82E-06	1.08E-05	1.64E-05	2.58E-05
Cm248	0.00E+00	0.00E+00	7.70E-07	1.25E-06	2.13E-06
H 3	0.007767	0.009733	0.010567	0.0114	0.012433
Li 6	1.53E-05	1.78E-05	1.87E-05	1.95E-05	2.05E-05
Li 7	6.73E-07	8.56E-07	9.36E-07	1.02E-06	1.12E-06
Be 9	1.01E-06	1.28E-06	1.4E-06	1.52E-06	1.68E-06
Be 10	6.04E-06	7.69E-06	8.41E-06	9.14E-06	0.00001
C 14	8.71E-07	1.11E-06	1.21E-06	1.32E-06	1.45E-06
Zn 70	5.6E-08	7E-08	7.66E-08	8.3E-08	9.07E-08
Ga 71	5.31E-07	6.65E-07	7.27E-07	7.89E-07	8.62E-07
Ge 72	3.21E-05	4.06E-05	4.43E-05	4.81E-05	5.28E-05
Ge 73	9.33E-05	0.000117	0.000127	0.000137	0.000149

Isotope	Burnup (GWd-th/MTU)				
	Base Case (33 GWd + 25 years storge)	42	46	50	55
Ge 74	7.97E-05	0.000102	0.000112	0.000122	0.000135
As 75	0.000699	0.00088	0.000957	0.001035	0.001131
Ge 76	0.002092	0.002658	0.002895	0.003145	0.003447
Se 76	2.2E-05	3.41E-05	4.04E-05	4.71E-05	5.62E-05
Se 77	0.004675	0.005883	0.006416	0.006922	0.007584
Se 78	0.015256	0.019359	0.021154	0.023077	0.025256
Se 79	0.028481	0.036076	0.039494	0.042785	0.046962
Br 79	8.58E-08	1.3E-07	1.53E-07	1.77E-07	2.09E-07
Se 80	0.077625	0.098375	0.1075	0.116625	0.1275
Kr 80	3.34E-07	4.16E-07	4.55E-07	4.93E-07	5.39E-07
Br 81	0.113457	0.14321	0.155556	0.167901	0.183951
Kr 81	2.46E-08	3.74E-08	4.44E-08	5.21E-08	6.26E-08
Se 82	0.181707	0.230488	0.252439	0.273171	0.3
Kr 82	0.003598	0.005378	0.006293	0.007256	0.008549
Kr 83	0.23012	0.283133	0.303614	0.325301	0.350602
Kr 84	0.62381	0.803571	0.883333	0.963095	1.065476
Kr 85	0.122353	0.152941	0.165882	0.178824	0.194118
Rb 85	0.496471	0.635294	0.695294	0.756471	0.832941
Kr 86	0.980233	1.244186	1.360465	1.476744	1.627907
Sr 86	0.001872	0.003012	0.003616	0.004267	0.005163
Rb 87	1.264368	1.609195	1.758621	1.908046	2.091954
Sr 87	9.46E-06	1.56E-05	1.92E-05	2.33E-05	2.92E-05
Sr 88	1.784091	2.272727	2.488636	2.693182	2.965909
Sr 89	0	0.158427	0.157303	0.155056	0.152809
Y 89	2.202247	2.842697	3.123596	3.404494	3.752809
Sr 90	2.755556	3.477778	3.777778	4.088889	4.466667
Y 90	0.000748	0.000942	0.001026	0.001108	0.001211
Zr 90	0.101111	0.158889	0.188889	0.22	0.263333
Y 91	0	0.243956	0.241758	0.23956	0.237363
Zr 91	2.758242	3.571429	3.934066	4.285714	4.736264
Zr 92	3.173913	4.043478	4.423913	4.804348	5.282609
Zr 93	2.322581	2.946237	3.215054	3.483871	3.817204
Nb 93	1.09E-07	1.73E-07	2.1E-07	2.52E-07	3.11E-07
Nb 93m	1.41E-06	2.2E-06	2.6E-06	3.03E-06	3.61E-06
Zr 94	3.744681	4.776596	5.234043	5.691489	6.255319
Nb 94	2.36E-06	2.94E-06	3.19E-06	3.45E-06	3.74E-06
Zr 95	0	0.386316	0.385263	0.383158	0.382105
Nb 95	0	0.210526	0.210526	0.210526	0.209474
Nb 95m	0	0.000247	0.000246	0.000245	0.000243
Mo 95	3.094737	4.031579	4.442105	4.842105	5.347368
Zr 96	3.864583	4.90625	5.364583	5.833333	6.40625
Mo 96	0.172917	0.276042	0.329167	0.386458	0.4625
Mo 97	3.618557	4.587629	5.020619	5.453608	5.989691
Mo 98	3.897959	4.959184	5.438776	5.908163	6.5
Tc 98	3.37E-05	5.36E-05	6.41E-05	7.54E-05	9.07E-05
Tc 99	3.646465	4.535354	4.919192	5.282828	5.747475
Ru 99	0.000142	0.000183	0.000201	0.000219	0.000242

	Burnup (GWd-th/MTU)				
Isotope	Base Case (33 GWd + 25 years storge)	42	46	50	55
Mo100	4.33	5.5	6.02	6.54	7.19
Ru100	0.483	0.727	0.85	0.981	1.15
Ru101	3.524752	4.435644	4.831683	5.227723	5.722772
Ru102	3.54902	4.558824	5.019608	5.480392	6.058824
Rh102	5.86E-06	8.82E-06	1.03E-05	1.18E-05	1.37E-05
Ru103	0	0.248544	0.250485	0.250485	0.251456
Rh103	1.970874	2.378641	2.543689	2.699029	2.873786
Rh103m	0	0.000247	0.000248	0.000249	0.00025
Ru104	2.461538	3.125	3.423077	3.730769	4.096154
Pd104	0.930769	1.365385	1.586538	1.807692	2.096154
Pd105	1.714286	2.180952	2.390476	2.6	2.866667
Ru106	0.778302	0.884906	0.929245	0.971698	1.009434
Rh106	0	9.14E-07	9.53E-07	9.91E-07	1.03E-06
Pd106	0.878302	1.226415	1.396226	1.566038	1.792453
Pd107	0.990654	1.261682	1.383178	1.504673	1.654206
Ag107	1.03E-07	1.6E-07	1.9E-07	2.21E-07	2.64E-07
Pd108	0.639815	0.812963	0.89537	0.972222	1.074074
Ag108m	9.44E-07	1.48E-06	1.77E-06	2.07E-06	2.47E-06
Cd108	9.63E-07	1.5E-06	1.79E-06	2.09E-06	2.49E-06
Ag109	0.387156	0.473394	0.511927	0.549541	0.593578
Pd110	0.187273	0.24	0.265455	0.29	0.320909
Ag110m	0	0.004645	0.005173	0.005691	0.006291
Cd110	0.166364	0.244545	0.285455	0.328182	0.381818
Cd111	0.094595	0.125225	0.138739	0.152252	0.169369
Cd112	0.049018	0.063482	0.070357	0.077232	0.085714
Cd113	0.000439	0.000497	0.000519	0.000541	0.000566
Cd113m	0.000542	0.000719	0.000806	0.000894	0.001009
In113	2.58E-05	4.11E-05	4.92E-05	5.81E-05	7.01E-05
Cd114	0.049737	0.06386	0.070351	0.076754	0.084561
Sn114	1.32E-06	2.64E-06	3.46E-06	4.44E-06	5.87E-06
Cd115m	0	7.3E-05	7.48E-05	7.65E-05	7.84E-05
In115	0.006209	0.006965	0.007252	0.007522	0.007817
Sn115	0.000718	0.000913	0.001	0.001087	0.0012
Cd116	0.020086	0.025431	0.027759	0.030172	0.033103
Sn116	0.008793	0.012328	0.013966	0.015603	0.017759
Sn117	0.018803	0.023675	0.025897	0.028205	0.030855
Sn118	0.015	0.018983	0.020763	0.022627	0.024831
Sn119	0.015546	0.019664	0.021597	0.023445	0.025714
Sn119m	0	0.000116	0.000129	0.000144	0.000161
Sn120	0.015167	0.019167	0.021	0.02275	0.025
Sn121	0	3.69E-05	3.69E-05	3.69E-05	3.69E-05
Sn121m	0.000168	0.00021	0.00023	0.000249	0.000272
Sb121	0.014959	0.018595	0.020248	0.021818	0.023719
Sn122	0.019262	0.024344	0.026639	0.028934	0.031721
Te122	0.001	0.001533	0.00182	0.002115	0.002508
Sn123	0	0.00031	0.000312	0.000314	0.000315
Sb123	0.017073	0.021463	0.023333	0.025285	0.027561

	Burnup (GWd-th/MTU)				
Isotope	Base Case (33 GWd + 25 years storge)	42	46	50	55
Te123	8.46E-06	1.46E-05	1.8E-05	2.17E-05	2.68E-05
Te123m	0	5.59E-06	6.82E-06	8.21E-06	0.00001
Sn124	0.031694	0.039919	0.043629	0.047339	0.051855
Sb124	0	0.000239	0.000263	0.000288	0.000317
Te124	0.000726	0.001177	0.001427	0.001694	0.002048
Sb125	0.0292	0.03464	0.03688	0.03912	0.04152
Te125	0.00896	0.01344	0.01568	0.01824	0.02128
Te125m	0.000356	0.000435	0.00047	0.000504	0.000541
Sn126	0.071746	0.090476	0.098413	0.107143	0.11746
Sb126	0	0	0	0	2.43E-05
Te126	0.001317	0.001778	0.002	0.002246	0.002548
Te127	0	0.000135	0.000135	0.000135	0.000135
Te127m	0	0.006181	0.00626	0.006323	0.006378
I127	0.149606	0.186614	0.203937	0.220472	0.240157
Te128	0.328125	0.414844	0.453906	0.492969	0.541406
Xe128	0.009297	0.014609	0.017422	0.020391	0.024375
Te129	0	5.74E-05	0	0	0
Te129m	0	0.00814	0.00814	0.00814	0.008062
I129	0.647287	0.813953	0.891473	0.968992	1.054264
Xe129	5.22E-05	9.77E-05	0.000126	0.000157	0.000202
Te130	1.292308	1.646154	1.8	1.953846	2.146154
Xe130	0.024923	0.036615	0.042615	0.049	0.057308
Xe131	1.450382	1.732824	1.839695	1.938931	2.053435
Xe132	3.840909	5.022727	5.560606	6.098485	6.780303
Ba132	8.41E-07	1.35E-06	1.61E-06	1.89E-06	2.28E-06
Cs133	3.932331	4.87218	5.270677	5.661654	6.135338
Xe134	5.231343	6.649254	7.283582	7.910448	8.731343
Cs134	0.41194	0.576866	0.652985	0.730597	0.828358
Ba134	0.125373	0.221642	0.273881	0.332836	0.414179
Cs135	1.162963	1.674074	1.911111	2.155556	2.488889
Ba135	0.000956	0.002089	0.002815	0.003696	0.00503
Xe136	7.867647	9.779412	10.66176	11.47059	12.5
Ba136	0.055662	0.089706	0.108088	0.128676	0.157353
Cs137	4.20438	5.306569	5.79562	6.277372	6.868613
Ba137	0.129197	0.20146	0.238686	0.278832	0.333577
Ba137m	6.48E-07	8.18E-07	8.91E-07	9.64E-07	1.06E-06
Ba138	4.297101	5.463768	5.985507	6.5	7.152174
La138	2.86E-05	3.71E-05	4.1E-05	4.49E-05	0.00005
La139	4.021583	5.107914	5.582734	6.057554	6.654676
Ce139	0	1.35E-07	1.47E-07	1.59E-07	1.73E-07
Ce140	4.128571	5.264286	5.764286	6.271429	6.9
Ce141	0	0.199291	0.198582	0.197872	0.197163
Pr141	3.460993	4.439716	4.87234	5.304965	5.843972
Ce142	3.669014	4.669014	5.112676	5.549296	6.098592
Nd142	0.06	0.091549	0.107746	0.124648	0.147183
Nd143	2.573427	3.167832	3.412587	3.643357	3.937063
Ce144	1.222222	1.305556	1.333333	1.347222	1.368056

Isotope	Burnup (GWd-th/MTU)				
	Base Case (33 GWd + 25 years storge)	42	46	50	55
Pr144	0	5.55E-05	5.65E-05	5.73E-05	5.8E-05
Pr144m	0	3.22E-07	3.28E-07	3.33E-07	3.37E-07
Nd144	2.888889	4.048611	4.590278	5.145833	5.854167
Nd145	2.131034	2.655172	2.875862	3.089655	3.358621
Pm145	7.86E-08	1.16E-07	1.34E-07	1.53E-07	1.81E-07
Sm145	0	0	0	1.19E-08	1.43E-08
Nd146	2.184932	2.849315	3.150685	3.452055	3.842466
Pm146	2.8E-05	3.97E-05	4.52E-05	5.07E-05	5.86E-05
Sm146	1.84E-05	3.28E-05	4.07E-05	4.95E-05	6.29E-05
Pm147	0.559864	0.611565	0.627211	0.640816	0.653061
Sm147	0.202041	0.270748	0.29932	0.327211	0.367347
Nd148	1.148649	1.459459	1.594595	1.72973	1.898649
Pm148	0	0.003905	0.003973	0.004027	0.004068
Pm148m	0	0.004608	0.004723	0.004818	0.004905
Sm148	0.356081	0.519595	0.597973	0.682432	0.804054
Sm149	0.008658	0.009866	0.010268	0.010671	0.011208
Nd150	0.553333	0.7	0.766667	0.833333	0.92
Sm150	0.96	1.213333	1.326667	1.433333	1.566667
Sm151	0.052384	0.064106	0.068874	0.07351	0.080132
Eu151	5.04E-05	6.69E-05	7.35E-05	8.01E-05	8.94E-05
Sm152	0.396053	0.473026	0.505263	0.535526	0.573026
Eu152	0.000116	0.000152	0.000166	0.000181	0.000201
Gd152	0.000155	0.000232	0.000268	0.000308	0.000361
Eu153	0.360131	0.466013	0.512418	0.55817	0.613072
Gd153	0	2.22E-05	2.69E-05	3.22E-05	3.95E-05
Sm154	0.112987	0.144156	0.158442	0.172078	0.18961
Eu154	0.075325	0.107143	0.121429	0.136364	0.155844
Gd154	0.004929	0.008766	0.010844	0.013182	0.016429
Eu155	0.016774	0.022323	0.024968	0.027548	0.030774
Gd155	0.000126	0.000203	0.000241	0.000283	0.000342
Gd156	0.208974	0.31859	0.377564	0.440385	0.523077
Gd157	0.000359	0.000486	0.000549	0.000617	0.000707
Gd158	0.054557	0.074684	0.085443	0.096835	0.111392
Tb159	0.006918	0.008931	0.009937	0.010943	0.012201
Gd160	0.003025	0.003875	0.004275	0.004681	0.005163
Tb160	0	0.000368	0.000414	0.000463	0.000523
Dy160	0.000523	0.000819	0.000969	0.001138	0.001344
Dy161	0.001019	0.001342	0.001497	0.001658	0.001863
Dy162	0.000778	0.001025	0.001136	0.001253	0.001401
Dy163	0.00062	0.000871	0.000994	0.001123	0.001282
Dy164	0.000141	0.00021	0.000246	0.000284	0.000333
Ho165	0.000183	0.000277	0.000328	0.000384	0.000456
Ho166m	6.33E-07	1.09E-06	1.37E-06	1.69E-06	2.13E-06
Er166	4.04E-05	6.87E-05	8.61E-05	0.000105	0.000133
Er167	7.9E-07	1.43E-06	1.83E-06	2.3E-06	2.97E-06
Er168	9.64E-07	1.99E-06	2.68E-06	3.54E-06	4.82E-06
Tm169	8.76E-09	1.1E-08	1.25E-08	1.36E-08	1.48E-08

Isotope	Burnup (GWd-th/MTU)				
	Base Case (33 GWd + 25 years storge)	42	46	50	55
Er170	9.65E-09	1.22E-08	1.34E-08	1.45E-08	1.59E-08
Tm171	0	1.06E-08	1.13E-08	1.19E-08	1.26E-08
Yb171	3.57E-09	5.26E-09	6.08E-09	7.02E-09	8.13E-09
Yb172	8.14E-09	1.03E-08	1.13E-08	1.23E-08	1.35E-08

APPENDIX J

FUSION TRANSMUTATION OF WASTE REACTOR DATA

Table 126 - Transuranic Burnup Chains Used in REBUS Model

Isotope	Reaction Type	Product Isotope	Yield	Product Isotope	Yield	Product Isotope	Yield
U-232	1	U-233	1				
U-232	2	FP235	1	RE235	1		
U-232	5	DUMP1	1				
U-232	8	DUMP1	1				
U-233	1	U-234	1				
U-233	2	FP235	1	RE235	1		
U-233	5	U-232	1				
U-233	8	DUMP1	1				
U-234	1	U-235	1				
U-234	2	FP235	1	RE235	1		
U-234	5	U-233	1				
U-234	8	DUMP1	1				
U-235	1	U-236	1				
U-235	2	FP235	1	RE235	1		
U-235	5	U-234	1				
U-235	8	DUMP1	1				
U-236	1	U-237	1				
U-236	2	FP235	1	RE235	1		
U-236	5	U-235	1				
U-236	8	DUMP1	1				
U-237	1	U-238	1				
U-237	2	FP238	1	RE238	1		
U-237	5	U-236	1				
U-237	6	NP237	1				
U-238	1	PU239	1				
U-238	2	FP238	1	RE238	1		
U-238	5	U-237	1				
U-238	8	DUMP1	1				
NP237	1	NP238	1				
NP237	2	FP238	1	RE238	1		
NP237	5	U-236	0.374	PU236	0.346	DUMP1	0.28
NP237	8	DUMP1	1				
NP238	1	PU239	1				
NP238	2	FP238	1	RE238	1		
NP238	5	NP237	1				
NP238	6	PU238	1				
PU236	1	NP237	1				
PU236	2	FP235	1	RE235	1		
PU236	5	U-235	1				

Isotope	Reaction Type	Product Isotope	Yield	Product Isotope	Yield	Product Isotope	Yield
PU236	8	U-232	1				
PU238	1	PU239	1				
PU238	2	FP238	1	RE238	1		
PU238	5	NP237	1				
PU238	8	U-234	1				
PU239	1	PU240	1				
PU239	2	FP239	1	RE239	1		
PU239	5	PU238	1				
PU239	8	U-235	1				
PU240	1	PU241	1				
PU240	2	FP240	1	RE240	1		
PU240	5	PU239	1				
PU240	8	U-236	1				
PU241	1	PU242	1				
PU241	2	FP241	1	RE241	1		
PU241	5	PU240	1				
PU241	6	AM241	1				
PU242	1	PU243	1				
PU242	2	FP241	1	RE241	1		
PU242	5	PU241	1				
PU242	8	U-238	1				
PU243	1	PU244	1				
PU243	2	FP241	1	RE241	1		
PU243	5	PU242	1				
PU243	6	AM243	1				
PU244	1	CM245	1				
PU244	2	FP241	1	RE241	1		
PU244	5	PU243	1				
PU244	6	DUMP1	1				
PU244	8	PU240	1				
AM241	1	AM242	0.8	AM24M	0.2		
AM241	2	FP241	1	RE241	1		
AM241	5	PU240	1				
AM241	8	NP237	1				
AM242	1	AM243	1				
AM242	2	FP241	1	RE241	1		
AM242	5	AM241	1				
AM242	6	CM242	1				
AM242	7	PU242	1				
AM24M	1	AM243	1				
AM24M	2	FP241	1	RE241	1		
AM24M	5	AM241	1				
AM24M	6	AM242	1				
AM24M	8	PU238	1				
AM243	1	CM244	1				
AM243	2	FP241	1	RE241	1		
AM243	5	AM24M	0.5	PU242	0.086	CM242	0.414
AM243	8	PU239	1				

Isotope	Reaction Type	Product Isotope	Yield	Product Isotope	Yield	Product Isotope	Yield
CM242	1	CM243	1				
CM242	2	FP241	1	RE241	1		
CM242	5	AM241	0.99	NP237	0.01		
CM242	8	PU238	1				
CM243	1	CM244	1				
CM243	2	FP241	1	RE241	1		
CM243	5	CM242	1				
CM243	7	AM243	1				
CM243	8	PU239	1				
CM244	1	CM245	1				
CM244	2	FP241	1	RE241	1		
CM244	5	CM243	1				
CM244	8	PU240	1				
CM245	1	CM246	1				
CM245	2	FP241	1	RE241	1		
CM245	5	CM244	1				
CM245	8	PU241	1				
CM246	1	CM247	1				
CM246	2	FP241	1	RE241	1		
CM246	5	CM245	1				
CM246	8	PU242	1				
CM247	1	CM248	1				
CM247	2	FP241	1	RE241	1		
CM247	5	CM246	1				
CM247	8	AM243	1				
CM248	1	BK249	1				
CM248	2	FP241	1	RE241	1		
CM248	5	CM247	1				
CM248	6	DUMP1	1				
CM248	8	PU244	1				
BK249	1	CF250	1				
BK249	2	FP241	1	RE241	1		
BK249	5	CM244	1				
BK249	6	CF249	1				
BK249	8	CM245	1				
CF249	1	CF250	1				
CF249	2	FP241	1	RE241	1		
CF249	5	CM244	1				
CF249	8	CM245	1				
CF250	1	CF251	1				
CF250	2	FP241	1	RE241	1		
CF250	5	CF249	1				
CF250	6	DUMP1	1				
CF250	8	CM246	1				
CF251	1	CF252	1				
CF251	2	FP241	1	RE241	1		
CF251	5	CF250	1				
CF251	8	CM247	1				

Isotope	Reaction Type	Product Isotope	Yield	Product Isotope	Yield	Product Isotope	Yield
CF252	1	BK249	1				
CF252	2	FP241	1	RE241	1		
CF252	5	CF251	1				
CF252	6	DUMP1	1				
CF252	8	CM248	1				
ZR	0						
FP239	0						
FP240	0						
FP241	0						
FP235	0						
FP238	0						
FPLWR	0						
RELWR	0						
RE239	0						
RE240	0						
RE241	0						
RE235	0						
RE238	0						
DUMP1	0						

Table 127 - Solid Breeder Depletion Chains Used in REBUS Model

Isotope	Reaction Type	Product Isotope	Yield
LI-7	0		
LI-6	4	H-3	1
H-3	6	HE3	1
HE3	3	H-3	1
O-16	0		

Table 128 - Nuclear Reaction Types For REBUS Model

Reaction Type	Reaction
0	None
1	n,γ
2	n,f
3	n,p
4	n,α
5	n,2n
6	β^- decay
7	β^+ decay
8	α decay

Table 129 - Decay Chains Used For REBUS Model

Isotope	Reaction Type	Product Isotope	Decay Constant (1/sec)
U-232	8	DUMP1	3.149E-10
U-233	8	DUMP1	1.381E-13
U-234	8	DUMP1	8.978E-14
U-235	8	DUMP1	3.120E-17
U-236	8	DUMP1	9.379E-16
U-237	6	NP237	1.188E-06
U-238	8	DUMP1	4.915E-18
NP237	8	DUMP1	1.026E-14
NP238	6	PU238	3.789E-06
PU236	8	U-232	7.703E-09
PU238	8	U-234	2.503E-10
PU239	8	U-235	9.109E-13
PU240	8	U-236	3.353E-12
PU241	6	AM241	1.494E-09
PU242	8	U-238	5.833E-14
PU243	6	AM243	3.885E-05
PU244	6	FP241	3.262E-19
PU244	8	PU240	2.715E-16
AM241	8	NP237	5.081E-11
AM242	6	CM242	9.940E-06
AM242	7	PU242	2.079E-06
AM24M	6	AM242	1.551E-10
AM24M	8	PU238	7.166E-13
AM243	8	PU239	2.976E-12
CM242	8	PU238	4.924E-08
CM243	7	AM243	2.003E-12
CM243	8	PU239	7.685E-10
CM244	8	PU240	1.213E-09
CM245	8	PU241	2.592E-12
CM246	8	PU242	4.642E-12
CM247	8	AM243	1.410E-15
CM248	6	FP241	5.336E-15
CM248	8	PU244	5.927E-14
BK249	6	CF249	2.507E-08
BK249	8	CM245	3.510E-13
CF249	8	CM245	6.258E-11
CF250	6	FP241	1.343E-12
CF250	8	CM246	1.678E-09
CF251	8	CM247	2.446E-11
CF252	6	FP241	2.574E-10
CF252	8	CM246	8.047E-09
H-3	6	HE3	1.781E-09

Table 130 - Composition of Fission Product Lumps in Atoms per Lump

Fission Product Lump	FP239	FP240	FP241	FP235	FP238	FPLWR
Fissioning Isotope	PU239	PU240	PU241	U235	U238	LWR
GE73 5	7.39E-06	3.28E-06	4.65E-06	5.90E-06	4.71E-07	1.41E-06
GE74 5	1.77E-05	8.74E-06	1.11E-05	1.45E-05	9.38E-07	1.20E-06
GE76 5	5.86E-05	1.46E-05	8.06E-06	1.60E-04	8.05E-06	3.16E-05
AS75 5	2.67E-05	5.29E-06	4.54E-06	8.92E-05	2.37E-06	1.05E-05
SE76 5	6.58E-07	1.24E-07	1.05E-07	2.24E-06	5.60E-08	3.31E-07
SE77 5	1.36E-04	1.27E-04	9.35E-05	3.42E-04	3.24E-05	7.05E-05
SE78 5	3.76E-04	2.72E-04	1.83E-04	6.49E-04	1.12E-04	2.30E-04
SE80 5	1.06E-03	8.53E-04	6.45E-04	1.76E-03	6.90E-04	1.17E-03
SE82 5	2.13E-03	2.00E-03	1.43E-03	3.80E-03	2.38E-03	2.74E-03
BR79 5	8.07E-09	6.27E-09	4.39E-09	1.32E-08	4.12E-09	1.29E-09
BR81 5	1.39E-03	1.38E-03	9.35E-04	2.46E-03	1.39E-03	1.71E-03
KR80 5	1.21E-08	2.45E-09	5.82E-10	2.11E-09	1.25E-10	5.03E-09
KR82 5	4.44E-05	3.86E-05	2.51E-05	7.18E-05	3.75E-05	5.43E-05
KR83 5	3.03E-03	2.97E-03	1.93E-03	5.56E-03	3.75E-03	3.47E-03
KR84 5	4.80E-03	4.15E-03	3.31E-03	9.72E-03	7.64E-03	9.41E-03
KR85 5	1.25E-03	1.18E-03	8.24E-04	2.72E-03	1.55E-03	1.85E-03
KR86 5	7.59E-03	7.35E-03	5.67E-03	1.87E-02	1.24E-02	1.48E-02
RB85 5	4.80E-03	4.62E-03	3.27E-03	1.09E-02	6.19E-03	7.49E-03
RB86 5	4.71E-06	6.01E-06	6.02E-06	3.21E-05	7.01E-06	
RB87 5	9.84E-03	9.66E-03	7.30E-03	2.37E-02	1.53E-02	1.91E-02
SR86 5	8.11E-05	1.26E-04	1.51E-04	9.32E-04	1.34E-04	2.82E-05
SR87 5	3.05E-07	4.51E-07	5.63E-07	3.67E-06	4.27E-07	1.43E-07
SR88 5	1.31E-02	1.22E-02	9.35E-03	3.39E-02	1.94E-02	2.69E-02
SR89 5	1.38E-03	1.27E-03	1.10E-03	3.25E-03	2.42E-03	
SR90 5	2.00E-02	1.86E-02	1.52E-02	5.40E-02	3.28E-02	4.16E-02
Y89 5	1.63E-02	1.36E-02	1.15E-02	4.23E-02	2.64E-02	3.32E-02
Y90 5	5.52E-06	5.14E-06	4.30E-06	1.57E-05	9.09E-06	1.13E-05
Y91 5	2.15E-03	2.21E-03	1.90E-03	4.88E-03	3.89E-03	
ZR90 5	6.53E-04	5.96E-04	5.03E-04	2.03E-03	1.05E-03	1.53E-03
ZR91 5	2.21E-02	2.07E-02	1.75E-02	5.50E-02	3.71E-02	4.16E-02
ZR92 5	2.96E-02	2.85E-02	2.30E-02	5.69E-02	4.45E-02	4.79E-02
ZR93 5	3.65E-02	3.69E-02	2.86E-02	5.90E-02	4.75E-02	3.50E-02
ZR94 5	4.27E-02	4.19E-02	3.49E-02	6.33E-02	5.16E-02	5.65E-02
ZR95 5	4.64E-03	4.76E-03	4.30E-03	5.78E-03	5.49E-03	
ZR96 5	4.80E-02	4.92E-02	4.37E-02	6.08E-02	5.97E-02	5.83E-02

Fission Product Lump	FP239	FP240	FP241	FP235	FP238	FPLWR
Fissioning Isotope	PU239	PU240	PU241	U235	U238	LWR
NB93 5	4.22E-09	3.18E-09	2.30E-09	5.24E-09	3.86E-09	1.64E-09
NB94 5	5.81E-08	1.23E-08	2.59E-09	6.06E-09	4.41E-10	3.56E-08
NB95 5	2.51E-03	2.54E-03	2.30E-03	3.17E-03	2.93E-03	
MO95 5	3.90E-02	3.61E-02	3.21E-02	5.37E-02	4.27E-02	4.67E-02
MO96 5	8.83E-04	7.97E-04	6.89E-04	1.21E-03	9.16E-04	2.61E-03
MO97 5	5.18E-02	5.05E-02	4.56E-02	5.78E-02	5.42E-02	5.46E-02
MO98 5	5.71E-02	5.55E-02	5.01E-02	5.92E-02	5.86E-02	5.88E-02
MO99 5	2.46E-04	2.73E-04	2.56E-04	2.10E-04	2.77E-04	
MO1005	6.53E-02	6.06E-02	6.29E-02	6.28E-02	6.68E-02	6.53E-02
TC99 5	5.71E-02	5.76E-02	5.27E-02	5.45E-02	5.93E-02	5.50E-02
RU99 5	2.31E-07	2.23E-07	2.03E-07	2.27E-07	2.33E-07	2.15E-06
RU1005	2.70E-03	2.60E-03	2.38E-03	2.66E-03	2.73E-03	7.29E-03
RU1015	6.24E-02	5.76E-02	6.02E-02	5.06E-02	5.79E-02	5.32E-02
RU1025	6.91E-02	6.32E-02	6.93E-02	4.75E-02	6.57E-02	5.35E-02
RU1035	4.12E-03	4.44E-03	4.31E-03	1.82E-03	4.04E-03	
RU1045	6.48E-02	5.86E-02	7.05E-02	2.25E-02	4.93E-02	3.71E-02
RU1055	1.51E-05	1.72E-05	2.03E-05	3.08E-06	1.22E-05	
RU1065	2.06E-02	2.43E-02	2.99E-02	2.57E-03	1.23E-02	1.17E-02
RH1035	6.14E-02	6.01E-02	5.74E-02	2.97E-02	5.60E-02	2.97E-02
RH1055	1.21E-04	1.38E-04	1.62E-04	2.47E-05	9.72E-05	
PD1045	3.14E-03	2.96E-03	2.81E-03	1.56E-03	2.77E-03	1.40E-02
PD1055	5.09E-02	5.24E-02	6.07E-02	1.15E-02	3.78E-02	2.59E-02
PD1065	2.61E-02	2.86E-02	3.47E-02	3.79E-03	1.54E-02	1.32E-02
PD1075	2.91E-02	3.96E-02	4.65E-02	3.12E-03	1.25E-02	1.49E-02
PD1085	2.06E-02	3.22E-02	3.70E-02	1.88E-03	6.68E-03	9.65E-03
PD1105	6.14E-03	1.17E-02	1.41E-02	8.92E-04	1.35E-03	2.82E-03
AG1075	3.79E-09	4.97E-09	5.80E-09	4.19E-10	1.58E-09	1.55E-09
AG1095	1.84E-02	1.75E-02	2.45E-02	1.11E-03	2.65E-03	5.84E-03
AG1115	4.09E-05	6.53E-05	9.71E-05	4.49E-06	1.01E-05	
CD1085	1.26E-09	7.91E-10	2.71E-10	4.54E-11	5.45E-11	1.45E-08
CD1105	1.08E-03	9.76E-04	1.37E-03	6.67E-05	1.49E-04	2.51E-03
CD1115	3.49E-03	4.97E-03	7.35E-03	4.23E-04	7.90E-04	1.43E-03
CD1125	2.00E-03	2.50E-03	3.77E-03	3.86E-04	6.64E-04	7.39E-04
CD1135	1.21E-03	1.53E-03	2.02E-03	3.21E-04	5.04E-04	6.62E-06
CD1145	9.46E-04	1.01E-03	1.20E-03	3.29E-04	4.01E-04	7.50E-04

Fission Product Lump	FP239	FP240	FP241	FP235	FP238	FPLWR
Fissioning Isotope	PU239	PU240	PU241	U235	U238	LWR
CD115M	7.39E-06	7.35E-06	1.12E-05	2.62E-06	3.51E-06	
CD1165	5.90E-04	7.86E-04	9.53E-04	3.42E-04	4.12E-04	3.03E-04
IN1135	2.53E-06	3.02E-06	4.26E-06	5.89E-07	8.98E-07	3.88E-07
IN1155	7.01E-04	6.53E-04	9.98E-04	2.85E-04	3.30E-04	9.36E-05
SN1155	2.40E-05	2.24E-05	3.43E-05	9.86E-06	1.14E-05	1.08E-05
SN1165	2.66E-05	2.38E-05	3.64E-05	1.12E-05	1.22E-05	1.33E-04
SN1175	7.83E-04	7.81E-04	8.69E-04	3.35E-04	3.66E-04	2.84E-04
SN1185	6.34E-04	7.45E-04	8.31E-04	3.32E-04	3.97E-04	2.26E-04
SN1195	6.29E-04	7.35E-04	8.13E-04	3.37E-04	3.56E-04	2.34E-04
SN1205	6.14E-04	7.81E-04	8.28E-04	3.42E-04	3.58E-04	2.29E-04
SN1225	7.59E-04	8.74E-04	9.04E-04	4.01E-04	3.75E-04	2.91E-04
SN1235	8.69E-05	1.08E-04	1.04E-04	4.16E-05	4.23E-05	
SN1245	1.33E-03	1.15E-03	1.07E-03	6.55E-04	4.45E-04	4.78E-04
SN1255	7.06E-06	4.99E-06	3.76E-06	2.29E-06	1.88E-06	
SN1265	3.04E-03	2.78E-03	1.87E-03	1.37E-03	6.31E-04	1.08E-03
SB1215	6.62E-04	7.61E-04	8.47E-04	3.37E-04	4.19E-04	2.26E-04
SB1235	7.59E-04	8.94E-04	8.60E-04	4.02E-04	3.61E-04	2.58E-04
SB1245	2.39E-06	2.68E-06	2.56E-06	1.22E-06	1.08E-06	
SB1255	1.08E-03	7.76E-04	6.76E-04	5.07E-04	3.86E-04	4.40E-04
SB1265	1.48E-06	8.58E-07	6.41E-07	4.69E-07	3.30E-07	
TE1225	2.20E-05	2.44E-05	2.70E-05	1.17E-05	1.36E-05	1.51E-05
TE1235	3.35E-07	3.62E-07	4.01E-07	1.79E-07	2.03E-07	1.28E-07
TE1245	1.10E-05	1.15E-05	1.09E-05	5.49E-06	4.60E-06	1.09E-05
TE1255	3.59E-04	2.47E-04	2.14E-04	1.76E-04	1.25E-04	1.35E-04
TE1265	9.12E-05	4.04E-05	2.47E-05	1.97E-05	1.09E-05	1.99E-05
TE127M	1.45E-04	1.18E-04	8.87E-05	6.77E-05	3.48E-05	
TE1285	9.41E-03	6.68E-03	5.92E-03	6.77E-03	4.60E-03	4.95E-03
TE129M	2.01E-04	1.43E-04	1.24E-04	1.39E-04	1.08E-04	
TE1305	2.56E-02	1.99E-02	1.69E-02	1.92E-02	1.87E-02	1.95E-02
TE1325	2.43E-04	2.52E-04	2.50E-04	1.94E-04	2.67E-04	
I1275	5.14E-03	3.89E-03	2.90E-03	2.59E-03	1.17E-03	2.26E-03
I1295	1.55E-02	1.03E-02	8.93E-03	8.58E-03	8.12E-03	9.76E-03
I1305	6.05E-07	3.89E-07	3.35E-07	3.23E-07	3.05E-07	
I1315	4.58E-04	4.68E-04	4.32E-04	3.35E-04	4.15E-04	
I1355	2.44E-05	3.04E-05	3.22E-05	2.25E-05	3.02E-05	

Fission Product Lump	FP239	FP240	FP241	FP235	FP238	FPLWR
Fissioning Isotope	PU239	PU240	PU241	U235	U238	LWR
XE1285	1.93E-04	1.41E-04	1.04E-04	9.99E-05	4.27E-05	1.40E-04
XE1295	1.73E-06	1.24E-06	9.26E-07	9.99E-07	3.82E-07	7.88E-07
XE1305	3.84E-04	2.27E-04	1.93E-04	2.00E-04	1.78E-04	3.76E-04
XE1315	3.76E-02	3.44E-02	3.13E-02	3.08E-02	3.15E-02	2.19E-02
XE1325	5.33E-02	4.81E-02	4.65E-02	4.59E-02	5.16E-02	5.79E-02
XE1335	5.42E-04	6.12E-04	5.94E-04	4.71E-04	5.60E-04	
XE1345	7.35E-02	6.99E-02	7.69E-02	7.51E-02	7.60E-02	7.89E-02
XE1355	4.21E-05	4.69E-05	4.70E-05	3.33E-05	4.23E-05	
XE1365	6.77E-02	6.58E-02	6.53E-02	5.88E-02	6.49E-02	1.19E-01
CS1335	6.62E-02	6.73E-02	6.45E-02	6.44E-02	6.31E-02	5.93E-02
CS1345	1.69E-03	1.67E-03	1.60E-03	1.85E-03	1.57E-03	6.21E-03
CS1355	7.44E-02	7.45E-02	7.37E-02	6.91E-02	6.90E-02	1.75E-02
CS1365	3.72E-05	2.48E-05	1.51E-05	1.40E-05	1.17E-05	
CS1375	6.38E-02	6.42E-02	6.61E-02	6.14E-02	6.16E-02	6.34E-02
BA1345	4.94E-04	4.79E-04	4.60E-04	5.81E-04	4.53E-04	1.89E-03
BA1355	2.45E-06	2.38E-06	2.40E-06	4.94E-06	2.19E-06	1.44E-05
BA1365	1.56E-03	8.48E-04	4.02E-04	4.22E-04	2.72E-04	8.40E-04
BA1375	1.91E-03	1.81E-03	1.83E-03	1.84E-03	1.72E-03	1.95E-03
BA1385	6.10E-02	6.53E-02	6.40E-02	6.50E-02	5.60E-02	6.48E-02
BA1405	1.00E-03	1.07E-03	1.15E-03	1.03E-03	1.23E-03	

Table 131 - Composition of Fission Product Lumps in Atoms per Lump

Fission Product Lump	RE239	RE240	RE241	RE235	RE238	RELWR
Fissioning Isotope	PU239	PU240	PU241	U235	U238	LWR
LA1395	5.62E-02	5.86E-02	6.20E-02	6.32E-02	6.05E-02	6.07E-02
LA1405	1.32E-04	1.41E-04	1.52E-04	1.35E-04	1.62E-04	
CE1405	5.28E-02	5.05E-02	5.34E-02	6.06E-02	5.93E-02	6.23E-02
CE1415	2.54E-03	2.55E-03	2.70E-03	2.60E-03	2.88E-03	
CE1425	4.76E-02	4.94E-02	4.63E-02	5.61E-02	4.71E-02	5.53E-02
CE1435	8.74E-05	1.07E-04	1.05E-04	1.03E-04	1.01E-04	
CE1445	1.44E-02	1.68E-02	1.73E-02	2.01E-02	1.84E-02	1.84E-02
PR1415	4.94E-02	4.48E-02	4.69E-02	5.63E-02	5.19E-02	5.22E-02
PR1425	9.07E-07	8.22E-07	8.60E-07	1.03E-06	9.53E-07	
PR1435	8.64E-04	1.06E-03	1.04E-03	1.02E-03	9.98E-04	
ND1425	3.39E-04	2.97E-04	3.09E-04	3.98E-04	3.47E-04	9.05E-04
ND1435	4.14E-02	4.54E-02	4.40E-02	5.46E-02	4.38E-02	3.88E-02
ND1445	2.26E-02	2.47E-02	2.52E-02	3.33E-02	2.74E-02	4.36E-02
ND1455	2.89E-02	3.21E-02	3.18E-02	3.65E-02	3.71E-02	3.21E-02
ND1465	2.50E-02	2.80E-02	2.80E-02	2.97E-02	3.48E-02	3.30E-02
ND1475	3.27E-04	4.11E-04	4.18E-04	3.11E-04	4.56E-04	
ND1485	1.62E-02	1.90E-02	1.89E-02	1.65E-02	2.06E-02	1.73E-02
ND1505	9.70E-03	1.13E-02	1.18E-02	6.71E-03	1.25E-02	8.35E-03
PM1475	1.35E-02	1.54E-02	1.55E-02	1.41E-02	1.75E-02	8.44E-03
PM1485	8.88E-06	1.01E-05	1.02E-05	9.25E-06	1.15E-05	
PM148M	6.29E-05	7.14E-05	7.18E-05	6.63E-05	8.12E-05	
PM1495	4.18E-05	5.14E-05	5.53E-05	3.14E-05	5.90E-05	
PM1515	1.39E-05	1.69E-05	1.85E-05	6.61E-06	1.57E-05	
SM1475	4.73E-03	5.19E-03	5.16E-03	5.14E-03	5.93E-03	3.05E-03
SM1485	1.31E-03	1.42E-03	1.42E-03	1.43E-03	1.63E-03	5.37E-03
SM1495	1.09E-02	1.21E-02	1.29E-02	9.05E-03	1.42E-02	1.31E-04
SM1505	1.69E-03	1.77E-03	1.86E-03	1.41E-03	2.10E-03	1.45E-02
SM1515	6.72E-03	7.35E-03	7.93E-03	3.52E-03	6.97E-03	7.90E-04
SM1525	6.91E-03	7.50E-03	8.06E-03	3.27E-03	6.12E-03	5.97E-03
SM1535	1.40E-05	2.02E-05	1.93E-05	5.22E-06	1.42E-05	
SM1545	2.70E-03	3.09E-03	3.62E-03	7.24E-04	2.08E-03	1.70E-03
EU1515	5.52E-05	5.81E-05	6.25E-05	2.98E-05	5.56E-05	7.60E-07
EU1525	5.76E-06	5.91E-06	6.37E-06	3.15E-06	5.75E-06	1.76E-06
EU1535	3.88E-03	5.14E-03	4.82E-03	1.57E-03	3.67E-03	5.43E-03

Fission Product Lump	RE239	RE240	RE241	RE235	RE238	RELWR
Fissioning Isotope	PU239	PU240	PU241	U235	U238	LWR
EU1545	5.81E-04	7.45E-04	6.93E-04	2.41E-04	5.38E-04	1.14E-03
EU1555	1.73E-03	1.93E-03	2.48E-03	4.36E-04	1.05E-03	2.53E-04
EU1565	4.63E-05	5.86E-05	7.80E-05	7.24E-06	2.44E-05	
EU1575	1.05E-06	1.36E-06	1.65E-06	9.32E-08	3.93E-07	
GD1525	2.52E-06	2.58E-06	2.78E-06	1.38E-06	2.50E-06	2.34E-06
GD1545	3.90E-05	4.91E-05	4.54E-05	1.64E-05	3.54E-05	7.43E-05
GD1555	3.07E-04	3.28E-04	4.19E-04	7.91E-05	1.80E-04	1.91E-06
GD1565	1.70E-03	1.98E-03	2.63E-03	2.63E-04	8.20E-04	3.15E-03
GD1575	1.10E-03	1.27E-03	1.53E-03	1.13E-04	3.86E-04	5.41E-06
GD1585	8.02E-04	9.30E-04	1.16E-03	7.51E-05	1.98E-04	8.23E-04
GD1605	2.57E-04	3.01E-04	3.76E-04	1.16E-05	3.20E-05	4.56E-05
TB1595	3.91E-04	3.47E-04	5.85E-04	2.88E-05	7.68E-05	1.04E-04
TB1605	8.64E-06	7.55E-06	1.27E-05	6.38E-07	1.67E-06	
DY1605	3.17E-05	2.67E-05	4.49E-05	2.39E-06	5.97E-06	7.88E-06
DY1615	8.40E-05	1.10E-04	2.06E-04	3.46E-06	1.21E-05	1.54E-05
DY1625	7.68E-05	7.61E-05	1.22E-04	9.86E-07	6.05E-06	1.17E-05
DY1635	4.01E-05	2.57E-05	6.23E-05	1.47E-07	1.46E-06	9.35E-06
DY1645	2.53E-05	1.24E-05	3.28E-05	6.67E-08	4.53E-07	2.13E-06
HO1655	1.06E-05	5.45E-06	1.39E-05	2.37E-08	1.47E-07	2.76E-06
ER1665	3.09E-06	1.51E-06	1.70E-06	3.19E-09	1.34E-08	6.10E-07
ER1675	8.69E-08	4.10E-08	3.92E-08	7.85E-11	2.79E-10	1.19E-08

Table 132 - Equilibrium FTWR Composition (Moles per MTU SNF)

	HELE		SB	
Isotope	BOC Fuel	EOC Fuel	BOC Fuel	EOC Fuel
U232	3.93E-04	3.07E-04	4.30E-04	3.39E-04
U233	1.87E-03	1.87E-03	1.91E-03	1.91E-03
U234	2.80E+00	2.64E+00	2.78E+00	2.63E+00
U235	6.06E-01	6.03E-01	6.31E-01	6.27E-01
U236	7.72E-01	7.60E-01	7.75E-01	7.64E-01
U237	1.15E-15	3.03E-04	1.11E-15	3.37E-04
U238	2.00E+00	1.80E+00	2.09E+00	1.90E+00
Np237	5.56E+00	3.39E+00	5.89E+00	3.81E+00
Np238	0.00E+00	1.09E-03	0.00E+00	1.30E-03
Pu236	1.06E-04	2.01E-04	1.19E-04	2.21E-04
Pu238	8.02E+00	7.39E+00	8.00E+00	7.36E+00
Pu239	5.16E+01	2.54E+01	5.23E+01	2.72E+01
Pu240	5.09E+01	4.05E+01	5.04E+01	4.04E+01
Pu241	5.60E+00	4.28E+00	5.64E+00	4.38E+00
Pu242	1.50E+01	1.28E+01	1.51E+01	1.29E+01
Pu243	0.00E+00	1.04E-04	0.00E+00	1.14E-04
Pu244	5.36E-04	4.61E-04	5.28E-04	4.56E-04
Am241	1.51E+01	1.02E+01	1.57E+01	1.10E+01
Am242	1.03E-05	8.93E-04	1.07E-05	1.03E-03
Am242m	7.95E-01	8.03E-01	8.27E-01	8.36E-01
Am243	4.71E+00	4.23E+00	4.71E+00	4.25E+00
Cm242	4.96E-03	1.80E-01	6.11E-03	2.08E-01
Cm243	1.09E-02	1.07E-02	1.10E-02	1.08E-02
Cm244	1.40E+00	1.49E+00	1.29E+00	1.37E+00
Cm245	3.35E-01	3.30E-01	2.93E-01	2.88E-01
Cm246	1.27E-01	1.27E-01	9.82E-02	9.79E-02
Cm247	8.83E-03	8.84E-03	6.51E-03	6.51E-03
Cm248	2.97E-03	2.98E-03	1.94E-03	1.94E-03
Bk249	2.87E-06	2.35E-05	2.35E-06	1.76E-05
Cf249	2.12E-04	1.93E-04	1.39E-04	1.25E-04
Cf250	1.34E-05	1.55E-05	8.34E-06	9.55E-06
Cf251	1.54E-06	1.54E-06	9.25E-07	9.22E-07
Cf252	3.39E-07	3.33E-07	1.96E-07	1.90E-07
FP239		5.99E+01		5.77E+01
FP240		2.24E+01		2.16E+01
FP241		2.48E+01		2.33E+01
FP235		2.14E+00		2.05E+00
FP238		1.07E+01		1.03E+01
RELWR	3.15E+00	3.15E+00	3.02E+00	3.02E+00
RE239	4.54E-01	9.09E+00	4.38E-01	8.75E+00
RE240	1.83E-01	3.65E+00	1.76E-01	3.52E+00
RE241	2.07E-01	4.15E+00	1.94E-01	3.89E+00
RE235	1.93E-02	3.86E-01	1.85E-02	3.70E-01
RE238	9.64E-02	1.93E+00	9.27E-02	1.85E+00

APPENDIX K

URANIUM ORE DATA

Table 133 - Radioactive Decay Chain Data for Natural Uranium

	Half-life					Daughters			
Parent	years	days	hours	minutes	seconds	Isotope	yield	Isotope	yield
U238	4,468,000,000					Th234	100%		
Th234		24.1				Pa234m	100%		
Pa234m				1.17		U234	99.87%	Pa234	0.13%
Pa234			6.7			U234	100%		
U234	245,500					Th230	100%		
Th230	75,380					Ra226	100%		
Ra226	1,600					Rn222	100%		
Rn222		3.8235				Po218	100%		
Po218				3.1		Pb214	99.98%	At218	0.02%
Pb214				26.8		Bi214	100%		
At218					1.5	Bi214	99.9%	Rn218	0.1%
Bi214				19.9		Pb210	100%		
Rn218					0.035	Po214	100%		
Pb210	23.3					Bi210	99.99981%	Hg206	0.00019%
Po214					0.00016	Pb210	100%		
Hg206				8.15		Tl206	100%		
Tl206				4.199		Pb206	100%		
Pb206	Stable								
Bi209	Stable								
Bi210		5.013				Po210	99.99987%	Tl206	0.000132%
Pb209			3.253			Bi209	100%		
Po210		138.376				Pb206	100%		
Tl210				1.3		Pb210	99.993%	Pb209	0.007%
U235	703,800,000					Th231	100%		
Ac227	21.773					Th227	98.62%	Fr223	1.38%
At215					0.0001	Bi211	100%		
At219					56	Bi215	97%	Rn219	3%
Bi211				2.14		Tl207	99.72%	Po211	0.28%
Bi215				7.6		Po215	100%		
Fr223				22		Ra223	99.994%	At219	0.006%
Pa231	32,760					Ac227	100%		
Pb207	Stable								
Pb211				36.1		Bi211	100%		
Po211					0.516	Pb207	100%		
Po215					0.00178	Pb211	99.99977%	At215	0.00023%
Ra223		11.435				Rn219	100%		
Ra227				42.2		Ac227	100%		
Rn219					3.96	Po215	100%		
Th227		18.72				Ra223	100%		
Th231			25.52			Pa231	99.99999999%	Ra227	0.00000001%
Tl207				4.77		Pb207	100%		

APPENDIX L

SINGLE MOX RECYCLE (MOX1) RESULTS

Table 134 - Composition of discharge LWR SNF (Moles per MTU SNF)

Isotope	LWR Waste	MOX Fuel	MOX SNF	Isotope	LWR Waste	MOX Fuel	MOX SNF
Th230	4.95E-06		5.10E-07	Cd113	9.50E-04		6.31E-04
Th232	7.72E-07			Cd113m	1.17E-03		6.97E-04
Pa231	1.31E-06			In113	5.57E-05		5.50E-05
U232	5.94E-11	7.01E-07	7.01E-07	Cd114	1.08E-01		5.42E-02
U233	4.66E-10	5.76E-07	5.76E-07	Sn114	2.85E-06		4.15E-06
U234	3.45E-05	4.64E-02	4.64E-02	In115	1.34E-02		5.41E-03
U235	1.82E-03	7.01E-01	7.01E-01	Sn115	1.55E-03		6.96E-04
U236	8.31E-04	2.30E-01	2.30E-01	Cd116	4.35E-02		1.63E-02
U238	1.98E-01	6.92E+02	6.93E+02	Sn116	1.90E-02		9.15E-03
Np236	3.20E-06		4.73E-07	Sn117	4.07E-02		1.73E-02
Np237	1.87E+00		1.52E-01	Sn118	3.25E-02		1.28E-02
Pu238	3.21E-05	6.42E-01	8.21E-01	Sn119	3.36E-02		1.31E-02
Pu239	1.23E-03	2.47E+01	1.13E+01	Sn120	3.28E-02		1.26E-02
Pu240	4.90E-04	9.80E+00	8.46E+00	Sn121			1.54E-05
Pu241	2.99E-04	5.97E+00	4.44E+00	Sn121m	3.63E-04		1.58E-04
Pu242	1.08E-04	2.15E+00	3.44E+00	Sb121	3.24E-02		1.17E-02
Pu244	3.65E-09	7.29E-05	1.27E-04	Sn122	4.17E-02		1.59E-02
Am241	1.60E-01		1.40E+00	Te122	2.16E-03		1.19E-03
Am242m	3.48E-03		1.23E-02	Sb123	3.69E-02		1.34E-02
Am243	4.69E-01		1.09E+00	Te123	1.83E-05		1.38E-05
Cm242	5.56E-02		2.06E-04	Sn124	6.86E-02		2.57E-02
Cm243	1.49E-03		4.85E-03	Te124	1.57E-03		9.56E-04
Cm244	1.37E-01		5.60E-01	Sb125	6.32E-02		2.06E-02
Cm245	5.69E-03		6.05E-02	Te125	1.94E-02		1.18E-02
Cm246	4.52E-04		5.89E-03	Te125m	7.70E-04		2.73E-04
Cm247	4.54E-06		1.24E-04	Sn126	1.55E-01		6.58E-02
Cm248			9.87E-06	Sb126			1.07E-05
H 3	1.68E-02		4.89E-03	Te126	2.85E-03		1.50E-03
Li 6	3.30E-05		1.10E-05	I127	3.24E-01		1.29E-01
Li 7	1.46E-06		3.84E-07	Te128	7.10E-01		2.36E-01
Be 9	2.18E-06		5.76E-07	Xe128	2.01E-02		1.32E-02
Be 10	1.31E-05		3.45E-06	I129	1.40E+00		4.60E-01
C 14	1.89E-06		4.98E-07	Xe129	1.13E-04		8.87E-05
Zn 70	1.21E-07		5.68E-08	Te130	2.80E+00		7.97E-01
Ga 71	1.15E-06		5.06E-07	Xe130	5.39E-02		1.81E-02
Ge 72	6.94E-05		2.64E-05	Xe131	3.14E+00		8.33E-01
Ge 73	2.02E-04		6.08E-05	Xe132	8.31E+00		2.44E+00
Ge 74	1.72E-04		4.83E-05	Ba132	1.82E-06		7.92E-07
As 75	1.51E-03		3.32E-04	Cs133	8.51E+00		2.20E+00

Isotope	LWR Waste	MOX Fuel	MOX SNF	Isotope	LWR Waste	MOX Fuel	MOX SNF
Ge 76	4.53E-03		8.24E-04	Xe134	1.13E+01		2.93E+00
Se 76	4.75E-05		1.49E-05	Cs134	8.91E-01		2.67E-01
Se 77	1.01E-02		2.06E-03	Ba134	2.71E-01		1.29E-01
Se 78	3.30E-02		8.45E-03	Cs135	2.52E+00		1.43E+00
Se 79	6.16E-02		1.42E-02	Ba135	2.07E-03		1.35E-03
Br 79	1.86E-07		6.51E-08	Xe136	1.70E+01		3.93E+00
Se 80	1.68E-01		3.39E-02	Ba136	1.20E-01		8.14E-02
Kr 80	7.22E-07		3.42E-07	Cs137	9.10E+00		2.47E+00
Br 81	2.45E-01		5.12E-02	Ba137	2.80E-01		1.15E-01
Kr 81	5.31E-08		3.35E-08	Ba137m	1.40E-06		3.81E-07
Se 82	3.93E-01		7.28E-02	Ba138	9.30E+00		2.37E+00
Kr 82	7.78E-03		2.56E-03	La138	6.19E-05		1.75E-05
Kr 83	4.98E-01		9.24E-02	La139	8.70E+00		2.18E+00
Kr 84	1.35E+00		2.18E-01	Ce140	8.93E+00		2.26E+00
Kr 85	2.65E-01		3.92E-02	Pr141	7.49E+00		1.89E+00
Rb 85	1.07E+00		1.62E-01	Ce142	7.94E+00		1.92E+00
Kr 86	2.12E+00		3.07E-01	Nd142	1.30E-01		3.27E-02
Sr 86	4.05E-03		8.44E-04	Nd143	5.57E+00		1.40E+00
Rb 87	2.74E+00		3.91E-01	Ce144	2.64E+00		4.38E-01
Sr 87	2.05E-05		5.10E-06	Nd144	6.25E+00		1.41E+00
Sr 88	3.86E+00		5.32E-01	Nd145	4.61E+00		1.06E+00
Y 89	4.76E+00		6.38E-01	Pm145	1.70E-07		6.29E-08
Sr 90	5.96E+00		7.83E-01	Nd146	4.73E+00		1.18E+00
Y 90	1.62E-03		2.09E-04	Pm146	6.06E-05		2.05E-05
Zr 90	2.19E-01		3.95E-02	Sm146	3.99E-05		2.02E-05
Zr 91	5.97E+00		9.16E-01	Pm147	1.21E+00		2.51E-01
Zr 92	6.87E+00		1.17E+00	Sm147	4.37E-01		1.31E-01
Zr 93	5.02E+00		9.59E-01	Nd148	2.48E+00		6.75E-01
Nb 93	2.35E-07		9.41E-08	Sm148	7.70E-01		2.58E-01
Nb 93m	3.05E-06		8.25E-07	Sm149	1.87E-02		8.46E-03
Zr 94	8.10E+00		1.67E+00	Nd150	1.20E+00		4.01E-01
Nb 94	5.11E-06		1.98E-06	Sm150	2.08E+00		5.94E-01
Mo 95	6.70E+00		1.51E+00	Sm151	1.13E-01		5.33E-02
Zr 96	8.36E+00		1.93E+00	Eu151	1.09E-04		1.05E-04
Mo 96	3.74E-01		1.10E-01	Sm152	8.57E-01		2.57E-01
Mo 97	7.83E+00		1.93E+00	Eu152	2.52E-04		2.07E-04
Mo 98	8.43E+00		2.19E+00	Gd152	3.36E-04		2.57E-04
Tc 98	7.28E-05		3.08E-05	Eu153	7.79E-01		2.85E-01
Tc 99	7.89E+00		2.02E+00	Sm154	2.44E-01		1.13E-01
Ru 99	3.08E-04		8.42E-05	Eu154	1.63E-01		9.10E-02
Mo100	9.37E+00		2.54E+00	Gd154	1.07E-02		9.64E-03
Ru100	1.04E+00		3.56E-01	Eu155	3.63E-02		1.57E-02
Ru101	7.63E+00		2.14E+00	Gd155	2.74E-04		3.48E-04
Ru102	7.68E+00		2.46E+00	Gd156	4.52E-01		2.15E-01
Rh102	1.27E-05		7.77E-06	Gd157	7.76E-04		5.97E-04
Rh103	4.26E+00		1.63E+00	Gd158	1.18E-01		6.80E-02
Ru104	5.33E+00		2.30E+00	Tb159	1.50E-02		9.73E-03
Pd104	2.01E+00		7.86E-01	Gd160	6.54E-03		4.35E-03

Isotope	LWR Waste	MOX Fuel	MOX SNF	Isotope	LWR Waste	MOX Fuel	MOX SNF
Pd105	3.71E+00		1.87E+00	Dy160	1.13E-03		1.29E-03
Ru106	1.68E+00		6.22E-01	Dy161	2.20E-03		1.71E-03
Pd106	1.90E+00		1.32E+00	Dy162	1.68E-03		1.06E-03
Pd107	2.14E+00		1.31E+00	Dy163	1.34E-03		1.10E-03
Ag107	2.22E-07		2.63E-07	Dy164	3.06E-04		3.59E-04
Pd108	1.38E+00		8.91E-01	Ho165	3.96E-04		2.79E-04
Ag108m	2.04E-06		2.47E-06	Ho166m	1.37E-06		1.28E-06
Cd108	2.08E-06		2.47E-06	Er166	8.74E-05		8.02E-05
Ag109	8.38E-01		4.60E-01	Er167	1.71E-06		1.90E-06
Pd110	4.05E-01		2.67E-01	Er168	2.09E-06		2.41E-06
Cd110	3.60E-01		3.41E-01	Tm169	1.89E-08		1.06E-08
Cd111	2.05E-01		1.37E-01	Er170	2.09E-08		1.22E-08
Cd112	1.06E-01		6.33E-02	Yb171	7.73E-09		7.25E-09

APPENDIX M

INTEGRAL FAST REACTOR (IFR) RESULTS

Table 135 - Equilibrium Composition of IFR Fuel (Moles per MTU SNF)

Isotope	Charged	Discharge	Isotope	Charged	Discharge
U232	1.79E-04	1.40E-04	Cm243	6.69E-02	6.83E-02
U233	2.62E-04	2.58E-04	Cm244	6.36E+00	6.74E+00
U234	3.71E+00	3.36E+00	Cm245	1.64E+00	1.63E+00
U235	2.82E+00	1.65E+00	Cm246	8.10E-01	8.10E-01
U236	6.67E+00	5.69E+00	Cm247	6.27E-02	6.28E-02
U237	3.15E-14	9.12E-03	Cm248	2.67E-02	2.67E-02
U238	1.50E+03	1.34E+03	Bk249	9.98E-05	4.85E-04
Np237	1.36E+01	8.88E+00	Cf249	2.46E-03	2.09E-03
Np238	1.36E-24	6.05E-03	Cf250	3.02E-04	3.36E-04
Pu236	6.23E-05	1.01E-04	Cf251	4.27E-05	4.28E-05
Pu238	2.13E+01	1.95E+01	Cf252	1.16E-05	1.16E-05
Pu239	2.58E+02	2.01E+02	FP239		1.18E+02
Pu240	1.76E+02	1.53E+02	FP240		2.10E+01
Pu241	2.25E+01	2.03E+01	FP241		2.51E+01
Pu242	4.05E+01	3.55E+01	FP235		1.69E+00
Pu243	0.00E+00	6.55E-04	FP238		2.76E+01
Pu244	1.58E-03	1.41E-03	RE239	2.18E+00	4.35E+01
Am241	3.25E+01	2.08E+01	RE240	4.17E-01	8.33E+00
Am242	2.24E-05	3.94E-03	RE241	5.08E-01	1.02E+01
Am242m	1.73E+00	1.75E+00	RE235	3.70E-02	7.39E-01
Am243	1.27E+01	1.17E+01	RE238	6.03E-01	1.21E+01
Cm242	4.11E-02	8.18E-01			

APPENDIX N

ACCELERATOR TRANSMUTATION OF WASTE (ATW) RESULTS

Table 136 - Equilibrium Composition of ATW Reactor Fuel (Moles per MTU SNF)

Isotope	Charged	Dischrage	Isotope	Charged	Dischrage
U232	7.57E-05	5.04E-05	Cm243	1.58E-01	1.64E-01
U233	8.86E-05	8.87E-05	Cm244	9.14E+00	9.73E+00
U234	1.80E+00	1.53E+00	Cm245	2.70E+00	2.68E+00
U235	4.38E-01	4.31E-01	Cm246	1.51E+00	1.51E+00
U236	5.80E-01	5.56E-01	Cm247	1.62E-01	1.62E-01
U237	9.95E-17	1.21E-03	Cm248	7.65E-02	7.66E-02
U238	3.26E+00	2.76E+00	Bk249	6.61E-04	3.22E-03
Np237	9.85E+00	4.66E+00	Cf249	8.63E-03	6.11E-03
Np238	1.52E-24	8.26E-03	Cf250	2.27E-03	2.53E-03
Pu236	4.33E-05	7.04E-05	Cf251	4.27E-04	4.28E-04
Pu238	1.88E+01	1.63E+01	Cf252	1.29E-04	1.29E-04
Pu239	1.14E+02	4.99E+01	FP239		4.06E+01
Pu240	1.24E+02	9.80E+01	FP240		1.31E+01
Pu241	2.08E+01	1.80E+01	FP241		2.53E+01
Pu242	4.03E+01	3.47E+01	FP235		4.28E-01
Pu243	0.00E+00	1.68E-03	FP238		6.52E+00
Pu244	2.44E-03	2.25E-03	RE239	7.48E-01	1.50E+01
Am241	2.62E+01	1.37E+01	RE240	2.59E-01	5.19E+00
Am242	1.68E-05	6.46E-03	RE241	5.13E-01	1.03E+01
Am242m	1.30E+00	1.30E+00	RE235	9.37E-03	1.87E-01
Am243	1.29E+01	1.17E+01	RE238	1.43E-01	2.85E+00
Cm242	6.69E-02	1.42E+00			

REFERENCES

1 "First Phase P&T Systems Study: Status and Assessment Report on Actinide and Fission Product Partitioning and Transmutation", OECD/NEA, Paris (1999).

2 "Proc. 1st-5th NEA International Exchange Meetings", OECD/NEA, Paris (1990,92,94,96,98).

3 "Nuclear Wastes--Technologies for Separations and Transmutations", National Research Council, National Academy Press, Washington (1996).

4 R.N. Hill, et. al., "Multiple Tier Fuel Cycle Studies for Waste Transmutation," Proceedings of ICONE 10: 10th International Conference on Nuclear Engineering, April 14-18, 2002, Arlington, VA, USA.

5 C. D. Bowman, et al., "Nuclear Energy Generation and Waste Transmutation Using Accelerator-Driven Intense Thermal Neutron Source", *Nucl. Instr. Methods, A320*, 336 (1992).

6 W. C. Sailor, et al., "Comparison of Accelerator-Based with Reactor-Based Nuclear Waste Transmutation Schemes", *Progress in Nuclear Energy, 28*, 359 (1994).

7 "A Roadmap for Developing Accelerator Transmutation of Waste (ATW) Technology", US Dept. Energy report DOE/RW-0519 (1999).

8 E.T. Cheng, et. al., "Actinide Transmutation with Small Tokamak Fusion Reactors," Proc. Int. Conf. Eval. Emerging Nuclear Fuel Cycle Systems, Versailles, France (1995).

9 E.T. Cheng and R.J. Cerbone, "Prospect of Nuclear Waste Transmutation and Power Production in Fusion Reactors," Fusion Technology, 30, 1654 (1996).

10 Y. Gohar, "Fusion Option to Dispose of Spent Nuclear Fuel and Transuranic Elements," Argonne National Laboratory report ANL/TD/TM00-09 (2000).

11 W.M. Stacey, "Capabilities of a DT Tokamak Fusion Neutron Source for Driving a Spent Nuclear Fuel Transmutation Reactor," Nucl. Fusion, 41, 135 (2001).

12 W.M. Stacey, et. al., "A Fusion Transmutation of Waste Reactor," Fusion Science and Technology, Volume 41, March 2002.

13 E.A. Hoffman and W.M. Stacey, " Nuclear And Fuel Cycle Analysis For A Fusion Transmutation Of Waste Reactor ", Fusion Eng. Des., to be published (2002); also "Nuclear Design and Safety Analysis of the Fusion Transmutation of Waste Reactor," Fusion Sci. Technol., in preparation (2002).

14 Office of Civilian Radioactive Waste Management Web Site (http://www.rw.doe.gov)

15 DOE Report DOE/RW-0006, Integrated Data Base Report – 1996: US Spent Nuclear Fuel and Radioactive Waste Inventories, Projections, and Characteristics, 1-7 (1997).

16 F. Najmabadi, et al., "ARIES-I Tokamak Reactor Study Final Report", Univ. California Los Angeles report UCLA-PPG-1323, (1991)

17 Y. Severi, et. al. "Water-Cooled Lithium-Lead Box-Shaped Blanket Concept for Demo: Thermo-mechanical Optimization and Manufacturing Sequence Proposal," Fusion Technology, 1992, pp. 1484-1488.

18 F. Venneri et al., "A Roadmap for the Developing ATW Technology: Target-Blanket Technology," Los Alamos National Laboratory Report LA-UR-99-3022, September 1999.

19 Nuclear Reactor Physics, p 235

20 National Research Council, "Nuclear Wastes Technology for Separations and Transmutation," Washington D.C., National Academy Press, 1996.

21 Domenici, Pete V., Inaugural Symposium, Belfer Center for Science and International Affairs, Harvard University, October 31, 1997.

22 "A Roadmap for Developing Accelerator Transmutation of Waste (ATW) Technology A Report to Congress," DOE/RW-0519, October 1999.

23 T.R. England, and B.F. Rider, "ENDF-349 Evaluation and Compilation of Fission Product Yields 1993," Los Alamos National Laboratory, LA-UR-94-3106, October, 1994.

24 "Table of Nuclides," Korea Atomic Energy Research Institute, http://atom.kaeri.re.kr/.

25 "Viability Assessment of a Repository at Yucca Mountain," DOE/RW-0508, December 1998.

26 Wachter, J.W., Croff, A.G., "Actinide Partitioning-Transmutation Program Final Report. III. Transmutation Studies," Oak Ridge National Laboratory, ORNL/TM-6983, July 1980.
27 Salvatores, M., Prunier, C., "Transmutation and Nuclear Radioactive Waste Management: a Perspective," Endeavour, New Series, Volume 17, No. 3, 1993.
28 Hermann, O.W., Westfall, R.M., "ORIGEN-S: SCALE System Module to Calculate Fuel Depletion, Actinide Transmutation, Fission Product Buildup and Decay, and Associated Radiation Source Terms," NUREG/CR-0200, Revision 6, Volume 2, Section F7, ORNL/NUREG/CSD-2/V2/R6, September 1998.
29 Ryman, J.C., Hermann, O.W., "ORIGEN-S Data Libraries," NUREG/CR-0200, Revision 6, Volume 3, Section M6, ORNL/NUREG/CSD-2/V3/R6, September 1998.
30 Croff, Allen G., "A Concept for Increasing the Effective Capacity of a Unit Area of a Geologic Repository," Radioactive Waste Management and Environmental Restoration, Vol. 18, 1994, pp. 155-180.
31 "MCNP™ - A General Monet Carlo N-Particle Transport Code, Version 4B," Briesmeister, H.F., Ed., Los Alamos Nation Laboratory, LA-1265-M, Version 4B Manual, March 1997.
32 D.E. Beller, and R.A. Krakowski, "Burnup Dependence of Proliferation Attributes of Plutonium from Spent LWR Fuel," Los Alamos National Laboratory, LA-UR-99-751, February 1999.
33 Office of Civilian Radioactive Waste Management Web Site (http://www.rw.doe.gov)
34 DOE Report DOE/RW-0006, Integrated Data Base Report – 1996: US Spent Nuclear Fuel and Radioactive Waste Inventories, Projections, and Characteristics, 1-7 (1997).
35 DoE Office of Civilian Radioactive Waste Management, "Draft Environmental Impact Statement for a Geologic Repository - Appendix A: Inventory and Characteristics of Spent Nuclear Fuel, High-Level Radioactive Waste, and Other Materials," DOE/EIS-0250D, July 1999.
36 R.N. Hill, "LWR Feed Inventory Specifications for ATW System Studies," internal memo, Argonne National Laboratory, June 12, 2000.
37 NEI Nuclear Energy Insight, June 1999.
38 "North Anna Unit 2, Cycle 9 Design Report," Technical Report NE-885 - Rev. 0, Virginia Power, April 1992.
39 R.G. Cochran, N. Tsoulfanidis, "The Nuclear Fuel Cycle: Analysis and Management," American Nuclear Society, 1990.
40 F. Rahnema, D. Ilas, S Sitaraman, "Boiling Water Reactor Benchmark Calculations," Nuclear Technology, Volume 117, February 1997.
41 " Universal Nuclide Chart and Radioactive Decay Applet," European Communities, January 24, 2001, http://www.nuclides.net/applets/radioactive_decay.htm.
42 "SCALE: A Modular Code System for Performing Standardized Computer Analyses for Licensing Evaluation," NUREG/CR-0200, Rev. 5 (ORNL/NUREG/CSD-2/R5), Vols I, II, and III, March 1997.
43 W.M. Stacey, et. al., "A Fusion Transmutation of Waste Reactor," Fusion Science and Technology, Volume 41, March 2002.
44 WebElements™, the periodic table on the WWW, URL: http://www.webelements.com/ Copyright 1993-2002 Mark Winter [The University of Sheffield and WebElements Ltd, UK]. All rights reserved. Document modification date: 03 April 2002
45 DIII-D paper that had density profile
46 E.A. Hoffman, W.M. Stacey, N.E. Hertel, "Radioactive Waste Disposal Characteristics of Candidate Tokamak Demonstration Reactors," Fusion Research Center, Georgia Institute of Technology, GTFR 119, August, 1995.
47 S.J. Zinkle, "Summary of Physical Properties for Lithium, Pb-17Li, and $(LiF)_n \bullet BeF_2$ Coolants," APEX Study Meeting, Sandia National Lab, July 27-28, 1998.
48 P.N. Martynov, K.D. Ivanov, "Properties of Lead-Bismuth Cooland and Perspectives of Non-Electric Applications of Lead-Bismuth Reactors," IAEA-TECDOC--1056, International Atomic Energy Agency.
49 B.J. Toppel, "A User's Guide to the REBUS-3 Fuel Cycle Analysis Capability," ANL-83-2, Argonne National Laboratory (1983)
50 "DANTSYS: A Diffusion Accelerated Neutral Particle Transport Code System," LA-12969-M MANUAL UC-705, March 1997.

51 H. Henryson II, et al., "MC^2-2: A Code to Calculate Fast Neutron Spectra and Multigroup Cross Sections," ANL-8144, Argonne National Laboratory (1976).
52 W.M. Stacey, Jr., et al., "A New Space-Dependent Fast-Neutron Multigroup Cross Section Processing Capability," Trans. Am. Nucl. Soc., 15, 292, (1972).
53 M.A. Abdou, E.L. Vold, C.Y. Gung, M.Z. Youssef, and K. Shin, "Deuterium-Tritium Fuel Self-Sufficiency in Fusion Reactors," Fusion Technol. 9, 250 (1986).
54 W. S. Yang and H. Khalil, "ATW System Point Design Employing LBE Cooled Blanket Design", Argonne National Laboratory Report (2000).
55 J. Buongiorno, N.E. Todreas, and M. Kazimi, "Thermal Design of Lead-Bismuth Cooled Reactors for Actinide Burning and Power Production," Massachusetts Institute of Technology, MIT-ANP-TR-066, July 1999.
56 Lamarsh, Introduction to Nuclear Engineering
57 D.S. Gelles, "Microstructural Examination of Commercial Ferritic Alloys at 200 DPA," Semiannual Progress Report, DOE/ER-0313/16, (1994).
58 Mohamed Sawan, University of Wisconsin, personal communication, March 2001.
59 W. M. Stacey, Nuclear Reactor Physics, Wiley-Interscience, New York (2001) p 168-177.
60 H.U. Wider and J. Karlsson, "Safety Aspects of Heavy Metal-Cooled Accelerator-Driven Waste," Journal De Physique IV, Vol. 9, 1999, pp. 127-131.
61 W. Maschek and D. Struwe, "Accident Analysis and Passive Measures Reducing the Consequence of a Core-Melt in CAPRA/CADRA Reactor Cores," Nuclear Engineering and Design, Vol. 202, 2000, pp. 311-324.
62 R.N. Hill and H. Khalil, "ATW System Point Design Employing Sodium Cooled Blanket Design", Draft ATW Report, Argonne National Laboratory, July 21, 2000.
63 R.N. Hill, Argonne National Laboratory, personal communication.
64 W. S. Yang and H. Khalil, "ATW System Point Design Employing LBE Cooled Blanket Design", Argonne National Laboratory Report (2000).
65 Nuclear Reactor Physics, p 235
66 "Plutonium Recycling in Pressurized-water Reactors Benchmark Results Analysis," Physics of Plutonium Recycling Volume II, A report by the Working Party on the Physics of Plutonium Recycling of the NEA Nuclear Science Committee (1995).
67 R.N. Hill, D.C. Wade, J.R. Liaw, and E.K. Fujita, "Physics Studies of Weapons Plutonium Disposition in the Integral Fast Reactor Closed Fuel Cycle," Nuclear Science and Engineering, Vol. 121, September 1995.
68 B.J. Toppel, "A User's Guide to the REBUS-3 Fuel Cycle Analysis Capability," ANL-83-2, Argonne National Laboratory (1983)
69 "DANTSYS: A Diffusion Accelerated Neutral Particle Transport Code System," LA-12969-M MANUAL UC-705, March 1997.
70 H. Henryson II, et al., "MC^2-2: A Code to Calculate Fast Neutron Spectra and Multigroup Cross Sections," ANL-8144, Argonne National Laboratory (1976).
71 W.M. Stacey, Jr., et al., "A New Space-Dependent Fast-Neutron Multigroup Cross Section Processing Capability," Trans. Am. Nucl. Soc., 15, 292, (1972).
72 R.N. Hill, and H.S. Khalil, "Physic Studies for Sodium Cooled ATW Blanket," Proc. IAEA Mtg. on Emerging Nuclear Energy Systems, Argonne, Illinois, 2000.
73 B.J. Toppel, "A User's Guide to the REBUS-3 Fuel Cycle Analysis Capability," ANL-83-2, Argonne National Laboratory (1983)
74 "DANTSYS: A Diffusion Accelerated Neutral Particle Transport Code System," LA-12969-M MANUAL UC-705, March 1997.
75 H. Henryson II, et al., "MC^2-2: A Code to Calculate Fast Neutron Spectra and Multigroup Cross Sections," ANL-8144, Argonne National Laboratory (1976).
76 W.M. Stacey, Jr., et al., "A New Space-Dependent Fast-Neutron Multigroup Cross Section Processing Capability," Trans. Am. Nucl. Soc., 15, 292, (1972).
77 "Viability Assessment of a Repository at Yucca Mountain," DOE/RW-0508, December 1998.
78 D.E. Beller, and R.A. Krakowski, "Burnup Dependence of Proliferation Attributes of Plutonium from Spent LWR Fuel," Los Alamos National Laboratory, LA-UR-99-751, February 1999.